UNIVERSITY OF CALIFORNIA, MERCED

Community ecology, stable isotope ecology, and taxonomy of small mammal fossils from Rancho La Brea, Los Angeles, CA

A dissertation submitted in partial satisfaction of the requirements
for the degree Doctor of Philosophy

in

Environmental Systems

by

Nathaniel S. Fox

Committee in charge:

Dr. Stephen C. Hart, Chair
Dr. Jessica L. Blois
Dr. Sora Kim
Dr. Emily L. Lindsey
Dr. Justin D. Yeakel

2020

The Dissertation of Nathaniel S. Fox is approved, and it is acceptable in quality and form for publication on microfilm and electronically:

_____
Jessica L. Blois, Advisor

_____
Stephen C. Hart, Chair

_____
Sora Kim

_____
Emily L. Lindsey

_____
Justin D. Yeakel

Table of Contents

List of Tables

List of Figures

Acknowledgements

This dissertation has MANY contributors. First, I thank my awesome family: Kris, Than, Elizabeth, David, and Nat Fox; Grisel, Guadalupe, Trinidad Sr., and Trinidad Aguiniga Lopez; and Judy Wright for their continuous support and encouragement over the last five years.

Next, I thank my amazing advisor, Jessica Blois, for her guidance, time, feedback, and endless patience throughout my graduate career at UC Merced. I also thank dissertation committee members: Emily Lindsey, Justin Yeakel, Sora Kim, and Stephen Hart for their mentorship and suggestions that enriched my research. Past and present Blois Lab members: Robert Boria, Danaan DeNeve Weeks, Mairin Balisi, Kinsey Brock, Laura Van Vranken, Eric Williams, Giovanni Rapacciuolo, Kaitlin Maguire, Paulo Ricardo de Oliveira Roth, and Sarah Brown are thanked for their professional and personal support. I am lucky to have such great colleagues and friends.

This project would not have been possible without the collective contributions of La Brea Tar Pits and Museum staff and volunteers: Aisling Farrell, Barbara Hill, Beau Campbell, Bob Yeager, Chris McCrystal, Christine Mazzello, Dixie Swift, Gary Takeuchi, Gene Poppe, Geneva Rangel, Jack Schwellenback, Joe DelVecchio, Judith Sydner-Gordon, Karin Rice, Lahari Indraganti, Laura Tewksbury, Lauren Fabia, London Ruff, Lynne Schneider, Marsha Lenox, Mary Ellen Friedman, Mary Simun, Matt Hooper, Nika Aroustamian, Nola Milner, Paul Byrne, Paul Eppleston, Ruth Cohen, Safi Alia Shabaik, Sean Campbell, Sheila Pressman, Sherree Strong, Stephany Potze, Stevie Morley, Susan Masters, Tara Thara, and Carrie Howard who excavated, sorted, prepared, organized, and archived the thousands of fossils included in these studies. I am indebted to you all.

Many thanks to Marilyn Fogel for introducing me to the world of stable isotope ecology and encouraging me to pursue isotopic research. I am also grateful to research mentors: Alexis Mychajliw, Benjamin Fuller, Emily Jane McTavish, Jenny McGuire, John Southon, Robin Trayler, and research mentees: Chris Jorgensen, Iheoma Chieke, and Joseph Veneracion who assisted this project. Finally, I thank my research hosts and grant collaborators: Alex Lentz, Chris Conroy, Jacquelyn Gill, Jim Dines, John Romano, Josh Meyers, Katherine Glover, Libby Ellwood, Luis Chiappe, Mark Omura, Pat Holroyd, and Taran Rallings.

This project was funded in part by National Science Foundation grants EAR-1623852 and EAR-1623885, the American Society of Mammologists 2017 Grant-in-Aid of research, and the Paleontological Society 2018 N. Gary Lane award.

Chapter 1 is a full reprint of the material as it appears in PaleoBios: https://escholarship.org/uc/item/9tr0d3wq. © 2019 PaleoBios CC BY-NC-SA 4.0. The dissertation author, Nathaniel Fox, designed the study, led the acquisition, analysis, and

interpretation of data, and wrote the article. Gary Takeuchi and Aisling Farrell helped acquire and manage data and revised the manuscript. Jessica Blois directed and supervised this research, which forms the basis for the dissertation, and revised the manuscript.

Chapter 2 is a full reprint of the material as it appears in Ecology and Evolution: https://doi.org/10.1002/ece3.6063. © 2020 Wiley Open Access CC BY. Nathaniel Fox designed the study, led the acquisition, analysis, and interpretation of data, and wrote the article. Joseph Veneracion helped acquire data and performed data analyses supervised by Nathaniel Fox. Jessica Blois directed and supervised this research, which forms the basis for the dissertation, provided analytical support, and revised the manuscript.

Curriculum Vitae

EDUCATION

University of California, Merced (UCM) — **Merced, CA**
Doctor of Philosophy in Environmental Systems — Expected August 2020

East Tennessee State University (ETSU) — **Johnson City, TN**
Master of Science in Geosciences, concentration in Paleontology — May 2014

University of Massachusetts, Amherst (UMass) — **Amherst, MA**
Bachelor of Science in Biology, minor in Geology — May 2011

RECENT PROFESSIONAL APPOINTMENTS AND EXPERIENCE

UCM Graduate Division — Merced, CA
Research Assistant — *August 2016 – Present*
Teaching Assistant
- Evolution and Development discussions (spring 2016) — *January 2016 – May 2016*
- Introductory Biology labs (fall 2015) — *August 2015 – December 2015*

Undergraduate Research Mentor — *September 2016–May 2020*

Neotoma Paleoecology Database
Data steward — January 2019 – *May 2020*

La Brea Tar Pits and Museum — Los Angeles, CA
Assistant Collections Manager — *June 2018 – August 2018*

SWCA Environmental Consultants — Sheridan, WY
Paleontological Specialist I, SWPPP Inspector — *June 2014 – July 2015*

ETSU Natural History Museum and Gray Fossil Site — Johnson City, TN
Research Associate — *May 2014 – Present*

ETSU Department of Geosciences — Johnson City, TN
Teaching Assistant — *January 2012 - May 2014*
- Introductory geology labs (fall 2012, spring 2013, fall 2013, spring 2014)

Research Assistant — *May 2012 - May 2014*
- Vertebrate collections and field assistant

Rockport Public Schools; Gloucester Public Schools — Rockport, MA; Gloucester, MA
Substitute Teacher — *September 2011 - May 2014*

Denver Museum of Nature and Science — Snowmass, CO
Intern for Project Snowmastodon — *May 2011 - July 2011*

The Mammoth Site of Hot Springs, South Dakota — Hot Springs, SD
Summer Intern — *May 2010 - August 2010*

PEER-REVIEWED PUBLICATIONS

Fox, N.S., J.J. Veneracion, and J.L. Blois. 2020. Are geometric morphometric analyses

replicable? Evaluating landmark measurement error and its impact on extant and fossil *Microtus* classification. Ecology and Evolution 10(7): 3260-3275. https://doi.org/10.1002/ece3.6063

Fox, N.S., G.T. Takeuchi, A.B. Farrell, and J.L. Blois. 2019. A protocol for differentiating late Quaternary leporid species in southern California with remarks on Project 23 lagomorphs at Rancho La Brea, Los Angeles, California, USA. PaleoBios 36:1-20. https://escholarship.org/uc/item/9tr0d3wq

Fox, N.S., S.C. Wallace, and J.I. Mead. 2017. Fossil *Mustela nigripes* from Snake Creek Burial Cave, Nevada, and implications for black-footed ferret paleoecology. Western North American Naturalist 77:137-151. https://doi.org/10.3398/064.077.0202

Getty, P., C. Aucoin, **N.S. Fox**, A. Judge, L. Hardy, and A. Bush. 2017. Perennial lakes as an environmental control on theropod movement in the Jurassic of the Hartford Basin. Geosciences 7:13. https://doi:10.3390/geosciences7010013

Getty, P., and **N.S. Fox**. 2015. An Isolated *Eubrontes giganteus* Trackway from the Gary Gaulin Dinosaur Track Site (Early Jurassic, East Berlin Formation), Holyoke, Massachusetts. Northeastern Geoscience 33:16-21.

THESES

Fox, N.S. Community Ecology, Stable Isotope Ecology, and Taxonomy of Small Mammal Fossils from Rancho La Brea, Los Angeles, CA. Doctoral dissertation, University of California, Merced, California.

Fox. N.S. 2014. Analysis of Snake Creek Burial Cave *Mustela* fossils using Linear & Landmark-based Morphometrics: Implications for Weasel Classification & Black-footed Ferret Conservation. Master's thesis, East Tennessee State University, Johnson City, Tennessee.

RECENT GRANTS, FELLOWSHIPS, AND AWARDS

UC Merced 2020, Graduate Dean's Dissertation Fellowship

UC Merced 2019, ES Graduate Student Professional Development Fellowship

Paleontological Society 2018, N. Gary Lane Award

UC Merced 2018, ES Graduate Student Professional Development Fellowship

UC Merced 2017-18, Research & Travel Fellowship

American Society of Mammologists 2017, Grant-in-Aid of Research

UC Merced 2017, Environmental Systems Summer Travel Fellowship

UC Merced 2016, Environmental Systems Summer Research Fellowship

SELECTED CONFERENCE ABSTRACTS

Fox, N.S., J.R. Southon, G.T. Takeuchi, A.B. Farrell, E.L. Lindsey, and J.L. Blois. Baseline shifts in small mammal communities at Rancho La Brea track late Quaternary environmental changes in southern California. To be presented orally at the 79th Annual Society of Vertebrate Paleontology Meeting, Brisbane, Queensland. October 2019.

Fox, N.S., J.R. Southon, G.T. Takeuchi, A.B. Farrell, E.L. Lindsey, T. Rallings, J.D. Yeakel, K.C. Glover, J.L. Gill, and J.L. Blois. Identification and analysis of small mammal fossils at Rancho La Brea elucidate responses to late Quaternary environmental change in southern

California**.** Oral Presentation at the 11th North American Paleontological Convention, Riverside, CA. June 2019.

Blois, J.L., **N.S. Fox**, K. Glover, J. Gill, T. Rallings, J. Yeakel, J. Southon, G.T. Takeuchi, A.B. Farrell, and E.L. Lindsey. Small mammal population and assemblage dynamics at the Rancho La Brea Tar Pits. Poster presented at the International Biogeography Society Meeting, Málaga, Spain. January 2019.

Fox, N.S., J.R. Southon, G.T. Takeuchi, A.B. Farrell, E.L. Lindsey, and J.L. Blois. Small mammal community dynamics and isotope ecology at Rancho La Brea: millennial-scale stability or change? Poster presented at the 98th Annual Meeting of the American Society of Mammalogists, Manhattan, KS. June 2018.

Blois, J.L., **N.S. Fox**, K. Glover, J. Gill, T. Rallings, J. Yeakel, B.T. Fuller, J. Southon, G.T. Takeuchi, A.B. Farrell, and E. Lindsey. Assessing drivers of millennial-scale small mammal community structure and dynamics at the Rancho La Brea Tar Pits. Co-author on oral presentation at the Biogeography Society annual meeting, Évora, Portugal. March 2018.

Fox, N.S., J.R. Southon, B.T Fuller, G.T. Takeuchi, A.B. Farrell, E.L. Lindsey, and J.L. Blois. A Tale of Two Faunas: Small Mammal Paleoecology within and among Project 23 Deposits at Rancho La Brea. Poster presented at the 77th Annual Society of Vertebrate Paleontology Meeting, Calgary, AB. August 2017.

Fox, N.S. and J.L. Blois. Preliminary Analysis of Small Mammal Fossils from "Project 23" at Rancho La Brea, Los Angeles, CA. Poster presented at the Western Association of Vertebrate Paleontology Annual Meeting, Anza-Borrego Desert State Park, Borrego Springs, CA. February 2016.

Knauss, G.E., S.L. Johnson, L. Hall, **N.S. Fox**, and V.L. Meyers. From Grasslands to Well Pad: A Mitigation Paleontological Discovery, Lance Formation (Maastrichtian), Wyoming Proves the Value of Implementing Best Practices. Poster presented at the 75th Annual Society of Vertebrate Paleontology Meeting, Dallas, TX. October 2015.

Fox, N.S. Morphometric analysis of black-footed ferret dentaries from Snake Creek Burial Cave, Nevada. Oral presentation at the 40th Anniversary Mammoth Site Mini-Symposium, Hot Springs, SD. June 2014.

Fox, N.S. Interpretation of Early Mesozoic Ichnology in Holyoke, MA**.** Oral presentation at the Southeast Association of Vertebrate Paleontology Meeting, Boone, NC. August 2012.

PROFESSIONAL SERVICE AND OUTREACH

ad hoc peer reviewer for interdisciplinary journals: Ecography, Global Ecology and Biogeography, PaleoBios, and Quaternary Science Reviews

Oral presenter for the La Brea Tar Pits lunch talk, Los Angeles, CA. August 2019

Member of Quest[X], a non-profit scientific outreach organization. Spring 2016 – present.

Ada Givens Elementary School S.T.E.A.M Center guest speaker, Merced, CA. Oct. 2018.

Oral presenter for La Brea Tar Pits Summer Field School, Los Angeles, CA. June 2018.

Oral presenter for the La Brea Tar Pits "Digging Deeper" lecture series, Los Angeles, CA. June 2017.

Oral presenter at the National GIS Day Gray Fossil Site public lecture series, Johnson City, TN. November 2013.

Abstract of the Dissertation

Community ecology, stable isotope ecology, and taxonomy of small mammal fossils from Rancho La Brea, Los Angeles, CA

by

Nathaniel S. Fox

Doctor of Philosophy, Environmental Systems
University of California, Merced 2020
Dr. Jessica L. Blois, Graduate Advisor
Dr. Stephen C. Hart, Chair

Contemporary species are undergoing population declines and extinction at rates unprecedented in recorded history. These ongoing global biodiversity losses are largely caused by human overpopulation and other anthropogenic impacts on the environment such as natural habitat destruction driven by urbanization, deforestation, agriculture, pollution, overconsumption of natural resources, and climate change. Understanding how species are influenced by – and respond to – various changes in their environment is critical for predicting and mitigating future biodiversity loss. These predictions are challenging, however, because humans have been heavily modifying ecosystems for centuries – well before the advent of modern ecology as a field of study. Disentangling species responses to naturally occurring changes in their environment versus anthropogenic changes is thus extremely challenging.

Paleoecological studies of fossil organisms can help establish the baseline responses of biota to natural environmental changes at times before humans dominated terrestrial ecosystems. However, these studies have their own set of challenges. For example, it can be difficult to determine how representative a preserved fossil community is of the original living community because the fossil record is inherently incomplete and often biased. It is also difficult to quantify species-specific responses to environmental change if the identity of species is unknown or imprecise; and due to the fragmentary nature of the fossil record, it can be difficult to identify isolated elements to species. The incompleteness of the fossil record does not only apply to the organisms preserved, but also to the environmental data documenting the contexts in which they operated while alive and during preservation. Most paleontological assemblages are affected by time-averaging and incomplete depositional sequences to some degree. Depending on the severity of time averaging, and the resolution of data collected, these temporal gaps can

erase fine-scale and geologically rapid events that are important for understanding ecological patterns and processes.

These unique opportunities and challenges of working with paleoecological data are what motivate my research. Within the scope of my dissertation, my goals are twofold. Foremost, I strive to quantify long-term biotic composition, diversity, and trait changes in response to pre-anthropogenic environmental change at population and community levels to establish baselines of organismal responses to natural ecosystem perturbations. However, to accomplish this, it is first necessary to quantify the strengths and limitations of paleontological data in these systems and maximize data resolution to mitigate erroneous interpretations. The main data types I focus on improving here are those of taxonomic fidelity and age control. The first three chapters of my dissertation focus on the former, using morphometric techniques to improve identification accuracy of closely related and morphologically similar species, thus extending paleoecological data resolution from genus to species for several taxa. The last two chapters of my dissertation focus on the latter, examining paleoecological data at various levels of temporal precision using a combination of radiocarbon-dated and time-averaged data to determine how analytical results and conclusions are affected by time-averaging. Once these limitations have been quantified and mitigated to the extent possible, I determine how the focal taxa of my study system were impacted by long-term environmental changes using multidisciplinary approaches. Chapter 3 focuses on intraspecific phenotypic responses to climate change using geometric morphometrics, Chapter 4 evaluates long-term changes in biotic community structure using diversity and trait metrics, and Chapter 5 quantifies the relative impacts of climate and biotic interactions on species niches over the last 50,000 years using stable isotope analysis. My study system for addressing all these topics is Rancho La Brea (RLB), a world renowned late Quaternary paleontological locality in Los Angeles, California, USA. I specifically examine the small mammals (e.g., rodents, lagomorphs, and soricomorphs) of this locality because they are ubiquitous across most Quaternary fossil assemblages, thus facilitating large sample sizes. In addition, small mammals are generally short lived and confined to small home ranges, so I am relatively certain that the paleoecological signals I track within samples are local and geologically instantaneous rather than substantially spatially or temporally averaged.

Results of the three taxonomic studies indicate that, although closely related and speciose small mammals are difficult to differentiate due to morphological variation and overlap, they can be identified to species with relatively good accuracy, usually > 80%, using quantitative techniques including morphometric and geometric morphometric measurements and statistical grouping analyses (Chapters 1-3). However, results can deviate considerably if data acquisition processes are not standardized. For example, geometric morphometric data collected by different personnel and, to a lesser extent, with different instruments can generate substantially different classification statistics (Chapter 2). It is therefore recommended that data acquisition procedures are standardized as much

as possible to facilitate analytical replicability. Comparisons of time-averaged trait datasets (Chapters 4 and 5) to those with good age control (Chapter 5) further show that much information can be lost from geologically rapid events when data is time-averaged or time-binned versus continuous data. Such loss of information can then result in profoundly different interpretations regarding the probable drivers of observed paleoecological patterns (Chapter 5).

With these insights and limitations in mind, I show that local environments of RLB during the last glacial period (specifically Marine Isotope Stage (MIS) 3, ~60,000 to 29,000 years BP) were generally similar to that of the Los Angeles Basin today based on overall similarities between contemporary and fossil small mammal faunas (Chapter 4). Changes in taxonomic abundances and trait diversity among deposits of different mean ages suggest that the small mammal communities of RLB were responding to slight or moderate changes in temperature and precipitation during that time (Chapter 4). Unfortunately, precise information on the timing and pattern of environmental changes cannot be discerned at the community level due to the time-averaged nature of the deposits and faunas examined, combined with the variable climates during MIS 3. By subsequently examining the isotopic niches of individually-dated specimens, however, it becomes clear that geologically rapid environmental changes were occurring at RLB throughout the late Quaternary that largely reflect regional climate patterns (Chapter 5). Further, the isotopic niches of small mammals appear to be shaped more strongly by those climatic oscillations than by biotic interactions over the last 50,000 years. Insights on the paleoenvironments of RLB (Chapter 4) and climatic changes that likely occurred there during the late Quaternary (Chapter 5) have significant implications for studies of other RLB biota in that species responses to changing environments can be better contextualized now that those changes are better understood. In a broader context, my work quantifying geometric morphometric error (Chapter 2) and time-averaging error (Chapter 5) may facilitate best practices protocols for similar study systems. Finally, my taxonomic identification protocols for lagomorphs (Chapter 1) and woodrats (Chapter 3) should be useful for other small mammal studies because lagomorph remains are common at most late Quaternary sites and woodrat species are good indicators of paleoecological conditions and change.

Chapter 1: A protocol for differentiating late Quaternary leporids in southern California with remarks on Project 23 lagomorphs at Rancho La Brea, Los Angeles, California

1.1 Abstract

Leporid remains are common in Quaternary fossil assemblages and are useful paleoenvironmental indicators. Identifying leporid fossils to species is challenging, though previous work has shown that identifications are more feasible if fossils can be narrowed down to a subset of potential species occurring across limited spatial scales. I sampled 120 adult and nine juvenile dentaries of six extant western North American species (*Lepus americanus, L. californicus, L. townsendii, Sylvilagus audubonii, S. bachmani*, and *S. nuttallii*) to establish useful characters for genus and species-level identification of late Quaternary leporid fossils in California. Most individuals can be differentiated from individuals of other species using a combination of lower third premolar enamel folding patterns and dental measurements. However, it is difficult to discriminate dental elements among *L. californicus* and *L. townsendii* and elements of *S. nuttallii* from *S. audubonii*, *S. bachmani*, and *L. americanus*. Here I present criteria for differentiating western leporid dental remains, apply the criteria to identify specimens recovered from several late Quaternary fossil deposits at Rancho La Brea (RLB), California, collectively known as Project 23, and reconstruct changes in relative fossil leporid abundances there. Using these criteria, I identified two extant species, *S. audubonii* and *S. bachmani*, among the Project 23 fossils. In addition to relative abundance changes across several RLB deposits, *S. audubonii* and *S. bachmani* generally become larger through time, possibly in response to local environmental changes. Establishing region-specific identification criteria as done here may prove useful for discerning morphologically similar species at prehistoric sites elsewhere.

1.2 Introduction

Leporids (rabbits and hares) occupy diverse habitats, provide important ecosystem services, and are prevalent in Quaternary paleofaunas throughout North America (Kurtén & Anderson, 1980; Smith et al., 2018). As such, their fossils are useful indicators of paleoenvironments and for tracking environmental changes through time (e.g., Driver & Woiderski, 2008; Hulbert, 1984; Somerville et al., 2018; Wicks et al., 2015). Identifying isolated leporid fossils to species is challenging, however, due to extensive morphological variation and range overlap among taxa (Dalquest, 1979; Hall & Kelson, 1959; White, 1991). Useful characters for differentiating species in one region are not always useful for differentiating the same species in another region due to intraspecific variation across spatial gradients (Hall & Kelson, 1959); this problem is compounded across temporal gradients due to changing climates and shifting geographic ranges. Isolated elements of common North American leporids, including *Lepus* Linnaeus (1758) spp. and *Sylvilagus* Gray (1867) spp., generally cannot be differentiated using

morphology alone (Dalquest, 1979; Jass, 2009; Kurtén & Anderson 1980), with some exceptions. Individuals of some species can be differentiated based on the degree of enamel folding (crenulation) across the posterobuccal re-entrant of the lower third premolar (p3) (Dalquest et al., 1989) and the addition of craniomandibular size measurements can sometimes help differentiate species of *Lepus* and *Sylvilagus* (Pettus, 1956). Most individuals, however, cannot be differentiated using this method exclusively (Jass, 2009; White, 1991), in the absence of additional contextual information.

Despite the difficulty of identifying isolated leporid elements to species, studies have been more successful at discriminating leporid taxa within limited spatial scales. For example, Hulbert (1984) found no size overlap in maxillary and mandibular measurements of recent *Lepus californicus*/*Sylvilagus aquaticus* and *S. audubonii*/*S. floridanus* collected throughout the state of Texas. Leporid fossils from central Texas were differentiated between those taxonomic pairs using size alone, though discriminant analyses were needed to differentiate *L. californicus* Gray (1837) from *S. aquaticus* and *S. audubonii* Baird (1857) from *S. floridanus* (Hulbert, 1984). Dice (1925) examined extant leporids near San Francisco and San Diego, California, and observed that p3 enamel crenulation is usually "smooth" in *L. californicus* and *S. bachmani* Waterhouse (1838) and highly crenulated or "wavy" in *S. audubonii*. Those criteria and size were used to identify leporid fossils from Pits 1059, 2050, and 2051 at Rancho La Brea in Los Angeles, CA.

The taxonomic resolution at which isolated leporid fossils can be identified is thus dependent on the extent of size/shape variation within and among taxa that occur (or occurred) in the focal region of study. Since there is no one set of criteria for identifying North American leporid fossils, region-specific "keys" must be employed using characters relevant to those locations. One fundamental assumption that should be acknowledged when implementing region-specific protocols is that the geographic range and morphology of the fossil taxa of interest have not shifted temporally to the extent that comparative specimens within the study region are no longer representative of the fossil taxon. Indeed, some small mammals have undergone considerable range shifts during the late Quaternary (Graham, 1986). It may therefore be necessary to include extralimital taxa and/or extralimital individuals of focal taxa to mitigate the chance of excluding representative specimens from the comparative identification pool. Deciding whether this assumption is appropriate or not will depend on several factors including the size of the study region, the temporal distance between comparative and fossil taxa, and the ecology of the focal taxa (e.g., their dispersal ability and rate of morphological change among generations). I focus on developing a set of criteria for identifying isolated leporid elements in California that, given this assumption and the known ecology of the focal taxa today, is likely reasonable to apply to identify late Pleistocene fossils from Rancho La Brea (RLB).

1.3 Methods

1.3.1 Extant taxa

Three leporid species are distributed in low-elevation areas of southern California today: *Lepus californicus* (black-tailed jackrabbit), *Sylvilagus audubonii* (desert cottontail), and *S. bachmani* (brush rabbit) (Fig. 1.1). To determine whether leporid fossils from this region can be differentiated among the species, I collected comparative morphometric data and observed p3 enamel crenulation patterns in 30 extant adult specimens each of *L. californicus*, *S. audubonii*, and *S. bachmani* from California at the Natural History Museum of Los Angeles County (LACM) and Museum of Vertebrate Zoology at Berkeley (MVZ) (Fig. 1.1; Appendix Table 1.12.1). In addition, I collected comparative data on ten adult individuals each of *L. americanus* Erxleben (1777) (snowshoe hare), *L. townsendii* Bachman (1839) (white-tailed jackrabbit) and *S. nuttallii* Bachman (1837) (mountain cottontail) from western North America at the Harvard Museum of Comparative Zoology (MCZ) and MVZ (Fig. 1.1, Appendix Table 1.12.1). The latter three species occur today only along the eastern periphery of northern and central California (Chapman, 1975; Lim, 1987) (Fig. 1.1); however, their presence should be considered at extralimital fossil localities since some mammalian ranges have shifted markedly throughout the late Quaternary (Graham, 1986). I also observed the dental morphology of six *Brachylagus idahoensis* Merriam (1891) (pygmy rabbit) individuals (Appendix Table 1.12.1). *Brachylagus idahoensis* presently occurs along the eastern fringes of northern and central California; however, its tooth shape and size is distinctive from all other extant North American leporids (Green & Flinders, 1980; Jass, 2009; Kurtén & Anderson, 1980) so it does not warrant further consideration for this study.

Modifying the categories of Dalquest et al. (1989), I sorted p3 crenulation patterns of each specimen into one of four grouping conditions: “simple,” “moderate,” “complex,” or “alternate” and obtained linear measurements of p3 length/p3 width (Fig. 1.2), diastema length, and toothrow length. Measurements were conducted using Fisherbrand Traceable ISO 17025 calibrated digital calipers as follows: p3 length=length from the apex of the anterior-most projection of the anterolophid (buccal to the anterior re-entrant) to the posterior edge of the posterolophid where enamel thickness begins to taper (Fig. 1.2); p3 width=buccolingual width from the apex of the buccal projection of the anterolophid (between the anterobuccal and posterobuccal re-entrants) to its lingual edge (Fig. 1.2); diastema length=length from the posterior edge of the incisor alveolus to the anterior edge of the p3 alveolus; toothrow length=length from the anterior edge of the p3 alveolus to the posterior edge of the m3 alveolus. I measured each feature three times and recorded the average of the three measurements. Measurements of juvenile specimens were not considered for taxonomic identifications, though p3 crenulation patterns were observed in juveniles to determine if ontogenetic differences in enamel patterning are present (Appendix Table 1.12.1).

All p3 crenulation types exhibit a thick enamel band at the buccal-most edge of the anterolophid, forming a semicircular curve or “hook,” which extends lingually across the anterior wall of the posterobuccal re-entrant. In specimens with “simple” crenulation, the band often extends posterolingually prior to the midline of the tooth, then reorients anterolingually towards the lingual edge, sometimes forming a checkmark-like pattern

(Fig. 1.3A). Apart from this anteroposterior reorientation, termed the "central angle" by Dalquest et al. (1989), specimens with simple crenulation exhibit relatively smooth enamel with no prominent folding. Specimens with "moderate" crenulation exhibit two prominent anteriorly-oriented "loop" folds referred to here as the double anterior loop (DAL) lingual to the central angle (Fig. 1.2). The remainder of enamel lingual to the DAL is relatively smooth in specimens with moderate crenulation (Fig. 1.3B). Specimens with "complex" crenulation exhibit a DAL, as seen in the moderate condition, with additional folds extending from the DAL toward the lingual edge of the tooth (Fig. 1.3C). Finally, specimens with "alternate" crenulation exhibit prominent buccolingual folding across the anterior wall of the posterobuccal re-entrant but lack the DAL seen in specimens with moderate or complex crenulation (Fig. 1.3D).

Next, I employed random forest classification trees, an ensemble learning technique, to determine how accurately the six extant leporid species can be binned in their respective species-groups using the dental measurements and crenulation observations. Measurements of p3 length, p3 width, p3 length-to-width ratio (l/w), diastema length, toothrow length, and crenulation patterning were entered in the analysis. Only adult and suspected adult specimens of each species were included. Random forests were conducted on two datasets. The first dataset included only species that presently occur in low elevation areas of southern California (i.e., *Lepus californicus*, *Sylvilagus audubonii*, and *S. bachmani*) and the second dataset included all six species observed in this study. Both datasets were analyzed twice in the R programming package "randomForest" (Liaw & Wiener, 2002), first using all six predictor variables and again with only p3 variables of length, width, l/w, and crenulation pattern. The latter modification was performed because isolated teeth are frequently recovered from vertebrate assemblages, limiting the availability of diastema and toothrow measurements. All dataset trials were run on 1000 trees with the number of variables for splitting at each tree node set to six or four depending on how many variables were entered in the analysis. All analyses were conducted using R (version 3.6.1, R Core Team (2019)).

1.3.2 Fossil taxa

Rancho La Brea today is a protected National Natural Landmark with a long (>100 year) history of fossil collection. The oil-impregnated sands near the surface have resulted in the accumulation and preservation of over 600 species of late Quaternary plants and animals, all housed at La Brea Tar Pits Museum. In 2006, during the building of a new underground parking structure at the Los Angeles County Museum of Art, sixteen new asphalt fossil deposits were discovered. They were removed in twenty-three wooden crates for subsequent excavation and are collectively referred to as Project 23 (Fuller et al., 2014). Several deposits were too large for a single crate and thus were divided into multiple crates. Systematic excavation of each Project 23 deposit in $1m^2$ x 25cm grids has resulted in thousands of well-preserved fossils. I screened approximately 4.5kg of matrix from various grids within Project 23 Deposits 1, 7B, 13, and 14. This resulted in fifty-nine leporid p3s (including partial dentaries with p3s). Fossils were

subsequently cataloged and housed in the Los Angeles County Museum Project 23 (LACMP23) collections.

I evaluated the fossil samples to determine likely taxonomic affinity according to the protocol I developed based on extant specimens, the chronological range of leporids in each deposit, and potential changes in body size through time. Radiocarbon dating of Project 23 materials was conducted at the University of California Irvine Keck Carbon Cycle AMS Laboratory using the ultrafiltration protocol of Fuller et al. (2015) to remove asphaltic contaminants. Dates were also obtained from Project 23 fossils not collected in this study to increase sample size. Potential body size changes were determined using a Welch two-sample t-test in R (version 3.6.1, R Core Team (2019)) to determine if significant size differences occur between fossil samples and their assumed extant species representatives from southern California. Only non-juvenile, complete, fossil p3s from which length and width measurements could be obtained were included in size analyses (Appendix Table 1.12.2).

1.4 Interspecific morphology

Most individuals of extant leporids in southern California exhibit only one or two of the four defined p3 crenulation conditions per species, although intraspecific variation does occur in these patterns. Approximately 90% of *Lepus californicus* have simple or alternate crenulation, 97% of *Sylvilagus audubonii* have moderate or complex crenulation, and 86% of *S. bachmani* have simple crenulation (Table 1.1). Crenulation-based identifications are least effective for discriminating *L. californicus* from *S. bachmani* since individuals of both taxa often exhibit simple crenulation – 57% and 86% of sampled individuals of *L. californicus* and *S. bachmani* exhibit this condition respectively (Table 1.1). Since only sampled individuals of *Lepus* exhibit alternate crenulation, this morphotype likely indicates some form of *Lepus* in southern California specimens.

Sylvilagus bachmani exhibits the narrowest p3s of the five leporid species overall (mean p3 l/w=1.27) (Table 1.1; Fig. 1.4). Further, there is no overlap between *L. californicus* and *S. bachmani* in the ranges of different measurements, except for the p3 l/w (Table 1.1; Fig. 1.4A). Samples of extant *L. californicus* are, on average, ~42% larger than extant *S. bachmani* and even the smallest *L. californicus* individual is >10% larger than the largest *S. bachmani* (Table 1.1; Fig. 1.4A). Of course, pre- and post-glacial populations of some small mammal species exhibit significant body size shifts (e.g., Blois et al., 2008; Smith et al., 1995) and mandibular features of fossil *Sylvilagus floridanus* Allen (1890) from south-central Texas are significantly larger than those of recent populations (Pettus, 1956). However, temporal populations of *S. floridanus* do not exceed a 10% change in size measurements overall (Pettus, 1956). It is acknowledged that size overlap among recent or fossil *S. bachmani* and *L. californicus* may have occurred in the past due to unknown selective pressures. Therefore, I use relative tooth width and crenulation patterning (if alternate) to differentiate these species in addition to size and find that, based on this sample, misclassification does not occur between these

two taxa if all three conditions are examined (Table 1.2). Overall, observed dental characters are quite effective at differentiating leporids when only the three low-elevation southern California taxa are considered. Out-of-bag error is 5.88% and 9.41% for random forest classifications of *L. californicus, S. audubonii,* and *S. bachmani* using all dental variables and only p3 variables respectively (Table 1.2).

Differentiating southern California leporid species is more difficult when extralimital taxa (i.e., *L. americanus, L. townsendii,* and *S. nuttallii*) are considered. Random forest classification out-of-bag error is 14.91% and 24.56% for all variables and p3 variables respectively; though, in some cases, individual species misclassifications are substantially greater (Table 1.2). Crenulation patterns of *L. americanus and L. townsendii* are comparable to those of *L. californicus*, though *L. townsendii* exhibits overall wider p3s, longer toothrows, and shorter diastemas than *L. californicus* (Table 1.1, Fig. 1.4B). Nevertheless, misclassification between *L. californicus* and *L. townsendii* is high due to the general similarity of their dental characters (Table 1.2). *Lepus americanus* has the greatest relative p3 width of all observed leporids overall (mean l/w=1.08) and is obviously smaller than the other two *Lepus* species – there is no overlap in p3 length, diastema length, or toothrow length and no random forest misclassification between *L. americanus* and *L. californicus*/*L. townsendii* (Tables 1.1, 1.2; Fig. 1.4A). However, measurements of *L. americanus* do overlap in size with all three *Sylvilagus* species examined, occasionally resulting in their misclassification (Tables 1.1, 1.2; Fig. 1.4A). The simple or alternate p3 crenulation pattern of *L. americanus* can distinguish it from *S. audubonii*, and it can be differentiated from *S. bachmani* based on relative dentition width (mean p3 l/w=1.08 and 1.27 for *L. americanus* and *S. bachmani* respectively) (Tables 1.1, 1.2; Fig. 1.4B). Though, some specimens of *S. nuttallii* and *L. americanus* overlap in size and morphology (Table 1.2; Fig. 1.4).

Concerningly, size measurements and p3 crenulation patterns of *S. nuttallii* fall within the observed range of *S. audubonii*, *S. bachmani,* and *L. americanus* (Tables 1.1, 1.2; Fig. 1.4). *Sylvilagus nuttallii* p3s are proportionally wider than *S. bachmani* overall, though not as wide as *L. americanus*, and comparable in width to *S. audubonii* (Table 1.1; Fig. 1.4B). Of the six focal species, *S. nuttallii* is by far the most difficult to differentiate from others. Approximately 67% of *S. nuttallii* individuals are misclassified in random forests as *L. americanus, S. audubonii,* or *S. bachmani* (Table 1.2). Measured characters of *S. nuttallii* are marginally smaller than those of *S. audubonii*, overall, and the former taxon exhibits simple p3 crenulation more often than the latter (Table 1.1; Fig. 1.4). However, those differences are unlikely to be useful for specific identification unless fossil sample sizes are large.

1.5 Ontogenetic morphology

Juvenile samples were limited (n=9); nevertheless, ontogenetic differences in crenulation patterns of *S. audubonii* were observed. Juvenile *S. audubonii* individuals tend to exhibit simple crenulation more frequently than adult individuals, a phenomenon also noted by Dice (1925). Further, juvenile *S. audubonii* with loose p3s that permit

tooth-base examination, and other relativity small individuals of *S. audubonii* that may be juvenile or subadult, tend to exhibit more complex crenulation at the tooth base versus the occlusal surface (Fig. 1.5, Appendix Table 1.12.1). No p3s in my observation (extant or fossil) exhibit more complex crenulation at the tooth surface than at the base. Therefore, I hypothesize that adult p3 posterobuccal re-entrant enamel patterning forms at the tooth base and gradually moves towards the surface with ontogeny/wear. Leporid teeth are hypselodont and relatively fast-growing (Ungar, 2010). I could not find more specific information on the ontogenetic timing of leporid enamel growth-patterning in the literature, though it would be useful for paleontological identifications. Therefore, if this inference is true, crenulation at the p3 base is a more reliable species indicator than crenulation at the surface and crenulation discrepancies between the tooth surface and base may indicate juvenile and/or young adult individuals. Until such research is conducted, I tentatively refer to isolated leporid p3s with obviously dissimilar base-surface crenulation complexity (e.g., "complex" versus "simple") as juvenile. Isolated p3s with slight changes in base-surface crenulation complexity (e.g., "complex" versus "moderate") tend to be larger than those with more extreme crenulation changes and may indicate young adults or subadults; however, this is speculative. I tentatively refer to specimens with slight changes in crenulation complexity as "subadult?".

1.6 Identification criteria

Due to suspected ontogenetic variation, enamel crenulation patterns should be observed at the tooth base when possible, and length/width measurements of juvenile specimens (i.e., specimens with markedly dissimilar p3 base-surface widths or crenulation complexity) should not be considered for species identification. Even when excluding juveniles, dentary measurements alone cannot differentiate the three southern California leporid species due to size overlap among adult *L. californicus*/*S. audubonii* and *S. audubonii*/*S. bachmani*. However, a combination of size-based measurements, p3 l/w, and p3 crenulation patterns can differentiate these taxa within a relatively small range of error (Table 1.2; Fig. 1.4). When the extralimital species *L. americanus, L. townsendii,* and *S. nuttallii* are included, species-level identification becomes more difficult due to increased morphometric and crenulation pattern overlap (Table 1.2; Fig. 1.4). *Lepus americanus* can be differentiated from *L. californicus* and *L. townsendii* via dentary and tooth dimensions, but not via crenulation patterning, and individual elements of *L. californicus* are difficult to differentiate from *L. townsendii* aside from a proportionally wider p3 exhibited by the latter species overall (Tables 1.1, 1.2; Fig. 1.4). Individuals of *Sylvilagus nuttallii* often cannot be differentiated from *S. bachmani* and *L. americanus* based on observed dental characters (Table 1.2). Consequently, one may need to consider site-specific geographic probabilities to determine whether *S. nuttallii* is likely present at a locality. If so, specific identification of isolated leporid elements may not be feasible.

From these findings, I employ the following general criteria for identification of leporid fossils in southern California, recognizing there may still be some uncertainty in

the final identifications and that protocol applicability may differ depending on site and study-specific conditions:

- p3s >3.1mm in length and >2.5 mm in width that exhibit simple (Fig. 1.3A) or alternate (Fig. 1.3D) crenulation – or, alternatively, dentaries with diastema and toothrow lengths >18.2mm and >15.5mm respectively – can be attributed to *Lepus*. Diastema and toothrow size thresholds assume that some individuals of the next largest taxon, *S. audubonii*, may be up to 10% larger than the largest extant individual(s) sampled in this study (Table 1.1).

- p3s <3.1mm in length that exhibit simple crenulation can be attributed to *Lepus americanus/Sylvilagus bachmani/S. nuttallii*. *Lepus americanus* and *Sylvilagus bachmani* can be further differentiated statistically and/or using relative tooth width if multiple individuals are present – i.e., with multiple individuals, whether the relative tooth widths of those individuals cluster within the range of variation of *S. bachmani* versus *L. americanus* may become more apparent (Table 1.2; Fig. 1.4). *Lepus americanus* has the widest dentition of the six observed species and *S. bachmani* has the narrowest, and there is little p3 l/w overlap and no statistical misclassification among individuals of these two species (Tables 1.1, 1.2; Fig. 1.4B). Individuals of *S. nuttallii* can exhibit size and morphological characters within the observed range of *L. americanus* and *S. bachmani* and are therefore difficult to identify.

- p3s with moderate (Fig. 1.2B) or complex (Fig. 1.2C) crenulation and mean l/w ~1.20 can be attributed to *S. audubonii*/*S. nuttallii*. *Sylvilagus nuttallii* exhibit simple crenulation more frequently than *S. audubonii* (Table 1.1; Fig. 1.4B). However, differentiating *S. audubonii* and *S. nuttallii* is difficult without large sample sizes, especially if *S. bachmani* and/or *L. americanus* is present, since different individuals of *S. nuttallii* can be misidentified as any one of those three species (Table 1.2).

1.7 Systematic paleontology

Though some uncertainty remains when using the criteria outlined above to determine the taxonomic affinity of individual fossil specimens and the number of identified specimens per taxon (NISP) (Tables 1.1, 1.2), large sample sizes should allow taxon occurrences to be inferred assuming that spatiotemporal shifts in species distributions and morphology are minimal among the extant and fossil specimens examined. In other words, if several recent or fossil specimens of unknown taxonomic affinity cluster within the morphological range of a known, extant, taxon-group (e.g., Fig. 1.4), one can be reasonably certain that the extant taxon is present in the unknown sample pool even if there are morphological outliers that impact abundance calculations. These findings show that some leporid species are more morphologically distinct than others. Individuals of *Sylvilagus nuttallii*, for example, share physical characteristics with *S. audubonii*, *S. bachmani*, and/or *L. americanus* and thus are often misclassified (Table

1.2; Fig. 1.4). Consequently, estimating *S. nuttallii* NISP is often impractical since its range largely overlaps with one or more of those other species (Fig. 1.1). However, it may be possible to detect *S. nuttallii* presence at localities in California if fossil sample sizes are large. With large sample sizes, one may infer *S. nuttallii* presence via a process of elimination if several leporid p3s are 1) relatively small (i.e., are < 3.1mm and therefore not likely *L. californicus* or *L. townsendii*), 2) exhibit l/w between 1.15 and 1.25 (i.e., are likely not *L. americanus* or *S. bachmani*), and 3) exhibit simple crenulation (i.e., are likely not *S. audubonii*). This criterion is not suitable for identification of individual specimens or detecting *S. nuttallii* if it is rare within a fauna and/or if there are few individuals sampled; though, it should facilitate detection of *S. nuttallii* if it is common and well-sampled at a locality. Using these criteria, I identified the 59 fossil leporid specimens sampled from Project 23 at RLB as the following:

LAGOMORPHA Brandt, 1855
LEPORIDAE Fischer 1817
SYLVILAGUS Gray 1867
Sylvilagus audubonii Baird 1857

Referred specimens: LACMP23-39811, left dentary fragment with p3, p4, m2. LACMP23-32047, right dentary fragment with p3-m1; LACMP23-39819, right dentary fragment with p3-m1; LACMP23-39820, right dentary fragment with partial p3-m2. The following specimens represent complete left p3s: LACMP23-28084, LACMP23-28555, LACMP23-28661, LACMP23-31781, LACMP23-35608, LACMP23-35763, LACMP23-35847, LACMP23-35885, LACMP23-35937, LACMP23-40167, LACMP23-40209, LACMP23-40284, LACMP23-40285, LACMP23-40286, LACMP23-40287. The following specimens represent complete right p3s: LACMP23-28341, LACMP23-28519, LACMP23-28556, LACMP23-28858, LACMP23-33962, LACMP23-34117, LACMP23-35614, LACMP23-35696, LACMP23-35836, LACMP23-35839, LACMP23-35840, LACMP23-35881, LACMP23-35883, LACMP23-39874, LACMP23-40166, LACMP23-40210, LACMP23-40211. The following specimens represent partial left p3s and left p3 fragments: LACMP23-28266, LACMP23-31782, LACMP23-34259, LACMP23-34260, LACMP23-35771, LACMP23-40039, LACMP23-40288. The following specimens represent partial right p3s and right p3 fragments: LACMP23-28105, LACMP23-35618, LACMP23-35619, LACMP23-35645, LACMP23-39929, LACMP23-40110, LACMP23-40168, LACMP23-40212, LACMP23-40291.

Remarks: Fifty-two specimens from Project 23 are assigned to *S. audubonii* based on moderate or complex p3 crenulation (Table 1.2; Figs. 1.4, 1.5C). The possibility that some specimens belong to *S. nuttallii* cannot be eliminated; however, I consider this unlikely since most p3s with l/w <1.25 (i.e., those not likely belonging to *S. bachmani*) exhibit moderate or complex crenulation at the tooth surface and/or base (Fig. 1.4; Appendix Table 1.12.2). If *S. nuttalli* was present and common in the local region encompassing Project 23, I would expect proportionally more non-narrow p3s to exhibit simple crenulation. Further, *S. nuttallii* is currently restricted to intermountain regions >100 miles from Los Angeles (Chapman 1975; Hall & Kelson 1959). All specimens with

more complex crenulation at the tooth base relative to the occlusal surface are considered juvenile individuals of *S. audubonii*. Excluding suspected juveniles, p3s from Project 23 are, overall, ~9% smaller than extant *S. audubonii* (mean=2.55mm, 2.14mm, and 1.19 for p3 length, width, and l/w respectively; Fig. 1.4; Appendix Table 1.12.2). Size changes between extant (n=30) and fossil (n=25) *S. audubonii* are statistically significant ($t=4.6205$, $df=48.06$, $p<0.001$ for p3 length; $t=4.5672$, $df=51.154$, $p<0.001$ for p3 width).

LAGOMORPHA Brandt 1855
LEPORIDAE Fischer 1817
SYLVILAGUS Gray 1867
Sylvilagus bachmani Waterhouse 1838

Referred specimens: LACMP23-32045, left dentary fragment with p3. The following specimens represent complete left p3s: LACMP23-29229, LACM-P23 33861. The following specimens represent complete right p3s: LACMP23-28082, LACMP23-34262, LACMP23- 35844, LACMP23-36615.

Remarks: Seven specimens from Project 23 are assigned to *S. bachmani* based on simple p3 crenulation at the occlusal surface and base of the tooth, p3 lengths <3.1 mm, and a mean p3 l/w >1.25 (Table 1.2; Figs. 1.4 & 1.5D). Since adult individuals of this species usually exhibit simple crenulation (Table 1.1; Fig. 1.4), it is difficult to identify juveniles from surface-base changes in crenulation complexity. However, specimens can be identified as juvenile if the width at the occlusal surface is less than the width at the tooth base (White, 1991). Excluding potential juvenile p3s of *S. bachmani* from Project 23, the sample is ~11% smaller than recent *S. bachmani* (mean=2.19mm, 1.71mm, and 1.28 for p3 length, width, and l/w respectively; Fig. 1.4; Appendix Table 1.12.2). Size changes between extant (n=30) and fossil (n=7) *S. bachmani* are statistically significant ($t=2.8861$, $df=8.2077$, $p=0.0198$ for p3 length; $t=4.6124$, $df=12.923$, $p<0.001$ for p3 width).

1.8 Paleoecological implications

Here I present a region-specific protocol for identifying leporid dental remains to genus and species in California and demonstrate its utility and limitations for identifying Project 23 leporid fossils at RLB. Determining the spatial and taxonomic boundaries of comparative specimen pools to use when developing such a protocol, and whether the assumptions and limitations therein are appropriate, is a study-specific decision based, in part, on the spatial and temporal breadth of the unknown specimens in question and their ecology and evolution. Assumptions of relative morphological and geographic range stasis are inherent to many such protocols. In this study, for example, I assume 1) that intraspecific dental crenulation patterning and morphology of the extant and fossil leporids from Project 23 has not changed substantially in southern California over the last 50,000 years and 2) that leporid ranges have not shifted during that time to the extent that extralimital species not included in this study, such as *Sylvilagus floridanus*, whose westernmost distribution is currently hundreds of kilometers east of Los Angeles, resided

there during the late Pleistocene. The limitations of those assumptions are dependent, in part, on the spatial and morphological breadth of the comparative specimens examined and the spatial and temporal distance between comparative specimens and the unknown specimens of interest. Increasing the spatial and taxonomic/morphological coverage of comparative specimen pools will improve identification fidelity of unknowns (i.e., one can be more certain that all potential taxonomic representatives of unknown specimens are included). However, a trade-off may also occur between the spatial and morphological breadth of comparative sample coverage and specimen identification accuracy, as shown in classification results of local specimen pools versus local and extralimital specimen pools (Table 1.2; Fig 1.4).

Facilitating species-level identifications is imperative for increasing the resolution at which (paleo)ecological questions can be addressed (e.g., how organisms interact with each another and their environment and how taxon-specific habitats or entire ecosystems change over time). Assuming that the assumptions outlined for this protocol are true, I identified two unique leporid species from Project 23 (*S. audubonii* and *S. bachmani*) and observed differences in their relative abundance among Project 23 deposits (Table 1.3). Radiocarbon dating of Project 23 fossils shows that *S. bachmani* is less abundant in overall younger deposits than older ones (Table 1.3; Appendix Table 1.12.3). Further, *Lepus californicus* is thus far absent from excavated Project 23 deposits that pre-date the Last Glacial Maximum but present in deposits that yield glacial and post-glacial dates within the RLB Hancock Collection (O'Keefe et al., 2009; Stock & Harris, 1992). This faunal change may have significant paleoenvironmental implications for Los Angeles since *S. bachmani*, as its common name implies, requires dense brushy habitats while *L. californicus* avoids dense vegetation. The contemporary range of *S. bachmani* is restricted to the Pacific coast of North America from Washington to Baja California and inhabits coastal chaparral and forest biomes with dense brush cover (Chapman, 1974). Conversely, extant *L. californicus* occupy coastal chaparral, desert, savannah, and grassland biomes (Best, 1996). *Lepus californicus* prefer open, arid habitats – including those with shortgrass, sagebrush, and juniper vegetation – and avoid tall grasses and forests where visibility is reduced (Best, 1996). *Sylvilagus audubonii* also occupy coastal chaparral, desert, savannah, and grassland biomes and prefer arid areas with relatively sparse vegetation (Chapman & Willner, 1978). Though, individuals of *Sylvilagus* generally require more vegetation cover than *Lepus* to escape predation since the former taxon usually hides from predators and the latter tends to run (Chapman et al., 1982; Driver & Woiderski, 2008). Considering the ecologies of extant members of these species, RLB may have become more sparsely vegetated and possibly more arid towards the Last Glacial Maximum.

In contrast to the smaller sizes observed among recent individuals of *S. floridanus* relative to fossil specimens from Friesenhahn Cave, TX (Pettus, 1956), recent *S. audubonii* and *S. bachmani* from southern California are generally larger than fossil specimens from RLB (Fig. 1.4A). Differences in the directionality of size change among S. *audubonii*/*S. bachmani* and *S. floridanus* could be influenced by several factors including differences in the behavioral ecologies of the focal taxa and/or spatiotemporal

differences in the late Quaternary environments and associated selective pressures of south-central Texas and southern California. More extensive research on microvertebrate faunas and floras is needed to reconstruct the late Quaternary environments of Los Angeles and other parts of California through time. However, exploratory inferences such as these and comprehensive paleoecological studies alike benefit from species-level data. Building regional keys for identifying speciose, morphologically variable, or otherwise difficult fossil taxa is advocated to improve site-specific paleoecological inferences, so long as the inherent assumptions of doing so are considered appropriate for study-specific systems and objectives.

1.9 References

Allen, J.A. (1890) Descriptions of a new species and a new subspecies of the genus *Lepus*. *Bulletin of the American Museum of Natural History*, *3*(8), 159–160.

Bachman, J. (1837) Observations on the different species of hares (genus *Lepus*) inhabiting the United States and Canada. *Journal of the Academy of Natural Sciences of Philadelphia*, *7*, 282–361.

Bachman, J. (1839) Additional remarks on the genus *Lepus*, with corrections of a former paper, and descriptions of other species of quadrupeds found in North America. *Journal of the Academy of Natural Sciences of Philadelphia*, *8*, 75–105.

Baird, S.F. (1857) Mammals: General report upon the zoology of the several Pacific railroad routes. Vol. 8, part 1. *Reports of explorations and surveys to ascertain the most practicable and economical route for a railroad from the Mississippi River to the Pacific Ocean*. Senate executive document no. 78, Washington, D.C.

Best, T.L. (1996) *Lepus californicus*. *Mammalian Species*, (530), 1-10, https://doi.org/10.2307/3504151.

Blois, J.L., Feranec, R.S., & Hadly, E.A. (2008) Environmental influences on spatial and temporal patterns of body-size variation in California ground squirrels (*Spermophilus beecheyi*). *Journal of Biogeography*, *35*, 602-613, https://doi.org/10.1111/j.1365-2699.2007.01836.x.

Brandt, J.F. (1855) Beitrage zur nahern Kenntniss der Säugethiere Russland's. *Kaiserlichen Akademie der Wissenschaften, Saint Petersburg, Mémoires Mathématiques, Physiques et Naturelles*, *7*, 1–365.

Chapman, J.A. (1974) *Sylvilagus bachmani*. *Mammalian Species*, (34), 1-4, https://doi.org/0.2307/3503777.

Chapman, J.A. (1975) *Sylvilagus nuttallii*. *Mammalian Species*, (56), 1-3, https://doi.org/10.2307/3503902.

Chapman, J.A., & Willner, G.R. (1978) *Sylvilagus audubonii*. *Mammalian Species*, (106), 1-4.

Chapman, J.A., Hockman, J.G. & Edwards, W.R. (1982) Cottontails: *Sylvilagus floridanus* and allies. *Wild Mammals of North America: Biology, Management, and Economics* (ed. by J.A Chapman and G.A. Feldhamer), pp. 83-123. John Hopkins University Press, Baltimore.

Dalquest, W.W. (1979) Identification of genera of American rabbits of Blancan age. *The Southwestern Naturalist, 24*, 275-278, https://doi.org/10.2307/3670925.

Dalquest, W.W., Stangl Jr, F.B., & Grimes, J.V. (1989) The third lower premolar of the cottontail, genus *Sylvilagus*, and its value in the discrimination of three species. *American Midland Naturalist, 121*, 293-301, https://doi.org/10.2307/2426033.

Dice, L.R. (1925) Rodents and lagomorphs of the Rancho la Brea deposits. *Carnegie Institution of Washington, 349*, 119-130.

Driver, J.C. & Woiderski, J.R. (2008) Interpretation of the ‘‘lagomorph index’’ in the American Southwest. *Quaternary International, 185*, 3-11, https://doi.org/10.1016/j.quaint.2007.09.022.

Erxleben, J.C.P. (1777) *Systema regni animalis per classes, ordines, genera, species, varietates, cum synonymia et historia animalium. Classis I. Mammalia*. Weygandianis, Lipsiae.

Fischer de Waldheim, G. (1817) Adversaria zoologica. *Memoires de la Société Impériale des Naturalistes du Moscou, 5*, 357–428.

Fuller, B.T., Fahrni, S.M., Harris, J.M., Farrell, A.B., Coltrain, J.B., Gerhart, L.M., Ward, J.K., Taylor, R.E., & Southon, J.R. (2014) Ultrafiltration for asphalt removal from bone collagen for radiocarbon dating and isotopic analysis of Pleistocene fauna at the tar pits of Rancho La Brea, Los Angeles, California. *Quaternary Geochronology*, *22*, 85-98, https://doi.org/10.1016/j.quageo.2014.03.002.

Fuller, B.T., Harris, J.M., Farrell, A.B., & Takeuchi, G.T. (2015) Sample preparation for radiocarbon dating and isotopic analysis of bone from Rancho La Brea. *Science Series*, *42*, 151-167.

Graham, R.W. (1986) Response of mammalian communities to environmental changes during the Late Quaternary. *Community ecology* (ed. by J. Diamond and T.J. Case), pp. 300-313. Harper and Row, New York.

Gray, J.E. (1837) Description of some new or little known Mammalia, principally in the British Museum Collection. The Magazine of Natural History, and Journal of

Zoology, Botany, Mineralogy, Geology, and Meteorology, New Series, *1*, 577–587.

Gray, J.E. (1867) On the skulls of hares and picas. *The Annals and Magazine of Natural History; Zoology, Botany, and Geology, Series 3*, *20*, 219–225.

Green, J.S., & Flinders, J.T. (1980) *Brachylagus idahoensis*. *Mammalian Species*, (125), 1-4, https://doi.org/10.2307/3503856.

Hall, E.R., & Kelson, K.R. (1959) *The mammals of North America*. Volume 1. Ronald Press, New York.

Hulbert Jr, R.C. (1984) Latest Pleistocene and Holocene leporid faunas from Texas: their composition, distribution and climatic implications. *The Southwestern Naturalist*, *29*, 197-210, https://doi.org/10.2307/3671026.

Jass, C.N. (2009) Pleistocene lagomorphs from Cathedral Cave, Nevada. *PaleoBios*, *29*(1), 1-12.

Kurtén, B., & Anderson, E. (1980) *Pleistocene mammals of North America*. Columbia University Press, New York.

Liaw, A., & Wiener, M. (2002) Classification and Regression by randomForest. *R News*, *2*(3), 18-22.

Lim, B.K. (1987) *Lepus townsendii*. *Mammalian Species*, (288), 1-6, https://doi.org/10.2307/3504001

Linnaeus, C. (1758) *Systema Naturae per regna tria naturae, secundum classis, ordines, genera, species cum characteribus, differentiis, synonymis, locis*. Tenth edition volume 1. Laurentii Salvii, Stockholm.

Merriam, C.H. (1891) Results of a biological reconnoissance [sic] of southcentral Idaho. *North American Fauna*, *5*, 1–113.

O'Keefe, F.R., Fet, E.V. & Harris, J.M. (2009) Compilation, calibration, and synthesis of faunal and floral radiocarbon dates, Rancho La Brea, California. *Contributions in Science (Los Angeles)*, *518*, 1-16.

Patterson, B.D., Ceballos, G., Sechrest, W., Tognelli, M.F., Brooks, T., Luna, L., Ortega, P., Salazar, I. & Young, B.E. (2007) Digital distribution maps of the mammals of the western hemisphere, version 3.0. NatureServe, Arlington, Virginia, USA.

Pettus, D. (1956) Fossil rabbits (Lagomorpha) of the Friesenhahn Cave deposit, Texas. *The Southwestern Naturalist*, *1*, 109-115, https://doi.org/10.2307/3669132.

R Core Team (2019) R: A language and environment for statistical computing. R Foundation for Statistical Computing, Vienna, Austria, https://www.R-project.org/.

Smith, F.A., Betancourt, J.L., & Brown, J.H. (1995) Evolution of body size in the woodrat over the past 25,000 years of climate change. *Science, 270*, 2012-2014, https://doi.org/10.1126/science.270.5244.2012.

Smith, A.T., Johnston, C.H., Alves, P.C., & Hackländer, K., eds. (2018) *Lagomorphs: Pikas, rabbits, and hares of the World*. John Hopkins University Press, Baltimore.

Somerville, A.D., Froehle, A.W., & Schoeninger, M.J. (2018) Environmental influences on rabbit and hare bone isotope abundances: Implications for paleoenvironmental research. *Palaeogeography, Palaeoclimatology, Palaeoecology, 497*, 91-104, https://doi.org/10.1016/j.palaeo.2018.02.008.

Stock, C., & Harris, J.M. (1992) Rancho La Brea: A record of Pleistocene life in California. *Science Series, 37*, 1-113.

Ungar, P.S. (2010) *Mammal teeth: origin, evolution and diversity*. John Hopkins University Press, Baltimore.

Waterhouse, G.R. (1838) Original description of *Lepus bachmani*, pp. 103–105. *Proceedings of the Zoological Society of London*.

Wicks, T.Z., Thirumalai, K., Shanahan, T.M., & Bell, C.J. (2015) The use of $\delta^{13}C$ values of leporid teeth as indicators of past vegetation. *Palaeogeography, Palaeoclimatology, Palaeoecology, 418*, 245-260, https://doi.org/10.1016/j.palaeo.2014.11.017.

White, J.A. (1991) North American Leporinae (Mammalia: Lagomorpha) from late Miocene (Clarendonian) to latest Pliocene (Blancan). *Journal of Vertebrate Paleontology, 11*, 67-89, https://doi.org/10.1080/02724634.1991.10011376.

1.10 Tables

Table 1.1: Linear dentary measurements and p3 crenulation patterns of recent *Lepus californicus*, *L. townsendii*, *Sylvilagus audubonii*, *S. bachmani*, and *S. nuttallii*. Asterisks indicate taxa that are currently extralimital from Los Angeles County and most of southern California. Data collected from juvenile and inferred juvenile individuals are not included. See Appendix Table 1.12.1 for measurements of individual specimens.

Measurements (mm)	**p3 length**	**p3 width**	**p3 l/w**	**Diastema length**	**Toothrow length**	**Crenulation pattern (n)**	
L. californicus (n=30)							
Maximum	3.96	3.39	1.37	25.48	19.19	Simple	17 (57%)
Minimum	3.09	2.52	1.02	15.3	14.78	Alternate	10 (33%)
Mean	3.47	2.91	1.20	19.64	16.28	Moderate	2 (7%)
Standard Deviation	0.22	0.23	0.08	1.90	0.98	Complex	1 (3%)
**L. townsendii* (n=10)							
Maximum	3.65	3.32	1.21	20.31	18.16	Simple	9 (90%)
Minimum	3.25	2.79	1.05	17.72	16.06	Alternate	1 (10%)
Mean	3.45	3.04	1.14	19.38	17.09	Moderate	0 (0%)
Standard Deviation	0.15	0.17	0.05	0.74	0.74	Complex	0 (0%)
L. americanus (n=10)							
Maximum	2.90	2.60	1.16	15.15	13.89	Simple	8 (80%)
Minimum	2.40	2.32	1.00	13.49	12.19	Alternate	2 (20%)
Mean	2.61	2.41	1.08	14.41	13.11	Moderate	0 (0%)
Standard Deviation	0.18	0.09	0.06	0.51	0.51	Complex	0 (0%)
S. audubonii (n=30)							
Maximum	3.19	2.81	1.35	16.51	14.13	Simple	1 (3%)
Minimum	2.30	1.99	1.02	11.94	11.47	Alternate	0 (0%)
Mean	2.82	2.35	1.20	14.15	12.71	Moderate	10 (33%)
Standard Deviation	0.21	0.18	0.10	1.07	0.63	Complex	19 (63%)
S. bachmani (n=30)							
Maximum	2.80	2.26	1.44	14.20	13.29	Simple	26 (86%)
Minimum	2.09	1.68	1.14	10.34	10.11	Alternate	0 (0%)
Mean	2.44	1.93	1.27	12.17	11.58	Moderate	2 (7%)

Standard Deviation	0.19	0.15	0.08	0.92	0.71	Complex	2 (7%)
**S. nuttallii* (n=10)							
Maximum	2.98	2.47	1.31	14.66	13.35	Simple	6 (60%)
Minimum	2.2	1.68	1.10	11.29	10.21	Alternate	0 (0%)
Mean	2.50	2.09	1.20	12.97	11.94	Moderate	0 (0%)
Standard Deviation	0.24	0.26	0.06	1.19	0.97	Complex	4 (40%)

Table 1.2: Confusion matrices depicting random forest classification results of four leporid dataset trials. Trials titled "Three species" show classification results for species currently distributed in low-elevation areas of southern California only (i.e., *L. californicus*, *S. audubonii*, and *S. bachmani*). Trials titled "Six species" show results for all species observed in this study. Trials titled "all variables" indicate that all six measured variables of p3 length, p3 width, p3 length-to-width-ratio, p3 crenulation pattern, diastema length, and toothrow length are included in the analysis. Trials titled "p3 variables only" indicate that only the first four p3 variables are included. The number of variables for splitting at each node was set to six for "all variables" and four for "p3 variables only". All trials were run on 1000 trees.

Three species, all variables: Out-of-Bag estimate of error = 5.88%							
	L. californicus	*S. audubonii*	*S. bachmani*				Taxon-specific error
L. californicus	29	0	0				0.0%
S. audubonii	0	24	3				10.11%
S. bachmani	0	2	27				6.90%
Three species, p3 variables only: Out-of-Bag estimate of error = 9.41%							
	L. californicus	*S. audubonii*	*S. bachmani*				Taxon-specific error
L. californicus	28	1	0				3.45%
S. audubonii	2	22	3				18.52%
S. bachmani	0	2	27				6.90%
Six species, all variables: Out-of-Bag estimate of error = 14.91%							
	L. americanus	*L. californicus*	*L. townsendii*	*S. audubonii*	*S. bachmani*	*S. nuttallii*	Taxon-specific error
L. americanus	9	0	0	0	0	1	10.0%
L. californicus	0	27	2	0	0	0	6.90%
L. townsendii	0	4	6	0	0	0	40.0%
S. audubonii	1	0	0	25	0	1	7.41%
S. bachmani	0	0	0	2	27	0	6.90%
S. nuttallii	2	0	0	2	2	3	66.67%
Six species, p3 variables only: Out-of-Bag estimate of error = 24.56%							
	L. americanus	*L. californicus*	*L. townsendii*	*S. audubonii*	*S. bachmani*	*S. nuttallii*	Taxon-specific error
L. americanus	8	0	0	0	0	2	20.0%
L. californicus	1	23	5	0	0	0	20.69%

L. townsendii	0	6	4	0	0	0	60.0%
S. audubonii	1	2	0	22	1	1	18.52%
S. bachmani	0	0	0	2	26	1	10.35%
S. nuttallii	2	0	0	1	3	3	66.67%

Table 1.3: Number of sampled p3s from Project 23 (n=59) assigned to each California leporid species per deposit. Mean deposit-specific radiocarbon ages are calculated from specimen dates in Appendix Table 1.12.3. The percentage of p3s assigned to each species relative to the total number of identifiable p3s recovered from each deposit is listed in parentheses. See Appendix Table 1.12.2 for measurements, crenulation patterns, and inferred life stages of individual fossil specimens.

p3 NISPs per Deposit	***L. californicus***	***S. audubonii***	***S. bachmani***
Deposit 1, ~37 ka BP	- (0%)	9 (82%)	2 (18%)
Deposit 13, ~37 ka BP	- (0%)	20 (100%)	- (0%)
Deposit 7B, ~45 ka BP	- (0%)	16 (94%)	1 (6%)
Deposit 14, >45 ka BP	- (0%)	7 (64%)	4 (36%)

1.11 Figures

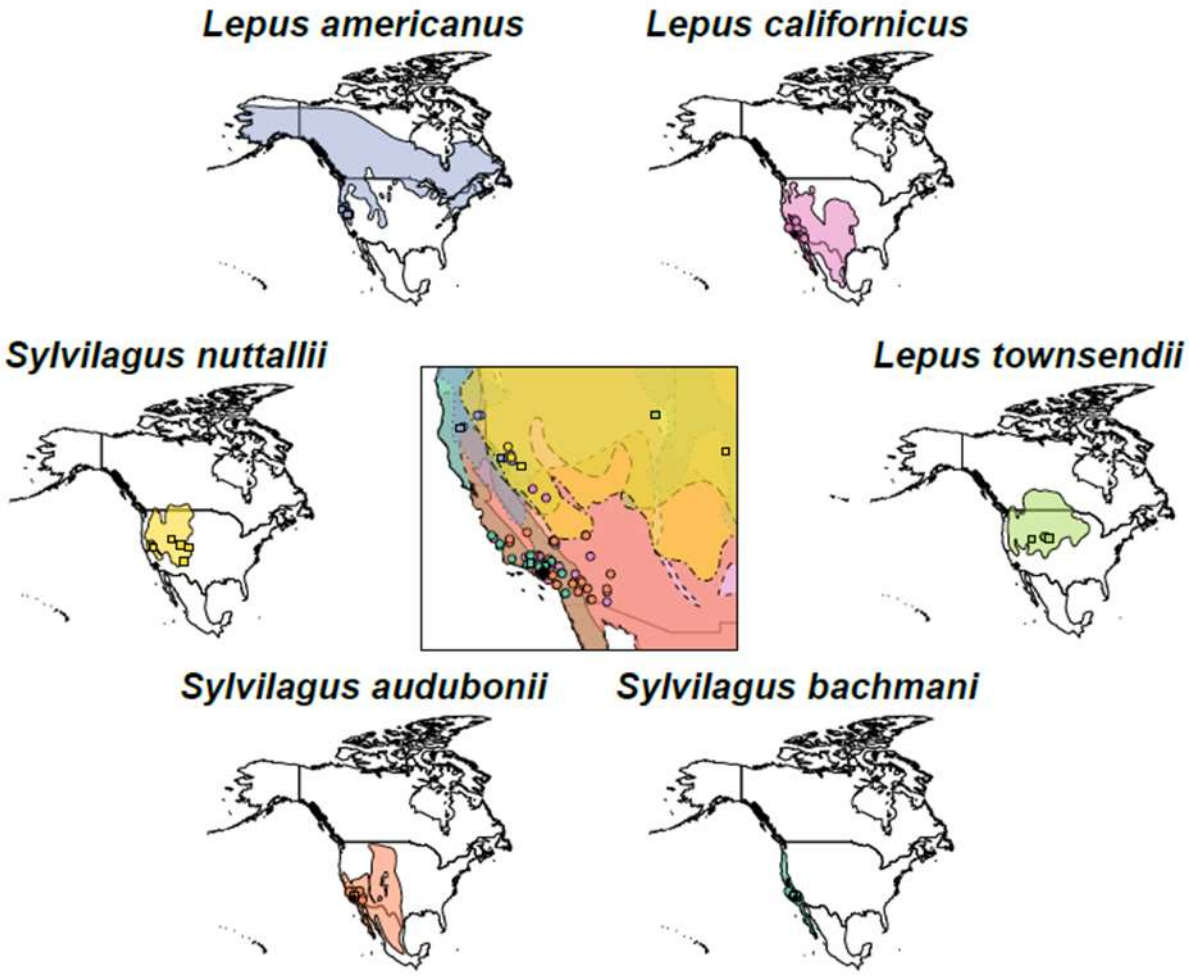

Figure 1.1: Map illustrating the modern distributions of the six extant leporid species examined. Points indicate sampling locations of individual specimens. Rancho La Brea, the fossil locality where unknown leporid specimens were collected, is marked by a black diamond. Species range data were obtained from (Patterson et al., 2007).

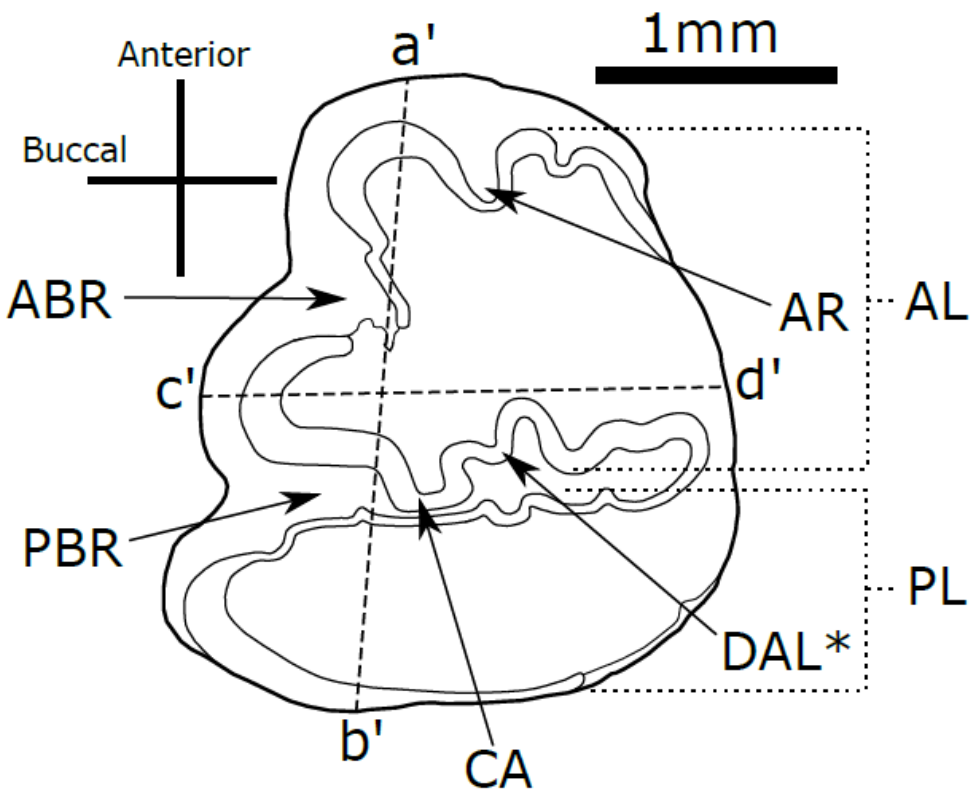

Figure 1.2: Lower left third premolar (p3) outline of LACM-53879 *Sylvilagus audubonii* (also pictured in Fig. 3B) illustrating tooth terminology and applied length (a'- b') and width (c'- d') measurements. AL=anterolophid, PL=posterolophid, AR=anterior re-entrant, ABR=anterobuccal re-entrant, PBR=posterobuccal re-entrant, CA=central angle, DAL=double anterior loop. Asterisk=not present on all specimens.

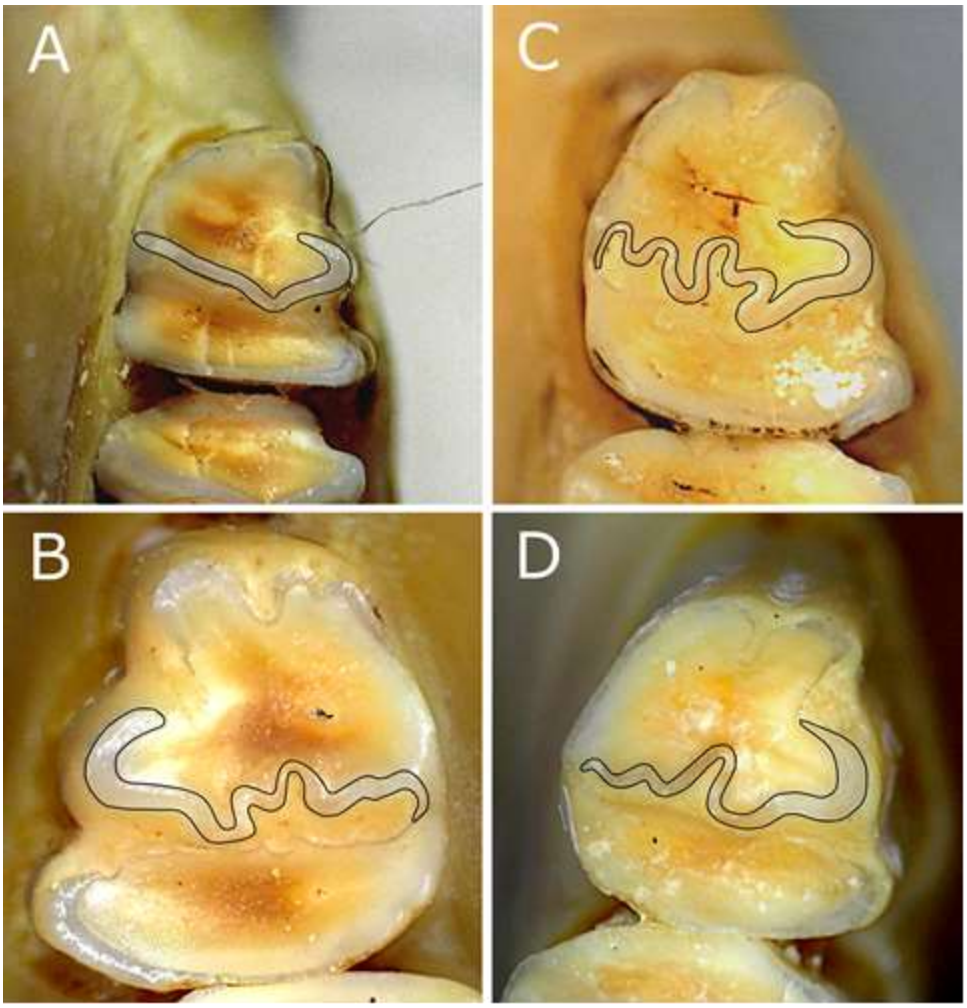

Figure 1.3: Occlusal views of extant leporid p3s illustrating the four enamel crenulation grouping patterns used in this study. Crenulation along the anterior and anterolateral wall of the posterobuccal re-entrant is outlined on each specimen. A) Right p3 of LACM-21374 *Sylvilagus bachmani* with "simple" crenulation; B) Left p3 of LACM-53879 *S. audubonii* with "moderate" crenulation; C) Right p3 of LACM-44966 *S. audubonii* with "complex" crenulation; D) Right p3 of LACM-29048 *Lepus californicus* with "alternate" crenulation. Images are magnified to illustrate crenulation patterns only and are not shown at a standardized scale.

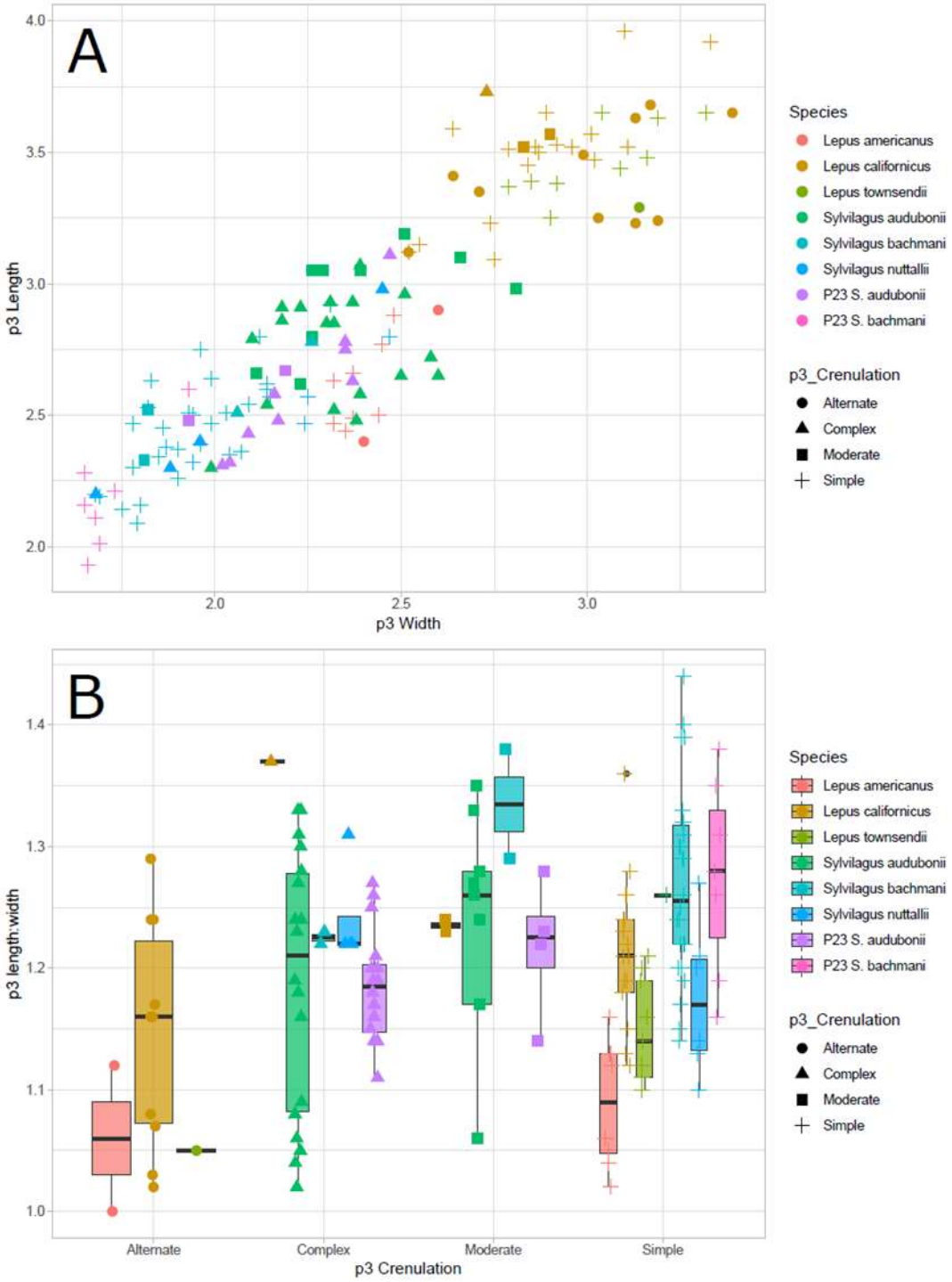

Figure 1.4: A) p3 length and width measurements of extant and Project 23 fossil leporids included in this study. All measurements are in millimeters. Juvenile and inferred juvenile individuals are not included. B) Boxplot of p3 l/w of the same recent and Project 23 fossil leporids grouped by crenulation pattern.

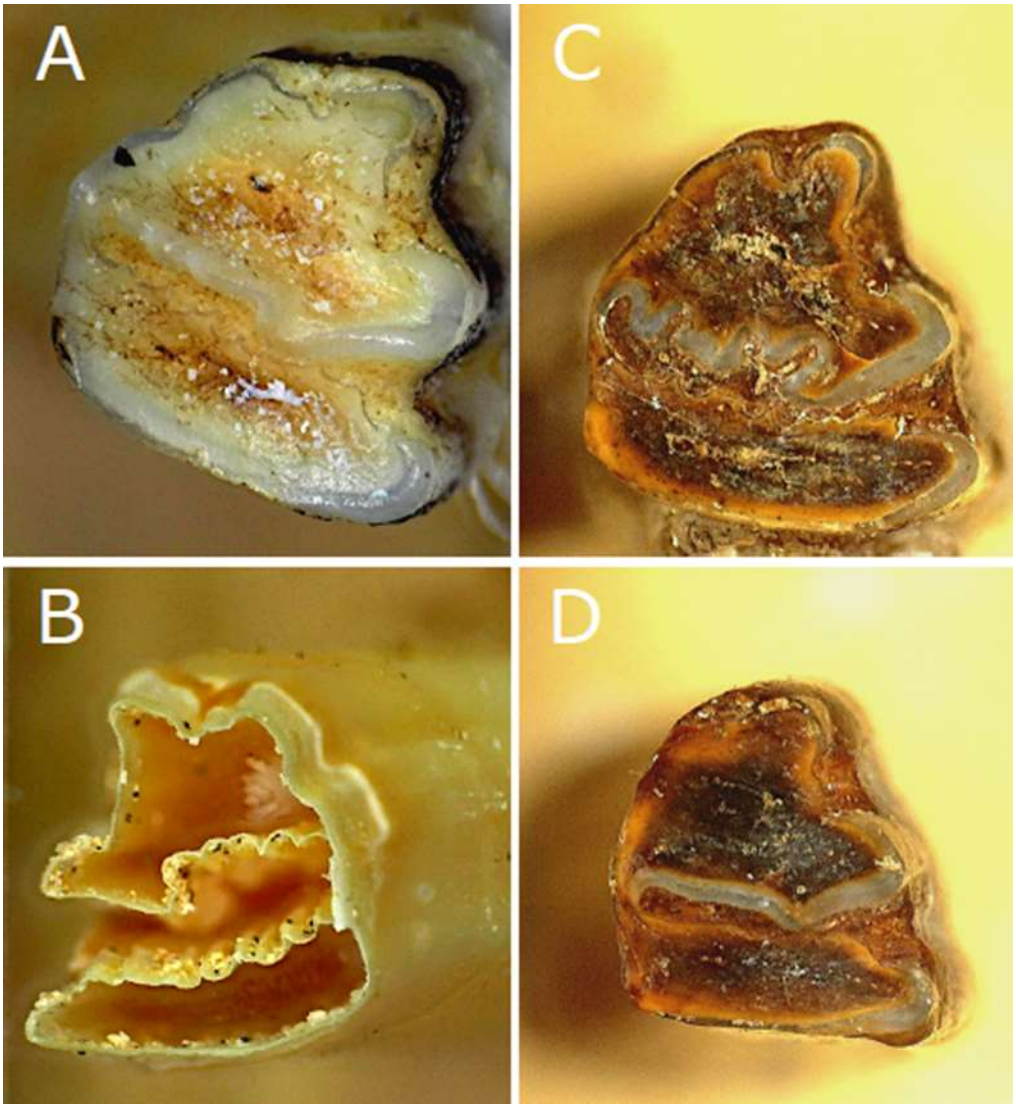

Figure 1.5: A-B: Right p3 of recent LACM-20731 *Sylvilagus audubonii* exhibiting simple crenulation at the surface of the tooth (A), and complex crenulation at the base of the tooth (B). C) Fossilized right p3 of LACMP23-30238 *S. audubonii* from Deposit 1 with complex crenulation at the occlusal surface. D) Fossilized right p3 of LACMP23-18270 *S. bachmani* from Deposit 1 at RLB with simple crenulation at the occlusal surface.

1.12 Appendix

Table 1.12.1: Dental measurements and p3 crenulation observations of all recent leporids sampled in this study. Specimens with two crenulation patterns (X; X) exhibit discrepancies between the tooth surface and base respectively. All measurements are in millimeters and measurements of juvenile or inferred juvenile specimens are not considered for species identification protocols.

Museum number	Species	Life Stage	p3 length	p3 width	p3 l/w ratio	Diastema length	Toothrow length	p3 Crenulation
LACM-3713	*Lepus californicus*	Adult	3.51	2.79	1.26	18.39	16.25	Simple
LACM-3822	*Lepus californicus*	Adult	3.96	3.10	1.28	20.37	17.57	Simple
LACM-6410	*Lepus californicus*	Adult	3.12	2.52	1.24	15.30	15.06	Alternate
LACM-21235	*Lepus californicus*	Adult	3.09	2.75	1.12	17.73	15.73	Simple
LACM-28172	*Lepus californicus*	Adult	3.50	2.87	1.22	19.17	15.31	Simple
LACM-28184	*Lepus californicus*	Adult	3.52	2.83	1.24	19.58	15.46	Moderate
LACM-28233	*Lepus californicus*	Adult	3.73	2.73	1.37	17.90	14.78	Complex
LACM-29047	*Lepus californicus*	Adult	3.52	2.96	1.19	19.27	15.09	Simple
LACM-29048	*Lepus californicus*	Adult	3.49	2.99	1.17	18.58	16.00	Alternate
LACM-29049	*Lepus californicus*	Adult	3.57	2.90	1.23	19.41	15.13	Moderate
LACM-30729	*Lepus californicus*	Adult	3.41	2.64	1.29	21.41	16.07	Alternate
LACM-30802	*Lepus californicus*	Adult	3.47	3.02	1.15	20.29	16.63	Simple
LACM-49513	*Lepus californicus*	Adult	3.12	2.52	1.24	15.30	15.31	Simple
LACM-49514	*Lepus californicus*	Adult	3.53	2.92	1.21	19.78	16.17	Simple
LACM-49515	*Lepus californicus*	Juvenile?	2.52	2.03	1.24	NA	12.63	Simple
LACM-49519	*Lepus californicus*	Adult	3.57	3.01	1.19	20.41	16.67	Simple

LACM-67485	*Lepus californicus*	Adult	3.45	2.84	1.21	18.16	15.54	Simple
LACM-84807	*Lepus californicus*	Adult	3.52	2.86	1.23	20.99	16.25	Simple
LACM-87443	*Lepus californicus*	Adult	3.35	2.71	1.24	19.13	15.70	Alternate
LACM-88149	*Lepus californicus*	Adult	3.15	2.55	1.24	NA	16.17	Simple
LACM-90240	*Lepus californicus*	Adult	3.65	2.89	1.26	20.72	16.75	Simple
LACM-95608	*Lepus californicus*	Adult	3.59	2.64	1.36	20.00	16.59	Simple
LACM-R6	*Lepus californicus*	Adult	3.23	3.13	1.03	25.48	19.19	Alternate
MVZ-1900	*Lepus californicus*	Adult	3.23	2.74	1.18	18.64	16.31	Simple
MVZ-7166	*Lepus californicus*	Adult	3.24	3.19	1.02	20.48	16.48	Alternate
MVZ-10683	*Lepus californicus*	Adult	3.63	3.13	1.16	20.77	16.99	Alternate
MVZ-10684	*Lepus californicus*	Adult	3.92	3.33	1.18	19.73	17.33	Simple
MVZ-24147	*Lepus californicus*	Adult	3.52	3.11	1.13	19.68	17.21	Simple
MVZ-27627	*Lepus californicus*	Adult	3.68	3.17	1.16	20.82	16.59	Alternate
MVZ-29158	*Lepus californicus*	Adult	3.65	3.39	1.08	20.54	18.25	Alternate
MVZ-29160	*Lepus californicus*	Adult	3.25	3.03	1.07	21.65	15.95	Alternate
MCZBOM-183	*Lepus townsendii*	Adult	3.25	2.90	1.12	18.83	16.06	Simple
MCZBOM-184	*Lepus townsendii*	Adult	3.39	2.85	1.19	19.02	16.83	Simple
MCZBOM-185	*Lepus townsendii*	Adult	3.29	3.14	1.05	19.65	16.48	Alternate
MCZBOM-186	*Lepus townsendii*	Adult	3.37	2.79	1.21	20.31	16.18	Simple
MCZBOM-221	*Lepus townsendii*	Adult	3.38	2.92	1.16	19.92	16.69	Simple
MCZBOM-222	*Lepus townsendii*	Adult	3.63	3.19	1.14	19.17	18.16	Simple
MCZBOM-223	*Lepus townsendii*	Adult	3.65	3.32	1.10	19.60	17.93	Simple
MCZBOM-224	*Lepus townsendii*	Adult	3.48	3.16	1.10	19.84	17.71	Simple

MCZBOM-225	*Lepus townsendii*	Adult	3.65	3.04	1.20	19.77	17.46	Simple
MCZBOM-964	*Lepus townsendii*	Adult	3.44	3.09	1.11	17.72	17.36	Simple
MVZ-13759	*Lepus americanus*	Adult	2.88	2.48	1.16	14.64	13.61	Simple
MVZ-20901	*Lepus americanus*	Adult	2.63	2.32	1.13	14.83	13.89	Simple
MVZ-23649	*Lepus americanus*	Adult	2.49	2.37	1.05	15.15	13.26	Simple
MVZ-23896	*Lepus americanus*	Adult	2.40	2.40	1.00	14.35	13.00	Alternate
MVZ-31899	*Lepus americanus*	Adult	2.90	2.60	1.12	14.64	13.57	Alternate
MVZ-32186	*Lepus americanus*	Adult	2.77	2.45	1.13	13.62	13.01	Simple
MVZ-33081	*Lepus americanus*	Adult	2.47	2.32	1.06	14.42	12.19	Simple
MVZ-36577	*Lepus americanus*	Adult	2.44	2.35	1.04	14.59	12.76	Simple
MVZ-119485	*Lepus americanus*	Adult	2.50	2.44	1.02	13.49	12.64	Simple
MVZ-165872	*Lepus americanus*	Adult	2.66	2.37	1.12	14.40	13.18	Simple
LACM-158	*Sylvilagus audubonii*	Adult	3.10	2.66	1.17	15.30	13.90	Moderate
LACM-254	*Sylvilagus audubonii*	Juvenile?	1.90	1.57	1.21	8.67	9.06	Simple
LACM-446	*Sylvilagus audubonii*	Adult	2.66	2.11	1.26	13.29	11.81	Moderate
LACM-653	*Sylvilagus audubonii*	Adult	2.79	2.10	1.33	13.23	12.02	Complex
LACM-916	*Sylvilagus audubonii*	Adult	2.96	2.51	1.18	12.88	12.93	Complex
LACM-3811	*Sylvilagus audubonii*	Adult	2.98	2.81	1.06	14.44	13.40	Moderate
LACM-4154	*Sylvilagus audubonii*	Juvenile	NA	NA	NA	NA	NA	Simple
LACM-5479	*Sylvilagus audubonii*	Subadult?	2.91	2.51	1.16	14.92	13.43	Moderate; Complex
LACM-7986	*Sylvilagus audubonii*	Adult	2.80	2.26	1.24	14.04	12.30	Moderate
LACM-90208	*Sylvilagus audubonii*	Adult	2.85	2.32	1.23	14.21	13.04	Complex

LACM-20731	*Sylvilagus audubonii*	Subadult?	2.84	2.42	1.17	15.12	13.54	Simple; Complex
LACM-21803	*Sylvilagus audubonii*	Adult	2.85	2.30	1.24	15.21	12.55	Complex
LACM-29050	*Sylvilagus audubonii*	Adult	2.93	2.31	1.27	14.19	12.64	Complex
LACM-32961	*Sylvilagus audubonii*	Adult	3.07	2.39	1.28	14.36	12.62	Complex
LACM-44966	*Sylvilagus audubonii*	Adult	2.86	2.18	1.31	14.48	12.45	Complex
LACM-44967	*Sylvilagus audubonii*	Adult	3.05	2.39	1.28	16.51	13.67	Moderate
LACM-49525	*Sylvilagus audubonii*	Adult	3.19	2.51	1.27	15.23	14.13	Moderate
LACM-49526	*Sylvilagus audubonii*	Adult	2.54	2.14	1.19	14.30	12.08	Complex
LACM-53876	*Sylvilagus audubonii*	Adult	2.92	2.31	1.26	13.04	12.96	Simple
LACM-53879	*Sylvilagus audubonii*	Adult	3.05	2.29	1.33	12.98	12.57	Moderate
LACM-73039	*Sylvilagus audubonii*	Adult	2.91	2.18	1.33	13.39	12.63	Complex
LACM-85733	*Sylvilagus audubonii*	Adult	2.91	2.23	1.30	NA	12.52	Complex
LACM-90015	*Sylvilagus audubonii*	Adult	3.05	2.26	1.35	NA	13.12	Moderate
LACM-90207	*Sylvilagus audubonii*	Adult	2.93	2.37	1.24	15.38	12.91	Complex
LACM-97340	*Sylvilagus audubonii*	Juvenile	NA	NA	NA	NA	NA	Simple; Complex
MVZ-5318	*Sylvilagus audubonii*	Juvenile	NA	NA	NA	NA	NA	Simple
MVZ-6385	*Sylvilagus audubonii*	Adult	2.30	1.99	1.16	12.07	11.47	Complex
MVZ-7025	*Sylvilagus audubonii*	Adult	2.58	2.39	1.08	15.21	12.39	Complex
MVZ-7168	*Sylvilagus audubonii*	Adult	2.62	2.23	1.17	13.29	11.87	Moderate
MVZ-7170	*Sylvilagus audubonii*	Adult	2.52	2.32	1.09	11.94	12.18	Complex
MVZ-7171	*Sylvilagus audubonii*	Juvenile?	NA	NA	NA	NA	NA	Simple

MVZ-10673	*Sylvilagus audubonii*	Adult	2.72	2.58	1.05	14.11	12.45	Complex
MVZ-28714	*Sylvilagus audubonii*	Juvenile	NA	NA	NA	NA	NA	Simple
MVZ-107653	*Sylvilagus audubonii*	Adult	2.65	2.60	1.02	13.66	12.68	Complex
MVZ-107654	*Sylvilagus audubonii*	Adult	2.65	2.50	1.06	15.07	12.98	Complex
MVZ-107655	*Sylvilagus audubonii*	Adult	2.48	2.38	1.04	14.37	12.17	Complex
LACM-192	*Sylvilagus bachmani*	Adult	2.75	1.96	1.40	12.55	12.95	Simple
LACM-193	*Sylvilagus bachmani*	Adult	2.51	2.03	1.24	NA	11.15	Simple
LACM-252	*Sylvilagus bachmani*	Adult	2.63	1.83	1.44	12.75	12.09	Simple
LACM-364	*Sylvilagus bachmani*	Adult	2.47	1.78	1.39	11.82	11.21	Simple
LACM-6403	*Sylvilagus bachmani*	Adult	2.53	1.82	1.39	11.46	11.20	Simple
LACM-6406	*Sylvilagus bachmani*	Adult	2.19	1.69	1.30	12.03	11.41	Simple
LACM-6407	*Sylvilagus bachmani*	Adult	2.20	1.68	1.31	10.83	10.11	Simple
LACM-6408	*Sylvilagus bachmani*	Adult	2.80	2.12	1.32	12.19	11.89	Simple
LACM-7314	*Sylvilagus bachmani*	Adult	2.54	2.09	1.22	11.61	11.68	Simple
LACM-21374	*Sylvilagus bachmani*	Adult	2.37	1.90	1.25	10.86	11.31	Simple
LACM-21375	*Sylvilagus bachmani*	Adult	2.45	1.86	1.32	11.97	11.03	Simple
LACM-21376	*Sylvilagus bachmani*	Adult	2.14	1.75	1.22	10.34	10.35	Simple
LACM-21377	*Sylvilagus bachmani*	Adult	2.33	1.81	1.29	10.67	10.86	Moderate
LACM-30032	*Sylvilagus bachmani*	Adult	2.78	2.26	1.23	14.20	13.29	Complex
LACM-30780	*Sylvilagus bachmani*	Adult	2.50	1.94	1.29	12.80	11.57	Simple
LACM-49529	*Sylvilagus bachmani*	Adult	2.52	1.82	1.38	11.97	11.67	Moderate
LACM-49531	*Sylvilagus bachmani*	Adult	2.62	2.14	1.22	13.02	12.05	Simple
LACM-91507	*Sylvilagus bachmani*	Adult	2.51	1.93	1.30	12.78	11.64	Simple

MVZ-2699	*Sylvilagus bachmani*	Adult	2.30	1.78	1.29	11.40	10.95	Simple
MVZ-2700	*Sylvilagus bachmani*	Adult	2.16	1.80	1.20	12.92	11.41	Simple
MVZ-3888	*Sylvilagus bachmani*	Adult	2.35	2.04	1.15	13.76	12.5	Simple
MVZ-3889	*Sylvilagus bachmani*	Adult	2.47	1.99	1.24	13.59	11.26	Simple
MVZ-3891	*Sylvilagus bachmani*	Adult	2.09	1.79	1.17	11.71	10.82	Simple
MVZ-5315	*Sylvilagus bachmani*	Adult	2.39	1.96	1.22	11.90	12.27	Simple
MVZ-6364	*Sylvilagus bachmani*	Adult	2.36	2.07	1.14	12.85	11.76	Simple
MVZ-24459	*Sylvilagus bachmani*	Adult	2.26	1.90	1.19	11.80	10.91	Simple
MVZ-29187	*Sylvilagus bachmani*	Adult	2.34	1.85	1.26	11.61	11.43	Simple
MVZ-29188	*Sylvilagus bachmani*	Adult	2.64	1.99	1.33	12.32	12.39	Simple
MVZ-29189	*Sylvilagus bachmani*	Adult	2.57	2.15	1.20	12.29	11.89	Simple
MVZ-182871	*Sylvilagus bachmani*	Adult	2.51	2.06	1.22	12.84	12.38	Complex
MCZBOM-187	*Sylvilagus nuttallii*	Juvenile?	2.16	1.75	1.23	11.45	10.82	Simple
MCZBOM-188	*Sylvilagus nuttallii*	Adult	2.38	1.87	1.27	12.55	11.86	Simple
MCZBOM-189	*Sylvilagus nuttallii*	Adult	2.80	2.47	1.13	14.66	13.35	Simple
MCZ-7678	*Sylvilagus nuttallii*	Adult	2.47	2.24	1.10	14.43	12.51	Simple
MCZ-7747	*Sylvilagus nuttallii*	Adult	2.57	2.25	1.14	12.58	12.09	Simple
MCZBANGS-9347	*Sylvilagus nuttallii*	Adult	2.40	1.96	1.22	12.24	11.33	Complex
MCZBANGS-9348	*Sylvilagus nuttallii*	Juvenile?	2.13	1.67	1.28	10.71	10.59	Complex
MCZBANGS-9349	*Sylvilagus nuttallii*	Adult	2.30	1.88	1.22	12.15	11.63	Complex

MCZBANGS-9350	*Sylvilagus nuttallii*	Adult	2.20	1.68	1.31	11.29	10.21	Complex
MCZ-10517	*Sylvilagus nuttallii*	Adult	2.98	2.45	1.22	14.40	13.32	Complex
MVZ-11315	*Sylvilagus nuttallii*	Adult	2.32	1.94	1.20	11.90	11.11	Simple
MVZ-66012	*Sylvilagus nuttallii*	Adult	2.60	2.14	1.21	13.50	11.98	Simple
MVZ-36347	*Brachylagus idahoensis*	Adult	1.64	1.52	1.08	10.50	8.93	Simple
MVZ-36348	*Brachylagus idahoensis*	Adult	1.69	1.63	1.04	10.55	9.40	Simple
MVZ-36349	*Brachylagus idahoensis*	Adult	1.70	1.60	1.06	10.59	9.05	Simple
MVZ-36350	*Brachylagus idahoensis*	Adult	1.63	1.47	1.11	10.41	9.24	Simple
MVZ-36351	*Brachylagus idahoensis*	Adult	1.81	1.53	1.18	11.38	9.28	Simple
MVZ-36352	*Brachylagus idahoensis*	Adult	1.73	1.57	1.10	10.30	9.09	Simple

Table 1.12.2: Dental measurements and p3 crenulation observations of all fossil leporids sampled from Project 23 deposits at Rancho La Brea. Specimens with two crenulation patterns (X; X) exhibit discrepancies between the tooth surface and base respectively. All measurements are in millimeters and measurements of inferred juveniles are not considered for estimating mean fossil species sizes. * indicates specimens included in t-test statistics for size comparison with extant specimens.

LACMP23 Number	Deposit	Element	Assigned Species	Assigned Life Stage	p3 length	p3 width	l/w ratio	p3 Crenulation
28082*	1	rt p3	*Sylvilagus bachmani*	Adult	2.21	1.73	1.28	Simple
28084*	1	lt p3	*Sylvilagus audubonii*	Adult	2.48	1.93	1.28	Moderate
28105	1	partial rt p3	*Sylvilagus audubonii*	Adult	NA	NA	NA	Complex?
28266	1	partial lt p3	*Sylvilagus audubonii*	Juvenile	NA	1.75	NA	Simple; Complex
28341	1	rt p3	*Sylvilagus audubonii*	Juvenile	1.97	1.67	1.18	Simple; Complex
28519	1	rt p3	*Sylvilagus audubonii*	Juvenile	2.16	1.73	1.25	Moderate
28555*	1	lt p3	*Sylvilagus audubonii*	Adult	2.32	2.04	1.14	Complex
28556	1	rt p3	*Sylvilagus audubonii*	Juvenile	1.74	1.36	1.28	Simple; Moderate
28661*	1	lt p3	*Sylvilagus audubonii*	Subadult?	2.42	1.94	1.25	Moderate; Complex
28858	1	rt p3	*Sylvilagus audubonii*	Juvenile	2.26	1.77	1.28	Simple; Moderate
29229*	1	lt p3	*Sylvilagus bachmani*	Adult	2.16	1.65	1.31	Simple
31781	14	lt p3	*Sylvilagus audubonii*	Juvenile	1.86	1.70	1.09	Simple; Complex

31782	14	partial lt p3	*Sylvilagus audubonii*	Juvenile	NA	1.93	NA	Simple; Moderate
32045*	14	lt dentary frag. with p3	*Sylvilagus bachmani*	Adult	2.60	1.93	1.35	Simple
32047*	14	rt dentary frag. with p3-m1	*Sylvilagus audubonii*	Adult	2.67	2.19	1.22	Moderate
33861*	14	lt p3	*Sylvilagus bachmani*	Adult	2.28	1.65	1.38	Simple
33962	14	rt p3	*Sylvilagus audubonii*	Juvenile	2.01	1.62	1.24	Simple; Moderate
34117*	14	rt p3	*Sylvilagus audubonii*	Subadult?	2.27	2.01	1.13	Moderate; Complex
34259	14	partial lt p3	*Sylvilagus audubonii*	Juvenile	2.07	1.64	1.26	Complex
34260	14	partial lt p3	*Sylvilagus audubonii*	Juvenile	NA	1.55	NA	Simple; Complex
34262*	14	rt p3	*Sylvilagus bachmani*	Adult	2.11	1.68	1.26	Simple
35608*	7B	lt p3	*Sylvilagus audubonii*	Subadult?	2.64	2.23	1.18	Moderate; Complex
35614*	7B	rt p3	*Sylvilagus audubonii*	Adult	2.66	NA	NA	Complex
35618	7B	rt p3 frag.	*Sylvilagus audubonii*	Adult	NA	NA	NA	Complex
35619*	7B	partial rt p3	*Sylvilagus audubonii*	Adult	2.58	2.16	1.19	Complex
35645	7B	rt p3 frag.	*Sylvilagus audubonii*	Adult	NA	NA	NA	Complex
35696*	7B	rt p3	*Sylvilagus audubonii*	Adult	2.63	2.37	1.11	Complex
35763*	7B	lt p3	*Sylvilagus audubonii*	Adult	2.31	2.02	1.14	Complex

35771	7B	lt p3 frag.	*Sylvilagus audubonii*	Adult	NA	NA	NA	Complex
35836*	7B	rt p3	*Sylvilagus audubonii*	Adult	3.11	2.47	1.26	Complex
35839*	7B	rt p3	*Sylvilagus audubonii*	Adult	2.78	2.35	1.18	Complex
35840*	7B	rt p3	*Sylvilagus audubonii*	Adult	2.43	2.09	1.16	Complex
35844*	7B	rt p3	*Sylvilagus bachmani*	Adult	1.93	1.66	1.16	Simple
35847*	7B	lt p3	*Sylvilagus audubonii*	Adult	2.48	2.17	1.14	Complex
35881	7B	rt p3	*Sylvilagus audubonii*	Juvenile	2.12	1.82	1.16	Simple; Complex
35883*	7B	rt p3	*Sylvilagus audubonii*	Adult	2.75	2.35	1.17	Complex
35885	7B	lt p3	*Sylvilagus audubonii*	Juvenile	1.98	1.72	1.15	Simple; Complex
35937	7B	lt p3	*Sylvilagus audubonii*	Juvenile	1.80	1.50	1.20	Simple; Complex
36615*	14	rt p3	*Sylvilagus bachmani*	Adult	2.01	1.69	1.19	Simple
39811*	13	lt dentary frag. with p3, p4, m2	*Sylvilagus audubonii*	Adult	2.59	2.04	1.27	Complex
39819*	13	rt dentary frag. with p3-m1	*Sylvilagus audubonii*	Adult	3.01	2.40	1.25	Complex
39820	13	rt dentary frag. w/ partial p3-m2	*Sylvilagus audubonii*	Adult	2.56	NA	NA	Complex
39874*	13	rt p3	*Sylvilagus audubonii*	Subadult?	2.22	1.89	1.18	Moderate; Complex
39929	13	rt p3 frag.	*Sylvilagus audubonii*	Unknown	NA	NA	NA	Complex?
40039	13	partial lt p3	*Sylvilagus audubonii*	Adult	NA	NA	NA	Complex

40110	13	partial rt p3	*Sylvilagus audubonii*	Adult	NA	NA	NA	Complex
40166*	13	rt p3	*Sylvilagus audubonii*	Adult	2.61	2.19	1.19	Complex
40167	13	lt p3	*Sylvilagus audubonii*	Juvenile/Subadult	2.12	1.72	1.23	Moderate; Complex
40168	13	rt p3 frag.	*Sylvilagus audubonii*	Adult	NA	NA	NA	Complex
40209*	13	lt p3	*Sylvilagus audubonii*	Adult	2.63	2.19	1.20	Complex
40210*	13	rt p3	*Sylvilagus audubonii*	Adult	2.49	2.05	1.21	Complex
40211*	13	rt p3	*Sylvilagus audubonii*	Adult	2.44	2.13	1.15	Complex
40212	13	worn rt p3 frag.	*Sylvilagus audubonii*	Adult	NA	NA	NA	Complex?
40284	13	worn lt p3	*Sylvilagus audubonii*	Adult	3.03	NA	NA	Complex
40285*	13	worn lt p3	*Sylvilagus audubonii*	Adult	2.34	2.06	1.14	Moderate
40286*	13	lt p3	*Sylvilagus audubonii*	Adult	2.65	2.15	1.23	Moderate
40287*	13	lt p3	*Sylvilagus audubonii*	Adult	2.26	1.89	1.20	Complex
40288	13	lt p3 frag.	*Sylvilagus audubonii*	Adult	NA	NA	NA	Complex
40291	13	rt p3 frag.	*Sylvilagus audubonii*	Adult	NA	NA	NA	Complex?

Table 1.12.3: Carbon-14 data from leporid specimens sampled from Project 23 Deposits 1, 7B, 13, and 14. All specimens were analyzed at the University of California Irvine Keck Carbon Cycle AMS Laboratory (UCIAMS).

UCIAMS Number	LACMP23 Number	Deposit	Element	C/N (atomic)	^{14}C age (years BP)	^{14}C age error
191095	5233	1	rt dentary frag. w/ p3-m1	3.33	35750	610
191096	18270	1	rt dentary frag. w/ p3-m2	3.48	35440	580
191097	22009	1	rt dentary frag. w/ p3-m3	3.60	35150	580
191098	25476	1	rt anterior dentary w/ p3-m2	3.38	36050	630
191099	28903	1	rt dentary frag. w/ p3-p4	3.34	33830	480
191100	30238	1	rt anterior dentary w/ p3-m2	3.59	35780	600
191101	31269	1	rt anterior dentary w/ p3-m2	3.26	46200	2200
191102	31423	1	rt anterior dentary	3.46	35420	580
198294	28902	1	lt partial dentary w/ p3-m2	3.45	39700	810
216783	35774	7B	rt maxilla frag.	3.34	42600	1400
216784	36332	7B	lt distal humerus	3.24	41500	1200
216785	36336	7B	rt anterior dentary w/ p4-m1	3.32	50200	3500
217079	36331	7B	lt anterior dentary frag.	3.31	46200	2400
223495	35541	13	lt posterior dentary w/p4-m2	3.31	39220	460
223497	36693	13	lt dentary frag. w/p4-m2	3.46	39240	670
223499	36896	13	lt dentary frag. w/ m1-m2	3.33	33590	340
223502	36989	13	lt anterior dentary w/p4	3.48	44000	1200
223503	37612	13	lt dentary w/ p4-m2	3.40	46200	1600
223505	39811	13	lt anterior dentary frag. w/ p3, p4, m2	3.39	33260	320
223506	39812	13	lt posterior dentary w/ m1-m2	3.35	36260	470
223507	39818	13	lt posterior dentary frag.	3.49	31230	270
223508	39822	13	lt dentary frag. w/ p4-m2	3.36	31980	280
191103	31033	14	rt anterior dentary w/ p3-m2	3.47	>47800	NA
191104	31036	14	rt anterior dentary w/ p3-m1	5.56	>49900	NA
191105	31056	14	rt anterior dentary w/ p3-m2	4.04	>49900	NA
191242	31031	14	rt anterior dentary w/ p3-m2	3.51	>50800	NA
223516	40637	14	rt humerus	3.30	26780	160

Chapter 2: Are geometric morphometric analyses replicable? Evaluating landmark measurement error and its impact on extant and fossil *Microtus* classification

2.1 Abstract

Geometric morphometric analyses are frequently employed to quantify biological shape and shape variation. Despite the popularity of this technique, quantification of measurement error in geometric morphometric datasets and its impact on statistical results is seldom assessed in the literature. Here, I evaluate error on 2D landmark coordinate configurations of the lower first molar of five North American *Microtus* (vole) species. I acquired data from the same specimens several times to quantify error from four data acquisition sources: specimen presentation, imaging devices, interobserver variation, and intraobserver variation. I then evaluated the impact of those errors on linear discriminant analysis-based classifications of the five species using recent specimens of known species affinity and fossil specimens of unknown species affinity. Results indicate that data acquisition error can be substantial, sometimes explaining >30% of the total variation among datasets. Comparisons of datasets digitized by different individuals exhibit the greatest discrepancies in landmark precision and comparison of datasets photographed from different presentation angles yield the greatest discrepancies in species classification results. All error sources impact statistical classification to some extent. For example, no two landmark dataset replicates exhibit the same predicted group memberships of recent or fossil specimens. These findings emphasize the need to mitigate error as much as possible during geometric morphometric data collection. Though the impact of measurement error on statistical fidelity is likely analysis-specific, it is recommended that all geometric morphometric studies standardize specimen imaging equipment, specimen presentations (if analyses are 2D), and landmark digitizers to reduce error and subsequent analytical misinterpretations.

2.2 Introduction

Geometric morphometrics (GM) is a popular technique for evaluating shape and shape change among biological specimens. It is often used in ecology, archeology, and paleontology to address a variety of topics including: taxonomy (De Meulemeester et al., 2012; Jansky et al., 2016; Wallace, 2006), ecomorphology (Cassini, 2013; Curran, 2012; Figueirido et al., 2009; Gómez Cano et al., 2013; Meachen et al., 2014), evolution and development (Lawing & Polly, 2010), and population history (Baumgartner & Hoffman, 2019; Bignon et al., 2005; Gaubert et al., 2005; Nicholson & Harvati, 2006). Geometric morphometric "shape" is quantified via Cartesian landmark coordinate configurations positioned on discreet, biological loci (Zelditch et al., 2004). The scale, location, and rotational orientation of these landmark configurations are then standardized via Generalized Procrustes Analysis (GPA) superimposition to isolate and compare object shape (Kendall, 1977; Rohlf & Slice, 1990). Geometric morphometric analysis of specimens projected on 2D and 3D surfaces can be advantageous over qualitative morphological descriptions and traditional morphometrics (e.g., linear measurements)

since the former is often subjective and the latter is correlated with object size (Schmieder et al., 2015). Unlike traditional morphometrics, GM also excels at shape visualization which facilitates communication of empirical results (Zelditch et al., 2004).

Despite its analytical advantages and broad utility, replicating GM results can be challenging due to the variety of research equipment used to image the samples, variation in specimen positioning, and variation in landmark digitization within and among operators, all of which can generate data discrepancies. Each phase of GM data acquisition can introduce a unique form of random and/or systematic measurement error. When compounded, these errors may lead to inconsistency among repeated measures and obscure the distinction between biological and artificial variation among specimens (Fruciano, 2016; Robinson & Terhune, 2017). Three general types of GM-based measurement error are acknowledged (methodological, instrumental, and personal), which can be subdivided into more specific error sources (Arnqvist & Mårtensson, 1998). Here, I address four sources of measurement error encountered during landmark data acquisition:

Imaging device (error type – instrumental): use of different instruments for projecting 3D objects on 2D and 3D surfaces (e.g., digitizing tablets, digital images, scanners, etc.) can generate dissimilar morphological reconstructions of original specimens (Arnqvist & Mårtensson, 1998). Variation can occur within equipment types as well. Camera lenses, for example, generate 2D image distortion based on the magnification of an object and its distance and position from the camera; the extent of image distortion varies among lens types due to factors such as lens curvature (Zelditch et al., 2004). The resolution of an image will also vary depending on the number of photodetectors in a camera (Zelditch et al., 2004); some anatomical loci may be obscured in lower-resolution images which can impact the precision of landmark placement. Error facilitated by dimensional loss is specific to 2D GM analyses; though, other forms of instrumental error can occur in 3D systems as well (Fruciano et al., 2017; Robinson & Terhune, 2017). The configuration of landmarks placed on specimen images may, therefore, be inconsistent when different equipment is used and/or when data from different imaging protocols are combined.

Specimen presentation (error type – methodological): operators digitizing specimens in two dimensions should be cautious of their presentations (i.e., the projected orientation of specimens) since some degree of distortion is usually unavoidable when projecting 3D objects. Differential shifting of three-dimensional features can be problematic in 2D systems because z-axes are not retained and, therefore, projected locations of landmark loci can be displaced relative to their true position among other loci (Buser et al., 2018; Cardini, 2014; Zelditch et al., 2004). Effects of such displacement can be exacerbated if landmark loci shift towards the edges of a camera field where image distortion is greatest (Fruciano, 2016; Zelditch et al., 2004). If all objects are projected from similar orientations and with the same equipment, any projection distortions should be similar among specimens and are thus unlikely to generate substantial artificial variation. If presentations are dissimilar among species, however, associated interspecimen variation in landmark coordinates may appear biological in downstream analysis when it is in fact artificial. Presentation error may be particularly substantial in situations where interspecimen orientations are difficult to standardize (e.g., when

comparing within-cranium teeth of recent specimens to isolated teeth of fossil specimens).

Interobserver error (error type – personal): after specimens have been selected, presented, and projected, error can occur during landmark digitization. For example, one individual may position a landmark differently than another individual, even when digitizing the same locus of the same specimen. Error among landmark digitizers is referred to as interobserver error.

Intraobserver error (error type – personal): Digitizing error occurs within observers as well. An individual may place a landmark on a locus differently from one specimen to another or from one digitizing session to another. This is referred to as intraobserver error. Intra and interobserver error can be affected by factors such as variation in digitizing experience among observers, the number of digitizing sessions conducted per observer, and ease of landmark loci visualization (Fruciano, 2016; Osis et al., 2015). Observer errors may be exacerbated by variation in specimen projection, and/or presentation as well.

Measurement error introduced at various phases of landmark data acquisition can be substantial; however, their collective impacts on GM analyses are underreported (Fruciano, 2016). It is not uncommon for studies to report inter- and intraobserver error (e.g., Dujardin et al., 2010; Gonzalez et al., 2011; Nicholson and Harvati, 2006; Ross and Williams, 2008), possibly because landmark digitization does not require presentation and projection replications and because it can be conducted any time after projected specimen data collection. Personal digitizing errors are therefore more convenient to quantify than most other error types (Fruciano, 2016). Quantification of presentation and projection error requires replication which generally must be conducted at specimen housing facilities, and are seldom assessed in the literature (but see Fruciano, 2016; Fruciano et al., 2017; Robinson and Terhune, 2017) though their potential for obscuring biologically-meaningful shape variation is considerable (Fruciano, 2016; Zelditch et al., 2004). Few studies demonstrate how several of these error types can combine to impact statistical result-based inferences (but see Fruciano et al., 2017, 2020; Robinson and Terhune, 2017; Vergara-Solana et al., 2014). This context is important because ecological, archeological, and paleontological studies often use statistical grouping analyses (e.g., linear discriminant analysis (LDA)/canonical variate analysis) to determine the taxonomic or ecological affinity of unknown specimens (Kovarovic et al., 2011; Webster & Sheets, 2010). Despite the frequency of GM-based classification analyses in the literature (e.g., Baumgartner and Hoffman, 2019; Cassini, 2013; Curran, 2012; De Meulemeester et al., 2012; Gómez Cano et al., 2013; Wallace, 2006), the impacts of multiple sources of measurement error on statistically-derived group membership predictions are largely untested.

Here, I evaluate the relative contribution of GM measurement error from different landmark data acquisition sources and their impact on LDA group membership predictions. I specifically quantify error introduced from four sources—specimen presentation, specimen imaging devices, interobserver digitization, and intraobserver digitization—and determine how the accuracy and replicability of 2D landmark-based identifications of five closely-related extant species, and the predicted group membership

replicability of congeneric specimens of unknown species affinity, are affected by each error source. For this study, "replicable" is defined as achieving the same group membership predictions of individual specimens among repeated data acquisition iterations. I do this so future researchers classifying specimens via landmark analysis are aware of 1) the data acquisition sources that may introduce non-negligible amounts of measurement error and 2) the precautions that can be employed to mitigate those errors and their impacts on statistical results.

2.3 Methods

2.3.1 Study system

Recent work on observer and method-based GM error suggests that error may have a substantial impact on statistical results when variation among similar (e.g., intraspecific) groups is analyzed because morphological differences among those groups is likely to be subtle (Robinson & Terhune, 2017). Thus, artificial variation introduced via GM error may be more likely to impact classification statistics, and bias subsequent inferences of biological variation, when among-group variation is low (Robinson & Terhune, 2017). Comprehensive analysis of different types of measurement error and their impact on closely related/morphologically similar group differentiation is seldomly conducted. To explore this, I examine five *Microtus* (vole) species (*M. californicus*, *M. longicaudus*, *M. montanus*, *M. oregoni*, and *M. townsendii*) distributed throughout western North America. Voles are frequently used as biochronologic and paleoenvironmental indicators at fossil sites due to their habitat specificity and ubiquity in modern and prehistoric biotic assemblages (Bell & Bever, 2006; Bell & Repenning, 1999; McGuire, 2011; Smartt, 1977; Wallace, 2019). However, identifying voles to species is challenging due to high morphological variability, high diversity, and sympatry of species throughout much of North America (Barnosky, 1990; Bell & Bever, 2006; Smartt, 1977; Wallace, 2006). Over the past two decades, more advanced research techniques including landmark-based LDA of *Microtus* lower first molars (m1s) has improved vole species identification accuracy (Wallace, 2006), but it is still imperfect when applied to study regions such as western North America due to marked geographic range and shape overlap among the many members that reside there today (McGuire, 2011). Western North American voles are therefore an appropriate system for evaluating GM measurement error on classification statistics when intergroup variation is low.

2.3.2 Study design

I replicated 2D digital specimen images (n=247) and m1 landmark configurations (n=21 landmarks; Fig. 2.1) of (McGuire, 2011) to quantify measurement error from four data acquisition sources and its impact on *Microtus* species classification. All photographed specimens are from the University of California Museum of Vertebrate Zoology (MVZ); see Appendix I of (McGuire, 2011) for a list of the recent *Microtus* specimens included. I was unable to acquire four of the 251 original specimens from McGuire (2011) (MVZ: 68521, 83519, 96735, 99283) so the final number of individuals analyzed per species is as follows: *M. californicus* (n=49), *M. longicaudus* (n=49), *M. montanus* (n=48), *M. oregoni* (n=50), *M. townsendii* (n=51). Each species group thus

meets ideal LDA conditions that 1) predictor variables (i.e., x and y Cartesian landmark coordinates, n=42) do not exceed n of the smallest group and 2) that group samples sizes are approximately equal (Kovarovic et al., 2011). Each phase of landmark data acquisition (i.e., specimen presentation, specimen imaging, and inter/intra observer digitization) was repeated to quantify error from those sources. The study design for quantifying error from each source was as follows:

Imaging device: I assembled two datasets using specimen images obtained from two different cameras to evaluate inter-instrument variation (hereafter "imaging device" or simply "device" variation). The first image set included the original *Microtus* dentary images photographed with a Nikon D70s (hereafter Nikon) from (McGuire, 2011). The second image set included the same specimens photographed with a Dino-Lite Edge AM4815ZTL Digital Microscope (hereafter Dino-Lite). Efforts were made to replicate the original Nikon specimen orientations, especially projected angles of occlusal tooth surfaces and specimen distances from the camera lens, to minimize presentation error during this iteration. However, presentation error is necessarily a residual component of imaging device error in 2D systems.

Specimen presentation: After an initial Dino-Lite photograph was taken, each *Microtus* specimen was tilted haphazardly along its anteroposterior and/or labiolingual axis and re-photographed with all landmark loci still visible. This was done to simulate specimen orientation changes that may occur when comparing dissimilar specimens such as *in situ* teeth and isolated teeth. That scenario is not uncommon when comparing fossil specimens to recent specimens since complete preservation of fossilized craniodental remains is rare. When loose m1s were available from recent *Microtus* specimens, those teeth were photographed in isolation rather than *in situ* during this iteration. Note, however, that intentionally tilting specimens potentially exacerbates presentation error relative to the amount of error typically introduced when specimen orientations are standardized. The intent of this modification is to quantify potential presentation error rather than expected error since presentation error will vary by study (Fruciano, 2016).

Inter/intra observer error: To quantify observer variation, the original Nikon *Microtus* m1 images and Dino-Lite resampled images were digitized by two observers using the 21-landmark protocol of Wallace (2006) and McGuire (2011) (Fig. 2.1). Those observers also allowed us to evaluate methodological experience, a variable suggested (but rarely tested) to impact the magnitude of observer error (Fruciano, 2016). It is perhaps expected that experience will reduce digitizing error, but recent studies have shown that is not always true (Engelkes et al., 2019) thus warranting its quantification here. One observer, hereafter referred to as the experienced observer (EO), had previous experience conducting 2D landmark analyses at the time this study was initiated while the other observer, hereafter referred to as the new observer (NO), did not. Each image set was then digitized a second time by the EO and NO with at least one week between iterations to evaluate intraobserver variation on landmark placement.

2.3.3 Data preparation

Nine unique landmark datasets were assembled in total to evaluate measurement error from the four focal data acquisition sources. First, Nikon and Dino-Lite image sets

were assembled to quantify imaging device variation. Those image sets were digitized twice by each observer to evaluate inter and intraobserver error (two image sets and two digitizing iterations per observer = eight datasets, Appendix Fig. 2.9.1). A "tilted" Dino-Lite image set was then assembled and digitized by the EO to quantify data variation due to changes in specimen presentation resulting in a total of nine datasets. All image sets were assembled and digitized using TpsUtil 32 (Rohlf, 2018a) and TpsDig 2.32 (Rohlf, 2018b) software respectively. Each landmark dataset was superimposed via GPA to standardize effects of rotation, orientation, and scale among specimens using the gpagen function in the R package "geomorph" (version 3.1.3, Adams et al., 2019). During GPA, all specimens are translated to the origin, scaled to unit-centroid size, and optimally rotated via a generalized least-squares algorithm to align them along a common coordinate system (Rohlf & Slice, 1990).

2.3.4 Quantifying measurement error

Procrustes ANOVA models were run using the procD.lm function in geomorph to analyze source-specific variation in the nine GPA-transformed landmark datasets. Analyses were conducted on 22 unique pairwise dataset comparisons (see dataset comparison names in Table 2.1 for specific comparisons) and cumulatively across 8 datasets using the following nested hierarchal levels: species > individuals > imaging device> interobservers > intraobservers (Appendix Fig. 2.9.1). Specimen presentation was only evaluated via pairwise comparison of tilted versus non-tilted Dino-Lite datasets because tilted presentations were not included in the original Nikon-image study design of (McGuire, 2011). All Procrustes ANOVAs were conducted using a residual randomization procedure with 999 iterations. Dataset comparisons were grouped according to the specific data acquisition iterations they encompassed using a four-part naming system. For example, "Dinolite_NoTilt_EO_T1" indicates that 1) the images were photographed with a Dino-Lite camera, 2) the images were not randomly tilted, 3) images were digitized by the EO, and 4) it was the EO's first digitizing iteration. Thus, pairwise comparison of datasets "Dinolite_Notilt_EO_T1" and "Dinolite_Notilt_EO_T2" quantifies intraobserver variation between digitizing iterations one and two for the EO since all other source components are equivalent. In addition, repeatability was calculated among these datasets using pairwise Procrustes ANOVA mean squares based on the protocol and equations of Arnqvist and Mårtensson (1998) and Fruciano (2016). Repeatability quantifies the variability of repeated measurements within the same samples, in this case the resampled *Microtus* datasets, relative to the variability among samples, in this case the biological variation among specimens, on a zero to one scale. Values closer to one indicate higher repeatability and values closer to zero indicate lower repeatability (Arnqvist & Mårtensson, 1998; Fruciano, 2016).

2.3.5 Quantifying measurement error impacts on classification statistics

To determine how source-specific measurement error impacts *Microtus* species classification, I ran LDAs on each of the nine GPA-transformed landmark trial datasets using the lda function in the R package "MASS" (version 7.3, Venables and Ripley, 2002). Forty-two x, y coordinates from the 21 digitized landmarks were used as predictor variables to classify each specimen into a predicted species group. Leave-one-out cross-

validation was used to determine the percentage of specimens correctly classified within their respective species groups since it reduces standard LDA-group overfitting (Kovarovic et al., 2011). Prior probabilities of group membership were assigned using the default lda argument based on the proportion of group samples which, in this case, are nearly equal due to similar sample sizes among species. Linear discriminant analysis predicted group membership (PGM) error percentages were calculated for each landmark dataset by dividing the number of misclassified individuals across all five species by the total number of individuals (n=247) multiplied by 100. Differences in absolute PGM error percentages among the 22 pairwise dataset comparisons were then recorded. Additionally, a stepwise discriminant analysis was performed on a subset of trials to evaluate whether the significance of different landmark variables for discriminating extant *Microtus* species groups change among data acquisition iterations. A standard LDA was performed in all other cases unless specified otherwise.

Next, a set of 31 fossil *Microtus* m1 images of unknown species identity was digitized by the EO, using the same 21-landmark protocol, and appended to each dataset of recent *Microtus* specimens to evaluate error impacts on the PGM of unknown specimens. Fossil specimens included mostly isolated m1s and were photographed with the same Dino-Lite camera as recent *Microtus* specimens. Each of the nine recent *Microtus* landmark datasets served as a unique discriminant function training set to classify the unknown fossils into one or more of the five extant species groups. All fossil specimens are from Project 23, Deposit 1, at Rancho La Brea in Los Angeles, CA and are late Pleistocene in age (~46,000 to ~31,000 radiocarbon years before present (Fox et al., 2019; Fuller et al., 2020)). Due to their geographic and temporal location, it is unlikely that the fossils belong to a species of *Microtus* other than the five included in the LDA training sets. Linear discriminant analyses were run on landmark coordinate variables of each dataset with fossils entered as unknowns and the PGM of each fossil specimen in each trial was recorded.

2.3.6 Species occurrence likelihood

Since LDA of western North American vole species is less than 100% accurate (McGuire, 2011), it may be difficult to determine whether some PGMs are “real” or altered by error within the LDA training set, especially when the number of individuals assigned to a species-group is small. Therefore, I consider a species occurrence “likely” if the percentage of unknown individuals classified to a species-group, relative to the total number of individuals within the unknown dataset, exceeds the percentage of cross-validated classification error within the LDA training set. For example, a dataset that misclassifies 40 of the 247 recent *Microtus* specimens (16.2%) must assign more than 16.2% of the total unknown specimens to a particular species group for that species to be considered “likely present”. Thus, if 15 of the 31 unknown specimens were assigned to *M. californicus* (48.3%), four were assigned to *M. montanus* (12.9%), and two were assigned to *M. townsendii* (6.5%), only *M. californicus* would be considered “likely present” since the percentage of specimens assigned to the other two species falls within the range of classification error for that dataset (see Results). To further vet false occurrences, I removed all fossil individuals with PGM posterior probabilities less than 0.95 prior to these likelihood calculations.

2.4 Results

2.4.1 Source-specific variation

Pairwise and nested Procrustes ANOVA of the landmark datasets show that all potential error sources generate significant error (Tables 2.1 & 2.2). Of the four sources, interobserver error is the most substantial and explains ~27% of the variation among datasets, on average, in pairwise comparisons (see R^2 values, Table 2.1). The next greatest sources of error in the pairwise comparisons are seen among specimen presentations and imaging devices, both of which explain ~20% of the variation on average, followed by intraobserver error which explains ~12% of pairwise variation on average (Table 2.1). The combined model shows similar patterns for different contributions to variation (Table 2.2): interobserver error accounts for ~21% of the variation, whereas device and intraobserver error explain ~8% and 10% of among-dataset variation respectively in the nested Procrustes ANOVA model. These data acquisition error sources together explain ~39% of the total variation among datasets while biological variation among individuals and species explain ~53% and ~8% of the total variation respectively (Table 2.2). Error source-specific repeatability is similar to patterns of Procrustes ANOVA R^2 variation – interobserver pairwise comparisons are the least repeatable overall (mean = 0.30), followed by presentation comparisons (mean = 0.45), device comparisons (mean = 0.46) and intraobserver comparisons (mean = 0.66) (Table 2.1).

2.4.2 Classification accuracy

Cross-validated PGM error varies substantially among the 22 pairwise LDA comparisons with 0%-24.3% discrepancies in absolute error among landmark datasets (Table 2.1). Contrary to Procrustes ANOVA results, differences in PGM error are greatest between datasets of differential presentation (i.e., between tilted versus non-tilted specimen images), which exhibit a mean pairwise PGM accuracy difference of 18.8% (Table 2.1). Datasets digitized by different observers generate the next greatest amount of variation in pairwise PGM error overall (mean difference = 15.2%) followed by device error and intraobserver error which yield mean PGM accuracy shifts of 5.9% and 2.7% respectively among pairwise comparisons (Table 2.1). Cross-validated PGM error of all extant *Microtus* species ranges from 13.8% to 38.1% among the nine datasets, with a mean error of 26.3% among datasets overall (Table 2.3). Predicted group membership errors are substantially lower in non-cross-validated analyses of the same datasets (PGM error = 2.8% to 20.6%, Appendix Table 2.9.1), likely due to PGM overfitting (Kovarovic et al., 2011). Variables selected for discriminating extant *Microtus* species groups in stepwise discriminant analysis also vary among datasets, even among datasets collected with the same imaging device and digitized by the same observer (Appendix Table 2.9.2).

2.4.3 Predicted group membership replicability

Predicted group memberships of unknown *Microtus* fossils from Project 23, Deposit 1, at Rancho La Brea vary substantially among the nine landmark datasets (Tables 2.1 & 2.3; Appendix Table 2.9.1). Individual fossil PGM discrepancies range from 9.7% to 45.2% among the 22 pairwise dataset comparisons (Table 2.1). As with

differences in PGM error of recent specimens, PGM differences among the unknown fossils is greatest between trials of differential presentation (mean PGM variation = 43.6%) followed by different imaging devices (32.7%), different observers (29.5%), and within-observers (22.6%) (Table 2.1). *Microtus californicus* is the most frequently assigned species; the number of fossil individuals classified as *M. californicus* with predicted probabilities >0.95 range from three to 20 among datasets (Table 2.3). *Microtus californicus* is considered "likely present" in four of the nine datasets according to my likelihood criterion. *Microtus longicaudus* is the second most frequently assigned species; 0 to eight individuals are classified as this species within datasets after probability vetting, and it is considered "likely present" in one of the nine datasets (Table 2.3). Individual specimens assigned to the other three species range from 0, 0-2, and 0-1 for *M. montanus*, *M. oregoni*, and *M. townsendii* respectively after probability vetting. None of those species are considered "likely present" in any dataset using this likelihood criterion (Table 2.3). Relative proportions of fossil individuals assigned to each species group are similar across datasets when posterior probability vetting and leave-one out cross-validation is not employed, though the number of individuals retained in each species group is greater. The number of datasets with *M. californicus* and *M. longicaudus* considered likely present increases to nine and eight respectively using this procedure (Appendix Table 2.9.1).

2.5 Discussion

2.5.1 Landmark data acquisition error

I have shown that error introduced from various landmark data acquisition sources can be substantial and, in some cases, explains >30% of non-biological variation among datasets (Tables 2.1 & 2.2). This is concerning for geometric morphometric analyses aiming to quantify shape change among biological groups – including studies of taxonomy, functional ecology, and population history – because large amounts of error may impact hypothesis testing outcomes and/or lead to erroneous interpretations of focal-group relationships (Buser et al., 2018). It is therefore necessary to identify source-specific causes of error and establish protocols to mitigate error as much as possible.

I find interobserver error to be greatest among datasets, overall, followed by error among specimen presentations, within observers, and among different types of imaging equipment (Tables 2.1 & 2.2; Fig. 2.2), though the relative importance of device versus intraobserver error differs among pairwise versus nested Procrustes ANOVA analyses (Tables 2.1 & 2.2). Such discrepancies are not unexpected since intraobserver error is an inextricable component of device error, presentation error, and interobserver error in pairwise analysis and therefore its impact is best captured by the nested analysis. In all cases, variation attributed to data acquisition error sources is less than biological variation among individuals but greater than or approximately equal to variation among species (Tables 2.1 & 2.2). These findings generally agree with quantifications of interobserver and device error in other studies (e.g., Fruciano et al., 2017; Robinson and Terhune, 2017). For example, Fruciano et al. (2017) found interobserver error to be greater than device error or biological asymmetry, explaining up to 10.2% and 5.4% of the variation

within datasets respectively. Similarly, Robinson and Terhune (2017) found observer error to be the greatest non-biological source of variation. Interobserver variation in this study may have been exacerbated by differences in digitizing experience among operators and device error may be elevated by residual presentation error despite controlling for this. Indeed, pairwise Procrustes ANOVA of datasets digitized by the EO and NO yielded considerable differences in R^2 and repeatability, with less error and higher repeatability of datasets digitized by the EO, suggesting that experience does reduce digitizing error here. Mean intraobserver R^2 is 9.84% and 13.72%, and repeatability is 0.72 and 0.61, for the EO and NO respectively (Table 2.1). Changes in specimen presentation yield the second greatest amount of landmark data variation in pairwise comparisons (Table 2.1). Although presentation error may have been exacerbated by the intentional titling of specimens in this treatment, Fruciano (2016) also found presentation-based variation to be significant and substantially greater than intraobserver error on 2D landmark configurations of fish body shape.

2.5.2 Impacts on group classification statistics

As with Procrustes ANOVA variation, LDA PGM error of extant *Microtus* varies substantially among datasets, with up to 24% variation in absolute PGM accuracy among pairwise trial comparisons (Table 2.1). Unlike Procrustes ANOVA results, however, PGM error changes were greatest among specimens of differential presentation (mean PGM error difference=18.8% among tilted and non-tilted trials) rather than among observers (mean PGM error difference=15.2% between EO and NO trials) (Table 2.1). Procrustes ANOVA variation and LDA error variation are both used as proxies of error in this study; though, they are not necessarily equivalent. Procrustes ANOVA variation reflects changes in landmark precision among datasets and PGM error variation reflects changes in landmark accuracy relative to the biological loci and groups of interest, which may partly explain these discrepancies. As with Procrustes ANOVA R^2, PGM error and pairwise differences in absolute PGM error were lower among EO datasets and greater among NO datasets overall (Tables 2.1 & 2.3; Fig. 2.3A). Mean cross-validated PGM error variation of pairwise intraobserver comparisons, excluding tilted trials, is 1.8% and 3.5% among EO and NO trials respectively (Table 2.1) and the mean PGM error among 8 datasets digitized by each author, excluding the tilted trial, is 17.9% and 32.7% for the EO and NO respectively (Table 2.3; Fig. 2.3A). These results suggest that, in this case, digitizing experience improves downstream classification accuracy in addition to increasing landmark precision. In future studies, it would be informative to test the rate at which landmark accuracy and precision improves with experience by conducting further EO and NO digitizing iterations.

The greatest difference in PGM of fossil specimens is observed among pairwise comparisons of different presentations followed by different imaging devices, observers, and iterations within observers (Table 2.1). Unlike recent specimens of known species affinity, experience-based intraobserver variation in fossil PGM is similar among observers and trials overall (mean fossil PGM change = 22.6% among both EO and NO trials, Table 2.1). Pairwise differences in fossil PGM are often large, ranging from 9.7% to 45.2%, even when Procrustes ANOVA R^2 values and/or extant species PGM

differences among pairwise comparisons are small (e.g., between Nikon_NoTilt_EO_T1 and Nikon_NoTilt_EO_T2, Table 2.1). Data of unknown specimens may be especially sensitive to measurement error because they are often acquired, appended, and/or analyzed only after a meaningful group-binning protocol has been established among training groups (e.g., Cassini, 2013; De Meulemeester et al., 2012; Figueirido et al., 2015; this study). Thus, data acquisition processes and their associated errors may be repeated during unknown specimen data collection, which may exacerbate the amount of artificial variation present among unknowns relative to specimens in the training set. For example, replicating the orientation of recent specimen teeth projected from within jaws could be difficult when projecting isolated teeth of fossil specimens. Indeed, these data show that orientation changes among specimens captured in 2D images can profoundly impact recent and fossil specimen classification statistics (Table 2.1; Fig. 2.3B&D). Differences in digitizing personnel and/or imaging instruments used to obtain recent and fossil specimen data could accentuate those errors.

Data acquisition error is not only problematic for evaluating the number of specimens classified within a group, it can also lead to erroneous inferences of taxonomic occurrences at sites when PGM is performed on specimens of unknown taxonomic affinities. Such issues are most likely to arise when comparing morphologically similar groups and/or when PGM error of the training set is large. For example, it may be difficult to determine whether the fossil *M. longicaudus, M. montaus, M. oregoni*, and *M. townsendii* predicted as present by some LDA training sets in this study actually occur within Project 23, Deposit 1, at Rancho La Brea or whether the few individuals assigned to those species-groups are simply an artifact of PGM error (Appendix Table 2.9.1). Increasing sample sizes of training and unknown specimen groups, re-running analyses on multiple landmark iterations, and employing error-based occurrence and PGM probability vetting can help elucidate which group occurrences are likely real and which are likely attributable to non-biological error sources (e.g., Table 2.3). Even with those measures, however, the presence of some groups may be uncertain depending on analysis-specific intergroup similarity and PGM accuracy. For example, the few individuals assigned to *M. montanus, M. oregoni,* and *M. townsendii* must be viewed with skepticism since they fall within the range of cross-validated PGM error of all recent specimen training sets using my species likelihood criterion (Table 2.3). However, *M. longicaudus* is considered likely present in one or eight of the nine landmark datasets depending on which likelihood criterion is used (Table 2.3; Appendix Table 2.9.1). This is interesting since an isolated, high-elevation population of *M. longicaudus* is present in the San Bernardino mountains today (Patterson et al., 2003). Nevertheless, the occurrence of *M. longicaudus* in Deposit 1 at Rancho La Brea is uncertain until a larger fossil sample size is acquired.

2.5.3 Relationships among error proxies and data replicability

Results indicate that some landmark data acquisition sources contribute relatively large amounts of variation across error proxies (e.g., interobserver error quantified by Procrustes ANOVA and LDA) (Tables 2.1, 2.2; Fig. 2.2). Though, all error sources are significant and impact classification statistics of recent and fossil *Microtus* specimens to

some extent (Table 2.1; Fig. 2.3). The fact that source-specific measurement error is significant, alone, does not indicate that it will substantially impact downstream classification results. For example, Fruciano et al (2020) found significant differences in fish body shape attributed to different preservation treatments. However, the impact of preservation treatment on LDA fish-group classification was minimal. The authors attributed that discrepancy to differences in shape change direction between the fish groups of interest and preservation-based error (i.e., shape change due to preservation and biological shape change was not parallel in that system) (Fruciano et al., 2020).

In this study, extant *Microtus* PGM accuracy and consistency generally align with Procrustes ANOVA variation such that pairwise comparisons of datasets with lower R^2 values and higher repeatability values exhibit greater PGM agreement (Table 2.1; Fig. 2.4A). The trend suggests that measurement error in this system alters shape in a similar direction to biological shape variation among *Microtus* species. However, the trend does not hold for pairwise comparisons of fossils. Predicted group membership disagreement is substantial for most pairwise comparisons; though, no obvious relationship is observed between Procrustes ANOVA R^2/repeatability values and fossil PGM affinity differences (Table 2.1; Fig. 2.4B). The latter trend is possibly due to the additional data acquisition phases, and thus greater error potential, inherent of classifying unknowns as mentioned. One notable exception to the overall trend of recent and fossil specimen pairwise data is observed in presentation-based error. Procrustes ANOVA variation and repeatability among tilted versus non-tilted trials is moderate relative to the other three error sources (R^2 =20.1-20.4%, repeatability = 0.44-0.45) (Table 2.1; Fig. 2.2B). Major discrepancies occur, however, in PGM accuracy of recent specimens and PGM affinity of fossil specimens between tilted and non-tilted datasets (Table 2.1; Fig. 2.3B&D, Fig. 2.4). Conversely, pairwise intraobserver PGM differences, and to a lesser extent pairwise imaging device PGM differences, are much lower than pairwise presentation and interobserver PGM differences relative to their Procrustes ANOVA R^2 and repeatability values overall (Table 2.1; Fig. 2.4A). In other words, measurement error attributed to different devices and within-observers does not have as strong of an effect on classification results as measurement error between specimen presentations and among-observers. This suggests that the direction of biological shape variation among *Microtus* species is more dissimilar to the direction of artificial shape variation attributed to device and intraobserver differences than it is to presentation and interobserver differences.

While reduced pairwise PGM error discrepancies among devices and within observes may be caused by differences in biological and artificial shape change directionality, elevated pairwise PGM error among different specimen presentations relative to other error sources could be explained, in part, by the different proxies used to quantify error since pairwise Procrustes ANOVA comparisons quantify landmark precision and LDA PGMs quantify landmark accuracy. However, the inconsistency of presentation error quantified among those proxies is far greater than that of any other error source (Table 2.1; Fig. 2.4) so it is unlikely that this is entirely explained by the different proxies of error. Another possible explanation for the presentation error discrepancy observed in this study is image distortion-facilitated changes in specimen landmark configurations. Rotational changes among 3D specimens in “tilted” trials may

distort certain tooth loci captured in 2D images. Such distortions would then displace subsequent landmarks on those loci. Although orientation changes among landmark configurations are mitigated during GPA, the generalized least-squares algorithm that aligns the configurations to a common coordinate system does not adjust error based on individual point-variation. Rather, corrections are distributed randomly across the entire configuration to reduce residual variation of less precise landmarks and increases variation of more precise landmarks to minimize error overall (von Cramon-Taubadel et al., 2007). This "spreading" of landmark coordinate error during GPA, termed the "Pinocchio effect" (Chapman, 1990; von Cramon-Taubadel et al., 2007), may alter total specimen shape and thus biological variation among specimens captured via landmarks. The Pinocchio effect could be particularly detrimental for statistical grouping analyses because some shape variables are more relevant for group separation than others. For example, variables that are highly inconsistent within groups are not likely to be selected for LDA since variables that maximize among-group separation are preferentially selected (Kovarovic et al., 2011). Distributing the error of highly variable landmarks (e.g., those facilitated by presentation inconstancies) across all landmarks may reduce overall error quantified by analyses of variance, but also inhibit the discriminatory power of classification analyses since the most significant among group-separating variables may be altered by doing so. Indeed, stepwise LDA indicates that variables selected for discriminating *Microtus* species are dissimilar among tilted versus non-tilted trials (Appendix Table 2.9.2). It is perhaps relevant that differences between variables entered in stepwise LDA of tilted versus non-tilted trials often occur among landmarks positioned on tooth extremities (e.g., Landmarks 3, 13, and 21; Fig. 2.1; Appendix Table 2.9.2), which are closest to the image edges where distortion is generally greatest (Zelditch et al., 2004).

Overall, these results indicate that GM classification results of morphologically similar taxa are not always replicable due, in part, to multiple sources of data acquisition error. No two iterations among the nine resampled specimen datasets of this study exhibit the same intragroup classification results, and many datasets yield dissimilar predictions of fossil species occurrences (Table 2.3, Appendix Table 2.9.1). However, these findings may be different from those of other studies since the impact of measurement error on data replicability will likely vary based on analysis-specific objectives, inter- and intragroup similarity, and statistical classification accuracy (Robinson & Terhune, 2017). For example, small to moderate amounts of measurement error may be negligible for studies classifying organisms at the family level because among-group biological variation may surpass any artificial variation introduced to that system. Similarly, small amounts of measurement error and classification inaccuracy may be acceptable for quantifying interspecific occurrences, but not for quantifying intraspecific abundances within the same system. The amount of introduced error that surpasses an acceptable threshold will likely vary case-by-case depending on the respective analytical design, focal system, and questions/objectives of the study (Fruciano, 2016; Robinson & Terhune, 2017). Nevertheless, there are general measures that can be taken to mitigate error in any system.

2.5.4 Mitigating error and error impacts

It is impossible to eliminate GM error completely (Fruciano, 2016), but there are several ways to lessen the amount of error introduced. Presentation error, for example, has the most egregious impact on group classification replicability in this study. Although presentation error may have been exacerbated by intentional tilting of specimens in the "tilted" data acquisition trial, these findings indicate that it can impact landmark-based classification statistics considerably if not properly managed (Table 2.1; Figs. 2.3 & 2.4). Of further concern is the fact that this error source is less detectable through common error-quantifying methods (i.e., Procrustes ANOVA) than other data acquisition sources that introduce large amounts of error (e.g., interobservers) (Table 2.1; Fig. 2.2), possibly due to the Pinocchio effect of GPA. Presentation error can be mitigated by using 3D GM which bypasses error associated with dimensional loss (Buser et al., 2018; Cardini, 2014). Three-dimensional GM technology has improved greatly over the past two decades with respect to its data resolution and cost (Cardini, 2014). High-resolution 3D analyses that were previously restricted to larger specimens are becoming increasingly applicable to small objects (e.g., Cornette et al., 2013), such as the *Microtus* molars evaluated in this study. However, 2D GM will be more feasible for some projects since it is generally more affordable and can be conducted faster and with more versatile analytical equipment than 3D GM (Cardini, 2014). Researchers interested in conducting 2D GM analyses should therefore standardize specimen projection orientations as much as possible to mitigate presentation error.

For 2D and 3D GM analyses, I recommend that researchers avoid mixing observers due to the considerable amount of digitization error that can be generated among them (Tables 2.1 & 2.2; Figs. 2.2 & 2.4). After such precautions have been taken, determining the fidelity of statistical results, and/or whether the amount of error introduced is negligible, will be study-specific and dependent on inter-group data similarity and the overall accuracy of the analysis. These findings suggest that, in general, groups with low numbers of unknown individuals assigned to them should be considered with caution, especially when classification accuracy and/or among-group variation is relatively low (Tables 2.2 & 2.3; Fig. 2.3; Appendix Table 2.9.1). Including relatively large sample sizes, posterior probability thresholds, and multiple (intraobserver) digitizing iterations may help infer group occurrence fidelity.

In conclusion, GM measurement error from different landmark data acquisition sources has the potential to obscure biologically meaningful shape variation, facilitate statistical misclassification, and negatively impact data replicability. I do not discourage using GM for biological group classification since it is among the most powerful techniques available for quantifying shape and shape variability among groups. Rather, I hope this study provides an informative, if cautionary, example of why GM error should be mitigated to the greatest feasible extent. After precautions have been taken to reduce measurement error, repeated measurements and statistical evaluations can be employed to facilitate decisions of whether the amount of residual error is acceptable for study-specific research objectives.

2.6 References

Adams, D. C., Collyer, M. L., & Kaliontzopoulou, A. (2019). *Geomorph: Software for geometric morphometric analyses. R package version 3.1.0*. https://cran.r-project.org/package=geomorph

Arnqvist, G., & Mårtensson, T. (1998). Measurement error in geometric morphometrics: Empirical strategies to assess and reduce its impact on measures of shape. *Zoologica Academiae Scientiarum Hungaricae*, *44*(1–2), 73–96.

Barnosky, A. D. (1990). Evolution of Dental Traits Since Latest Pleistocene in Meadow Voles (*Microtus Pennsylvanicus*) from Virginia. *Paleobiology*, *16*(3), 370–383.

Bates, D., Mächler, M., Bolker, B., & Walker, S. (2015). Fitting Linear Mixed-Effects Models Using lme4. *Journal of Statistical Software*, *67*(1), 1–48. https://doi.org/10.18637/jss.v067.i01

Baumgartner, J. M., & Hoffman, S. M. G. (2019). Comparison of the responses of two Great Lakes lineages of *Peromyscus leucopus* to climate change. *Journal of Mammalogy*, *100*(2), 354–364. https://doi.org/10.1093/jmammal/gyz063

Bell, C. J., & Bever, G. S. (2006). Description and significance of the *Microtus* (Rodentia: Arvicolinae) from the type Irvington fauna, Alameda County, California. *Journal of Vertebrate Paleontology*, *26*(2), 371–380. https://doi.org/10.1671/0272-4634(2006)26[371:DASOTM]2.0.CO;2

Bell, C. J., & Repenning, C. A. (1999). Observations on dental variation in *Microtus* from the Cudahy Ash Pit Fauna, Meade County, Kansas and implications for Irvingtonian microtine rodent biochronology. *Journal of Vertebrate Paleontology*, *19*(4), 757–766. https://doi.org/10.1080/02724634.1999.10011188

Bignon, O., Baylac, M., Vigne, J.-D., & Eisenmann, V. (2005). Geometric morphometrics and the population diversity of Late Glacial horses in Western Europe (*Equus caballus arcelini*): Phylogeographic and anthropological implications. *Journal of Archaeological Science*, *32*(3), 375–391. https://doi.org/10.1016/j.jas.2004.02.016

Buser, T. J., Sidlauskas, B. L., & Summers, A. P. (2018). 2D or Not 2D? Testing the Utility of 2D Vs. 3D Landmark Data in Geometric Morphometrics of the Sculpin Subfamily Oligocottinae (Pisces; Cottoidea). *The Anatomical Record*, *301*(5), 806–818. https://doi.org/10.1002/ar.23752

Cardini, A. (2014). Missing the third dimension in geometric morphometrics: How to assess if 2D images really are a good proxy for 3D structures? *Hystrix, the Italian Journal of Mammalogy*, *25*(2), 73–81. https://doi.org/10.4404/hystrix-25.2-10993

Cassini, G. H. (2013). Skull Geometric Morphometrics and Paleoecology of Santacrucian (Late Early Miocene; Patagonia) Native Ungulates (Astrapotheria, Litopterna, and Notoungulata). *Ameghiniana*, *50*(2), 193–216. https://doi.org/10.5710/AMGH.7.04.2013.606

Chapman, R. E. (1990). Conventional procrustes approaches. In F. J. Rohlf & F. L. Bookstein (Eds.), *Proceedings of the Michigan Morphometrics Workshop* (pp. 251–267). University of Michigan Museum of Zoology.

Cornette, R., Baylac, M., Souter, T., & Herrel, A. (2013). Does shape co-variation between the skull and the mandible have functional consequences? A 3D approach for a 3D problem. *Journal of Anatomy*, *223*(4), 329–336. https://doi.org/10.1111/joa.12086

Curran, S. C. (2012). Expanding ecomorphological methods: Geometric morphometric analysis of Cervidae post-crania. *Journal of Archaeological Science*, *39*(4), 1172–1182. https://doi.org/10.1016/j.jas.2011.12.028

De Meulemeester, T., Michez, D., Aytekin, A. M., & Danforth, B. N. (2012). Taxonomic affinity of halictid bee fossils (Hymenoptera: Anthophila) based on geometric morphometrics analyses of wing shape. *Journal of Systematic Palaeontology*, *10*(4), 755–764. https://doi.org/10.1080/14772019.2011.628701

Dujardin, J.-P. A., Kaba, D., & Henry, A. B. (2010). The exchangeability of shape. *BMC Research Notes*, *3*(1), 266. https://doi.org/10.1186/1756-0500-3-266

Engelkes, K., Helfsgott, J., Hammel, J. U., Büsse, S., Kleinteich, T., Beerlink, A., Gorb, S. N., & Haas, A. (2019). Measurement error in lCT-based three-dimensional geometric morphometrics introduced by surface generation and landmark data acquisition. *Journal of Anatomy*, *235*(2), 357–378. https://doi.org/10.1111/joa.12999

Figueirido, B., Martín-Serra, A., Tseng, Z. J., & Janis, C. M. (2015). Habitat changes and changing predatory habits in North American fossil canids. *Nature Communications*, *6*(1), 7976. https://doi.org/10.1038/ncomms8976

Figueirido, B., Palmqvist, P., & Pérez-Claros, J. A. (2009). Ecomorphological correlates of craniodental variation in bears and paleobiological implications for extinct taxa: An approach based on geometric morphometrics. *Journal of Zoology*, *277*(1), 70–80. https://doi.org/10.1111/j.1469-7998.2008.00511.x

Fox, N. S., Takeuchi, G. T., Farrell, A. B., & Blois, J. L. (2019). A protocol for differentiating late Quaternary leporids in southern California with remarks on Project 23 lagomorphs at Rancho La Brea, Los Angeles, California, USA. *PaleoBios*, *36*, 1–20.

Fruciano, C. (2016). Measurement error in geometric morphometrics. *Development Genes and Evolution*, *226*(3), 139–158. https://doi.org/10.1007/s00427-016-0537-4

Fruciano, C., Celik, M. A., Butler, K., Dooley, T., Weisbecker, V., & Phillips, M. J. (2017). Sharing is caring? Measurement error and the issues arising from combining 3D morphometric datasets. *Ecology and Evolution*, *7*(17), 7034–7046. https://doi.org/10.1002/ece3.3256

Fruciano, C., Schmidt, D., Ramírez Sanchez, M. M., Morek, W., Avila Valle, Z., Talijančić, I., Pecoraro, C., & Schermann Legionnet, A. (2020). Tissue preservation can affect geometric morphometric analyses: A case study using fish body shape. *Zoological Journal of the Linnean Society*, *188*(1), 148–162. https://doi.org/10.1093/zoolinnean/zlz069

Fuller, B. T., Southon, J. R., Fahrni, S. M., Farrell, A. B., Takeuchi, G. T., Nehlich, O., Guiry, E. J., Richards, M. P., Lindsey, E. L., & Harris, J. M. (2020). Pleistocene paleoecology and feeding behavior of terrestrial vertebrates recorded in a pre-LGM asphaltic deposit at Rancho La Brea, California. *Palaeogeography, Palaeoclimatology, Palaeoecology*, *537*, 109383. https://doi.org/10.1016/j.palaeo.2019.109383

Gaubert, P., Taylor, P. J., Fernandes, C. A., Bruford, M. W., & Veron, G. (2005). Patterns of cryptic hybridization revealed using an integrative approach: A case study on genets (Carnivora, Viverridae, *Genetta* spp.) from the southern African subregion. *Biological Journal of the Linnean Society*, *86*(1), 11–33. https://doi.org/10.1111/j.1095-8312.2005.00518.x

Gómez Cano, A. R., Hernández Fernández, M., & Álvarez-Sierra, M. Á. (2013). Dietary Ecology of Murinae (Muridae, Rodentia): A Geometric Morphometric Approach. *PLoS ONE*, *8*(11), e79080. https://doi.org/10.1371/journal.pone.0079080

Gonzalez, P. N., Bernal, V., & Perez, S. I. (2011). Analysis of sexual dimorphism of craniofacial traits using geometric morphometric techniques. *International Journal of Osteoarchaeology*, *21*(1), 82–91. https://doi.org/10.1002/oa.1109

Jansky, K., Schubert, B. W., & Wallace, S. C. (2016). Geometric morphometrics of dentaries in *Myotis*: Species identification and its implications for conservation and the fossil record. *Northeastern Naturalist*, *23*(1), 184–194. https://doi.org/10.1656/045.023.0115

Kendall, D. G. (1977). The diffusion of shape. *Advances in Applied Probability*, *9*(03), 428–430. https://doi.org/10.2307/1426091

Kovarovic, K., Aiello, L. C., Cardini, A., & Lockwood, C. A. (2011). Discriminant function analyses in archaeology: Are classification rates too good to be true?

Journal of Archaeological Science, *38*(11), 3006–3018. https://doi.org/10.1016/j.jas.2011.06.028

Lawing, A. M., & Polly, P. D. (2010). Geometric morphometrics: Recent applications to the study of evolution and development. *Journal of Zoology*, *280*(1), 1–7. https://doi.org/10.1111/j.1469-7998.2009.00620.x

McGuire, J. L. (2011). Identifying California *Microtus* species using geometric morphometrics documents Quaternary geographic range contractions. *Journal of Mammalogy*, *92*(6), 1383–1394. https://doi.org/10.1644/10-MAMM-A-280.1

Meachen, J. A., Janowicz, A. C., Avery, J. E., & Sadleir, R. W. (2014). Ecological Changes in Coyotes (*Canis latrans*) in Response to the Ice Age Megafaunal Extinctions. *PLoS ONE*, *9*(12), e116041. https://doi.org/10.1371/journal.pone.0116041

Nicholson, E., & Harvati, K. (2006). Quantitative analysis of human mandibular shape using three-dimensional geometric morphometrics. *American Journal of Physical Anthropology*, *131*(3), 368–383. https://doi.org/10.1002/ajpa.20425

Osis, S. T., Hettinga, B. A., Macdonald, S. L., & Ferber, R. (2015). A novel method to evaluate error in anatomical marker placement using a modified generalized Procrustes analysis. *Computer Methods in Biomechanics and Biomedical Engineering*, *18*(10), 1108–1116. https://doi.org/10.1080/10255842.2013.873034

Patterson, B. D., Ceballos, G., Sechrest, W., Tognelli, M. F., Brooks, T., Luna, L., Ortega, P., Salazar, I., & Young, B. E. (2003). *Digital Distribution Maps of the Mammals of the Western Hemisphere. NatureServe version 1.0.*

Robinson, C., & Terhune, C. E. (2017). Error in geometric morphometric data collection: Combining data from multiple sources. *American Journal of Physical Anthropology*, *164*(1), 62–75. https://doi.org/10.1002/ajpa.23257

Rohlf, F. J. (2018a). *TpsDig version 2.31*. Ecology & Evolution: (program).

Rohlf, F. J. (2018b). *TpsUtil version 1.76*. Ecology & Evolution: (program).

Rohlf, F. J., & Slice, D. (1990). Extensions of the procrustes method for the optimal superimposition of landmarks. *Systematic Zoology*, *39*(1), 40–59. https://doi.org/10.2307/2992207

Ross, A. H., & Williams, S. (2008). Testing repeatability and error of coordinate landmark data acquired from crania. *Journal of Forensic Sciences*, *53*(4), 782–785. https://doi.org/10.1111/j.1556-4029.2008.00751.x

Schmieder, D. A., Benítez, H. A., Borissov, I. M., & Fruciano, C. (2015). Bat species comparisons based on external morphology: A test of traditional versus geometric morphometric approaches. *PLOS ONE*, *10*(5), e0127043. https://doi.org/10.1371/journal.pone.0127043

Smartt, R. A. (1977). The ecology of late Pleistocene and recent *Microtus* from south-central and southwestern New Mexico. *The Southwestern Naturalist*, *22*(1), 1–19. https://doi.org/10.2307/3670460

Venables, W. N., & Ripley, B. D. (2002). *Modern Applied Statistics with S, Fourth edition*. Springer. http://www.stats.ox.ac.uk/pub/MASS4

Vergara-Solana, F., García-Rodríguez, F., & De La Cruz-Agüero, J. (2014). Effect of preservation procedures on the body shape of the golden mojarra, *Diapterus aureolus* (Actinopterygii: Perciformes: Gerreidae), and its repercussions in a taxonomic study. *Acta Ichthyologica et Piscatoria*, *44*(1), 65–70. https://doi.org/10.3750/AIP2014.44.1.08

von Cramon-Taubadel, N., Frazier, B. C., & Lahr, M. M. (2007). The problem of assessing landmark error in geometric morphometrics: Theory, methods, and modifications. *American Journal of Physical Anthropology*, *134*(1), 24–35. https://doi.org/10.1002/ajpa.20616

Wallace, S. C. (2006). Differentiating *Microtus xanthognathus* and *Microtus pennsylvanicus* Lower First Molars Using Discriminant Analysis of Landmark Data. *Journal of Mammalogy*, *87*(6), 1261–1269.

Wallace, S. C. (2019). Enamel microstructure and morphometric discrimination of sympatric species of *Microtus* (Rodentia). *Quaternary International*, *530–531*, 69–79. https://doi.org/10.1016/j.quaint.2019.10.014

Webster, M., & Sheets, H. D. (2010). A practical introduction to landmark-based geometric morphometrics. *The Paleontological Society Papers*, *16*, 163–188.

Zelditch, M., Swiderski, D.L., Sheets, H. D., & Fink, W.L (Eds.). (2004). *Geometric morphometrics for biologists: A primer*. Elsevier Academic Press.

2.7 Tables

Table 2.1: Pairwise analysis of landmark datasets comparing Procrustes ANOVA residual R^2 percentages (ProcANOVA R^2 (%)) and repeatability among datasets, absolute differences among comparisons in cross-validated linear discriminant analysis predicted group membership error (PGM Error Change (%)), and differences among comparisons in the percent of predicted group membership changes among individual Project 23 fossils of unknown species affinity (Fossil PGM Change (%)). Datasets are paired according to the respective error sources they quantify. Analyzed levels (i.e., error sources) of each comparison is bolded and mean differences among datasets for each level is underlined. Dataset name segments indicate the following: **Dinolite** = images photographed with a Dino-Lite camera are included; **Nikon** = images photographed with a Nikon camera are included; **NoTilt** = specimens photographed from a standardized orientation are included; **Tilted** = specimens photographed from haphazardly tilted orientations are included; **EO** = landmark configurations digitized by the experienced observer are included; **NO** = landmark configurations digitized by the new observer are included; **T1** = landmark data from the first digitizing iteration of the respective image set and observer are included; **T2** = landmark data from the second digitizing iteration of the respective image set and observer are included.

Dataset Comparisons (trials)	**Error Source Quantified**	**Repeatability**	**ProcANOVA R^2 (%)**	**PGM Error Change (%)**	**Fossil PGM Change (%)**
Dinolite_NoTilt_EO_**T1**-Dinolite_NoTilt_EO_**T2**	Intraobserver	0.80	6.99	3.6	9.7
Dinolite_NoTilt_NO_**T1**-Dinolite_NoTilt_NO_**T2**	Intraobserver	0.61	13.74	3.7	22.6
Nikon_NoTilt_EO_**T1**-Nikon_NoTilt_EO_**T2**	Intraobserver	0.64	12.69	0.0	35.5
Nikon_NoTilt_NO_**T1**-Nikon_NoTilt_NO_**T2**	Intraobserver	0.61	13.70	3.3	22.6
<u>Mean among all intraobserver dataset comparisons</u>		<u>0.66</u>	<u>11.78</u>	<u>2.7</u>	<u>22.6</u>
Dinolite_NoTilt_**EO**_T1-Dinolite_NoTilt_**NO**_T1	Interobserver	0.21	31.01	20.6	32.3
Dinolite_NoTilt_**EO**_T2-Dinolite_NoTilt_**NO**_T2	Interobserver	0.19	32.24	20.7	16.1
Dinolite_NoTilt_**EO**_T1-Dinolite_NoTilt_**NO**_T2	Interobserver	0.18	32.66	24.3	25.8

Dinolite_NoTilt_**EO**_T2-Dinolite_NoTilt_**NO**_T1	Interobserver	0.21	31.32	19.8	32.3
Nikon_NoTilt_**EO**_T1-Nikon_NoTilt_**NO**_T1	Interobserver	0.58	14.84	7.3	32.3
Nikon_NoTilt_**EO**_T2-Nikon_NoTilt_**NO**_T2	Interobserver	0.25	28.87	10.6	32.3
Nikon_NoTilt_**EO**_T1-Nikon_NoTilt_**NO**_T2	Interobserver	0.42	21.31	10.6	29.0
Nikon_NoTilt_**EO**_T2-Nikon_NoTilt_**NO**_T1	Interobserver	0.39	22.78	7.3	35.5
Mean among all interobserver dataset comparisons		0.30	26.88	15.2	29.5
Dinolite_NoTilt_EO_T1-**Nikon**_NoTilt_EO_T1	Device	0.54	16.56	6.4	35.5
Dinolite_NoTilt_EO_T2-**Nikon**_NoTilt_EO_T2	Device	0.65	12.36	2.8	32.3
Dinolite_NoTilt_EO_T1-**Nikon**_NoTilt_EO_T2	Device	0.63	12.87	6.4	41.9
Dinolite_NoTilt_EO_T2-**Nikon**_NoTilt_EO_T1	Device	0.55	15.97	2.8	25.8
Dinolite_NoTilt_NO_T1-**Nikon**_NoTilt_NO_T1	Device	0.30	26.65	6.9	29.0
Dinolite_NoTilt_NO_T2-**Nikon**_NoTilt_NO_T2	Device	0.35	24.11	7.3	32.3
Dinolite_NoTilt_NO_T1-**Nikon**_NoTilt_NO_T2	Device	0.39	22.72	3.6	29.0
Dinolite_NoTilt_NO_T2-**Nikon**_NoTilt_NO_T1	Device	0.27	27.84	10.6	35.5
Mean among all imaging device dataset comparisons		0.46	19.89	5.9	32.7
Dinolite_**NoTilt**_EO_T1-Dinolite_**Tilted**_EO_T1	Presentation	0.44	20.36	20.6	45.2

Dinolite_**NoTilt**_EO_T2-Dinolite_**Tilted**_EO_T1	Presentation	0.45	20.08	17.0	41.9
Mean among all presentation dataset comparisons		0.45	20.22	18.8	43.6

Table 2.2: Nested Procrustes ANOVA summary statistics of variation attributed to biological factors (i.e., among species and individual specimens) and three data acquisition error sources: imaging device, interobserver digitization, and intraobserver digitization across eight landmark datasets. The "Dinolite_Tilted_EO_T1" dataset was not included since it did not fit into the nested analytical hierarchy (Appendix Fig. 2.9.1).

Error source	**Df**	**SS**	**R^2**	**Z**	***p* value**
Species	4	0.7619	0.07818	16.265	0.001
Individuals	247	5.1919	0.53276	28.423	0.001
Device	242	0.7302	0.07493	11.767	0.001
Interobservers	494	2.0661	0.21201	24.689	0.001
Intraobservers	988	0.9953	0.10213	29.826	0.001
Total	1975	9.7453			

Table 2.3: Cross-validated linear discriminant analysis (LDA) classification statistics of 31 fossil *Microtus* m1s from Project 23 at Rancho La Brea. Column values indicate the number of fossil specimens assigned to each extant species per landmark dataset. Specimens with predicted group membership probabilities <0.95 are not included. "Error (%)" indicates the percentage of recent *Microtus* specimens (n = 247) misclassified within the LDA training set. Underlined values mark a species' presence as "likely" according to the accuracy of its respective LDA training set. See main text and Table 1 for explanations of species likelihood calculations and dataset naming respectively.

Landmark Dataset	***M. californicus***	***M. longicaudus***	***M. montanus***	***M. oregoni***	***M. townsendii***	**Error (%)**
Dinolite_NoTilt_EO_T1	<u>20</u>	1	0	2	1	13.8
Dinolite_NoTilt_EO_T2	<u>14</u>	1	0	2	0	17.4
Nikon_NoTilt_EO_T1	6	3	0	1	0	20.2
Nikon_NoTilt_EO_T2	3	<u>8</u>	0	1	0	20.2
Nikon_NoTilt_NO_T1	10	1	0	1	0	27.5
Nikon_NoTilt_NO_T2	6	3	0	0	0	30.8
Dinolite_NoTilt_NO_T1	<u>12</u>	1	0	0	0	34.4
Dinolite_Tilted_EO_T1	3	1	0	0	0	34.4
Dinolite_NoTilt_NO_T2	<u>13</u>	0	0	0	0	38.1
Mean:	**9.7**	**2.1**	**0**	**0.8**	**0.1**	**26.3**
Range:	**3-20**	**0-8**	**0**	**0-2**	**0-1**	**13.8-38.1**

2.8 Figures

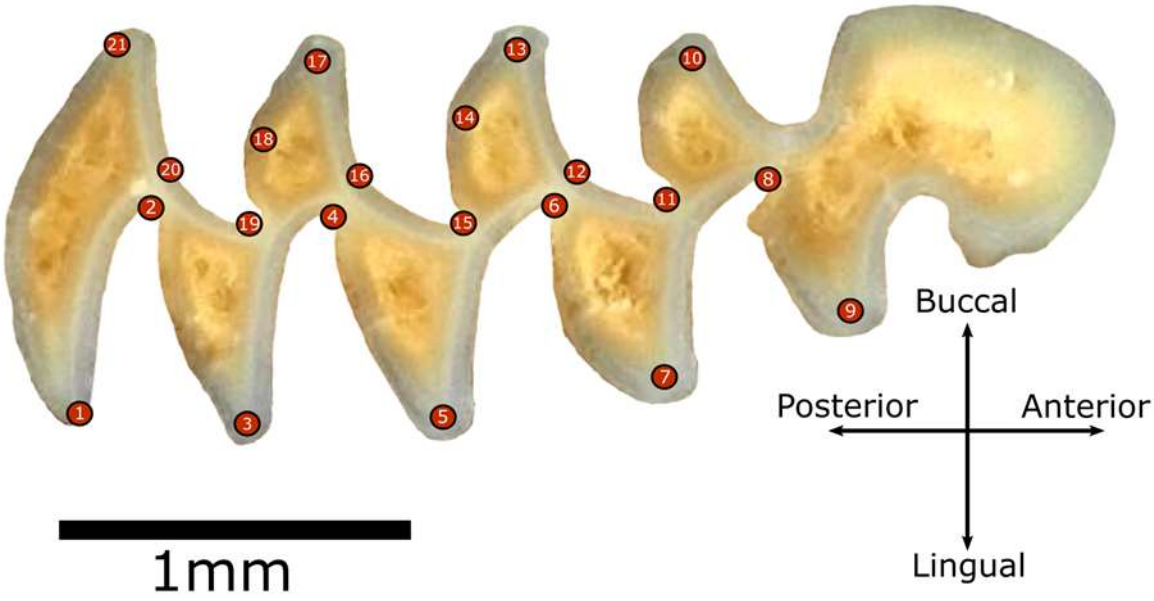

Figure 2.1: Lower left first molar occlusal surface of MVZ-132727 *Microtus californicus* illustrating the 21-landmark configuration used to quantify shape variation among extant and fossil *Microtus* species. See (Wallace, 2006) for landmark definitions.

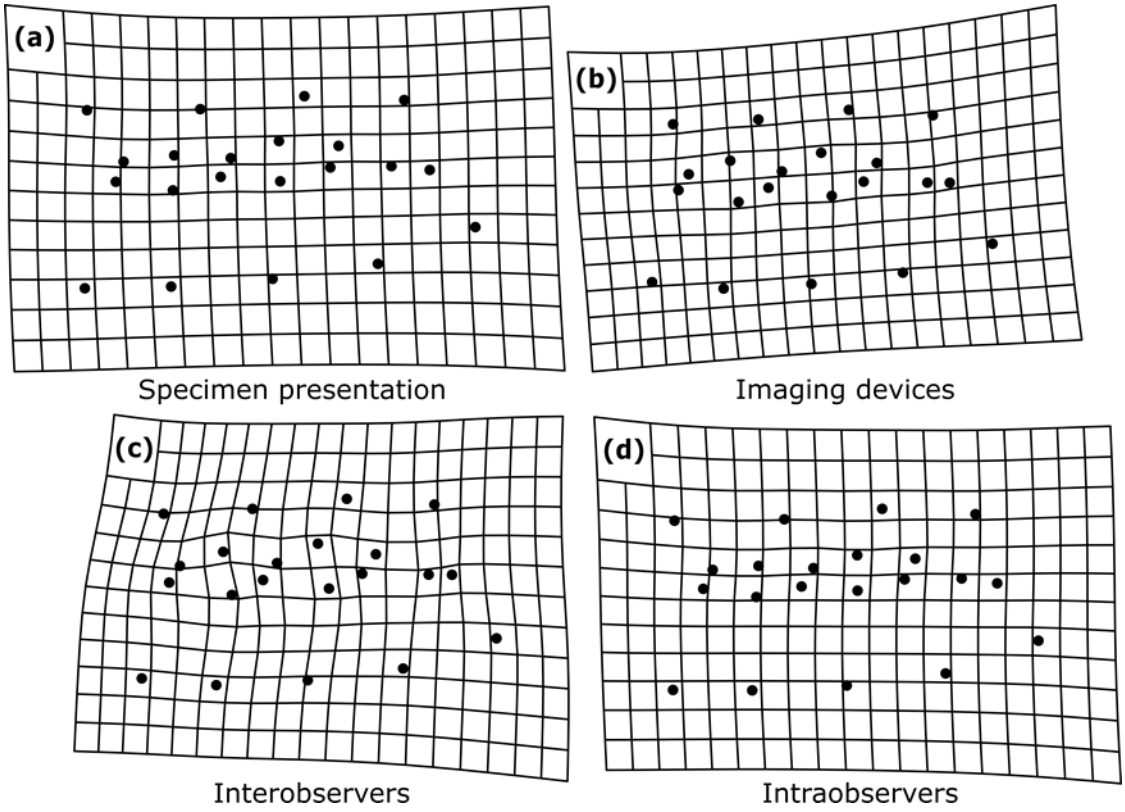

Figure 2.2: Thin-plate spline deformation grids illustrating mean shape changes between reference dataset and target dataset landmark configurations of *Microtus* lower first molars. A) Specimen presentation impacts on overall landmark coordinate shape between datasets "Dinolite_Notilt_EO_T1" and "Dinolite_Tilt_EO_T1". B) Imaging device impacts on overall landmark coordinate shape between datasets "Nikon_NoTilt_NO_T2" and "Dinolite_NoTilt_NO_T2". C) Interobserver impacts on overall landmark coordinate shape between datasets "Dinolite_NoTilt_EO_T2" and "Dinolite_NoTilt_NO_T2". D) Intraobserver impacts on overall landmark coordinate shape between datasets "Dinolite_NoTilt_EO_T1" and "Dinolite_NoTilt_EO_T2". See Table 2.1 for dataset name explanations.

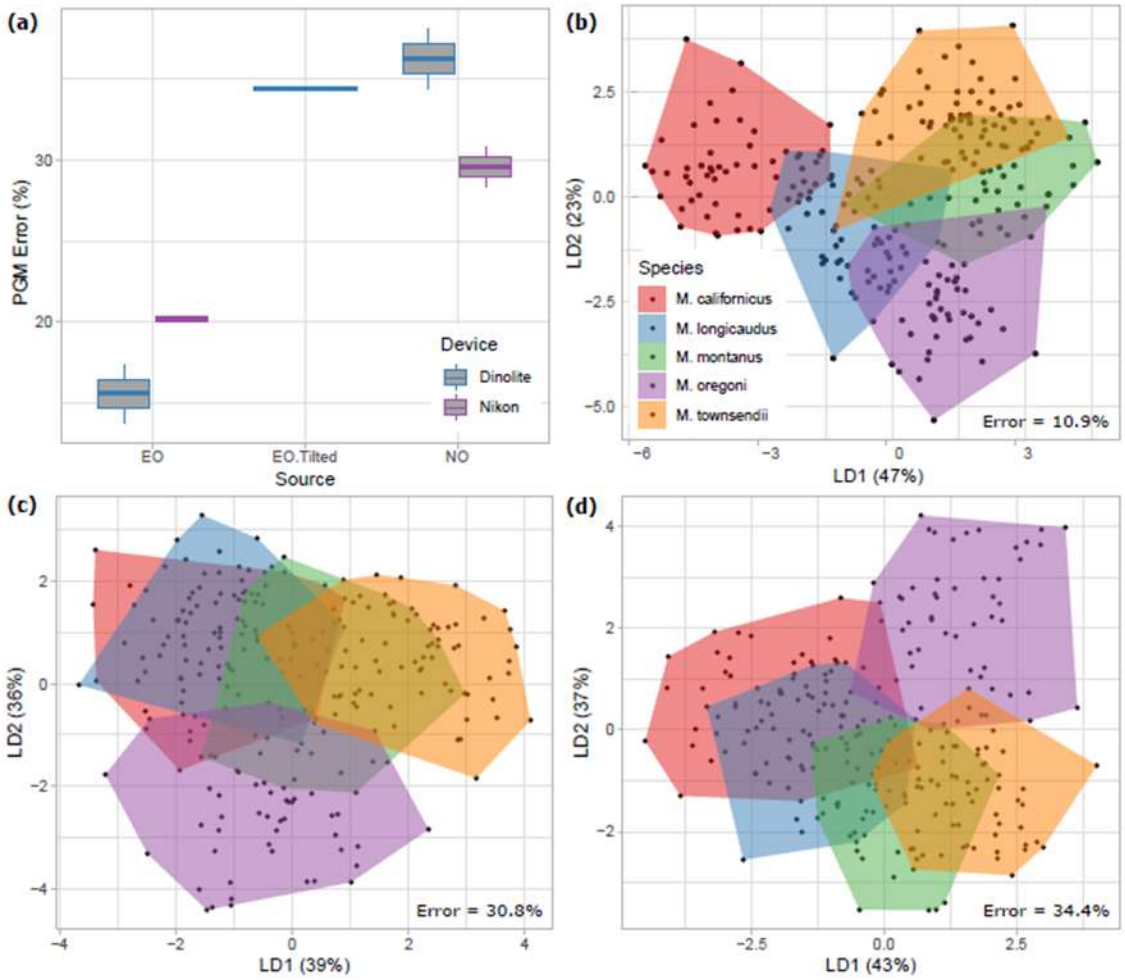

Figure 2.3: A) Boxplot of linear discriminant analysis predicted group membership error percentages using leave-one-out cross-validation across all extant *Microtus* species for each dataset in this study (n=9) grouped by observer, imaging device, and specimen orientation. See Table 3 for error values generated from individual datasets. B-D) Plot of linear discriminant functions one (LD1) and two (LD2) from a subset of the nine landmark datasets: B) EO intraobserver mean of coordinates "Dinolite_NoTilt_EO_T1" and "Dinolite_NoTilt_EO_T2", C) NO intraobserver mean of coordinates "Dinolite_NoTilt_NO_T1" and "Dinolite_NoTilt_NO_T2" D) "Tilted" specimen presentations "Dinolite_Tilt_EO_T1". All 247 recent *Microtus* individuals are grouped according to species affinity: "Mc" = *Microtus californicus*, "Ml" = M. *longicaudus*, "Mm" = *M. montanus*, "Mo" = *M. oregoni*, "Mt" = *M. townsendii*. "Error" = the percentage of cross-validated predicted group membership error across all species.

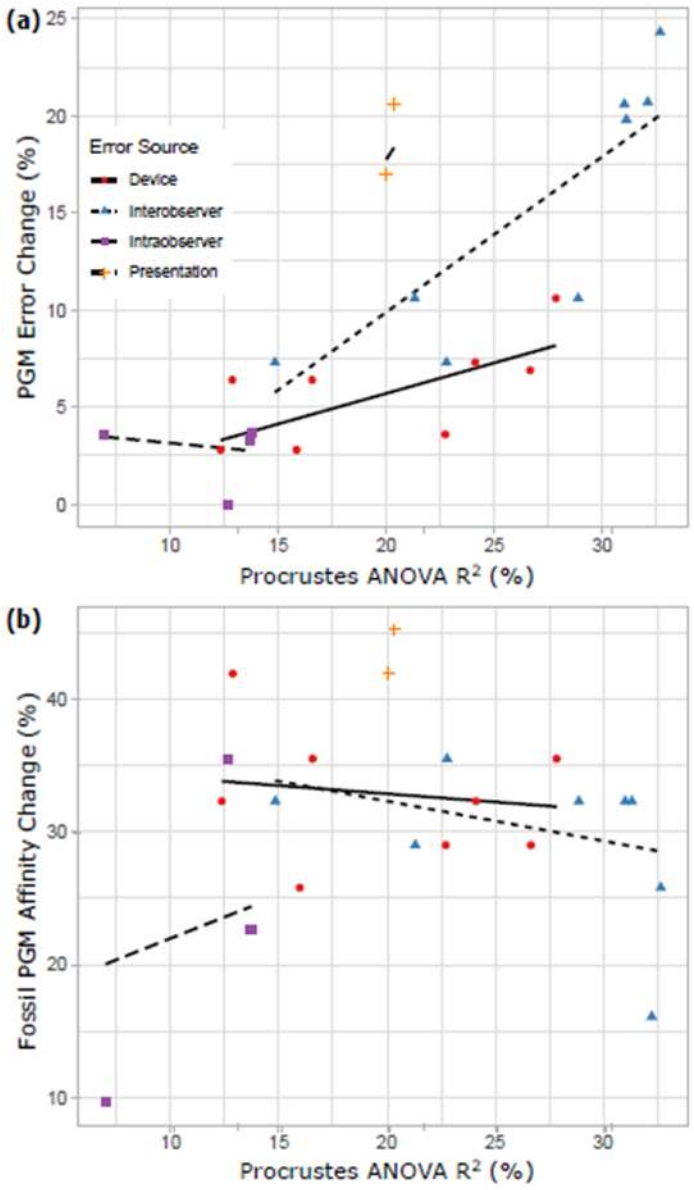

Figure 2.4: A) Linear mixed model of pairwise Procrustes ANOVA residual R^2 (error) percentages and pairwise differences in linear discriminant analysis (LDA) predicted group membership (PGM) absolute error percentages of extant *Microtus* species. B) Plot of Procrustes ANOVA residual R^2 percentages and percentages of LDA PGM affinity differences of fossil *Microtus* from Rancho La Brea, Project 23, Deposit 1 using the same pairwise dataset comparisons as A). Points are colored according to error source and all pairwise dataset comparisons are listed in Table 2.1. Models were run using the lmer function in the R package "lme4" (Bates et al., 2015).

2.9 Appendix

Table 2.9.1: Linear discriminant analysis (LDA) classification statistics of 31 fossil *Microtus* m1s from Project 23 at Rancho La Brea using the same landmark datasets reported in Table 3 without leave-one out cross-valuation or posterior probability vetting. Column values indicate the number of fossil specimens assigned to each extant species per landmark dataset. Underlined values mark a species' presence as "likely" according to the accuracy of its respective LDA training set. See main text and Table 2.1 for explanations of species likelihood calculations and dataset naming respectively.

Landmark Dataset	***M. califonicus***	***M. longicaudus***	***M. montanus***	***M. oregoni***	***M. townsendii***	**Error (%)**
Dinolite_NoTilt_EO_T1	25	3	0	2	1	2.8
Dinolite_NoTilt_EO_T2	24	5	0	2	0	5.7
Nikon_NoTilt_EO_T1	16	9	3	3	0	9.3
Nikon_NoTilt_EO_T2	16	14	0	1	0	9.3
Nikon_NoTilt_NO_T1	22	5	0	3	1	12.2
Nikon_NoTilt_NO_T2	19	9	0	2	1	15.0
Dinolite_NoTilt_NO_T1	20	7	0	4	0	18.6
Dinolite_Tilted_EO_T1	17	11	1	2	0	14.6
Dinolite_NoTilt_NO_T2	25	5	0	1	0	20.6
Mean:	**20.4**	**7.6**	**0.4**	**2.2**	**0.3**	**12.0**
Range:	**16-25**	**3-14**	**0-3**	**1-4**	**0-1**	**2.8-20.6**

Table 2.9.2: Comparison of landmarks entered in stepwise discriminant analysis of the five extant *Microtus* species between digitizing iterations of the experienced observer using standardized Dino-Lite presentation images (Dinolite_NoTilt_EO_T1 and Dinolite_NoTilt_EO_T2) and haphazardly tilted Dino-Lite presentation images (Dinolite_Tilted_EO_T1). Landmarks are labeled as "included" if their x coordinate variable, y coordinate variable, or both were entered in the analysis. See Table 2.1 for dataset name explanations.

Landmark	**Dinolite_NoTilt_EO_T1**	**Dinolite_NoTilt_EO_T2**	**Dinolite_Tilted_EO_T1**
LM1	Included	-	-
LM2	Included	Included	Included
LM3	-	-	Included
LM4	-	Included	Included
LM5	Included	-	-
LM6	-	Included	Included
LM7	Included	Included	Included
LM8	Included	Included	Included
LM9	-	Included	Included
LM10	-	Included	Included
LM11	Included	-	Included
LM12	Included	-	-
LM13	Included	Included	-
LM14	Included	Included	-
LM15	-	Included	-
LM16	-	-	Included
LM17	Included	Included	Included
LM18	Included	Included	-
LM19	Included	Included	Included
LM20	Included	Included	Included
LM21	Included	Included	-

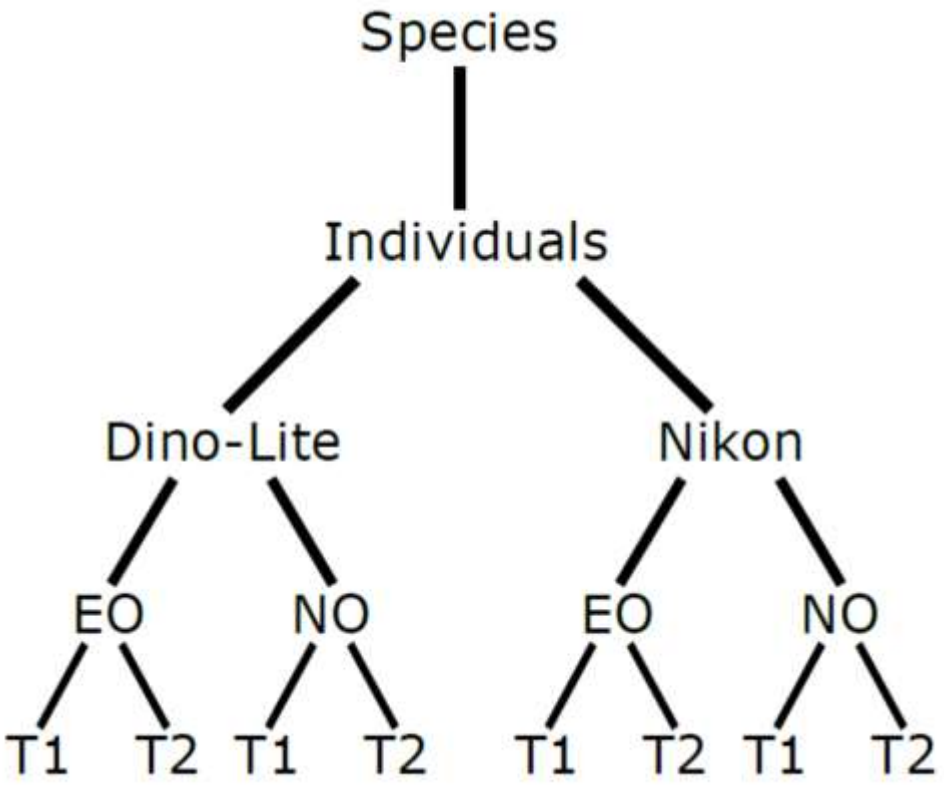

Figure 2.9.1. Hierarchical structure for the nested Procrustes ANOVA with results depicted in Table 2.2.

Chapter 3: Midden or molar? A geometric morphometric approach for identifying woodrat remains (genus *Neotoma*) and evaluating their ecology

3.1 Abstract

Woodrats of the genus *Neotoma* are good paleoecological indicators because their middens preserve materials from the surrounding environment and are well represented in Quaternary fossil assemblages. Moreover, intergenerational body size of several extant species fluctuates in response to changes in ambient temperature and precipitation, tracking climate across space and time. Woodrats are thus an important system for ecological and paleoecological research; however, such studies are hindered by the difficulty of identifying woodrat remains to species. Identifications are often inferred based on skeletal element size, fecal pellet size, and contemporary species distributions rather than diagnostic morphological features. To address this limitation, I use 2D geometric morphometrics to differentiate the lower first molar (m1) of five extant western North American woodrat species (*N. albigula*, *N. cinerea*, *N. fuscipes*, *N. lepida*, and *N. macrotis*) collected throughout California and apply the new protocol to identify fossils from the Rancho La Brea Tar Pits in Los Angeles, CA. I then use m1 centroid size as a proxy for body size and evaluate its sensitivity to 10 temperature and precipitation variables. Cross-validated linear discriminant analysis (LDA) of landmark data correctly classifies ~84% of 199 recent individuals by species and most misclassifications occur between sister taxa *N. fuscipes* and *N. macrotis*. As with body and fecal pellet size, m1 size of most species tracks climate; though, patterns are species and variable specific. For example, *N. cinerea* exhibits a negative size relationship with January temperature while *N. macrotis* exhibits a positive size relationship with the same variable. When applied to fossil specimens from Rancho La Brea, landmark based LDA classifies most unknowns as *N. macrotis*. Overall, geometric morphometric analyses are effective at quantitatively differentiating m1s of closely related *Neotoma* species and for tracking their size-climate responses through space and potentially time.

3.2 Introduction

Understanding how terrestrial organisms respond to environmental change is essential for predicting and mitigating global warming effects. However, organismal responses can be individualistic, gradual, and may lag behind environmental baseline shifts (Blois & Hadly, 2009; Svenning & Sandel, 2013). For these reasons, estimating relationships between organismal ecology and environmental change from contemporary data alone can be challenging – depending on the species and the nature of the forcing, changes may be difficult to detect with only ~100 years of observational data. The fossil record can help overcome those observational limitations by extending the timescales at which environments and associated biotic changes can be observed; though, some taxa better track paleoecological patterns and processes than others.

Small mammals (e.g., rodents, lagomorphs, and soricomorphs) are good (paleo)ecological indicators because they often occupy small home ranges and specific

habitats and are therefore sensitive to local disturbances (Cuenca-Bescós et al., 2009; Grayson, 2006; Samuels & Hopkins, 2017; Smartt, 1977; Somerville et al., 2018). Responses to environmental changes can vary across taxa, space, and time. For example, some small mammals exhibit long-term changes in range distributions and community composition (Graham et al., 1996) while others exhibit changes taxonomic diversity (Blois et al., 2010) and functional traits (Samuels & Hopkins, 2017) including body size (Smith et al., 1995). One particularly useful group of small mammals for reconstructing past environments and tracking long-term changes therein via behavioral and size-based traits are woodrats of the genus *Neotoma*.

Woodrats are a group of medium-sized North American rodents with broad geographic and habitat distributions extending from southern Mexico to northern Canada (Cordero & Epps, 2012; Coyner et al., 2015; Soberón & Martínez-Gordillo, 2012). Species within this genus construct complex multichambered dens (middens) using local vegetation and animal remains consolidated with crystalized urine (Smith et al., 1995, 2009; Smith & Betancourt, 2006). Members of *Neotoma* are considered keystone species because their middens create nutrient-rich microhabitats that help maintain local biodiversity (Matocq, 2009; Whitford & Steinberger, 2010). In addition, these species are important indicators of paleoecosystem function. Woodrat middens, and the plant and animal remains within, often fossilize in arid regions and preserve aspects of local biotic communities over millennia (Cordero & Epps, 2012; Smith et al., 1995). Woodrats also have been used as a "paleothermometer" for tracking long-term climate change because the intergenerational body size of some species is highly sensitive to changes in ambient temperature (Smith & Betancourt, 1998, 2003). For these reasons, woodrats are a coveted system for studies of environmental change and adaptive responses to environmental change across space and time (Brooke McEachern et al., 2006; Cordero & Epps, 2012; Lyman & O'Brien, 2005; Smith et al., 1995, 2009; Smith & Betancourt, 2006).

Since different species of woodrat exhibit different habitat and climatic tolerances (Lyman & O'Brien, 2005; Smith et al., 2009; Soberón & Martínez-Gordillo, 2012), species-level identification of their remains is critical for ecological and paleoecological research. Studies of fossil woodrat ecology has largely focused on paleomidden analysis (Mychajliw et al., 2020; Smith et al., 1995, 2009; Smith & Betancourt, 2003). However, midden preservation tends to be biased both spatially and temporally, which limits the geographic scope of such studies. Geologically younger middens are generally more abundant than older middens and are most often preserved in arid environments (Smith et al., 2009; Smith & Betancourt, 2006). Consequently, most paleoecological work on woodrats has focused on low elevation areas of western interior North America (Jackson et al., 2005; Smith et al., 2009; Smith & Betancourt, 1998, 2003), while comparatively little is known about the paleoecology of woodrats in coastal, eastern, and northern regions of North America (but see Mychajliw et al., 2020).

Despite the spatiotemporal bias of paleomidden preservation, other type of woodrat remains such as teeth and bones preserve across a broader spatial and temporal range and in other depositional environments (Betancourt et al., 1990; Zakrzewski, 1993). Unfortunately, specific identification of those materials is difficult (Betancourt et al., 1990; Harris, 1984). Most species-level identifications of woodrat teeth, bones, and fecal pellets are size-based and thus only relevant when observing species near the size

minima and maxima of the genus where little or no size overlap occurs (e.g., *N. albigula* and *N. cinerea* (Lyman & O'Brien, 2005); *N. lepida* and *N. cinerea* (Smith et al., 2009)). Even when such methods are applicable, they can limit paleoecological observations of size change across space and time (Lyman & O'Brien, 2005). Still, shape-based identification of woodrat teeth and bones has been attempted. For example, Zakrzewski (1993) described morphological characters of extant and fossil woodrat dentition and inferred general biostratigraphic, phylogenetic, and evolutionary patterns based on those characters. It was acknowledged, however, that specific relationships among fossil taxa could not be inferred in part because some features (e.g., spatial relationships between different tooth reentrant folds) are difficult to quantify via direct observation (Zakrzewski, 1993). Harris (1984) attempted to discriminate eight extant woodrat species to facilitate fossil woodrat identification using a combination of linear measurements and qualitative characters of the lower first molar. It was shown that most specimens can be correctly sorted into their respective species groups, but only when split into species-pairs for statistical analysis (Harris, 1984). Pairwise species comparisons were constructed using several qualitative dental characters and analyzed after statistical corrections were implemented to account for tooth wear differences (Harris, 1984). While informative, those criteria may be difficult to replicate for other *Neotoma* study systems.

More recently, geometric morphometric analyses have been employed to quantify shape and shape change among objects. This technique has made differentiating some closely related and morphologically similar small mammal species more feasible (e.g., Jansky et al., 2016; Wallace, 2006, but see Fox et al. 2020) and has facilitated studies of phenotypic change across space (Cordero & Epps, 2012; McGuire, 2010) and time (Meachen et al., 2014). Geometric morphometric analyses are less subjective than qualitative character observations and offer several advantages over traditional linear morphometrics, including the ability to partition object shape from size and to capture spatial distributions of shape change (Zelditch et al., 2004). This technique allows entire shape configurations to be visualized and analyzed collectively; therefore, it is therefore appropriate for quantifying complex morphological conditions such as the relationships between woodrat tooth lophs and folds. Geometric morphometric analyses have been applied to woodrat anatomical features (Cordero & Epps, 2012; Soberón & Martínez-Gordillo, 2012), but these analyses usually focus on the cranium which is seldom preserved in paleontological assemblages and therefore has limited utility for analyzing fossil specimens.

To facilitate shape and size comparison of extant and fossil woodrats, I developed a landmark protocol using individual teeth that are frequently preserved in fossil assemblages (Betancourt et al., 1990). Specifically, I quantified shape and shape change in the lower dentition of five extant western North American species, in part, to facilitate species-level differentiation and identification. I then applied the landmark protocol to identify fossil woodrat teeth from a near-coastal late Pleistocene locality in southern California and track intraspecific changes across climate gradients, space, and time. To evaluate inter and intraspecific morphological variation in woodrat dentition, I addressed the following questions:

1) Can the lower dentition of five closely related *Neotoma* species be differentiated using geometric morphometrics?

2) Does lower first molar (m1) centroid size track intraspecific responses to climate across space and time?

3.3 Methods

3.3.1 Study system

I examine all five western North American woodrat species that currently occur in California: *Neotoma albigula* (white-throated woodrat), *N. cinerea* (bushy-tailed woodrat), *N. fuscipes* (dusky-footed woodrat), *N. lepida* (desert woodrat) and *N. macrotis* (big-eared woodrat). Collectively, these five species occupy broad geographic distributions and habitats ranging from boreal forest to desert (Smith et al., 2009). I sampled 39 individuals of *N. cinerea* and 40 individuals of the other four species (n=199) collected throughout the state of California between 1904 and 2015 (Fig. 3.1; Appendix Table 3.9.1) from the University of California Museum of Vertebrate Zoology (MVZ) and analyzed the morphology of their m1s because the first lower cheek tooth tends to vary most among closely related small mammal species (Dalquest et al., 1989; Dalquest & Stangl Jr., 1983; Harris, 1984; Thaeler, 1980; Wallace, 2006). In addition, *Neotoma* first molars are among the most common elements found in fossil assemblages because they are larger and more robust than other cheek teeth (Harris, 1984). Lower first molars are therefore ideal for analyzing shape and shape change in extant and prehistoric specimens.

Fourteen fossilized left and right m1s were also sampled from four Project 23 (P23) Deposits (1, 7B, 13 and 14) at the Rancho La Brea Tar Pits in Los Angeles, CA (Fig. 3.1; Appendix Table 3.9.1), which range from >50,000 to ~27,000 radiocarbon years before present in age (Fox et al., 2019; Fuller et al., 2020). *Neotoma* fossils are uncommon at RLB (Dice, 1925) so this m1 sample exhausts what is currently available from those deposits. Due to their geographic and temporal position, it is unlikely that the Rancho La Brea fossils belong to a woodrat species other than the five extant species examined in this study, so comparison of fossil molars with recent specimens from California is appropriate. By doing this, however, I assume that: 1) geographic ranges of woodrats have not shifted drastically over the last 50,000 years such that species currently residing hundreds of miles from Los Angeles (e.g., *N. mexicana*) were present there in the past; and 2) that intraspecific tooth morphology has not changed substantially in that time.

3.3.2 Geometric morphometric analysis

Recent and fossil woodrat dentaries were photographed using a Dino-Lite Edge AM4815ZTL Digital Microscope. To mitigate specimen presentation and imaging error (see Arnqvist and Mårtensson, 1998; Fox et al., 2020; Fruciano, 2016), the orientation of the occlusal surface of each specimen and distance from the camera lens was standardized to the extent possible. No sampling filters (e.g., by age, sex, or tooth wear stage) were implemented aside from omitting very juvenile specimens with unerupted or partially erupted dentition. Recent and fossil specimen image sets were assembled in

TpsUtil 32 (Rohlf, 2018a) and digitized in TpsDig 2.32 (Rohlf, 2018a). Images of fossil left m1s were flipped to imitate right dentition prior to landmark digitization.

Fourteen landmarks were analyzed along the occlusal periphery of the right m1 of each specimen (see Table 3.1 & Fig. 3.2 for landmark definitions and placement respectively). Landmarks can be grouped into three general types: 1, 2, and 3. Type 1 landmarks were defined by the intersection of three or more structures (e.g., cranial sutures), type 2 landmarks were defied by maxima/minima of curvatures (e.g., the tip of a canine tooth), and type 3 landmarks were extremal points (e.g., the anterior-most point of a jaw; Bookstein, 1997). Type 1 landmarks are most desirable because their positions are highly localized. Type 3 landmarks are least desirable because their positions are the least localized, most subjective, and most prone to error of the three types (Bookstein, 1997; Zelditch et al., 2004). Type 1 and 2 landmarks were mainly used; however, some type 3 landmarks are included due to the somewhat simplistic morphology of the woodrat tooth periphery (Fig. 3.2). Some landmarks also vary in type among specimens (i.e., landmarks 1, 4, and 14) depending on wear stage and species (Fig. 3.2). In such cases, different definitions are used depending on which condition occurs (Table 3.1). Each specimen was digitized twice with several weeks between sessions to quantify intraobserver error and evaluate the replicability of this landmark configuration for species classification. Error was quantified among datasets using the procD.lm function in the R package "geomorph" (Adams et al., 2019). All landmark datasets were superimposed via Generalized Procrustes analysis (GPA) in geomorph. Generalized Procrustes analysis translates all specimens to unit centroid size and optimally rotates them along a common coordinate system using a generalized least-squares algorithm to standardize specimen rotation, orientation, and scale (Adams et al., 2019; Rohlf & Slice, 1990).

3.3.3 Species classification

Linear discriminant analyses (LDA) were conducted on GPA-transformed datasets using the lda function in the R package "MASS" (Venables & Ripley, 2002) to differentiate extant species and predict the species affinity of unknown (fossil) specimens. Twenty-eight x and y landmark coordinate variables and centroid size, the square root of the sum of squared distances from the centroid of each landmark configuration, were entered as predictor variables for species-group classification. Leave-one-out cross-validation was implemented to determine the percentage of recent specimens correctly classified within their species-groups since it mitigates standard LDA overfitting (Kovarovic et al., 2011). Prior probabilities of group membership were calculated based on the proportion of group samples that are approximately equal due to similar sample sizes among species. Linear discriminant analysis predicted group membership (PGM) error percentages were calculated by dividing the number of misclassified individuals across all five species by the total number of individuals (n=199) multiplied by 100%. Landmark data of fossil specimens were appended to each extant *Neotoma* dataset, entered in LDA analyses as unknowns, and classified using the five extant woodrat species as grouping variables. Predicted species-group membership and posterior probability of group membership was evaluated for each fossil specimen in each dataset to determine specimen-specific PGM fidelity. Discriminant analysis of

principle components (DAPC) was performed in the R package "adegenet" to visualize morphological positions of fossils relative to the five extant species (Jombart, 2008). The optimal number of principal components to include in DAPC was determined via *a*-score optimization using the optim.a.score function in adegenet. The *a*-score is a measure of tradeoff between discriminatory power and overfitting based on the number of principle components included in the analysis. Too few principle components will not adequately capture intergroup variation and lead to poor group separation. Conversely, too many principle components will cause overfitting to occur and the model will lose predictive power for sorting unknowns (Jombart & Collins, 2015).

3.3.4 Tooth size and climate

In addition to identifying morphological changes among species, I determine whether intraspecific woodrat m1 size tracks geographic climate gradients across space, similar to the temperature tracking through time found for woodrat fecal pellet size (e.g., Smith et al., 1995). Lower first molar size closely approximates relative size differences among individuals because m1s are highly correlated with body size in cricetid rodents (Damuth & MacFadden, 1990). To evaluate size sensitivity to climate, I extracted 10 climate variables at the geographic coordinates where each extant woodrat specimen was collected: mean January temperature, minimum January temperature, mean July temperature, maximum July temperature, mean January precipitation, mean July precipitation, temperature seasonality, precipitation seasonality, and annual precipitation. The first six variables were obtained from monthly climate averages between 1970 and 2000 from WorldClim Version 2.1 at 30 second (~1 km^2) grid resolution (Fick & Hijmans, 2017). Annual mean temperature, temperature seasonality, precipitation seasonality, and annual precipitation was obtained from BioClim variables 1, 4, 15, and 12 respectively at 30 second grid resolution, from WorldClim Version 2. I then fitted linear models to associate the climate data with the corresponding m1 centroid size. *Neotoma albigula* was excluded from this analysis due to its very limited range in southeastern California (Macedo and Mares, 1988) (Fig. 4.2).

3.3.4 Fossil and contemporary comparisons

Welch two-sample t-tests were performed to evaluate potential size differences between recent and fossil *Neotoma* specimens in R (version 3.6.1) (R Core Team, 2019).

3.4 Results

Procrustes ANOVA comparison of two digitizing iterations of the same dataset indicate that intraobserver error is relatively low (i.e., ~3.2% of the total variation, see Table 3.2 residual R^2 values). Linear discriminant analysis correctly classifies 84.9% and 83.4% of specimens within their respective species group using leave-one-out cross-validation in digitizing iterations one and two, respectively (Table 3.3). Most fossil specimens of unknown species affinity from P23 are classified as *Neotoma macrotis* (Table 3.4), and DAPC shows most clustering within or near the morphospace of extant *N. macrotis* (Fig. 3.3). Some specimens are classified as *N. albigula* or *N. fuscipes*, but

those counts are low, inconsistent among data replicates, and often have relatively low posterior probability support (Table 3.4).

Linear models of m1 centroid size and monthly climate variables show statistically significant relationships in most extant *Neotoma* species throughout California (Fig. 3.4; Table 5). However, the variables of significance, and strength and direction of size-climate trends, are dissimilar among species (Table 3.5; Fig. 3.4). For example, *N. cinerea* m1 size exhibits significant relationships with several temperature and precipitation variables while *N. lepida* m1s do not change significantly in size with any climate variable (Table 3.5; Fig. 3.4). Excluding seasonality, *N. fuscipes* exhibits significant size relationships with variables of precipitation but not temperature and *N. macrotis* exhibits a significant relationship with temperature but not precipitation (Table 3.5; Fig. 3.4). No significant size differences are observed between extant *N. macrotis* from southern California (Appendix Table 3.9.1) and P23 fossil individuals (Fig. 3.5).

3.5 Discussion

3.5.1 Biological and non-biological variation

Procrustes ANOVA indicates that m1 morphological differences among *Neotoma* species explains ~29% of the total variation among datasets and is substantially lower than variation among individuals (~68%; Table 3.2). A similar pattern of less biological variation among species than among individuals is observed in the m1 of other closely related cricetid rodent species (Fox et al., 2020), suggesting that interspecific variation is low relative to intraspecific variation among members of this group overall. These findings are expected given the challenges of identifying many members of the diverse Family Cricetidae to species based on tooth morphology (Dalquest & Stangl Jr., 1983; Harris, 1984; Wallace, 2006). Variation among digitizing iterations (i.e., intraobserver error) is relatively low and explains only ~3% of the total variation among datasets (Table 3.2). However, recent studies show that even small amounts of artificial error can substantially impact downstream statistics and statistical replicability when intergroup variation is low (Fox et al., 2020; Robinson and Terhune, 2017; but see Fruciano et al., 2020).

3.5.2 Classification results

Linear discriminant analysis of the 28 m1 landmark variables and centroid size was conducted to determine if the five extant woodrat species can be differentiated by tooth morphology and whether the landmarks are useful for identifying fossils of unknown species affinity. Linear discriminant was performed on both data replicates to evaluate statistical sensitivity due to high within-to-among group variation and inherent digitization error (Table 3.2). Results correctly predicted species affinities of 83.4-84.9% of the 199 recent specimens using leave-on-out cross validation (Table 3.3).

Predicted group memberships of unknowns are consistent among iterations in ten of fourteen fossil individuals (71%, Table 3.4) despite some intraobserver error (Table 3.2) and extant group misclassification (Table 3.3) among datasets. Most PGM inconsistencies occur between *Neotoma fuscipes* and *N. macrotis* (Tables 3.3 & 3.4). This is unsurprising because *N. macrotis* was considered a subspecies of *N. fuscipes* until its recent elevation to species following morphological and molecular-based phylogenetic work (Matocq, 2002). Indeed, DAPC plots of landmark data show considerably more morphological overlap between *N. fuscipes* and *N. macrotis* than any other two species (Fig. 3.3). Most fossil specimens from RLB are classified as *N. macrotis*; though, 1-2 specimens are classified as *N. albigula* and 2-5 specimens are classified as *N. fuscipes* within each dataset (Table 3.4). Because the percent of predicted *N. albigula* counts fall within the range of recent specimen classification error (Table 3.3), and because some morphological overlap occurs between *N. albigula*, *N. fuscipes*, and *N. macrotis* (Fig. 3.3), I do not consider the occurrence of *N. albigula* to be strongly supported in this sample. Many fossil specimens classified as *N. macrotis* exhibit relatively high posterior probabilities of group membership (Table 3.4), so this taxon is undoubtedly present in the P23 faunas of RLB. However, it is difficult to discern whether *N. fuscipes* is present in this fauna as well or whether its predicted occurrence is an artifact of elevated misclassification rates and morphological overlap among extant *N. fuscipes* and *N. macrotis* due to their close ancestry (Table 3.3; Fig. 3.3).

3.5.3 Biogeographic implications

This study is the first to report *N. macrotis* remains at a prehistoric locality, to my knowledge, likely due to the recent elevation of *N. macrotis* to species and the challenges of identifying isolated elements of *Neotoma* to species overall. Rancho La Brea is located within the contemporary range of *N. macrotis* (Fig. 3.1), so its presence in these paleofauanas is expected. However, RLB is also less than 150 km from the southernmost *N. fuscipes/N. macrotis* contact zone (Matocq, 2002) (Fig. 3.1), and it is possible that the range of *N. fuscipes* extended further south during the late Pleistocene because more extreme Quaternary range shifts have been documented in other small mammal species (Graham et al., 1996; McGuire, 2011). Recent projections of the geographic distribution of *N. fuscipes* place it in southern California at the Last Glacial Maximum, 21,000 years before present (Boria et al., In Review), representing a second line of evidence that it was potentially in the region around RLB in the slightly earlier glacial times captured by the fossil specimens. Interpreting whether *N. fuscipes* and *N. macrotis*, or *N. macrotis* alone, is present at RLB is further complicated by the fact that these two species are known to hybridize in parts of California (Coyner et al., 2015; Matocq, 2002). Even within *N. fuscipes*, there is marked genotypic (Boria et al., In Review; Matocq, 2002) and phenotypic (Hooper, 1938; Matocq, 2002) variation among geographic populations in California. Indeed, more variation occurs in the m1 morphological ellipse of extant *N. fuscipes* than in any other California *Neotoma* species examined in this sample, some of which overlaps with *N. macrotis* (Fig. 3.3). Due to these complications, caution is advised when calculating species-level NISP (number of identified specimens) via this protocol if *N. fuscipes* and *N. macrotis* are both detected in an unknown sample pool, especially at localities near their contemporary range intersections. In such cases this

protocol may only be appropriate for detecting the dominant taxon within an unknown sample (e.g., *N. macrotis* this study), and data replicates should be performed when assigning individuals to a species. For example, it may be concluded that the seven fossil individuals classified as *N. macrotis* in both landmark data replicates of this study are *N. macrotis* and the other seven are of uncertain species affinity (Table 3.4). Nevertheless, this landmark protocol is efficient at differentiating m1s of all other *Neotoma* species examined here (Table 3.3; Fig. 3.2) and should be quite useful for identifying fossil woodrat dentition further from *N. fuscipes*/*N. macrotis* contact zones.

3.5.4 Implications for (paleo)climate and (paleo)ecology

Patterns of m1 centroid size and climate differ markedly in direction and strength within and among species. *Neotoma cinerea*, for example, exhibits a significant negative relationship with January temperature (Table 3.5) in accordance with Bergmann's rule. Bergmann's rule proposes that endothermic vertebrates are larger in colder climates and at higher latitudes because larger bodies have lower surface-area-to-volume ratios which increases thermoregulatory efficiency (Bergmann, 1847; Mayr, 1956). Extensive work on *N. cinerea* ecology and paleoecology show similar negative size-temperature patterns (Brown & Lee, 1969; Smith et al., 1995, 2009; Smith & Betancourt, 2003, 2006). However, *N. cinerea* m1 size in this study also exhibits a significant positive relationship with summer temperature, such that individuals from areas with higher maximum July temperatures are larger than individuals from areas with lower maximum July temperatures (Table 3.5). These apparently conflicting size-climate trends are potentially explained by this taxon's sensitivity to temperature seasonality in which size significantly increases with temperature variability (Table 3.5). Because sampling focused on specimens from California, and the range of *N. cinerea* is quite broad, further work will be needed to determine whether this pattern is a general feature of the species or specific to the localities observed in California. Conversely, *N. macrotis* exhibits a significant and positive relationship with January temperature (contrary to Bergmann's rule) and significantly decreases in size with temperature seasonality (Table 5; Fig. 3.4).

In addition to changes in direction, the strength of size-climate relationships differs markedly among the examined species – R^2 values of the most significant climate variable associated with m1 centroid size range from ~0.07 in *N. lepida* (with temperature seasonality, $p = 0.081$) to ~0.45 in *N. fuscipes* (with annual precipitation, $p < 0.001$; Table 3.5; Fig. 3.4). Minimal size-climate sensitivity in *N. lepida* is at odds with previous research that has shown strong negative relationships between *N. lepida* size and July temperature across space and potentially time (Smith & Betancourt, 2003, 2006). Such discrepancies suggest that size-climate relationships may vary regionally within taxa as well as locally among taxa. Even the most closely related species examined here (i.e., *N. fuscipes* and *N. macrotis*) exhibit very different size responses to climate. *Neotoma macrotis* is significantly larger in parts of California with warmer January temperatures versus locations with cooler January temperatures; however, *N. fuscipes* does not exhibit a significant size relationship with any temperature variable except seasonality (Table 3.5). On the other hand, *N. fuscipes* m1 centroid size is negatively related to annual precipitation and winter precipitation throughout California, while *N.*

macrotis m1 centroid size does not significantly track any precipitation variable except seasonality (Table 3.5; Fig. 3.4). These data suggest that environmental drivers of size can be highly specific, differing even among very closely related species. Teeth of *N. cinerea*, *N. fuscipes*, and *N. macrotis* should be useful for tracking different aspects of climate through time as well as through space, if specific identification of their fossils can be achieved, given the significant size-climate relationships observed here. For example, differences in the m1 centroid size of extant versus fossil *N. macrotis* could indicate differences in seasonality and winter temperature between prehistoric and historic times (Table 3.5; Fig. 3.4).

I compared RLB fossil *Neotoma* m1s to the size of recent *N. macrotis* m1s from southern California (Appendix Table 3.9.1) and evaluated these differences in a paleoclimatic context. Fossil m1s were split into two groups representing two taxonomic scenarios. Scenario 1 assumes that all fossil specimens are of the most common LDA-classified taxon, *N. macrotis*, and that predicted occurrences of other taxa are due to analytical error, not true occurrences. All 14 fossil individuals were therefore included in this comparison. Scenario 2 assumes that the RLB *Neotoma* fauna is potentially polytypic and that only the seven individuals classified as *N. macrotis* in both landmark data replicates can be accepted as this taxon; the other seven specimens are considered unidentifiable and removed from the analysis. I found non-significant size differences between recent and fossil populations in both scenarios (Fig. 3.4); though size differences are more discernable for scenario 2 (Fig. 3.4B). Interpreting these results in a paleoclimatic context is complicated by small sample sizes, *N. fuscipes*/*N. macrotis* taxonomic uncertainty, and time-averaging, but I address several scenarios that researchers should potentially consider when interpreting fossil versus modern size differences in other systems.

Scenario 1A: all 14 fossil specimens are *N. macrotis* and no size differences occur between recent and fossil populations overall (Fig. 3.5A). Climatically, this could suggest that winter temperatures and seasonality were similar in Los Angeles between the late Pleistocene and present (Table 3.5; Figs. 3.4D & 3.5A). In scenario 1A, size differences between classification vetted and non-vetted fossil samples could be attributed to subsampling bias (Fig. 3.5A versus 3.5B).

Scenario 1B: all fossil specimens are *N. macrotis* and no size differences occur between recent and fossil populations overall. However, rapid climatic oscillations occurred during the late Pleistocene in California (Hendy et al., 2002; Hendy & Kennett, 1999), so it is possible that some specimens were smaller or larger depending on the specific climates at the time they were deposited, which could result in greater size variability but no average size differences from contemporary populations. Indeed, there is greater size variability in the fossil population than in the modern sample (Fig. 3.5A). P23 faunas are also time-averaged (Fox et al., 2019; Fuller et al., 2020), so age and climate variability must be considered for the RLB sample.

Scenario 2: the full fossil sample represents multiple species of *Neotoma*, *N. macrotis* and at least one larger taxon (e.g., *N. fuscipes*, Table 3.4; Fig. 3.5B). Scenario 2 could explain why size differences occur between the classification vetted and non-vetted fossil samples as well (Table 3.4; Fig. 3.5). Under this scenario, winter temperatures

and/or seasonality may have been cooler and greater in Los Angeles respectfully during the late Pleistocene versus today based on contemporary size-climate patterns in *N. macrotis* (Table 3.5; Fig. 3.4) if only the classification-vetted sample is considered (Fig. 3.5B).

Scenario 3: different combinations of environmental forcings in the past could complicate size-climate patterns regardless of species composition and thus limit the utility of size as a climate tracer. For example, concurrent decreases in winter temperature and temperature seasonality may nullify size shifts in *N. macrotis* since the former has a positive effect on size and the latter has a negative effect (Table 3.5; Fig. 3.4). Distinguishing among these scenarios would be aided by individually dated fossil *Neotoma* specimens from multiple different times in the past, but those data are not available for *Neotoma* fossils from RLB due to their scarcity in these asphaltic deposits.

The potential impact of biotic interactions on size, which may have been different in the Pleistocene versus today, is also not considered here. In fact, geographic differences in unmeasured abiotic and biotic variables may explain why different size-climate responses are observed in some taxa (e.g., *N. lepida*) among studies. It is therefore perhaps best to evaluate fossil *Neotoma* size in tandem with other climate proxies (if available) for paleoenvironmental reconstruction, and only if those remains can be identified to species.

3.5.5 Summary and conclusions

Here, I show that 2D landmark analysis of *Neotoma* m1s is effective at morphologically differentiating five western North American species overall. Most individuals are correctly classified within their respective species groups via LDA; though, higher rates of misclassification occur between the two most recently diverged species, *N. fuscipes* and *N. macrotis* (Table 3.3). As demonstrated with fresh capture weights (Brown & Lee, 1969), and fecal pellet size (Smith et al., 1995, 2009; Smith & Betancourt, 2003), *Neotoma* m1 size is a good tracer of climate in most species. However, the specific aspects of climate that affect tooth size and the direction and magnitude of those effects is species – and potentially location – specific (Table 3.5; Fig. 3.4). Because fossil teeth tend to preserve over a wider range of climates and time periods than fossil middens, this protocol could extend the spatiotemporal range of *Neotoma* species occurrences and further our understanding of their biogeography and paleoecology. Even at prehistoric localities where middens are present, landmark-based tooth identifications can provide a size and contemporary range-independent method of identifying species occupants.

By applying this landmark protocol to identify fossil *Neotoma* m1s at RLB, I confirmed the presence of *N. macrotis*, which supports inferences of (Mychajliw et al., 2020) that either *N. lepida* or *N. macrotis* likely occurred there based on fecal pellet analysis of a midden recovered from Deposit 1 of P23. Finally, I evaluated size differences between extant and fossil *N. macrotis* samples to infer long-term climate patterns at RLB. Such inferences are complicated by small sample sizes, time-averaging, and uncertainty in whether *N. fuscipes* and/or hybrid individuals are present at this site.

Paleoclimate applications of m1 size change through time will likely be more feasible at sites with greater *Neotoma* sample sizes and better chronological control, especially at sites far from *N. fuscipes*/*N. macrotis* contact zones.

In conclusion, geometric morphometric analysis of *Neotoma* molars is useful for identifying species and tracking (paleo)ecological patterns in California. This relatively simple landmark identification protocol may be applicable to other study systems and locations. Though, researchers should independently evaluate size-climate relationships of extant *Neotoma* species in those systems before making paleoecological assessments due to the variability of responses observed within and among species here. These findings emphasize the importance of species-level fossil identifications since evolutionary responses to environmental pressures can be individualistic – even among very closely related taxa.

3.6 References

Adams, D. C., Collyer, M. L., & Kaliontzopoulou, A. (2019). *Geomorph: Software for geometric morphometric analyses. R package version 3.1.0.* https://cran.r-project.org/package=geomorph

Arnqvist, G., & Mårtensson, T. (1998). Measurement error in geometric morphometrics: Empirical strategies to assess and reduce its impact on measures of shape. *Zoologica Academiae Scientiarum Hungaricae*, *44*(1–2), 73–96.

Bergmann, C. (1847). Über die Verhältnisse der Wärmeökonomie der Thiere zu ihrer Grösse. *Göttinger Studien*, *3*, 595–708.

Betancourt, J. L., Devender, T. R. V., & Martin, P. S. (1990). *Packrat Middens: The Last 40,000 Years of Biotic Change*. University of Arizona Press.

Blois, J. L., & Hadly, E. A. (2009). Mammalian Response to Cenozoic Climatic Change. *Annual Review of Earth and Planetary Sciences*, *37*(1), 181–208. https://doi.org/10.1146/annurev.earth.031208.100055

Blois, J. L., McGuire, J. L., & Hadly, E. A. (2010). Small mammal diversity loss in response to late-Pleistocene climatic change. *Nature*, *465*(7299), 771–774. https://doi.org/10.1038/nature09077

Bookstein, F. L. (1997). *Morphometric Tools for Landmark Data: Geometry and Biology*. Cambridge University Press.

Boria, R. A., Brown, S. K., Matocq, M. D., & Blois, J. L. (In Review). Genome-wide genetic variation coupled with demographic and ecological niche modeling of the dusky-footed woodrat (*Neotoma fuscipes*) reveal patterns of deep divergence and widespread Holocene expansions across northern California. *Heredity*.

Brooke McEachern, M., A. Eagles-Smith, C., M. Efferson, C., & H. Van Vuren, D. (2006). Evidence for local specialization in a generalist mammalian herbivore, *Neotoma fuscipes*. *Oikos*, *113*(3), 440–448. https://doi.org/10.1111/j.2006.0030-1299.14176.x

Brown, J. H., & Lee, A. K. (1969). Bergmann's Rule and Climatic Adaptation in Woodrats (Neotoma). *Evolution*, *23*(2), 329–338.

Cordero, G. A., & Epps, C. W. (2012). From Desert to Rainforest: Phenotypic Variation in Functionally Important Traits of Bushy-Tailed Woodrats (*Neotoma cinerea*) Across Two Climatic Extremes. *Journal of Mammalian Evolution*, *19*(2), 135–153. https://doi.org/10.1007/s10914-012-9187-0

Coyner, B. S., Murphy, P. J., & Matocq, M. D. (2015). Hybridization and asymmetric introgression across a narrow zone of contact between *Neotoma fuscipes* and *N. macrotis* (Rodentia: Cricetidae): Hybridization in *Neotoma*. *Biological Journal of the Linnean Society*, *115*(1), 162–172. https://doi.org/10.1111/bij.12487

Cuenca-Bescós, G., Straus, L. G., González Morales, M. R., & García Pimienta, J. C. (2009). The reconstruction of past environments through small mammals: From the Mousterian to the Bronze Age in El Mirón Cave (Cantabria, Spain). *Journal of Archaeological Science*, *36*(4), 947–955. https://doi.org/10.1016/j.jas.2008.09.025

Dalquest, W. W., Stangl, F. B., & Grimes, J. V. (1989). The Third Lower Premolar of the Cottontail, Genus *Sylvilagus*, and Its Value in the Discrimination of Three Species. *American Midland Naturalist*, *121*(2), 293. https://doi.org/10.2307/2426033

Dalquest, W. W., & Stangl Jr., F. B. (1983). Identification of Seven Species of *Peromyscus* from Trans-Pecos Texas by Characteristics of the Lower Jaws. *Occasional Papers of the Museum, Texas Tech University, no. 90*, 1–12.

Damuth, J. D., & MacFadden, B. J. (1990). *Body Size in Mammalian Paleobiology: Estimation and Biological Implications*. Cambridge University Press.

Dice, L. R. (1925). Rodents and lagomorphs of the Rancho la Brea deposits. *Carnegie Institution of Washington*, *349*, 119–130.

Fick, S. E., & Hijmans, R. J. (2017). WorldClim 2: New 1-km spatial resolution climate surfaces for global land areas. *International Journal of Climatology*, *37*, 4302–4315.

Fox, N. S., Takeuchi, G. T., Farrell, A. B., & Blois, J. L. (2019). A protocol for differentiating late Quaternary leporids in southern California with remarks on

Project 23 lagomorphs at Rancho La Brea, Los Angeles, California, USA. *PaleoBios*, *36*, 1–20.

Fox, N. S., Veneracion, J. J., & Blois, J. L. (2020). Are geometric morphometric analyses replicable? Evaluating landmark measurement error and its impact on extant and fossil *Microtus* classification. *Ecology and Evolution*, *10*(7), 3260–3275. https://doi.org/10.1002/ece3.6063

Fruciano, C. (2016). Measurement error in geometric morphometrics. *Development Genes and Evolution*, *226*(3), 139–158. https://doi.org/10.1007/s00427-016-0537-4

Fruciano, C., Schmidt, D., Ramírez Sanchez, M. M., Morek, W., Avila Valle, Z., Talijančić, I., Pecoraro, C., & Schermann Legionnet, A. (2020). Tissue preservation can affect geometric morphometric analyses: A case study using fish body shape. *Zoological Journal of the Linnean Society*, *188*(1), 148–162. https://doi.org/10.1093/zoolinnean/zlz069

Fuller, B. T., Southon, J. R., Fahrni, S. M., Farrell, A. B., Takeuchi, G. T., Nehlich, O., Guiry, E. J., Richards, M. P., Lindsey, E. L., & Harris, J. M. (2020). Pleistocene paleoecology and feeding behavior of terrestrial vertebrates recorded in a pre-LGM asphaltic deposit at Rancho La Brea, California. *Palaeogeography, Palaeoclimatology, Palaeoecology*, *537*, 109383. https://doi.org/10.1016/j.palaeo.2019.109383

Graham, R. W., Lundelius, E. L., Graham, M. A., Schroeder, E. K., Toomey, R. S., Anderson, E., Barnosky, A. D., Burns, J. A., Churcher, C. S., Grayson, D. K., Guthrie, R. D., Harington, C. R., Jefferson, G. T., Martin, L. D., McDonald, H. G., Morlan, R. E., Semken, H. A., Webb, S. D., Werdelin, L., & Wilson, M. C. (1996). Spatial Response of Mammals to Late Quaternary Environmental Fluctuations. *Science*, *272*(5268), 1601–1606.

Grayson, D. K. (2006). The Late Quaternary biogeographic histories of some Great Basin mammals (western USA). *Quaternary Science Reviews*, *25*(21), 2964–2991. https://doi.org/10.1016/j.quascirev.2006.03.004

Harris, A. H. (1984). *Neotoma* in the late Pleistocene of New Mexico and Chihuahua. *Special Publications, Carnegie Museum of Natural History*, *8*, 164–178.

Hendy, I. L., & Kennett, J. P. (1999). Latest Quaternary North Pacific surface-water responses imply atmosphere-driven climate instability. *Geology*, *27*(4), 291–294. https://doi.org/10.1130/0091-7613(1999)027<0291:LQNPSW>2.3.CO;2

Hendy, I. L., Kennett, J. P., Roark, E. B., & Ingram, B. L. (2002). Apparent synchroneity of submillennial scale climate events between Greenland and Santa Barbara

Basin, California from 30–10ka. *Quaternary Science Reviews*, *21*(10), 1167–1184. https://doi.org/10.1016/S0277-3791(01)00138-X

Hooper, E. T. (1938). *Geographical variation in wood rats of the species Neotoma fuscipes*. University of California Press.

Jackson, S. T., Betancourt, J. L., Lyford, M. E., Gray, S. T., & Rylander, K. A. (2005). A 40,000-year woodrat-midden record of vegetational and biogeographical dynamics in north-eastern Utah, USA: Vegetational and biogeographical dynamics in north-eastern Utah. *Journal of Biogeography*, *32*(6), 1085–1106. https://doi.org/10.1111/j.1365-2699.2005.01251.x

Jansky, K., Schubert, B. W., & Wallace, S. C. (2016). Geometric morphometrics of dentaries in *Myotis*: Species identification and its implications for conservation and the fossil record. *Northeastern Naturalist*, *23*(1), 184–194. https://doi.org/10.1656/045.023.0115

Jombart, T. (2008). adegenet: A R package for the multivariate analysis of genetic markers. *Bioinformatics*, *24*(11), 1403–1405. https://doi.org/10.1093/bioinformatics/btn129

Jombart, T., & Collins, C. (2015). *A tutorial for Discriminant Analysis of Principal Components (DAPC) using adegenet 2.0.0*. 43.

Kovarovic, K., Aiello, L. C., Cardini, A., & Lockwood, C. A. (2011). Discriminant function analyses in archaeology: Are classification rates too good to be true? *Journal of Archaeological Science*, *38*(11), 3006–3018. https://doi.org/10.1016/j.jas.2011.06.028

Lyman, R. L., & O'Brien, M. J. (2005). Within-taxon morphological diversity in late-Quaternary *Neotoma* as a paleoenvironmental indicator, Bonneville Basin, Northwestern Utah, USA. *Quaternary Research*, *63*(3), 274–282. https://doi.org/10.1016/j.yqres.2005.02.013

Macedo, R. H., & Mares, M. A. (1988). Neotoma albigula. *Mammalian Species*, *310*, 1. https://doi.org/10.2307/3504165

Matocq, M. D. (2002). Phylogeographical structure and regional history of the dusky-footed woodrat, *Neotoma fuscipes*. *Molecular Ecology*, *11*(2), 229–242. https://doi.org/10.1046/j.0962-1083.2001.01430.x

Matocq, M. D. (2009). A microarray's view of life in the desert: Adding a powerful evolutionary genomics tool to the packrat's midden. *Molecular Ecology*, *18*(11), 2310–2312. https://doi.org/10.1111/j.1365-294X.2009.04172.x

Mayr, E. (1956). Geographical Character Gradients and Climatic Adaptation. *Evolution*, *10*(1), 105–108. https://doi.org/10.1111/j.1558-5646.1956.tb02836.x

McGuire, J. L. (2010). Geometric morphometrics of vole (*Microtus californicus*) dentition as a new paleoclimate proxy: Shape change along geographic and climatic clines. *Quaternary International*, *212*(2), 198–205. https://doi.org/10.1016/j.quaint.2009.09.004

McGuire, J. L. (2011). Identifying California *Microtus* species using geometric morphometrics documents Quaternary geographic range contractions. *Journal of Mammalogy*, *92*(6), 1383–1394. https://doi.org/10.1644/10-MAMM-A-280.1

Meachen, J. A., Janowicz, A. C., Avery, J. E., & Sadleir, R. W. (2014). Ecological Changes in Coyotes (*Canis latrans*) in Response to the Ice Age Megafaunal Extinctions. *PLoS ONE*, *9*(12), e116041. https://doi.org/10.1371/journal.pone.0116041

Mychajliw, A. M., Rice, K. A., Tewksbury, L. R., Southon, J. R., & Lindsey, E. L. (2020). Exceptionally preserved asphaltic coprolites expand the spatiotemporal range of a North American paleoecological proxy. *Scientific Reports*, *10*(1), 5069. https://doi.org/10.1038/s41598-020-61996-y

Patterson, B. D., Ceballos, G., Sechrest, W., Tognelli, M. F., Brooks, T., Luna, L., Ortega, P., Salazar, I., & Young, B. E. (2007). *Digital Distribution Maps of the Mammals of the Western Hemisphere. NatureServe version 3.0.*

R Core Team. (2019). *R: A language and environment for statistical computing. R Foundation for Statistical Computing* (Version 3.6.1) [Computer software]. https://www.R-project.org/

Robinson, C., & Terhune, C. E. (2017). Error in geometric morphometric data collection: Combining data from multiple sources. *American Journal of Physical Anthropology*, *164*(1), 62–75. https://doi.org/10.1002/ajpa.23257

Rohlf, F. J. (2018a). *TpsDig version 2.31*. Ecology & Evolution: (program).

Rohlf, F. J. (2018b). *TpsUtil version 1.76*. Ecology & Evolution: (program).

Rohlf, F. J., & Slice, D. (1990). Extensions of the procrustes method for the optimal superimposition of landmarks. *Systematic Zoology*, *39*(1), 40–59. https://doi.org/10.2307/2992207

Samuels, J. X., & Hopkins, S. S. B. (2017). The impacts of Cenozoic climate and habitat changes on small mammal diversity of North America. *Global and Planetary Change*, *149*, 36–52. https://doi.org/10.1016/j.gloplacha.2016.12.014

Smartt, R. A. (1977). The ecology of late Pleistocene and recent *Microtus* from south-central and southwestern New Mexico. *The Southwestern Naturalist*, *22*(1), 1–19. https://doi.org/10.2307/3670460

Smith, F. A., & Betancourt, J. L. (1998). Response of Bushy-Tailed Woodrats (*Neotoma cinerea*) to Late Quaternary Climatic Change in the Colorado Plateau. *Quaternary Research*, *50*(1), 1–11. https://doi.org/10.1006/qres.1998.1982

Smith, F. A., & Betancourt, J. L. (2003). The effect of Holocene temperature fluctuations on the evolution and ecology of *Neotoma* (woodrats) in Idaho and northwestern Utah. *Quaternary Research*, *59*(2), 160–171. https://doi.org/10.1016/S0033-5894(03)00004-8

Smith, F. A., & Betancourt, J. L. (2006). Predicting woodrat (*Neotoma*) responses to anthropogenic warming from studies of the palaeomidden record. *Journal of Biogeography*, *33*(12), 2061–2076. https://doi.org/10.1111/j.1365-2699.2006.01631.x

Smith, F. A., Betancourt, J. L., & Brown, J. H. (1995). Evolution of Body Size in the Woodrat over the Past 25,000 Years of Climate Change. *Science*, *270*(5244), 2012–2014. https://doi.org/10.1126/science.270.5244.2012

Smith, F. A., Crawford, D. L., Harding, L. E., Lease, H. M., Murray, I. W., Raniszewski, A., & Youberg, K. M. (2009). A tale of two species: Extirpation and range expansion during the late Quaternary in an extreme environment. *Global and Planetary Change*, *65*(3–4), 122–133. https://doi.org/10.1016/j.gloplacha.2008.10.015

Soberón, J., & Martínez-Gordillo, D. (2012). Occupation of environmental and morphological space: Climatic niche and skull shape in *Neotoma* woodrats. *Evolutionary Ecology Research*, *14*, 503–517.

Somerville, A. D., Froehle, A. W., & Schoeninger, M. J. (2018). Environmental influences on rabbit and hare bone isotope abundances: Implications for paleoenvironmental research. *Palaeogeography, Palaeoclimatology, Palaeoecology*, *497*, 91–104. https://doi.org/10.1016/j.palaeo.2018.02.008

Svenning, J.-C., & Sandel, B. (2013). Disequilibrium vegetation dynamics under future climate change. *American Journal of Botany*, *100*(7), 1266–1286. https://doi.org/10.3732/ajb.1200469

Thaeler, C. S. (1980). Chromosome Numbers and Systematic Relations in the Genus *Thomomys* (Rodentia: Geomyidae). *Journal of Mammalogy*, *61*(3), 414–422. https://doi.org/10.2307/1379835

Venables, W. N., & Ripley, B. D. (2002). *Modern Applied Statistics with S, Fourth edition*. Springer. http://www.stats.ox.ac.uk/pub/MASS4

Wallace, S. C. (2006). Differentiating *Microtus xanthognathus* and *Microtus pennsylvanicus* Lower First Molars Using Discriminant Analysis of Landmark Data. *Journal of Mammalogy, 87*(6), 1261–1269.

Whitford, W. G., & Steinberger, Y. (2010). Pack rats (*Neotoma* spp.): Keystone ecological engineers? *Journal of Arid Environments*, *74*(11), 1450–1455. https://doi.org/10.1016/j.jaridenv.2010.05.025

Zakrzewski, R. J. (1993). Morphological change in woodrat (Rodentia: Cricetidae) molars. In R. A. Martin & A. D. Barnosky (Eds.), *Morphological Change in Quaternary Mammals of North America* (pp. 392–409). Cambridge University Press.

Zelditch, M., Swiderski, D.L., Sheets, H. D., & Fink, W.L (Eds.). (2004). *Geometric morphometrics for biologists: A primer*. Elsevier Academic Press.

3.7 Tables

Table 3.1: Definitions of the 14-landmark configuration employed for specific differentiation of western North American *Neotoma* spp. right m1s. Landmark types (i.e., 1, 2, 3; (Bookstein, 1997)) are listed as well.

Landmark #	Type	Description
1	1;2	Intersection of leading and trailing enamel edges at the enamel-dentine contact of the posterobuccal projection apex of the anterolophid (Fig. 3.1A); maxima of curvature at the enamel-dentine contact if the posterobuccal projection is not well-defined (Fig. 3.1B)
2	2	Maxima of curvature along the leading edge of the anterobuccal reentrant at the enamel-reentrant contact
3	2	Maxima of curvature along the training edge of the anterobuccal reentrant at the enamel-reentrant contact
4	1;2	Intersection of leading and trailing enamel edges at the enamel-dentine contact of the buccal projection apex of the mesolophid (Fig. 3.1A); maxima of curvature at the enamel-dentine contact along the buccal edge of the mesolophid if the apex is blunt and intersections are not well-defined (Fig. 3.1B)
5	3	Medial-most extent of the posterobuccal reentrant at the enamel- reentrant contact
6	1	Intersection of leading and trailing enamel edges at the enamel-dentine contact of the buccal projection apex of the posterolophid
7	1	Intersection of leading and trailing enamel edges at the enamel-dentine contact of the lingual projection apex of the posterolophid
8	3	Medial-most extent of the posterolingual reentrant at the enamel- reentrant contact
9	1	Intersection of leading and trailing enamel edges at the enamel-dentine contact of the lingual projection apex of the mesolophid
10	2	Maxima of curvature along the trailing edge of the mesolingual reentrant at the enamel-reentrant contact
11	2	Maxima of curvature along the leading edge of the mesolingual reentrant at the enamel-reentrant contact
12	2	Maxima of curvature along the trailing edge of the anterolophid lingual projection at the enamel-dentine contact
13	1	Intersection of leading and trailing enamel edges at the enamel-dentine contact of the lingual projection apex of the anterolophid

14	1;2	Intersection of leading and trailing enamel edges at the enamel-dentine contact of the anterolingual projection apex of the anterolophid (Fig. 3.1A); maxima of curvature at the enamel-dentine contact if the anterolingual projection is not well-defined (Fig. 3.1B)

Table 3.2: Procrustes ANOVA summary statistics of biological variation among *Neotoma* species and individuals, and intraobserver digitizing error, among the two landmark datasets.

	Df	**SS**	**MS**	**R^2**	**F**	**Z**	***p*-value**
Species	4	1.4082	0.35205	0.28786	449.940	11.935	0.001
Individuals	194	3.3280	0.01715	0.68031	21.925	20.693	0.001
Residuals (error)	199	0.1557	0.00078	0.03183			
Total	397	4.8919					

Table 3.3: Cross-validated linear discriminant analysis classification statistics of extant *Neotoma* from the first (top) and second (bottom) digitizing iteration. Rows indicate predicted species affinities; columns indicate actual species affinities.

Iteration 1	**Na**	**Nc**	**Nf**	**Nl**	**Nm**
Na	35	1	1	2	1
Nc	1	38	0	0	0
Nf	1	0	29	0	9
Nl	2	0	1	38	1
Nm	1	0	9	0	29
Total predicted group membership accuracy = 84.9%					
Iteration 2	**Na**	**Nc**	**Nf**	**Nl**	**Nm**
Na	31	1	2	2	1
Nc	1	38	0	0	0
Nf	1	0	30	0	9
Nl	4	0	0	38	1
Nm	3	0	8	0	29
Total predicted group membership accuracy = 83.4%					

Table 3.4: Classification results of 14 fossil *Neotoma* m1s from Project 23 Deposits: 1, 7B, 13, and 14 at Rancho La Brea. Predicted species-group memberships (PGMs) of each specimen are listed for each dataset trial (T1 and T2) followed by their 0-1 posterior probabilities (PP) of group membership. Values closer to one indicate higher probabilities of belonging to a particular species than values closer to 0. Underlined text indicates fossil specimens assigned to the same extant species in both LDA training sets.

LACMP23 number	**T1 PGM**	**T1 PP**	**T2 PGM**	**T2 PP**
40158	*N. macrotis*	0.898	*N. fuscipes*	0.736
40402	*N. macrotis*	0.757	*N. fuscipes*	0.718
28509	*N. albigula*	0.597	*N. macrotis*	0.842
31175	*N. albigula*	0.696	*N. albigula*	0.527
31976	*N. macrotis*	0.911	*N. macrotis*	0.671
33922	*N. fuscipes*	0.643	*N. fuscipes*	0.932
34168	*N. macrotis*	0.902	*N. fuscipes*	0.523
35665	*N. macrotis*	0.999	*N. macrotis*	0.918
35668	*N. macrotis*	0.988	*N. macrotis*	0.990
35780	*N. macrotis*	0.890	*N. macrotis*	0.961
35782	*N. macrotis*	0.656	*N. macrotis*	0.842
35806	*N. macrotis*	0.877	*N. macrotis*	0.871
35934	*N. macrotis*	0.992	*N. macrotis*	0.996
36312	*N. fuscipes*	0.968	*N. fuscipes*	0.725

Table 3.5: Linear model summary statistics of 10 temperature and precipitation variables examined against the m1 centroid size of four extant *Neotoma* species. Variables explaining the most size variation in each species, plotted in Fig. 3.3, are bolded and variables exhibiting a positive relationship with size are underlined. * indicates statistically significant relationships between climate variables and tooth size

Species	**Predictor variable**	**Intercept**	**Slope**	**R^2**	***p*-value**
N. cinerea (n=39)	Mean Jan Temp*	3.5070	-0.0247	0.1494	0.0151
	Mean July Temp	3.2662	0.0177	0.0468	0.1860
	Mean Jan Precip*	**3.8444**	**-0.0019**	**0.4343**	**<0.0001**
	Mean July Precip	3.4977	0.0026	0.0027	0.7540
	Min Jan Temp*	3.2820	-0.0299	0.2587	0.0010
	Max July Temp*	2.9269	0.0290	0.1696	0.0092
	Temp Seasonality*	2.5498	0.0016	0.3771	<0.0001
	Precip Seasonality*	4.2231	-0.0102	0.2628	0.0009
	Annual Temp	3.5687	-0.0068	0.0072	0.6070
	Annual Precip*	3.8395	-0.0003	0.4011	<0.0001
N. fuscipes (n=40)	Mean Jan Temp	3.4748	0.0121	0.0349	0.2480
	Mean July Temp	4.1820	-0.0304	0.0798	0.0774
	Mean Jan Precip*	3.8076	-0.0020	0.3388	<0.0001
	Mean July Precip	3.6270	-0.0240	0.0819	0.0734
	Min Jan Temp	3.5713	0.0097	0.0278	0.3040
	Max July Temp	3.7924	-0.0089	0.0089	0.5620
	Temp Seasonality*	3.9789	-0.0008	0.1695	0.0083
	Precip Seasonality	3.4232	0.0015	0.0125	0.4920
	Annual Temp	3.4405	0.0081	0.0086	0.5690
	Annual Precip*	**3.8708**	**-0.0005**	**0.4451**	**<0.0001**
N. lepida (n=40)	Mean Jan Temp	3.0401	-0.0020	0.0107	0.5260
	Mean July Temp	3.1134	-0.0032	0.0261	0.3190
	Mean Jan Precip	2.9810	0.0012	0.0642	0.1150
	Mean July Precip	3.0541	-0.0032	0.0304	0.2820
	Min Jan Temp	3.0246	-0.0016	0.0067	0.6160
	Max July Temp	3.1296	-0.0030	0.0223	0.3570
	Temp Seasonality	**3.6267**	**-0.0008**	**0.0739**	**0.0810**
	Precip Seasonality	2.9401	0.0015	0.0739	0.0898
	Annual Temp	3.0679	-0.0026	0.0176	0.4150
	Annual Precip	2.9908	0.0002	0.0268	0.3130
N. macrotis (n=40)	Mean Jan Temp*	3.1955	0.0256	0.2393	0.0016
	Mean July Temp	3.5333	-0.0071	0.0157	0.4470

	Mean Jan Precip	3.4450	-0.0006	0.0309	0.2840
	Mean July Precip	3.4162	-0.0119	0.0620	0.1260
	Min Jan Temp*	3.3967	0.0199	0.2115	0.0032
	Max July Temp	3.4607	-0.0029	0.0034	0.7260
	Temp Seasonality*	**3.7455**	**-0.0007**	**0.2745**	**0.0006**
	Precip Seasonality*	2.6776	0.0079	0.1804	0.0070
	Annual Temp	3.1005	0.0198	0.0874	0.0677
	Annual Precip	3.4639	-0.0002	0.0562	0.1460

3.8 Figures

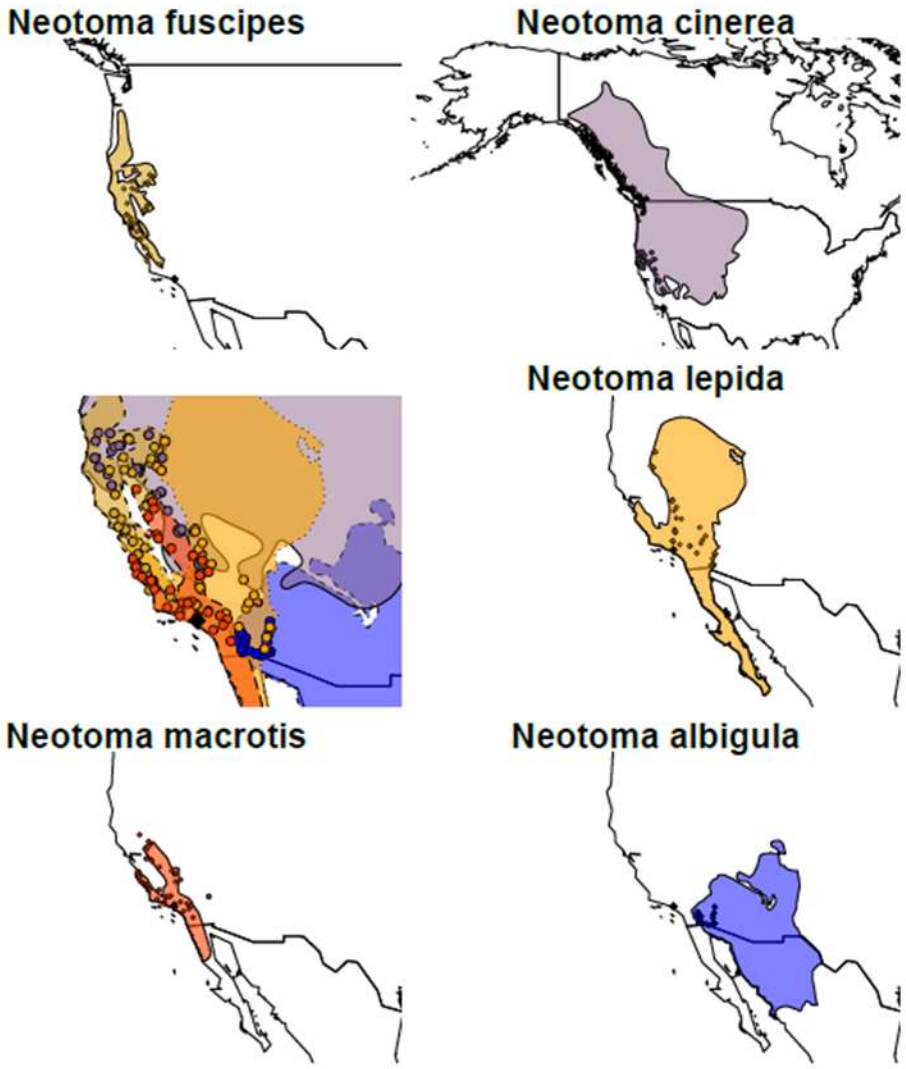

Figure 3.1: Distribution maps of the five extant *Neotoma* species examined here. Points indicate sampling locations of individual specimens. Rancho La Brea, the locality where fossil *Neotoma* specimens were collected, is marked by a black diamond in the North American west coast inset. Species range data obtained from (Patterson et al., 2007).

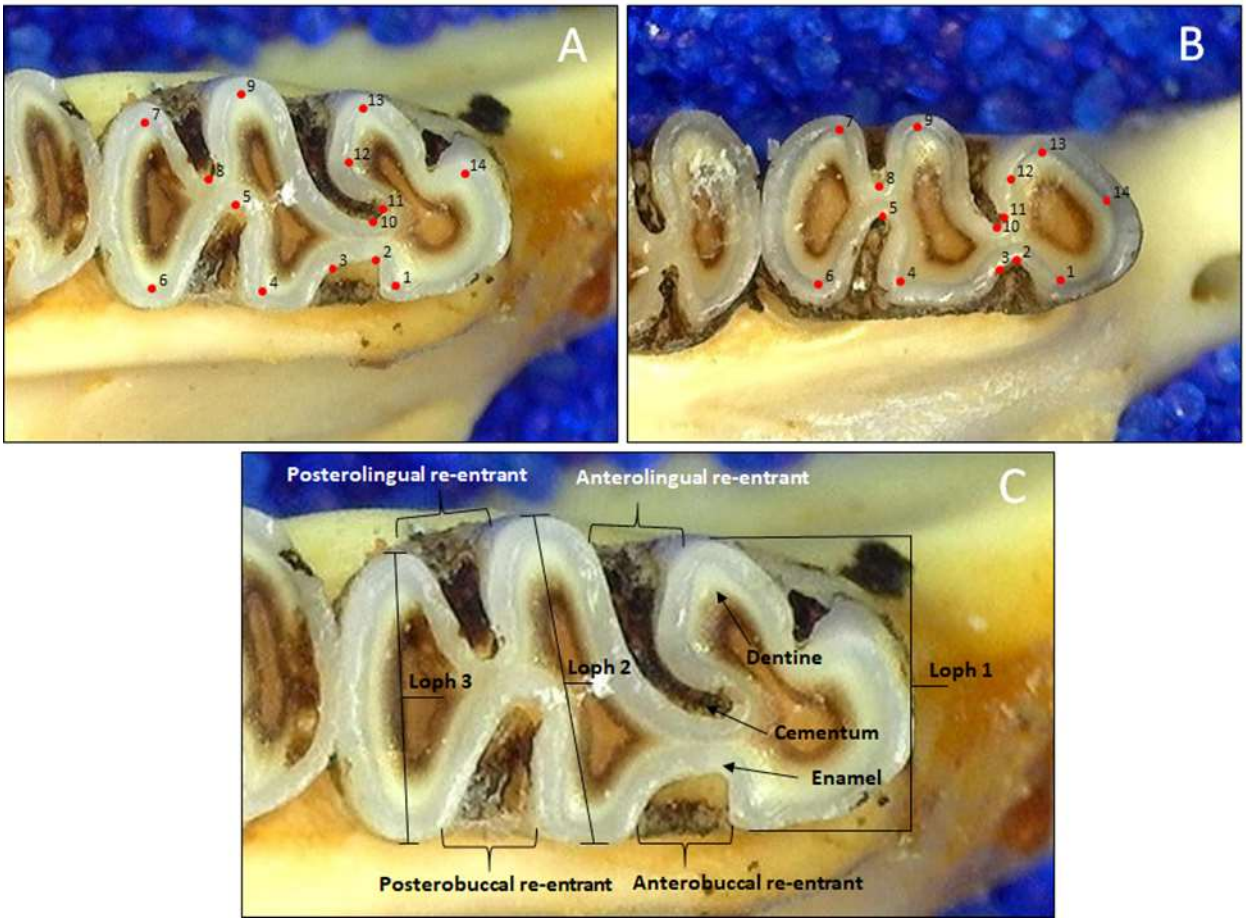

Figure 3.2: A) Landmark configuration employed on the right m1 of MVZ-3925 *Neotoma macrotis* with well-defined posterobuccal and anterolingual anterolophid projections (landmarks 1 and 14 respectively). B). Landmark configuration employed on the right m1 of MVZ-199799 *N. lepida* which lacks well-defined posterobuccal and anterolingual anterolophid projections. C) Right m1 of MVZ-3925 *N. macrotis* illustrating the tooth terminology adapted from Zakrzewski (1993) for use in this study.

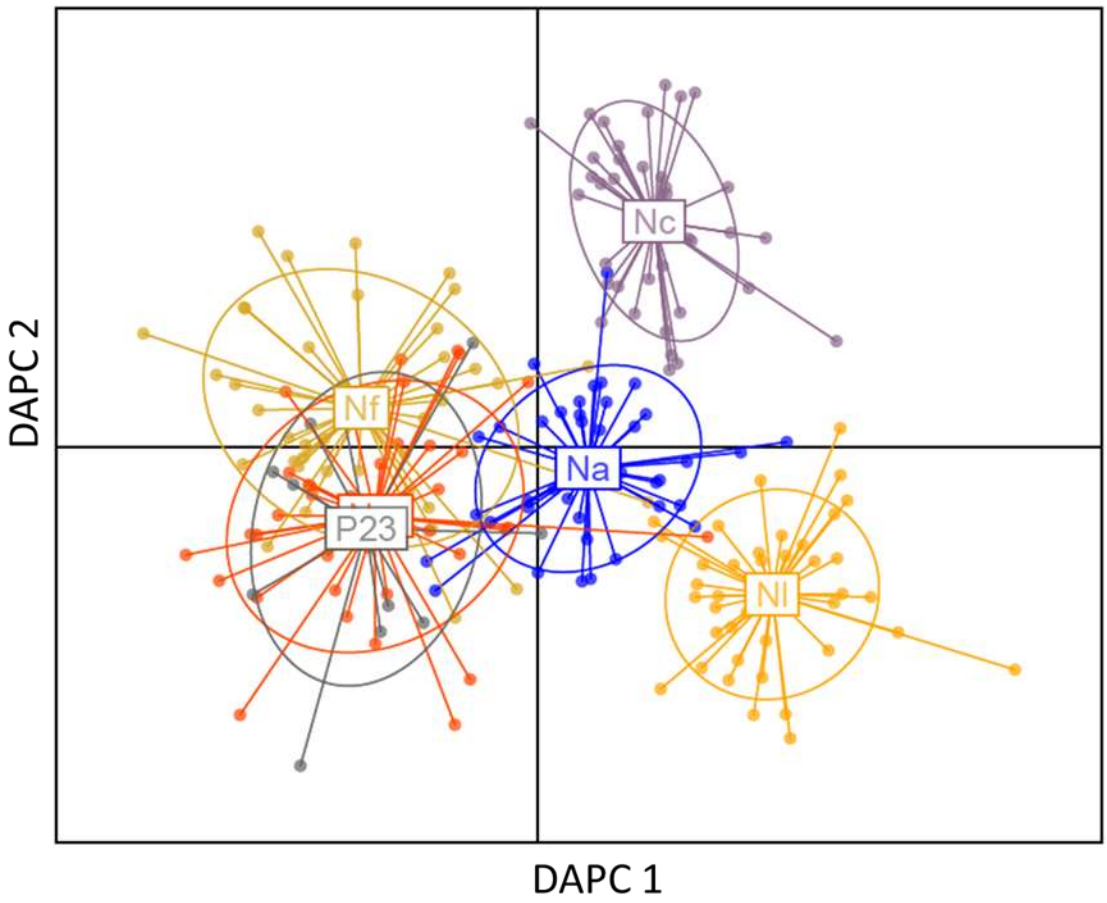

Figure 3.3: Plot of DAPC scores one and two obtained from m1 landmark data of five recent *Neotoma* species: *N. albigula* (Na), *N. cinerea* (Nc), *N. fuscipes* (Nf), *N. lepida* (Nl), *N. macrotis*, and Project 23 fossils from Rancho La Brea (P23, overlapping with *N. macrotis*). The first eight of 25 principle components are included based on optim.a.score function calculations in the R package "adegenet".

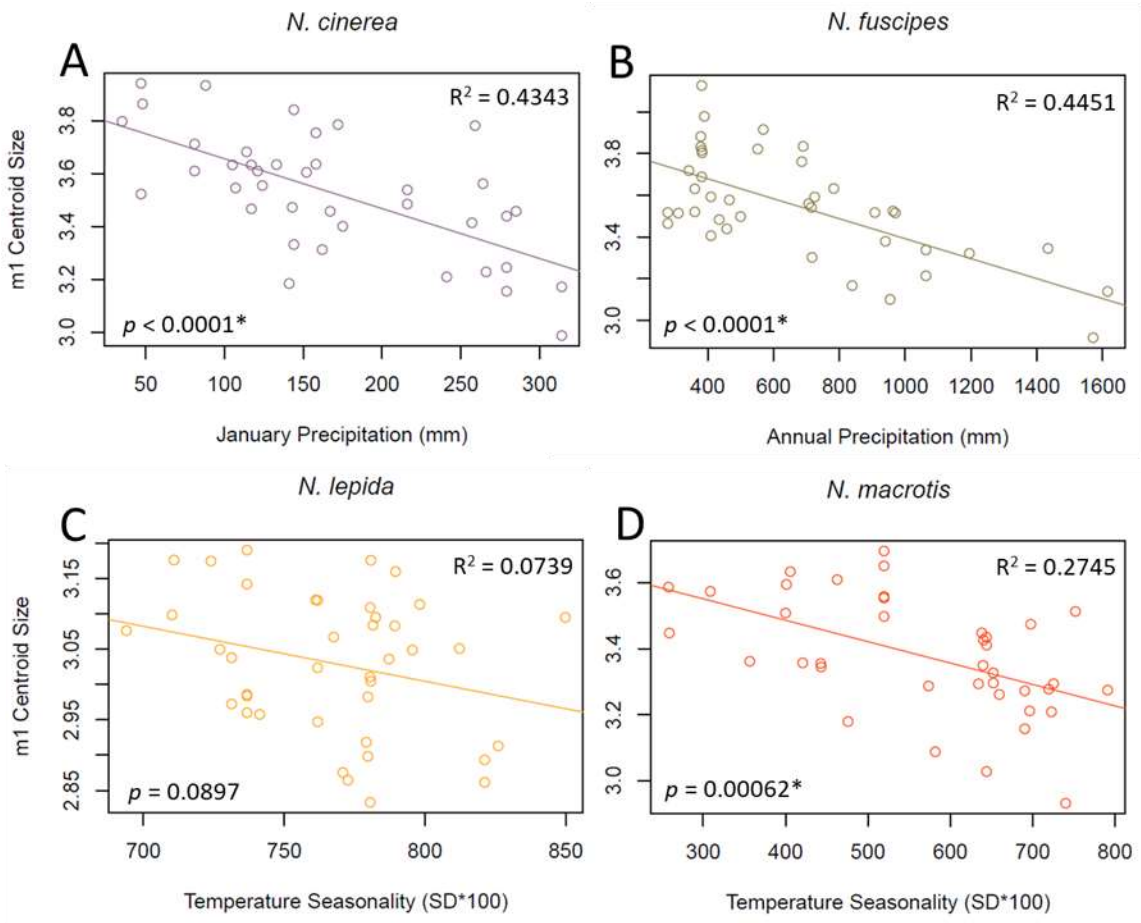

Figure 3.4: Linear models of the most significant climate variable for explaining m1 centroid size variation in four *Neotoma* species. A) *Neotoma cinerea* m1 size against mean January precipitation, B) *N. fuscipes* m1 size against total annual precipitation, C) *N. lepida* m1 size against temperature seasonality (BioClim variable 4), D) *N. macrotis* m1 size against temperature seasonality. See Table 3.5 for statistics of all 10 climate variable models of each species.

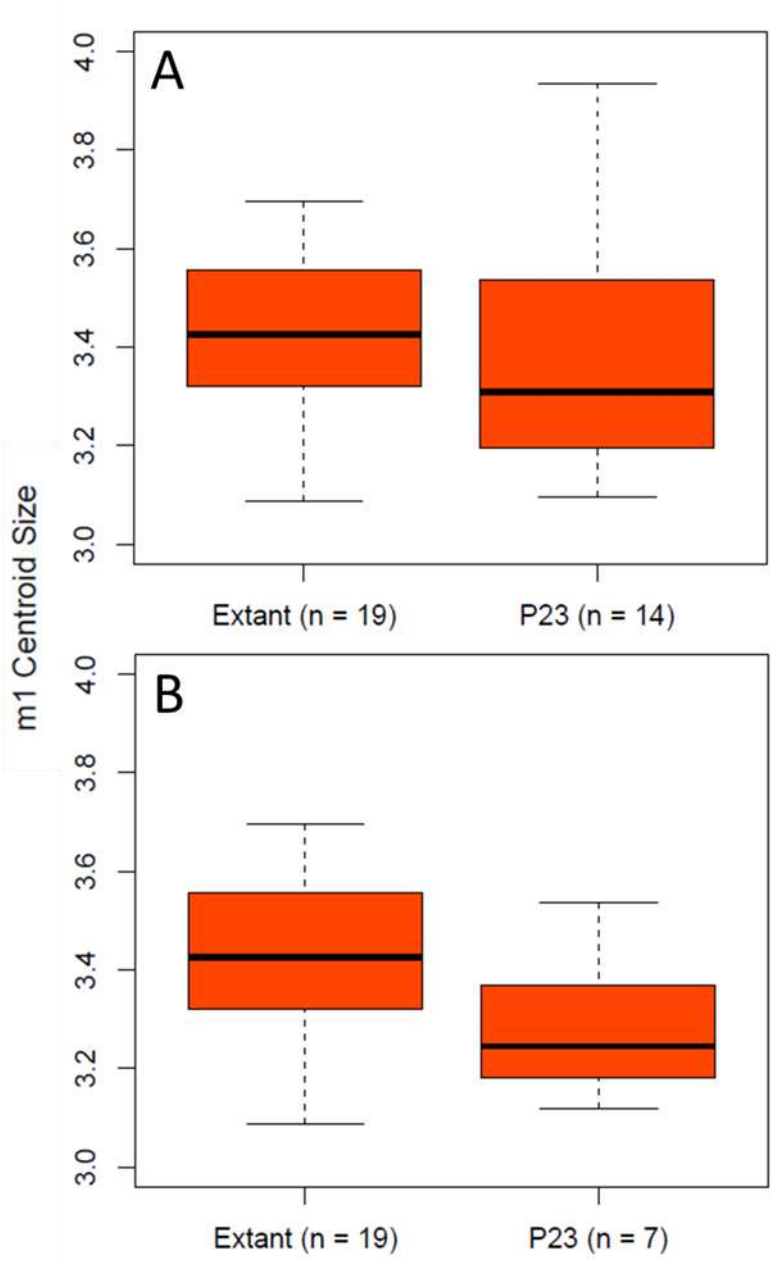

Figure 3.5: Boxplot of m1 centroid size comparisons between 19 recent individuals of *Neotoma macrotis* sampled from southern California counites (Appendix Table 3.9.1) and fossil specimens sampled from P23 deposits at Rancho La Brea. A) Recent *N. macrotis* from southern California compared to all 14 fossil individuals. B) Recent *N. macrotis* compared to only the seven fossil individuals classified as *N. macrotis* in both landmark data replicates (Table 3.4). In both cases, recent and fossil individuals are not significantly different in m1 centroid size based on a t-test (A: t = 0.07159, df = 20.691, p = 0.9436; B: t = 1.8359, df = 12.926, p = 0.0895).

3.9 Appendix

Table 3.9.1: List of all extant and fossil *Neotoma* species examined. The University of California Museum of Vertebrate Zoology number (MVZ #), latitudinal coordinate, (Lat.), longitudinal coordinate (Long.), lower first molar centroid size (m1 size) year of capture (year), and California county of each specimen is included. For each fossil specimen, the Natural History Museum of Los Angeles County Project 23 number (LACMP23 #), anatomical element, and associated Project 23 deposit is listed as well.

MVZ #	Species	Lat.	Long.	m1 size	year	County
1160	*N. albigula*	33.57277	-116.067	3.431	1908	Riverside
1161	*N. albigula*	33.57277	-116.067	3.570	1908	Riverside
7174	*N. albigula*	33.1426	-115.865	3.137	1909	Imperial
7189	*N. albigula*	32.7352	-115.967	3.193	1909	Imperial
7321	*N. albigula*	33.333	-115.833	3.506	1909	Imperial
7323	*N. albigula*	33.333	-115.833	3.275	1909	Imperial
7325	*N. albigula*	33.333	-115.833	3.561	1909	Imperial
7326	*N. albigula*	33.333	-115.833	3.335	1909	Imperial
7479	*N. albigula*	32.7923	-115.606	3.277	1909	Imperial
7558	*N. albigula*	32.87883	-116.044	3.511	1909	San Diego
10463	*N. albigula*	34.023	-114.541	3.220	1910	Riverside
10464	*N. albigula*	34.023	-114.541	3.410	1910	Riverside
10465	*N. albigula*	33.4167	-114.685	3.599	1910	Imperial
10466	*N. albigula*	33.4167	-114.685	3.294	1910	Imperial
10467	*N. albigula*	33.18	-114.7	3.612	1910	Imperial
10471	*N. albigula*	33.18	-114.7	3.451	1910	Imperial
10477	*N. albigula*	32.7654	-114.529	3.186	1910	Imperial
10479	*N. albigula*	32.7654	-114.529	3.353	1910	Imperial
10481	*N. albigula*	32.7654	-114.529	3.055	1910	Imperial
10482	*N. albigula*	32.7654	-114.529	3.178	1910	Imperial

10483	*N. albigula*	32.7654	-114.529	3.163	1910	Imperial
10486	*N. albigula*	32.7314	-114.749	3.275	1910	Imperial
10487	*N. albigula*	32.7314	-114.749	3.496	1910	Imperial
161983	*N. albigula*	33.0994	-115.923	3.590	1980	Imperial
234515	*N. albigula*	33.64	-116.139	3.354	2014	Riverside
234517	*N. albigula*	33.64	-116.139	3.359	2015	Riverside
234520	*N. albigula*	33.53999	-116.079	3.465	2015	Riverside
234521	*N. albigula*	33.53999	-116.079	3.358	2015	Riverside
27864	*N. albigula*	32.87883	-116.044	3.077	1918	San Diego
39621	*N. albigula*	32.60139	-115.00	3.640	1928	Baja California
62601	*N. albigula*	33.60856	-114.593	3.357	1934	Riverside
7559	*N. albigula*	32.87883	-116.044	3.423	1909	San Diego
7577	*N. albigula*	32.87883	-116.044	3.453	1909	San Diego
7578	*N. albigula*	32.87883	-116.044	3.372	1909	San Diego
7579	*N. albigula*	32.87883	-116.044	3.769	1909	San Diego
84637	*N. albigula*	32.6827	-115.251	3.502	1938	Imperial
84638	*N. albigula*	32.6827	-115.251	3.379	1938	Imperial
84639	*N. albigula*	32.6827	-115.251	3.231	1938	Imperial
84803	*N. albigula*	32.6827	-115.251	3.587	1938	Imperial
95009	*N. albigula*	33.22694	-116.33	3.384	1941	San Diego
13370	*N. cinerea*	41.16756	-122.861	3.400	1911	Trinity
13381	*N. cinerea*	41.34264	-122.692	3.609	1911	Siskiyou
15539	*N. cinerea*	36.09286	-118.226	3.633	1911	Tulare
15546	*N. cinerea*	36.48861	-118.208	3.466	1911	Inyo
15551	*N. cinerea*	36.48861	-118.208	3.632	1911	Inyo
22330	*N. cinerea*	37.77411	-119.26	3.554	1915	Tuolumne
22332	*N. cinerea*	37.8785	-119.367	3.545	1915	Tuolumne

23103	*N. cinerea*	37.78762	-119.341	3.331	1915	Mariposa
23109	*N. cinerea*	37.78762	-119.341	3.841	1915	Mariposa
23111	*N. cinerea*	37.87338	-119.171	3.609	1915	Mono
121991	*N. cinerea*	41.58702	-123.692	3.561	1957	Del Norte
121993	*N. cinerea*	41.93184	-123.543	3.228	1957	Siskiyou
128770	*N. cinerea*	39.43165	-120.248	3.604	1955	Nevada
132508	*N. cinerea*	41.84132	-120.904	3.940	1963	Modoc
132509	*N. cinerea*	41.84132	-120.904	3.522	1963	Modoc
132714	*N. cinerea*	39.72751	-122.844	3.172	1949	Glenn
132715	*N. cinerea*	39.72751	-122.844	2.987	1952	Glenn
218378	*N. cinerea*	40.88837	-120.181	3.797	2006	Lassen
220747	*N. cinerea*	40.40637	-121.361	3.635	2007	Plumas
220748	*N. cinerea*	40.40637	-121.361	3.753	2007	Plumas
222826	*N. cinerea*	39.46031	-120.285	3.312	2008	Sierra
224334	*N. cinerea*	36.43453	-118.283	3.682	2009	Tulare
224650	*N. cinerea*	39.3057	-120.517	3.781	2009	Placer
23112	*N. cinerea*	37.87338	-119.171	3.711	1915	Mono
232199	*N. cinerea*	38.66816	-119.91	3.184	2009	Alpine
24997	*N. cinerea*	36.7938	-118.581	3.933	1916	Fresno
33719	*N. cinerea*	40.45969	-121.442	3.457	1923	Shasta
34865	*N. cinerea*	40.4147	-121.532	3.785	1924	Tehama
35207	*N. cinerea*	40.801	-120.612	3.863	1924	Lassen
57071	*N. cinerea*	40.49	-123.523	3.414	1932	Trinity
57072	*N. cinerea*	40.48086	-123.481	3.457	1932	Trinity
59068	*N. cinerea*	40.87485	-123.732	3.439	1933	Humboldt
59072	*N. cinerea*	40.87485	-123.732	3.155	1933	Humboldt
59073	*N. cinerea*	40.87485	-123.732	3.245	1933	Humboldt

64967	*N. cinerea*	40.18778	-123.045	3.209	1932	Trinity
65425	*N. cinerea*	41.39539	-122.378	3.472	1935	Siskiyou
65495	*N. cinerea*	41.40182	-122.454	3.633	1934	Siskiyou
69443	*N. cinerea*	41.91065	-122.926	3.538	1935	Siskiyou
69446	*N. cinerea*	41.91065	-122.926	3.484	1935	Siskiyou
195212	*N. fuscipes*	36.27004	-121.064	3.517	2000	Monterey
195213	*N. fuscipes*	36.27004	-121.064	3.464	2000	Monterey
195986	*N. fuscipes*	37.11999	-121.1	3.514	1999	Merced
196356	*N. fuscipes*	37.86557	-122.152	3.835	1999	Contra Costa
196360	*N. fuscipes*	35.7504	-120.773	3.832	2000	San Luis Obispo
196363	*N. fuscipes*	35.7504	-120.773	3.882	2000	San Luis Obispo
196371	*N. fuscipes*	35.72531	-120.654	3.718	2000	San Luis Obispo
196382	*N. fuscipes*	35.61446	-120.688	3.978	2000	San Luis Obispo
196388	*N. fuscipes*	41.70796	-121.981	3.592	1998	Siskiyou
196391	*N. fuscipes*	41.70796	-121.981	3.406	1998	Siskiyou
196392	*N. fuscipes*	41.66421	-121.94	3.439	1998	Siskiyou
196400	*N. fuscipes*	40.36344	-122.958	3.524	1998	Shasta
196404	*N. fuscipes*	39.34502	-122.665	3.542	1998	Colusa
196415	*N. fuscipes*	40.26732	-121.773	3.321	1998	Tehama
196416	*N. fuscipes*	38.57045	-122.716	3.214	1998	Sonoma
196417	*N. fuscipes*	38.57045	-122.716	3.338	1998	Sonoma
196564	*N. fuscipes*	36.84171	-121.476	3.688	1999	San Benito
196565	*N. fuscipes*	36.84171	-121.476	4.126	1999	San Benito
196566	*N. fuscipes*	36.84171	-121.476	3.815	1999	San Benito
197373	*N. fuscipes*	35.08698	-119.776	3.498	2000	San Luis Obispo
206894	*N. fuscipes*	37.78888	-122.146	3.592	2003	Alameda
216804	*N. fuscipes*	37.9043	-122.175	3.761	2004	Contra Costa

217863	*N. fuscipes*	40.66361	-120.793	3.577	2006	Lassen
218015	*N. fuscipes*	37.88603	-122.125	3.821	2004	Contra Costa
218708	*N. fuscipes*	37.38171	-121.737	3.302	2004	Santa Clara
219021	*N. fuscipes*	38.0054	-122.475	3.379	2006	Marin
219027	*N. fuscipes*	38.00053	-122.491	3.515	2006	Marin
219537	*N. fuscipes*	41.2311	-120.398	3.520	2006	Modoc
219572	*N. fuscipes*	41.2311	-120.398	3.631	2006	Modoc
219598	*N. fuscipes*	40.38944	-122.183	3.632	2007	Tehama
220636	*N. fuscipes*	40.84853	-120.768	3.483	2007	Lassen
221488	*N. fuscipes*	38.90445	-121.015	3.517	2008	El Dorado
221493	*N. fuscipes*	38.91554	-121.011	3.167	2008	El Dorado
221496	*N. fuscipes*	38.89364	-121.023	3.100	2008	El Dorado
221614	*N. fuscipes*	39.23901	-120.754	3.138	2008	Placer
221625	*N. fuscipes*	39.19489	-120.832	3.345	2008	Placer
223078	*N. fuscipes*	41.34133	-120.605	3.803	2008	Modoc
225109	*N. fuscipes*	40.9176	-122.24	2.917	2008	Shasta
225235	*N. fuscipes*	38.31666	-122.339	3.559	2006	Napa
230700	*N. fuscipes*	35.32762	-120.864	3.915	2007	San Luis Obispo
15510	*N. lepida*	36.5051	-118.102	3.120	1911	Inyo
16789	*N. lepida*	37.80021	-118.529	3.036	1912	Mono
26336	*N. lepida*	37.79747	-118.568	3.067	1917	Mono
26337	*N. lepida*	36.43934	-117.611	2.865	1917	Inyo
5370	*N. lepida*	34.7347	-118.424	2.986	1904	Los Angeles
5371	*N. lepida*	34.7347	-118.424	3.190	1904	Los Angeles
5383	*N. lepida*	34.7347	-118.424	2.960	1904	Los Angeles
5384	*N. lepida*	34.7347	-118.424	2.984	1904	Los Angeles
6182	*N. lepida*	34.3628	-116.858	2.973	1905	San Bernardino

6968	*N. lepida*	34.7347	-118.424	3.142	1904	Los Angeles
114334	*N. lepida*	40.3619	-120.232	3.176	1950	Lassen
149261	*N. lepida*	33.7457	-114.504	2.893	1974	Riverside
149264	*N. lepida*	33.7457	-114.504	2.861	1974	Riverside
195260	*N. lepida*	32.88713	-114.828	3.024	2000	Imperial
195262	*N. lepida*	32.88713	-114.828	2.947	2000	Imperial
195320	*N. lepida*	34.574	-115.796	3.095	2000	San Bernardino
195928	*N. lepida*	35.61617	-118.253	2.958	2000	Kern
196355	*N. lepida*	34.81681	-115.662	3.109	1998	San Bernardino
197160	*N. lepida*	41.58266	-120.033	2.898	2001	Modoc
197164	*N. lepida*	41.58266	-120.033	2.982	2001	Modoc
198672	*N. lepida*	34.36273	-116.856	3.038	2002	San Bernardino
199789	*N. lepida*	35.37369	-118.163	3.176	2002	Kern
199799	*N. lepida*	35.46656	-118.235	3.076	2002	Kern
202450	*N. lepida*	37.0694	-118.293	3.113	2003	Inyo
215634	*N. lepida*	32.88713	-114.828	3.119	2005	Imperial
215704	*N. lepida*	33.79832	-114.561	2.913	2005	Riverside
215714	*N. lepida*	33.80568	-116.18	3.050	2005	Riverside
219371	*N. lepida*	37.33035	-118.089	3.160	2007	Inyo
220815	*N. lepida*	40.52303	-120.473	3.084	2007	Lassen
220820	*N. lepida*	40.52438	-120.467	3.095	2007	Lassen
223713	*N. lepida*	37.91354	-118.459	2.918	2009	Mono
223717	*N. lepida*	37.80368	-118.456	3.083	2009	Mono
42463	*N. lepida*	34.4737	-117.785	3.175	1929	Los Angeles
60231	*N. lepida*	35.4609	-118.22	3.098	1933	Kern
77609	*N. lepida*	40.3619	-120.232	3.005	1936	Lassen
79371	*N. lepida*	41.5816	-120.072	3.011	1937	Modoc

79372	*N. lepida*	41.5816	-120.072	2.833	1937	Modoc
80245	*N. lepida*	35.1303	-115.386	2.875	1938	San Bernardino
86546	*N. lepida*	35.784	-115.931	3.049	1939	San Bernardino
95024	*N. lepida*	33.37102	-114.731	3.051	1940	Imperial
17971	*N. macrotis*	39.57029	-121.555	3.474	1912	Butte
196593	*N. macrotis*	39.04221	-120.71	3.411	1998	Placer
196594	*N. macrotis*	39.04221	-120.71	3.028	1998	Placer
24678	*N. macrotis*	38.75449	-120.635	3.327	1916	El Dorado
17966	*N. macrotis*	38.40863	-120.919	3.296	1912	Amador
207663	*N. macrotis*	37.66281	-120.48	3.272	2004	Stanislaus
207681	*N. macrotis*	37.51207	-120.398	3.211	2004	Merced
116723	*N. macrotis*	37.09064	-119.721	3.208	1952	Madera
24990	*N. macrotis*	36.7938	-118.581	3.277	1916	Fresno
108716	*N. macrotis*	36.66462	-121.741	3.586	1937	Monterey
16760	*N. macrotis*	36.58926	-118.11	3.274	1912	Inyo
196422	*N. macrotis*	36.37851	-121.557	3.633	1999	Monterey
108722	*N. macrotis*	36.31007	-121.568	3.344	1936	Monterey
231876	*N. macrotis*	36.11381	-117.757	3.513	2015	Inyo
108748	*N. macrotis*	36.01413	-121.515	3.573	1937	Monterey
222721	*N. macrotis*	35.96326	-118.231	2.931	2008	Tulare
196504	*N. macrotis*	35.89846	-121.259	3.508	2001	Monterey
196533	*N. macrotis*	35.7504	-120.773	3.696	2000	San Luis Obispo
196538	*N. macrotis*	35.7504	-120.773	3.554	2000	San Luis Obispo
196540	*N. macrotis*	35.7504	-120.773	3.651	2000	San Luis Obispo
196542	*N. macrotis*	35.7504	-120.773	3.498	2000	San Luis Obispo
14052	*N. macrotis*	35.38948	-120.607	3.355	1911	San Luis Obispo
107648	*N. macrotis*	35.34967	-119.765	3.261	1947	Kern

196780	*N. macrotis*	34.88378	-118.658	3.349	2001	Kern
5548	*N. macrotis*	34.818	-118.884	3.426	1904	Ventura
5340	*N. macrotis*	34.812	-119.146	3.087	1904	Ventura
198325	*N. macrotis*	34.79703	-118.861	3.448	2001	Los Angeles
196556	*N. macrotis*	34.61285	-119.927	3.357	1998	Santa Barbara
3925	*N. macrotis*	34.441	-119.26	3.595	1906	Ventura
125883	*N. macrotis*	34.41816	-117.789	3.294	1955	Los Angeles
125890	*N. macrotis*	34.28244	-117.166	3.157	1953	San Bernardino
3926	*N. macrotis*	34.27364	-119.266	3.447	1906	Ventura
5544	*N. macrotis*	34.26928	-118.336	3.609	1904	Los Angeles
176217	*N. macrotis*	34.13631	-116.768	3.434	1974	San Bernardino
114487	*N. macrotis*	34.10341	-118.444	3.362	1951	Los Angeles
84558	*N. macrotis*	33.88442	-116.994	3.287	1938	Riverside
2352	*N. macrotis*	33.67608	-117.517	3.179	1908	Orange
7573	*N. macrotis*	33.21	-116.6	3.293	1909	San Diego
196535	*N. macrotis*	35.7503974	-120.773	3.558	2000	San Luis Obispo
201919	*N. macrotis*	37.71515	-119.665	3.105	2003	Mariposa
LACMP23 #	**Element**	**Lat.**	**Long.**	**m1 size**	**Deposit**	**County**
28509	left m1	34.0638	-118.355	3.225	1	Los Angeles
31175	left m1	34.0638	-118.355	3.097	14	Los Angeles
31976	left m1	34.0638	-118.355	3.197	14	Los Angeles
33922	right m1	34.0638	-118.355	3.936	14	Los Angeles
34168	left m1	34.0638	-118.355	3.280	14	Los Angeles
35665	right m1	34.0638	-118.355	3.166	7B	Los Angeles
35668	right m1	34.0638	-118.355	3.120	7B	Los Angeles
35780	right m1	34.0638	-118.355	3.536	7B	Los Angeles
35782	left m1	34.0638	-118.355	3.340	7B	Los Angeles

35806	right m1	34.0638	-118.355	3.397	7B	Los Angeles
35934	left m1	34.0638	-118.355	3.245	7B	Los Angeles
36312	right m1	34.0638	-118.355	3.531	7B	Los Angeles
40158	right m1	34.0638	-118.355	3.810	13	Los Angeles
40402	left m1	34.0638	-118.355	3.804	13	Los Angeles

Chapter 4: Community ecology and geochronology of small mammal faunas at Rancho La Brea, Los Angeles, California

4.1 Abstract

Understanding biotic responses to long-term environmental change is critical for anticipating the consequences of anthropogenic disturbances. However, those gradual and sometimes lagged responses are difficult to measure with contemporary ecological data. The Rancho La Brea (RLB) tar pits in Los Angeles, California have produced millions of plant and animal fossils from the climatically unstable late Quaternary period (~50,000 years ago to present) and therefore provide a unique opportunity to study biotic responses to millennial-scale environmental changes before global human impacts. The extent of late Quaternary environmental changes in the local region around RLB, and its impact on the biotic communities of Los Angeles is uncertain due in part to a historical research bias focused on extinct mammalian megafauna. To accurately assess paleoenvironmental processes at RLB and elsewhere, it is critical to examine locally restricted biota. I therefore identified small mammal fossils from four RLB deposits (Project 23 Deposits 1, 7B, 13, and 14) and evaluated changes in their composition, taxonomic diversity, and trait diversity to estimate late Quaternary environmental changes in this region. I sampled over 2,000 small mammal specimens from at least 18 unique taxa among the four deposits. Sixty radiocarbon dates were obtained from a subset of specimens across deposits to establish the age boundaries of each. Overall, the composition of species present in Project 23 was similar to historic faunas of the Los Angeles (LA) Basin. However, differences in taxonomic diversity and trait diversity occurred among the deposits. Radiocarbon ages vary extensively within and among deposits and range from >50,000 to ~30,000 calibrated years BP, indicating an exclusively Marine Isotope Stage 3 (MIS 3) depositional period. Some deposits have different mean ages facilitating general assessments of long-term community change between them while others overlap extensively. Results indicated that overall younger deposits have communities with cooler, wetter, and larger body size traits than overall older deposits, and that taxonomic diversity and evenness generally decreases towards the Last Glacial Maximum. Together, these findings suggest that while no major biome shifts occurred in the LA Basin between MIS 3 and recent times, the organization of small mammal communities was measurably impacted by environmental changes over ~25,000 years during the last glacial period. Considering these results, the comparatively rapid environmental changes occurring in anthropogenically dominated landscapes of the LA Basin today could have a larger impact on the small mammal communities that reside there.

4.2 Introduction

Ecological communities are changing rapidly today in response to myriad global changes, including habitat loss and degradation, trophic downgrading due to targeted removal of large-bodied species, spread of invasive species, and climatic change (Barnosky et al., 2017; Blois et al., 2013; Estes et al., 2011). Attributing changes to

climate, as opposed to other potential drivers of diversity loss and species turnover, is important for understanding and predicting the extent to which biotic communities will continue to be affected by anthropogenic climate change. However, it can be difficult to determine the importance of climate in driving diversity change using contemporary time series alone, in part because it is difficult to determine the baseline composition against which to compare changes using short time series data, mostly collected when humans were already modifying the landscape substantially (e.g., Gonzalez et al., 2010; Vellend, 2010). The longer time series typically captured by paleoecological data is therefore useful to gain a better understanding of baseline community composition and the degree to which changes in composition are influenced by climate. A variety of studies have shown that communities changed substantially over the last twenty thousand years, particularly due to climatic changes at the transition from the last glacial to interglacial period (Blois et al., 2010; Grayson, 2006; Williams & Jackson, 2007). Yet this time period also coincided with increasing human impacts and landscape transformation resulting from human-driven loss of the megafauna. Such losses may drive changes in community composition of the surviving plants and animals independent of climate through their cascading effects on the broader ecosystem and food web (e.g., Gill et al., 2009; Malhi et al., 2016). Studies of compositional change, and the importance of climate in driving change, before the last Glacial Maximum (LGM, ~26,000 to 18,000 years before present (BP)) and prior to megafaunal extinctions are rare, but crucial for establishing baseline estimates of community composition and change. Here, I use a series of pre-LGM fossil deposits that capture a rich small mammal assemblage to answer two questions:

1) Did community composition and diversity systemically change through time during glacial conditions?

2) To what extent are compositional changes in communities reflective of past climatic changes?

One of the most prolific fossil localities in western North America, Rancho La Brea (RLB), is particularly well-suited for studies of biotic responses to millennial-scale environmental change. Asphalt deposits at RLB, a renowned late Quaternary lagerstätte in Los Angeles, California (34°03′48″N, 118°21′20″W), have yielded millions of well-preserved plant and animal fossils spanning >50 thousand years ago to the present (Fig. 4.1). The abundance of fossils accumulated at this site, coupled with the climatically unstable geologic period from which they were deposited, makes RLB an ideal site for studies of prehistoric biotic interactions (Coltrain et al., 2004; DeSantis et al., 2019; Feranec et al., 2009; Meachen et al., 2014a) and intraspecific responses to climate change (Desantis et al., 2011; Meachen et al., 2014b; O'Keefe et al., 2014; Prothero et al., 2012; Raymond & Prothero, 2011). Additionally, paleoclimate data from marine and lake sediment cores in and along the edge of western North America indicate that episodic warming and cooling intervals occurred in the region during the last 60,000 years (Glover et al., 2017, 2020; Hendy et al., 2002; Hendy & Kennett, 1999; Heusser, 1998; Heusser et al., 2015) (Fig. 4.2). Those oscillations fluctuated around a relatively stable and cool mean temperature until ~35 thousand years ago (ka) at which time the climate oscillated

towards a cooler system as the earth approached the LGM. Following the LGM, temperatures warmed rapidly from the start of the last deglaciation through the Pleistocene-Holocene transition (~18,000–11,000 BP) (Hendy et al., 2002; Hendy & Kennett, 1999) (Fig. 4.2). Thus, fossil deposits from RLB have the potential to capture rich ecological communities from climatically variable time periods that pre-date extensive human impacts as human occupation of North America is generally thought to have occurred after 16,000 BP.

Despite the longevity of paleoecological and paleoenvironmental research conducted at RLB over the last century, there is no consensus on the magnitude and direction of paleoenvironmental changes that occurred there (Holden et al., 2017; Stock & Harris, 1992). Paleoclimate patterns such as those obtained from the surrounding region (e.g., Baldwin Lake (Glover et al., 2017, 2020), Diamond Valley (Anderson et al., 2002), Lake Elsinore (Heusser et al., 2015), and the Santa Barbara Basin (Hendy et al., 2002; Hendy & Kennett, 1999) (Fig. 4.2) provide baseline estimates that support hypotheses and predictions of past biotic responses to climate change in California. But local environments can be dissimilar from regional signals due to small-scale changes in topography, vegetation, and atmospheric and oceanic conditions across space and time (Sandel et al., 2011). An alternative to relying on regional patterns of climate is to use the fauna itself to indicate paleoenvironment. Fossils of small mammals (e.g., rodents, lagomorphs, and soricomorphs) are often used for biostratigraphic, biogeographic, and paleoenvironmental research (Cuenca-Bescós et al., 2009; Grayson, 1987, 2006; Martin, 2019; Simonetti, 1989) because they are ubiquitous across Cenozoic fossil assemblages (Kurtén & Anderson, 1980; Martin, 2019). Further, these taxa tend to occupy small home ranges due to their size-mobility constraints and short lifespans (Grayson, 2006; Somerville et al., 2018), and many species are confined to specific habitats and/or narrow geographic ranges (Cuenca-Bescós et al., 2009; Samuels & Hopkins, 2017; Smartt, 1977). Small mammals are therefore sensitive to local environmental changes and their remains are good indicators of past environmental conditions. For example, small mammal community turnover has been shown to track major climatic events such as the last deglaciation (Blois et al., 2010), and early Holocene warming (Grayson, 2006). However, these taxa are an understudied component of paleontological faunas overall (Samuels & Hopkins, 2017; Stock & Harris, 1992). Despite their relative abundance and utility for understanding past environments and environmental change, research on small mammal fossils has been relatively limited at RLB (Stock & Harris, 1992) (but see Compton, 1937; Dice, 1925; Fox et al., 2019; Mychajliw et al., 2020; Whistler, 1989). All RLB small mammal studies published thus far lack large sample sizes of multiple environmentally informative taxa and good radiocarbon age-control, so comprehensive analyses of the RLB small mammal communities is warranted.

Here, I rely on the RLB small mammal faunas to first evaluate changes in taxonomic composition and diversity through time in the LA Basin. Then, I assess the extent to which community changes are reflective of past climatic changes by testing the relationships between regional climate and small mammal community structure. The fundamental assumption here is that Pleistocene small mammals were sensitive to any major long-term environmental changes that occurred in the focal region. Thus, if the

small mammal communities of RLB are relatively stable through time, then climates of the LA Basin will be stable during their entrapment period as well. Alternatively, if small mammal communities changed substantially during the late Quaternary, then climate will also change, and community diversity and trait changes will mirror regional climate changes through time. Mismatch between changes in the small mammal assemblage and regional climates could indicate differing local microclimate conditions, but also may be due to taphonomic or analytical factors.

4.3 Methods

4.3.1 Study system

To explore relationships between small mammal assemblage composition and environmental change, I examined a subset of recently discovered deposits at RLB collectively known as Project 23 (P23). Sixteen new fossiliferous asphalt seeps were discovered in 2006 during the construction of an underground parking structure at the Los Angeles County Museum of Art adjacent to the La Brea Tar Pits and Museum (LBTPM; Fig. 4.1). Due to time and budget constraints, the deposits were encased in twenty-three wooden crates (several deposits were too large for a single crate) and removed for subsequent excavation by LBTMP staff and volunteers in Hancock Park (Fox et al., 2019; Fuller et al., 2014; Holden et al., 2017; Mychajliw et al., 2020) (Fig. 4.1). These P23 deposits provide new opportunities to excavate *in situ* fossils of megafauna, microfauna, and flora with modern systematic sampling protocols and improved spatial context (Mychajliw et al., 2020). Project 23 research thus far has focused primarily on the faunas of Deposit 1 (Fuller et al., 2020; Holden et al., 2017; Mychajliw et al., 2020) and less is known about the paleoecology of other P23 deposits.

4.3.2 Sampling and identification

Each Project 23 deposit was systematically excavated in 1 m^2 x 0.25 m depth grids; this has resulted in thousands of well-preserved fossils (Fox et al., 2019). Fossiliferous matrix from each grid/level excavation is collected in 5-gallon metal buckets, heat-treated with biodiesel and *n*-propyl bromide to remove asphalt, and stored in one-gallon canisters for screening and sorting (Mychajliw et al., 2020; Rice et al., 2015). I selected and screened a subset of canisters from various grids within P23 Deposits 1, 7B, 13, and 14 following the sampling protocol of Fox et al. (2019). I systematically chose one canister per grid from Deposit 1 to assess variation in taxa and dates among grids but found no systematic differences in community composition or specimen ages among grid cells, supporting other observations of a lack of meaningful stratigraphy within RLB deposits (O'Keefe et al., 2009). For subsequent deposits, I haphazardly sampled canisters from a subset of the available grids for a deposit, stopping once the full diversity of the fauna was captured (assessed via rarefaction, see below). Matrix was screened in 4 (4760 μm), 8 (2380 μm), and 16 (1190 μm) mesh sieves; approximately 4.5 kg of matrix was screened per canister on average. Small mammal craniodental elements were then sorted from the residual material for taxonomic identification. Taxa were identified to subfamily or lower using diagnostic characters

from the literature and/or morphometric analysis (see Appendix 4.9.1, Systematic Paleontology for details). All identified fossils (Appendix Table 4.9.2) are cataloged and housed in Los Angeles County Museum Project 23 (LACMP23) collections.

4.3.3 Geochronology

A subset of small mammal fossils obtained from this study were radiocarbon dated to determine where each deposit's fauna is positioned temporally. Additional specimens from Project 23 Deposits 1, 7B, 13, and 14, acquired outside the sampling effort of this study, were radiocarbon dated to increase sample size. Large samples of dates are necessary to assess the age boundaries of each deposit because extensive time-averaging occurs in most RLB deposits, often spanning several thousand years or more (Fuller et al., 2014, 2020; O'Keefe et al., 2009). Further, age offsets can occur between different taxonomic groups within the same deposit (Holden et al., 2017), so age distributions obtained from megafauna, plants, or insects are not necessarily applicable to small mammal faunas. To establish a small mammal chronology for each deposit, 77 specimens were sampled in total. All specimens were radiocarbon dated at the UC Irvine Keck Carbon Cycle Accelerator Mass spectrometry (AMS) Laboratory using a National Electrostatics Corporation 0.5 MV 1.5SDH-1 Pelletron. Fossil elements were sampled either in full or sectioned with a handheld Dremel rotary tool depending on how much material was available. Only specimens with initial bone weights >200 mg were selected for destructive analysis since anything lighter is unlikely to yield enough collagen for AMS (J. Southon, UC Irvine, personal communication). All RLB fossils are contaminated with asphalt due to their depositional setting, but accurate radiocarbon dates are attainable from bone collagen through various petroleum removal measures (Fox-Dobbs et al., 2006; Friscia et al., 2008; Fuller et al., 2014, 2015; Marcus & Berger, 1984; O'Keefe et al., 2009). Specimens were prepared for AMS using the recent ultrafiltration procedure of Fuller et al. (2014) and analyzed as graphitized CO_2 acquired from ~2 mg of purified collagen. Following AMS, radiocarbon ages were calibrated in OxCal v.4.3.2 using the IntCal13 calibration curve (Reimer et al., 2013). The median of the Bayesian probability age distribution of each specimen was then used for paleoclimate comparisons.

4.3.4 Paleoclimate

To determine whether potential small mammal community changes between deposits and through time are reflective of climate change, I relied on a high-resolution paleoclimate dataset from the Santa Barbara Basin ODP Hole 893A (Hendy et al., 2007). I estimated deposit-specific paleoclimates based on the planktonic foraminifera (*Neogloboquadrina pachyderma*) $\delta^{18}O$ values (Hendy et al., 2007) from the small mammal age range of each P23 deposit. These isotopes reflect temperature changes near the base of the Pacific Ocean thermocline which record regional sea surface temperature patterns comparable to the Greenland Ice Core in direction and magnitude (Hendy & Kennett, 1999) (Fig. 4.2). Because there are multiple ways to calculate the age range of a deposit, I calculated several different age ranges to test analytical sensitivity. First, deposit age ranges were determined using the median of the OxCal calibrated age distribution of the oldest and youngest specimen from each. Deposits yielding oldest age

estimates >50,000 radiocarbon years BP were assigned an upper age of 50,000 cal BP for this estimate. I then extracted all $\delta^{18}O$ values available within this age range and calculated the mean $\delta^{18}O$ for that time interval. Second, I linearly interpolated the original $\delta^{18}O$ values, then extracted the estimated foraminiferal $\delta^{18}O$ corresponding to the mean and median calibrated age estimate of each dated specimen per deposit. Specimens with radiocarbon ages beyond the measurable limit of ~50,000 years were necessarily excluded from these estimates. I then calculated the mean $\delta^{18}O$ across all specimens in a deposit. Three different estimates of average paleoclimates for each deposit were thus measured: non-interpolated, mean-interpolated, and median-interpolated $\delta^{18}O$. *Neogloboquadrina pachyderma* $\delta^{18}O$ is negatively correlated with marine thermocline temperature (Hendy & Kennett, 1999) (Fig. 4.2). Therefore, deposits yielding lower mean $\delta^{18}O$ values indicate that they were active during overall warmer climates and higher mean $\delta^{18}O$ values indicate that deposition occurred during relatively colder climates.

4.3.5 Compositional diversity

Small mammals did not experience the elevated rate of extinction seen in larger mammals across the late Quaternary (Koch & Barnosky, 2006), so most fossil species are extant, and many contemporary LA Basin small mammals occur in a wide variety of habitats (Chapman & Willner, 1978; Smith et al., 2016). Therefore, fossil species occurrences alone may be inadequate for tracking local environmental changes through time if similar species are present in P23. Other metrics of community composition such as relative abundance can be useful for tracking paleoenvironments even if the analyzed taxa are environmental generalists (Simonetti, 1989), because small mammal abundance can vary across habitats, climate, and time within a species (Terry et al., 2011). In addition to determining the presence and richness of small mammal taxa in P23, deposit-specific faunas were evaluated based also on their relative abundance and diversity. Only elements of crania, dentaries, and cheek-teeth were considered for abundance and diversity analysis, because they tend to be the most diagnostic among taxa. Other elements such as incisors and postcrania were not considered because they are more diagnostic in some taxa (e.g., leporids) than others and therefore may skew relative abundance calculations. Due to time-averaging and the lack of stratigraphy within RLB deposits (Fuller et al., 2014, 2015; O'Keefe et al., 2009), community composition metrics were calculated based on the entire assemblage of each deposit. Relative abundance was calculated based on the number of individual specimens per taxon (NISP), per deposit, divided by the total NISP of all small mammal taxa per deposit. Rank and log abundance were calculated using the "rankabundance" and "rankabunplot" functions in the R package BiodiversityR (Kindt & Coe, 2005). In addition, rarified diversity was calculated via the Hill number $q = 1$ (i.e., Shannon diversity, (Chao et al., 2014; Hill, 1973)) in the R package iNeXT (Hsieh et al., 2020).

4.3.6 Trait diversity

To quantify trait diversity, I calculated the weighted community average of macroecological traits with links to climate (i.e., species temperature affinity and precipitation affinity) for each P23 deposit. Note that here I am using traits measured

across the contemporary range of each species to quantify environmental change, rather than more traditional morphology-based functional traits (e.g., tooth crown height). I extracted six bioclimatic variables from WorldClim (Fick & Hijmans, 2017) at 5' grid resolution: mean annual temperature (°C, BIO1), maximum temperature of the warmest month (°C, BIO5), minimum temperature of the coldest month (°C, BIO6), annual precipitation (mm, BIO12), precipitation of the wettest month (mm, BIO13), and precipitation of the driest month (mm, BIO14) from the contemporary range of each species identified in each deposit. Species range data were obtained from (Patterson et al., 2007). The median value across the range of each species was then used to calculate average community-weighted trait values for each bioclimatic variable.

In addition, normalized difference vegetation indices (NDVI) were quantified using the mean monthly NDVI raster dataset for North America at 10' spatial resolution in the R package "grassmapr" (Powell et al., 2019). NDVI is calculated from satellite measurements of near-infrared light (NIR) and red light (Red) reflected on Earth surfaces using the equation: (NIR - Red)/(NIR + Red) (Pettorelli et al., 2011). Those measurements are highly correlated with plant dry matter on terrestrial landscapes. For example, landscapes covered in green vegetation exhibit high near-infrared reflectance, and therefore have more positive NDVI values, while barren landscapes have values closer to zero (Pettorelli et al., 2011). NVDI was averaged across all months in the year 2001 (Powell et al., 2019) and extracted from species range polygons (Patterson et al., 2007). NDVI median values across the range of each taxon was then used to estimate relative vegetation cover, with higher NDVI values indicating a taxonomic affinity for more densely vegetated habitats than lower values. I expect relative NDVI patterns among taxa and deposits to mirror relative changes in precipitation affinity due to the correlation between precipitation and green vegetation density in many ecosystems (e.g., Wang et al., 2003).

One conventional phenotypic functional trait, body size, was also quantified because it varies climatically in some mammals over millennial scales (Smith et al., 1995). Bergmann's rule, proposed as a potential mechanism for the correlation between body size and climate, states that endothermic vertebrates living in colder climates are generally larger than their counterparts at lower latitudes and in warmer climates due to differences in thermoregulatory efficiency driven by size-based changes in surface area-to-volume ratios (Bergmann, 1847; Mayr, 1956). Bergmann's rule is usually tested on contemporary populations over a large geographic area, but it can be applied to measure *in situ* population responses to climate change over time (Meachen et al., 2014b; O'Keefe et al., 2014) and community-level size changes (Blackburn & Hawkins, 2004; Classen et al., 2017) as well. If Bergmann's rule is followed by the small mammal communities of P23, and if late Quaternary climates of the LA Basin changed through time, then I expect small mammal paleocommunities deposited during cooler time periods to be overall larger than those deposited during warmer time periods. To examine this, deposit-averaged body size was calculated for each community at the species level using average adult body size from PanTHERIA (Jones et al., 2009). Thus, any changes in mean body size among deposit communities from this calculation will reflect interspecific compositional change rather than intraspecific morphological change.

Quantifying mean trait diversity among deposit communities is useful for estimating the direction of environmental change that likely occurred within the depositional period of P23 (e.g., transitions from a warm system to an overall cooler system). However, those data provide little context for temperature and precipitation differences between the last glacial period and today. Species climate-limiting traits (i.e., the maximum value of maximum temperature of the warmest month (max_BIO5), the maximum value of annual precipitation (max_BIO12), the minimum value of minimum temperature of the coldest month (min_BIO6), and the minimum value of annual precipitation (min_BIO12) across the range of each species) was therefore recorded to identify paleoclimate-limiting conditions. These values indicate the minimum and maximum temperature and precipitation conditions that extant members of fossil species occur in today, which may inform overall niche-limiting conditions (recognizing that these values are based on realized rather than fundamental niches (Colwell & Rangel, 2009)). Species with the lowest observed maximum temperature and maximum precipitation tolerances, and highest observed minimum temperature and minimum precipitation tolerances, can inform paleoclimate-bounding conditions such that conditions were likely not above/below those thresholds in the past if the limiting species is present in that assemblage.

Because they are average values from across the contemporary distribution of species found in the past at RLB, all traits calculated here are reflective of the environmental conditions occupied by the species today. An inherent assumption I am making with these calculations is that the environmental affinity of each species has not changed substantially over the last 50 thousand years. Even if the geographic range of each identified P23 species, and environmental conditions within those ranges, were dissimilar during the late Pleistocene versus today, I assume that fossil members of extant small mammal species occupied similar niches during the late Pleistocene. If this assumption is true, then relative differences in trait values among taxa and deposits should be environmentally informative even if actual trait values vary between the past and today.

I calculated average community-weighted trait diversity as the weighted mean of each individual bioclimatic, NDVI, and size trait variable across all specimens in a deposit. Specifically, I multiplied the NISP of each species per deposit by its range-averaged contemporary trait value, summed across species, and then divided by the total NISP of each deposit. Species affinity was assumed for weighted trait analysis based on congeneric species identified from other P23 elements for elements only identifiable to genus. For example, all craniodental remains of *Microtus* are assumed to be *M. californicus* because *M. californicus* is the only definitive species identified from diagnostic elements in P23 (see Appendix 4.9.1, Systematic Paleontology). In the case of polytypic P23 taxa such as *Sylvilagus* spp., relative abundances of species were estimated based on the ratio of species-identifiable elements per deposit. For example, if seven species-diagnostic elements were identified as *S. audubonii* and three were identified as *S. bachmani* in a deposit, then 70% of non-species identifiable *Sylvilagus* elements would be assigned to *S. audubonii* and 30% would be assigned to *S. bachmani* for weighted trait analysis.

4.3.7 Sensitivity analyses

One limitation of using contemporary range-averaged trait values is that trait means may be unequally informative across species due to differences in the size of species geographic distributions. Some fossils at RLB may be from species with narrow contemporary distributions and others may be of cosmopolitan species that occur in many other parts of North America today. To test the sensitivity of trait diversity results on range size, I grouped the P23-identified species into three datasets based on the overall size of their distributions. The first dataset, hereafter referred to as the "continental" dataset, contained all identified fossil taxa regardless of range size. The second, hereafter referred to as the "regional" dataset, contained only taxa with >50% of their range occurring west of the Rockies. The third, hereafter referred to as the "local" dataset, contained only taxa with >50% of their range occurring west of the Sierra. Because identification confidence is also not equal across taxa (see Appendix 4.9.1, Systematic Paleontology), I also evaluated the impact of identification fidelity and taxonomic predictors (i.e., the number of taxa used to inform trait diversity) on community trait analyses. Here, datasets were split into three additional categories according to species identification criteria. A "known" species dataset was assembled that included only taxa that were confidently identified to species. Next, a "tentative" species dataset was assembled that included taxa identified to species and also taxa with "cf." species designations. Note that my use of "cf." before a Latin nominal in this study is not interchangeable with "?". Here, "cf." indicates that a specimen is comparable to the referred taxon while "?" indicates that the specimen is likely the referred taxon. Thus, "?" indicates greater taxonomic confidence than "cf.". Specimens with "?" identifications at the species-level (see Appendix 4.9.1, Systematic Paleontology) were binned as "known" rather than "tentative" for these analyses. Finally, an "estimated" species dataset was assembled that, in addition to including "known" and "tentative" species, assumed species-level identification of taxa only identified to genus in this study based on congeneric species identified in previous RLB small mammal studies (i.e., Compton, 1937; Dice, 1925; Whistler, 1989). For example, I am unable to identify *Dipodomys* to species (cf. or otherwise), so *Dipodomys* is not included in the "known" and "tentative" species lists. However, Dice (1925) identified *Dipodomys* from other RLB deposits as *D. agilis*, so I used range-averaged trait data of *D. agilis* in the "estimated" species dataset. These spatial and taxonomic sensitivity tests resulted in nine versions of the faunal assemblages at each P23 deposit, with the number of species per dataset ranging from four to 17. See Appendix Table 4.9.4 for a list of species and their trait values included in each dataset.

4.3.8 Relating compositional and trait diversity to climate

The average community-weighted trait of each deposit's fauna was compared with the mean $\delta^{18}O$ climate estimate of the same deposit to determine if a relationship occurs between climate and community traits across deposits. If the small mammal communities of RLB have changed in response to late Quaternary climate, then I expect the abiotic and biotic proxies of climate to show the same rank-order of change among deposits and through time overall. For the sensitivity test datasets, I expected that species

with the narrowest climate ranges (roughly corresponding to those with the smallest geographic distributions) to be most informative. However, the number of taxa and individuals is also lower, so I am only capturing a small portion of the community with these taxa. On the other hand, species with continental distributions may be so generalized as to be uninformative. I do not expect bias towards or against particular trait values based on estimates of taxonomic certainty in the sensitivity datasets, but sample size changes across the three taxonomic datasets may affect trait values. Because uncertainty in species assignments is greatest in the "estimated" dataset, trait values therein may be most dissimilar from true community traits if several species are misidentified.

4.4 Results

4.4.1 Community analysis

I identified 2,440 small mammal specimens to subfamily or lower across all four deposits, representing at least 18 unique taxa (Appendix 4.9.1 & Appendix Table 4.9.2). Overall, community composition of P23 is quite similar to the historic small mammal faunas of Los Angeles (Dice, 1925). All taxa identified to species are extant and many still reside in or near the LA Basin today. Taxonomic composition across deposits is generally similar, with some exceptions. Within this P23 sample, for example, *Onychomys* is tentatively identified only in Deposit 13 and *Scapanus* is only found in Deposit 7B (Table 4.1). Differences also occur in the relative abundance of taxa among deposits (Figs. 4.3 & 4.4). *Sylvilagus* is the most abundant genus in Deposits 1, 7B, and 13, but *Microtus* is most abundant in Deposit 14 (Table 4.1; Fig. 4.4), and the rank-order of the four most abundant genera are not congruent in any two deposits (Fig. 4.4). Taxonomic evenness (Fig. 4.4) and rarefied diversity (Fig. 4.5) are also dissimilar among the four deposits; Deposit 7B has the most diverse and most even fauna, and Deposit 1 has the least diverse and least even fauna.

4.4.2 Geochronology

Most P23 fossils yielded sufficient collagen for radiocarbon dating (Table 4.2). However, geochemical preservation in Deposit 14 was notably poorer than the other three deposits. Of the 77 specimens sampled, 17 yielded insufficient collagen for AMS (Appendix Table 4.9.3). All dated specimens produced ages between ~26,000 and >50,000 radiocarbon years BP, indicating an exclusively Marine Isotope Stage 3 (MIS 3) entrapment period (Siddall et al., 2008) (Table 4.2). Age distributions of all four deposits overlap, though some are narrower than others (Fig. 4.6). Deposit 1 exhibited the narrowest age distribution, with most specimens dating between ~30,000 and ~37,000 radiocarbon years BP (Table 4.2; Fig. 4.6) and Deposit 14 exhibits the most time-averaging. Dates from Deposit 14 range from ~26,000 to >50,000 radiocarbon years BP, spanning the entirely of the P23 age distribution, with two main clusters at ~25,000-29,000 and >45,000 radiocarbon years BP (Fig. 4.6). Median radiocarbon ages were 35,440 BP, 35,765 BP, >36,870 BP, and 42,050 BP for Deposits 1, 13, 14, and 7B respectively (Table 4.2; Fig. 4.6).

4.4.3 Paleoclimate

Averaged $\delta^{18}O$ data from the marine foraminifera climate dataset of Hendy et al. (2007) captured marginally different climate windows within the age range of each deposit, despite their vastly overlapping age distributions (Fig. 4.6; Appendix Table 4.9.7). $\delta^{18}O$ averages were similar among calculations using non-interpolated, mean-interpolated, and median-interpolated calibrated ages such that the rank order of values among deposits were concordant in each (Appendix Table 4.9.7). Hereafter, I refer to average $\delta^{18}O$ values based on median-age interpolations (i.e., $\delta^{18}O$ = 2.040, 1.938, 2.285, and 1.798 for Deposits 1, 13, 14, and 7B respectively) because interpolated values are more fitted to deposit-specific age distributions. $\delta^{18}O$ suggests that Deposit 7B captures the warmest climate overall and Deposit 14 captures the coldest climate overall (Appendix Table 4.9.7). However, many Deposit 14 dates were older than the AMS limit; interpolated $\delta^{18}O$ values could not be obtained from ~40% of Deposit 14 dates with mean and median calibrated ages >50,000 years (Table 4.2). Due to the bimodal distribution of Deposit 14 dates clustered near the upper and lower age limits of P23 (Fig. 4.6), $\delta^{18}O$ values from Deposit 14 were likely skewed much colder than their true value since they predominantly reflect dates nearest the LGM (~30,000 years calibrated BP; Table 4.2; Fig. 4.2). Thus, climate estimates for Deposit 14 are thus unlikely to reflect trait estimates inferred from the fauna, which presumably includes specimens entrapped during older and warmer times as well as during younger and colder times (Figs. 4.2 & 4.6). Consequently, Deposit 14 is excluded from subsequent community climate-trait comparisons.

4.4.4 Community traits

Average community-weighted trait data varied slightly among spatial and taxonomic species pool combinations, especially between spatial extremes (i.e., local versus continental scales) and taxonomic extremes (i.e., known versus estimated species identifications); however, results were relativity consistent within trait variables overall (Figs. 4.7-4.10, Appendix Figs. 4.9.3-4.9.6). Mismatches in the rank-order of difference between average climate estimates (marine foraminifera $\delta^{18}O$) and average community traits often occurred between Deposits 1 and 13 but are relatively consistent for Deposit 7B (Figs. 4.7-4.10; Appendix Figs. 4.9.3-4.9.6). For example, Deposit 13 exhibited the overall coldest and wettest community trait signal for some variables and species pool combinations, but Deposit 1 exhibits the coldest and wettest signal for others (Figs. 4.7-4.8; Appendix Figs. 4.9.3-4.9.6). However, in most cases Deposit 7B exhibited the warmest, driest, and least vegetated community trait signal regardless of variable and species pool combination (Figs. 4.7-4.9; Appendix Figs. 4.9.3-4.9.6). Similarly, Deposit 1 sometimes showed the overall largest body-sized small mammal community (based on PanTHERIA data), but other times Deposit 13 had the largest fauna depending on the species pool used. In all cases, the community-averaged body size of Deposit 7B was the smallest overall (Fig. 4.10).

Extraction of climate-limiting traits across the contemporary range of each identified P23 species suggested that *Neotamias merriami* occurs in locations with

coolest maximum temperatures (39.6 °C), *Sylvilagus bachmani* occurs in areas with warmest minimum temperatures (-9 °C), and *Dipodomys agilis* occurs in areas with both the least maximum annual precipitation (836 mm) and greatest minimum annual precipitation (77 mm; Appendix Table 4.9.4).

4.5 Discussion

Late Quaternary paleoenvironments of the LA Basin are poorly understood due, in part, to age uncertainties and time-averaging within and among deposits (Fuller et al., 2014; O'Keefe et al., 2009) and a historical research bias towards mammalian megafauna. Extinct megafauna provide little information about local environmental conditions due to their broad distributions throughout North America during the Pleistocene (Mychajliw et al., 2020; Stock & Harris, 1992). The few studies of taxa with local paleoenvironmental context for RLB have generated dissimilar conclusions on the magnitude and direction of environmental change that occurred between the late Quaternary and today. Research on some plant (Warter, 1976) and invertebrate (Lamb, 1989) fossils suggests that late Pleistocene environments of the LA Basin were substantially cooler and more mesic than today. Pollen data from marine sediment cores suggests that much of southern California may have been covered in closed-canopy vegetation during the late Pleistocene, with conifer forests and annual precipitation around 1000 mm (Heusser, 1995, 1998), rather than the more open and arid chaparral environments present throughout much of southern California today. However, research on other RLB microvertebrate and invertebrate faunas suggests that the LA Basin may have been a climatic refugia in which late Pleistocene environments are largely similar to contemporary environments (Dice, 1925; Doyen & Miller, 1980; Holden et al., 2017; Johnson, 1977), or even warmer and dryer than today (Compton, 1937).

To accurately assess responses of biota to past environmental changes, the extent and direction of those changes must be better resolved. To accomplish this, researchers must: 1) examine locality-confined faunas and floras that are sensitive to – and reflective of – habitat change; and 2) collect a large sample of individually dated specimens or collect specimens from deposits with good age control to manage time-averaging effects. Only one study of RLB biota has met both of these criteria, finding that environments of the LA Basin have been largely similar during the past 50,000 years based on the environmental tolerances of extant individuals of identified and dated fossil insect species (Holden et al., 2017). Additional research on other locally restricted biota is needed to better establish the local paleoenvironmental context of this site (Holden et al., 2017). To contribute to our understanding of past environments and environmental change through time, I sampled over 2,000 individual small mammal fossils from four well-dated RLB Deposits (P23 Deposits 1, 7B, 13, and 14) and evaluated their community composition, rarified diversity, and trait diversity. Those analyses were performed to determine whether the community structure of environmentally sensitive small mammals systemically changes with regional climate (a proxy for local climate) during the last glacial period.

4.5.1 Community composition

Fossil small mammal species identified in P23 were similar to contemporary faunas of the LA Basin (Dice, 1925; Stock & Harris, 1992). Extant members of most identified species inhabit relatively open and semiarid environments including those of the LA Basin today (Dice, 1925). Other taxa such as *Sylvilagus bachmani* and *Neotamias*/*Tamias* generally prefer more densely vegetated habitats (Best & Granai, 1994; Chapman, 1974), and *Sorex* and *Scapanus latimanus* prefer more mesic habitats, than other members of the P23 community (Owen & Hoffmann, 1983; Verts & Carraway, 2001). However, such requirements could be provided by microtopographic features such as stream channels and associated riparian vegetation that may have been present at RLB in the past (Stock & Harris, 1992). The apparent absence of arboreal (e.g., *Glaucomys*, *Sciurus*) and semiaquatic (e.g., *Castor*, *Ondatra*) taxa suggest that paleoenvironments of P23 were not dominated by woodlands or large bodies of freshwater.

In addition to their overall similarity with contemporary LA faunas, the small mammals of P23 were nearly identical in composition to those of other RLB localities, including Pits 1059, 2050, 2051, and 2052 (Compton, 1937; Dice, 1925), that are geologically younger than P23 (O'Keefe et al., 2009). Two exceptions include *Lepus californicus* (black-tailed jackrabbit) and *Notiosorex crawfordi* (Crawford's gray shrew) which have not been identified in P23 but are present in other RLB deposits (Compton, 1937; Dice, 1925; N. Fox personal observation, 2018). *Notiosorex crawfordi* is relatively common in Pit 2051 (Compton, 1937) and *L. californicus* is rare at RLB (Dice, 1925; N. Fox personal observation, 2018). Thus, it is possible that these taxa were only present intermittently at RLB, though absence data should be interpreted cautiously in the fossil record (Lyman, 2008). In any case, there was no evidence for substantial small mammal community turnover among the faunas of different RLB deposits or between the late Pleistocene and contemporary LA faunas overall, indicating relative climatic stability.

Some features of the LA Basin small mammal community suggest that there may not be a tight link between the small mammal community and environment. Many of the identified species at RLB are habitat generalists and therefore changes in the environment may not reflect changes that occurred locally in species occurrence data (though relative abundance and other diversity metrics can provide more insight; Simonetti, 1989). Marked differences in the relative abundance of some taxa occurred among P23 deposits and between P23 and non-P23 localities in general. For example, *Thomomys bottae* (Botta's pocket gopher) was the most common small mammal species found in Pit 2051 (Dice, 1925), which post-dates sampled P23 deposits overall (mean radiocarbon age = 22,692 (O'Keefe et al., 2009)) but it is relatively uncommon in all P23 deposits aside from Deposit 7B (Table 4.1; Fig. 4.6). Even among P23 deposits there are marked differences. For example, *Sylvilagus* is the most common genus in all Project 23 except Deposit 14, where *Microtus* is the dominant taxon, and no two P23 Deposits exhibit the same top four genus-rank abundances (Table 4.1; Fig. 4.6). *Scapanus* is also found only in Deposit 7B and *Onychomys* is only identified in Deposit 13 (Table 4.1). However, *Scapanus* and *Onychomys* are rare in P23, so it is possible that their absence in other deposits is due to taphonomic effects and/or unequal sampling efforts rather than true absences.

In addition to presence and abundance, diversity changes occurred among P23 Deposits. Results showed that Deposit 7B was the most diverse and Deposit 1 was the least diverse of the four deposits examined (Figs. 4.4 & 4.5). This is notable because P23 research thus far has largely focused on Deposit 1 (Fuller et al., 2020; Holden et al., 2017; Mychajliw et al., 2020). Changes in the presence, relative abundance, and diversity of taxa could be facilitated by many pre-and post-depositional factors, the latter of which is poorly understood for most RLB deposits (Friscia et al., 2008; Spencer et al., 2003). Quantifying deposit age distributions in tandem with climate and community trait analysis may help determine whether climate is likely a contributing factor to such changes.

4.5.2 Geochronology

Most small mammal elements sampled from Deposits 1, 7B, and 13 yielded good-quality collagen (Table 4.2), but preservation in Deposit 14 is notably poorer – 14 of 35 specimens sampled from Deposit 14 (40%) yield insufficient collagen for AMS (Table 4.2; Appendix Table 4.9.3). This may be due in part to the relatively advanced age of Deposit 14 overall; 9 of 21 AMS-analyzed specimens (~43%) date from 45,000 radiocarbon years BP to >50,000 years BP (Table 4.2). Non-P23 RLB deposits span MIS 3 through MIS 1 (~50,000 years BP to present) (Fuller et al., 2014; Holden et al., 2017; O'Keefe et al., 2009). Though, all 60 small mammal radiocarbon dates obtained here are within MIS 3 (Siddall et al., 2008) (Table 4.2), suggesting that the entrapment period of P23 is exclusively pre-LGM. Aside from this specificity, there was little age separation among the examined deposits of Project 23 overall. Deposit 14 captured the broadest age range, spanning the full >25,000-year entrapment period of P23 (Fig. 4.6). Deposit 1 exhibited the overall youngest and narrowest age distribution of the four deposits, but overlaps extensively in age with Deposit 13, and was similar to the Deposit 1 age distribution obtained by Fuller et al. (2020) (Fig. 4.6). It is thus possible that the comparatively low rarified taxonomic diversity of Deposit 1 measured here (Fig. 4.5) is due to its restricted age range relative to other deposits (Fig. 4.6) and not necessarily indicative of lower community diversity at equivalent snapshots in time. However, if temporal breadth alone drives deposit-community diversity, then Deposit 14 should exhibit the greatest taxonomic diversity of the four, which is not the case (Fig. 4.5).

Though only moderately diverse taxonomically, Deposit 14 was the most fossil-abundant deposit by far. Deposit 14 rarified diversity reached saturation at only a fraction of the grid levels sampled from the other three deposits (Fig. 4.5; Appendix Table 4.9.2) but it is also a challenging deposit to interpret due to limited age control and relatively poor fossil collagen preservation (Fig. 4.6; Appendix Table 4.9.3). Deposit 14 appears to have two main entrapment events from ~25,000 - 30,000 and ~45,000 - >50,000 radiocarbon years BP. A directional relationship was not observed between grid/level analysis units and the distribution of dates within this deposit. However, Deposit 14 could be useful for future paleoecological analyses if its geochronology is better resolved. At present, Deposit 7B appears to contain the only reasonably discrete temporal community of the four examined here (Fig. 4.6).

4.5.3 Paleoclimate and community traits

Average marine foraminifera $\delta^{18}O$ climate estimates and average community-weighted trait analysis both indicate that Deposit 7B has the warmest climate overall (Fig. 4.7; Appendix Table 4.9.7; Appendix Figs. 4.9.3 & 4.9.4). This is expected because Deposit 7B is the overall oldest, with a median radiocarbon age of 42,050 BP (~45,000 calibrated years BP; Table 4.2, Fig. 4.6), and regional climates around 50,000 years BP were generally warmer than those closer to the LGM (Fig. 4.2). Community trait data further suggested that climates were overall drier and less vegetated at the time Deposit 7B was active versus Deposits 1 and 13 (Figs. 4.8 & 4.9; Appendix Figs. 4.9.5 & 4.9.6). There was less rank-order agreement among $\delta^{18}O$ and community traits for Deposits 1 and 13. In some cases, Deposit 1 exhibited the coolest, wettest, and most vegetated community traits, but in other cases Deposit 13 exhibited those conditions depending on which species pools were examined (Figs. 4.7–4.9; Appendix Figs. 4.9.3–4.9.6). This is not surprising given the highly overlapping age distributions of those two deposits (Fig. 4.6). However, there was more rank-order agreement between climate and community trait proxies for variables of precipitation than variables of temperature across deposits and species pools overall (Fig. 4.7 and Appendix Fig. 4.9.3 versus Fig. 4.8 and Appendix Fig. 4.9.5). This could indicate that small mammal communities of RLB shifted more abruptly in response to changes in precipitation than changes in temperature, which has been observed in other small mammal assemblages (e.g., Grayson, 2000). Indeed, there is more overall disparity in precipitation trait affinities than temperature trait affinities among communities of the warmest versus coolest deposits (~0.5 °C or ~4% change in temperature), and the wettest versus driest (~42 mm or ~8.5% change in precipitation; Figs. 4.7 & 4.8; Appendix Figs. 4.9.3–4.9.6).

In all cases, community-averaged body size was smallest in Deposit 7B (Fig. 4.10). Though inconsistencies occur in whether Deposit 1 or 13 contains the largest fauna, likely due to their overall compositional and age similarity (Figs. 4.3 & 4.4, 4.6, 4.10). The observation that Deposit 7B exhibits the warmest and driest climate and contains the overall smallest fauna, while cooler and wetter Deposits 1 and 13 contain overall larger faunas, conforms with expectations of Bergmann's rule at the community level. Such trends also match contemporary patterns of increased mammalian diversity in warmer/lower latitude regions of North America too (Brodie, 2019; Jenkins et al., 2013; Marcot et al., 2016; Ricketts et al., 1999) given that Deposit 7B is the most taxonomically even and diverse of the three deposits (Figs. 4.4 & 4.5).

Regarding climate-bounding traits (i.e., the maximum value of BIO5, minimum value of BIO6, maximum value of BIO12, and minimum value of BIO12), limiting values were found within contemporary ranges of: *Dipodomys agilis*, *Neotamias merriami*, and *Sylvilagus bachmani*. *Neotamias merriami* does not occur in locations with maximum temperatures over ~39.6 °C (~103 °F) today and *S. bachmani* does not occur in locations with minimum temperatures under ~ -9 °C (~16 °F; Appendix Table 4.9.4). Further, *D. agilis* does not occur in locations with annual precipitation over 836 mm or under 77 mm (Appendix Table 4.9.4). *Dipodomys agilis* and *N. merriami* were inferred to be present in P23 based on previous RLB research (Dice, 1925; Whistler, 1989) but could not be confirmed in this study (see Appendix 4.9.1, Systematic Paleontology). *Sylvilagus*

bachmani and *N. macrotis* were the most limiting species for maximum temperature and annual precipitation, respectively, with confirmed occurrences in P23; *S. bachmani* does not occur in areas with maximum temperatures over ~ 43.1 °C (~110 °F) and *N. macrotis* does not occur in areas with annual precipitation over 1392 mm or under 69 mm (Appendix Table 4.9.4). Assuming these species were present continuously throughout the P23 entrapment period, and that their environmental tolerances during the late Pleistocene were similar to today, climates of RLB during MIS 3 were unlikely to exceed temperatures of 39.6-43.1 °C, fall below -9 °C, exceed 836-1392 mm of annual precipitation, or fall below 69-77 mm of annual precipitation (Appendix Table 4.9.4).

4.5.4 Paleoenvironmental and ecological synthesis

Identification of 18+ small mammal taxa from four P23 deposits indicate that small mammal communities of P23 were remarkably similar to historic LA faunas in overall composition (Dice, 1925) (Table 4.1; Appendix 4.9.1 & Appendix Table 4.9.2). Radiocarbon dates obtained from 60 specimens in those deposits yield ages ranging from >50,000 to ~ 30,000 calibrated years BP (Table 4.2), suggesting that fossils from P23 Deposits 1, 7B, 13, and 14 were deposited during MIS 3 exclusively. Therefore, little turnover is evident among contemporary LA small mammal faunas and those of the last glacial period. Two notable exceptions include *Lepus californicus* and *Notiosorex crawfordi* which are apparently absent from P23 but present in deposits from the RLB Hancock Collection spanning MIS 3-MIS 1 (Fox et al., 2019; Fuller et al., 2014; O'Keefe et al., 2009; Stock & Harris, 1992). Both species occupy relatively warm, open, and arid environments today (Armstrong & Jones, 1972; Best, 1996) so it is possible that southern California conditions were cooler and more mesic during MIS 3 than after the LGM (Heusser, 1995, 1998) and thus unsuitable for those desert-adapted species. However, this is speculative until ages of individual *L. californicus* and *N. crawfordi* specimens at RLB are better resolved. Both species are relatively rare in non-P23 deposits, so it is possible that further sampling efforts will recover them. In any case, most small mammal species identified in P23 occupy open and semiarid environments, including those typical of the LA Basin today, so any environmental changes that occurred at RLB during the late Quaternary were apparently not substantial enough to cause major biome shifts (e.g., from open conifer forest to the coastal sage scrub and oak landscapes of today; Heusser, 1998).

Lack of evidence for major biome shifts over the last 50,000 years in the LA Basin does not necessarily indicate that environmental changes did not occur or that RLB was a climatic refugia as suggested previously (Doyen & Miller, 1980; Johnson, 1977). Many small mammal species identified at RLB are habitat generalists that tolerate a broad range of environmental conditions (e.g., Chapman & Willner, 1978; Smith et al., 2016) so their presence alone may not reflect long-term microclimate dynamics (Simonetti, 1989). By examining changes in small mammal abundance, taxonomic diversity, and trait diversity among deposits, I found that taxonomic diversity and "warm" community traits generally decrease – and "mesic" community traits increase – from ~50,000 to ~30,000 years ago (Figs. 4.7 & 4.8; Appendix Figs. 4.3-4.6). Average community body size increases during this time as well (Fig. 4.10), following

Bergmann's rule expectations. However, physiological constraints such as the relationship between thermoregulatory efficiency and body mass cannot explain these size patterns at the community level given that size changes here reflect shifts in the relative abundance of different sized species rather than size shifts within populations. Nevertheless, similar patterns of increasing community body size with decreasing temperature are seen in other studies. For example, Blackburn and Hawkins (2004) found that mammalian communities of the Nearctic, including small mammal species, exhibit significant and negative body size relationships with temperature. On the other hand, Classen et al. (2017) found that intraspecific bee size increases with elevation and decreases with temperature in accordance with Bergman's rule at the population level but decreases in size with elevation at the community level. That outcome was driven by a decrease in large-bodied bee species present at higher elevations, presumably due to different physiological and energetic constraints acting on different levels of biological organization (Classen et al., 2017). Decreases in large-bodied bee species at higher elevations were attributed to decreases in flower resources needed to support larger communities (Classen et al., 2017). In this context, the opposing pattern observed in small mammal communities of RLB (i.e., larger-sized communities at lower temperatures) is expected because regions with warm Mediterranean climates such as southern California experience most of their annual plant growth during the relatively cool and wet months of late winter and spring (Montenegro et al., 1981). Mediterranean vegetation in California is projected to decline in the future due to climate warming (Lenihan et al., 2008) and has been shown to decline experimentally with drought (Potts et al., 2012). It therefore seems reasonable to assume that moderate decreases in temperature and/or moderate increases in precipitation over millennial timescales would facilitate larger-bodied small mammal communities by expanding the plant resources necessary to sustain them. Further, average community-weighted estimates of NDVI show positive relationships between vegetation cover and small mammal community size (Fig. 4.9).

Mean trait patterns of temperature affinity, precipitation affinity, vegetation cover affinity, and size elucidate the probable direction of environmental change within the entrapment window of P23, but they do not shed light on environmental differences between MIS 3 and today. Small mammal climate-limiting traits (i.e., the most extreme climatic conditions that contemporary individuals of identified P23 species can tolerate) suggest that maximum temperatures during MIS 3 did not exceed 39.6-43.1 °C, minimum temperatures were no lower than -9 °C, and annual precipitation was no greater than 836-1392 mm or less than 69-77 mm (Appendix Table 4.9.4). Extracting the same variables (BIO 5, BIO 6, and BIO 12) from the geographic coordinates of RLB yield maximum temperatures of 28.5°C, minimum temperatures of 8.3 °C, and annual precipitation of 357 mm. Those values occur within the contemporary ranges (realized niches) of all identified fossil species and suggest that RLB climates during MIS 3 were generally similar, though not necessarily equivalent, to its modern climate.

4.5.5 Conclusions

My expectation that the small mammal paleocommunity is reflective of the paleoenvironment was generally supported. I found that species presences among paleocommunities were relatively stable through time, indicating broad relative stability in climate from >50,000 to ~30,000 cal. BP. However, species abundances change markedly in directions that reflect the general transition from relatively warm glacial times to cooler glacial times (Fig. 4.2). Further, community diversity and trait changes coarsely mirror regional climate patterns among deposits that are furthest apart in age (e.g., Deposit 1 versus Deposit 7B), thus supporting the assumption that changes in climate are reflected in changes in small mammal assemblages. Deposits that are closer in age (e.g., Deposit 1 versus Deposit 13) did not show concordance in diversity or trait changes with climate (Figs. 4.3-4.10; Appendix Figs. 4.9.3-4.9.6), likely because both deposits are highly time-averaged and overlapping in age and climatic context. Observations that taxonomic diversity decreases – and average community body size increases – temporally with lower temperature, higher precipitation, and higher NDVI (Figs. 4.4-4.10; Appendix Figs. 4.9.3–4.9.6) suggest that slight to moderate changes in climate and resource availability impacted the long-term organization of small mammals within this system. Further research on RLB small mammal traits, and pollen and plant macrofossils, at more precise points in time may refine the probable abiotic and biotic drivers of these patterns in the future.

4.6 References

Akersten, W. (1979). New Mammalian Records from the Late Pleistocene of Rancho La Brea. *Bulletin of the Southern California Academy of Sciences, 78*(2), 141–143.

Anderson, R. S., Power, M. J., Smith, S. J., Springer, K., & Scott, E. (2002). Paleoecology of a Middle Wisconsin Deposit from Southern California. *Quaternary Research, 58*(3), 310–317. https://doi.org/10.1006/qres.2002.2388

Armstrong, D. M., & Jones, J. K. (1972). Notiosorex crawfordi. *Mammalian Species, 17*, 1–5. https://doi.org/10.2307/3504060

Barnosky, A. D., Hadly, E. A., Gonzalez, P., Head, J., Polly, P. D., Lawing, A. M., Eronen, J. T., Ackerly, D. D., Alex, K., Biber, E., Blois, J., Brashares, J., Ceballos, G., Davis, E., Dietl, G. P., Dirzo, R., Doremus, H., Fortelius, M., Greene, H. W., … Zhang, Z. (2017). Merging paleobiology with conservation biology to guide the future of terrestrial ecosystems. *Science, 355*(6325), eaah4787. https://doi.org/10.1126/science.aah4787

Bell, C., & Jass, C. (2004). Arvicoline Rodents from Kokoweef Cave, Ivanpah Mountains, San Bernardino County, California. *Bulletin of the Southern California Academy of Sciences, 103*(1), 1–11.

Bergmann, C. (1847). Über die Verhältnisse der Wärmeökonomie der Thiere zu ihrer Grösse. *Göttinger Studien, 3*, 595–708.

Best, T. L. (1996). Lepus californicus. *Mammalian Species*, *530*, 1–10. https://doi.org/10.2307/3504151

Best, T. L., & Granai, N. J. (1994). Tamias merriami. *Mammalian Species*, *476*, 1–9. https://doi.org/10.2307/3504203

Blackburn, T. M., & Hawkins, B. A. (2004). Bergmann's rule and the mammal fauna of northern North America. *Ecography*, *27*(6), 715–724. https://doi.org/10.1111/j.0906-7590.2004.03999.x

Blois, J. L., McGuire, J. L., & Hadly, E. A. (2010). Small mammal diversity loss in response to late-Pleistocene climatic change. *Nature*, *465*(7299), 771–774. https://doi.org/10.1038/nature09077

Blois, J. L., Zarnetske, P. L., Fitzpatrick, M. C., & Finnegan, S. (2013). Climate Change and the Past, Present, and Future of Biotic Interactions. *Science*, *341*(6145), 499–504. https://doi.org/10.1126/science.1237184

Brodie, J. F. (2019). Environmental limits to mammal diversity vary with latitude and global temperature. *Ecology Letters*, *22*(3), 480–485. https://doi.org/10.1111/ele.13206

Bryant, M. D. (1945). Phylogeny of Nearctic Sciuridae. *The American Midland Naturalist*, *33*(2), 257–390. https://doi.org/10.2307/2421337

Carrasco, M. A. (2000). Species Discrimination and Morphological Relationships of Kangaroo Rats (*Dipodomys*) Based on their Dentition. *Journal of Mammalogy*, *81*(1), 107–122. https://doi.org/10.1644/1545-1542(2000)081<0107:SDAMRO>2.0.CO;2

Chao, A., Gotelli, N. J., Hsieh, T. C., Sander, E. L., Ma, K. H., Colwell, R. K., & Ellison, A. M. (2014). Rarefaction and extrapolation with Hill numbers: A framework for sampling and estimation in species diversity studies. *Ecological Monographs*, *84*(1), 45–67. https://doi.org/10.1890/13-0133.1

Chapman, J. A. (1974). Sylvilagus bachmani. *Mammalian Species*, *34*, 1–4. https://doi.org/10.2307/3503777

Chapman, J. A., & Willner, G. R. (1978). Sylvilagus audubonii. *Mammalian Species*, *106*, 1–4.

Classen, A., Steffan-Dewenter, I., Kindeketa, W. J., & Peters, M. K. (2017). Integrating intraspecific variation in community ecology unifies theories on body size shifts along climatic gradients. *Functional Ecology*, *31*(3), 768–777. https://doi.org/10.1111/1365-2435.12786

Coltrain, J. B., Harris, J. M., Cerling, T. E., Ehleringer, J. R., Dearing, M.-D., Ward, J., & Allen, J. (2004). Rancho La Brea stable isotope biogeochemistry and its implications for the palaeoecology of late Pleistocene, coastal southern California. *Palaeogeography, Palaeoclimatology, Palaeoecology*, *205*(3), 199–219. https://doi.org/10.1016/j.palaeo.2003.12.008

Colwell, R. K., & Rangel, T. F. (2009). Hutchinson's duality: The once and future niche. *Proceedings of the National Academy of Sciences*, *106*(Supplement 2), 19651–19658. https://doi.org/10.1073/pnas.0901650106

Compton, L. V. (1937). Shrews from the Pleistocene of the Rancho La Brea asphalt. *University of California Press*, *24*, 85–90.

Cuenca-Bescós, G., Straus, L. G., González Morales, M. R., & García Pimienta, J. C. (2009). The reconstruction of past environments through small mammals: From the Mousterian to the Bronze Age in El Mirón Cave (Cantabria, Spain). *Journal of Archaeological Science*, *36*(4), 947–955. https://doi.org/10.1016/j.jas.2008.09.025

Dalquest, W. W., & Schultz, G. E. (1992). *Ice age mammals of northwestern Texas*. Midwestern State University Press.

Dalquest, W. W., & Stangl Jr., F. B. (1983). Identification of Seven Species of *Peromyscus* from Trans-Pecos Texas by Characteristics of the Lower Jaws. *Occasional Papers of the Museum, Texas Tech University, no. 90*, 1–12.

Deniro, M. J., Schoeninger, M. J., & Hastorf, C. A. (1985). Effect of heating on the stable carbon and nitrogen isotope ratios of bone collagen. *Journal of Archaeological Science*, *12*(1), 1–7. https://doi.org/10.1016/0305-4403(85)90011-1

DeSantis, L. R. G., Crites, J. M., Feranec, R. S., Fox-Dobbs, K., Farrell, A. B., Harris, J. M., Takeuchi, G. T., & Cerling, T. E. (2019). Causes and Consequences of Pleistocene Megafaunal Extinctions as Revealed from Rancho La Brea Mammals. *Current Biology*, *29*(15), 2488-2495.e2. https://doi.org/10.1016/j.cub.2019.06.059

Desantis, S., Prothero, D. R., & Gage, G. (2011). Size and shape stasis in late Pleistocene horses and camels from Rancho La Brea during the last glacial-interglacial cycle. *New Mexico Museum of Natural History Bulletin*, *53*, 505–510.

Dice, L. R. (1925). Rodents and lagomorphs of the Rancho la Brea deposits. *Carnegie Institution of Washington*, *349*, 119–130.

Doyen, J. T., & Miller, S. E. (1980). Review of Pleistocene darkling ground beetles of the California asphalt deposits (Coleoptera: Tenebrionidae, Zopheridae). *Pan-Pacific Entomologist*, *56*(1), 1–10.

Estes, J. A., Terborgh, J., Brashares, J. S., Power, M. E., Berger, J., Bond, W. J., Carpenter, S. R., Essington, T. E., Holt, R. D., Jackson, J. B. C., Marquis, R. J., Oksanen, L., Oksanen, T., Paine, R. T., Pikitch, E. K., Ripple, W. J., Sandin, S. A., Scheffer, M., Schoener, T. W., … Wardle, D. A. (2011). Trophic Downgrading of Planet Earth. *Science, 333*(6040), 301–306. https://doi.org/10.1126/science.1205106

Feranec, R. S., Hadly, E. A., & Paytan, A. (2009). Stable isotopes reveal seasonal competition for resources between late Pleistocene bison (*Bison*) and horse (*Equus*) from Rancho La Brea, southern California. *Palaeogeography, Palaeoclimatology, Palaeoecology*, *271*(1), 153–160. https://doi.org/10.1016/j.palaeo.2008.10.005

Fick, S. E., & Hijmans, R. J. (2017). WorldClim 2: New 1-km spatial resolution climate surfaces for global land areas. *International Journal of Climatology*, *37*, 4302–4315.

Fox, N. S., Takeuchi, G. T., Farrell, A. B., & Blois, J. L. (2019). A protocol for differentiating late Quaternary leporids in southern California with remarks on Project 23 lagomorphs at Rancho La Brea, Los Angeles, California, USA. *PaleoBios*, *36*, 1–20.

Fox, N. S., Veneracion, J. J., & Blois, J. L. (2020). Are geometric morphometric analyses replicable? Evaluating landmark measurement error and its impact on extant and fossil *Microtus* classification. *Ecology and Evolution*, *10*(7), 3260–3275. https://doi.org/10.1002/ece3.6063

Fox-Dobbs, K., Stidham, T. A., Bowen, G. J., Emslie, S. D., & Koch, P. L. (2006). Dietary controls on extinction versus survival among avian megafauna in the late Pleistocene. *Geology*, *34*(8), 685–688. https://doi.org/10.1130/G22571.1

Friscia, A. R., Van Valkenburgh, B., Spencer, L., & Harris, J. (2008). Chronology and Spatial Distribution of Large Mammal Bones in Pit 91, Rancho la Brea. *PALAIOS*, *23*, 35–42.

Fuller, B. T., Fahrni, S. M., Harris, J. M., Farrell, A. B., Coltrain, J. B., Gerhart, L. M., Ward, J. K., Taylor, R. E., & Southon, J. R. (2014). Ultrafiltration for asphalt removal from bone collagen for radiocarbon dating and isotopic analysis of Pleistocene fauna at the tar pits of Rancho La Brea, Los Angeles, California. *Quaternary Geochronology*, *22*, 85–98. https://doi.org/10.1016/j.quageo.2014.03.002

Fuller, B. T., Harris, J. M., Farrell, A. B., Takeuchi, G. T., & Southon, J. R. (2015). Sample Preparation for Radiocarbon Dating and Isotopic Analysis of Bone from Rancho La Brea. *Natural History Museum of Los Angeles County Science Series*, *42*, 151–167.

Fuller, B. T., Southon, J. R., Fahrni, S. M., Farrell, A. B., Takeuchi, G. T., Nehlich, O., Guiry, E. J., Richards, M. P., Lindsey, E. L., & Harris, J. M. (2020). Pleistocene paleoecology and feeding behavior of terrestrial vertebrates recorded in a pre-LGM asphaltic deposit at Rancho La Brea, California. *Palaeogeography, Palaeoclimatology, Palaeoecology, 537*, 109383. https://doi.org/10.1016/j.palaeo.2019.109383

Gill, J. L., Williams, J. W., Jackson, S. T., Lininger, K. B., & Robinson, G. S. (2009). Pleistocene Megafaunal Collapse, Novel Plant Communities, and Enhanced Fire Regimes in North America. *Science*, *326*(5956), 1100–1103. https://doi.org/10.1126/science.1179504

Glover, K. C., Chaney, A., Kirby, M. E., Patterson, W. P., & MacDonald, G. M. (2020). Southern California Vegetation, Wildfire, and Erosion Had Nonlinear Responses to Climatic Forcing During Marine Isotope Stages 5–2 (120–15 ka). *Paleoceanography and Paleoclimatology*, *35*(2), e2019PA003628. https://doi.org/10.1029/2019PA003628

Glover, K. C., MacDonald, G. M., Kirby, M. E., Rhodes, E. J., Stevens, L., Silveira, E., Whitaker, A., & Lydon, S. (2017). Evidence for orbital and North Atlantic climate forcing in alpine Southern California between 125 and 10 ka from multi-proxy analyses of Baldwin Lake. *Quaternary Science Reviews*, *167*, 47–62. https://doi.org/10.1016/j.quascirev.2017.04.028

Gonzalez, P., Neilson, R. P., Lenihan, J. M., & Drapek, R. J. (2010). Global patterns in the vulnerability of ecosystems to vegetation shifts due to climate change. *Global Ecology and Biogeography*, *19*(6), 755–768. https://doi.org/10.1111/j.1466-8238.2010.00558.x

Goodwin, H. T. (2004). Systematics and faunal dynamics of fossil squirrels (Rodentia, Sciuridae) from Porcupine Cave, Park County, Colorado. In A. D. Barnosky (Ed.), *Biodiversity response to climate change in the Middle Pleistocene: The Porcupine Cave fauna from Colorado* (pp. 172–192). The University of California Press.

Grayson, D. K. (1987). The Biogeographic History of Small Mammals in the Great Basin: Observations on the Last 20,000 Years. *Journal of Mammalogy*, *68*(2), 359–375. https://doi.org/10.2307/1381475

Grayson, D. K. (2000). Mammalian responses to Middle Holocene climatic change in the Great Basin of the western United States. *Journal of Biogeography*, *27*(1), 181–192. https://doi.org/10.1046/j.1365-2699.2000.00383.x

Grayson, D. K. (2006). The Late Quaternary biogeographic histories of some Great Basin mammals (western USA). *Quaternary Science Reviews*, *25*(21), 2964–2991. https://doi.org/10.1016/j.quascirev.2006.03.004

Hall, E. R., & Kelson, K. R. (1959). *The mammals of North America* (Vol. 1). Ronald Press.

Harris, A. H. (1984). *Neotoma* in the late Pleistocene of New Mexico and Chihuahua. *Special Publications, Carnegie Museum of Natural History*, *8*, 164–178.

Hendy, I. L. (2007). *Santa Barbara Basin ODP893A Planktonic Stable Isotope Data*. IGBP PAGES/World Data Center for Paleoclimatology Data Contribution Series # 2007-080. NOAA/NCDC Paleoclimatology Program, Boulder CO, USA.

Hendy, I. L., & Kennett, J. P. (1999). Latest Quaternary North Pacific surface-water responses imply atmosphere-driven climate instability. *Geology*, *27*(4), 291–294. https://doi.org/10.1130/0091-7613(1999)027<0291:LQNPSW>2.3.CO;2

Hendy, I. L., Kennett, J. P., Roark, E. B., & Ingram, B. L. (2002). Apparent synchroneity of submillennial scale climate events between Greenland and Santa Barbara Basin, California from 30–10ka. *Quaternary Science Reviews*, *21*(10), 1167–1184. https://doi.org/10.1016/S0277-3791(01)00138-X

Heusser, L. E. (1995). Pollen stratigraphy and paleoecologic interpretation of the 160-ky record from Santa Barbara Basin, Hole 893A. In J. P. Kennett, G. J. Baldauf, & M. Lyle (Eds.), *Proceedings of the ocean drilling program, scientific results* (Vols. 146–2, pp. 265–279).

Heusser, L. E. (1998). Direct correlation of millennial-scale changes in western North American vegetation and climate with changes in the California Current System over the past ~60 kyr. *Paleoceanography*, *13*(3), 252–262. https://doi.org/10.1029/98PA00670

Heusser, L. E., Kirby, M. E., & Nichols, J. E. (2015). Pollen-based evidence of extreme drought during the last Glacial (32.6–9.0 ka) in coastal southern California. *Quaternary Science Reviews*, *126*, 242–253. https://doi.org/10.1016/j.quascirev.2015.08.029

Hill, M. O. (1973). Diversity and Evenness: A Unifying Notation and Its Consequences. *Ecology*, *54*(2), 427–432. https://doi.org/10.2307/1934352

Hillson, S. (2005). *Teeth*. Cambridge University Press.

Hinesley, L. L. (1979). Systematics and Distribution of Two Chromosome Forms in the Southern Grasshopper Mouse, Genus *Onychomys*. *Journal of Mammalogy*, *60*(1), 117–128. https://doi.org/10.2307/1379763

Holden, A. R., Southon, J. R., Will, K., Kirby, M. E., Aalbu, R. L., & Markey, M. J. (2017). A 50,000 year insect record from Rancho La Brea, Southern California:

Insights into past climate and fossil deposition. *Quaternary Science Reviews, 168*, 123–136. https://doi.org/10.1016/j.quascirev.2017.05.001

Hooper, E. T. (1957). Dental patterns in mice of the genus *Peromyscus*. *Miscellaneous Publications Museum of Zoology, University of Michigan*, *99*, 1–59.

Hsieh, T. C., Ma, K. H., & Chao, A. (2020). *INEXT: Interpolation and Extrapolation for Species Diversity* (Version R package version 2.0.20) [Computer software]. http://chao.stat.nthu.edu.tw/wordpress/software_download/

Jenkins, C. N., Pimm, S. L., & Joppa, L. N. (2013). Global patterns of terrestrial vertebrate diversity and conservation. *Proceedings of the National Academy of Sciences*, *110*(28), E2602–E2610. https://doi.org/10.1073/pnas.1302251110

Johnson, D. L. (1977). The late Quaternary climate of coastal California: Evidence for an ice age refugium. *Quaternary Research*, *8*(2), 154–179.

Jones, C. A., & Baxter, C. N. (2004). Thomomys bottae. *Mammalian Species*, *2004*(742), 1–14. https://doi.org/10.1644/742

Jones, K. E., Bielby, J., Cardillo, M., Fritz, S. A., O'Dell, J., Orme, C. D. L., Safi, K., Sechrest, W., Boakes, E. H., Carbone, C., Connolly, C., Cutts, M. J., Foster, J. K., Grenyer, R., Habib, M., Plaster, C. A., Price, S. A., Rigby, E. A., Rist, J., … Purvis, A. (2009). PanTHERIA: A species-level database of life history, ecology, and geography of extant and recently extinct mammals. *Ecology*, *90*(9), 2648–2648. https://doi.org/10.1890/08-1494.1

Kindt, R., & Coe, R. (2005). *Tree diversity analysis. A manual and software for common statistical methods for ecological and biodiversity studies.* World Agroforestry Centre (ICRAF). http://www.worldagroforestry.org/output/tree-diversity-analysis

Koch, P. L., & Barnosky, A. D. (2006). Late Quaternary Extinctions: State of the Debate. *Annual Review of Ecology, Evolution, and Systematics*, *37*(1), 215–250. https://doi.org/10.1146/annurev.ecolsys.34.011802.132415

Kurtén, B., & Anderson, E. (1980). *Pleistocene mammals of North America*. Columbia University Press.

Lamb, R. V. (1989). *The nonmarine mollusks of Pit 91, Rancho La Brea, southern California, and their paleoecologic and biogeographic implications.* [Master's thesis]. California State University, Northridge.

Lenihan, J. M., Bachelet, D., Neilson, R. P., & Drapek, R. (2008). Response of vegetation distribution, ecosystem productivity, and fire to climate change scenarios for California. *Climatic Change*, *87*(1), 215–230. https://doi.org/10.1007/s10584-007-9362-0

Lyman, R. L. (2008). Estimating the magnitude of data asymmetry in palaeozoological biogeography. *International Journal of Osteoarchaeology*, *18*(1), 85–94. https://doi.org/10.1002/oa.921

Malhi, Y., Doughty, C. E., Galetti, M., Smith, F. A., Svenning, J.-C., & Terborgh, J. W. (2016). Megafauna and ecosystem function from the Pleistocene to the Anthropocene. *Proceedings of the National Academy of Sciences*, *113*(4), 838–846. https://doi.org/10.1073/pnas.1502540113

Marcot, J. D., Fox, D. L., & Niebuhr, S. R. (2016). Late Cenozoic onset of the latitudinal diversity gradient of North American mammals. *Proceedings of the National Academy of Sciences*, *113*(26), 7189–7194. https://doi.org/10.1073/pnas.1524750113

Marcus, L. F., & Berger, R. (1984). The significance of radiocarbon dates for Rancho La Brea. In P. S. Martin & R. G. Klein (Eds.), *Quarternary extinctions: A prehistoric revolution* (pp. 159–183). The University of Arizona Press.

Martin, R. A. (1968). Further Study of the Friesenhahn Cave *Peromyscus*. *The Southwestern Naturalist*, *13*(3), 253–266. https://doi.org/10.2307/3669219

Martin, R. A. (2019). Correlation of Pliocene and Pleistocene fossil assemblages from the central and eastern United States: Toward a continental rodent biochronology. *Historical Biology*, *0*(0), 1–17. https://doi.org/10.1080/08912963.2019.1666118

Mayr, E. (1956). Geographical Character Gradients and Climatic Adaptation. *Evolution*, *10*(1), 105–108. https://doi.org/10.1111/j.1558-5646.1956.tb02836.x

McCarty, R. (1975). Onychomys torridus. *Mammalian Species*, *59*, 1–5. https://doi.org/10.2307/3503863

McCarty, R. (1978). Onychomys leucogaster. *Mammalian Species*, *87*, 1–6. https://doi.org/10.2307/3503934

McGuire, J. L. (2011). Identifying California *Microtus* species using geometric morphometrics documents Quaternary geographic range contractions. *Journal of Mammalogy*, *92*(6), 1383–1394. https://doi.org/10.1644/10-MAMM-A-280.1

Meachen, J. A., Janowicz, A. C., Avery, J. E., & Sadleir, R. W. (2014a). Ecological Changes in Coyotes (*Canis latrans*) in Response to the Ice Age Megafaunal Extinctions. *PLoS ONE*, *9*(12), e116041. https://doi.org/10.1371/journal.pone.0116041

Meachen, J. A., O'Keefe, F. R., & Sadleir, R. W. (2014b). Evolution in the sabre-tooth cat, *Smilodon fatalis*, in response to Pleistocene climate change. *Journal of Evolutionary Biology*, *27*(4), 714–723. https://doi.org/10.1111/jeb.12340

Miller, W. E. (1976). Late Pleistocene vertebrates of the Silver Creek Local Fauna fom north central Utah. *The Great Basin Naturalist, 36*(4), 387–424.

Montenegro, G., Aljaro, M. E., Walkowiak, A., & Saenger, R. (1981). Seasonality, growth and net productivity of herbs and shrubs of the Chilean matorral. In C. C. Conrad & W. C. Oechel (Eds.), *Dynamics and Management of Mediterranean-Type Ecosystems* (pp. 135–141). USDA Forest Service, Gen. Tech. Rep. PSW 58.

Mychajliw, A. M., Rice, K. A., Tewksbury, L. R., Southon, J. R., & Lindsey, E. L. (2020). Exceptionally preserved asphaltic coprolites expand the spatiotemporal range of a North American paleoecological proxy. *Scientific Reports*, *10*(1), 5069. https://doi.org/10.1038/s41598-020-61996-y

Oaks, E. C., Young, P. J., Kirkland, G. L., & Schmidt, D. F. (1987). Spermophilus variegatus. *Mammalian Species*, *272*, 1–8. https://doi.org/10.2307/3503949

O'Keefe, F. R., Binder, W., Frost, S., Sadlier, R., & Valkenburgh, B. V. (2014). Cranial morphometrics of the dire wolf, *Canis dirus*, at Rancho La Brea: Temporal variability and its links to nutrient stress and climate. *Palaeontologia Electronica*, *17*, 1–24.

O'Keefe, F. R., Fet, E., & Harris, J. (2009). Compilation, Calibration, and Synthesis of Faunal and Floral Radiocarbon Dates, Rancho La Brea, California. *Contributions in Science*, *518*, 1–16.

Owen, J. G., & Hoffmann, R. S. (1983). Sorex ornatus. *Mammalian Species*, *212*, 1–5. https://doi.org/10.2307/3504070

Patterson, B. D., Ceballos, G., Sechrest, W., Tognelli, M. F., Brooks, T., Luna, L., Ortega, P., Salazar, I., & Young, B. E. (2007). *Digital Distribution Maps of the Mammals of the Western Hemisphere. NatureServe version 3.0.*

Pettorelli, N., Ryan, S., Mueller, T., Bunnefeld, N., Jedrzejewska, B., Lima, M., & Kausrud, K. (2011). The Normalized Difference Vegetation Index (NDVI): Unforeseen successes in animal ecology. *Climate Research*, *46*(1), 15–27. https://doi.org/10.3354/cr00936

Potts, D. L., Suding, K. N., Winston, G. C., Rocha, A. V., & Goulden, M. L. (2012). Ecological effects of experimental drought and prescribed fire in a southern California coastal grassland. *Journal of Arid Environments*, *81*, 59–66. https://doi.org/10.1016/j.jaridenv.2012.01.007

Powell, R. L. (2019). *Grassmapr, an R package to predict C3/C4 grass distributions and model terrestrial δ13C isoscapes.* https://github.com/rebeccalpowell/grassmapr

Prothero, D. R., Syverson, V. J., Raymond, K. R., Madan, M., Molina, S., Fragomeni, A., DeSantis, S., Sutyagina, A., & Gage, G. L. (2012). Size and shape stasis in late Pleistocene mammals and birds from Rancho La Brea during the Last Glacial–Interglacial cycle. *Quaternary Science Reviews*, *56*, 1–10. https://doi.org/10.1016/j.quascirev.2012.08.015

Raymond, K. R., & Prothero, D. R. (2011). Did climate changes affect size in late Pleistocene *Bison*? *New Mexico Museum of Natural History Bulletin*, *53*, 636–640.

Reimer, P. J., Bard, E., Bayliss, A., Beck, J. W., Blackwell, P. G., Ramsey, C. B., Buck, C. E., Cheng, H., Edwards, R. L., Friedrich, M., Grootes, P. M., Guilderson, T. P., Haflidason, H., Hajdas, I., Hatté, C., Heaton, T. J., Hoffmann, D. L., Hogg, A. G., Hughen, K. A., … Plicht, J. van der. (2013). IntCal13 and Marine13 Radiocarbon Age Calibration Curves 0–50,000 Years cal BP. *Radiocarbon*, *55*(4), 1869–1887. https://doi.org/10.2458/azu_js_rc.55.16947

Rice, K., Sessions, A., Lai, K., & Takeuchi, G. T. (2015). New technique to remove asphalt from microfossil-rich matrix from Rancho La Brea. *Natural History Museum of Los Angeles County Science Series*, *42*, 169–174.

Ricketts, T. H., Dinerstein, E., Olson, D. M., & Loucks, C. (1999). Who's Where in North America? *BioScience*, *49*(5), 369–381. https://doi.org/10.2307/1313630

Samuels, J. X., & Hopkins, S. S. B. (2017). The impacts of Cenozoic climate and habitat changes on small mammal diversity of North America. *Global and Planetary Change*, *149*, 36–52. https://doi.org/10.1016/j.gloplacha.2016.12.014

Sandel, B., Arge, L., Dalsgaard, B., Davies, R. G., Gaston, K. J., Sutherland, W. J., & Svenning, J.-C. (2011). The Influence of Late Quaternary Climate-Change Velocity on Species Endemism. *Science*, *334*(6056), 660–664. https://doi.org/10.1126/science.1210173

Shellhammer, H. (1982). Reithrodontomys raviventris. *Mammalian Species*, *169*, 1–3. https://doi.org/10.2307/3503874

Siddall, M., Rohling, E. J., Thompson, W. G., & Waelbroeck, C. (2008). Marine isotope stage 3 sea level fluctuations: Data synthesis and new outlook. *Reviews of Geophysics*, *46*(4). https://doi.org/10.1029/2007RG000226

Simonetti, J. A. (1989). Small mammals as paleoenvironmental indicators: Validation for species of central Chile. *Revista Chilena de Historia Natural*, *62*, 109–114.

Smartt, R. A. (1977). The ecology of late Pleistocene and recent *Microtus* from south-central and southwestern New Mexico. *The Southwestern Naturalist*, *22*(1), 1–19. https://doi.org/10.2307/3670460

Smith, F. A., Betancourt, J. L., & Brown, J. H. (1995). Evolution of Body Size in the Woodrat over the Past 25,000 Years of Climate Change. *Science*, *270*(5244), 2012–2014. https://doi.org/10.1126/science.270.5244.2012

Smith, J. E., Long, D. J., Russell, I. D., Newcomb, K. L., & Muñoz, V. D. (2016). Otospermophilus beecheyi (Rodentia: Sciuridae). *Mammalian Species*, *48*(939), 91–108. https://doi.org/10.1093/mspecies/sew010

Somerville, A. D., Froehle, A. W., & Schoeninger, M. J. (2018). Environmental influences on rabbit and hare bone isotope abundances: Implications for paleoenvironmental research. *Palaeogeography, Palaeoclimatology, Palaeoecology*, *497*, 91–104. https://doi.org/10.1016/j.palaeo.2018.02.008

Spencer, L. M., Valkenburgh, B. V., & Harris, J. M. (2003). Taphonomic analysis of large mammals recovered from the Pleistocene Rancho La Brea tar seeps. *Paleobiology*, *29*(4), 561–575. https://doi.org/10.1666/0094-8373(2003)029<0561:TAOLMR>2.0.CO;2

Stock, C., & Harris, J. M. (1992). Rancho La Brea: A record of Pleistocene life in California. *Science Series*, *37*, 1–113.

Terry, R. C., Li, C. (lily), & Hadly, E. A. (2011). Predicting small-mammal responses to climatic warming: Autecology, geographic range, and the Holocene fossil record. *Global Change Biology*, *17*(10), 3019–3034. https://doi.org/10.1111/j.1365-2486.2011.02438.x

Thaeler, C. S. (1980). Chromosome Numbers and Systematic Relations in the Genus *Thomomys* (Rodentia: Geomyidae). *Journal of Mammalogy*, *61*(3), 414–422. https://doi.org/10.2307/1379835

Vellend, M. (2010). Conceptual Synthesis in Community Ecology. *The Quarterly Review of Biology*, *85*(2), 183–206. https://doi.org/10.1086/652373

Verts, B. J., & Carraway, L. N. (2001). Scapanus latimanus. *Mammalian Species*, *2001*(666), 1–7. https://doi.org/10.1644/1545-1410(2001)666<0001:SL>2.0.CO;2

Verts, B. J., & Carraway, L. N. (2003). Thomomys townsendii. *Mammalian Species*, *2003*(719), 1–6. https://doi.org/10.1644/719

Wahlert, J. H. (1993). The fossil record. In H. H. Genoways & J. H. Brown (Eds.), *Biology of the Heteromyidae* (pp. 1–37). Special Publication, The American Society of Mammalogists.

Wallace, S. C. (2006). Differentiating *Microtus xanthognathus* and *Microtus pennsylvanicus* Lower First Molars Using Discriminant Analysis of Landmark Data. *Journal of Mammalogy*, *87*(6), 1261–1269.

Wang, J., Rich, P. M., & Price, K. P. (2003). Temporal responses of NDVI to precipitation and temperature in the central Great Plains, USA. *International Journal of Remote Sensing*, *24*(11), 2345–2364. https://doi.org/10.1080/01431160210154812

Warter, J. K. (1976). Late Pleistocene plant communities–evidence from the Rancho La Brea tar pits. In J. Latting (Ed.), *Plant Communities of Southern California* (pp. 32–39). California Native Plant Society Special Publication No. 2.

Whistler, D. P. (1989). Late Pleistocene Chipmunk, *Tamias* (Mammalia: Sciuridae), from Rancho La Brea, Los Angeles, California. *Bulletin of the Southern California Academy of Sciences*, *88*(3), 117–122.

Williams, J. W., & Jackson, S. T. (2007). Novel climates, no-analog communities, and ecological surprises. *Frontiers in Ecology and the Environment*, *5*(9), 475–482. https://doi.org/10.1890/070037

Wilson, D. E., & Reeder, D. M. (2005). *Mammal Species of the World: A Taxonomic and Geographic Reference*. Johns Hopkins University Press.

Wilson, R. W. (1933). Pleistocene Mammalian Fauna from the Carpinteria Asphalt. In *Contributions to Palaeontology* (pp. 59–76). Carnegie Institution of Washington. https://resolver.caltech.edu/CaltechAUTHORS:20200124-151834439

4.7 Tables

Table 4.1: Total number of individual specimens per taxon (NISP) obtained from the grid/level sampling effort of this study grouped by genus.

Taxon	Deposit 1	Deposit 13	Deposit 14	Deposit 7B	Total
Sylvilagus	158	235	196	95	725
Microtus	119	89	263	64	535
Peromyscus	32	116	137	69	354
Otospermophilus	51	68	49	17	185
Dipodomys	2	30	86	21	139
Thomomys	8	13	34	39	94
Neotoma	5	7	24	31	67
Mustela	3	18	4	3	28
Reithrodontomys	0	3	1	6	10
Neotamias/*Tamias*	1	5	2	1	9
Mephitis	3	3	0	3	9
Sorex	2	0	5	1	8
Onychomys	0	3	0	0	3
Spilogale	1	0	1	0	2
Scapanus	0	0	0	1	1
Deposit NISP sum	385	590	802	351	2128

Table 4.2: Radiocarbon ages (^{14}C age), radiocarbon age uncertainties (+/-), calibrated ages (Cal age median), and calibrated age uncertainties (SD) of all 60 AMS-analyzed P23 samples from which dates were obtained. Calibrated ages show the median of each specimens' Bayesian probability age distribution analyzed in OxCal v.4.3.2 using the IntCal13 calibration curve (Reimer et al., 2013). δ^{18}O values reflect *Neogloboquadrina pachyderma* δ^{18}O data from Hendy et al. (2007) linearly interpolated with the median calibrated age of each specimen. *= dates potentially affected by contamination (i.e., those with C:N ratios outside 2.9-3.6 (Deniro et al., 1985)).

UCIAMS	LACM	Deposit	Taxon	^{14}C age	+/-	Collagen yield %	C:N atomic	Cal age median	SD	δ^{18}O
191095	P23-5233	1	*Sylvilagus*	35750	610	2.7	3.33	40385	640	2.368
191096	P23-18270	1	*Sylvilagus*	35440	580	1.7	3.48	40058	637	2.223
191097	P23-22009	1	*Sylvilagus*	35150	580	1.1	3.6	39745	640	2.281
191098	P23-25476	1	*Sylvilagus*	36050	630	1.4	3.38	40678	623	2.232
191099	P23-28903	1	*Sylvilagus*	33830	480	1.2	3.34	38214	660	1.709
191100	P23-30238	1	*Sylvilagus*	35780	600	1.2	3.59	40416	628	2.125
191101	P23-31269	1	*Sylvilagus*	46200	2200	2	3.26	48507	1123	1.648
191102	P23-31423	1	*Sylvilagus*	35420	580	1.5	3.46	40036	638	2.407
191103	P23-31033	14	*Sylvilagus*	>47800	NA	0.8	3.47	NA	NA	NA
*191104	P23-31036	14	*Sylvilagus*	>49900	NA	1.8	5.56	NA	NA	NA
*191105	P23-31056	14	*Sylvilagus*	>49900	NA	1.1	4.04	NA	NA	NA
191242	P23-31031	14	*Sylvilagus*	>50800	NA	1.1	3.51	NA	NA	NA
198199	P23-2046	1	*Canis latrans*	35770	550	2.6	3.25	40409	587	2.064
198200	P23-11485	1	*Canis latrans*	35050	510	2	3.5	39625	571	2.473
198201	P23-17139	1	*Otospermophilus*	32500	370	1.3	3.33	36492	532	1.354
198202	P23-20172	1	*Otospermophilus*	35900	560	1.5	3.36	40539	581	2.234
198203	P23-26592	1	*Otospermophilus*	33100	620	1.1	3.37	37345	774	1.740
198204	P23-30796	1	*Otospermophilus*	36160	910	1.2	3.31	40752	846	2.195
*198205	P23-33227	1	*Otospermophilus*	36580	610	3.2	3.74	41162	552	1.537
*198206	P23-33228	1	*Otospermophilus*	30480	290	2.9	3.89	34454	260	2.144
198207	P23-33229	1	*Otospermophilus*	31830	340	2.4	3.42	35729	369	2.263
*198208	P23-33233	14	*Neotoma*	25620	160	1.4	3.77	29778	261	2.388

198294	P23-28902	1	*Sylvilagus*	39700	810	0.8	3.45	43526	676	2.108
*198295	P23-31113	14	*Otospermophilus*	33070	350	1.2	3.35	37260	535	1.748
198296	P23-31118	14	*Otospermophilus*	47400	2000	0.7	3.5	NA	NA	NA
*198297	P23-33232	14	*Thomomys*	28600	210	0.6	3.61	32643	381	2.315
198298	P23-33235	14	*Otospermophilus*	26310	150	2.3	3.36	30633	179	2.527
198302	P23-33228	1	*Otospermophilus*	30870	270	3.1	3.31	34795	274	1.650
216781	P23-35670	7B	*Otospermophilus*	30970	320	5	3.3	34900	326	1.550
216782	P23-35691	7B	*Mustela*	38750	840	3.1	3.2	42814	669	2.082
216783	P23-35774	7B	Leporidae	42600	1400	2.5	3.3	46221	1395	2.290
216784	P23-36332	7B	*Sylvilagus*	41500	1200	1.7	3.2	45104	1212	1.478
216785	P23-36336	7B	*Sylvilagus*	50200	3500	1	3.3	NA	NA	NA
217079	P23-36331	7B	*Sylvilagus*	46200	2400	1.2	3.3	48419	1178	1.588
223496	P23-36572	13	*Otospermophilus*	40640	800	1.9	3.5	44244	709	1.504
223497	P23-36693	13	*Sylvilagus*	39240	670	1.3	3.5	43123	549	2.140
223498	P23-36859	13	*Otospermophilus*	34800	390	5.0	3.4	39338	437	2.322
223499	P23-36896	13	*Sylvilagus*	33590	340	3.8	3.3	37934	502	1.830
223500	P23-36907	13	*Otospermophilus*	35230	410	1.9	3.4	39809	486	2.354
223501	P23-36910	13	*Otospermophilus*	35270	410	5.5	3.4	39855	487	2.411
223502	P23-36989	13	*Sylvilagus*	44000	1200	4.2	3.5	47439	1147	1.882
223503	P23-37612	13	*Sylvilagus*	46200	1600	3.0	3.4	48804	938	1.478
223504	P23-37651	13	*Otospermophilus*	47400	1800	4.3	3.4	NA	NA	NA
223505	P23-39811	13	*Sylvilagus*	33260	320	2.0	3.4	37505	506	1.720
223506	P23-39812	13	*Sylvilagus*	36260	470	3.5	3.3	40891	468	1.816
223507	P23-39818	13	*Sylvilagus*	31230	270	3.3	3.5	35132	286	1.649
223508	P23-39822	13	*Sylvilagus*	31980	280	2.7	3.4	35879	307	2.274
223509	P23-39825	13	*Otospermophilus*	32660	300	4.5	3.3	36660	460	1.516
223513	P23-40634	14	*Sylvilagus*	25830	140	3.1	3.3	30053	249	2.501
223514	P23-40635	14	*Sylvilagus*	>51700	NA	1.7	3.3	NA	NA	NA
223515	P23-40636	14	*Sylvilagus*	27200	160	0.5	NA	31152	110	2.247
223516	P23-40637	14	*Sylvilagus*	26780	160	2.7	3.3	30945	115	2.282

223517	P23-40638	14	*Sylvilagus*	36870	500	1.1	3.4	41434	434	1.981
223518	P23-40639	14	*Sylvilagus*	49800	2500	1.1	3.3	NA	NA	NA
*223519	P23-40640	14	*Sylvilagus*	49400	2400	0.3	NA	NA	NA	NA
*223520	P23-40641	14	*Neotoma*	28750	190	0.5	NA	32898	328	2.363
*223522	P23-40644	14	*Sylvilagus*	38490	610	0.4	NA	42572	442	2.334
223523	P23-40647	14	*Sylvilagus*	>49900	NA	1.8	3.4	NA	NA	NA
223585	P23-35541	13	*Sylvilagus*	39220	460	2.7	3.3	43041	376	2.097
223587	P23-40642	14	*Otospermophilus*	26710	110	4.0	3.3	30911	99	2.287

4.8 Figures

Figure 4.1: Map of Hancock Park showing the location of La Brea Tar Pits and Museum (LBTPM) and the adjacent Los Angeles County Museum of Art (LACMA) in central Los Angeles, CA. White boxes indicate the original salvage location of P23 asphalt deposits (left) and the current location of the wooden crates (center) where P23 excavation occurs. Figure adapted from (Mychajliw et al., 2020).

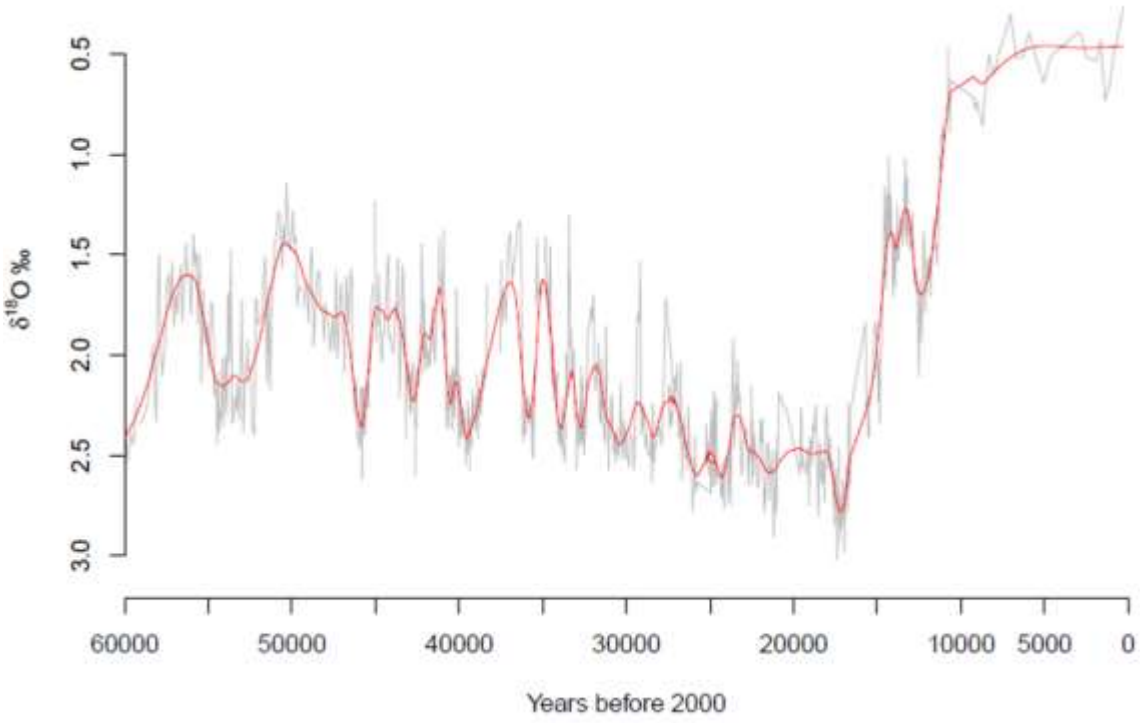

Figure 4.2: Marine foraminifera (*Neogloboquadrina pachyderma*) $\delta^{18}O$ climate record from Santa Barbara Basin ODP Hole 893A (Hendy et al., 2007). A locally estimated scatterplot smoothing (LOESS) polynomial (red line) is fitted over the original data (gray line) with a smoothing parameter $\alpha = 0.05$.

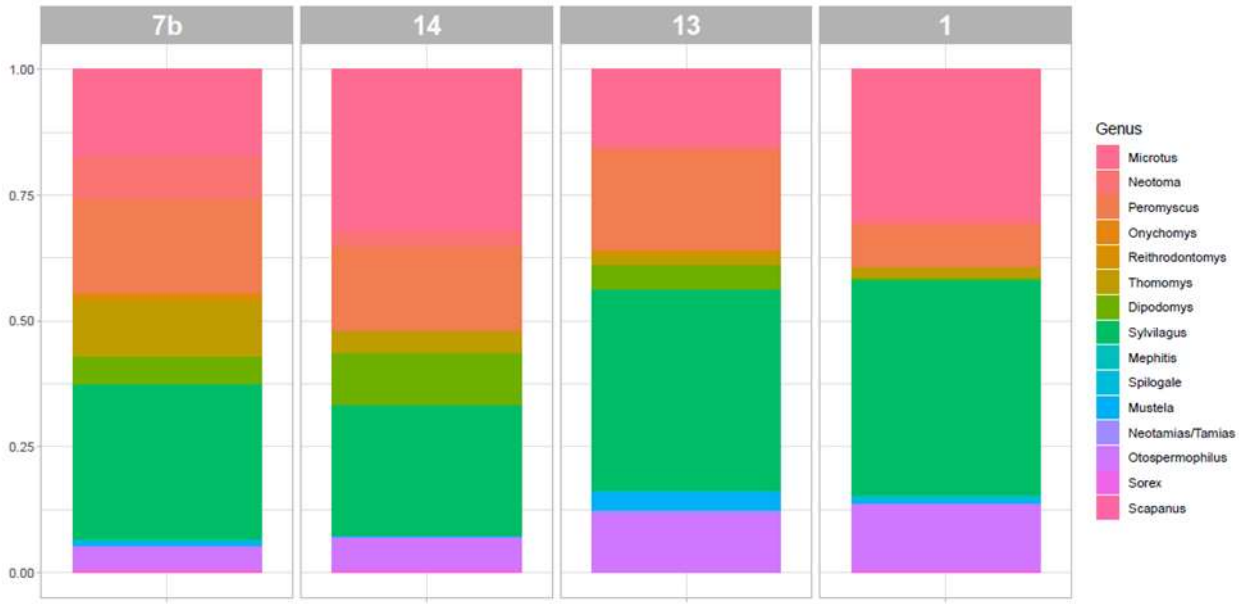

Figure 4.3: Genus-level relative abundance of taxa among the four deposits (Deposit 1, 13, 14, and 7b) based on NISP data from Table 4.1.

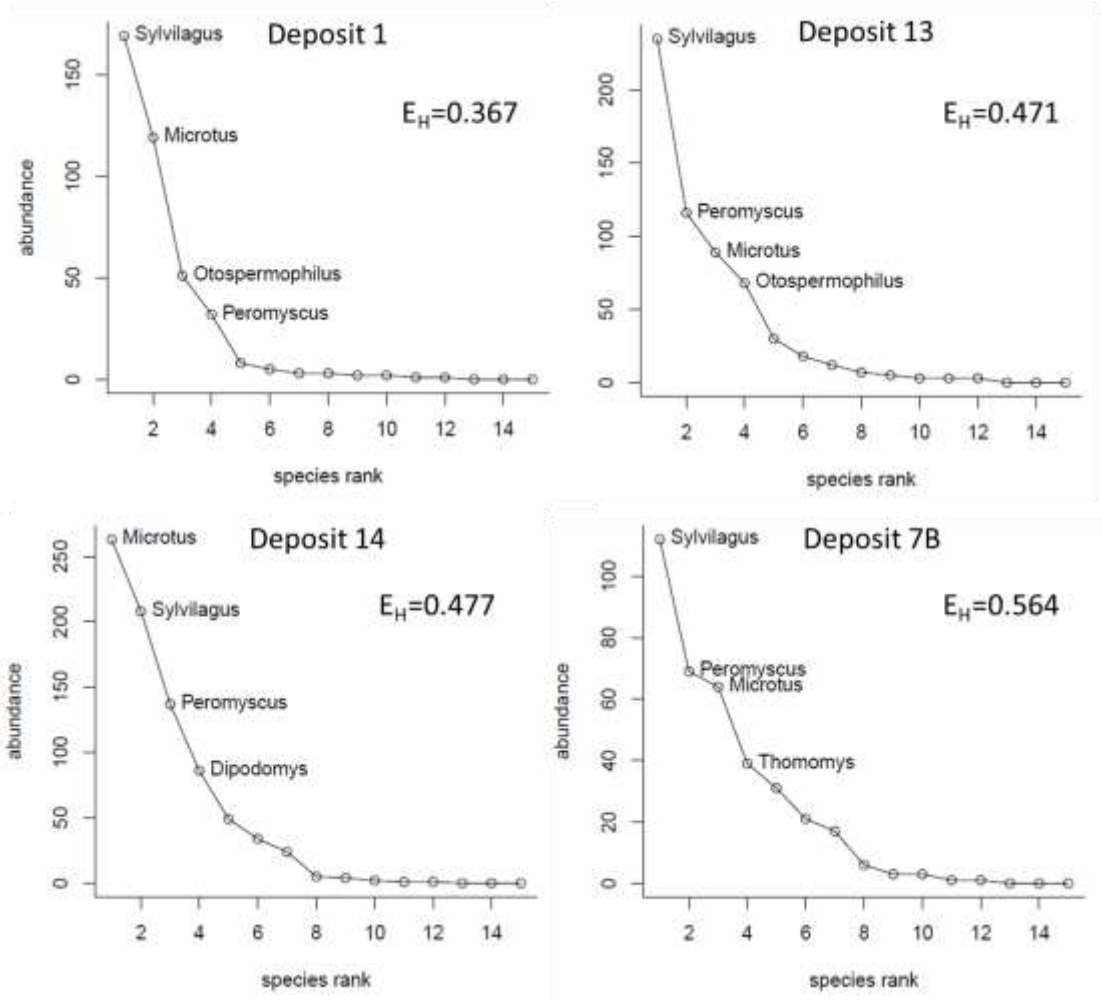

Figure 4.4: Rank abundance of genera among the four P23 deposits. The four most common genera and the generic evenness of each deposit based on the Shannon index (E_H) is labeled. Values closer to one and zero indicate greater and lesser evenness respectively. Plots were generated in the R package BiodiversityR (Kindt & Coe, 2005).

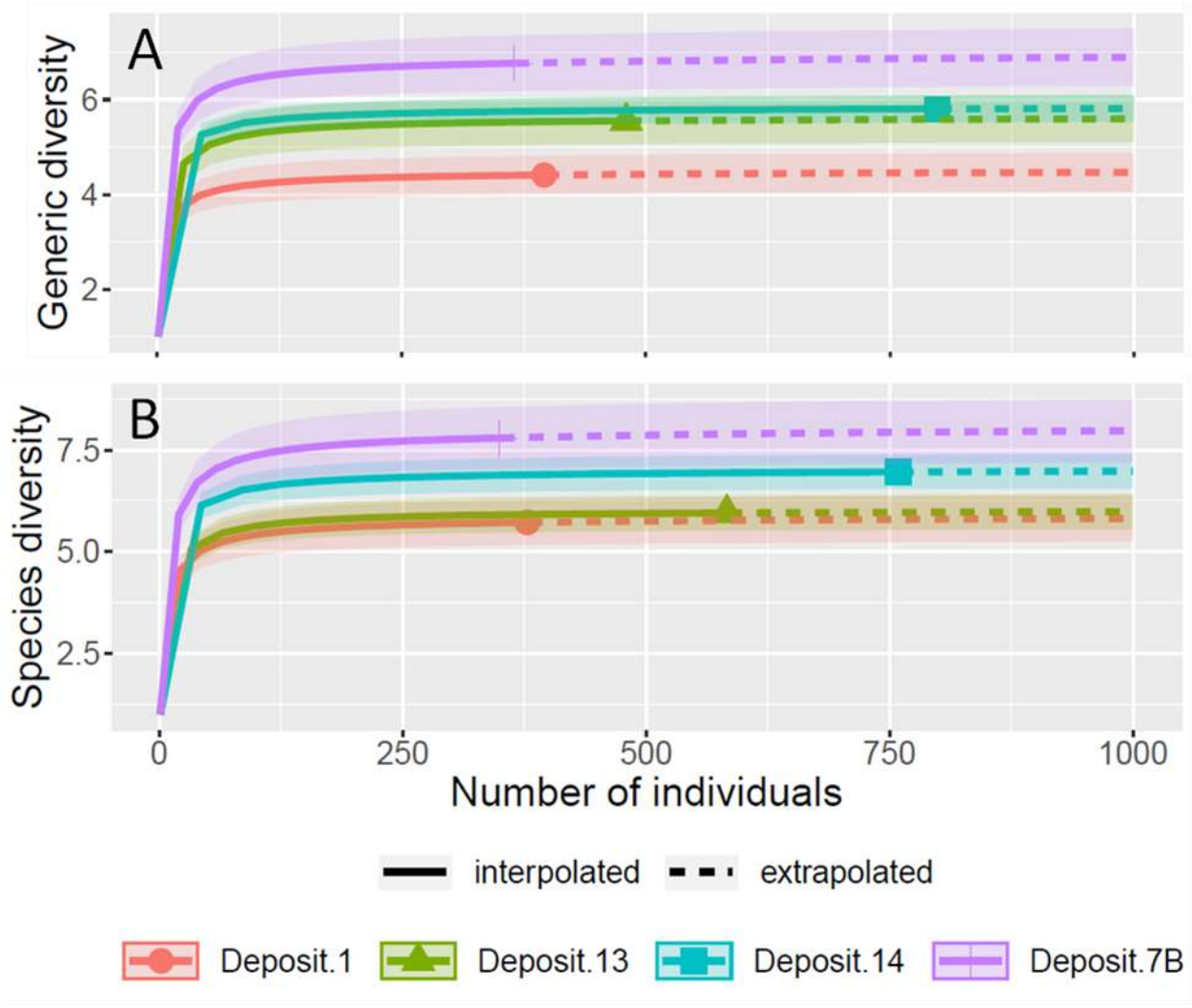

Figure 4.5: Rarified genus (A) and species (B) diversity of P23 taxa grouped by deposit. Species identifications in (B) were assumed for some taxa based on congeneric species identified at RLB in the literature (see "estimated" species pool conditions in the "Community traits" subsection of Methods and Appendix Table 4.4). Models were run using the Hill number $q = 1$ (i.e., Shannon diversity, (Chao et al., 2014)) in the R package iNeXT (Hsieh et al., 2020).

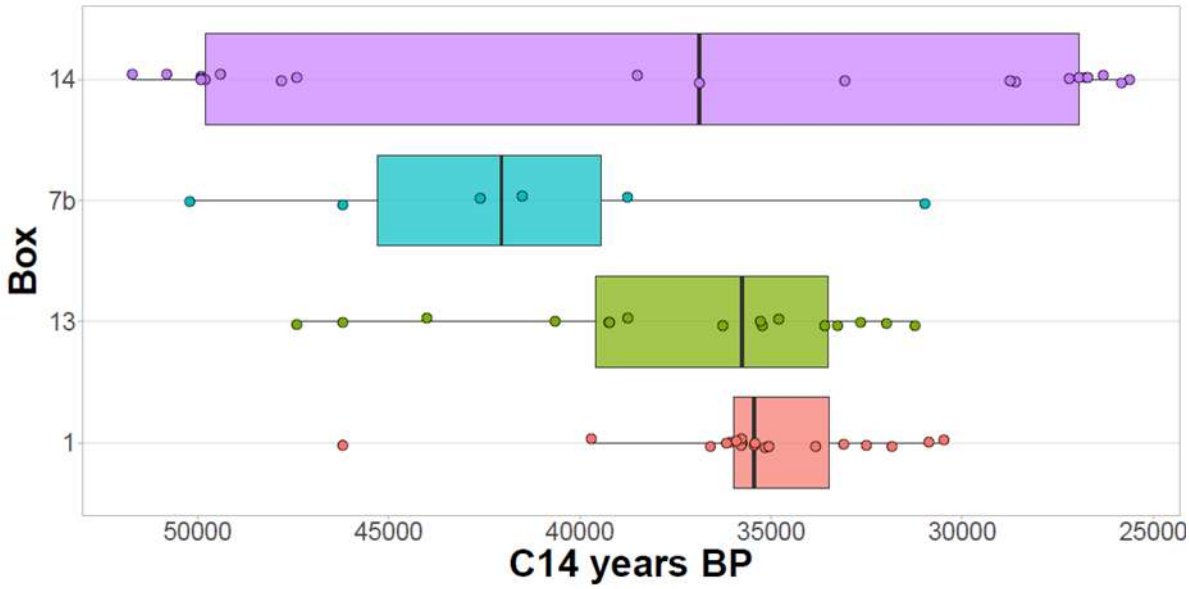

Figure 4.6: Age distribution of all radiocarbon dates obtained from P23 specimens reported in Table 4.2 grouped by deposit.

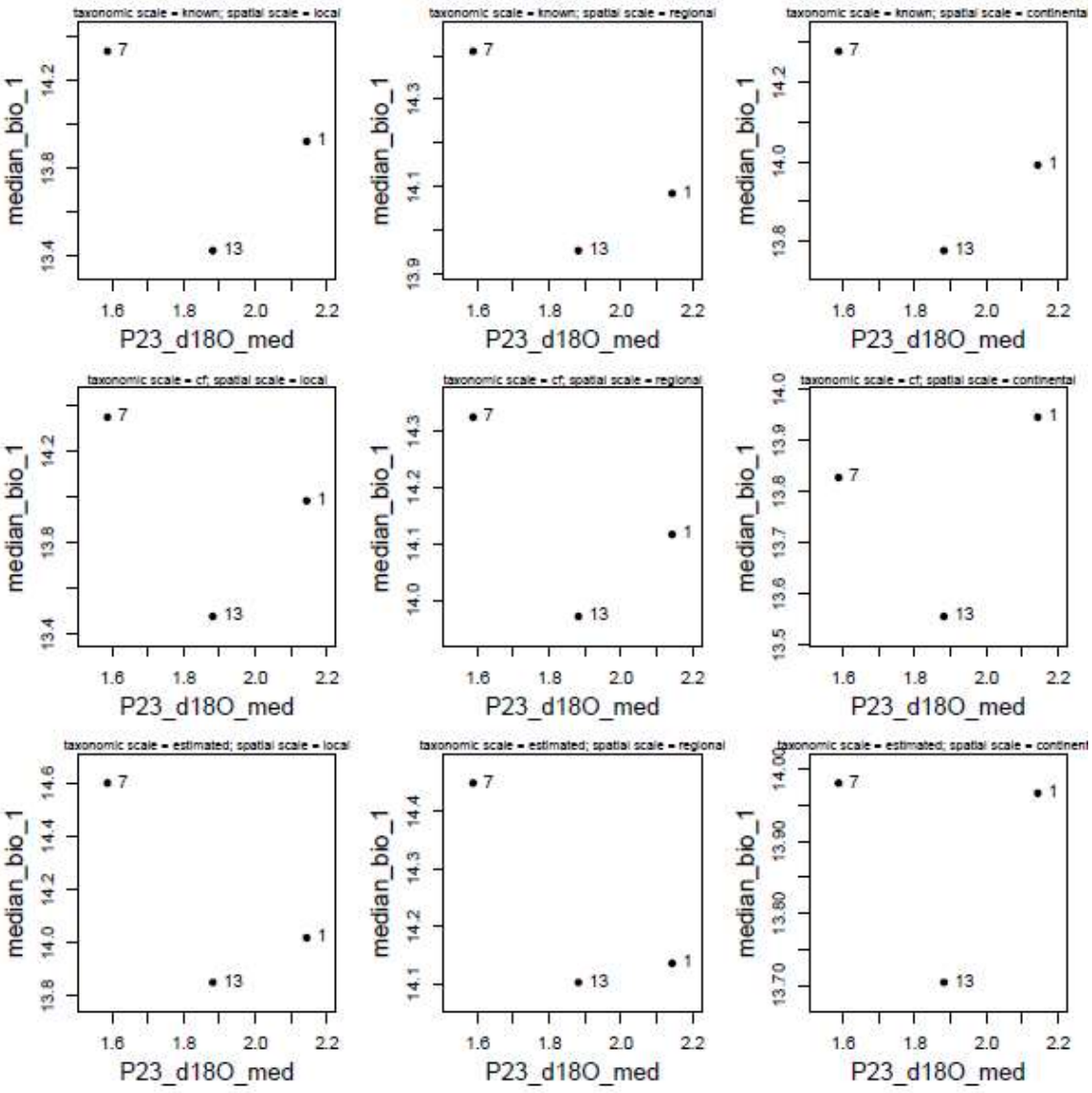

Figure 4.7: Results of nine spatial and taxonomic sensitivity simulations (see Methods) illustrating the relationship between average community-weighted temperature trait estimates, based on the median mean annual temperature value (BIO1) across the range of each identified species, and median interpolated $\delta^{18}O$ climate estimates for P23 Deposits: 1, 13, and 7B. $\delta^{18}O$ climate and community trait data were calculated from Hendy et al. (2007) and Fick and Hijmans (2017) respectively.

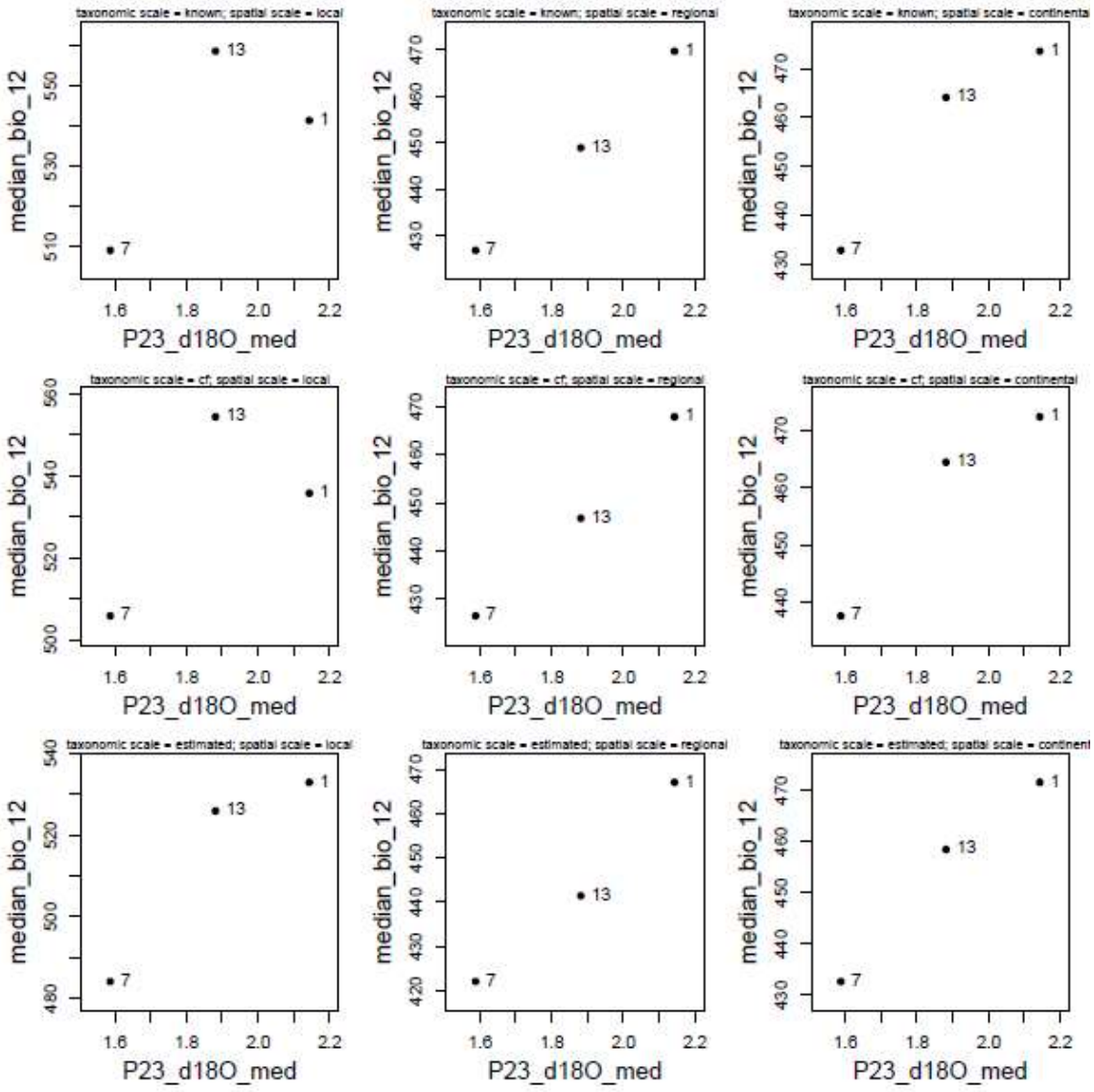

Figure 4.8: Results of nine spatial and taxonomic sensitivity simulations (see Methods) illustrating the relationship between average community-weighted precipitation trait estimates, based on the median annual precipitation value (BIO12) across the range of each identified species, and median interpolated $\delta^{18}O$ climate estimates for P23 Deposits: 1, 13, and 7B. $\delta^{18}O$ climate and community trait data were calculated from Hendy et al. (2007) and Fick and Hijmans (2017) respectively.

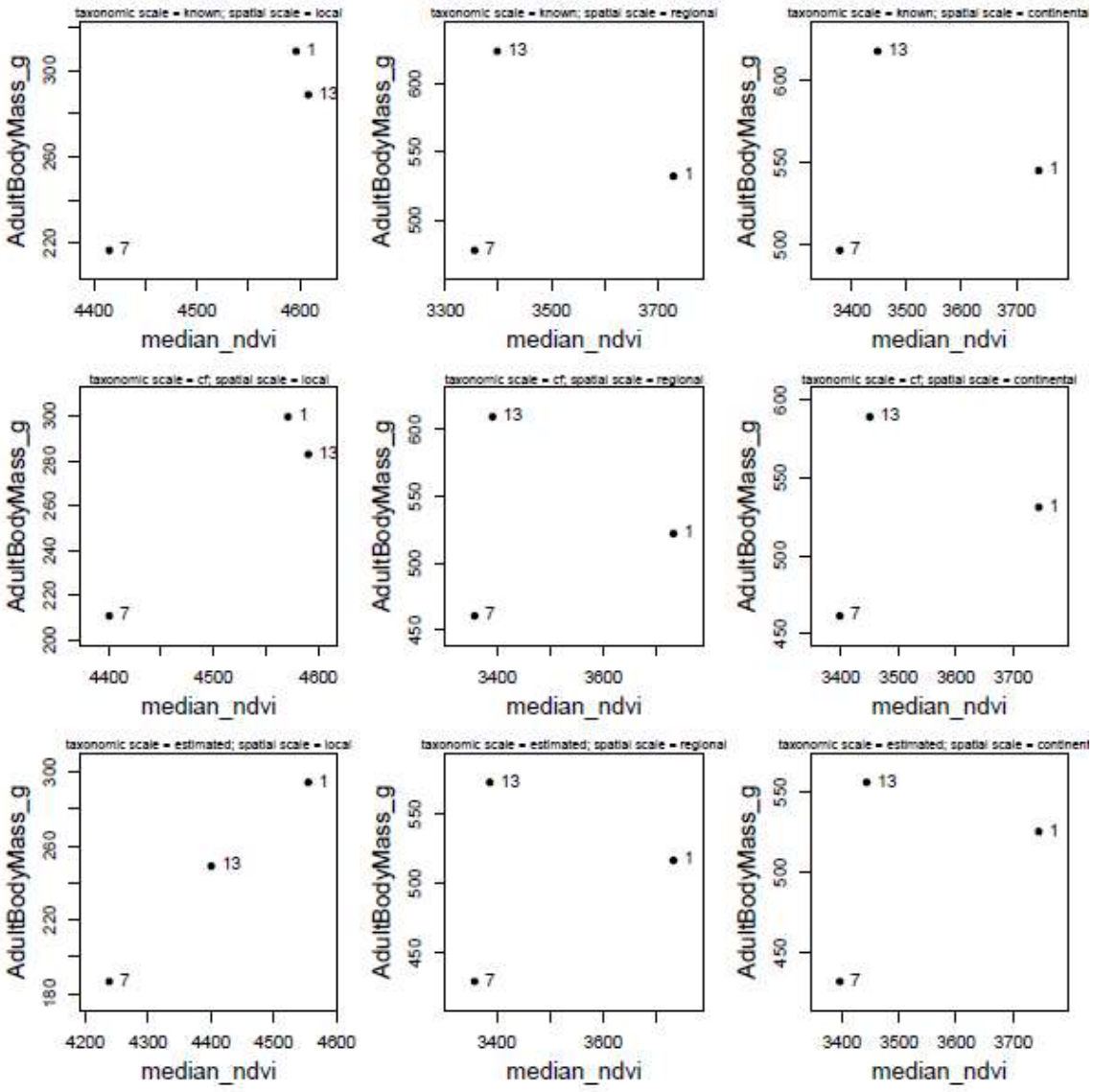

Figure 4.9: Results of nine spatial and taxonomic sensitivity simulations (see Methods) illustrating the relationship between average community-weighted adult body size estimates of each identified P23 species from PanTHERIA and average community-weighted NDVI estimates for P23 Deposits: 1, 13, and 7B. NDVI and body size data were calculated from Powell et al. (2019) and Jones et al. (2009) respectively.

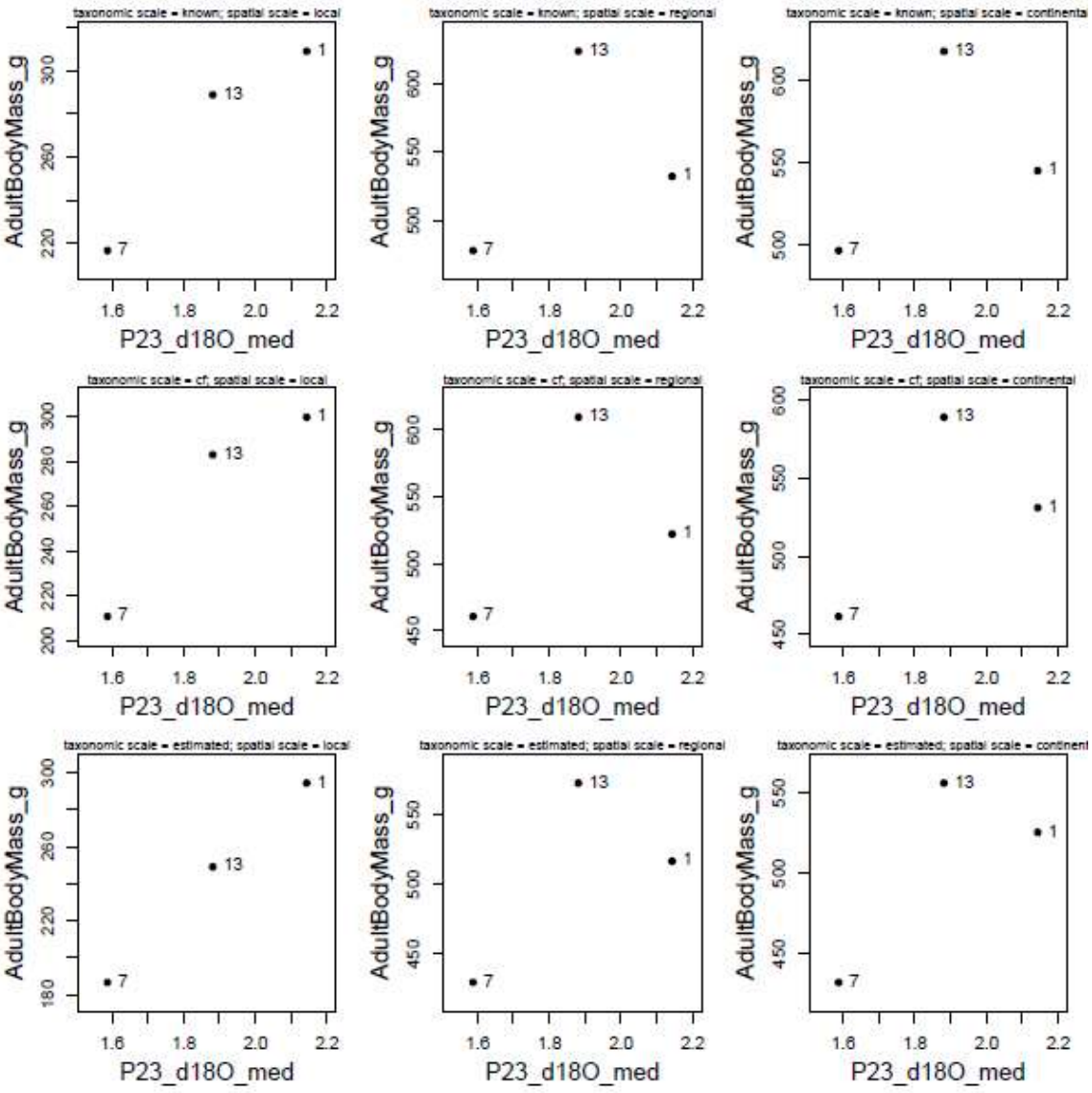

Figure 4.10: Results of nine spatial and taxonomic sensitivity simulations (see Methods) illustrating the relationship between average community-weighted adult body size estimates of each identified P23 species from PanTHERIA and median interpolated $\delta^{18}O$ climate estimates for P23 Deposits: 1, 13, and 7B. $\delta^{18}O$ climate and body size data were calculated from Hendy et al. (2007) and Jones et al. (2009) respectively.

4.9 Appendix

Appendix 4.9.1: Systematic paleontology descriptions of small mammal craniodental elements identified from P23 Deposits 1, 7B, 13, and 14 at Rancho La Brea. Referred specimens list counts of individual specimens reported in Appendix Table 4.9.2 and, for monotypic taxa, Table 4.1. Referenced comparative specimens are listed in Appendix Table 4.9.5. Element abbreviations: lt = left side elements, rt = right side elements, upper case letters indicate teeth in the upper toothrow, lowercase letters indicate teeth in the lower toothrow. C/c = canine, I/i = incisor, D/d = deciduous tooth; P/p = premolar; M/m = molar; 1-4 refers to tooth position. All identifications were made by Nathaniel Fox. Taxonomic names follow (Wilson & Reeder, 2005).

CARNIVORA Bowditch, 1821
MEPHITITADE Bonaparte, 1845
MEPHITIS MEPHITIS Schreber, 1776

Referred specimens – Nine specimens are assigned to *Mephitis mephitis* (3, 3, 3, and 0 from Deposits 1, 7B, 13, and 14 respectively; Table 4.1, Appendix Table 4.9.2).

Remarks – Specimens were identified as *Mephitis mephitis* (striped skunk) based on morphological features and size using recent comparative specimens of *M. mephitis* and *Spilogale gracilis* (spotted skunk) in the LBTPM research collection: *Mephitis mephitis* fossils have been found in other RLB deposits as well (Stock & Harris, 1992).

SPILOGALE GRACILIS Merriam, 1890

Referred specimens – Two specimens are assigned to *Spilogale gracilis* (1, 0, 0, and 1 from Deposits 1, 7B, 13, and 14 respectively; Table 4.1, Appendix Table 4.9.2).

Remarks – Adult elements of *Spilogale gracilis* exhibit the same general morphology as *Mephitis mephitis* but are obviously smaller. *Spilogle gracilis* is a relatively rare carnivore at RLB, but several fossils have been recovered from non-P23 deposits (Stock & Harris, 1992, N. Fox, personal observation 2018).

MUSTELIDAE Fischer 1817
MUSTELA FRENATA Lichtenstein, 1831

Referred specimens – 31 specimens are assigned to *Mustela frenata* (3, 3, 21, and 4 from Deposits 1, 7B, 13, and 14 respectively; Table 4.1, Appendix Table 4.9.2).

Remarks – Specimens were identified as *Mustela frenata* based on element sizes well above the upper range of extant *M. nivalis* and most examined individuals of *M. erminea* (Appendix Table 4.9.5). *Mustela frenata* is the most common small carnivore at RLB overall (Stock & Harris, 1992).

LAGOMORPHA Brandt, 1855
LEPORIDAE Fischer, 1817

SYLVILAGUS Gray, 1867

Referred specimens – 666 specimens are assigned to *Sylvilagus* sp. (158, 96, 215, and 197 from Deposits 1, 7B, 13, and 14 respectively; Appendix Table 4.9.2).

Remarks – Specimens were identified as *Sylvilagus* sp. based on element sizes well outside the size range of extant *Lepus californicus* and *Lepus townsendii*. Specimens of *Sylvilagus* other than p3s or dentaries with p3s preclude species-level identification. See (Fox et al., 2019) for the list of recent comparative leporid specimens examined.

SYLVILAGUS AUDUBONII Baird, 1857

Referred specimens – 52 craniodental elements with p3s and partial p3s are assigned to *S. audubonii* (9, 16, 20, and, 7 from Deposits 1, 7B, 13, and 14 respectively; Appendix Table 4.9.2).

Remarks – Using the protocol of (Fox et al., 2019), I identified fifty-two specimens as *S. audubonii* based on moderate to complex p3 enamel crenulation and p3 l/w ratios within the range of extant *S. audubonii* (i.e., 1.02-1.35, mean =~1.20). Differences in p3 crenulation patterning between the surface and base of the tooth occur in some specimens which I attribute to ontogeny/wear (Fox et al., 2019). 11 of the 52 specimens with more complex crenulation at the base of the tooth relative to the surface are considered juvenile individuals of *S. audubonii*. See (Fox et al., 2019) for the list of recent comparative leporid specimens examined.

SYLVILAGUS BACHMANI Waterhouse, 1839

Referred specimens – Seven specimens are assigned to *S. bachmani* (2, 1, 0, and, 4 p3 specimens from Deposits 1, 7B, 13, and 14 respectively; Appendix Table 4.9.2).

Remarks – Seven specimens are identified as *S. bachmani* based on simple crenulation at the surface and base of the p3, a p3 length < 3.0 mm, and l/w ratios within the range of extant *S. bachmani* (i.e., 1.14-1.44, mean =~1.25) (Fox et al., 2019). See (Fox et al., 2019) for the list of recent comparative leporid specimens examined.

RODENTIA Bowdich, 1821
CRICETIDAE Fischer, 1817
ARVICOLINAE Gray, 1821
***MICROTUS* Schrank, 1798**

Referred specimens – 503 specimens are assigned to *Microtus* sp. (108, 64, 89, and 242 from Deposits 1, 7B, 13, and 14 respectively; Appendix Table 4.9.2).

Remarks – Specimens exhibit rootless molars with reentrant angles are covered in cementum. The m1 exhibits a posterior loop, anterior cap, and five closed alternating triangles (Bell & Jass, 2004). *Microtus* M3s exhibit an anterior loop and two or three

closed alternating triangles (Bell & Jass, 2004). All edentulous *Microtus* jaws and isolated molars, other than m1s, preclude species-level identification.

MICROTUS CALIFORNICUS Peale, 1848

Referred specimens – 23 specimens are assigned to *Microtus californicus* (11, 0, 0, and 12 from Deposits 1, 7B, 13, and 14 respectively; Appendix Tables 4.9.2 & 4.9.6).

Remarks – I conducted linear discriminant analyses (LDA) on 2D landmark data from the lower first molar of five extant western North American *Microtus* species (i.e., *M. californicus*, *M. longicaudus*, *M. montanus*, *M. oregoni*, and *M. townsendii*, n = 247) using the protocol of (McGuire, 2011; Wallace, 2006). See (McGuire, 2011) for the list of recent *Microtus* specimens examined. Discriminant functions of the recent "training" specimens were then used to identify 60 P23 fossil *Microtus* molars of unknown species affinity. An exploratory analysis evaluating geometric morphometric error and classification sensitivity was conducted on 31 specimens from Deposit 1 (Fox et al., 2020). I expanded that dataset to include an additional 29 specimens from Deposit 14. Extant specimens were digitized twice (datasets "Dinolite_NoTilt_EO_T1" and "Dinolite_NoTilt_EO_T2" from (Fox et al., 2020)) and LDA of both datasets predict *M. californicus* as the dominant species in both deposits (Appendix Table 5). Specimens classified as *M. californicus* in both datasets are assigned to "*M. californicus*" while specimens classified as *M. californicus* in one or neither dataset are assigned to "*Microtus* sp." (Appendix Table 4.9.6). Since specimens from Deposits 7B and 13 were not included in the landmark analysis, it is likely that the absence the *M. californicus* in those deposits is a sampling effect rather than a true absence. It is unclear whether the predicted occurrences of less common *Microtus* species are actually present in P23 (Appendix Table 4.9.6) or if this is an artifact of classification error (Fox et al., 2020). Misclassification rates of 13.8-17.4% occur within the extant species LDA training sets listed above (Fox et al., 2020). Until further support is provided, I do not consider the presence of any other *Microtus* species at RLB likely. Dice (1925) attributed *Microtus* craniodental specimens from RLB localities 1059, 2051, and 2052 to *M. californicus*.

NEOTOMINAE Merriam, 1894
NEOTOMA Say & Ord, 1825

Referred specimens – 60 specimens are assigned to *Neotoma* sp. (5, 25, 7, and 23 from Deposits 1, 7B, 13, and 14 respectively; Appendix Table 4.9.2).

Remarks – Cricetid craniodental elements were assigned to *Neotoma* sp. based on relatively
large, hypsodont, robust, and rooted dentition with three upper and lower molars per side (Hillson, 2005). All elements lacking the diagnostic m1 (Harris, 1984; Fox, Chapter 3) and m1s with ambiguous morphology are assigned to *Neotoma* sp.

NEOTOMA MACROTIS Thomas, 1893

Referred specimens – Seven lower first molars are assigned to *Neotoma macrotis* (0, 6, 0, and 1 from Deposits 1, 7B, 13, and 14 respectively; Appendix Tables 4.9.2 & 4.9.6).

Remarks – As with *Microtus*, LDA of 2D landmarks was conducted on the lower first molar of five extant western North American *Neotoma* species (i.e., *N. albigula, N. cinerea, N. fuscipes, N. lepida,* and *N. macrotis*, n = 199) to identify 14 P23 fossils of unknown species affinity (Fox, Chapter 3). See Fox (Chapter 3) for the list of recent *Neotoma* specimens examined. *Neotoma* is relatively rare in P23 (Table 4.1) so those 14 specimens represent all complete m1s acquired from my sampling approach. Seven of the 14 fossils, classified as *N. macrotis* in both landmark data replicates of Fox (Chapter 3), are assigned to "*N. macrotis*" (Appendix Table 4.9.6). Specimens classified as *N. macrotis* in one or neither dataset are assigned to "*Neotoma* sp.". Classification accuracy of the two *Neotoma* dataset replicates is comparable to *Microtus* dataset replicates digitized by the same individual (15.1-16.6% versus 13.8-17.4% misclassification rates for extant *Neotoma* and *Microtus* species respectively, Appendix Table 4.9.6). Therefore, as with *Microtus*, I do not consider the few specimens assigned to other species of *Neotoma* (i.e., *N. albigula* and *N. fuscipes*, Appendix Table 4.9.6) likely present in P23 based on such limited samples.

cf. ONYCHOMYS TORRIDUS Coues, 1874

Referred specimens – Three specimens are assigned to cf. *Onychomys torridus* (0, 0, 3, and 0 from Deposits 1, 7B, 13, and 14 respectively; Table 4.1, Appendix Table 4.9.2). The following specimens are upper left first molars: LACMP23-40527, upper right first molars: LACMP23-40531, and lower right first molars: LACMP23-40522 respectively.

Remarks – Specimens are approximately equal in size to – or slightly larger than – molars of recent, medium-sized, *Peromyscus* species (e.g., *P. maniculatus*) but exhibit characteristics not seen in comparative specimens of those taxa (Appendix Table 4.9.5). For example, fossil upper first molars LACMP23-40527 and LACMP23-40531 exhibit more anteriorly protruding anterocones than *Peromyscus* which forms a prominent anterolingual angle with the body of the tooth in occlusal view (Appendix Figure 4.9.1A). M1 cusps of fossils are narrower and more pointed at the dorsal apex than *Peromyscus* which exhibits more blunted cusps, even in individuals with little occlusal wear (Figure 4.9.1A). Cusps of the referred fossil specimens also project medioventrally at a steeper angle than *Peromyscus*, forming a "v" shape (Appendix Figure 4.9.1A). In lateral view, re-entrants between cusps protrude deeper ventrally than *Peromyscus*. Together, these characters give a tooth a sharper and more "carnivorous" appearance than *Peromyscus*. The transverse ridges connecting molar cusps of the referred fossils are also less prominent than those of lightly to moderately worn specimens of *Peromyscus* (Appendix Figure 4.9.1A). Lastly, there is a marked gap between the mesiobuccal and posterobuccal cusps of the referred fossils relative to recent and referred fossils of *Peromyscus*.

As with the fossil upper molars, cusps of the lower first molar LACMP23-40522 slope more steeply, lack prominent transverse ridges, and are higher crowned than recent and referred fossil *Peromyscus* specimens (Appendix Figure 4.9.1B). The tooth is

proportionally longer than other *Peromyscus* and *Peromyscus*-referred specimens overall (Appendix Figure 4.9.1B). Unlike *Peromyscus*, which generally exhibits lower buccal cusps relative to lingual cusps, buccal and lingual cusp height is approximately equal in the referred fossil specimen. The first anterolateral cusp of the referred specimen is also positioned more anteriorly than in specimens of *Peromyscus* and it forms a tight notch between the anteroconid rather than a prominent gap (Appendix Figure 4.9.1B). This displacement, and the steeper and more ventrally protruding cusps, create a deeper and wider gap in the re-entrants between cusps than in *Peromyscus* – especially in the mesiolingual gap between the anterolingual and posterolingual cusps (Appendix Figure 4.9.1B). These characters compare more favorably with recent specimens of *Onychomys* that exhibit little occlusal wear than recent specimens of *Peromyscus*. However, due to the morphological variation present in members of *Peromyscus*, and my relatively small recent and fossil comparative sample size, identification of *Onychomys* is tentative. If these identifications are correct, the specimens most likely belong to *Onychomys torridus* based on the modern distribution of three extant species (*O. arenicola, O. leucogaster*, and *O. torridus*) in southwestern North America (Hinesley, 1979; McCarty, 1975, 1978). Dice (1925) assigned one specimen from RLB locality 2052 and another from a locality, possibly 2051, to *O. torridus*.

PEROMYSCUS Gloger, 1841

Referred specimens – 296 specimens are assigned to *Peromyscus* sp. (22, 55, 100, and 119 from Deposits 1, 7B, 13, and 14 respectively; Appendix Table 4.9.2).

Remarks – Specimens are assigned to two morphotypes (A and B) differentiated primarily by obvious size differences in adult specimens (Appendix Figure 4.9.1). These morphs likely represent two distinct species of *Peromyscus*. Due to the vast number of *Peromyscus* species that occur in North America and their morphological variability (Dalquest & Stangl Jr., 1983; Hooper, 1957; Martin, 1968; Miller, 1976), I was unable to assign many *Peromyscus* specimens to a particular species; though I consider a subset of species to be likely candidates. Morphotype A represents the larger and less common morph while morphotype B represents the smaller and more common morph. Specimens of morphotype A usually exhibit strongly differentiated m1 anteroconids (Appendix Figure 4.9.1B), small or absent accessory lophs and styles on upper molars (Appendix Figure 4.9.1A), and are overall larger than all extant *Peromyscus* species examined aside from *P. californicus* (Appendix Table 4.9.5). In morphotype B, the morphology of the m1 anteroconid is variable and ranges from undivided to highly divided (Appendix Figure 1, see Dalquest and Strangl (1983) for division categories). Individuals of morph B with highly divided m1 anteroconids tend to be slightly larger than those with weakly divided or undivided m1 anteroconids (Appendix Figure 4.9.1B). Such traits compare favorability with several individuals of extant *P. truei* examined here (Appendix Table 4.9.5). Individuals with weakly or undifferentiated m1 anteroconids tend to be slightly smaller than those with strongly differentiated anteroconids and often compare favorably in size and morphology with extant individuals of *P. eremicus* and *P. maniculatus* (Appendix Table 4.9.5). Due to potential ontogenetic differences among specimens, and the extensive morphological variability within and among members of this genus, morph B

could represent a single species or several species. At minimum, however, there appears to be two species of *Peromyscus* present within the faunas of Project 23 (morphotype A and morphotype B).

PEROMYSCUS cf. P. CALIFORNICUS Gambel, 1848

Referred specimens – 20 specimens are assigned to *Peromyscus* cf. *P. californicus* (7, 3, 4, and 6 from Deposits 1, 7B, 13, and 14 respectively; Appendix Table 4.9.2).

Remarks – Specimens of morphotype A are tentatively assigned to *Peromyscus* cf. *P. californicus*. These specimens are obviously larger than those of morphotype B (Appendix Figure 4.9.1) and examined individuals of extant species other than *P. californicus* (Appendix Table 4.9.5). The referred specimens usually exhibit strongly divided m1 anteroconids (Appendix Figure 1B) and small or absent accessory lophs and styles on upper molars (Appendix Figure 4.9.1A) which compares favorably with extant individuals of *P. californicus* (Hooper 1957) (Appendix Table 4.9.5). However, there is some uncertainty in these identifications since other members of *Peromyscus* can exhibit similar morphological characteristics (Dalquest & Stangl Jr., 1983; Hooper, 1957) and because intraspecific small mammal body size can change over millennia (e.g., Fox et al., 2019; Smith et al., 1995).

PEROMYSCUS cf. P. MANICULATUS Wagner, 1845

Referred specimens – 38 specimens are assigned to *Peromyscus* cf. *P. maniculatus* (3, 11, 12, and 12 from Deposits 1, 7B, 13, and 14 respectively; Appendix Table 4.9.2).

Remarks – A subset of specimens of morphotype B within the size range of extant *P. maniculatus* that exhibit prominent M1 anterobuccal accessory lophs/styles and diminutive, undifferentiated, m1 anteroconids are tentatively assigned to *P. maniculatus* (Appendix Figure 4.9.1). The morphology of *P. maniculatus* dentition is highly variable (Dalquest & Stangl Jr., 1983; Hooper, 1957). However, large M1 accessory lophs/styles and diminutive and undivided m1 anteroconids are common in extant *P. maniculatus* (Hooper, 1957; Miller, 1976), and most recent *Peromyscus* specimens examined here exhibiting those characters are of *P. maniculatus* (Appendix Table 4.9.5). Therefore, the subset of morphotype B specimens exhibiting characters typical of *P. maniculatus* were identified as "*Peromyscus* cf. *P. maniculatus*", recognizing that some uncertainty occurs in these identifications. Dice (1925) attributed *Peromyscus* fossils from RLB localities 1059, 2050, 2051, 2052 to an extinct taxon, *Peromyscus imperfectus*, approximately equal in size to *P. maniculatus*. However, *P. imperfectus* is now considered synonymous with *P. maniculatus* (https://www.itis.gov/servlet/SingleRpt/SingleRpt?search_topic=TSN&search_value=971494#null). Craniodental characters described in *P. imperfectus*, including "small accessory tubercules on the M1 and M2" (Dice, 1925), are commonly observed in recent specimens of *P. maniculatus* as mentioned. Consequently, fossils previously described as *P. imperfectus* from RLB likely belong to *P. maniculatus* or another extant *Peromyscus* species; though those specimens were not examined here.

cf. REITHRODONTOMYS MEGALOTIS Baird, 1857

Referred specimens – 10 specimens are assigned to cf. *Reithrodontomys megalotis* (0, 6, 3, and 1 from Deposits 1, 7B, 13, and 14 respectively; Appendix Table 4.9.2).

Remarks – Specimens obviously smaller than extant members of *Peromyscus* that do not appear juvenile are tentatively identified as *Reithodontomys megalotis* (western harvest mouse) (Appendix Figure 4.9.1). *Reithodontomys megalotis* is the only species of harvest mouse known from recent and late Quaternary sites in the Pacific West of North America aside from the endangered Salt Marsh Harvest Mouse (*Reithrodontomys raviventris*) endemic to the San Francisco Bay area (Hall & Kelson, 1959; Shellhammer, 1982). *Reithrodontomys* are morphologically similar to *Peromyscus* and many isolated elements of the two genera are only distinguishable based on size (Wilson, 1933). These diminutive molars are assigned to cf. *Reithrodontomys megalotis*. Though, identifications are tentative without other diagnostic morphological characters.

GEOMYIDAE Bonaparte, 1845
THOMOMYS Wied-Neuwied, 1839

Referred specimens – 87 specimens are assigned to *Thomomys* sp. (8, 36, 11, and 32 from Deposits 1, 7B, 13, and 14 respectively; Appendix Table 4.9.2).

Remarks – Dental elements of *Thomomys* can be differentiated from morphologically similar heteromyid dentition (e.g., *Dipodomys*) based on relatively large, robust, and teardrop-shaped molars in the former (Dalquest & Schultz, 1992). Conversely, heteromyid molars are comparatively smaller, more gracile, and more oval-shaped overall. Isolated geomyid dentition, excluding p4s, preclude species-level identification.

THOMOMYS ?BOTTAE Eydoux and Gervais, 1836

Referred specimens – Six specimens are assigned to *Thomomys* ?*bottae* (0, 3, 1, and 2 from Deposits 1, 7B, 13, and 14 respectively; Appendix Table 4.9.2).

Remarks – All p4s and posterior dentaries from P23 can be identified to the subgenus *Megascapheus* based on a conspicuous anterolingual gap between the anterior enamel plate and lateral enamel plate of the p4, a lack of recurvature along the anterior enamel plate of the p4, and a weakly-developed ventral flange along the dentary ramus (Thaeler, 1980). Within this subgenus, two species occur in the Pacific West today: *T. bottae* and *T. townsendii*. *Thomomys bottae* is broadly distributed throughout most of California while *T. townsendii* occurs only in a small part of northeastern California (Jones & Baxter, 2004; Verts & Carraway, 2003). Specimens from P23 compare more favorably in size with the smaller taxon, *T. bottae*, than the larger *T. townsendii*. Therefore, all referred specimens likely belong to *T. bottae*. Dice (1925) attributed geomyid specimens from RLB localities 1059, 2050, 2051, and 2052 to *T. bottae* as well.

HETEROMYIDAE Gray, 1868
DIPODOMYINAE Gervais, 1853
DIPODOMYS Gray, 1841

Referred specimens – 139 specimens are assigned to *Dipodomys* sp. (2, 21, 30, and 86 from Deposits 1, 7B, 13, and 14 respectively; Table 4.1; Appendix Table 4.9.2).

Remarks – Isolated heteromyid teeth are difficult to identify to species due to their lack of diagnostic qualitative characters and the high diversity of this taxonomic group (Carrasco, 2000; Wahlert, 1993). Therefore, all craniodental elements of *Dipodomys* are identified to genus only. Dice (1925), assigned heteromyid craniodental elements from RLB localities 1059 and 2051 to *Dipodomys agilis*, and the referred P23 specimens compare favorably in shape and size with *Dipodomys agilis* overall. However, I am unable to rule out other species due to the relatively simplistic morphology of these specimens.

PEROGNATHINAE Coues, 1875

Referred specimens – 17 specimens are assigned to Perognathinae (1, 12, 0, and 4 from Deposits 1, 7B, 13, and 14 respectively; Table 4.1; Appendix Table 4.9.2).

Remarks – As with other heteromyids such as *Dipodomys*, identifying isolated dental elements of pocket mice (subfamily Perognathinae) to species is difficult. Such identifications are further complicated in California by the two specious genera of pocket mice that reside there today (i.e., *Chaetodipus* and *Perognathus*). Dice (1925) referred craniodental elements from RLB localities 2051and 2052 to *Chaetodipus californicus*; though, I am unable to confidently assign the few pocket mouse elements recovered from P23 to genus or species.

SCIURIDAE Fischer de Waldheim, 1817
XERINAE Osborn, 1910

Referred specimens – 32 specimens are assigned to Xerinae (3, 3, 21, and 5 from Deposits 1, 7B, 13, and 14 respectively; Appendix Table 4.9.2).

Remarks – All sciurid cheek teeth and partial cheek teeth from P23 can be identified as terrestrial squirrels (subfamily Xerinae) based on a lingually-tapered protocone in upper molariform teeth creating an overall "triangular" occlusal profile, relatively high crown height, and well-defined proto- and metalophs (Bryant, 1945; Goodwin, 2004). Such characters are distinct from tree squirrels (subfamily Sciurinae) which exhibit lower crowned and more quadrate dentition with less prominent proto- and metalophs (Bryant, 1945; Goodwin, 2004).

OTOSPERMOPHILUS ?BEECHEYI Richardson, 1829

Referred specimens – 185 specimens are assigned to *Otospermophilus* ?*beecheyi* (51, 17, 68, and 49 from Deposits 1, 7B, 13, and 14 respectively; Table 4.1; Appendix Table 4.9.2).

Remarks – The referred specimens within the subfamily Xerinae are relatively large and exhibit size and shape characters (e.g., separation of the metaloph from the protocone, and a prominent metaconule, on P4s, M1s, and M2s and the absence of a mesoconid on m1s and m2s) that compare favorably with *Otospermophilus beechyi* (Bryant, 1945; Goodwin, 2004). However, there is some uncertainty with these identifications since such characters are shared with other relatively large ground squirrels (e.g., *O. variegatus*). *Otospermophilus variegatus* occurs only along the southeastern edge of California today (Oaks et al., 1987) while *O. beecheyi* is broadly distributed throughout much of California including the LA Basin (Smith et al., 2016). *Otospermophilus beechyi* has also been reported from RLB localities 1059, 2050, 2051, and 2052 (Dice, 1925).

NEOTAMIAS/TAMIAS Howell, 1929/ Illiger, 1811

Referred specimens – Nine specimens are assigned to *Neotamias*/*Tamias* (1, 1, 5, and 2 from Deposits 1, 7B, 13, and 14 respectively; Table 4.1; Appendix Table 4.9.2).

Remarks – In addition to obvious size differences, chipmunks (genera *Neotamias* and *Tamias*) can be differentiated from larger terrestrial squirrels based on their comparatively diminutive P4 anterior cingulum and valley, and an M1/M2 metaloph that is fully joined to the protocone without a prominent metaconule (Bryant, 1945). Lower molars of chipmunks exhibit a prominent mesoconid, and a conspicuous notch between the protoconid and anterior cingulum ridge, on the m1-m3 (Bryant, 1945; Goodwin, 2004). Due to the diversity of *Neotamias* and *Tamias* species in California and their morphological similarity (Goodwin, 2004), I cannot confidently assign P23 chipmunk specimens to either genus. However, Whistler (1989) tentatively assigned specimens from RLB Pit 91 to "*Neotamias* cf. *N. merriami*" and P23 fossils compare favorably with examined recent individuals of *N. merriami* overall (Appendix Table 4.9.5).

SORICOMORPHA Gregory, 1910
SORICIDAE Fischer, 1814
SORICINAE Fischer 1817

Referred specimens – 10 specimens are assigned to the subfamily Soricinae (0, 3, 3, and 4 from Deposits 1, 7B, 13, and 14 respectively; Table 4.1; Appendix Table 4.9.2).

Remarks – Isolated shrew dentition are difficult to identify to genus or species. Though, most molariform teeth compare favorably with the genus *Sorex*. Members of *Sorex* often exhibit marked enamel pigmentation (Appendix Figure 4.9.2A). This character can be difficult to ascertain in asphaltic fossils due to staining; however, it is obvious that many P23 specimens are pigmented even with asphaltic discoloration (N. Fox, personal observation 2018).

SOREX Linnaeus, 1758

Referred specimens – Eight specimens are assigned to the genus *Sorex* (2, 1, 0, and 5 from Deposits 1, 7B, 13, and 14 respectively; Table 4.1; Appendix Table 4.9.2).

Remarks – Posterior soricid dentaries can be differentiated between the genera *Sorex* and *Notiosorex*, both of which have been reported from other RLB localities (Compton, 1937), based on the slope of the ascending ramus and size/shape of the mandibular foramen. When viewed laterally from the lingual side, the anterior slope of the ramus of *Sorex* exhibits a conspicuous angle not seen in *Notiosorex* and the mandibular foremen of *Sorex* is obviously larger, encompassing much of the interior ramus (Appendix Figure 4.9.2). Such conditions are consistent in all 14 and 3 examined recent specimens of *Sorex* and *Notiosorex* respectively (Appendix Table 4.9.5). Compton (1937) identified *Sorex* specimens from RLB localities 2051 as "*Sorex* cf. *S. ornatus*". I could not reliably differentiate recent specimens of *S. ornatus* from other western North American *Sorex* species that occur in California today (e.g., *S. palustris*, *S. trowbridgii*, *S. vagrans*) and therefore could not confidently assign P23 fossils to any one species. However, most P23 specimens comparable favorably with recent individuals of *S. ornatus* overall. Thus far, no specimens of *Notiosorex* have been identified from P23.

TALPIDAE Pomel, 1848
SCAPANUS CF. S. LATIMANUS Bachman, 1842

Referred specimens – One lower left m1/m2 from P23 Deposit 7B is assigned to *Scapanus* cf. *S. latimanus*: LACMP23-35853 (Table 4.1; Appendix Table 4.9.2).

Remarks – The referred mole (genus *Scapanus*) tooth is easily distinguishable from other soricomorphs based on size and morphology (Appendix Figure 4.9.2D). The specimen compares favorably with *Scapanus latimanus* and is tentatively assigned to that taxon based on morphological similarity and the present distribution of *Scapanus* species in western North America – *S. latimanus* is broadly distributed throughout California and southern Oregon while *S. orarius* and *S. townsendii* occur only in the pacific Northwest today. However, I am unable to identify this single tooth to species confidently. LACMP23-35853 is the only mole specimen recovered from P23, but an isolated humerus identified as *Scapanus latimanus* has been recovered from RLB Pit 91 as well (Akersten, 1979).

Table 4.9.2: Listed of all sampled P23 small mammal specimens identified to subfamily or lower (n = 2,440). Element abbreviations follow Appendix Table 4.9.1

LACMP23 Number	Deposit	Grid/ Level	Order	Family	Subfamily	Genus	Species	Element
28065	1	A1/L1	Lagomorpha	Leporidae		Sylvilagus	sp	upper rt tooth
28066	1	A1/L1	Lagomorpha	Leporidae		Sylvilagus	sp	lower rt tooth
28067	1	A1/L1	Lagomorpha	Leporidae		Sylvilagus	sp	upper rt tooth
28068	1	A1/L1	Lagomorpha	Leporidae		Sylvilagus	sp	upper rt tooth
28069	1	A1/L1	Lagomorpha	Leporidae		Sylvilagus	sp	lower lt tooth
28070	1	A1/L1	Carnivora	Mephitidae		Mephitis	mephitis	lt p4
28073	1	A2/L2	Rodentia	Sciuridae	Xerinae	Otospermophilus	?beecheyi	lt maxilla and P4
28074	1	A1/L1	Lagomorpha	Leporidae		Sylvilagus	sp	lower rt tooth
28075	1	A1/L1	Lagomorpha	Leporidae		Sylvilagus	sp	lower rt tooth
28076	1	A1/L1	Lagomorpha	Leporidae		Sylvilagus	sp	partial upper tooth
28077	1	A1/L1	Rodentia	Cricetidae	Arvicolinae	Microtus	sp	rt M1 (2 frags)
28079	1	A2/L2	Rodentia	Sciuridae	Xerinae	Otospermophilus	?beecheyi	lt M3
28080	1	A2/L2	Lagomorpha	Leporidae		Sylvilagus	sp	upper tooth frag
28081	1	A2/L2	Lagomorpha	Leporidae		Sylvilagus	sp	upper tooth frag
28082	1	A2/L2	Lagomorpha	Leporidae		Sylvilagus	bachmani	rt p3
28083	1	A2/L2	Rodentia	Sciuridae	Xerinae	Otospermophilus	?beecheyi	rt m1
28084	1	A2/L2	Lagomorpha	Leporidae		Sylvilagus	cf audubonii	lt p3
28085	1	A2/L2	Rodentia	Sciuridae	Xerinae	Otospermophilus	?beecheyi	rt m1/m2
28096	1	B2/L2	Lagomorpha	Leporidae				rt tooth
28097	1	B2/L2	Rodentia	Sciuridae	Xerinae	Otospermophilus	?beecheyi	lt M3
28098	1	B2/L2	Rodentia	Sciuridae	Xerinae	Otospermophilus	?beecheyi	partial lower lt molar
28099	1	B2/L2	Lagomorpha	Leporidae		Sylvilagus	sp	lower rt tooth

28100	1	B2/L2	Rodentia	Cricetidae	Arvicolinae	Microtus	sp	lt M1
28101	1	B2/L2	Rodentia	Cricetidae	Arvicolinae	Microtus	sp	lt M2
28103	1	B2/L2	Rodentia	Sciuridae	Xerinae	Otospermophilus	?beecheyi	partial lower rt molar
28104	1	B2/L2	Rodentia	Sciuridae	Xerinae	Otospermophilus	?beecheyi	rt M3
28105	1	B2/L2	Lagomorpha	Leporidae		Sylvilagus	audubonii	rt p3
28106	1	B2/L2	Lagomorpha	Leporidae				tooth frag
28107	1	B2/L2	Rodentia	Sciuridae	Xerinae			lower molar frag
28108	1	B2/L2	Rodentia	Cricetidae	Arvicolinae	Microtus	sp	lower rt m3
28109	1	B2/L2	Lagomorpha	Leporidae		Sylvilagus	sp	partial p3
28111	1	B2/L2	Lagomorpha	Leporidae		?Sylvilagus	sp	upper tooth frag
28112	1	B2/L2	Rodentia	Cricetidae	Arvicolinae	Microtus	sp	lt M1
28113	1	B2/L2	Rodentia	Cricetidae	Arvicolinae	Microtus	sp	lt m2
28114	1	B2/L2	Lagomorpha	Leporidae		Sylvilagus	sp	M3
28116	1	B2/L2	Lagomorpha	Leporidae		?Sylvilagus	sp	partial tooth
28128	1	B2/L2	Rodentia	Cricetidae	Neotominae	cf Peromyscus		rt M1
28129	1	B2/L2	Rodentia	Cricetidae	Arvicolinae	Microtus	sp	partial m1
28130	1	B2/L2	Lagomorpha	Leporidae		?Sylvilagus	sp	partial tooth
28131	1	B2/L2	Rodentia	Cricetidae	Arvicolinae	Microtus	sp	molar frag
28133	1	B2/L2	Rodentia	Cricetidae	Neotominae	cf Peromyscus	sp	lt m1
28134	1	B2/L2	Rodentia	Cricetidae	Arvicolinae	Microtus	sp	rt M1
28135	1	B2/L2	Rodentia	Cricetidae	Neotominae	Peromyscus	sp	lt M1
28136	1	B2/L2	Rodentia	Cricetidae	Neotominae			rt M2
28137	1	B2/L2	Rodentia	Sciuridae	Xerinae	Otospermophilus	?beecheyi	lt P4
28138	1	B2/L2	Rodentia	Heteromyidae	Dipodomyinae	Dipodomys	sp	molar
28139	1	B2/L2	Rodentia	Cricetidae	Arvicolinae	Microtus	sp	molar frag
28140	1	B2/L2	Rodentia	Cricetidae	Arvicolinae	Microtus	sp	molar frag
28141	1	B2/L2	Rodentia	Cricetidae	Arvicolinae	Microtus	sp	molar frag
28142	1	B2/L2	Rodentia	Cricetidae	Arvicolinae	Microtus	sp	partial lower rt molar

28143	1	B2/L2	Lagomorpha	Leporidae		Sylvilagus	sp	upper rt tooth
28144	1	B2/L2	Lagomorpha	Leporidae		?Sylvilagus	sp	upper tooth frag
28146	1	B2/L2	Lagomorpha	Leporidae		Sylvilagus	sp	lt P2
28147	1	A1/L3	Rodentia	Cricetidae	Arvicolinae	Microtus	sp	partial lt m1
28148	1	A1/L3	Rodentia	Sciuridae	Xerinae	Otospermophilus	?beecheyi	lt M1/M2
28150	1	A1/L3	Lagomorpha	Leporidae		Sylvilagus	sp	upper lt tooth
28151	1	A1/L3	Rodentia	Cricetidae	Neotominae	Peromyscus	sp	lt m2
28152	1	A2/L3	Carnivora	Mustelidae	Mustelinae	Mustela	frenata	lt dentary w/ p3, m1
28155	1	A2/L3	Rodentia	Cricetidae	Neotominae	Peromyscus	sp	lt dentary
28156	1	A2/L3	Rodentia	Cricetidae	Arvicolinae	Microtus	sp	lt M1
28157	1	A2/L3	Rodentia	Cricetidae	Arvicolinae	Microtus	sp	rt m1
28158	1	A2/L3	Rodentia	Cricetidae	Arvicolinae	Microtus	californicus	rt m1
28159	1	A2/L3	Rodentia	Cricetidae	Arvicolinae	Microtus	sp	rt m1
28160	1	A2/L3	Rodentia	Cricetidae	Arvicolinae	Microtus	californicus	lt m1
28161	1	A2/L3	Rodentia	Sciuridae	Xerinae	Otospermophilus	?beecheyi	rt M3
28162	1	A2/L3	Rodentia	Sciuridae	Xerinae	Otospermophilus	?beecheyi	lt m3
28163	1	A2/L3	Rodentia	Sciuridae	Xerinae	Otospermophilus	?beecheyi	rt M1/M2
28164	1	A2/L3	Rodentia	Sciuridae	Xerinae	Otospermophilus	?beecheyi	rt M1/M2
28165	1	A2/L3	Rodentia	Sciuridae	Xerinae	Otospermophilus	?beecheyi	rt p4
28166	1	A2/L3	Lagomorpha	Leporidae		Sylvilagus	sp	upper rt tooth
28167	1	A2/L3	Lagomorpha	Leporidae		Sylvilagus	sp	lower rt tooth
28168	1	A2/L3	Lagomorpha	Leporidae		Sylvilagus	sp	lower rt tooth
28169	1	A2/L3	Lagomorpha	Leporidae		Sylvilagus	sp	lower rt tooth
28176	1	A2/L3	Lagomorpha	Leporidae		Sylvilagus	sp	tooth frag
28178	1	A2/L3	Rodentia	Cricetidae	Arvicolinae	Microtus	sp	lt M2
28179	1	A2/L3	Rodentia	Cricetidae	Arvicolinae	Microtus	sp	rt M2
28180	1	A2/L3	Rodentia	Cricetidae	Neotominae	Peromyscus	sp	lt m1
28181	1	A2/L3	Lagomorpha	Leporidae		?Sylvilagus	sp	upper tooth frag
28182	1	A2/L3	Rodentia	Cricetidae	Neotominae	Peromyscus	sp	lt M2

28183	1	A2/L3	Rodentia	Geomyidae	Thomomyinae	Thomomys	sp	rt m1/m2
28184	1	A2/L3	Rodentia	Cricetidae	Arvicolinae	Microtus	sp	rt M1
28186	1	A2/L3	Rodentia	Cricetidae	Neotominae	Peromyscus	sp	lt M1
28187	1	A2/L3	Lagomorpha	Leporidae		Sylvilagus	sp	rt p3
28188	1	A2/L3	Rodentia	Cricetidae	Arvicolinae	Microtus	sp	lt M2
28189	1	A2/L3	Rodentia	Cricetidae	Neotominae			lt m2
28190	1	A2/L3	Rodentia	Cricetidae	Neotominae	cf Peromyscus	sp	rt m1
28191	1	A2/L3	Rodentia	Cricetidae	Arvicolinae	Microtus	sp	rt M1
28192	1	A2/L3	Rodentia	Cricetidae	Arvicolinae	Microtus	sp	partial molar
28193	1	A2/L3	Rodentia	Sciuridae	Xerinae	Otospermophilus	?beecheyi	lower molar frag
28195	1	A2/L3	Rodentia	Cricetidae	Arvicolinae	Microtus	sp	lt M2
28196	1	A2/L3	Rodentia	Cricetidae	Arvicolinae	Microtus	sp	lower molar frag
28197	1	A2/L3	Lagomorpha	Leporidae		Sylvilagus	sp	lower tooth frag
28198	1	A2/L3	Rodentia	Geomyidae	Thomomyinae	Thomomys	sp	m1/m2
28199	1	A2/L3	Rodentia	Cricetidae	Arvicolinae	Microtus	sp	partial rt m1
28200	1	A2/L3	Rodentia	Cricetidae	Neotominae			rt M1
28201	1	A2/L3	Rodentia	Geomyidae	Thomomyinae	Thomomys	sp	lt P4
28202	1	A2/L3	Lagomorpha	Leporidae		Sylvilagus	sp	lt P2
28203	1	A2/L3	Rodentia	Cricetidae	Arvicolinae	Microtus	sp	molar frag
28204	1	A2/L3	Rodentia	Cricetidae	Neotominae			lt m2
28204	1	A2/L4	Rodentia	Cricetidae	Arvicolinae	Microtus	sp	rt M1
28205	1	A2/L3	Rodentia	Cricetidae	Neotominae	cf Peromyscus	sp	rt M1
28224	1	A2/L3	Rodentia	Cricetidae	Arvicolinae	Microtus	sp	partial upper molar
28225	1	B2/L3	Rodentia	Cricetidae	Arvicolinae	Microtus	sp	rt m1
28226	1	B2/L3	Rodentia	Cricetidae	Arvicolinae	Microtus	californicus	lt m1
28227	1	B2/L3	Rodentia	Cricetidae	Arvicolinae	cf Microtus	sp	lt dentary frag
28228	1	B2/L3	Lagomorpha	Leporidae		Sylvilagus	sp	upper tooth
28229	1	B2/L3	Lagomorpha	Leporidae		?Sylvilagus	sp	upper tooth frag

28230	1	B2/L3	Lagomorpha	Leporidae		Sylvilagus	sp	upper tooth
28231	1	B2/L3	Lagomorpha	Leporidae		Sylvilagus	sp	upper tooth
28232	1	B2/L3	Lagomorpha	Leporidae		Sylvilagus	sp	lower rt tooth
28233	1	B2/L3	Lagomorpha	Leporidae		Sylvilagus	sp	lower rt tooth
28234	1	B2/L3	Lagomorpha	Leporidae		Sylvilagus	sp	p3
28235	1	B2/L3	Lagomorpha	Leporidae		Sylvilagus	sp	lower lt tooth
28236	1	B2/L3	Lagomorpha	Leporidae		?Sylvilagus	sp	upper tooth frag
28237	1	B2/L3	Rodentia	Cricetidae	Neotominae	Peromyscus	cf maniculatus	rt M1
28238	1	B2/L3	Rodentia	Cricetidae	Neotominae	Peromyscus	cf californicus	lt M2
28239	1	B2/L3	Rodentia	Cricetidae	Arvicolinae	Microtus	sp	rt m2
28240	1	B2/L3	Rodentia	Cricetidae	Arvicolinae	Microtus	sp	lt M3
28241	1	B2/L3	Lagomorpha	Leporidae		Sylvilagus	sp	upper rt tooth
28242	1	B2/L3	Lagomorpha	Leporidae		?Sylvilagus	sp	upper tooth frag
28243	1	B2/L3	Rodentia	Cricetidae	Neotominae	Peromyscus	cf maniculatus	lt M1
28244	1	B2/L3	Rodentia	Cricetidae	Neotominae	Peromyscus	sp	rt M2
28245	1	B2/L3	Rodentia	Cricetidae	Arvicolinae	Microtus	sp	lt M1
28247	1	B2/L3	Lagomorpha	Leporidae		?Sylvilagus	sp	tooth frag
28248	1	B2/L3	Lagomorpha	Leporidae		?Sylvilagus	sp	upper tooth frag
28249	1	B2/L3	Lagomorpha	Leporidae		?Sylvilagus	sp	tooth frag
28250	1	B2/L3	Rodentia	Cricetidae	Neotominae	Peromyscus	cf californicus	lt m1
28251	1	B2/L3	Rodentia	Cricetidae	Neotominae	Peromyscus	cf californicus	rt m2
28252	1	B2/L3	Rodentia	Cricetidae	Arvicolinae	Microtus	sp	lt M2
28253	1	B2/L3	Lagomorpha	Leporidae		Sylvilagus	sp	rt p3
28254	1	B2/L3	Lagomorpha	Leporidae		Sylvilagus	sp	lower tooth
28255	1	B2/L3	Rodentia	Cricetidae	Neotominae	Peromyscus	cf californicus	rt M2
28256	1	B2/L3	Lagomorpha	Leporidae				tooth frag
28257	1	B2/L3	Rodentia	Cricetidae	Neotominae	Peromyscus	sp	rt M1

28258	1	B2/L3	Rodentia	Cricetidae	Neotominae	Peromyscus	cf californicus	rt m1
28259	1	B2/L3	Lagomorpha	Leporidae		Sylvilagus	sp	lt? p3
28261	1	A1/L4	Rodentia	Sciuridae	Xerinae	Otospermophilus	?beecheyi	lt M3
28262	1	A1/L4	Lagomorpha	Leporidae		Sylvilagus	sp	lower lt tooth
28263	1	A1/L4	Lagomorpha	Leporidae		Sylvilagus	sp	lower lt tooth
28266	1	A1/L4	Lagomorpha	Leporidae		Sylvilagus	audubonii	partial lt p3
28267	1	A2/L4	Rodentia	Cricetidae	Neotominae	Neotoma	sp	rt m2
28268	1	A2/L4	Rodentia	Cricetidae	Arvicolinae	Microtus	californicus	rt m1
28269	1	A2/L4	Rodentia	Cricetidae	Arvicolinae	Microtus	californicus	lt m1
28270	1	A2/L4	Rodentia	Cricetidae	Arvicolinae	Microtus	californicus	rt m1
28271	1	A2/L4	Rodentia	Cricetidae	Arvicolinae	Microtus	sp	rt M1
28272	1	A2/L4	Rodentia	Cricetidae	Arvicolinae	Microtus	sp	lt M2
28273	1	A2/L4	Lagomorpha	Leporidae		Sylvilagus	sp	m3
28274	1	A2/L4	Rodentia	Sciuridae	Xerinae	Otospermophilus	?beecheyi	lt m3
28275	1	A2/L4	Rodentia	Sciuridae	Xerinae	Otospermophilus	?beecheyi	rt m1/m2
28276	1	A2/L4	Lagomorpha	Leporidae		Sylvilagus	sp	lt P2
28277	1	A2/L4	Lagomorpha	Leporidae		Sylvilagus	sp	rt P2
28278	1	A2/L4	Lagomorpha	Leporidae		Sylvilagus	sp	upper tooth
28280	1	A2/L4	Lagomorpha	Leporidae		Sylvilagus	sp	upper tooth frag
28281	1	A2/L4	Lagomorpha	Leporidae		Sylvilagus	sp	upper rt tooth frag
28283	1	A2/L4	Lagomorpha	Leporidae		Sylvilagus	sp	upper tooth frag
28293	1	A2/L4	Rodentia	Cricetidae	Neotominae	Peromyscus	cf maniculatus	rt M1
28294	1	A2/L4	Rodentia	Cricetidae	Arvicolinae	Microtus	sp	molar frag
28295	1	A2/L4	Rodentia	Sciuridae	Xerinae	Otospermophilus	?beecheyi	partial lt M1/M2
28297	1	A2/L4	Lagomorpha	Leporidae		Sylvilagus	sp	partial upper tooth
28300	1	A2/L4	Rodentia	Cricetidae	Arvicolinae	Microtus	sp	lt M3
28301	1	A2/L4	Rodentia	Cricetidae	Arvicolinae	Microtus	sp	lower molar frag

28302	1	A2/L4	Rodentia	Heteromyidae	Perognathinae			lt m1/m2
28305	1	A2/L4	Rodentia	Cricetidae	Arvicolinae	Microtus	sp	rt M2
28306	1	A2/L4	Rodentia	Cricetidae	Arvicolinae	Microtus	sp	rt M3
28307	1	A2/L4	Rodentia	Cricetidae	Arvicolinae	Microtus	sp	lt M3
28308	1	A2/L4	Rodentia	Geomyidae	Thomomyinae	Thomomys	sp	lt m1/m2
28309	1	A2/L4	Rodentia	Cricetidae	Arvicolinae	Microtus	sp	rt M2
28310	1	A2/L4	Rodentia	Cricetidae	Arvicolinae	Microtus	sp	rt M2
28312	1	A2/L4	Rodentia	Cricetidae	Arvicolinae	Microtus	sp	lt m2
28313	1	A2/L4	Rodentia	Cricetidae	Neotominae	Peromyscus	sp	lt m2
28314	1	A2/L4	Rodentia	Sciuridae	Xerinae	Otospermophilus	?beecheyi	partial rt P4
28315	1	A2/L4	Lagomorpha	Leporidae		Sylvilagus	sp	lower lt tooth
28316	1	A2/L4	Rodentia	Cricetidae	Arvicolinae	Microtus	sp	rt M1
28317	1	A2/L4	Lagomorpha	Leporidae		Sylvilagus	sp	upper lt tooth
28318	1	A2/L4	Rodentia	Cricetidae	Arvicolinae	Microtus	sp	partial M3
28319	1	A2/L4	Rodentia	Cricetidae	Arvicolinae	Microtus	sp	upper molar frag
28320	1	A2/L4	Rodentia	Cricetidae	Arvicolinae	Microtus	sp	lt M2
28321	1	A2/L4	Rodentia	Cricetidae	Arvicolinae	Microtus	sp	rt M1 frag
28322	1	A2/L4	Lagomorpha	Leporidae		Sylvilagus	sp	lower lt tooth (2 frags)
28325	1	A2/L5	Rodentia	Cricetidae	Arvicolinae	Microtus	californicus	rt m1
28326	1	A2/L5	Rodentia	Cricetidae	Arvicolinae	Microtus	sp	rt m1
28327	1	A2/L5	Rodentia	Cricetidae	Arvicolinae	Microtus	californicus	rt m1
28328	1	A2/L5	Rodentia	Cricetidae	Arvicolinae	Microtus	californicus	lt m1
28329	1	A2/L5	Rodentia	Cricetidae	Arvicolinae	Microtus	sp	rt M1
28330	1	A2/L5	Rodentia	Cricetidae	Arvicolinae	Microtus	sp	lt M1
28331	1	A2/L5	Rodentia	Cricetidae	Arvicolinae	Microtus	sp	rt M3
28332	1	A2/L5	Lagomorpha	Leporidae		Sylvilagus	sp	lower lt tooth
28333	1	A2/L5	Rodentia	Cricetidae	Arvicolinae	Microtus	sp	lt M3
28334	1	A2/L5	Rodentia	Sciuridae	Xerinae	Otospermophilus	?beecheyi	lt DP4
28335	1	A2/L5	Rodentia	Sciuridae	Xerinae	Otospermophilus	?beecheyi	lt M3

28336	1	A2/L5	Rodentia	Sciuridae	Xerinae	Otospermophilus	?beecheyi	partial rt DP4
28337	1	A2/L5	Lagomorpha	Leporidae		Sylvilagus	sp	rt maxilla w/ P3
28338	1	A2/L5	Lagomorpha	Leporidae		Sylvilagus	sp	upper rt tooth
28339	1	A2/L5	Lagomorpha	Leporidae		Sylvilagus	sp	upper rt tooth
28340	1	A2/L5	Rodentia	Geomyidae	Thomomyinae	Thomomys	sp	rt P4
28341	1	A2/L5	Lagomorpha	Leporidae		Sylvilagus	audubonii	rt p3
28342	1	A2/L5	Lagomorpha	Leporidae		Sylvilagus	sp	upper rt tooth
28343	1	A2/L5	Lagomorpha	Leporidae		Sylvilagus	sp	maxilla frag
28344	1	A2/L5	Rodentia	Cricetidae	Arvicolinae	Microtus	sp	rt M3
28345	1	A2/L5	Lagomorpha	Leporidae		Sylvilagus	sp	m3
28390	1	A2/L5	Carnivora	Mustelidae	Mustelinae	Mustela	frenata	rt m2
28391	1	A2/L5	Lagomorpha	Leporidae		?Sylvilagus	sp	partial tooth
28392	1	A2/L5	Rodentia	Cricetidae	Arvicolinae	Microtus	sp	molar frag
28393	1	A2/L5	Rodentia	Cricetidae	Arvicolinae	Microtus	sp	molar frag
28394	1	A2/L5	Rodentia	Cricetidae	Arvicolinae	Microtus	sp	partial molar
28395	1	A2/L5	Rodentia	Cricetidae	Arvicolinae	Microtus	sp	rt M2
28397	1	A2/L5	Rodentia	Cricetidae	Arvicolinae	Microtus	sp	rt M2
28400	1	A2/L5	Rodentia	Cricetidae	Arvicolinae	Microtus	sp	rt m2
28401	1	A2/L5	Rodentia	Cricetidae	Neotominae	Peromyscus	sp	lt M1
28402	1	A2/L5	Lagomorpha	Leporidae		?Sylvilagus	sp	partial tooth
28403	1	A2/L5	Rodentia	Cricetidae	Arvicolinae	Microtus	sp	molar frag
28404	1	A2/L5	Rodentia	Cricetidae	Arvicolinae	Microtus	sp	molar frag
28503	1	A2/L5	Rodentia	Cricetidae	Arvicolinae	Microtus	sp	lt M2
28504	1	A2/L5	Rodentia	Cricetidae	Arvicolinae	Microtus	sp	lt M3
28505	1	A2/L5	Rodentia	Sciuridae	Xerinae	Otospermophilus	?beecheyi	lt M1/M2
28506	1	A2/L5	Rodentia	Cricetidae	Arvicolinae	Microtus	sp	rt m2
28507	1	A2/L5	Rodentia	Cricetidae	Arvicolinae	Microtus	sp	molar frag
28508	1	A2/L5	Lagomorpha	Leporidae		Sylvilagus	sp	upper lt tooth frag
28509	1	B1/L3	Rodentia	Cricetidae	Neotominae	Neotoma	sp	lt m1

28510	1	B1/L3	Rodentia	Cricetidae	Arvicolinae	Microtus	sp	rt m2
28511	1	B1/L3	Rodentia	Cricetidae	Arvicolinae	Microtus	sp	lt m3
28512	1	B1/L3	Rodentia	Cricetidae	Arvicolinae	Microtus	sp	molar frag
28513	1	B1/L3	Rodentia	Cricetidae	Neotominae			partial rt dentary
28514	1	B1/L3	Rodentia	Cricetidae	Neotominae	Peromyscus	cf californicus	lt M2
28515	1	B1/L3	Rodentia	Cricetidae	Neotominae	cf Peromyscus	sp	rt m1
28516	1	B1/L3	Rodentia	Cricetidae	Neotominae	Peromyscus	sp	lt m2
28517	1	B1/L3	Rodentia	Cricetidae	Neotominae	Peromyscus	sp	lt m2 frag
28519	1	B1/L3	Lagomorpha	Leporidae		Sylvilagus	audubonii	rt p3
28520	1	B1/L3	Lagomorpha	Leporidae		?Sylvilagus	sp	upper rt tooth
28521	1	B1/L3	Lagomorpha	Leporidae		Sylvilagus	sp	upper tooth frag
28522	1	B1/L2	Carnivora	Mephitidae		Mephitis	mephitis	lt m2
28524	1	B1/L2	Rodentia	Cricetidae	Arvicolinae	Microtus	sp	partial molar
28525	1	B1/L2	Rodentia	Cricetidae	Neotominae	cf Peromyscus		rt m1
28527	1	B1/L2	Rodentia	Sciuridae	Xerinae	Otospermophilus	?beecheyi	rt m1/m2
28528	1	B1/L2	Rodentia	Sciuridae	Xerinae	Otospermophilus	?beecheyi	lt DP4
28529	1	B1/L2	Lagomorpha	Leporidae		Sylvilagus	sp	lt dentary frag
28530	1	B1/L2	Lagomorpha	Leporidae		Sylvilagus	sp	lower tooth
28531	1	B1/L2	Lagomorpha	Leporidae		Sylvilagus	sp	upper lt tooth frag
28532	1	B1/L2	Lagomorpha	Leporidae		Sylvilagus	sp	upper lt tooth frag
28533	1	B1/L2	Lagomorpha	Leporidae		Sylvilagus	sp	upper tooth frag
28534	1	B1/L2	Lagomorpha	Leporidae		Sylvilagus	sp	upper lt tooth frag
28535	1	B1/L2	Lagomorpha	Leporidae		Sylvilagus	sp	upper tooth frag
28536	1	B1/L2	Lagomorpha	Leporidae		Sylvilagus	sp	upper tooth frag
28537	1	B1/L2	Lagomorpha	Leporidae		Sylvilagus	sp	rt P2
28538	1	B1/L4	Rodentia	Cricetidae	Arvicolinae	Microtus	sp	lt m1
28539	1	B1/L4	Rodentia	Cricetidae	Arvicolinae	Microtus	sp	rt M1

28540	1	B1/L4	Rodentia	Cricetidae	Arvicolinae	Microtus	sp	lt M1
28541	1	B1/L4	Rodentia	Cricetidae	Arvicolinae	Microtus	sp	lt m2
28542	1	B1/L4	Rodentia	Cricetidae	Arvicolinae	Microtus	sp	lt m2
28543	1	B1/L4	Rodentia	Cricetidae	Arvicolinae	Microtus	sp	molar frag
28544	1	B1/L4	Rodentia	Cricetidae	Arvicolinae	Microtus	sp	rt dentary frag
28545	1	B1/L4	Rodentia	Cricetidae	Arvicolinae	Microtus	sp	rt dentary frag
28546	1	B1/L4	Rodentia	Cricetidae	Neotominae	cf Peromyscus	sp	lt m1
28547	1	B1/L4	Rodentia	Geomyidae	Thomomyinae	Thomomys	sp	rt P4
28548	1	B1/L4	Rodentia	Geomyidae	Thomomyinae	Thomomys	sp	lt M1/M2
28549	1	B1/L4	Rodentia	Sciuridae	Xerinae	Otospermophilus	?beecheyi	lt M3
28550	1	B1/L4	Rodentia	Sciuridae	Xerinae	Otospermophilus	?beecheyi	partial lt m3
28551	1	B1/L4	Rodentia	Sciuridae	Xerinae	Otospermophilus	?beecheyi	lt p4
28552	1	B1/L4	Rodentia	Sciuridae	Xerinae			partial rt p4
28554	1	B1/L4	Lagomorpha	Leporidae		Sylvilagus	sp	upper tooth
28555	1	B1/L4	Lagomorpha	Leporidae		Sylvilagus	audubonii	lt p3
28556	1	B1/L4	Lagomorpha	Leporidae		Sylvilagus	audubonii	rt p3
28557	1	B1/L4	Lagomorpha	Leporidae		Sylvilagus	sp	upper lt tooth
28558	1	B1/L4	Lagomorpha	Leporidae		Sylvilagus	sp	rt premaxilla
28559	1	B1/L4	Lagomorpha	Leporidae		Sylvilagus	sp	lt maxilla
28560	1	B1/L4	Lagomorpha	Leporidae		Sylvilagus	sp	rt maxilla frag
28561	1	A1/L5	Rodentia	Cricetidae	Arvicolinae	Microtus	sp	rt M2
28562	1	A1/L5	Lagomorpha	Leporidae		Sylvilagus	sp	rt maxilla frag
28563	1	A1/L5	Lagomorpha	Leporidae		Sylvilagus	sp	rt P2
28592	1	B1/L8	Lagomorpha	Leporidae		Sylvilagus	sp	lt p3
28593	1	B1/L8	Lagomorpha	Leporidae		Sylvilagus	sp	lt maxilla w/ P3
28594	1	B1/L8	Lagomorpha	Leporidae		Sylvilagus	sp	rt maxilla frag
28595	1	B1/L8	Lagomorpha	Leporidae		Sylvilagus	sp	lt dentary frag w/ p4-m1
28596	1	B1/L8	Lagomorpha	Leporidae		Sylvilagus	sp	upper lt tooth
28597	1	B1/L8	Lagomorpha	Leporidae		Sylvilagus	sp	upper lt tooth

28598	1	B1/L8	Lagomorpha	Leporidae		Sylvilagus	sp	lower lt tooth
28599	1	B1/L8	Lagomorpha	Leporidae		Sylvilagus	sp	lower rt tooth
28600	1	B1/L8	Carnivora	Mephitidae		Spilogale	gracilis	lt dentary frag
28601	1	B1/L8	Rodentia	Cricetidae	Arvicolinae	Microtus	sp	partial rt dentary
28602	1	B1/L8	Rodentia	Cricetidae	Arvicolinae	Microtus	sp	rt m2
28603	1	B1/L8	Rodentia	Cricetidae	Arvicolinae	Microtus	sp	rt m3
28604	1	B1/L8	Rodentia	Cricetidae	Neotominae	cf Peromyscus	sp	lt maxilla frag
28605	1	B1/L8	Rodentia	Sciuridae	Xerinae			rt maxilla
28606	1	B1/L8	Rodentia	Sciuridae	Xerinae	Otospermophilus	?beecheyi	rt m1
28607	1	B1/L8	Rodentia	Cricetidae	Arvicolinae	Microtus	californicus	rt dentary frag w/ m1
28608	1	B1/L8	Rodentia	Cricetidae	Arvicolinae	Microtus	sp	lt M1
28609	1	B1/L8	Lagomorpha	Leporidae		Sylvilagus	sp	anterior rt dentary frag
28610	1	B1/L8	Lagomorpha	Leporidae		Sylvilagus	sp	lt premaxilla with I1
28611	1	B1/L8	Lagomorpha	Leporidae		Sylvilagus	sp	upper rt tooth
28612	1	B1/L8	Lagomorpha	Leporidae		Sylvilagus	sp	upper rt tooth
28613	1	B1/L8	Lagomorpha	Leporidae		Sylvilagus	sp	upper lt tooth
28614	1	B1/L8	Lagomorpha	Leporidae		Sylvilagus	sp	upper rt tooth
28615	1	B1/L8	Lagomorpha	Leporidae		Sylvilagus	sp	upper tooth frag
28616	1	B1/L8	Lagomorpha	Leporidae		Sylvilagus	sp	lower rt tooth
28617	1	B1/L8	Lagomorpha	Leporidae		Sylvilagus	sp	lower rt tooth
28618	1	B1/L8	Lagomorpha	Leporidae		Sylvilagus	sp	lower rt tooth
28619	1	B1/L8	Carnivora	Mustelidae	Mustelinae	?Mustela	frenata	lt P3
28622	1	B1/L5	Rodentia	Cricetidae	Arvicolinae	Microtus	sp	lt M3
28623	1	B1/L5	Rodentia	Cricetidae	Neotominae			rt dentary frag
28624	1	B1/L5	Rodentia	Sciuridae	Xerinae	Otospermophilus	?beecheyi	rt m1/m2
28625	1	B1/L5	Rodentia	Sciuridae	Xerinae	Otospermophilus	?beecheyi	lt m1/m2
28626	1	B1/L5	Lagomorpha	Leporidae		Sylvilagus	sp	upper tooth frag
28627	1	B1/L5	Lagomorpha	Leporidae		Sylvilagus	sp	upper tooth frag

28640	1	A1/L6	Rodentia	Sciuridae	Xerinae	Neotamias/Tamias	sp	lt p4
28641	1	A1/L6	Rodentia	Sciuridae	Xerinae	Otospermophilus	?beecheyi	lt P4
28642	1	A1/L6	Rodentia	Cricetidae	Neotominae			lt maxilla frag
28643	1	A1/L6	Rodentia	Sciuridae	Xerinae	Otospermophilus	?beecheyi	rt p4
28644	1	A1/L6	Rodentia	Sciuridae	Xerinae	Otospermophilus	?beecheyi	lt p4
28645	1	A1/L6	Rodentia	Sciuridae	Xerinae	Otospermophilus	?beecheyi	partial lt M1/M2
28646	1	A1/L6	Rodentia	Sciuridae	Xerinae	Otospermophilus	?beecheyi	lt DP4
28647	1	A1/L6	Rodentia	Sciuridae	Xerinae	Otospermophilus	?beecheyi	lower lt molar frag
28649	1	A1/L6	Rodentia	Cricetidae	Arvicolinae	Microtus	sp	rt m1
28650	1	A1/L6	Rodentia	Cricetidae	Arvicolinae	Microtus	sp	lt M3
28651	1	A1/L6	Rodentia	Cricetidae	Arvicolinae	Microtus	sp	rt M3
28652	1	A1/L6	Rodentia	Cricetidae	Arvicolinae	Microtus	sp	lt m2
28653	1	A1/L6	Rodentia	Cricetidae	Arvicolinae	Microtus	sp	molar frag
28654	1	A1/L6	Rodentia	Cricetidae	Arvicolinae	Microtus	sp	rt M2
28655	1	A1/L6	Rodentia	Cricetidae	Arvicolinae	Microtus	sp	rt m2
28656	1	A1/L6	Rodentia	Cricetidae	Neotominae	Neotoma	sp	molar - lt m2?
28657	1	A1/L6	Rodentia	Cricetidae	Neotominae	cf Peromyscus	sp	rt M1 frag
28658	1	A1/L6	Rodentia	Cricetidae	Neotominae			molar frag
28659	1	A1/L6	Lagomorpha	Leporidae		Sylvilagus	sp	m3
28660	1	A1/L6	Lagomorpha	Leporidae		Sylvilagus	sp	m3
28661	1	A1/L6	Lagomorpha	Leporidae		Sylvilagus	audubonii	lt p3
28662	1	A1/L6	Lagomorpha	Leporidae		Sylvilagus	sp	dentary frag
28663	1	A1/L6	Lagomorpha	Leporidae		Sylvilagus	sp	rt dentary frag
28664	1	A1/L6	Lagomorpha	Leporidae		Sylvilagus	sp	upper lt tooth
28665	1	A1/L6	Lagomorpha	Leporidae		Sylvilagus	sp	upper tooth frag
28666	1	A1/L6	Lagomorpha	Leporidae		Sylvilagus	sp	upper tooth frag
28667	1	A1/L6	Lagomorpha	Leporidae		Sylvilagus	sp	lower tooth
28668	1	A1/L6	Lagomorpha	Leporidae		Sylvilagus	sp	lower tooth
28669	1	A1/L6	Lagomorpha	Leporidae		Sylvilagus	sp	lower lt tooth

28670	1	A1/L6	Lagomorpha	Leporidae		Sylvilagus	sp	lower lt tooth
28671	1	A1/L6	Rodentia	Leporidae		Sylvilagus	sp	M3
28673	1	A1/L7	Rodentia	Cricetidae	Arvicolinae	Microtus	sp	rt M1
28674	1	A1/L7	Rodentia	Cricetidae	Neotominae	Peromyscus	sp	rt dentary w/ m2
28675	1	A1/L7	Rodentia	Cricetidae	Neotominae			rt m1
28676	1	A1/L7	Rodentia	Sciuridae	Xerinae	Otospermophilus	?beecheyi	lt M3
28677	1	A1/L7	Rodentia	Sciuridae	Xerinae	Otospermophilus	?beecheyi	lt m1/m2
28678	1	A1/L7	Carnivora	Mephitidae		Mephitis	mephitis	lt m2
28679	1	A1/L7	Lagomorpha	Leporidae		Sylvilagus	sp	upper rt tooth
28680	1	A1/L7	Lagomorpha	Leporidae		Sylvilagus	sp	upper tooth frag
28681	1	A1/L7	Lagomorpha	Leporidae		Sylvilagus	sp	upper tooth frag
28682	1	A1/L7	Lagomorpha	Leporidae		Sylvilagus	sp	lower lt tooth
28683	1	A1/L7	Lagomorpha	Leporidae		Sylvilagus	sp	lower rt tooth
28840	1	B2/L4	Rodentia	Cricetidae	Arvicolinae	Microtus	californicus	lt dentary w/ m1-m3
28841	1	B2/L4	Rodentia	Cricetidae	Arvicolinae	Microtus	californicus	rt m1
28842	1	B2/L4	Rodentia	Cricetidae	Arvicolinae	Microtus	sp	lower lt m1
28843	1	B2/L4	Rodentia	Cricetidae	Arvicolinae	Microtus	sp	rt M2
28844	1	B2/L4	Rodentia	Cricetidae	Arvicolinae	Microtus	sp	tooth frag
28845	1	B2/L4	Rodentia	Cricetidae	Arvicolinae	Microtus	sp	tooth frag
28846	1	B2/L4	Rodentia	Cricetidae	Arvicolinae	Microtus	sp	tooth frag
28847	1	B2/L4	Rodentia	Cricetidae	Neotominae	Peromyscus	cf californicus	rt M2
28848	1	B2/L4	Rodentia	Cricetidae	Neotominae	cf Peromyscus	sp	lt m1
28849	1	B2/L4	Rodentia	Cricetidae	Neotominae	cf Peromyscus		rt m2
28850	1	B2/L4	Rodentia	Cricetidae	Neotominae	Neotoma	sp	lt M3
28854	1	B2/L4	Rodentia	Sciuridae	Xerinae	Otospermophilus	?beecheyi	rt m2
28855	1	B2/L4	Rodentia	Sciuridae	Xerinae	Otospermophilus	?beecheyi	lt m3
28856	1	B2/L4	Rodentia	Sciuridae	Xerinae	Otospermophilus	?beecheyi	partial rt M3
28857	1	B2/L4	Rodentia	Sciuridae	Xerinae	Otospermophilus	?beecheyi	lt M1/M2

28858	1	B2/L4	Lagomorpha	Leporidae		Sylvilagus	audubonii	rt p3
28859	1	B2/L4	Lagomorpha	Leporidae		Sylvilagus	sp	upper rt tooth
28860	1	B2/L4	Lagomorpha	Leporidae		Sylvilagus	sp	partial lower rt tooth
28861	1	B2/L4	Lagomorpha	Leporidae		Sylvilagus	sp	upper tooth frag
28862	1	B2/L4	Lagomorpha	Leporidae		Sylvilagus	sp	tooth frag
28863	1	B2/L4	Lagomorpha	Leporidae		Sylvilagus	sp	upper tooth frag
28864	1	B2/L4	Lagomorpha	Leporidae		Sylvilagus	sp	lower rt tooth frag
28865	1	B2/L4	Lagomorpha	Leporidae		Sylvilagus	sp	tooth frag
28866	1	B2/L4	Lagomorpha	Leporidae		Sylvilagus	sp	upper lt tooth
28867	1	B2/L4	Lagomorpha	Leporidae		Sylvilagus	sp	m3
28868	1	B2/L4	Lagomorpha	Leporidae		?Sylvilagus	sp	rt maxilla frag
28869	1	B2/L4	Soricomorpha	Soricidae	Soricinae	?Sorex	sp	partial rt dentary w/ molar
28870	1	B2/L5	Rodentia	Cricetidae	Neotominae	Peromyscus	sp	rt dentary
28871	1	B2/L5	Rodentia	Cricetidae	Arvicolinae	Microtus	sp	lt anterior dentary
28872	1	B2/L5	Rodentia	Cricetidae	Arvicolinae	Microtus	sp	lt M1
28873	1	B2/L5	Rodentia	Cricetidae	Arvicolinae	Microtus	sp	partial molar
28874	1	B2/L5	Rodentia	Cricetidae	Arvicolinae	Microtus	sp	molar frag
28875	1	B2/L5	Rodentia	Cricetidae	Arvicolinae	Microtus	sp	molar frag
28876	1	B2/L5	Rodentia	Sciuridae	Xerinae	Otospermophilus	?beecheyi	rt M1/M2
28878	1	B2/L5	Lagomorpha	Leporidae		Sylvilagus	sp	upper lt tooth
28879	1	B2/L6	Rodentia	Heteromyidae	Dipodomyinae	Dipodomys	sp	molar
28880	1	B2/L6	Rodentia	Geomyidae	Thomomyinae	?Thomomys	sp	tooth frag
28881	1	B2/L6	Lagomorpha	Leporidae		Sylvilagus	sp	M3
28882	1	B2/L6	Lagomorpha	Leporidae		Sylvilagus	sp	rt P2
29225	1	A2/L6	Lagomorpha	Leporidae		Sylvilagus	sp	lower tooth
29227	1	A1/L9+10	Rodentia	Cricetidae	Neotominae			dentary frag
29229	1	A1/L9+10	Lagomorpha	Leporidae		Sylvilagus	bachmani	lt p3

29230	1	A1/L9+10	Lagomorpha	Leporidae		Sylvilagus	sp	lower lt tooth
31426	1	B1/L6	Lagomorpha	Leporidae		Sylvilagus	sp	partial rt maxilla
31427	1	B1/L6	Lagomorpha	Leporidae		Sylvilagus	sp	lower rt tooth
31428	1	B1/L6	Lagomorpha	Leporidae		Sylvilagus	sp	lt dentary frag
31429	1	B1/L6	Lagomorpha	Leporidae		Sylvilagus	sp	dentary frag
31430	1	B1/L6	Lagomorpha	Leporidae		Sylvilagus	sp	rt dentary frag
31431	1	B1/L6	Lagomorpha	Leporidae		Sylvilagus	sp	lower lt tooth
31432	1	B1/L6	Lagomorpha	Leporidae		Sylvilagus	sp	lower rt tooth
31433	1	B1/L6	Lagomorpha	Leporidae		Sylvilagus	sp	lower lt tooth
31434	1	B1/L6	Lagomorpha	Leporidae		Sylvilagus	sp	lower rt tooth
31435	1	B1/L6	Lagomorpha	Leporidae		Sylvilagus	sp	tooth - P2?
31436	1	B1/L6	Lagomorpha	Leporidae		Sylvilagus	sp	lower rt tooth
31437	1	B1/L6	Lagomorpha	Leporidae		Sylvilagus	sp	tooth frag
31438	1	B1/L6	Lagomorpha	Leporidae		Sylvilagus	sp	tooth frag
31439	1	B1/L6	Lagomorpha	Leporidae		?Sylvilagus	sp	tooth frag
31440	1	B1/L6	Lagomorpha	Leporidae		Sylvilagus	sp	tooth frag
31441	1	B1/L6	Lagomorpha	Leporidae		Sylvilagus	sp	lower rt tooth
31442	1	B1/L6	Lagomorpha	Leporidae		?Sylvilagus	sp	tooth frag
31443	1	B1/L6	Rodentia	Sciuridae	Xerinae	Otospermophilus	?beecheyi	lt dentary
31444	1	B1/L6	Rodentia	Sciuridae	Xerinae	Otospermophilus	?beecheyi	rt m1/m2
31445	1	B1/L6	Rodentia	Sciuridae	Xerinae	Otospermophilus	?beecheyi	rt m1/m2
31446	1	B1/L6	Rodentia	Sciuridae	Xerinae	Otospermophilus	?beecheyi	partial lower rt molar
31447	1	B1/L6	Rodentia	Sciuridae	Xerinae	Otospermophilus	?beecheyi	partial rt p4
31448	1	B1/L6	Rodentia	Cricetidae	Neotominae	Neotoma	sp	molar
31449	1	B1/L6	Rodentia	Cricetidae	Arvicolinae	Microtus	sp	lt M2
31450	1	B1/L6	Lagomorpha	Leporidae		?Sylvilagus	sp	tooth frag
31451	1	B1/L6	Soricomorpha	Soricidae	Soricinae	?Sorex	sp	lt maxilla w/ 2 teeth
31501	14	C3/L5	Rodentia	Sciuridae	Xerinae	Otospermophilus	?beecheyi	rt M3

31502	14	C3/L5	Rodentia	Sciuridae	Xerinae	Otospermophilus	?beecheyi	lt m3
31503	14	C3/L5	Rodentia	Heteromyidae	Dipodomyinae	Dipodomys	sp	p4?
31504	14	C3/L5	Rodentia	Heteromyidae	Dipodomyinae	Dipodomys	sp	molar
31505	14	C3/L5	Rodentia	Heteromyidae	Dipodomyinae	?Dipodomys	sp	molar
31506	14	C3/L5	Rodentia	Heteromyidae	Dipodomyinae	?Dipodomys	sp	P4/p4?
31507	14	C3/L5	Rodentia	Heteromyidae	Dipodomyinae	?Dipodomys	sp	molar
31508	14	C3/L5	Rodentia	Heteromyidae	Dipodomyinae	?Dipodomys	sp	molar
31509	14	C3/L5	Rodentia	Geomyidae	Thomomyinae	Thomomys	sp	rt m3?
31510	14	C3/L5	Rodentia	Cricetidae	Neotominae	Neotoma	sp	rt M1
31511	14	C3/L5	Rodentia	Cricetidae	Neotominae	Neotoma	sp	upper molar frag
31512	14	C3/L5	Rodentia	Cricetidae	Neotominae			rt m2
31513	14	C3/L5	Rodentia	Cricetidae	Neotominae	Peromyscus	sp	rt m1
31514	14	C3/L5	Rodentia	Cricetidae	Neotominae			lt M2
31515	14	C3/L5	Rodentia	Cricetidae	Neotominae	Peromyscus	cf maniculatus	lt m1
31516	14	C3/L5	Rodentia	Cricetidae	Neotominae	Peromyscus	cf maniculatus	lt m1
31517	14	C3/L5	Rodentia	Cricetidae	Neotominae	Peromyscus	cf californicus	lt M1
31518	14	C3/L5	Rodentia	Cricetidae	Neotominae			lower lt molar - m2?
31519	14	C3/L5	Rodentia	Cricetidae	Neotominae	?Peromyscus	sp	partial rt M1
31520	14	C3/L5	Rodentia	Cricetidae	Neotominae			rt m2
31521	14	C3/L5	Rodentia	Cricetidae	Arvicolinae	Microtus	sp	rt m2
31522	14	C3/L5	Rodentia	Cricetidae	Arvicolinae	Microtus	sp	partial rt m1
31523	14	C3/L5	Rodentia	Cricetidae	Arvicolinae	Microtus	sp	rt M3
31524	14	C3/L5	Rodentia	Cricetidae	Arvicolinae	Microtus	sp	rt m2
31525	14	C3/L5	Rodentia	Cricetidae	Arvicolinae	Microtus	sp	lt M2
31526	14	C3/L5	Rodentia	Cricetidae	Arvicolinae	Microtus	sp	rt m2
31527	14	C3/L5	Rodentia	Cricetidae	Arvicolinae	Microtus	sp	molar frag
31528	14	C3/L5	Rodentia	Cricetidae	Arvicolinae	Microtus	sp	rt M3

31529	14	C3/L5	Rodentia	Cricetidae	Arvicolinae	Microtus	sp	rt M1
31530	14	C3/L5	Rodentia	Cricetidae	Arvicolinae	Microtus	sp	lt M2
31531	14	C3/L5	Rodentia	Cricetidae	Arvicolinae	Microtus	sp	rt m2
31532	14	C3/L5	Rodentia	Cricetidae	Arvicolinae	Microtus	sp	molar frag
31533	14	C3/L5	Rodentia	Cricetidae	Arvicolinae	Microtus	sp	rt M2
31534	14	C3/L5	Rodentia	Cricetidae	Arvicolinae	Microtus	sp	rt M1
31535	14	C3/L5	Rodentia	Cricetidae	Arvicolinae	Microtus	sp	rt m2
31536	14	C3/L5	Rodentia	Cricetidae	Arvicolinae	Microtus	sp	rt M2
31537	14	C3/L5	Rodentia	Cricetidae	Arvicolinae	Microtus	sp	partial lt m1
31538	14	C3/L5	Rodentia	Cricetidae	Arvicolinae	Microtus	sp	lt M1
31539	14	C3/L5	Rodentia	Cricetidae	Arvicolinae	Microtus	sp	rt m2
31540	14	C3/L5	Rodentia	Cricetidae	Arvicolinae	Microtus	sp	lt m1
31541	14	C3/L5	Rodentia	Cricetidae	Arvicolinae	Microtus	sp	lt m1
31542	14	C3/L5	Rodentia	Cricetidae	Arvicolinae	Microtus	sp	rt M2
31543	14	C3/L5	Rodentia	Cricetidae	Arvicolinae	Microtus	sp	partial rt M2
31544	14	C3/L5	Rodentia	Cricetidae	Neotominae	cf Peromyscus	sp	rt dentary
31545	14	C3/L5	Rodentia	Cricetidae	Neotominae	cf Peromyscus	sp	rt dentary
31546	14	C3/L5	Rodentia	Cricetidae	Neotominae	cf Peromyscus	sp	rt dentary
31547	14	C3/L5	Rodentia	Cricetidae	Neotominae	cf Peromyscus	sp	rt dentary
31548	14	C3/L5	Rodentia	Cricetidae	Neotominae	cf Peromyscus	sp	partial lt dentary
31549	14	C3/L5	Rodentia	Cricetidae	Neotominae			partial lt dentary
31550	14	C3/L5	Rodentia	Cricetidae	Neotominae			dentary frag
31551	14	C3/L5	Rodentia	Cricetidae	Neotominae	Peromyscus	cf maniculatus	lt M1
31552	14	C3/L5	Rodentia	Cricetidae	Neotominae			partial molar
31553	14	C3/L5	Rodentia	Cricetidae	Neotominae			molar frag
31554	14	C3/L5	Rodentia	Cricetidae	Neotominae			lower molar - lt m2?
31555	14	C3/L5	Rodentia	Cricetidae	Neotominae			molar frag
31556	14	C3/L5	Rodentia	Cricetidae	Neotominae			M3

31557	14	C3/L5	Rodentia	Cricetidae	Neotominae			rt M2
31558	14	C3/L5	Rodentia	Cricetidae	Neotominae			lt m2
31559	14	C3/L5	Rodentia	Cricetidae	Neotominae	Peromyscus	sp	rt m1
31560	14	C3/L5	Rodentia	Cricetidae	Neotominae			rt m2
31561	14	C3/L5	Rodentia	Cricetidae	Neotominae	?Peromyscus	sp	rt m1
31562	14	C3/L5	Rodentia	Cricetidae	Neotominae			rt m1
31563	14	C3/L5	Rodentia	Cricetidae	Neotominae	Peromyscus	sp	lt M1
31564	14	C3/L5	Rodentia	Cricetidae	Neotominae			lt m2
31565	14	C3/L5	Rodentia	Cricetidae	Neotominae	Peromyscus	sp	lt m1
31566	14	C3/L5	Rodentia	Cricetidae	Neotominae	Peromyscus	sp	rt M1
31567	14	C3/L5	Rodentia	Cricetidae	Neotominae			molar frag
31568	14	C3/L5	Rodentia	Cricetidae	Neotominae			lt M2
31569	14	C3/L5	Rodentia	Cricetidae	Neotominae			rt m2
31570	14	C3/L5	Rodentia	Cricetidae	Neotominae			rt m2
31571	14	C3/L5	Rodentia	Cricetidae	Neotominae	Peromyscus	sp	lt m1
31572	14	C3/L5	Rodentia	Cricetidae	Neotominae			lt? m3
31573	14	C3/L5	Rodentia	Cricetidae	Neotominae			rt m2
31574	14	C3/L5	Rodentia	Cricetidae	Neotominae	Peromyscus	sp	rt m1
31575	14	C3/L5	Rodentia	Cricetidae	Neotominae			rt m2
31576	14	C3/L5	Rodentia	Cricetidae	Neotominae	Peromyscus	sp	rt M1
31577	14	C3/L5	Rodentia	Cricetidae	Neotominae	Peromyscus	sp	lt m1
31578	14	C3/L5	Rodentia	Cricetidae	Neotominae			lt M2
31579	14	C3/L5	Rodentia	Cricetidae	Neotominae			rt m2
31580	14	C3/L5	Rodentia	Cricetidae	Neotominae			molar frag
31581	14	C3/L5	Rodentia	Cricetidae	Neotominae	Peromyscus	sp	lt m1
31582	14	C3/L5	Rodentia	Cricetidae	Neotominae	Peromyscus	sp	rt m2
31583	14	C3/L5	Rodentia	Cricetidae	Neotominae	Peromyscus	sp	rt M2
31584	14	C3/L5	Rodentia	Cricetidae	Neotominae	Peromyscus	sp	lt M2
31585	14	C3/L5	Rodentia	Cricetidae	Neotominae			broken molar
31586	14	C3/L5	Rodentia	Cricetidae	Neotominae			lt M2

31587	14	C3/L5	Rodentia	Cricetidae	Neotominae	Peromyscus	sp	lt M1
31588	14	C3/L5	Rodentia	Cricetidae	Neotominae	Peromyscus	sp	lt m1
31589	14	C3/L5	Rodentia	Cricetidae	Neotominae			lt m2
31590	14	C3/L5	Rodentia	Cricetidae	Neotominae	Peromyscus	sp	lt M1
31591	14	C3/L5	Rodentia	Cricetidae	Neotominae	Peromyscus	sp	lt M1
31592	14	C3/L5	Rodentia	Cricetidae	Neotominae	Peromyscus	sp	rt M1
31593	14	C3/L5	Rodentia	Cricetidae	Neotominae	Peromyscus	sp	rt m1
31594	14	C3/L5	Rodentia	Cricetidae	Neotominae	?Peromyscus	sp	lt M1
31595	14	C3/L5	Rodentia	Cricetidae	Neotominae			molar frag
31596	14	C3/L5	Rodentia	Cricetidae	Neotominae	Peromyscus	cf maniculatus	lt M1
31597	14	C3/L5	Rodentia	Cricetidae	Neotominae	?Peromyscus	sp	lt m1
31598	14	C3/L5	Rodentia	Cricetidae	Neotominae			molar frag
31599	14	C3/L5	Rodentia	Cricetidae	Neotominae			lt m1 - multiple frags
31600	14	C3/L5	Rodentia	Cricetidae	Neotominae			partial molar
31601	14	C3/L5	Rodentia	Cricetidae	Neotominae			rt M2
31602	14	C3/L5	Rodentia	Cricetidae	Neotominae	Peromyscus	sp	lt m1
31603	14	C3/L5	Rodentia	Cricetidae	Neotominae			lt M2
31604	14	C3/L5	Rodentia	Cricetidae	Neotominae			rt m3
31605	14	C3/L5	Rodentia	Cricetidae	Neotominae	Peromyscus	sp	lt M1
31606	14	C3/L5	Rodentia	Cricetidae	Neotominae			lt M2
31607	14	C3/L5	Rodentia	Cricetidae	Neotominae			rt M2
31608	14	C3/L5	Rodentia	Cricetidae	Neotominae			partial tooth
31609	14	C3/L5	Rodentia	Cricetidae	Neotominae			rt M2
31610	14	C3/L5	Rodentia	Cricetidae	Arvicolinae	Microtus	sp	rt m1
31611	14	C3/L5	Rodentia	Cricetidae	Arvicolinae	cf Microtus	sp	maxilla frag
31612	14	C3/L5	Rodentia	Cricetidae	Arvicolinae	cf Microtus	sp	partial rt dentary
31613	14	C3/L5	Rodentia	Cricetidae	Arvicolinae	cf Microtus	sp	partial rt dentary
31614	14	C3/L5	Rodentia	Cricetidae	Arvicolinae	cf Microtus	sp	maxilla frag

31615	14	C3/L5	Rodentia	Cricetidae	Neotominae	Neotoma	sp	molar frag
31616	14	C3/L5	Rodentia	Cricetidae	Neotominae	Peromyscus	sp	lt m2
31617	14	C3/L5	Rodentia	Cricetidae	Neotominae	Neotoma	sp	rt M3
31618	14	C3/L5	Rodentia	Cricetidae	Neotominae			broken molar
31619	14	C3/L5	Rodentia	Cricetidae	Neotominae	Peromyscus	sp	lt m2
31620	14	C3/L5	Rodentia	Cricetidae	Arvicolinae	Microtus	sp	rt m1
31621	14	C3/L5	Rodentia	Cricetidae	Arvicolinae	Microtus	sp	lt M1
31622	14	C3/L5	Rodentia	Cricetidae	Arvicolinae	Microtus	sp	partial lt m1
31623	14	C3/L5	Rodentia	Cricetidae	Arvicolinae	Microtus	sp	lt M1
31624	14	C3/L5	Rodentia	Cricetidae	Arvicolinae	Microtus	sp	rt M1
31625	14	C3/L5	Rodentia	Cricetidae	Arvicolinae	Microtus	sp	molar frag
31626	14	C3/L5	Rodentia	Cricetidae	Arvicolinae	Microtus	sp	molar frag
31627	14	C3/L5	Rodentia	Cricetidae	Arvicolinae	Microtus	sp	rt M3
31628	14	C3/L5	Rodentia	Cricetidae	Arvicolinae	Microtus	sp	rt m2
31629	14	C3/L5	Rodentia	Cricetidae	Arvicolinae	Microtus	sp	molar frag
31630	14	C3/L5	Rodentia	Cricetidae	Arvicolinae	Microtus	sp	broken molar
31631	14	C3/L5	Rodentia	Cricetidae	Arvicolinae	Microtus	sp	rt m2
31632	14	C3/L5	Rodentia	Cricetidae	Arvicolinae	Microtus	sp	rt M2
31633	14	C3/L5	Rodentia	Cricetidae	Arvicolinae	Microtus	sp	rt M2
31634	14	C3/L5	Rodentia	Cricetidae	Arvicolinae	Microtus	sp	lt M3
31636	14	C3/L5	Rodentia	Cricetidae	Arvicolinae	Microtus	sp	rt m1 frag
31637	14	C3/L5	Rodentia	Cricetidae	Arvicolinae	Microtus	sp	molar frag
31638	14	C3/L5	Rodentia	Cricetidae	Arvicolinae	Microtus	sp	rt M2
31639	14	C3/L5	Rodentia	Cricetidae	Arvicolinae	Microtus	sp	broken molar
31640	14	C3/L5	Rodentia	Cricetidae	Arvicolinae	Microtus	sp	lt m2
31641	14	C3/L5	Rodentia	Cricetidae	Arvicolinae	Microtus	sp	rt M2
31642	14	C3/L5	Rodentia	Cricetidae	Arvicolinae	Microtus	sp	lt m2
31643	14	C3/L5	Rodentia	Cricetidae	Arvicolinae	Microtus	sp	rt m3
31644	14	C3/L5	Rodentia	Cricetidae	Arvicolinae	Microtus	sp	lt M3
31645	14	C3/L5	Rodentia	Cricetidae	Arvicolinae	Microtus	sp	rt M3

31646	14	C3/L5	Rodentia	Cricetidae	Arvicolinae	Microtus	sp	molar frag
31647	14	C3/L5	Rodentia	Cricetidae	Arvicolinae	Microtus	sp	molar frag
31648	14	C3/L5	Rodentia	Cricetidae	Arvicolinae	Microtus	sp	molar frag
31649	14	C3/L5	Rodentia	Cricetidae	Arvicolinae	Microtus	sp	molar frag
31650	14	C3/L5	Rodentia	Cricetidae	Arvicolinae	Microtus	sp	molar frag
31651	14	C3/L5	Rodentia	Cricetidae	Arvicolinae	Microtus	sp	molar frag
31652	14	C3/L5	Rodentia	Cricetidae	Arvicolinae	Microtus	sp	molar frag
31653	14	C3/L5	Rodentia	Cricetidae	Arvicolinae	Microtus	sp	molar frag
31654	14	C3/L5	Rodentia	Cricetidae	Arvicolinae	Microtus	sp	molar frag
31655	14	C3/L5	Rodentia	Cricetidae	Arvicolinae	Microtus	sp	molar frag
31656	14	C3/L5	Rodentia	Cricetidae	Arvicolinae	Microtus	sp	molar frag
31657	14	C3/L5	Rodentia	Cricetidae	Arvicolinae	Microtus	sp	molar frag
31658	14	C3/L5	Rodentia	Cricetidae	Arvicolinae	Microtus	sp	molar frag
31659	14	C3/L5	Rodentia	Cricetidae	Arvicolinae	Microtus	sp	molar frag
31660	14	C3/L5	Rodentia	Cricetidae	Arvicolinae	Microtus	sp	molar frag
31661	14	C3/L5	Rodentia	Cricetidae	Arvicolinae	Microtus	sp	molar frag
31662	14	C3/L5	Rodentia	Cricetidae	Arvicolinae	Microtus	sp	molar frag
31663	14	C3/L5	Rodentia	Cricetidae	Arvicolinae	Microtus	sp	molar frag
31664	14	C3/L5	Rodentia	Cricetidae	Arvicolinae	Microtus	sp	rt M3
31665	14	C3/L5	Rodentia	Cricetidae	Arvicolinae	Microtus	sp	partial lt M2
31666	14	C3/L5	Rodentia	Cricetidae	Arvicolinae	Microtus	sp	rt M1
31667	14	C3/L5	Rodentia	Cricetidae	Arvicolinae	Microtus	sp	partial lt m1
31668	14	C3/L5	Rodentia	Cricetidae	Arvicolinae	Microtus	sp	partial lt m2
31669	14	C3/L5	Rodentia	Cricetidae	Arvicolinae	Microtus	sp	partial rt M2
31670	14	C3/L5	Rodentia	Cricetidae	Arvicolinae	Microtus	sp	molar frag
31671	14	C3/L5	Rodentia	Cricetidae	Arvicolinae	Microtus	sp	partial rt m2
31672	14	C3/L5	Rodentia	Cricetidae	Arvicolinae	Microtus	sp	lt M2
31673	14	C3/L5	Lagomorpha	Leporidae		?Sylvilagus	sp	rt dentary frag
31674	14	C3/L5	Lagomorpha	Leporidae		Sylvilagus	sp	lt P2
31675	14	C3/L5	Lagomorpha	Leporidae		?Sylvilagus	sp	tooth frag

31676	14	C3/L5	Lagomorpha	Leporidae		?Sylvilagus	sp	tooth frag
31677	14	C3/L5	Lagomorpha	Leporidae		?Sylvilagus	sp	tooth frag
31678	14	C3/L5	Lagomorpha	Leporidae		?Sylvilagus	sp	tooth frag
31679	14	C3/L5	Lagomorpha	Leporidae		Sylvilagus	sp	upper rt? tooth
31680	14	C3/L5	Lagomorpha	Leporidae		Sylvilagus	sp	rt P2
31681	14	C3/L5	Lagomorpha	Leporidae		Sylvilagus	sp	lower tooth
31682	14	C3/L5	Lagomorpha	Leporidae		Sylvilagus	sp	upper rt tooth
31683	14	C3/L5	Lagomorpha	Leporidae		?Sylvilagus	sp	M3
31684	14	C3/L5	Lagomorpha	Leporidae		Sylvilagus	sp	upper tooth
31685	14	C3/L5	Lagomorpha	Leporidae		Sylvilagus	sp	lower tooth
31686	14	C3/L5	Lagomorpha	Leporidae		Sylvilagus	sp	lower rt tooth
31687	14	C3/L5	Lagomorpha	Leporidae		?Sylvilagus	sp	tooth
31688	14	C3/L5	Lagomorpha	Leporidae		?Sylvilagus	sp	broken tooth
31689	14	C3/L5	Lagomorpha	Leporidae		Sylvilagus	sp	upper rt tooth
31690	14	C3/L5	Lagomorpha	Leporidae		?Sylvilagus	sp	tooth frag
31691	14	C3/L5	Lagomorpha	Leporidae		?Sylvilagus	sp	partial upper tooth
31692	14	C3/L5	Lagomorpha	Leporidae		Sylvilagus	sp	M3
31693	14	C3/L5	Rodentia	Geomyidae	Thomomyinae	Thomomys	sp	lt M1/M2
31694	14	C3/L5	Rodentia	Heteromyidae	Dipodomyinae	Dipodomys	sp	lt m1
31695	14	C3/L5	Rodentia	Heteromyidae	Dipodomyinae	?Dipodomys	sp	lt M1/M2
31696	14	C3/L5	Rodentia	Heteromyidae	Dipodomyinae	?Dipodomys	sp	rt m1
31697	14	C3/L5	Rodentia	Geomyidae	Dipodomyinae	?Dipodomys	sp	partial tooth
31698	14	C3/L5	Rodentia	Heteromyidae	Dipodomyinae	?Dipodomys	sp	molar
31699	14	C3/L5	Rodentia	Heteromyidae	Dipodomyinae	Dipodomys	sp	molar
31700	14	C3/L5	Rodentia	Heteromyidae	Dipodomyinae	Dipodomys	sp	rt p4
31701	14	C3/L5	Rodentia	Heteromyidae	Dipodomyinae	?Dipodomys	sp	tooth
31702	14	C3/L5	Rodentia	Heteromyidae	Dipodomyinae	?Dipodomys	sp	tooth
31703	14	C3/L5	Rodentia	Heteromyidae	Dipodomyinae	?Dipodomys	sp	tooth
31704	14	C3/L5	Rodentia	Heteromyidae	Dipodomyinae	?Dipodomys	sp	tooth

31705	14	C3/L5	Rodentia	Heteromyidae	Dipodomyinae	Dipodomys	sp	m3
31706	14	C3/L5	Rodentia	Heteromyidae	Dipodomyinae	?Dipodomys	sp	tooth
31709	14	C3/L5	Rodentia	Heteromyidae	Dipodomyinae	Dipodomys	sp	rt P4
31710	14	C3/L5	Rodentia	Sciuridae	Xerinae	Otospermophilus	?beecheyi	rt m3
31711	14	C3/L5	Eulipotyphla	Soricidae	Soricinae			rt M1
31712	14	C3/L5	Eulipotyphla	Soricidae	Soricinae			dentary frag
31713	14	C3/L5	Carnivora	Mephitidae		?Spilogale	gracilis	partial lt P3
31714	14	C3/L5	Rodentia	Sciuridae	Xerinae			upper molar frag
31716	14	C3/L5	Rodentia	Cricetidae	?Neotominae			dentary frag
31723	14	B3/L5	Lagomorpha	Leporidae		?Sylvilagus	sp	lt maxilla frag w/ p3
31724	14	B3/L5	Lagomorpha	Leporidae		?Sylvilagus	sp	maxilla frag
31725	14	B3/L5	Lagomorpha	Leporidae		?Sylvilagus	sp	upper tooth frag
31726	14	B3/L5	Lagomorpha	Leporidae		Sylvilagus	sp	lower tooth
31727	14	B3/L5	Rodentia	Geomyidae	Thomomyinae	Thomomys	sp	rt dentary with i1
31728	14	B3/L5	Rodentia	Cricetidae	Neotominae	Peromyscus	sp	rt dentary w/ i1-m3
31729	14	B3/L5	Rodentia	Cricetidae	Neotominae	cf Peromyscus	sp	rt dentary
31730	14	B3/L5	Rodentia	Cricetidae	Neotominae	cf Peromyscus	sp	rt dentary frag
31731	14	B3/L5	Rodentia	Cricetidae	Neotominae	?Peromyscus	sp	rt dentary
31732	14	B3/L5	Rodentia	Cricetidae	Neotominae			lt dentary
31733	14	B3/L5	Rodentia	Cricetidae	Neotominae			lt dentary
31734	14	B3/L5	Rodentia	Cricetidae	Neotominae			lt dentary
31735	14	B3/L5	Rodentia	Cricetidae	?Neotominae			lt maxilla frag
31736	14	B3/L5	Rodentia	Cricetidae	Neotominae	Peromyscus	sp	rt m1
31737	14	B3/L5	Rodentia	Cricetidae	Neotominae	Peromyscus	sp	lt M1
31738	14	B3/L5	Rodentia	Cricetidae	Neotominae	Peromyscus	cf maniculatus	lt m1
31739	14	B3/L5	Rodentia	Cricetidae	Neotominae			rt m2
31740	14	B3/L5	Rodentia	Cricetidae	Neotominae			rt M2

31741	14	B3/L5	Rodentia	Cricetidae	Neotominae			rt M2
31742	14	B3/L5	Rodentia	Cricetidae	Neotominae			lt M2
31743	14	B3/L5	Rodentia	Cricetidae	Arvicolinae	cf Microtus	sp	lt maxilla frag
31744	14	B3/L5	Rodentia	Cricetidae	Arvicolinae	Microtus	sp	lt m1
31745	14	B3/L5	Rodentia	Cricetidae	Arvicolinae	Microtus	sp	rt M1
31746	14	B3/L5	Rodentia	Cricetidae	Arvicolinae	Microtus	sp	rt m2
31747	14	B3/L5	Rodentia	Cricetidae	Arvicolinae	Microtus	sp	rt M2
31748	14	B3/L5	Rodentia	Cricetidae	Arvicolinae	Microtus	sp	lt M3
31749	14	B3/L5	Rodentia	Cricetidae	Arvicolinae	Microtus	sp	rt M2
31750	14	B3/L5	Rodentia	Cricetidae	Arvicolinae	Microtus	sp	rt m3
31751	14	B3/L5	Rodentia	Cricetidae	Arvicolinae	Microtus	sp	rt m3
31752	14	B3/L5	Rodentia	Cricetidae	Arvicolinae	Microtus	sp	lt m3
31753	14	B3/L5	Rodentia	Heteromyidae	Dipodomyinae	?Dipodomys	sp	rt p4 frag
31754	14	B3/L5	Rodentia	Heteromyidae	Dipodomyinae	Dipodomys	sp	rt m1/m2
31755	14	B3/L5	Rodentia	Heteromyidae	Dipodomyinae	Dipodomys	sp	molar
31756	14	B3/L5	Rodentia	Heteromyidae	Dipodomyinae	?Dipodomys	sp	tooth
31758	14	B3/L5	Rodentia	Heteromyidae	Dipodomyinae	Dipodomys	sp	lt m2
31759	14	B3/L5	Rodentia	Heteromyidae	Dipodomyinae	Dipodomys	sp	partial lower tooth
31760	14	B3/L5	Rodentia	Sciuridae	Xerinae	Otospermophilus	?beecheyi	rt P4
31763	14	D2/L4	Lagomorpha	Leporidae		?Sylvilagus	sp	lt dentary frag
31764	14	D2/L4	Lagomorpha	Leporidae		?Sylvilagus	sp	rt dentary frag
31767	14	D2/L4	Lagomorpha	Leporidae		Sylvilagus	sp	upper lt tooth
31768	14	D2/L4	Lagomorpha	Leporidae		Sylvilagus	sp	partial upper tooth
31769	14	D2/L4	Lagomorpha	Leporidae		Sylvilagus	sp	upper rt tooth
31770	14	D2/L4	Lagomorpha	Leporidae		Sylvilagus	sp	upper tooth frag
31771	14	D2/L4	Lagomorpha	Leporidae		Sylvilagus	sp	partial upper tooth
31772	14	D2/L4	Lagomorpha	Leporidae		Sylvilagus	sp	lt P2
31773	14	D2/L4	Lagomorpha	Leporidae		Sylvilagus	sp	partial upper tooth

31774	14	D2/L4	Lagomorpha	Leporidae		Sylvilagus	sp	rt P2
31775	14	D2/L4	Lagomorpha	Leporidae		?Sylvilagus	sp	upper tooth frag
31776	14	D2/L4	Lagomorpha	Leporidae		Sylvilagus	sp	upper tooth
31781	14	D2/L4	Lagomorpha	Leporidae		Sylvilagus	audubonii	lt p3
31782	14	D2/L4	Lagomorpha	Leporidae		Sylvilagus	audubonii	lt p3
31783	14	D2/L4	Lagomorpha	Leporidae		Sylvilagus	sp	rt p3
31784	14	D2/L4	Lagomorpha	Leporidae		Sylvilagus	sp	rt p3
31785	14	D2/L4	Lagomorpha	Leporidae		Sylvilagus	sp	m3
31786	14	D2/L4	Lagomorpha	Leporidae		Sylvilagus	sp	lower lt tooth
31787	14	D2/L4	Lagomorpha	Leporidae		Sylvilagus	sp	lower rt tooth
31788	14	D2/L4	Lagomorpha	Leporidae		Sylvilagus	sp	lower lt tooth
31789	14	D2/L4	Lagomorpha	Leporidae		Sylvilagus	sp	lower lt tooth
31790	14	D2/L4	Lagomorpha	Leporidae		Sylvilagus	sp	partial lower tooth
31791	14	D2/L4	Lagomorpha	Leporidae		Sylvilagus	sp	lower rt tooth
31792	14	D2/L4	Lagomorpha	Leporidae		Sylvilagus	sp	lower rt tooth
31793	14	D2/L4	Lagomorpha	Leporidae		Sylvilagus	sp	lower lt tooth
31794	14	D2/L4	Lagomorpha	Leporidae		Sylvilagus	sp	lower lt tooth
31795	14	D2/L4	Lagomorpha	Leporidae		Sylvilagus	sp	lower lt tooth
31796	14	D2/L4	Lagomorpha	Leporidae		Sylvilagus	sp	lower lt tooth
31797	14	D2/L4	Lagomorpha	Leporidae		Sylvilagus	sp	lower lt tooth
31798	14	D2/L4	Lagomorpha	Leporidae		Sylvilagus	sp	lower rt tooth
31799	14	D2/L4	Lagomorpha	Leporidae		Sylvilagus	sp	lower lt tooth
31800	14	D2/L4	Lagomorpha	Leporidae		?Sylvilagus	sp	lower tooth frag
31801	14	D2/L4	Lagomorpha	Leporidae		Sylvilagus	sp	partial lower rt tooth
31802	14	D2/L4	Lagomorpha	Leporidae		?Sylvilagus	sp	partial lower tooth
31803	14	D2/L4	Rodentia	Geomyidae	Thomomyinae	Thomomys	sp	rt m1/m2
31804	14	D2/L4	Rodentia	Geomyidae	Thomomyinae	Thomomys	sp	rt m1/m2
31806	14	D2/L4	Rodentia	Geomyidae	Thomomyinae	Thomomys	sp	lt m1/m2

31807	14	D2/L4	Rodentia	Heteromyidae	Dipodomyinae	?Dipodomys	sp	lower molar
31808	14	D2/L4	Rodentia	Geomyidae	Thomomyinae	Thomomys	sp	rt m1/m2
31809	14	D2/L4	Rodentia	Heteromyidae	Dipodomyinae	Dipodomys	sp	rt m1/m2
31810	14	D2/L4	Rodentia	Heteromyidae	Dipodomyinae	Dipodomys	sp	M1/M2
31811	14	D2/L4	Rodentia	Heteromyidae	Dipodomyinae	?Dipodomys	sp	rt m1/m2
31812	14	D2/L4	Rodentia	Geomyidae	Thomomyinae	Thomomys	sp	M3/m3
31813	14	D2/L4	Rodentia	Heteromyidae	Dipodomyinae	Dipodomys	sp	upper rt tooth
31814	14	D2/L4	Rodentia	Heteromyidae	Dipodomyinae	Dipodomys	sp	p4
31815	14	D2/L4	Rodentia	Heteromyidae	Dipodomyinae	Dipodomys	sp	lt p4
31816	14	D2/L4	Rodentia	Heteromyidae	Dipodomyinae	Dipodomys	sp	molar
31817	14	D2/L4	Rodentia	Heteromyidae	Dipodomyinae	?Dipodomys	sp	lower molar
31818	14	D2/L4	Rodentia	Heteromyidae	Dipodomyinae	Dipodomys	sp	molar
31819	14	D2/L4	Rodentia	Heteromyidae	Dipodomyinae	?Dipodomys	sp	molar
31820	14	D2/L4	Rodentia	Heteromyidae	Dipodomyinae	?Dipodomys	sp	molar
31821	14	D2/L4	Rodentia	Heteromyidae	Dipodomyinae	Dipodomys	sp	lt P4
31822	14	D2/L4	Rodentia	Heteromyidae	Dipodomyinae	Dipodomys	sp	upper tooth
31823	14	D2/L4	Rodentia	Heteromyidae	Dipodomyinae	Dipodomys	sp	rt m1/m2
31824	14	D2/L4	Rodentia	Heteromyidae	Dipodomyinae	Dipodomys	sp	molar
31826	14	D2/L4	Rodentia	Heteromyidae	Dipodomyinae	Dipodomys	sp	molar
31827	14	D2/L4	Rodentia	Geomyidae	Thomomyinae	Thomomys	sp	rt M1/M2
31828	14	D2/L4	Rodentia	Geomyidae	Thomomyinae	?Thomomys	sp	rt m1/m2
31829	14	D2/L4	Rodentia	Geomyidae	Thomomyinae	?Thomomys	sp	tooth
31830	14	D2/L4	Rodentia	Geomyidae	Thomomyinae	Thomomys	sp	lt m1/m2
31834	14	D2/L4	Rodentia	Heteromyidae	Dipodomyinae	?Dipodomys	sp	partial tooth
31837	14	D2/L4	Rodentia	Geomyidae	Thomomyinae	Thomomys	sp	rt M1/M2
31839	14	D2/L4	Rodentia	Heteromyidae	Dipodomyinae	Dipodomys	sp	tooth
31840	14	D2/L4	Rodentia	Heteromyidae	Dipodomyinae	Dipodomys	sp	p4
31841	14	D2/L4	Rodentia	Heteromyidae	Dipodomyinae	Dipodomys	sp	tooth
31845	14	D2/L4	Rodentia	Heteromyidae	Dipodomyinae	Dipodomys	sp	p4
31863	14	D2/L4	Rodentia	Cricetidae	Arvicolinae	Microtus	sp	rt m1

31864	14	D2/L4	Rodentia	Cricetidae	Arvicolinae	Microtus	californicus	lt m1
31865	14	D2/L4	Rodentia	Cricetidae	Arvicolinae	Microtus	sp	lt M1
31866	14	D2/L4	Rodentia	Cricetidae	Arvicolinae	Microtus	californicus	lt m1
31867	14	D2/L4	Rodentia	Cricetidae	Arvicolinae	Microtus	sp	molar frag
31868	14	D2/L4	Rodentia	Cricetidae	Arvicolinae	Microtus	sp	molar frag
31869	14	D2/L4	Rodentia	Cricetidae	Arvicolinae	Microtus	californicus	rt m1
31870	14	D2/L4	Rodentia	Cricetidae	Arvicolinae	Microtus	californicus	lt m1
31871	14	D2/L4	Rodentia	Cricetidae	Arvicolinae	Microtus	sp	lt M1
31872	14	D2/L4	Rodentia	Cricetidae	Arvicolinae	Microtus	sp	rt M1
31873	14	D2/L4	Rodentia	Cricetidae	Arvicolinae	Microtus	sp	rt M1
31874	14	D2/L4	Rodentia	Cricetidae	Arvicolinae	Microtus	sp	rt M2
31875	14	D2/L4	Rodentia	Cricetidae	Arvicolinae	Microtus	sp	lt dentary frag
31876	14	D2/L4	Rodentia	Cricetidae	Arvicolinae	Microtus	sp	rt m2
31877	14	D2/L4	Rodentia	Cricetidae	Arvicolinae	Microtus	sp	lt m2
31878	14	D2/L4	Rodentia	Cricetidae	Arvicolinae	Microtus	sp	partial lt m1
31879	14	D2/L4	Rodentia	Cricetidae	Arvicolinae	Microtus	sp	lt M2
31880	14	D2/L4	Rodentia	Cricetidae	Arvicolinae	cf Microtus	sp	rt dentary
31881	14	D2/L4	Rodentia	Cricetidae	Arvicolinae	Microtus	sp	rt m2
31882	14	D2/L4	Rodentia	Cricetidae	Arvicolinae	Microtus	sp	lt m2
31883	14	D2/L4	Rodentia	Cricetidae	Arvicolinae	Microtus	sp	partial lt M1
31884	14	D2/L4	Rodentia	Cricetidae	Arvicolinae	Microtus	sp	rt m2
31885	14	D2/L4	Rodentia	Cricetidae	Arvicolinae	Microtus	sp	rt m3
31886	14	D2/L4	Rodentia	Cricetidae	Arvicolinae	Microtus	sp	rt m3
31887	14	D2/L4	Rodentia	Cricetidae	Neotominae	Peromyscus	cf californicus	lt M1
31888	14	D2/L4	Rodentia	Cricetidae	Neotominae	Peromyscus	sp	rt M1
31889	14	D2/L4	Rodentia	Cricetidae	Neotominae	Peromyscus	sp	rt M1
31890	14	D2/L4	Rodentia	Cricetidae	Neotominae	Peromyscus	sp	rt m1
31891	14	D2/L4	Rodentia	Cricetidae	Neotominae	Peromyscus	sp	lt m1
31892	14	D2/L4	Rodentia	Cricetidae	Neotominae	Peromyscus	sp	rt m1

31893	14	D2/L4	Rodentia	Cricetidae	Neotominae	Peromyscus	sp	rt m1
31894	14	D2/L4	Rodentia	Cricetidae	Neotominae	Peromyscus	sp	rt M1
31895	14	D2/L4	Rodentia	Cricetidae	Neotominae	Peromyscus	sp	lt m1
31896	14	D2/L4	Rodentia	Cricetidae	Neotominae	Peromyscus	sp	rt m1
31897	14	D2/L4	Rodentia	Cricetidae	Neotominae			rt m2
31898	14	D2/L4	Rodentia	Cricetidae	Neotominae			rt m1
31899	14	D2/L4	Rodentia	Cricetidae	Neotominae	Peromyscus	sp	lt m1
31900	14	D2/L4	Rodentia	Cricetidae	Neotominae	Peromyscus	sp	lt m1
31901	14	D2/L4	Rodentia	Cricetidae	Neotominae			lt M2
31902	14	D2/L4	Rodentia	Cricetidae	Neotominae	Peromyscus	cf maniculatus	rt M1
31903	14	D2/L4	Rodentia	Cricetidae	Neotominae			rt m2
31904	14	D2/L4	Rodentia	Cricetidae	Neotominae			rt m1
31905	14	D2/L4	Rodentia	Cricetidae	Neotominae			lt m2
31906	14	D2/L4	Rodentia	Cricetidae	Neotominae			lt m2
31907	14	D2/L4	Rodentia	Cricetidae	Neotominae			rt m2
31908	14	D2/L4	Rodentia	Cricetidae	Neotominae			lt m2
31909	14	D2/L4	Rodentia	Cricetidae	Neotominae			rt m2
31911	14	D2/L4	Rodentia	Cricetidae	Neotominae			lt M1
31912	14	D2/L4	Rodentia	Cricetidae	Neotominae			rt M2
31913	14	D2/L4	Rodentia	Cricetidae	Neotominae			lt m1
31914	14	D2/L4	Rodentia	Cricetidae	Neotominae	Peromyscus	sp	rt m1
31915	14	D2/L4	Rodentia	Cricetidae	Neotominae			lt dentary
31916	14	D2/L4	Rodentia	Cricetidae	Neotominae			rt dentary frag
31917	14	D2/L4	Rodentia	Cricetidae	Neotominae			lt dentary frag
31918	14	D2/L4	Rodentia	Cricetidae	Neotominae	Peromyscus	sp	rt dentary w/ m2-m3
31919	14	D2/L4	Rodentia	Cricetidae	?Neotominae			lt dentary frag
31920	14	D2/L4	Rodentia	Cricetidae	Neotominae	Peromyscus	cf maniculatus	lt dentary w/ m2
31921	14	D2/L4	Rodentia	Cricetidae	Neotominae			lt dentary frag

31922	14	D2/L4	Rodentia	Cricetidae	Neotominae	?Peromyscus	sp	lt dentary with m2
31923	14	D2/L4	Rodentia	Cricetidae	?Neotominae			lt maxilla frag
31924	14	D2/L4	Rodentia	Cricetidae	Neotominae			lt dentary frag
31925	14	D2/L4	Rodentia	Cricetidae	Neotominae			lt m1
31926	14	D2/L4	Rodentia	Cricetidae	Neotominae			lt m2
31927	14	D2/L4	Rodentia	Cricetidae	Neotominae	Peromyscus	sp	rt m1
31928	14	D2/L4	Rodentia	Heteromyidae	Perognathinae			lt M1/M2
31929	14	D2/L4	Rodentia	Cricetidae	Neotominae			rt M2
31930	14	D2/L4	Rodentia	Cricetidae	Neotominae			rt M2
31931	14	D2/L4	Rodentia	Heteromyidae	Perognathinae			rt M1/M2
31932	14	D2/L4	Rodentia	Cricetidae	?Neotominae			rt maxilla frag
31933	14	D2/L4	Rodentia	Cricetidae	Neotominae			lt M2
31934	14	D2/L4	Rodentia	Cricetidae	Neotominae	Peromyscus	sp	lt M1
31935	14	D2/L4	Rodentia	Cricetidae	Neotominae			lt M2
31936	14	D2/L4	Rodentia	Cricetidae	Neotominae	Peromyscus	cf maniculatus	rt M1
31937	14	D2/L4	Rodentia	Cricetidae	Neotominae	Peromyscus	sp	lt M1
31938	14	D2/L4	Rodentia	Cricetidae	Neotominae			rt m2
31939	14	D2/L4	Rodentia	Cricetidae	Neotominae	cf Reithrodontomys	megalotis	lt M1
31940	14	D2/L4	Rodentia	Cricetidae	?Neotominae			rt maxilla frag
31941	14	D2/L4	Rodentia	Cricetidae	?Neotominae			lt dentary frag
31942	14	D2/L4	Rodentia	Cricetidae	Neotominae			rt dentary frag
31943	14	D2/L4	Rodentia	Cricetidae	?Neotominae			lt maxilla frag
31944	14	D2/L4	Rodentia	Cricetidae	Neotominae	?Peromyscus	sp	lt M1 frag
31945	14	D2/L4	Rodentia	Cricetidae	Neotominae			rt M2
31946	14	D2/L4	Rodentia	Cricetidae	Neotominae			lt M2
31947	14	D2/L4	Rodentia	Cricetidae	Arvicolinae	cf Microtus	sp	rt dentary frag
31948	14	D2/L4	Rodentia	Cricetidae	Arvicolinae	cf Microtus	sp	dentary frag
31949	14	D2/L4	Rodentia	Cricetidae	Arvicolinae	Microtus	sp	molar frag
31950	14	D2/L4	Rodentia	Cricetidae	Arvicolinae	Microtus	sp	molar frag

31951	14	D2/L4	Rodentia	Cricetidae	Arvicolinae	Microtus	sp	molar frag
31952	14	D2/L4	Rodentia	Cricetidae	Arvicolinae	Microtus	sp	molar frag
31953	14	D2/L4	Rodentia	Cricetidae	Arvicolinae	Microtus	sp	molar frag
31954	14	D2/L4	Rodentia	Cricetidae	Arvicolinae	Microtus	sp	molar frag
31955	14	D2/L4	Rodentia	Cricetidae	Arvicolinae	Microtus	sp	molar frag
31956	14	D2/L4	Rodentia	Cricetidae	Neotominae			lt M2
31957	14	D2/L4	Rodentia	Cricetidae	Neotominae	?Peromyscus	sp	lt M1
31958	14	D2/L4	Rodentia	Cricetidae	Neotominae			rt m2
31959	14	D2/L4	Rodentia	Cricetidae	Neotominae	Peromyscus	sp	lt m1
31960	14	D2/L4	Rodentia	Cricetidae	Neotominae			lt dentary frag
31961	14	D2/L4	Rodentia	Cricetidae	?Neotominae			maxilla frag
31962	14	D2/L4	Rodentia	Cricetidae	Neotominae			lt maxilla frag
31963	14	D2/L4	Rodentia	Sciuridae	Xerinae	Otospermophilus	?beecheyi	lt m2
31964	14	D2/L4	Rodentia	Sciuridae	Xerinae	Otospermophilus	?beecheyi	lt m1
31965	14	D2/L4	Rodentia	Sciuridae	Xerinae	Otospermophilus	?beecheyi	rt m2
31966	14	D2/L4	Rodentia	Sciuridae	Xerinae	Otospermophilus	?beecheyi	lt M1/M2
31967	14	D2/L4	Rodentia	Sciuridae	Xerinae	Otospermophilus	?beecheyi	lt P4
31968	14	D2/L4	Rodentia	Sciuridae	Xerinae	Otospermophilus	?beecheyi	rt P4
31969	14	D2/L4	Rodentia	Sciuridae	Xerinae	Otospermophilus	?beecheyi	rt M3
31970	14	D2/L4	Rodentia	Sciuridae	Xerinae			upper tooth frag
31971	14	D2/L4	Rodentia	Sciuridae	Xerinae	Otospermophilus	?beecheyi	rt P4
31972	14	D2/L4	Rodentia	Sciuridae	Xerinae	Otospermophilus	?beecheyi	rt P4
31973	14	D2/L4	Rodentia	Sciuridae	Xerinae	Otospermophilus	?beecheyi	rt M3
31974	14	D2/L4	Rodentia	Sciuridae	Xerinae	Otospermophilus	?beecheyi	lt P4
31975	14	D2/L4	Rodentia	Cricetidae	Neotominae	Neotoma	sp	rt M1
31976	14	D2/L4	Rodentia	Cricetidae	Neotominae	Neotoma	macrotis	lt m1
31977	14	D2/L4	Rodentia	Cricetidae	Neotominae	Neotoma	sp	rt M1
31978	14	D2/L4	Rodentia	Cricetidae	Neotominae	Neotoma	sp	lt M1 frag
31979	14	D2/L4	Rodentia	Cricetidae	Neotominae	Neotoma	sp	lt M2
31980	14	D2/L4	Rodentia	Cricetidae	Neotominae	Neotoma	sp	lt m1 frag

31981	14	D2/L4	Rodentia	Geomyidae	Thomomyinae	Thomomys	?bottae	lt p4
31982	14	D2/L4	Rodentia	Cricetidae	Neotominae	Neotoma	sp	lt M3
31983	14	D2/L4	Rodentia	Geomyidae	Thomomyinae	?Thomomys	sp	P4/p4
31984	14	D2/L4	Rodentia	Cricetidae	Neotominae	Neotoma	sp	lt M3
31985	14	D2/L4	Rodentia	Cricetidae	Neotominae	?Neotoma	sp	molar frag
31986	14	D2/L4	Rodentia	Cricetidae	Neotominae	?Neotoma	sp	molar frag
31987	14	D2/L4	Rodentia	Heteromyidae	Dipodomyinae	?Dipodomys	sp	rt p4 frag
31988	14	D2/L4	Rodentia	Heteromyidae	Perognathinae			lt? P4
31989	14	D2/L4	Rodentia	Heteromyidae	Dipodomyinae	?Dipodomys	sp	p4
31990	14	D2/L4	Rodentia	Heteromyidae	Perognathinae			rt m1/m2
31993	14	D2/L4	Rodentia	Heteromyidae	Perognathinae			upper molar - rt M3?
31995	14	D2/L4	Rodentia	Heteromyidae	Dipodomyinae	?Dipodomys	sp	maxilla frag
31998	14	D2/L4	Rodentia	Cricetidae	?Neotominae			maxilla frag
31999	14	D2/L4	Rodentia	Cricetidae	Arvicolinae	Microtus	sp	molar frag
32000	14	D2/L4	Rodentia	Cricetidae	Arvicolinae	Microtus	sp	molar frag
32002	14	C2/L4	Rodentia	Cricetidae	Arvicolinae	Microtus	californicus	lt m1
32003	14	C2/L4	Rodentia	Cricetidae	Arvicolinae	Microtus	sp	lt m1
32004	14	C2/L4	Rodentia	Cricetidae	Arvicolinae	Microtus	californicus	rt m1
32005	14	C2/L4	Rodentia	Cricetidae	Arvicolinae	Microtus	sp	lt m1
32006	14	C2/L4	Rodentia	Cricetidae	Arvicolinae	Microtus	californicus	lt m1
32007	14	C2/L4	Rodentia	Cricetidae	Arvicolinae	Microtus	sp	rt M1
32008	14	C2/L4	Rodentia	Cricetidae	Arvicolinae	Microtus	sp	partial rt m1
32009	14	C2/L4	Rodentia	Cricetidae	Arvicolinae	Microtus	sp	rt M1
32010	14	C2/L4	Rodentia	Cricetidae	Arvicolinae	Microtus	californicus	lt m1
32011	14	C2/L4	Rodentia	Cricetidae	Arvicolinae	Microtus	sp	rt m1
32012	14	C2/L4	Rodentia	Cricetidae	Arvicolinae	Microtus	sp	rt m1 frag
32013	14	C2/L4	Rodentia	Cricetidae	Arvicolinae	Microtus	sp	rt m1
32014	14	C2/L4	Rodentia	Cricetidae	Arvicolinae	Microtus	sp	rt m1
32015	14	C2/L4	Rodentia	Cricetidae	Arvicolinae	Microtus	sp	lt M1

32016	14	C2/L4	Rodentia	Cricetidae	Arvicolinae	Microtus	sp	lt M1
32017	14	C2/L4	Rodentia	Cricetidae	Arvicolinae	Microtus	sp	lt M1
32018	14	C2/L4	Rodentia	Cricetidae	Arvicolinae	Microtus	sp	lt M3
32019	14	C2/L4	Rodentia	Cricetidae	Arvicolinae	Microtus	sp	rt M2
32020	14	C2/L4	Rodentia	Cricetidae	Arvicolinae	Microtus	sp	lt M2
32021	14	C2/L4	Rodentia	Cricetidae	Arvicolinae	Microtus	sp	lt M1
32022	14	C2/L4	Rodentia	Cricetidae	Arvicolinae	Microtus	sp	rt M2
32023	14	C2/L4	Rodentia	Cricetidae	Arvicolinae	Microtus	sp	rt M3
32024	14	C2/L4	Rodentia	Cricetidae	Arvicolinae	Microtus	sp	lt M2
32025	14	C2/L4	Rodentia	Cricetidae	Arvicolinae	Microtus	sp	rt M2
32026	14	C2/L4	Rodentia	Cricetidae	Arvicolinae	Microtus	sp	rt M2
32027	14	C2/L4	Rodentia	Cricetidae	Arvicolinae	Microtus	sp	lt M2
32028	14	C2/L4	Rodentia	Cricetidae	Arvicolinae	Microtus	sp	rt m3
32029	14	C2/L4	Rodentia	Cricetidae	Arvicolinae	Microtus	sp	lt M2
32030	14	C2/L4	Rodentia	Cricetidae	Arvicolinae	Microtus	sp	lt M2
32031	14	C2/L4	Rodentia	Cricetidae	Arvicolinae	Microtus	sp	molar frag
32032	14	C2/L4	Rodentia	Cricetidae	Arvicolinae	Microtus	sp	rt m2
32033	14	C2/L4	Rodentia	Cricetidae	Arvicolinae	Microtus	sp	lt M2
32034	14	C2/L4	Rodentia	Cricetidae	Arvicolinae	Microtus	sp	lt m2
32035	14	C2/L4	Rodentia	Cricetidae	Arvicolinae	Microtus	sp	molar frag
32036	14	C2/L4	Rodentia	Cricetidae	Arvicolinae	Microtus	sp	rt m2
32037	14	C2/L4	Lagomorpha	Leporidae		Sylvilagus	sp	lower rt tooth
32038	14	C2/L4	Rodentia	Cricetidae	Arvicolinae	Microtus	sp	lt m1
32039	14	C2/L4	Rodentia	Cricetidae	Arvicolinae	Microtus	sp	molar frag
32040	14	C2/L4	Rodentia	Cricetidae	Arvicolinae	Microtus	sp	lt m2
32041	14	C2/L4	Rodentia	Cricetidae	Arvicolinae	Microtus	sp	molar frag
32042	14	C2/L4	Rodentia	Cricetidae	Arvicolinae	Microtus	sp	rt m3
32043	14	C2/L4	Rodentia	Cricetidae	Arvicolinae	Microtus	sp	rt M2
32044	14	C2/L4	Rodentia	Cricetidae	Arvicolinae	Microtus	sp	rt m3

32045	14	B2/L5	Lagomorpha	Leporidae		Sylvilagus	bachmani	lt dentary frag w/ p3
32046	14	C2/L3	Rodentia	Sciuridae	Xerinae	Otospermophilus	?beecheyi	partial rt maxilla w/ P4
32047	14	B2/L6	Lagomorpha	Leporidae		Sylvilagus	audubonii	rt dentary frag w/ p3-m1
32048	14	B2/L6	Rodentia	Sciuridae	Xerinae	Otospermophilus	?beecheyi	rt maxilla
32049	14	B2/L6	Rodentia	Sciuridae	Xerinae	Otospermophilus	?beecheyi	rt dentary
32050	14	D2/L6	Rodentia	Sciuridae	Xerinae	Otospermophilus	?beecheyi	lt dentary
33773	14	C2/L4	Rodentia	Cricetidae	Arvicolinae	Microtus	sp	lt dentary frag
33774	14	C2/L4	Rodentia	Cricetidae	Arvicolinae	Microtus	sp	lt dentary frag
33775	14	C2/L4	Rodentia	Cricetidae	Arvicolinae	Microtus	sp	lt m2
33776	14	C2/L4	Rodentia	Cricetidae	Arvicolinae	Microtus	sp	lt M2
33777	14	C2/L4	Rodentia	Cricetidae	Arvicolinae	Microtus	sp	rt m3
33778	14	C2/L4	Rodentia	Cricetidae	Arvicolinae	Microtus	sp	rt m3
33779	14	C2/L4	Rodentia	Cricetidae	Arvicolinae	Microtus	sp	rt m3
33780	14	C2/L4	Rodentia	Cricetidae	Arvicolinae	Microtus	sp	upper molar frag
33781	14	C2/L4	Rodentia	Cricetidae	Arvicolinae	Microtus	sp	molar frag
33782	14	C2/L4	Rodentia	Cricetidae	Arvicolinae	Microtus	sp	molar frag
33783	14	C2/L4	Rodentia	Cricetidae	Arvicolinae	Microtus	sp	molar frag
33784	14	C2/L4	Rodentia	Cricetidae	Neotominae	Peromyscus	sp	rt m1
33785	14	C2/L4	Rodentia	Heteromyidae	Dipodomyinae	Dipodomys	sp	lt dp4
33786	14	C2/L4	Rodentia	Cricetidae	Neotominae	?Peromyscus	sp	rt m1
33787	14	C2/L4	Rodentia	Cricetidae	Neotominae	Peromyscus	sp	lt m1
33788	14	C2/L4	Rodentia	Cricetidae	Neotominae			lt m2
33789	14	C2/L4	Rodentia	Cricetidae	Neotominae			lt m2
33790	14	C2/L4	Rodentia	Cricetidae	Neotominae			rt m2
33791	14	C2/L4	Rodentia	Cricetidae	Neotominae			rt m2
33792	14	C2/L4	Rodentia	Cricetidae	Neotominae	Peromyscus	sp	rt m1
33793	14	C2/L4	Rodentia	Cricetidae	Neotominae	Peromyscus	sp	rt M1
33794	14	C2/L4	Rodentia	Cricetidae	Neotominae			lt m2

33795	14	C2/L4	Rodentia	Cricetidae	Neotominae	Peromyscus	sp	lt m1
33796	14	C2/L4	Rodentia	Cricetidae	Neotominae			lt m2
33797	14	C2/L4	Rodentia	Cricetidae	Neotominae	Peromyscus	sp	lt m1
33798	14	C2/L4	Rodentia	Cricetidae	Neotominae			rt m2
33799	14	C2/L4	Rodentia	Cricetidae	Neotominae	Peromyscus	sp	rt M1
33800	14	C2/L4	Rodentia	Cricetidae	Neotominae	Peromyscus	sp	lt m1
33801	14	C2/L4	Rodentia	Cricetidae	Neotominae	cf Peromyscus	sp	lt dentary frag
33802	14	C2/L4	Rodentia	Cricetidae	Neotominae			lt dentary frag
33803	14	C2/L4	Rodentia	Cricetidae	Neotominae			rt dentary frag
33804	14	C2/L4	Rodentia	Cricetidae	Neotominae	cf Peromyscus	sp	rt anterior dentary
33805	14	C2/L4	Rodentia	Cricetidae	Neotominae			lt dentary
33806	14	C2/L4	Rodentia	Cricetidae	Neotominae			rt anterior dentary
33807	14	C2/L4	Rodentia	Cricetidae	Neotominae			rt anterior dentary
33808	14	C2/L4	Rodentia	Cricetidae	Neotominae			rt anterior dentary
33809	14	C2/L4	Rodentia	Cricetidae	Neotominae			lt anterior dentary
33810	14	C2/L4	Rodentia	Cricetidae	Neotominae			lt maxilla
33811	14	C2/L4	Rodentia	Cricetidae	Neotominae			rt anterior dentary
33812	14	C2/L4	Rodentia	Cricetidae	Neotominae			lt anterior dentary
33813	14	C2/L4	Rodentia	Cricetidae	Neotominae			rt dentary frag
33814	14	C2/L4	Rodentia	Cricetidae	Neotominae			lt dentary frag
33815	14	C2/L4	Rodentia	Cricetidae	Neotominae			rt dentary frag
33816	14	C2/L4	Rodentia	Cricetidae	Neotominae			rt dentary frag
33817	14	C2/L4	Rodentia	Cricetidae	Neotominae			lt maxilla frag
33818	14	C2/L4	Rodentia	Cricetidae	Neotominae			rt dentary frag
33819	14	C2/L4	Rodentia	Cricetidae	Neotominae			lt maxilla frag
33820	14	C2/L4	Rodentia	Cricetidae	Neotominae	Peromyscus	sp	lt m1

33821	14	C2/L4	Rodentia	Cricetidae	Neotominae			lt M2
33822	14	C2/L4	Rodentia	Cricetidae	Neotominae	Peromyscus	sp	rt M1
33824	14	C2/L4	Rodentia	Cricetidae	Neotominae	Peromyscus	cf californicus	lt M1
33825	14	C2/L4	Rodentia	Cricetidae	Neotominae	Peromyscus	sp	lt M1
33826	14	C2/L4	Rodentia	Cricetidae	Neotominae			rt M2
33827	14	C2/L4	Rodentia	Cricetidae	Neotominae			lt M1
33828	14	C2/L4	Rodentia	Cricetidae	Neotominae	Peromyscus	sp	rt M1
33829	14	C2/L4	Rodentia	Cricetidae	Neotominae			rt m2
33830	14	C2/L4	Rodentia	Cricetidae	Neotominae	Peromyscus	sp	lt m1
33831	14	C2/L4	Rodentia	Cricetidae	Neotominae			lt m2
33832	14	C2/L4	Rodentia	Cricetidae	Neotominae	Peromyscus	sp	lt m1
33833	14	C2/L4	Rodentia	Cricetidae	Neotominae	Peromyscus	sp	rt M1
33834	14	C2/L4	Rodentia	Cricetidae	Neotominae	Peromyscus	sp	lt M1
33835	14	C2/L4	Rodentia	Cricetidae	Neotominae			lt M2
33836	14	C2/L4	Rodentia	Cricetidae	Neotominae	?Peromyscus	sp	lt m1
33837	14	C2/L4	Rodentia	Cricetidae	Neotominae	Peromyscus	sp	rt m1
33838	14	C2/L4	Rodentia	Cricetidae	Neotominae	cf Peromyscus	cf californicus	rt maxilla
33839	14	C2/L4	Rodentia	Cricetidae	Neotominae	Peromyscus	sp	rt maxilla frag w/ M1
33840	14	C2/L4	Rodentia	Cricetidae	Neotominae			lt maxilla frag
33841	14	C2/L4	Rodentia	Cricetidae	Neotominae			lt maxilla frag
33842	14	C2/L4	Rodentia	Cricetidae	Neotominae			rt maxilla frag
33843	14	C2/L4	Rodentia	Cricetidae	Neotominae			lt maxilla
33844	14	C2/L4	Rodentia	Cricetidae	Neotominae			lt maxilla frag
33845	14	C2/L4	Rodentia	Cricetidae	Neotominae			lt maxilla frag
33846	14	C2/L4	Rodentia	Cricetidae	Neotominae			lt M2
33847	14	C2/L4	Rodentia	Cricetidae	Neotominae	?Peromyscus	sp	rt m1
33848	14	C2/L4	Rodentia	Cricetidae	Neotominae	Peromyscus	sp	rt M1
33849	14	C2/L4	Rodentia	Cricetidae	Neotominae			rt M2

33850	14	C2/L4	Rodentia	Cricetidae	Neotominae	?Peromyscus	sp	rt M1
33851	14	C2/L4	Rodentia	Cricetidae	Neotominae			rt m2
33852	14	C2/L4	Rodentia	Cricetidae	Neotominae			lt M2
33853	14	C2/L4	Rodentia	Cricetidae	Neotominae			lt maxilla
33854	14	C2/L4	Rodentia	Cricetidae	Neotominae			molar frag
33855	14	C2/L4	Rodentia	Cricetidae	Neotominae			rt M2
33856	14	C2/L4	Rodentia	Cricetidae	Neotominae			molar frag
33857	14	C2/L4	Rodentia	Cricetidae	Neotominae			molar
33858	14	C2/L4	Rodentia	Cricetidae	Neotominae	?Peromyscus	sp	rt M2
33859	14	C2/L4	Lagomorpha	Leporidae		Sylvilagus	sp	upper rt tooth
33860	14	C2/L4	Lagomorpha	Leporidae		Sylvilagus	audubonii	rt p3
33861	14	C2/L4	Lagomorpha	Leporidae		Sylvilagus	bachmani	lt p3
33862	14	C2/L4	Lagomorpha	Leporidae		Sylvilagus	sp	upper lt tooth
33863	14	C2/L4	Lagomorpha	Leporidae		Sylvilagus	sp	upper rt tooth
33864	14	C2/L4	Lagomorpha	Leporidae		Sylvilagus	sp	upper rt tooth
33865	14	C2/L4	Lagomorpha	Leporidae		Sylvilagus	sp	upper rt tooth
33866	14	C2/L4	Lagomorpha	Leporidae		Sylvilagus	sp	upper lt tooth
33867	14	C2/L4	Lagomorpha	Leporidae		Sylvilagus	sp	upper tooth
33868	14	C2/L4	Lagomorpha	Leporidae		Sylvilagus	sp	lower lt tooth
33869	14	C2/L4	Lagomorpha	Leporidae		Sylvilagus	sp	rt P2
33870	14	C2/L4	Lagomorpha	Leporidae		Sylvilagus	sp	partial rt P2
33871	14	C2/L4	Lagomorpha	Leporidae		Sylvilagus	sp	upper lt tooth
33872	14	C2/L4	Lagomorpha	Leporidae		Sylvilagus	sp	upper rt tooth
33873	14	C2/L4	Lagomorpha	Leporidae		Sylvilagus	sp	upper rt tooth
33874	14	C2/L4	Lagomorpha	Leporidae		Sylvilagus	sp	upper rt tooth
33875	14	C2/L4	Lagomorpha	Leporidae		Sylvilagus	sp	lower rt tooth
33876	14	C2/L4	Lagomorpha	Leporidae		?Sylvilagus	sp	M3
33877	14	C2/L4	Lagomorpha	Leporidae		Sylvilagus	sp	lt dentary frag
33878	14	C2/L4	Lagomorpha	Leporidae		Sylvilagus	sp	lt P2
33879	14	C2/L4	Lagomorpha	Leporidae		Sylvilagus	sp	upper lt tooth

33880	14	C2/L4	Lagomorpha	Leporidae		Sylvilagus	sp	rt? P2
33881	14	C2/L4	Lagomorpha	Leporidae		Sylvilagus	sp	partial upper rt tooth
33882	14	C2/L4	Lagomorpha	Leporidae		Sylvilagus	sp	partial upper rt tooth
33883	14	C2/L4	Lagomorpha	Leporidae		Sylvilagus	sp	lt maxilla
33884	14	C2/L4	Lagomorpha	Leporidae		Sylvilagus	sp	rt dentary frag w/ p4-m1
33885	14	C2/L4	Lagomorpha	Leporidae		Sylvilagus	sp	lt maxilla w/ P4, M2
33886	14	C2/L4	Lagomorpha	Leporidae		Sylvilagus	sp	lower tooth frag
33887	14	C2/L4	Lagomorpha	Leporidae		Sylvilagus	sp	lt maxilla
33888	14	C2/L4	Lagomorpha	Leporidae		Sylvilagus	sp	P2
33889	14	C2/L4	Lagomorpha	Leporidae		?Sylvilagus	sp	m3
33890	14	C2/L4	Lagomorpha	Leporidae		Sylvilagus	sp	upper tooth
33891	14	C2/L4	Lagomorpha	Leporidae		?Sylvilagus	sp	M3
33892	14	C2/L4	Rodentia	Geomyidae	Thomomyinae	Thomomys	sp	rt m1/m2
33893	14	C2/L4	Rodentia	Geomyidae	Thomomyinae	Thomomys	sp	rt m1/m2
33894	14	C2/L4	Rodentia	Geomyidae	Thomomyinae	Thomomys	?bottae	rt p4
33895	14	C2/L4	Rodentia	Geomyidae	Thomomyinae	Thomomys	sp	lt M1/M2
33896	14	C2/L4	Rodentia	Geomyidae	Thomomyinae	Thomomys	sp	partial rt p4
33897	14	C2/L4	Rodentia	Geomyidae	Thomomyinae	Thomomys	sp	rt m1/m2
33898	14	C2/L4	Rodentia	Geomyidae	Thomomyinae	?Thomomys	sp	tooth
33899	14	C2/L4	Rodentia	Geomyidae	Thomomyinae	?Thomomys	sp	partial tooth
33900	14	C2/L4	Rodentia	Geomyidae	Thomomyinae	Thomomys	sp	lt M1/M2
33901	14	C2/L4	Rodentia	Geomyidae	Thomomyinae	Thomomys	sp	rt m1/m2
33902	14	C2/L4	Rodentia	Geomyidae	Thomomyinae	Thomomys	sp	rt? M3
33909	14	C2/L4	Rodentia	Heteromyidae	Dipodomyinae	Dipodomys	sp	lt? p4
33915	14	C2/L4	Rodentia	Geomyidae	Thomomyinae	Thomomys	sp	partial M3/m3
33922	14	C2/L4	Rodentia	Cricetidae	Neotominae	Neotoma	sp	rt m1
33923	14	C2/L4	Rodentia	Cricetidae	Neotominae	Neotoma	sp	lt M1
33926	14	C2/L4	Rodentia	Heteromyidae	Perognathinae			rt P4

33927	14	C2/L4	Rodentia	Heteromyidae	Perognathinae			rt P4
33928	14	C2/L4	Rodentia	Heteromyidae	Perognathinae			rt M1/M2
33929	14	C2/L4	Lagomorpha	Leporidae		Sylvilagus	sp	tooth frag
33930	14	C2/L4	Lagomorpha	Leporidae		?Sylvilagus	sp	tooth frag
33931	14	C2/L4	Lagomorpha	Leporidae		Sylvilagus	sp	tooth frag
33932	14	C2/L4	Lagomorpha	Leporidae		?Sylvilagus	sp	upper tooth frag
33933	14	C2/L4	Rodentia	Sciuridae	Xerinae	Otospermophilus	?beecheyi	lt m1/m2
33934	14	C2/L4	Rodentia	Sciuridae	Xerinae	Otospermophilus	?beecheyi	lt M1/M2
33935	14	C2/L4	Rodentia	Sciuridae	Xerinae	Otospermophilus	?beecheyi	lt p4
33936	14	C2/L4	Rodentia	Sciuridae	Xerinae	Otospermophilus	?beecheyi	lt p4
33937	14	C2/L4	Rodentia	Sciuridae	Xerinae	Otospermophilus	?beecheyi	lt M1/M2
33938	14	C2/L4	Rodentia	Sciuridae	Xerinae	Otospermophilus	?beecheyi	partial lt m3
33939	14	C2/L4	Rodentia	Sciuridae	Xerinae	Otospermophilus	?beecheyi	lt P4
33940	14	C2/L4	Rodentia	Sciuridae	Xerinae	Otospermophilus	?beecheyi	lt M1/M2 frag
33941	14	C2/L4	Rodentia	Sciuridae	Xerinae			lower tooth frag
33942	14	C2/L4	Eulipotyphla	Soricidae	Soricinae			lt maxilla frag
33943	14	C2/L4	Eulipotyphla	Soricidae	Soricinae	Sorex	sp	lt dentary
33944	14	C2/L4	Eulipotyphla	Soricidae	Soricinae	Sorex	sp	partial rt dentary
33945	14	C2/L4	Eulipotyphla	Soricidae	Soricinae	Sorex	sp	partial lt dentary
33946	14	C2/L4	Eulipotyphla	Soricidae	Soricinae	Sorex	sp	lt dentary
33948	14	C2/L4	Lagomorpha	Leporidae		?Sylvilagus	sp	upper tooth frag
33949	14	C2/L4	Lagomorpha	Leporidae		?Sylvilagus	sp	tooth frag
33950	14	C2/L4	Rodentia	Cricetidae	Arvicolinae	?Microtus	sp	tooth frag
33951	14	C2/L4	Rodentia	Cricetidae	Neotominae			rt dentary frag
33952	14	C2/L4	Rodentia	Cricetidae	Neotominae			lt dentary frag
33953	14	C3/L6	Rodentia	Cricetidae	Arvicolinae	Microtus	sp	lt M1
33954	14	C3/L6	Rodentia	Cricetidae	Arvicolinae	Microtus	sp	lt M2
33955	14	C3/L6	Rodentia	Cricetidae	Arvicolinae	Microtus	sp	lt M1
33956	14	C3/L6	Rodentia	Cricetidae	Arvicolinae	Microtus	californicus	lt m1

33957	14	C3/L6	Rodentia	Cricetidae	Arvicolinae	Microtus	sp	rt M2
33958	14	C3/L6	Rodentia	Cricetidae	Arvicolinae	Microtus	sp	tooth frag
33959	14	C3/L6	Rodentia	Cricetidae	Arvicolinae	Microtus	sp	lt M1
33960	14	C3/L6	Rodentia	Cricetidae	Arvicolinae	Microtus	sp	lt M1
33961	14	C3/L6	Rodentia	Cricetidae	Arvicolinae	Microtus	sp	rt M2
33962	14	C3/L6	Lagomorpha	Leporidae		Sylvilagus	audubonii	rt p3
33963	14	C3/L6	Lagomorpha	Leporidae		Sylvilagus	sp	lower rt tooth
33964	14	C3/L6	Lagomorpha	Leporidae		Sylvilagus	sp	partial upper tooth
33965	14	C3/L6	Lagomorpha	Leporidae		?Sylvilagus	sp	tooth frag
33966	14	C3/L6	Lagomorpha	Leporidae		?Sylvilagus	sp	partial tooth
33967	14	C3/L6	Lagomorpha	Leporidae		Sylvilagus	sp	upper lt tooth
33968	14	C3/L6	Lagomorpha	Leporidae		Sylvilagus	sp	upper rt tooth
33969	14	C3/L6	Lagomorpha	Leporidae		Sylvilagus	sp	upper rt tooth
33970	14	C3/L6	Lagomorpha	Leporidae		Sylvilagus	sp	rt p3
33971	14	C3/L6	Lagomorpha	Leporidae		Sylvilagus	sp	lower rt tooth
33972	14	C3/L6	Lagomorpha	Leporidae		Sylvilagus	sp	lower rt tooth
33973	14	C3/L6	Lagomorpha	Leporidae		Sylvilagus	sp	lower rt tooth
33974	14	C3/L6	Lagomorpha	Leporidae		Sylvilagus	sp	upper lt tooth
33975	14	C3/L6	Lagomorpha	Leporidae		?Sylvilagus	sp	tooth frag
33976	14	C3/L6	Lagomorpha	Leporidae		Sylvilagus	sp	rt dentary frag
33977	14	C3/L6	Lagomorpha	Leporidae		Sylvilagus	sp	upper lt tooth
33978	14	C3/L6	Lagomorpha	Leporidae		Sylvilagus	sp	upper lt tooth
33979	14	C3/L6	Lagomorpha	Leporidae		Sylvilagus	sp	lower tooth frag
33980	14	C3/L6	Lagomorpha	Leporidae		Sylvilagus	sp	lower rt tooth
33981	14	C3/L6	Lagomorpha	Leporidae		?Sylvilagus	sp	upper tooth frag
33982	14	C3/L6	Lagomorpha	Leporidae		Sylvilagus	sp	upper rt tooth frag
33983	14	C3/L6	Lagomorpha	Leporidae		?Sylvilagus	sp	lower lt tooth frag
33984	14	C3/L6	Lagomorpha	Leporidae		Sylvilagus	sp	lower rt tooth frag

33986	14	C3/L6	Lagomorpha	Leporidae		Sylvilagus	sp	upper tooth frag
33987	14	C3/L6	Lagomorpha	Leporidae		Sylvilagus	sp	upper tooth frag
33989	14	C3/L6	Lagomorpha	Leporidae		?Sylvilagus	sp	tooth frag
33990	14	C3/L6	Lagomorpha	Leporidae		Sylvilagus	sp	upper tooth frag
33991	14	C3/L6	Lagomorpha	Leporidae		?Sylvilagus	sp	tooth frag
33992	14	C3/L6	Lagomorpha	Leporidae		?Sylvilagus	sp	tooth frag
33993	14	C3/L6	Lagomorpha	Leporidae		?Sylvilagus	sp	tooth frag
33995	14	C3/L6	Lagomorpha	Leporidae		?Sylvilagus	sp	tooth frag
33996	14	C3/L6	Lagomorpha	Leporidae		?Sylvilagus	sp	tooth frag
33997	14	C3/L6	Lagomorpha	Leporidae		?Sylvilagus	sp	tooth frag
33998	14	C3/L6	Lagomorpha	Leporidae		?Sylvilagus	sp	tooth frag
33999	14	C3/L6	Lagomorpha	Leporidae		?Sylvilagus	sp	tooth frag
34007	14	C3/L6	Rodentia	Cricetidae	Arvicolinae	Microtus	sp	lt M1
34008	14	C3/L6	Rodentia	Cricetidae	Arvicolinae	Microtus	sp	rt m1 frag
34009	14	C3/L6	Rodentia	Cricetidae	Arvicolinae	Microtus	sp	lt M1
34010	14	C3/L6	Rodentia	Cricetidae	Arvicolinae	Microtus	sp	molar frag
34011	14	C3/L6	Rodentia	Cricetidae	Arvicolinae	Microtus	sp	rt M2
34012	14	C3/L6	Rodentia	Cricetidae	Arvicolinae	Microtus	sp	rt M1
34013	14	C3/L6	Rodentia	Cricetidae	Arvicolinae	Microtus	sp	lt M3 frag
34014	14	C3/L6	Rodentia	Cricetidae	Arvicolinae	Microtus	sp	upper palate
34015	14	C3/L6	Rodentia	Cricetidae	Arvicolinae	Microtus	sp	rt dentary frag w/ i1
34016	14	C3/L6	Rodentia	Cricetidae	Arvicolinae	Microtus	sp	molar frag
34017	14	C3/L6	Rodentia	Cricetidae	Arvicolinae	Microtus	sp	rt m2
34018	14	C3/L6	Rodentia	Sciuridae	Xerinae	Otospermophilus	?beecheyi	rt m1/m2
34019	14	C3/L6	Rodentia	Sciuridae	Xerinae	Otospermophilus	?beecheyi	rt M1/M2
34020	14	C3/L6	Rodentia	Sciuridae	Xerinae	Otospermophilus	?beecheyi	lower tooth frag
34021	14	C3/L6	Rodentia	Sciuridae	Xerinae	Otospermophilus	?beecheyi	lt p4
34022	14	C3/L6	Rodentia	Sciuridae	Xerinae	Otospermophilus	?beecheyi	rt M1/M2
34023	14	C3/L6	Rodentia	Sciuridae	Xerinae	Otospermophilus	?beecheyi	upper tooth frag

34024	14	C3/L6	Rodentia	Sciuridae	Xerinae	Otospermophilus	?beecheyi	lower tooth frag
34025	14	C3/L6	Rodentia	Cricetidae	Neotominae	cf Peromyscus	sp	rt dentary
34026	14	C3/L6	Rodentia	Cricetidae	Neotominae	cf Peromyscus	sp	lt dentary w/ i1
34027	14	C3/L6	Rodentia	Cricetidae	Neotominae	Peromyscus	sp	rt M1
34028	14	C3/L6	Rodentia	Cricetidae	Neotominae	Peromyscus	sp	lt m1
34029	14	C3/L6	Rodentia	Cricetidae	Neotominae	Peromyscus	sp	rt M1
34030	14	C3/L6	Rodentia	Cricetidae	Neotominae	Peromyscus	cf maniculatus	rt m1
34031	14	C3/L6	Rodentia	Cricetidae	Neotominae			lt dentary frag
34032	14	C3/L6	Rodentia	Cricetidae	Neotominae			lt M1
34033	14	C3/L6	Rodentia	Cricetidae	Neotominae			rt m2
34034	14	C3/L6	Rodentia	Cricetidae	Neotominae	?Peromyscus	sp	partial lt m1
34035	14	C3/L6	Rodentia	Cricetidae	Neotominae	Peromyscus	sp	rt M1
34036	14	C3/L6	Rodentia	Cricetidae	Arvicolinae	Microtus	sp	molar frag
34037	14	C3/L6	Rodentia	Cricetidae	Arvicolinae	Microtus	sp	molar frag
34038	14	C3/L6	Rodentia	Cricetidae	Arvicolinae	Microtus	sp	molar frag
34039	14	C3/L6	Rodentia	Cricetidae	Arvicolinae	Microtus	sp	rt m3
34040	14	C3/L6	Rodentia	Cricetidae	Arvicolinae	Microtus	sp	lt m3 frag
34041	14	C3/L6	Rodentia	Cricetidae	Arvicolinae	cf Microtus	sp	rt dentary frag
34042	14	C3/L6	Rodentia	Cricetidae	Arvicolinae	cf Microtus	sp	lt dentary frag w/ i1
34043	14	C3/L6	Rodentia	Cricetidae	Arvicolinae	Microtus	sp	lt m1 frag
34044	14	C3/L6	Carnivora	Mustelidae	Mustelinae	Mustela	frenata	C1
34045	14	C3/L6	Carnivora	Mustelidae	Mustelinae	Mustela	frenata	rt M1
34047	14	C3/L6	Carnivora	Mustelidae	Mustelinae	?Mustela	frenata	m2?
34048	14	C3/L6	Rodentia	Cricetidae	Neotominae	?Neotoma	sp	broken molar
34049	14	C3/L6	Lagomorpha	Leporidae		?Sylvilagus	sp	tooth frag
34053	14	B3/L3	Rodentia	Cricetidae	Neotominae	Peromyscus	sp	lt m1
34054	14	B3/L3	Rodentia	Cricetidae	Neotominae	?Peromyscus	sp	lt m1
34055	14	B3/L3	Rodentia	Cricetidae	Neotominae			lt M2
34056	14	B3/L3	Rodentia	Cricetidae	Neotominae			lt m2

34057	14	B3/L3	Rodentia	Cricetidae	Neotominae			rt m2
34058	14	B3/L3	Rodentia	Cricetidae	Neotominae			lt m2
34059	14	B3/L3	Rodentia	Cricetidae	Neotominae			rt m2
34060	14	B3/L3	Rodentia	Cricetidae	Neotominae			lt m1
34061	14	B3/L3	Rodentia	Cricetidae	Neotominae			rt dentary frag
34062	14	B3/L3	Rodentia	Heteromyidae	Dipodomyinae	Dipodomys	sp	upper molar
34063	14	B3/L3	Rodentia	Heteromyidae	Dipodomyinae	Dipodomys	sp	molar
34064	14	B3/L3	Rodentia	Heteromyidae	Dipodomyinae	Dipodomys	sp	lower molar
34065	14	B3/L3	Rodentia	Heteromyidae	Dipodomyinae	Dipodomys	sp	upper molar
34066	14	B3/L3	Rodentia	Heteromyidae	Dipodomyinae	Dipodomys	sp	lower molar
34072	14	B3/L3	Rodentia	Cricetidae	Arvicolinae	Microtus	sp	lt M3
34073	14	B3/L3	Rodentia	Cricetidae	Arvicolinae	Microtus	sp	lt m3
34074	14	B3/L3	Rodentia	Sciuridae	Xerinae	Otospermophilus	?beecheyi	lt p4
34075	14	C2/L2	Lagomorpha	Leporidae		Sylvilagus	sp	upper rt tooth
34076	14	C2/L2	Lagomorpha	Leporidae		Sylvilagus	sp	upper lt tooth
34077	14	C2/L2	Rodentia	Cricetidae	Arvicolinae	Microtus	sp	lt m1
34078	14	C2/L2	Rodentia	Cricetidae	Arvicolinae	Microtus	sp	lt m1
34079	14	C2/L2	Rodentia	Cricetidae	Arvicolinae	Microtus	sp	rt m1
34080	14	C2/L2	Rodentia	Cricetidae	Arvicolinae	Microtus	sp	rt m1
34081	14	C2/L2	Rodentia	Cricetidae	Arvicolinae	Microtus	sp	lt M3
34082	14	C2/L2	Rodentia	Cricetidae	Arvicolinae	Microtus	sp	lt M2
34083	14	C2/L2	Rodentia	Cricetidae	Arvicolinae	Microtus	sp	rt M2
34084	14	C2/L2	Rodentia	Cricetidae	Arvicolinae	Microtus	sp	lt M2
34085	14	C2/L2	Rodentia	Cricetidae	Arvicolinae	Microtus	sp	lt M1
34086	14	C2/L2	Rodentia	Cricetidae	Arvicolinae	Microtus	sp	m1/m2 frag
34087	14	C2/L2	Rodentia	Cricetidae	Arvicolinae	Microtus	sp	rt m2
34088	14	C2/L2	Rodentia	Cricetidae	Neotominae	Neotoma	sp	rt M1
34089	14	C2/L2	Rodentia	Geomyidae	Thomomyinae	Thomomys	sp	lt m1/m2
34091	14	C2/L2	Rodentia	Cricetidae	Neotominae	Peromyscus	cf maniculatus	rt m1

34092	14	C2/L2	Rodentia	Cricetidae	Neotominae	Peromyscus	sp	rt M1
34093	14	C2/L2	Rodentia	Cricetidae	Neotominae	Peromyscus	sp	rt m1
34094	14	C2/L2	Rodentia	Cricetidae	Neotominae	Peromyscus	sp	rt m1
34095	14	C2/L2	Rodentia	Cricetidae	Neotominae			rt m2
34096	14	C2/L2	Rodentia	Cricetidae	Neotominae			rt m2
34097	14	C2/L2	Rodentia	Cricetidae	Neotominae	Peromyscus	sp	lt M1
34098	14	C2/L2	Rodentia	Cricetidae	Neotominae			partial rt dentary
34100	14	C2/L2	Rodentia	Cricetidae	Neotominae			lt M2
34102	14	D3/L6	Rodentia	Cricetidae	Arvicolinae	Microtus	sp	molar frag
34103	14	D3/L6	Rodentia	Cricetidae	Arvicolinae	Microtus	sp	molar frag
34104	14	D3/L6	Rodentia	Cricetidae	Arvicolinae	Microtus	sp	lt m3
34105	14	D3/L6	Rodentia	Cricetidae	Neotominae	Peromyscus	sp	lt m1
34106	14	D3/L6	Rodentia	Cricetidae	Neotominae	?Peromyscus	sp	partial rt m1
34107	14	D3/L6	Rodentia	Cricetidae	Neotominae	Neotoma	sp	rt M3
34108	14	D3/L6	Rodentia	Cricetidae	Neotominae			maxilla frag
34109	14	D3/L6	Rodentia	Cricetidae	Neotominae			molar frag
34110	14	D3/L6	Rodentia	Cricetidae	Neotominae	Peromyscus	sp	rt m1
34111	14	D3/L6	Lagomorpha	Leporidae		Sylvilagus	sp	upper lt tooth
34112	14	D3/L6	Lagomorpha	Leporidae		Sylvilagus	sp	partial upper tooth
34113	14	D3/L6	Lagomorpha	Leporidae		Sylvilagus	sp	upper lt tooth
34114	14	D3/L6	Lagomorpha	Leporidae		Sylvilagus	sp	upper rt tooth
34115	14	D3/L6	Lagomorpha	Leporidae		Sylvilagus	sp	upper rt tooth
34116	14	D3/L6	Lagomorpha	Leporidae		Sylvilagus	sp	partial lower lt tooth
34117	14	D3/L6	Lagomorpha	Leporidae		Sylvilagus	audubonii	rt p3
34118	14	D3/L6	Rodentia	Heteromyidae	Dipodomyinae	Dipodomys	sp	rt? m1/m2
34119	14	D3/L6	Rodentia	Heteromyidae	Dipodomyinae	Dipodomys	sp	rt m1/m2
34122	14	D3/L6	Rodentia	?Heteromyidae	Dipodomyinae	?Dipodomys	sp	tooth, p4?
34128	14	D3/L6	Rodentia	Sciuridae	Xerinae	Neotamias/Tamias	sp	lower tooth frag

34129	14	D3/L6	Rodentia	Sciuridae	Xerinae	Otospermophilus	?beecheyi	rt m1/m2
34130	14	D3/L6	Rodentia	Sciuridae	Xerinae	Otospermophilus	?beecheyi	rt m1/m2
34131	14	D3/L6	Rodentia	Sciuridae	Xerinae	Otospermophilus	?beecheyi	rt m1/m2 frag
34132	14	D3/L6	Rodentia	Sciuridae	Xerinae	Otospermophilus	?beecheyi	rt M1/M2 frag
34133	14	D3/L6	Rodentia	Sciuridae	Xerinae			lower tooth frag
34136	14	B2/L6	Lagomorpha	Leporidae		Sylvilagus	sp	upper lt tooth
34137	14	B2/L6	Lagomorpha	Leporidae		Sylvilagus	sp	upper rt tooth
34138	14	B2/L6	Lagomorpha	Leporidae		Sylvilagus	sp	partial upper rt tooth
34139	14	B2/L6	Lagomorpha	Leporidae		Sylvilagus	sp	lower rt tooth
34140	14	B2/L6	Lagomorpha	Leporidae		Sylvilagus	sp	lower rt tooth
34141	14	B2/L6	Lagomorpha	Leporidae		Sylvilagus	sp	lower lt tooth
34142	14	B2/L6	Lagomorpha	Leporidae		Sylvilagus	sp	lt P2
34143	14	B2/L6	Lagomorpha	Leporidae		Sylvilagus	sp	upper lt tooth
34144	14	B2/L6	Lagomorpha	Leporidae		Sylvilagus	sp	upper rt? tooth
34145	14	B2/L6	Lagomorpha	Leporidae		Sylvilagus	sp	lower lt tooth
34146	14	B2/L6	Lagomorpha	Leporidae		Sylvilagus	sp	upper rt tooth
34147	14	B2/L6	Lagomorpha	Leporidae		Sylvilagus	sp	upper rt tooth
34148	14	B2/L6	Lagomorpha	Leporidae		Sylvilagus	sp	partial upper tooth
34149	14	B2/L6	Lagomorpha	Leporidae		Sylvilagus	sp	upper tooth
34150	14	B2/L6	Lagomorpha	Leporidae		Sylvilagus	sp	rt dentary frag w/ p4-m2
34151	14	B2/L6	Lagomorpha	Leporidae		Sylvilagus	sp	rt maxilla w/ P3-M2
34152	14	B2/L6	Lagomorpha	Leporidae		Sylvilagus	sp	lt maxilla frag w/ cheek tooth
34153	14	B2/L6	Lagomorpha	Leporidae		Sylvilagus	sp	lt dentary frag
34154	14	B2/L6	Lagomorpha	Leporidae		Sylvilagus	sp	lower rt tooth
34155	14	B2/L6	Lagomorpha	Leporidae		Sylvilagus	sp	lower lt p3
34156	14	B2/L6	Lagomorpha	Leporidae		Sylvilagus	sp	lower lt tooth
34157	14	B2/L6	Lagomorpha	Leporidae		Sylvilagus	sp	lower lt tooth

34158	14	B2/L6	Lagomorpha	Leporidae		Sylvilagus	sp	lower rt tooth
34159	14	B2/L6	Lagomorpha	Leporidae		Sylvilagus	sp	m3
34160	14	B2/L6	Lagomorpha	Leporidae		Sylvilagus	sp	upper rt tooth
34161	14	B2/L6	Lagomorpha	Leporidae		Sylvilagus	sp	lt P2
34162	14	B2/L6	Lagomorpha	Leporidae		Sylvilagus	sp	m3
34163	14	B2/L6	Lagomorpha	Leporidae		Sylvilagus	sp	upper tooth frag
34164	14	B2/L6	Lagomorpha	Leporidae		Sylvilagus	sp	upper rt maxilla
34165	14	B2/L6	Lagomorpha	Leporidae		Sylvilagus	sp	lt dentary frag
34166	14	B2/L6	Lagomorpha	Leporidae		Sylvilagus	sp	lt dentary frag
34167	14	B2/L6	Rodentia	Cricetidae	Neotominae	Neotoma	sp	lt m2
34168	14	B2/L6	Rodentia	Cricetidae	Neotominae	Neotoma	sp	lt m1
34169	14	B2/L6	Rodentia	Cricetidae	Neotominae	Neotoma	sp	rt M3
34170	14	B2/L6	Rodentia	Sciuridae	Xerinae	Otospermophilus	?beecheyi	rt M1/M2
34171	14	B2/L6	Rodentia	Sciuridae	Xerinae	Otospermophilus	?beecheyi	lt m1/m2
34173	14	B2/L6	Eulipotyphla	Soricidae	Soricinae			partial rt dentary
34174	14	B2/L6	Rodentia	Cricetidae	Arvicolinae	Microtus	sp	lt m1
34175	14	B2/L6	Rodentia	Cricetidae	Arvicolinae	Microtus	californicus	lt m1
34176	14	B2/L6	Rodentia	Cricetidae	Arvicolinae	Microtus	sp	partial rt m1
34177	14	B2/L6	Rodentia	Cricetidae	Arvicolinae	Microtus	californicus	rt m1
34178	14	B2/L6	Rodentia	Cricetidae	Arvicolinae	Microtus	sp	lt m1
34179	14	B2/L6	Rodentia	Cricetidae	Arvicolinae	Microtus	sp	lt m1 frag
34180	14	B2/L6	Rodentia	Cricetidae	Arvicolinae	Microtus	sp	rt M1
34181	14	B2/L6	Rodentia	Cricetidae	Arvicolinae	Microtus	sp	rt M3
34182	14	B2/L6	Rodentia	Cricetidae	Arvicolinae	Microtus	sp	rt m2
34183	14	B2/L6	Rodentia	Cricetidae	Arvicolinae	Microtus	sp	lt M1
34184	14	B2/L6	Rodentia	Cricetidae	Arvicolinae	Microtus	sp	rt m2
34185	14	B2/L6	Rodentia	Cricetidae	Arvicolinae	Microtus	sp	lt M1
34186	14	B2/L6	Rodentia	Cricetidae	Arvicolinae	Microtus	sp	lt dentary frag
34187	14	B2/L6	Rodentia	Cricetidae	Arvicolinae	Microtus	sp	lt dentary frag

34188	14	B2/L6	Rodentia	Cricetidae	Arvicolinae	Microtus	sp	lt m2
34189	14	B2/L6	Rodentia	Cricetidae	Arvicolinae	Microtus	sp	partial lt M1
34190	14	B2/L6	Rodentia	Cricetidae	Arvicolinae	Microtus	sp	partial rt dentary w/ i1
34191	14	B2/L6	Rodentia	Heteromyidae	Dipodomyinae	Dipodomys	sp	rt? m1/m2
34192	14	B2/L6	Rodentia	Heteromyidae	Dipodomyinae	Dipodomys	sp	lt? p4
34194	14	B2/L6	Rodentia	Heteromyidae	Dipodomyinae	Dipodomys	sp	molar
34197	14	B2/L6	Rodentia	Heteromyidae	Dipodomyinae	Dipodomys	sp	rt? molar
34198	14	B2/L6	Rodentia	Heteromyidae	Dipodomyinae	Dipodomys	sp	rt? M1/M2
34200	14	B2/L6	Rodentia	Heteromyidae	Dipodomyinae	Dipodomys	sp	molar
34201	14	B2/L6	Rodentia	Heteromyidae	Dipodomyinae	Dipodomys	sp	m1/m2
34202	14	B2/L6	Rodentia	Geomyidae	Thomomyinae	Thomomys	sp	rt m1/m2
34204	14	B2/L6	Rodentia	Cricetidae	Neotominae	Peromyscus	sp	lt m1
34205	14	B2/L6	Rodentia	Cricetidae	Neotominae			partial rt m1
34206	14	B2/L6	Rodentia	Cricetidae	Neotominae	?Peromyscus	sp	lt M1
34207	14	B2/L6	Rodentia	Cricetidae	Neotominae			rt m2
34208	14	B2/L6	Rodentia	Cricetidae	Neotominae			lt M2
34209	14	B2/L6	Rodentia	Cricetidae	Neotominae			rt dentary
34210	14	B2/L6	Rodentia	Cricetidae	Neotominae			rt dentary frag
34211	14	B2/L6	Rodentia	Cricetidae	Neotominae			maxilla frag
34212	14	B2/L6	Rodentia	Cricetidae	Neotominae			lt maxilla frag
34213	14	B2/L6	Rodentia	Cricetidae	Neotominae	cf Peromyscus	sp	lt dentary w/ i1
34214	14	B2/L6	Rodentia	Cricetidae	Neotominae			lt dentary w/ i1
34215	14	B2/L6	Rodentia	Cricetidae	Neotominae	Peromyscus	cf californicus	lt m1
34216	14	B2/L6	Rodentia	Cricetidae	Neotominae	Peromyscus	sp	lt M1
34217	14	B2/L6	Rodentia	Cricetidae	Neotominae			rt M2
34218	14	B2/L6	Rodentia	Cricetidae	?Neotominae			tooth frag
34219	14	B2/L6	Rodentia	Cricetidae	?Neotominae			molar
34223	14	C3/L6	Rodentia	Cricetidae	Arvicolinae	Microtus	sp	lt dentary frag
34225	14	B3/L6	Lagomorpha	Leporidae		?Sylvilagus	sp	tooth frag

34229	14	B3/L6	Rodentia	Cricetidae	Arvicolinae	Microtus	sp	partial lt m1
34230	14	B3/L6	Rodentia	Cricetidae	Arvicolinae	Microtus	sp	rt m1
34231	14	B3/L6	Rodentia	Cricetidae	Arvicolinae	Microtus	sp	rt m1
34232	14	B3/L6	Rodentia	Cricetidae	Arvicolinae	Microtus	sp	rt m1
34233	14	B3/L6	Rodentia	Cricetidae	Arvicolinae	Microtus	sp	partial rt m1
34234	14	B3/L6	Rodentia	Cricetidae	Arvicolinae	Microtus	sp	rt m2
34235	14	B3/L6	Rodentia	Cricetidae	Arvicolinae	Microtus	sp	lt dentary
34236	14	B3/L6	Rodentia	Cricetidae	Arvicolinae	Microtus	sp	rt m2
34237	14	B3/L6	Rodentia	Cricetidae	Arvicolinae	cf Microtus	sp	rt dentary frag
34238	14	B3/L6	Rodentia	Heteromyidae	Dipodomyinae	Dipodomys	sp	lt p4
34239	14	B3/L6	Rodentia	Heteromyidae	Dipodomyinae	Dipodomys	sp	lt? m1/m2
34240	14	B3/L6	Rodentia	Heteromyidae	Dipodomyinae	Dipodomys	sp	rt? m1/m2
34241	14	B3/L6	Rodentia	Heteromyidae	Dipodomyinae	Dipodomys	sp	rt? m1/m2
34242	14	B3/L6	Rodentia	Geomyidae	Thomomyinae	Thomomys	sp	rt m1/m2
34243	14	B3/L6	Rodentia	Heteromyidae	Dipodomyinae	Dipodomys	sp	rt? M1/M2
34244	14	B3/L6	Rodentia	Heteromyidae	Dipodomyinae	?Dipodomys	sp	partial P4
34245	14	B3/L6	Rodentia	Heteromyidae	Dipodomyinae	Dipodomys	sp	lt m1/m2
34247	14	B3/L6	Rodentia	Heteromyidae	Dipodomyinae	Dipodomys	sp	molar
34248	14	B3/L6	Rodentia	Heteromyidae	Dipodomyinae	Dipodomys	sp	rt p4
34250	14	B3/L6	Rodentia	Heteromyidae	Dipodomyinae	Dipodomys	sp	partial lower tooth
34251	14	B3/L6	Lagomorpha	Leporidae		Sylvilagus	sp	upper lt tooth
34252	14	B3/L6	Lagomorpha	Leporidae		Sylvilagus	sp	lower rt tooth
34253	14	B3/L6	Lagomorpha	Leporidae		Sylvilagus	sp	lower rt tooth
34254	14	B3/L6	Lagomorpha	Leporidae		Sylvilagus	sp	lower lt tooth
34255	14	B3/L6	Lagomorpha	Leporidae		Sylvilagus	sp	lower lt tooth
34256	14	B3/L6	Lagomorpha	Leporidae		Sylvilagus	sp	rt p3
34257	14	B3/L6	Lagomorpha	Leporidae		Sylvilagus	sp	lower lt tooth
34258	14	B3/L6	Lagomorpha	Leporidae		Sylvilagus	sp	lower lt tooth
34259	14	B3/L6	Lagomorpha	Leporidae		Sylvilagus	audubonii	lt p3 frag

34260	14	B3/L6	Lagomorpha	Leporidae		Sylvilagus	audubonii	lt p3
34261	14	B3/L6	Lagomorpha	Leporidae		Sylvilagus	sp	lower lt tooth
34262	14	B3/L6	Lagomorpha	Leporidae		Sylvilagus	bachmani	rt p3
34263	14	B3/L6	Lagomorpha	Leporidae		Sylvilagus	sp	rt dentary frag
34264	14	B3/L6	Lagomorpha	Leporidae		Sylvilagus	sp	dentary frag
34265	14	B3/L6	Rodentia	Heteromyidae	Perognathinae			
34266	14	B3/L6	Rodentia	Sciuridae	Xerinae	Otospermophilus	?beecheyi	rt M1/M2 frag
34267	14	B3/L6	Rodentia	Sciuridae	Xerinae	Otospermophilus	?beecheyi	lower molar frag
34268	14	B3/L6	Rodentia	Sciuridae	Xerinae	Otospermophilus	?beecheyi	lower molar frag
34269	14	B3/L6	Rodentia	?Sciuridae	Xerinae			tooth frag
34270	14	B3/L6	Rodentia	Cricetidae	Neotominae	Neotoma	sp	lt M3
34271	14	B3/L6	Eulipotyphla	Soricidae	Soricinae	Sorex	sp	rt posterior dentary w/ partial teeth
34272	14	B3/L6	Rodentia	Cricetidae	Neotominae			rt dentary
34273	14	B3/L6	Rodentia	Cricetidae	Neotominae	cf Peromyscus	sp	lt dentary
34274	14	B3/L6	Rodentia	Cricetidae	Neotominae	Peromyscus	sp	lt m1
34277	14	B3/L6	Carnivora	Mustelidae	Mustelinae	Mustela	frenata	rt p3
34281	14	C3/L4	Rodentia	Sciuridae	Xerinae	Otospermophilus	?beecheyi	lt m1/m2
34282	14	C3/L4	Rodentia	Sciuridae	Xerinae	Otospermophilus	?beecheyi	rt m3
34283	14	C3/L4	Rodentia	Sciuridae	Xerinae	Otospermophilus	?beecheyi	lower molar frag
34284	14	C3/L4	Rodentia	Sciuridae	Xerinae	Otospermophilus	?beecheyi	rt M1/M2 frag
34285	14	C3/L4	Rodentia	cf Sciuridae	Xerinae	Otospermophilus	?beecheyi	tooth
34286	14	C3/L4	Rodentia	Cricetidae	Neotominae	Neotoma	sp	partial rt m2
34287	14	C3/L4	Rodentia	Heteromyidae	Perognathinae			rt? m1/m2
34288	14	C3/L4	Rodentia	Heteromyidae	Perognathinae			lt m1/m2
34289	14	C3/L4	Rodentia	Heteromyidae	Perognathinae			rt m1/m2
34290	14	C3/L4	Rodentia	Cricetidae	Neotominae	Peromyscus	cf maniculatus	lt m1

34291	14	C3/L4	Rodentia	Cricetidae	Neotominae	Peromyscus	sp	lt M1
34292	14	C3/L4	Rodentia	Cricetidae	Neotominae	Peromyscus	sp	rt M1
34293	14	C3/L4	Rodentia	Cricetidae	Neotominae	Peromyscus	cf californicus	rt M1
34294	14	C3/L4	Rodentia	Cricetidae	Neotominae	Peromyscus	sp	lt m1
34295	14	C3/L4	Rodentia	Sciuridae	Xerinae	Neotamias/Tamias	sp	lt p4
34296	14	C3/L4	Rodentia	Cricetidae	Neotominae	Peromyscus	cf maniculatus	rt M1
34297	14	C3/L4	Rodentia	Cricetidae	Neotominae	Peromyscus	sp	rt M1
34298	14	C3/L4	Rodentia	Cricetidae	?Neotominae			tooth
34299	14	C3/L4	Rodentia	Cricetidae	?Neotominae			tooth
34300	14	C3/L4	Rodentia	Cricetidae	Neotominae	?Peromyscus	sp	lt m1 frag
34301	14	C3/L4	Rodentia	Cricetidae	Neotominae	Peromyscus	sp	lt m1
34302	14	C3/L4	Rodentia	Cricetidae	Neotominae	Peromyscus	sp	lt m1
34303	14	C3/L4	Rodentia	Cricetidae	Neotominae	Peromyscus	sp	lt m1
34304	14	C3/L4	Rodentia	Cricetidae	Neotominae	?Peromyscus	sp	lt m1
34305	14	C3/L4	Rodentia	Cricetidae	Neotominae	Peromyscus	sp	lt m1
34306	14	C3/L4	Rodentia	Cricetidae	Neotominae			molar frag
34307	14	C3/L4	Rodentia	Cricetidae	Neotominae			lt dentary w/ i1
34308	14	C3/L4	Rodentia	Cricetidae	Neotominae			partial lt dentary
34309	14	C3/L4	Rodentia	Cricetidae	Neotominae			rt dentary frag
34310	14	C3/L4	Rodentia	Cricetidae	?Neotominae			tooth frag
34311	14	C3/L4	Rodentia	Cricetidae	Neotominae	?Peromyscus	sp	lt M1
34313	14	C3/L4	Lagomorpha	Leporidae		Sylvilagus	sp	lt P2
34316	14	C3/L4	Rodentia	Geomyidae	Thomomyinae	Thomomys	sp	partial M1/M2
34317	14	C3/L4	Rodentia	Geomyidae	Thomomyinae	?Thomomys	sp	M1/M2
34318	14	C3/L4	Rodentia	Heteromyidae	Dipodomyinae	?Dipodomys	sp	p4
34319	14	C3/L4	Rodentia	Heteromyidae	Dipodomyinae	Dipodomys	sp	molar
34320	14	C3/L4	Rodentia	Heteromyidae	Dipodomyinae	Dipodomys	sp	p4
34321	14	C3/L4	Rodentia	Heteromyidae	Dipodomyinae	Dipodomys	sp	lt m1/m2

34322	14	C3/L4	Rodentia	Heteromyidae	Dipodomyinae	?Dipodomys	sp	molar
34323	14	C3/L4	Rodentia	?Geomyidae	Thomomyinae	?Thomomys	sp	M1/M2
34324	14	C3/L4	Rodentia	Heteromyidae	Dipodomyinae	Dipodomys	sp	M1/M2
34326	14	C3/L4	Rodentia	Heteromyidae	Dipodomyinae	Dipodomys	sp	m1/m2
34334	14	C3/L4	Lagomorpha	Leporidae		Sylvilagus	sp	upper lt tooth
34335	14	C3/L4	Lagomorpha	Leporidae		Sylvilagus	sp	upper lt tooth
34336	14	C3/L4	Lagomorpha	Leporidae		?Sylvilagus	sp	tooth frag
34337	14	C3/L4	Lagomorpha	Leporidae		Sylvilagus	sp	upper lt tooth
34338	14	C3/L4	Lagomorpha	Leporidae		Sylvilagus	sp	tooth frag
34339	14	C3/L4	Lagomorpha	Leporidae		Sylvilagus	sp	lower rt tooth
34340	14	C3/L4	Lagomorpha	Leporidae		?Sylvilagus	sp	tooth frag
34341	14	C3/L4	Lagomorpha	Leporidae		?Sylvilagus	sp	tooth frag
34342	14	C3/L4	Lagomorpha	Leporidae		Sylvilagus	sp	upper tooth
34343	14	C3/L4	Lagomorpha	Leporidae		?Sylvilagus	sp	tooth frag
34344	14	C3/L4	Lagomorpha	Leporidae		?Sylvilagus	sp	tooth frag
34345	14	C3/L4	Lagomorpha	Leporidae		?Sylvilagus	sp	tooth frag
34346	14	C3/L4	Rodentia	Cricetidae	Arvicolinae	Microtus	sp	lt m2
34347	14	C3/L4	Rodentia	Cricetidae	Arvicolinae	Microtus	sp	lt M2
34348	14	C3/L4	Rodentia	Cricetidae	Arvicolinae	Microtus	sp	lt M1
34349	14	C3/L4	Rodentia	Cricetidae	Arvicolinae	Microtus	sp	rt M1
34350	14	C3/L4	Rodentia	Cricetidae	Arvicolinae	Microtus	sp	lt m2
34351	14	C3/L4	Rodentia	Cricetidae	Arvicolinae	Microtus	sp	lt m3
34352	14	C3/L4	Rodentia	Cricetidae	Arvicolinae	Microtus	sp	tooth frag
34353	14	C3/L4	Rodentia	Cricetidae	Arvicolinae	Microtus	sp	partial rt m2
34354	14	C3/L4	Rodentia	Cricetidae	Arvicolinae	Microtus	sp	lt M2
34355	14	C3/L4	Rodentia	Cricetidae	Arvicolinae	Microtus	sp	molar frag
34359	14	C2/L4	Rodentia	Cricetidae	Neotominae	Peromyscus	sp	rt M1
35552	7B	B1/L1	Rodentia	Cricetidae	Arvicolinae	Microtus	sp	lt M1
35553	7B	B1/L1	Rodentia	Cricetidae	Neotominae	Neotoma	sp	rt M1
35554	7B	B1/L1	Rodentia	Cricetidae	Neotominae	Neotoma	sp	rt M2

35555	7B	B1/L1	Rodentia	Cricetidae	Neotominae	Neotoma	sp	lt M1 frag
35556	7B	B1/L1	Lagomorpha	Leporidae		Sylvilagus	sp	upper rt tooth
35557	7B	B1/L1	Lagomorpha	Leporidae		Sylvilagus	sp	lt P2
35558	7B	B1/L1	Lagomorpha	Leporidae		Sylvilagus	sp	lt tooth
35559	7B	B1/L1	Lagomorpha	Leporidae		?Sylvilagus	sp	lt dentary frag
35560	7B	B1/L1	Lagomorpha	Leporidae		Sylvilagus	sp	tooth frag
35561	7B	B1/L1	Lagomorpha	Leporidae		Sylvilagus	sp	tooth frag
35563	7B	B1/L1	Carnivora	Mephitidae		?Mephitis	mephitis	lt P3 frag
35564	7B	B1/L1	Rodentia	Cricetidae	Neotominae	Peromyscus	cf californicus	lt m1
35565	7B	B1/L1	Rodentia	Cricetidae	Neotominae			lt m2
35566	7B	B1/L1	Rodentia	Cricetidae	Neotominae	Peromyscus	sp	rt m2
35567	7B	B1/L1	Rodentia	Cricetidae	Neotominae	Peromyscus	sp	lt M2
35568	7B	B1/L1	Rodentia	Cricetidae	Neotominae	Peromyscus	cf californicus	lt m1
35569	7B	B1/L1	Rodentia	Cricetidae	Neotominae	?Peromyscus	sp	rt m2
35570	7B	B1/L1	Rodentia	Cricetidae	Neotominae	?Peromyscus	sp	lt M1 frag
35571	7B	B1/L1	Rodentia	Cricetidae	Neotominae			lt dentary frag
35572	7B	B1/L1	Rodentia	Cricetidae	?Neotominae			rt dentary frag
35573	7B	B1/L1	Rodentia	Cricetidae	Arvicolinae	cf Microtus	sp	rt dentary frag
35574	7B	A2/L1	Rodentia	Cricetidae	Neotominae	Peromyscus	sp	rt m2
35575	7B	A2/L1	Rodentia	Cricetidae	Neotominae	Peromyscus	sp	rt m2
35576	7B	A2/L1	Rodentia	Cricetidae	Neotominae	Neotoma	sp	rt M2
35577	7B	A2/L1	Rodentia	Cricetidae	Arvicolinae	Microtus	sp	rt M1
35578	7B	A2/L1	Rodentia	Cricetidae	Arvicolinae	Microtus	sp	tooth frag
35579	7B	A2/L1	Rodentia	Cricetidae	Arvicolinae	Microtus	sp	rt m3
35580	7B	A2/L1	Rodentia	Cricetidae	Arvicolinae	Microtus	sp	tooth frag
35581	7B	A2/L1	Rodentia	Cricetidae	Arvicolinae	Microtus	sp	lt m1 frag
35582	7B	A2/L1	Rodentia	Cricetidae	Arvicolinae	Microtus	sp	lt m3
35583	7B	A2/L1	Lagomorpha	Leporidae		?Sylvilagus	sp	tooth frag
35584	7B	A2/L1	Lagomorpha	Leporidae		Sylvilagus	sp	upper tooth frag

35585	7B	A2/L1	Lagomorpha	Leporidae		Sylvilagus	sp	upper rt tooth
35586	7B	A2/L1	Lagomorpha	Leporidae		Sylvilagus	sp	lower rt tooth
35587	7B	A2/L1	Lagomorpha	Leporidae		Sylvilagus	sp	upper lt tooth
35588	7B	A2/L1	Lagomorpha	Leporidae		Sylvilagus	sp	partial upper tooth
35589	7B	A2/L1	Lagomorpha	Leporidae		?Sylvilagus	sp	lt dentary frag
35590	7B	A2/L1	Eulipotyphla	Soricidae	Soricinae	?Sorex	sp	dentary frag
35591	7B	A2/L1	Rodentia	Sciuridae	Xerinae	Otospermophilus	?beecheyi	lt M1/M2 frag
35592	7B	A2/L1	Rodentia	Geomyidae	Thomomyinae	Thomomys	sp	rt m1/m2
35594	7B	A2/L1	Rodentia	Geomyidae	Thomomyinae	Thomomys	sp	partial P4/p4
35597	7B	A2/L1	Lagomorpha	Leporidae		?Sylvilagus	sp	tooth frag
35599	7B	A3/L2	Rodentia	Cricetidae	Neotominae	cf Reithrodontomys	megalotis	lt M1
35599	7B	A3/L2	Rodentia	Cricetidae	Neotominae	?Peromyscus	sp	lt M1
35600	7B	A3/L2	Rodentia	Cricetidae	Neotominae	?Peromyscus	sp	rt m2
35602	7B	A3/L2	Rodentia	Cricetidae	Arvicolinae	Microtus	sp	molar frag
35603	7B	A3/L2	Rodentia	Cricetidae	Arvicolinae	cf Microtus	sp	molar frag
35604	7B	A2/L2	Rodentia	Geomyidae	Thomomyinae	Thomomys	sp	lt M1/M2
35605	7B	A2/L2	Rodentia	Geomyidae	Thomomyinae	Thomomys	sp	P4/p4 frag
35608	7B	A2/L2	Lagomorpha	Leporidae		Sylvilagus	audubonii	lt p3
35609	7B	A2/L2	Lagomorpha	Leporidae		Sylvilagus	sp	lower tooth frag
35610	7B	A2/L2	Rodentia	Sciuridae	Xerinae			rt M1/M2 frag
35611	7B	A2/L2	Rodentia	Cricetidae	Arvicolinae	Microtus	sp	lt m1
35612	7B	A2/L2	Rodentia	Cricetidae	Arvicolinae	cf Microtus	sp	molar frag
35613	7B	A2/L2	Rodentia	Cricetidae	Arvicolinae	Microtus	sp	rt m1 frag
35614	7B	B2/L1	Lagomorpha	Leporidae		Sylvilagus	audubonii	rt p3
35615	7B	B2/L1	Lagomorpha	Leporidae		Sylvilagus	sp	lower rt tooth
35616	7B	B2/L1	Lagomorpha	Leporidae		Sylvilagus	sp	upper rt tooth
35617	7B	B2/L1	Lagomorpha	Leporidae		Sylvilagus	sp	rt P2
35618	7B	B2/L1	Lagomorpha	Leporidae		Sylvilagus	audubonii	partial rt p3
35619	7B	B2/L1	Lagomorpha	Leporidae		Sylvilagus	audubonii	partial rt p3

35620	7B	B2/L1	Lagomorpha	Leporidae		Sylvilagus	sp	upper tooth frag
35621	7B	B2/L1	Lagomorpha	Leporidae		?Sylvilagus	sp	upper tooth frag
35622	7B	B2/L1	Lagomorpha	Leporidae		Sylvilagus	sp	lower rt tooth frag
35623	7B	B2/L1	Rodentia	Cricetidae	Neotominae	Neotoma	sp	lt m2
35624	7B	B2/L1	Rodentia	Cricetidae	Neotominae	Neotoma	sp	rt M1
35626	7B	B2/L1	Carnivora	Mephitidae		Mephitis	mephitis	rt p3
35627	7B	B2/L1	Eulipotyphla	Soricidae	Soricinae			rt maxilla frag w/ P4
35630	7B	B2/L1	Rodentia	Cricetidae	Neotominae	Peromyscus	cf maniculatus	rt M1
35631	7B	B2/L1	Rodentia	Cricetidae	Neotominae	?Peromyscus	sp	lt m1
35632	7B	B2/L1	Rodentia	Cricetidae	Neotominae	?Peromyscus	sp	rt m1
35633	7B	B2/L1	Rodentia	Cricetidae	Neotominae	Peromyscus	sp	rt M1
35634	7B	B2/L1	Rodentia	Cricetidae	Neotominae	Peromyscus	cf maniculatus	rt M1
35635	7B	B2/L1	Rodentia	Cricetidae	Neotominae	Peromyscus	sp	lt M1
35636	7B	B2/L1	Rodentia	Cricetidae	Arvicolinae	Microtus	sp	lt m1
35637	7B	B2/L1	Rodentia	Cricetidae	Arvicolinae	Microtus	sp	rt m1
35638	7B	B2/L1	Rodentia	Cricetidae	Arvicolinae	Microtus	sp	lt dentary frag w/ i1
35639	7B	B2/L1	Rodentia	Cricetidae	Arvicolinae	Microtus	sp	rt m1
35640	7B	B2/L1	Rodentia	Cricetidae	Arvicolinae	Microtus	sp	lt m1
35641	7B	B2/L1	Rodentia	Cricetidae	Arvicolinae	Microtus	sp	lt m1
35642	7B	B2/L1	Rodentia	?Geomyidae		?Thomomys	sp	molar
35643	7B	B2/L1	Rodentia	Heteromyidae	Dipodomyinae	Dipodomys	sp	molar
35645	7B	B2/L1	Lagomorpha	Leporidae		Sylvilagus	audubonii	rt p3 frag
35646	7B	B2/L1	Lagomorpha	Leporidae		?Sylvilagus	sp	upper tooth frag
35648	7B	B2/L2	Rodentia	Cricetidae	Arvicolinae	Microtus	sp	lt M1
35649	7B	B2/L2	Rodentia	Cricetidae	Arvicolinae	Microtus	sp	rt m1
35650	7B	B2/L2	Rodentia	Cricetidae	Arvicolinae	Microtus	sp	lt m1
35651	7B	B2/L2	Rodentia	Cricetidae	Arvicolinae	Microtus	sp	rt m1

35652	7B	B2/L2	Rodentia	Cricetidae	Arvicolinae	Microtus	sp	lt m1 frag
35653	7B	B2/L2	Rodentia	Cricetidae	Arvicolinae	Microtus	sp	lt M1
35654	7B	B2/L2	Rodentia	Cricetidae	Arvicolinae	Microtus	sp	rt M2
35655	7B	B2/L2	Rodentia	Cricetidae	Arvicolinae	Microtus	sp	lt m2
35656	7B	B2/L2	Rodentia	Cricetidae	Arvicolinae	Microtus	sp	rt m2
35657	7B	B2/L2	Rodentia	Cricetidae	Arvicolinae	Microtus	sp	lt M3
35658	7B	B2/L2	Rodentia	Cricetidae	Arvicolinae	Microtus	sp	lt m1 frag
35659	7B	B2/L2	Rodentia	Cricetidae	Arvicolinae	Microtus	sp	lt M3
35660	7B	B2/L2	Rodentia	Cricetidae	Arvicolinae	Microtus	sp	lt m3
35661	7B	B2/L2	Rodentia	Cricetidae	Arvicolinae	Microtus	sp	lt m2
35662	7B	B2/L2	Rodentia	Cricetidae	Arvicolinae	Microtus	sp	rt m2
35663	7B	B2/L2	Rodentia	Cricetidae	Neotominae	Neotoma	sp	lt m2
35664	7B	B2/L2	Rodentia	Cricetidae	Neotominae	Neotoma	sp	rt m2
35665	7B	B2/L2	Rodentia	Cricetidae	Neotominae	Neotoma	macrotis	rt m1
35666	7B	B2/L2	Rodentia	Cricetidae	Neotominae	Neotoma	sp	rt M3
35667	7B	B2/L2	Rodentia	Cricetidae	Neotominae	Neotoma	sp	lt M2
35668	7B	B2/L2	Rodentia	Cricetidae	Neotominae	Neotoma	macrotis	rt m1
35669	7B	B2/L2	Rodentia	Cricetidae	Neotominae	Neotoma	sp	lt? m3
35670	7B	B2/L2	Rodentia	Sciuridae	Xerinae	Otospermophilus	?beecheyi	rt dentary frag
35671	7B	B2/L2	Rodentia	Sciuridae	Xerinae			dentary frag
35672	7B	B2/L2	Rodentia	Sciuridae	Xerinae	Otospermophilus	?beecheyi	lt dentary frag
35673	7B	B2/L2	Rodentia	Sciuridae	Xerinae	Otospermophilus	?beecheyi	rt m1/m2
35674	7B	B2/L2	Rodentia	Sciuridae	Xerinae	Otospermophilus	?beecheyi	lt m1/m2
35675	7B	B2/L2	Rodentia	Sciuridae	Xerinae	Otospermophilus	?beecheyi	lt p4
35676	7B	B2/L2	Rodentia	Sciuridae	Xerinae	Otospermophilus	?beecheyi	lt m1/m2
35677	7B	B2/L2	Rodentia	Sciuridae	Xerinae	Otospermophilus	?beecheyi	lt M3
35678	7B	B2/L2	Rodentia	Sciuridae	Xerinae	Otospermophilus	?beecheyi	rt M1/M2 frag
35679	7B	B2/L2	Rodentia	Sciuridae	Xerinae	Otospermophilus	?beecheyi	partial lt p4
35680	7B	B2/L2	Rodentia	Sciuridae	Xerinae	Otospermophilus	?beecheyi	lt M1/M2
35681	7B	B2/L2	Rodentia	Geomyidae	Thomomyinae	Thomomys	sp	P4/p4

35682	7B	B2/L2	Rodentia	Geomyidae	Thomomyinae	Thomomys	sp	rt M1/M2
35683	7B	B2/L2	Lagomorpha	Leporidae		Sylvilagus	sp	lt P2
35685	7B	B2/L2	Rodentia	Heteromyidae	Dipodomyinae	Dipodomys	sp	rt P4
35689	7B	B2/L2	Rodentia	Geomyidae	Thomomyinae	Thomomys	sp	lt? M1/M2
35690	7B	B2/L2	Carnivora	Mephitidae		Mephitis	mephitis	lt m2
35691	7B	B2/L2	Carnivora	Mustelidae	Mustelinae	Mustela	frenata	partial rt dentary
35692	7B	B2/L2	Carnivora	Mustelidae	Mustelinae	?Mustela	frenata	rt dentary frag
35693	7B	B2/L2	Lagomorpha	Leporidae		Sylvilagus	sp	upper lt tooth
35694	7B	B2/L2	Lagomorpha	Leporidae		Sylvilagus	sp	lower rt tooth
35695	7B	B2/L2	Lagomorpha	Leporidae		Sylvilagus	sp	lower lt tooth
35696	7B	B2/L2	Lagomorpha	Leporidae		Sylvilagus	audubonii	rt p3
35697	7B	B2/L2	Lagomorpha	Leporidae		Sylvilagus	sp	lower rt tooth
35698	7B	B2/L2	Lagomorpha	Leporidae		Sylvilagus	sp	lower lt tooth
35699	7B	B2/L2	Lagomorpha	Leporidae		Sylvilagus	sp	lower rt tooth
35700	7B	B2/L2	Lagomorpha	Leporidae		Sylvilagus	sp	m3
35701	7B	B2/L2	Lagomorpha	Leporidae		Sylvilagus	sp	lower rt tooth
35702	7B	B2/L2	Lagomorpha	Leporidae		Sylvilagus	sp	lower lt tooth
35703	7B	B2/L2	Lagomorpha	Leporidae		Sylvilagus	sp	upper lt? tooth
35704	7B	B2/L2	Lagomorpha	Leporidae		Sylvilagus	sp	upper lt tooth
35705	7B	B2/L2	Lagomorpha	Leporidae		Sylvilagus	sp	upper tooth frag
35706	7B	B2/L2	Lagomorpha	Leporidae		?Sylvilagus	sp	upper tooth frag
35707	7B	B2/L2	Rodentia	Cricetidae	Neotominae			rt dentary w/ i1
35708	7B	B2/L2	Rodentia	Cricetidae	Neotominae			lt dentary frag
35709	7B	B2/L2	Rodentia	Cricetidae	Neotominae			rt dentary frag
35710	7B	B2/L2	Rodentia	Cricetidae	Neotominae			rt dentary frag
35711	7B	B2/L2	Rodentia	Cricetidae	Neotominae			rt dentary frag
35712	7B	B2/L2	Rodentia	Cricetidae	Neotominae	Peromyscus	cf maniculatus	lt M1
35713	7B	B2/L2	Rodentia	Cricetidae	Neotominae	?Peromyscus	sp	lt m1
35714	7B	B2/L2	Rodentia	Cricetidae	Neotominae	Peromyscus	sp	lt m1

35715	7B	B2/L2	Rodentia	Cricetidae	Neotominae	Peromyscus	sp	rt M1
35716	7B	B2/L2	Rodentia	Cricetidae	Neotominae	Peromyscus	sp	rt M1
35717	7B	B2/L2	Rodentia	Cricetidae	Neotominae	Peromyscus	sp	lt m1
35718	7B	B2/L2	Rodentia	Cricetidae	Neotominae	Peromyscus	sp	lt m2
35719	7B	B2/L2	Rodentia	Cricetidae	Neotominae	Peromyscus	sp	lt M1
35720	7B	B2/L2	Rodentia	Cricetidae	Neotominae	Peromyscus	sp	lt M1
35721	7B	B2/L2	Rodentia	Cricetidae	Neotominae	Peromyscus	sp	lt m1
35722	7B	B2/L2	Rodentia	Cricetidae	Neotominae	Peromyscus	sp	lt M2
35723	7B	B2/L2	Rodentia	Cricetidae	Neotominae	Peromyscus	cf maniculatus	rt M1
35724	7B	B2/L2	Rodentia	Heteromyidae	Perognathinae			rt anterior dentary w/ p4
35725	7B	B2/L2	Rodentia	?Neotominae				dentary frag
35726	7B	B2/L2	Lagomorpha	Leporidae		?Sylvilagus	sp	rt dentary frag
35727	7B	B2/L2	Lagomorpha	Leporidae		Sylvilagus	sp	partial rt p3
35728	7B	B2/L2	Lagomorpha	Leporidae		?Sylvilagus	sp	tooth frag
35731	7B	A3/L3	Rodentia	Heteromyidae	Dipodomyinae	?Dipodomys	sp	tooth
35734	7B	A3/L3	Rodentia	Heteromyidae	Dipodomyinae	Dipodomys	sp	partial rt? p4
35735	7B	A3/L3	Rodentia	Cricetidae	Neotominae	Peromyscus	sp	lt m1
35736	7B	A3/L3	Rodentia	Cricetidae	Neotominae	?Peromyscus	sp	lt M1 frag
35737	7B	A3/L3	Lagomorpha	Leporidae		?Sylvilagus	sp	upper tooth frag
35738	7B	A3/L3	Rodentia	Cricetidae	Arvicolinae	Microtus	sp	lt M1
35740	7B	A2/L3	Rodentia	Cricetidae	Arvicolinae	cf Microtus	sp	tooth frag
35741	7B	A2/L3	Lagomorpha	Leporidae		Sylvilagus	sp	lower lt tooth
35742	7B	A2/L3	Rodentia	Cricetidae	Neotominae	Peromyscus	sp	lt M1
35743	7B	A2/L3	Rodentia	Cricetidae	Neotominae			rt m2
35744	7B	A2/L3	Rodentia	Geomyidae	Thomomyinae	Thomomys	sp	lt P4
35745	7B	A2/L3	Rodentia	Heteromyidae	Dipodomyinae	Dipodomys	sp	lt? M1
35746	7B	A2/L3	Rodentia	Heteromyidae	Dipodomyinae	Dipodomys	sp	p4 frag
35747	7B	A2/L3	Rodentia	Heteromyidae	Dipodomyinae	Dipodomys	sp	molar
35748	7B	A2/L3	Rodentia	Heteromyidae	Dipodomyinae	?Dipodomys	sp	tooth frag

35749	7B	A2/L3	Rodentia	Heteromyidae	Dipodomyinae	?Dipodomys	sp	tooth frag
35750	7B	B2/L3	Rodentia	Cricetidae	Neotominae	cf Peromyscus	sp	lt m1
35751	7B	B2/L3	Rodentia	Cricetidae	Neotominae			lt m2
35752	7B	B2/L3	Rodentia	Cricetidae	Neotominae	Peromyscus	cf maniculatus	lt M1
35753	7B	B2/L3	Rodentia	Cricetidae	Neotominae			lt m2
35754	7B	B2/L3	Rodentia	Cricetidae	Neotominae	cf Reithrodontomys	megalotis	lower rt m1
35755	7B	B2/L3	Rodentia	Cricetidae	Neotominae			rt anterior dentary w/ i1
35756	7B	B2/L3	Rodentia	Cricetidae	Neotominae			rt M2
35757	7B	B2/L3	Rodentia	Cricetidae	Neotominae			lt M2
35758	7B	B2/L3	Rodentia	Cricetidae	Arvicolinae	Microtus	sp	rt M2
35759	7B	B2/L3	Rodentia	Cricetidae	Arvicolinae	Microtus	sp	rt m1
35760	7B	B2/L3	Rodentia	Cricetidae	Arvicolinae	Microtus	sp	lt M3
35761	7B	B2/L3	Rodentia	Cricetidae	Arvicolinae	Microtus	sp	lt dentary frag
35762	7B	B2/L3	Lagomorpha	Leporidae		Sylvilagus	sp	upper lt tooth
35763	7B	B2/L3	Lagomorpha	Leporidae		Sylvilagus	audubonii	lt p3
35764	7B	B2/L3	Lagomorpha	Leporidae		Sylvilagus	sp	lower lt tooth
35765	7B	B2/L3	Lagomorpha	Leporidae		Sylvilagus	sp	upper lt tooth
35766	7B	B2/L3	Lagomorpha	Leporidae		Sylvilagus	sp	lower lt tooth
35767	7B	B2/L3	Lagomorpha	Leporidae		Sylvilagus	sp	upper rt tooth
35768	7B	B2/L3	Lagomorpha	Leporidae		?Sylvilagus	sp	lower tooth frag
35769	7B	B2/L3	Lagomorpha	Leporidae		Sylvilagus	sp	upper lt tooth
35770	7B	B2/L3	Lagomorpha	Leporidae		Sylvilagus	sp	upper tooth
35771	7B	B2/L3	Lagomorpha	Leporidae		Sylvilagus	audubonii	lt p3 frag
35772	7B	B2/L3	Lagomorpha	Leporidae		Sylvilagus	sp	upper tooth
35773	7B	B2/L3	Lagomorpha	Leporidae		Sylvilagus	sp	dentary frag
35775	7B	B2/L3	Rodentia	Geomyidae	Thomomyinae	Thomomys	sp	lt m1/m2
35776	7B	B2/L3	Rodentia	Geomyidae	Thomomyinae	Thomomys	?bottae	lt p4
35777	7B	B2/L3	Rodentia	Geomyidae	Thomomyinae	Thomomys	sp	rt m1/m2
35778	7B	B2/L3	Rodentia	Geomyidae	Thomomyinae	Thomomys	sp	lower molar

35779	7B	B2/L3	Rodentia	Sciuridae	Xerinae	Otospermophilus	?beecheyi	rt p4
35780	7B	B2/L3	Rodentia	Cricetidae	Neotominae	Neotoma	macrotis	rt m1
35781	7B	B2/L3	Rodentia	Cricetidae	Neotominae	Neotoma	sp	rt m2
35782	7B	B2/L3	Rodentia	Cricetidae	Neotominae	Neotoma	macrotis	lt m1
35783	7B	B2/L3	Rodentia	Cricetidae	Neotominae	Neotoma	sp	molar - m3?
35784	7B	B2/L3	Rodentia	Cricetidae	?Neotominae			lt dentary frag
35785	7B	B2/L3	Rodentia	Geomyidae	Thomomyinae	?Thomomys	sp	tooth frag
35786	7B	B2/L3	Rodentia	Geomyidae	Thomomyinae	?Thomomys	sp	tooth frag
35787	7B	B2/L3	Lagomorpha	Leporidae		?Sylvilagus	sp	tooth cap
35788	7B	B2/L3	Rodentia	Cricetidae	Neotominae	?Neotoma	sp	molar frag
35789	7B	B2/L3	Rodentia	Cricetidae	Arvicolinae	cf Microtus	sp	molar frag
35793	7B	A3/L4	Rodentia	Geomyidae	Thomomyinae	Thomomys	sp	rt M1/M2
35794	7B	A3/L4	Rodentia	Neotominae				lt M1
35795	7B	A3/L4	Rodentia	?Neotominae				molar frag
35796	7B	A3/L4	Rodentia	Cricetidae	Arvicolinae	cf Microtus	sp	lt dentary frag
35797	7B	A3/L4	Rodentia	Cricetidae	Arvicolinae	cf Microtus	sp	tooth frag
35798	7B	A2/L4	Rodentia	Cricetidae	Neotominae	Peromyscus	sp	rt M1
35799	7B	A2/L4	Rodentia	Cricetidae	Neotominae	cf Reithrodontomys	megalotis	rt M1
35800	7B	A2/L4	Rodentia	Cricetidae	Neotominae	cf Reithrodontomys	megalotis	lt M1
35801	7B	A2/L4	Rodentia	Cricetidae	Arvicolinae	Microtus	sp	rt m3
35802	7B	A2/L4	Rodentia	Cricetidae	Arvicolinae	Microtus	sp	lt M1
35804	7B	B2/L4	Rodentia	Cricetidae	Neotominae	Neotoma	sp	rt m2
35805	7B	B2/L4	Rodentia	Cricetidae	Neotominae	Neotoma	sp	rt M1
35806	7B	B2/L4	Rodentia	Cricetidae	Neotominae	Neotoma	macrotis	rt m1
35807	7B	B2/L4	Rodentia	Cricetidae	Neotominae	Neotoma	sp	lt? m3
35808	7B	B2/L4	Rodentia	Cricetidae	Neotominae	Neotoma	sp	lt? m3
35809	7B	B2/L4	Rodentia	Sciuridae	Xerinae	Otospermophilus	?beecheyi	lt M1/M2
35811	7B	B2/L4	Rodentia	Cricetidae	Arvicolinae	Microtus	sp	rt M1
35812	7B	B2/L4	Rodentia	Cricetidae	Arvicolinae	Microtus	sp	rt m1
35813	7B	B2/L4	Rodentia	Cricetidae	Arvicolinae	Microtus	sp	lt m3

35814	7B	B2/L4	Rodentia	Cricetidae	Arvicolinae	Microtus	sp	molar frag
35815	7B	B2/L4	Rodentia	Cricetidae	Arvicolinae	Microtus	sp	lt dentary frag
35816	7B	B2/L4	Rodentia	Cricetidae	Arvicolinae	Microtus	sp	rt M3 frag
35817	7B	B2/L4	Rodentia	Cricetidae	Arvicolinae	Microtus	sp	molar frag
35818	7B	B2/L4	Rodentia	Geomyidae	Thomomyinae	Thomomys	sp	M1/M2
35819	7B	B2/L4	Rodentia	Heteromyidae	Dipodomyinae	Dipodomys	sp	m1/m2
35820	7B	B2/L4	Rodentia	Geomyidae	Thomomyinae	Thomomys	sp	M1/M2
35821	7B	B2/L4	Rodentia	?Heteromyidae	Dipodomyinae	?Dipodomys	sp	molar
35822	7B	B2/L4	Rodentia	Geomyidae	Thomomyinae	Thomomys	sp	P4/p4 frag
35823	7B	B2/L4	Rodentia	Geomyidae	Thomomyinae	Thomomys	sp	P4/p4 frag
35825	7B	B2/L4	Rodentia	Geomyidae	Thomomyinae	Thomomys	sp	molar frag
35826	7B	B2/L4	Rodentia	Geomyidae	Thomomyinae	Thomomys	sp	molar frag
35827	7B	B2/L4	Rodentia	Heteromyidae	Perognathinae			upper molar
35828	7B	B2/L4	Rodentia	Cricetidae	Neotominae	Peromyscus	sp	lt m1
35829	7B	B2/L4	Rodentia	Cricetidae	Neotominae			rt dentary frag
35830	7B	B2/L4	Rodentia	Cricetidae	Neotominae			rt maxilla frag
35831	7B	B2/L4	Rodentia	Cricetidae	Neotominae	Peromyscus	cf californicus	lt m1
35832	7B	B2/L4	Rodentia	Cricetidae	Neotominae	Peromyscus	cf maniculatus	lt m1
35833	7B	B2/L4	Rodentia	Cricetidae	Neotominae	Peromyscus	sp	lt m2
35834	7B	B2/L4	Rodentia	Cricetidae	Neotominae	Peromyscus	sp	rt m2
35835	7B	B2/L4	Rodentia	Cricetidae	Neotominae	Peromyscus	sp	rt M2
35836	7B	B2/L4	Lagomorpha	Leporidae		Sylvilagus	audubonii	rt p3
35837	7B	B2/L4	Lagomorpha	Leporidae		Sylvilagus	sp	upper (rt?) tooth
35838	7B	B2/L4	Lagomorpha	Leporidae		Sylvilagus	sp	upper lt tooth
35839	7B	B2/L4	Lagomorpha	Leporidae		Sylvilagus	audubonii	rt p3
35840	7B	B2/L4	Lagomorpha	Leporidae		Sylvilagus	audubonii	rt p3
35841	7B	B2/L4	Lagomorpha	Leporidae		Sylvilagus	sp	upper rt tooth
35842	7B	B2/L4	Lagomorpha	Leporidae		Sylvilagus	sp	upper rt tooth
35843	7B	B2/L4	Lagomorpha	Leporidae		Sylvilagus	sp	lower lt tooth

35844	7B	B2/L4	Lagomorpha	Leporidae		Sylvilagus	bachmani	rt p3
35845	7B	B2/L4	Lagomorpha	Leporidae		Sylvilagus	sp	upper tooth
35846	7B	B2/L4	Lagomorpha	Leporidae		Sylvilagus	sp	lower rt tooth
35847	7B	B2/L4	Lagomorpha	Leporidae		Sylvilagus	audubonii	rt p3
35848	7B	B2/L4	Lagomorpha	Leporidae		Sylvilagus	sp	upper rt tooth
35849	7B	B2/L4	Lagomorpha	Leporidae		Sylvilagus	sp	lower rt tooth
35850	7B	B2/L4	Lagomorpha	Leporidae		Sylvilagus	sp	lower rt tooth
35851	7B	B2/L4	Lagomorpha	Leporidae		Sylvilagus	sp	lower lt tooth
35852	7B	B2/L4	Lagomorpha	Leporidae		Sylvilagus	sp	upper lt tooth
35853	7B	B2/L4	Eulipotyphla	Talpidae	Scalopini	Scapanus	cf latimanus	lt m1/m2
35854	7B	B2/L4	Lagomorpha	Leporidae		?Sylvilagus	sp	rt dentary frag
35855	7B	B2/L4	Lagomorpha	Leporidae		?Sylvilagus	sp	lt dentary frag
35858	7B	B2/L4	Rodentia	?Cricetidae				rt maxilla
35860	7B	B2/L5	Rodentia	Cricetidae	Neotominae	Neotoma	sp	lt m2
35861	7B	B2/L5	Rodentia	Cricetidae	Neotominae	Neotoma	sp	rt M3
35862	7B	B2/L5	Rodentia	Cricetidae	Neotominae	Neotoma	sp	lt? m3
35863	7B	B2/L5	Rodentia	Cricetidae	Neotominae	Peromyscus	sp	rt m1
35864	7B	B2/L5	Rodentia	Cricetidae	Neotominae	Peromyscus	sp	rt m1
35865	7B	B2/L5	Rodentia	Cricetidae	Neotominae	Peromyscus	cf maniculatus	rt M1
35866	7B	B2/L5	Rodentia	Cricetidae	Neotominae	Peromyscus	cf maniculatus	rt m1
35867	7B	B2/L5	Rodentia	Cricetidae	Neotominae	Peromyscus	sp	rt m2
35868	7B	B2/L5	Rodentia	Cricetidae	Neotominae	Peromyscus	sp	lt m2
35869	7B	B2/L5	Rodentia	Cricetidae	Neotominae	Peromyscus	sp	lt M2
35870	7B	B2/L5	Rodentia	Cricetidae	Neotominae	Peromyscus	sp	lt M1
35871	7B	B2/L5	Rodentia	Cricetidae	Neotominae	cf Reithrodontomys	megalotis	rt m1
35872	7B	B2/L5	Rodentia	Cricetidae	Neotominae	Peromyscus	sp	rt m2
35873	7B	B2/L5	Rodentia	Cricetidae	Neotominae	Peromyscus	sp	lt m2
35874	7B	B2/L5	Rodentia	Cricetidae	Arvicolinae	Microtus	sp	rt M3

35875	7B	B2/L5	Rodentia	Cricetidae	Arvicolinae	Microtus	sp	rt m3
35876	7B	B2/L5	Rodentia	Cricetidae	Arvicolinae	Microtus	sp	rt m2
35877	7B	B2/L5	Rodentia	Cricetidae	Arvicolinae	Microtus	sp	lt M1
35878	7B	B2/L5	Rodentia	Heteromyidae	Dipodomyinae	Dipodomys	sp	lt P4
35880	7B	B2/L5	Lagomorpha	Leporidae		?Sylvilagus	sp	lt maxilla frag
35881	7B	B2/L5	Lagomorpha	Leporidae		Sylvilagus	audubonii	rt p3
35882	7B	B2/L5	Lagomorpha	Leporidae		Sylvilagus	sp	upper rt tooth
35883	7B	B2/L5	Lagomorpha	Leporidae		Sylvilagus	audubonii	rt p3
35884	7B	B2/L5	Lagomorpha	Leporidae		Sylvilagus	sp	upper lt tooth
35885	7B	B2/L5	Lagomorpha	Leporidae		Sylvilagus	audubonii	lt p3
35886	7B	B2/L5	Lagomorpha	Leporidae		Sylvilagus	sp	upper rt? tooth
35887	7B	B2/L5	Lagomorpha	Leporidae		Sylvilagus	sp	upper lt tooth
35888	7B	B2/L5	Lagomorpha	Leporidae		Sylvilagus	sp	upper lt tooth
35889	7B	B2/L5	Lagomorpha	Leporidae		Sylvilagus	sp	lt P2
35890	7B	B2/L5	Lagomorpha	Leporidae		Sylvilagus	sp	m3
35891	7B	B2/L5	Lagomorpha	Leporidae		Sylvilagus	sp	lower rt tooth
35892	7B	B2/L5	Lagomorpha	Leporidae		Sylvilagus	sp	partial tooth
35893	7B	B2/L5	Lagomorpha	Leporidae		Sylvilagus	sp	lt p3
35894	7B	B2/L5	Lagomorpha	Leporidae		?Sylvilagus	sp	upper rt maxilla frag
35895	7B	B2/L5	Rodentia	Heteromyidae	Dipodomyinae	Dipodomys	sp	lt m1/m2
35896	7B	B2/L5	Rodentia	Heteromyidae	Dipodomyinae	Dipodomys	sp	lt m1/m2
35897	7B	B2/L5	Rodentia	Heteromyidae	Dipodomyinae	Dipodomys	sp	lt? M1/M2
35898	7B	B2/L5	Rodentia	Geomyidae	Thomomyinae	Thomomys	sp	lt M1/M2
35899	7B	B2/L5	Rodentia	Geomyidae	Thomomyinae	?Thomomys	sp	molar
35900	7B	B2/L5	Rodentia	Heteromyidae	Dipodomyinae	Dipodomys	sp	molar
35901	7B	B2/L5	Rodentia	Geomyidae	Thomomyinae	Thomomys	sp	lt? M1/M2
35903	7B	B2/L5	Rodentia	Heteromyidae	Dipodomyinae	Dipodomys	sp	lt? p4
35904	7B	B2/L5	Rodentia	Heteromyidae	Dipodomyinae	?Dipodomys	sp	tooth
35905	7B	B2/L5	Rodentia	Geomyidae	Thomomyinae	Thomomys	sp	lt M3

35909	7B	B2/L5	Rodentia	Geomyidae	Thomomyinae	Thomomys	?bottae	rt dentary w/ broken i1
35911	7B	B2/L5	Carnivora	Mustelidae	Mustelinae	Mustela	frenata	lt dentary frag
35912	7B	B2/L5	Rodentia	Sciuridae	Xerinae	Neotamias/Tamias	sp	upper lt tooth - P4?
35913	7B	B1/L5+6	Rodentia	Cricetidae	Neotominae	Peromyscus	sp	lt M1
35914	7B	B1/L5+6	Rodentia	Cricetidae	Neotominae	Peromyscus	cf maniculatus	lt M1
35915	7B	B1/L5+6	Rodentia	Cricetidae	Neotominae	Peromyscus	sp	rt M2
35916	7B	B1/L5+6	Rodentia	Cricetidae	Neotominae	Peromyscus	sp	rt M2
35917	7B	B1/L5+6	Rodentia	Cricetidae	Neotominae	Peromyscus	sp	lt m1
35918	7B	B1/L5+6	Rodentia	Cricetidae	Neotominae	Neotoma	sp	lt M3
35919	7B	B1/L5+6	Rodentia	Heteromyidae	Dipodomyinae	Dipodomys	sp	molar
35920	7B	B1/L5+6	Rodentia	Heteromyidae	Dipodomyinae	?Dipodomys	sp	molar
35926	7B	B1/L5+6	Eulipotyphla	Soricidae	Soricinae			rt dentary frag
35927	7B	B1/L5+6	Rodentia	Cricetidae	Arvicolinae	Microtus	sp	molar frag
35928	7B	B1/L5+6	Lagomorpha	Leporidae		Sylvilagus	sp	lower rt tooth
35929	7B	B1/L5+6	Lagomorpha	Leporidae		Sylvilagus	sp	upper lt tooth
35930	7B	B1/L5+6	Lagomorpha	Leporidae		Sylvilagus	sp	lt P2
35931	7B	B1/L5+6	Lagomorpha	Leporidae		?Sylvilagus	sp	tooth frag
35934	7B	B2/L6	Rodentia	Cricetidae	Neotominae	Neotoma	macrotis	lt m1
35935	7B	B2/L6	Rodentia	Cricetidae	Neotominae	Neotoma	sp	lt m2
35937	7B	B2/L6	Lagomorpha	Leporidae		Sylvilagus	audubonii	lt p3
35938	7B	B2/L6	Lagomorpha	Leporidae		Sylvilagus	sp	lower lt tooth
35939	7B	B2/L6	Lagomorpha	Leporidae		Sylvilagus	sp	lower lt tooth
35940	7B	B2/L6	Lagomorpha	Leporidae		Sylvilagus	sp	upper rt tooth
35941	7B	B2/L6	Lagomorpha	Leporidae		Sylvilagus	sp	lower lt tooth
35942	7B	B2/L6	Rodentia	Heteromyidae	Dipodomyinae	Dipodomys	sp	rt P4
35943	7B	B2/L6	Rodentia	Sciuridae	Xerinae			lt P4
35944	7B	B2/L6	Rodentia	Sciuridae	Xerinae	Otospermophilus	?beecheyi	lt p4
35945	7B	B2/L6	Rodentia	Sciuridae	?Sciurinae			partial rt M1/M2

35946	7B	B2/L6	Rodentia	Sciuridae	Xerinae	Otospermophilus	?beecheyi	partial lt maxilla w/ P4
35947	7B	B2/L6	Rodentia	Cricetidae	Neotominae	Peromyscus	cf maniculatus	lt m1
35948	7B	B2/L6	Rodentia	Cricetidae	Neotominae	Peromyscus	sp	lt m2
35949	7B	B2/L6	Rodentia	Cricetidae	Neotominae	Peromyscus	sp	lt M1
35950	7B	B2/L6	Rodentia	Cricetidae	Neotominae	Peromyscus	sp	lt M1
35951	7B	B2/L6	Rodentia	Cricetidae	Neotominae	Peromyscus	sp	lt M2
35952	7B	B2/L6	Rodentia	Cricetidae	Neotominae	Peromyscus	sp	rt M2
35953	7B	B2/L6	Rodentia	Cricetidae	Neotominae	Peromyscus	sp	lt M2
35954	7B	B2/L6	Rodentia	Cricetidae	Neotominae	Peromyscus	sp	lt M1
35955	7B	B2/L6	Rodentia	Cricetidae	Neotominae	?Peromyscus	sp	rt M2
35956	7B	B2/L6	Rodentia	Cricetidae	Neotominae	Peromyscus	cf maniculatus	rt M1
35957	7B	B2/L6	Rodentia	Cricetidae	Neotominae			lt M2
35959	7B	B2/L6	Rodentia	Cricetidae	Arvicolinae	Microtus	sp	lt M2
35960	7B	B2/L6	Rodentia	Cricetidae	Arvicolinae	Microtus	sp	partial lt M2
35961	7B	B2/L6	Rodentia	Cricetidae	Arvicolinae	cf Microtus	sp	molar frag
35962	7B	B2/L6	Rodentia	Cricetidae	Arvicolinae	Microtus	sp	lt dentary w/ i1
35963	7B	B2/L6	Rodentia	Cricetidae	Arvicolinae	Microtus	sp	rt anterior dentary w/ m1-m2
35964	7B	B2/L6	Rodentia	Geomyidae	Thomomyinae	Thomomys	sp	rt? M1/M2
35966	7B	B2/L6	Rodentia	Geomyidae	Thomomyinae	Thomomys	sp	lt M1/M2
35968	7B	B2/L6	Rodentia	Geomyidae	Thomomyinae	Thomomys	sp	rt m1/m2
35974	7B	B2/L6	Rodentia	Geomyidae	Thomomyinae	Thomomys	sp	molar frag
35981	7B	B2/L6	Rodentia	Heteromyidae	?Perognathinae			tooth frag
36310	7B	B2/L3	Lagomorpha	Leporidae		?Sylvilagus	sp	lower tooth frag
36311	7B	B2/L3	Rodentia	Geomyidae	Thomomyinae	Thomomys	sp	molar frag
36312	7B	B2/L3	Rodentia	Cricetidae	Neotominae	Neotoma	sp	rt m1
36314	7B	B2/L3	Rodentia	Geomyidae	Thomomyinae	Thomomys	sp	m1/m2
36315	7B	B2/L3	Lagomorpha	Leporidae		Sylvilagus	sp	lower lt tooth

36316	7B	B2/L3	Rodentia	Geomyidae	Thomomyinae	Thomomys	sp	M1/M2 frag
36318	7B	B2/L3	Lagomorpha	Leporidae		Sylvilagus	sp	upper rt tooth
36319	7B	B2/L6	Lagomorpha	Leporidae		?Sylvilagus	sp	upper rt tooth
36320	7B	B2/L6	Rodentia	Cricetidae	Neotominae			partial rt dentary
36321	7B	B2/L6	Rodentia	Cricetidae	Neotominae			lt M2
36322	7B	B2/L6	Rodentia	Heteromyidae	Perognathinae			upper rt? molar
36323	7B	B2/L6	Rodentia	Cricetidae	Neotominae	cf Reithrodontomys	megalotis	lt M1
36325	7B	B2/L6	Eulipotyphla	Soricidae	Soricinae			lower lt molar
36326	7B	B2/L3	Rodentia	Cricetidae	Neotominae	?Peromyscus	sp	lt M2
36327	7B	B2/L3	Rodentia	Geomyidae	Thomomyinae	Thomomys	sp	P4/p4
36328	7B	B2/L3	Rodentia	Cricetidae	Neotominae	Peromyscus	sp	lt m1
36329	7B	B2/L3	Rodentia	Cricetidae	Neotominae	Peromyscus	sp	lt M1
36333	7B	B2/L3	Rodentia	Sciuridae	Xerinae	Otospermophilus	?beecheyi	rt dentary w/ m1 frag
36335	7B	B2/L4	Lagomorpha	Leporidae		Sylvilagus	sp	rt anterior dentary w/ p4-m1
36600	7B	B2/L3	Lagomorpha	Leporidae		Sylvilagus	sp	upper rt tooth
36601	7B	B2/L3	Lagomorpha	Leporidae		Sylvilagus	sp	lower cheek tooth
36602	7B	B2/L3	Lagomorpha	Leporidae		Sylvilagus	sp	upper rt cheek tooth
36603	7B	B2/L3	Lagomorpha	Leporidae		Sylvilagus	sp	lower lt cheek tooth
36604	7B	B2/L3	Rodentia	Geomyidae	Thomomyinae	Thomomys	?bottae	rt p4
36605	7B	B2/L3	Rodentia	Geomyidae	Thomomyinae	Thomomys	sp	lt M3
36606	7B	B2/L3	Rodentia	Geomyidae	Thomomyinae	Thomomys	sp	lt M1/M2
36607	7B	B2/L3	Rodentia	Geomyidae	Thomomyinae	Thomomys	sp	rt M1
36608	7B	B2/L3	Rodentia	Cricetidae	Arvicolinae	Microtus	sp	molar frag
36609	7B	B2/L3	Rodentia	Cricetidae	Arvicolinae	Microtus	sp	lt m3
36610	7B	B2/L3	Rodentia	Cricetidae	Neotominae	Peromyscus	sp	rt m1
36611	7B	B2/L3	Rodentia	Cricetidae	Neotominae			rt M2

36612	7B	B2/L3	Rodentia	Cricetidae	Neotominae	Neotoma	sp	rt M1 frag
36613	7B	B2/L3	Rodentia	Sciuridae	Xerinae	Otospermophilus	?beecheyi	rt p4
36615	14	C3/L7	Lagomorpha	Leporidae		Sylvilagus	bachmani	rt p3
36616	14	C3/L7	Rodentia	Cricetidae	Arvicolinae	Microtus	sp	rt M1
36617	14	C3/L7	Rodentia	Cricetidae	Arvicolinae	Microtus	californicus	lt m1
36618	14	C3/L7	Rodentia	Cricetidae	Arvicolinae	Microtus	sp	partial lt m1
39811	13	B2/L3	Lagomorpha	Leporidae		Sylvilagus	audubonii	lt dentary frag w/ p3, p4, m2
39812	13	B2/L3	Lagomorpha	Leporidae		Sylvilagus	sp	lt dentary frag w/ m1-m2
39813	13	B2/L3	Lagomorpha	Leporidae		Sylvilagus	sp	rt dentary frag w/ m1
39814	13	B2/L3	Lagomorpha	Leporidae		Sylvilagus	sp	lt dentary frag
39815	13	B2/L3	Lagomorpha	Leporidae		Sylvilagus	cf audubonii	lt maxilla w/ P3-M2
39816	13	B2/L3	Lagomorpha	Leporidae		Sylvilagus	sp	rt maxilla w/ P3, M1
39817	13	B2/L3	Rodentia	Sciuridae	Xerinae	Otospermophilus	?beecheyi	rt maxilla frag
39818	13	B3/L2-T1	Lagomorpha	Leporidae		Sylvilagus	sp	lt dentary frag w/ p4
39819	13	B3/L2-T1	Lagomorpha	Leporidae		Sylvilagus	audubonii	rt dentary frag w/ p3-m1
39820	13	B3/L2-T1	Lagomorpha	Leporidae		Sylvilagus	audubonii	rt dentary frag w/ p3-m2
39821	13	B3/L2-T1	Lagomorpha	Leporidae		Sylvilagus	sp	rt dentary frag w/ m1
39822	13	B3/L2-T1	Lagomorpha	Leporidae		Sylvilagus	sp	lt dentary frag w/ p4-m2
39823	13	B3/L2-T1	Lagomorpha	Leporidae		Sylvilagus	sp	rt dentary frag w/ m1-m2
39824	13	B3/L2-T1	Rodentia	Sciuridae	Xerinae	Otospermophilus	?beecheyi	lt dentary frag w/ p4
39825	13	B3/L2-T2	Rodentia	Sciuridae	Xerinae	Otospermophilus	?beecheyi	lt dentary w/ i1
39826	13	B3/L2-T2	Lagomorpha	Leporidae		Sylvilagus	sp	rt maxilla frag w/ P4
39827	13	B3/L2-T1	Rodentia	Sciuridae	Xerinae	Otospermophilus	?beecheyi	lt dentary frag

39828	13	B3/L3-T1	Lagomorpha	Leporidae		Sylvilagus	sp	lt maxilla w/ P3, M1
39829	13	B3/L3-T1	Lagomorpha	Leporidae		Sylvilagus	sp	rt maxilla
39830	13	B3/L3-T1	Rodentia	Sciuridae	Xerinae	Otospermophilus	?beecheyi	lt dentary w/ m1
39831	13	B3/L3-T1	Rodentia	Sciuridae	Xerinae	Otospermophilus	?beecheyi	rt maxilla w/ dP4, unerupted P4, and M1
39832	13	B3/L3-T1	Rodentia	Sciuridae	Xerinae	Otospermophilus	?beecheyi	rt maxilla frag
39833	13	B3/L3-T1	Carnivora	Mustelidae	Mustelinae	Mustela	frenata	rt dentary w/ m1
39834	13	B3/L3-T1	Carnivora	Mustelidae	Mustelinae	Mustela	frenata	lt dentary frag w/ m1
39835	13	B2/L2	Lagomorpha	Leporidae		Sylvilagus	sp	partial lt dentary w/ m1
39836	13	B2/L2	Lagomorpha	Leporidae		Sylvilagus	sp	lt dentary frag w/ p4, m2
39837	13	A3/L3	Rodentia	Cricetidae	Arvicolinae	Microtus	sp	lt m1
39838	13	A3/L3	Rodentia	Cricetidae	Arvicolinae	Microtus	sp	rt m1
39839	13	A3/L3	Rodentia	Cricetidae	Arvicolinae	Microtus	sp	lt m1
39840	13	A3/L3	Rodentia	Cricetidae	Arvicolinae	Microtus	sp	rt m1
39841	13	A3/L3	Rodentia	Cricetidae	Arvicolinae	Microtus	sp	lt m1
39842	13	A3/L3	Rodentia	Cricetidae	Arvicolinae	Microtus	sp	rt m2
39843	13	A3/L3	Rodentia	Cricetidae	Arvicolinae	Microtus	sp	lt M2
39844	13	A3/L3	Rodentia	Cricetidae	Arvicolinae	Microtus	sp	lt m2
39845	13	A3/L3	Rodentia	Cricetidae	Arvicolinae	Microtus	sp	rt M3
39846	13	A3/L3	Rodentia	Cricetidae	Arvicolinae	Microtus	sp	lt M1
39847	13	A3/L3	Rodentia	Cricetidae	Arvicolinae	?Microtus	sp	rt m1 frag
39848	13	A3/L3	Rodentia	Cricetidae	Arvicolinae	Microtus	sp	lt m2
39849	13	A3/L3	Rodentia	Cricetidae	Arvicolinae	Microtus	sp	rt m1 frag
39850	13	A3/L3	Rodentia	Cricetidae	Arvicolinae	Microtus	sp	lt m2
39851	13	A3/L3	Rodentia	Cricetidae	Arvicolinae	Microtus	sp	lt m1 frag
39852	13	A3/L3	Rodentia	Cricetidae	Arvicolinae	Microtus	sp	lt m2

39853	13	A3/L3	Rodentia	Cricetidae	Arvicolinae	Microtus	sp	rt M3
39854	13	A3/L3	Rodentia	Cricetidae	Arvicolinae	Microtus	sp	lt m3
39855	13	A3/L3	Rodentia	Cricetidae	Arvicolinae	?Microtus	sp	molar frag
39856	13	A3/L3	Rodentia	Cricetidae	Arvicolinae	Microtus	sp	molar frag
39857	13	A3/L3	Rodentia	Cricetidae	Arvicolinae	Microtus	sp	molar frag
39858	13	A3/L3	Rodentia	Cricetidae	Arvicolinae	Microtus	sp	lt dentary
39859	13	A3/L3	Rodentia	Cricetidae	Arvicolinae	Microtus	sp	rt M3 frag
39860	13	A3/L3	Rodentia	Cricetidae	Arvicolinae	Microtus	sp	molar frag
39861	13	A3/L3	Lagomorpha	Leporidae		Sylvilagus	sp	lt P2
39862	13	A3/L3	Rodentia	Heteromyidae	Dipodomyinae	Dipodomys	sp	lt m1/m2
39863	13	A3/L3	Lagomorpha	Leporidae		Sylvilagus	sp	lt P2
39864	13	A3/L3	Rodentia	Geomyidae	Thomomyinae	Thomomys	sp	lt? m1/m2
39865	13	A3/L3	Rodentia	Sciuridae	Xerinae	Otospermophilus	?beecheyi	lt m1/m2
39866	13	A3/L3	Lagomorpha	Leporidae		Sylvilagus	sp	lower rt tooth
39867	13	A3/L3	Lagomorpha	Leporidae		Sylvilagus	sp	upper lt tooth
39868	13	A3/L3	Lagomorpha	Leporidae		Sylvilagus	sp	lower rt tooth
39869	13	A3/L3	Lagomorpha	Leporidae		Sylvilagus	sp	upper rt tooth
39870	13	A3/L3	Lagomorpha	Leporidae		Sylvilagus	sp	lower rt tooth
39871	13	A3/L3	Lagomorpha	Leporidae		Sylvilagus	sp	upper lt tooth
39872	13	A3/L3	Lagomorpha	Leporidae		Sylvilagus	sp	upper tooth frag
39873	13	A3/L3	Lagomorpha	Leporidae		Sylvilagus	sp	lower lt tooth
39874	13	A3/L3	Lagomorpha	Leporidae		Sylvilagus	audubonii	rt p3
39875	13	A3/L3	Lagomorpha	Leporidae		Sylvilagus	sp	upper rt tooth
39876	13	A3/L3	Lagomorpha	Leporidae		Sylvilagus	sp	upper rt tooth
39877	13	A3/L3	Lagomorpha	Leporidae		Sylvilagus	sp	upper rt tooth
39878	13	A3/L3	Lagomorpha	Leporidae		Sylvilagus	sp	upper tooth
39879	13	A3/L3	Lagomorpha	Leporidae		Sylvilagus	sp	lower rt tooth
39880	13	A3/L3	Lagomorpha	Leporidae		Sylvilagus	sp	upper lt tooth
39881	13	A3/L3	Lagomorpha	Leporidae		Sylvilagus	sp	upper lt tooth
39882	13	A3/L3	Lagomorpha	Leporidae		Sylvilagus	sp	lower lt tooth

39883	13	A3/L3	Lagomorpha	Leporidae		Sylvilagus	sp	lower lt tooth
39884	13	A3/L3	Lagomorpha	Leporidae		Sylvilagus	sp	lower rt tooth
39885	13	A3/L3	Lagomorpha	Leporidae		Sylvilagus	sp	lower lt tooth
39886	13	A3/L3	Lagomorpha	Leporidae		Sylvilagus	sp	upper tooth
39887	13	A3/L3	Lagomorpha	Leporidae		Sylvilagus	sp	upper tooth frag
39888	13	A3/L3	Lagomorpha	Leporidae		Sylvilagus	sp	lower rt tooth
39889	13	A3/L3	Lagomorpha	Leporidae		Sylvilagus	sp	upper tooth frag
39890	13	A3/L3	Lagomorpha	Leporidae		Sylvilagus	sp	p3 frag
39891	13	A3/L3	Lagomorpha	Leporidae		Sylvilagus	sp	lower lt tooth
39892	13	A3/L3	Lagomorpha	Leporidae		Sylvilagus	sp	lower lt tooth
39893	13	A3/L3	Lagomorpha	Leporidae		Sylvilagus	sp	upper tooth frag
39894	13	A3/L3	Lagomorpha	Leporidae		Sylvilagus	sp	m3
39895	13	A3/L3	Lagomorpha	Leporidae		Sylvilagus	sp	lower rt tooth
39896	13	A3/L3	Lagomorpha	Leporidae		Sylvilagus	sp	upper tooth frag
39897	13	A3/L3	Lagomorpha	Leporidae		Sylvilagus	sp	lower tooth frag
39898	13	A3/L3	Lagomorpha	Leporidae		Sylvilagus	sp	lower tooth frag
39899	13	A3/L3	Lagomorpha	Leporidae		Sylvilagus	sp	lower tooth frag
39900	13	A3/L3	Lagomorpha	Leporidae		Sylvilagus	sp	lower tooth frag
39901	13	A3/L3	Rodentia	Cricetidae	Neotominae	Neotoma	sp	rt M3
39902	13	A3/L3	Lagomorpha	Leporidae		Sylvilagus	sp	m3 frag
39903	13	A3/L3	Carnivora	Mustelidae	Mustelinae	Mustela	frenata	lt P4 frag
39905	13	A3/L3	Carnivora	Mustelidae	Mustelinae	Mustela	frenata	rt M1
39906	13	A3/L3	Rodentia	Sciuridae	Xerinae	Otospermophilus	?beecheyi	lt m1/m2
39907	13	A3/L3	Rodentia	Sciuridae	Xerinae	Otospermophilus	?beecheyi	lt P4
39908	13	A3/L3	Rodentia	Sciuridae	Xerinae	Otospermophilus	?beecheyi	rt m1/m2
39909	13	A3/L3	Rodentia	Sciuridae	Xerinae	Otospermophilus	?beecheyi	lt m1/m2
39910	13	A3/L3	Rodentia	Sciuridae	Xerinae	Otospermophilus	?beecheyi	partial lower rt molar
39911	13	A3/L3	Rodentia	Sciuridae	Xerinae	Otospermophilus	?beecheyi	rt p4
39912	13	A3/L3	Rodentia	Sciuridae	Xerinae	Otospermophilus	?beecheyi	rt m3

39913	13	A3/L3	Rodentia	Sciuridae	Xerinae			lt p4
39914	13	A3/L3	Rodentia	Sciuridae	Xerinae	Otospermophilus	?beecheyi	lt m1/m2
39915	13	A3/L3	Rodentia	Sciuridae	Xerinae	Otospermophilus	?beecheyi	rt p4
39916	13	A3/L3	Rodentia	Sciuridae	Xerinae	Otospermophilus	?beecheyi	rt m3
39917	13	A3/L3	Rodentia	Sciuridae	Xerinae	Otospermophilus	?beecheyi	partial lower lt molar
39918	13	A3/L3	Rodentia	Sciuridae	Xerinae	Otospermophilus	?beecheyi	lt P4
39919	13	A3/L3	Rodentia	Geomyidae	Thomomyinae	Thomomys	sp	partial M1/M2
39920	13	A3/L3	Rodentia	Geomyidae	Thomomyinae	Thomomys	sp	lt m1/m2
39924	13	A3/L3	Rodentia	Geomyidae	Thomomyinae	?Thomomys	sp	molar frag
39926	13	A3/L3	Rodentia	Cricetidae	Arvicolinae	Microtus	sp	partial rt M1
39927	13	A3/L3	Rodentia	Cricetidae	Arvicolinae	Microtus	sp	lt m2
39929	13	A3/L1	Lagomorpha	Leporidae		Sylvilagus	audubonii	rt p3 frag
39930	13	A3/L1	Lagomorpha	Leporidae		Sylvilagus	sp	lt p3
39931	13	A3/L1	Lagomorpha	Leporidae		Sylvilagus	sp	upper tooth frag
39932	13	A3/L1	Lagomorpha	Leporidae		Sylvilagus	sp	lower lt tooth
39933	13	A3/L1	Lagomorpha	Leporidae		Sylvilagus	sp	lower rt tooth
39934	13	A3/L1	Lagomorpha	Leporidae		Sylvilagus	sp	lower rt tooth frag
39935	13	A3/L1	Lagomorpha	Leporidae		Sylvilagus	sp	upper tooth frag
39936	13	A3/L1	Lagomorpha	Leporidae		?Sylvilagus	sp	tooth frag
39937	13	A3/L1	Lagomorpha	Leporidae		Sylvilagus	sp	lower m3 frag
39938	13	A3/L1	Rodentia	Cricetidae	Arvicolinae	Microtus	sp	rt M3 frag
39939	13	A3/L1	Rodentia	Cricetidae	Arvicolinae	Microtus	sp	molar frag
39940	13	A3/L1	Rodentia	Cricetidae	Arvicolinae	Microtus	sp	molar frag
39941	13	A3/L1	Rodentia	Sciuridae	Xerinae	Otospermophilus	?beecheyi	upper rt P4
39942	13	A3/L1	Rodentia	Sciuridae	Xerinae			partial lt M1/M2
39943	13	A3/L1	Rodentia	Sciuridae	Xerinae	Otospermophilus	?beecheyi	rt M1/M2
39944	13	A3/L1	Rodentia	Sciuridae	Xerinae	Otospermophilus	?beecheyi	lt M3
39945	13	A3/L1	Rodentia	Sciuridae	Xerinae			lt p4

39946	13	A3/L1	Rodentia	Sciuridae	Xerinae	Neotamias/Tamias	sp	rt M1/M2
39947	13	A3/L1	Rodentia	?Sciuridae	Xerinae			tooth frag
39948	13	A3/L1	Carnivora	Mustelidae	Mustelinae	Mustela	frenata	rt P3
39950	13	A3/L1	Rodentia	Heteromyidae	Dipodomyinae	Dipodomys	sp	m1/m2
39951	13	A3/L1	Rodentia	Heteromyidae	Dipodomyinae	Dipodomys	sp	partial m1/m2
39956	13	A2/L1	Rodentia	Cricetidae	Arvicolinae	Microtus	sp	rt m1
39957	13	A2/L1	Rodentia	Cricetidae	Arvicolinae	cf Microtus	sp	molar frag
39958	13	A2/L1	Lagomorpha	Leporidae		Sylvilagus	sp	lower tooth frag
39959	13	A2/L1	Lagomorpha	Leporidae		Sylvilagus	sp	lower rt tooth
39960	13	A2/L1	Lagomorpha	Leporidae		Sylvilagus	sp	upper tooth frag
39961	13	A2/L1	Lagomorpha	Leporidae		Sylvilagus	sp	lower tooth frag
39962	13	A2/L1	Lagomorpha	Leporidae		Sylvilagus	sp	upper tooth frag
39963	13	A2/L1	Lagomorpha	Leporidae		?Sylvilagus	sp	tooth frag
39964	13	A2/L1	Lagomorpha	Leporidae		?Sylvilagus	sp	tooth frag
39965	13	A2/L1	Rodentia	Heteromyidae	Dipodomyinae	Dipodomys	sp	M1/M2
39968	13	A2/L1	Rodentia	Sciuridae	Xerinae	Otospermophilus	?beecheyi	lt p4
39969	13	A2/L1	Rodentia	Sciuridae	Xerinae			p4 frag
39971	13	A2/L1	Eulipotyphla	Soricidae	Soricinae			lt posterior dentary w/ m2
39974	13	B2/L1	Lagomorpha	Leporidae		Sylvilagus	sp	lower rt tooth
39975	13	B2/L1	Lagomorpha	Leporidae		Sylvilagus	sp	lower lt tooth
39976	13	B2/L1	Lagomorpha	Leporidae		Sylvilagus	sp	rt P2
39977	13	B2/L1	Lagomorpha	Leporidae		Sylvilagus	sp	upper tooth frag
39978	13	B2/L1	Lagomorpha	Leporidae		Sylvilagus	sp	rt p3
39979	13	B2/L1	Lagomorpha	Leporidae		Sylvilagus	sp	upper tooth frag
39980	13	B2/L1	Lagomorpha	Leporidae		Sylvilagus	sp	upper tooth frag
39981	13	B2/L1	Lagomorpha	Leporidae		Sylvilagus	sp	lower tooth frag
39982	13	B2/L1	Lagomorpha	Leporidae		Sylvilagus	sp	upper tooth frag
39983	13	B2/L1	Lagomorpha	Leporidae		Sylvilagus	sp	maxilla frag
39984	13	B2/L1	Lagomorpha	Leporidae		Sylvilagus	sp	lt maxilla frag

39985	13	B2/L1	Lagomorpha	Leporidae		Sylvilagus	sp	upper tooth frag
39986	13	B2/L1	Lagomorpha	Leporidae		Sylvilagus	sp	upper tooth frag
39987	13	B2/L1	Lagomorpha	Leporidae		?Sylvilagus	sp	tooth frag
39988	13	B2/L1	Lagomorpha	Leporidae		?Sylvilagus	sp	tooth frag
39989	13	B2/L1	Rodentia	Cricetidae	Neotominae	?Neotoma	sp	molar frag
39990	13	B2/L1	Rodentia	Sciuridae	Xerinae	Otospermophilus	?beecheyi	lt M1/M2
39991	13	B2/L1	Rodentia	Sciuridae	Xerinae	Otospermophilus	?beecheyi	rt M1/M2
39992	13	B2/L1	Rodentia	Sciuridae	Xerinae	Otospermophilus	?beecheyi	lt M3
39993	13	B2/L1	Rodentia	Sciuridae	Xerinae			upper tooth frag
39994	13	B2/L1	Rodentia	Sciuridae	Xerinae	Otospermophilus	?beecheyi	partial lt dentary
39997	13	B2/L1	Rodentia	Geomyidae	Thomomyinae	?Thomomys	sp	molar
39998	13	B2/L1	Rodentia	Heteromyidae	Dipodomyinae	Dipodomys	sp	lower molar
40001	13	B2/L1	Rodentia	Heteromyidae	Dipodomyinae	Dipodomys	sp	rt? p4
40008	13	B3/L1	Rodentia	Cricetidae	Arvicolinae	Microtus	sp	rt m1
40009	13	B3/L1	Rodentia	Heteromyidae	Dipodomyinae	Dipodomys	sp	rt p4
40011	13	B3/L1	Rodentia	Heteromyidae	Dipodomyinae	Dipodomys	sp	molar
40013	13	B3/L1	Lagomorpha	Leporidae		Sylvilagus	sp	upper tooth frag
40014	13	B3/L1	Rodentia	Cricetidae	Arvicolinae	Microtus	sp	lower rt m1 frag
40015	13	B3/L1	Lagomorpha	Leporidae		Sylvilagus	sp	tooth frag
40016	13	B3/L1	Rodentia	Sciuridae	Xerinae			rt p4
40017	13	B3/L1	Rodentia	Sciuridae	Xerinae			rt p4
40018	13	B3/L1	Rodentia	Sciuridae	Xerinae			lower molar frag
40019	13	B3/L1	Rodentia	Sciuridae	Xerinae			lower tooth frag
40022	13	A2/L2	Rodentia	Cricetidae	Arvicolinae	Microtus	sp	rt M1
40023	13	A2/L2	Rodentia	Cricetidae	Arvicolinae	Microtus	sp	partial lt m1
40024	13	A2/L2	Rodentia	Cricetidae	Arvicolinae	Microtus	sp	rt M2
40025	13	A2/L2	Rodentia	Cricetidae	Arvicolinae	Microtus	sp	rt dentary frag
40026	13	A2/L2	Rodentia	Cricetidae	Arvicolinae	Microtus	sp	rt m1 frag
40027	13	A2/L2	Rodentia	Cricetidae	Arvicolinae	cf Microtus	sp	molar frag

40028	13	A2/L2	Rodentia	Cricetidae	Arvicolinae	cf Microtus	sp	molar frag
40029	13	A2/L2	Rodentia	Sciuridae	Xerinae	Otospermophilus	?beecheyi	rt p4
40030	13	A2/L2	Rodentia	Sciuridae	Xerinae	Otospermophilus	?beecheyi	lt m1/m2
40031	13	A2/L2	Rodentia	Sciuridae	Xerinae	Neotamias/Tamias	sp	rt dp4
40032	13	A2/L2	Rodentia	Sciuridae	Xerinae			upper tooth frag
40033	13	A2/L2	Rodentia	Sciuridae	Xerinae			upper tooth frag
40034	13	A2/L2	Rodentia	Heteromyidae	Dipodomyinae	Dipodomys	sp	lt p4
40037	13	A2/L2	Lagomorpha	Leporidae		Sylvilagus	sp	upper tooth frag
40038	13	A2/L2	Lagomorpha	Leporidae		Sylvilagus	sp	lt P2
40039	13	A2/L2	Lagomorpha	Leporidae		Sylvilagus	audubonii	partial lt p3
40040	13	A2/L2	Lagomorpha	Leporidae		Sylvilagus	sp	upper rt tooth
40041	13	A2/L2	Lagomorpha	Leporidae		Sylvilagus	sp	lower tooth frag
40042	13	A2/L2	Lagomorpha	Leporidae		Sylvilagus	sp	lower tooth frag
40043	13	A2/L2	Lagomorpha	Leporidae		Sylvilagus	sp	m3
40044	13	A2/L2	Lagomorpha	Leporidae		Sylvilagus	sp	lower tooth frag
40045	13	A2/L2	Lagomorpha	Leporidae		Sylvilagus	sp	tooth frag
40046	13	A2/L2	Lagomorpha	Leporidae		Sylvilagus	sp	upper tooth frag
40047	13	A3/L2	Rodentia	Heteromyidae	Dipodomyinae	Dipodomys	sp	lt? p4
40048	13	A3/L2	Rodentia	Heteromyidae	Dipodomyinae	Dipodomys	sp	molar
40055	13	A3/L2	Rodentia	Sciuridae	Xerinae	Neotamias/Tamias	sp	rt p4
40056	13	A3/L2	Rodentia	Sciuridae	Xerinae	Otospermophilus	?beecheyi	rt dp4
40057	13	A3/L2	Rodentia	Sciuridae	Xerinae	Otospermophilus	?beecheyi	rt dp4
40058	13	A3/L2	Rodentia	Sciuridae	Xerinae	Otospermophilus	?beecheyi	rt m1/m2
40059	13	A3/L2	Rodentia	Sciuridae	Xerinae	Otospermophilus	?beecheyi	lt M1/M2
40060	13	A3/L2	Rodentia	Sciuridae	Xerinae	Otospermophilus	?beecheyi	lt M1/M2
40061	13	A3/L2	Rodentia	Sciuridae	Xerinae	Otospermophilus	?beecheyi	lt M1/M2
40062	13	A3/L2	Rodentia	Sciuridae	Xerinae	Otospermophilus	?beecheyi	lt M1/M2
40063	13	A3/L2	Rodentia	Sciuridae	Xerinae	Otospermophilus	?beecheyi	rt M3
40064	13	A3/L2	Rodentia	Sciuridae	Xerinae	Otospermophilus	?beecheyi	rt M3 frag
40065	13	A3/L2	Rodentia	Sciuridae	Xerinae	Otospermophilus	?beecheyi	lt M3 frag

40066	13	A3/L2	Rodentia	Sciuridae	Xerinae	Otospermophilus	?beecheyi	lt P4 frag
40067	13	A3/L2	Rodentia	Sciuridae	Xerinae	Otospermophilus	?beecheyi	rt P4
40068	13	A3/L2	Rodentia	Sciuridae	Xerinae	Otospermophilus	?beecheyi	rt P4 frag
40069	13	A3/L2	Rodentia	Sciuridae	Xerinae			upper tooth frag
40070	13	A3/L2	Rodentia	Sciuridae	Xerinae			upper tooth frag
40071	13	A3/L2	Rodentia	Sciuridae	Xerinae			upper tooth frag
40072	13	A3/L2	Rodentia	Sciuridae	Xerinae			upper tooth frag
40073	13	A3/L2	Rodentia	Geomyidae	Thomomyinae	Thomomys	?bottae	rt p4
40074	13	A3/L2	Lagomorpha	Leporidae		Sylvilagus	sp	upper tooth
40075	13	A3/L2	Rodentia	Cricetidae	Neotominae	Neotoma	sp	lt molar - m2?
40076	13	A3/L2	Rodentia	Cricetidae	Neotominae	Neotoma	sp	molar frag - lt M1?
40077	13	A3/L2	Rodentia	Cricetidae	Arvicolinae	Microtus	sp	lower molar frag
40078	13	A3/L2	Rodentia	Cricetidae	Arvicolinae	Microtus	sp	lower molar frag
40079	13	A3/L2	Rodentia	Cricetidae	Arvicolinae	Microtus	sp	lower molar frag
40080	13	A3/L2	Rodentia	Cricetidae	Arvicolinae	Microtus	sp	lower molar frag
40081	13	A3/L2	Rodentia	Cricetidae	Arvicolinae	Microtus	sp	lower molar frag
40082	13	A3/L2	Rodentia	Cricetidae	Arvicolinae	Microtus	sp	lower molar frag
40083	13	A3/L2	Rodentia	Cricetidae	Arvicolinae	Microtus	sp	lower molar frag
40084	13	A3/L2	Rodentia	Cricetidae	Arvicolinae	Microtus	sp	lower molar frag
40085	13	A3/L2	Rodentia	Cricetidae	Arvicolinae	Microtus	sp	lower molar frag
40086	13	A3/L2	Rodentia	Cricetidae	Arvicolinae	Microtus	sp	lower molar frag
40087	13	A3/L2	Rodentia	Cricetidae	Arvicolinae	Microtus	sp	lower molar frag
40088	13	A3/L2	Rodentia	Cricetidae	Arvicolinae	Microtus	sp	lower molar frag

40089	13	A3/L2	Rodentia	Cricetidae	Arvicolinae	Microtus	sp	lower molar frag
40090	13	A3/L2	Rodentia	Cricetidae	Arvicolinae	Microtus	sp	lt m1
40091	13	A3/L2	Rodentia	Cricetidae	Arvicolinae	Microtus	sp	lt m1
40092	13	A3/L2	Rodentia	Cricetidae	Arvicolinae	Microtus	sp	partial lt m1
40093	13	A3/L2	Rodentia	Cricetidae	Arvicolinae	Microtus	sp	partial rt m1
40094	13	A3/L2	Rodentia	Cricetidae	Arvicolinae	Microtus	sp	rt m1 frag
40095	13	A3/L2	Rodentia	Cricetidae	Arvicolinae	Microtus	sp	rt m1 frag
40096	13	A3/L2	Rodentia	Cricetidae	Arvicolinae	Microtus	sp	rt m3
40097	13	A3/L2	Rodentia	Cricetidae	Arvicolinae	Microtus	sp	lt M1
40098	13	A3/L2	Rodentia	Cricetidae	Arvicolinae	Microtus	sp	rt M1
40099	13	A3/L2	Rodentia	Cricetidae	Arvicolinae	Microtus	sp	lt M2
40100	13	A3/L2	Rodentia	Cricetidae	Arvicolinae	Microtus	sp	rt M2
40101	13	A3/L2	Rodentia	Cricetidae	Arvicolinae	Microtus	sp	rt M2
40102	13	A3/L2	Rodentia	Cricetidae	Arvicolinae	Microtus	sp	lt M3
40103	13	A3/L2	Rodentia	Cricetidae	Arvicolinae	Microtus	sp	lt M3
40104	13	A3/L2	Rodentia	Cricetidae	Arvicolinae	Microtus	sp	lt M3
40105	13	A3/L2	Rodentia	Cricetidae	Arvicolinae	Microtus	sp	rt M3
40106	13	A3/L2	Rodentia	Cricetidae	Arvicolinae	Microtus	sp	rt M3
40107	13	A3/L2	Rodentia	Cricetidae	Arvicolinae	Microtus	sp	molar frag
40108	13	A3/L2	Lagomorpha	Leporidae		?Sylvilagus	sp	tooth frag
40109	13	A3/L2	Lagomorpha	Leporidae		?Sylvilagus	sp	tooth frag
40110	13	A3/L2	Lagomorpha	Leporidae		Sylvilagus	audubonii	partial rt p3
40111	13	A3/L2	Lagomorpha	Leporidae		Sylvilagus	?audubonii	lt p3
40112	13	A3/L2	Lagomorpha	Leporidae		Sylvilagus	sp	lower lt tooth
40113	13	A3/L2	Lagomorpha	Leporidae		Sylvilagus	sp	lower rt tooth
40114	13	A3/L2	Lagomorpha	Leporidae		Sylvilagus	sp	lower lt tooth
40115	13	A3/L2	Lagomorpha	Leporidae		Sylvilagus	sp	lower rt tooth
40116	13	A3/L2	Lagomorpha	Leporidae		Sylvilagus	sp	m3
40117	13	A3/L2	Lagomorpha	Leporidae		Sylvilagus	sp	lower tooth frag

40118	13	A3/L2	Lagomorpha	Leporidae		Sylvilagus	sp	lower tooth frag
40119	13	A3/L2	Lagomorpha	Leporidae		Sylvilagus	sp	lower tooth frag
40120	13	A3/L2	Lagomorpha	Leporidae		Sylvilagus	sp	lower tooth frag
40121	13	A3/L2	Lagomorpha	Leporidae		Sylvilagus	sp	lower tooth frag
40122	13	A3/L2	Lagomorpha	Leporidae		Sylvilagus	sp	lower tooth frag
40123	13	A3/L2	Lagomorpha	Leporidae		Sylvilagus	sp	lower tooth frag
40124	13	A3/L2	Lagomorpha	Leporidae		Sylvilagus	sp	lt P2
40125	13	A3/L2	Lagomorpha	Leporidae		Sylvilagus	sp	lt P2
40126	13	A3/L2	Lagomorpha	Leporidae		Sylvilagus	sp	upper lt tooth
40127	13	A3/L2	Lagomorpha	Leporidae		Sylvilagus	sp	upper lt tooth
40128	13	A3/L2	Lagomorpha	Leporidae		Sylvilagus	sp	upper right tooth
40129	13	A3/L2	Lagomorpha	Leporidae		Sylvilagus	sp	upper tooth frag
40130	13	A3/L2	Lagomorpha	Leporidae		Sylvilagus	sp	upper tooth frag
40131	13	A3/L2	Lagomorpha	Leporidae		Sylvilagus	sp	upper tooth frag
40132	13	A3/L2	Lagomorpha	Leporidae		Sylvilagus	sp	upper tooth frag
40133	13	A3/L2	Lagomorpha	Leporidae		Sylvilagus	sp	upper tooth frag
40134	13	A3/L2	Lagomorpha	Leporidae		Sylvilagus	sp	upper tooth frag
40135	13	A3/L2	Lagomorpha	Leporidae		Sylvilagus	sp	upper tooth frag
40136	13	A3/L2	Lagomorpha	Leporidae		Sylvilagus	sp	upper tooth frag
40137	13	A3/L2	Lagomorpha	Leporidae		Sylvilagus	sp	upper tooth frag
40138	13	B2/L2	Rodentia	Geomyidae	Thomomyinae	Thomomys	sp	lt M1/M2
40140	13	B2/L2	Rodentia	Heteromyidae	Dipodomyinae	Dipodomys	sp	lt m1/m2
40141	13	B2/L2	Rodentia	Heteromyidae	Dipodomyinae	Dipodomys	sp	lt m1/m2
40142	13	B2/L2	Rodentia	Heteromyidae	Dipodomyinae	Dipodomys	sp	lower lt molar - m2?
40143	13	B2/L2	Rodentia	Heteromyidae	Dipodomyinae	Dipodomys	sp	lt M1/M2
40144	13	B2/L2	Rodentia	Heteromyidae	Dipodomyinae	?Dipodomys	sp	molar
40149	13	B2/L2	Rodentia	Sciuridae	Xerinae	Otospermophilus	?beecheyi	lt m3
40150	13	B2/L2	Rodentia	Sciuridae	Xerinae	Otospermophilus	?beecheyi	lt m1/m2
40152	13	B2/L2	Rodentia	Sciuridae	Xerinae	Neotamias/Tamias	sp	lt P4

40153	13	B2/L2	Rodentia	Sciuridae	Xerinae	?Neotamias/Tamias	sp	lt P4
40154	13	B2/L2	Rodentia	Sciuridae	Xerinae	Otospermophilus	?beecheyi	rt M1/M2
40155	13	B2/L2	Rodentia	Sciuridae	Xerinae			rt upper molar frag
40156	13	B2/L2	Rodentia	Sciuridae	Xerinae			lt upper molar frag
40157	13	B2/L2	Rodentia	Sciuridae	Xerinae	Otospermophilus	?beecheyi	rt M1/M2
40158	13	B2/L2	Rodentia	Cricetidae	Neotominae	Neotoma	sp	rt m1
40159	13	B2/L2	Rodentia	Cricetidae	Neotominae	Neotoma	sp	molar frag
40160	13	B2/L2	Rodentia	Cricetidae	Arvicolinae	cf Microtus	sp	rt anterior dentary frag
40161	13	B2/L2	Rodentia	Cricetidae	Arvicolinae	Microtus	sp	rt m1
40162	13	B2/L2	Rodentia	Cricetidae	Arvicolinae	Microtus	sp	rt M3
40163	13	B2/L2	Rodentia	Cricetidae	Arvicolinae	Microtus	sp	molar frag
40164	13	B2/L2	Rodentia	Cricetidae	Arvicolinae	Microtus	sp	molar frag
40165	13	B2/L2	Rodentia	Geomyidae	Thomomyinae	Thomomys	sp	lt M1/M2
40166	13	B2/L2	Lagomorpha	Leporidae		Sylvilagus	audubonii	rt p3
40167	13	B2/L2	Lagomorpha	Leporidae		Sylvilagus	audubonii	lt p3
40168	13	B2/L2	Lagomorpha	Leporidae		Sylvilagus	audubonii	partial rt p3
40169	13	B2/L2	Lagomorpha	Leporidae		Sylvilagus	sp	lower lt tooth
40170	13	B2/L2	Lagomorpha	Leporidae		Sylvilagus	sp	lower lt tooth
40171	13	B2/L2	Lagomorpha	Leporidae		Sylvilagus	sp	lower lt tooth
40172	13	B2/L2	Lagomorpha	Leporidae		Sylvilagus	sp	lower lt tooth
40173	13	B2/L2	Lagomorpha	Leporidae		Sylvilagus	sp	partial lower rt? tooth
40174	13	B2/L2	Lagomorpha	Leporidae		Sylvilagus	sp	lower lt tooth
40175	13	B2/L2	Lagomorpha	Leporidae		Sylvilagus	sp	m3
40176	13	B2/L2	Lagomorpha	Leporidae		Sylvilagus	sp	m3
40177	13	B2/L2	Lagomorpha	Leporidae		Sylvilagus	sp	lower tooth frag
40178	13	B2/L2	Lagomorpha	Leporidae		?Sylvilagus	sp	maxilla frag
40179	13	B2/L2	Lagomorpha	Leporidae		Sylvilagus	sp	lt P2
40180	13	B2/L2	Lagomorpha	Leporidae		Sylvilagus	sp	lt P2

40181	13	B2/L2	Lagomorpha	Leporidae		Sylvilagus	sp	lt P2
40182	13	B2/L2	Lagomorpha	Leporidae		Sylvilagus	sp	upper right tooth
40183	13	B2/L2	Lagomorpha	Leporidae		Sylvilagus	sp	partial upper lt tooth
40184	13	B2/L2	Lagomorpha	Leporidae		Sylvilagus	sp	upper tooth frag
40185	13	B2/L2	Lagomorpha	Leporidae		Sylvilagus	sp	upper tooth frag
40186	13	B2/L2	Lagomorpha	Leporidae		Sylvilagus	sp	upper tooth frag
40187	13	B2/L2	Lagomorpha	Leporidae		Sylvilagus	sp	upper tooth frag
40188	13	B2/L2	Lagomorpha	Leporidae		Sylvilagus	sp	upper tooth frag
40189	13	B2/L2	Lagomorpha	Leporidae		Sylvilagus	sp	lt p3 frag
40190	13	B2/L2	Lagomorpha	Leporidae		?Sylvilagus	sp	lower tooth frag
40196	13	B3/L2	Rodentia	Heteromyidae	Dipodomyinae	Dipodomys	sp	upper molar
40199	13	B3/L2	Rodentia	Cricetidae	Arvicolinae	Microtus	sp	rt m3
40200	13	B3/L2	Rodentia	Scuiridae	Xerinae	Otospermophilus	?beecheyi	lt dentary frag w/ m3
40201	13	B3/L2	Rodentia	Scuiridae	Xerinae	Otospermophilus	?beecheyi	rt p4
40202	13	B3/L2	Rodentia	Scuiridae	Xerinae	Otospermophilus	?beecheyi	rt m1/m2
40208	13	B3/L2	Lagomorpha	Leporidae		Sylvilagus	sp	rt dentary frag w/ p4
40209	13	B3/L2	Lagomorpha	Leporidae		Sylvilagus	audubonii	lt p3
40210	13	B3/L2	Lagomorpha	Leporidae		Sylvilagus	audubonii	rt p3
40211	13	B3/L2	Lagomorpha	Leporidae		Sylvilagus	audubonii	rt p3
40212	13	B3/L2	Lagomorpha	Leporidae		Sylvilagus	audubonii	rt p3 frag
40213	13	B3/L2	Lagomorpha	Leporidae		Sylvilagus	sp	lower lt tooth
40214	13	B3/L2	Lagomorpha	Leporidae		Sylvilagus	sp	lower lt tooth
40215	13	B3/L2	Lagomorpha	Leporidae		Sylvilagus	sp	lower lt tooth
40216	13	B3/L2	Lagomorpha	Leporidae		Sylvilagus	sp	lower lt tooth
40217	13	B3/L2	Lagomorpha	Leporidae		Sylvilagus	sp	lower lt tooth
40218	13	B3/L2	Lagomorpha	Leporidae		Sylvilagus	sp	lower lt tooth
40219	13	B3/L2	Lagomorpha	Leporidae		Sylvilagus	sp	lower rt tooth
40220	13	B3/L2	Lagomorpha	Leporidae		Sylvilagus	sp	lower rt tooth

40221	13	B3/L2	Lagomorpha	Leporidae		Sylvilagus	sp	lower rt tooth
40222	13	B3/L2	Lagomorpha	Leporidae		Sylvilagus	sp	m3
40223	13	B3/L2	Lagomorpha	Leporidae		Sylvilagus	sp	lower tooth frag
40224	13	B3/L2	Lagomorpha	Leporidae		Sylvilagus	sp	lower tooth frag
40225	13	B3/L2	Lagomorpha	Leporidae		Sylvilagus	sp	lower tooth frag
40226	13	B3/L2	Lagomorpha	Leporidae		Sylvilagus	sp	lower tooth frag
40227	13	B3/L2	Lagomorpha	Leporidae		Sylvilagus	sp	lower tooth frag
40228	13	B3/L2	Lagomorpha	Leporidae		Sylvilagus	sp	lower tooth frag
40229	13	B3/L2	Lagomorpha	Leporidae		Sylvilagus	sp	upper rt tooth
40230	13	B3/L2	Lagomorpha	Leporidae		Sylvilagus	sp	lt P2
40231	13	B3/L2	Lagomorpha	Leporidae		Sylvilagus	sp	upper tooth frag
40232	13	B3/L2	Lagomorpha	Leporidae		Sylvilagus	sp	upper tooth frag
40233	13	B3/L2	Lagomorpha	Leporidae		Sylvilagus	sp	upper tooth frag
40234	13	B3/L2	Lagomorpha	Leporidae		Sylvilagus	sp	upper tooth frag
40235	13	B3/L2	Lagomorpha	Leporidae		Sylvilagus	sp	upper tooth frag
40236	13	B3/L2	Lagomorpha	Leporidae		Sylvilagus	sp	upper tooth frag
40237	13	B3/L2	Lagomorpha	Leporidae		Sylvilagus	sp	upper tooth frag
40251	13	A3/L3	Carnivora	Mustelidae		Mustela	frenata	lt P2
40252	13	B2/L3	Rodentia	Cricetidae	Arvicolinae	Microtus	sp	parital lt m1
40253	13	B2/L3	Rodentia	Cricetidae	Arvicolinae	Microtus	sp	rt M2
40254	13	B2/L3	Rodentia	Cricetidae	Arvicolinae	Microtus	sp	rt M2
40255	13	B2/L3	Rodentia	Cricetidae	Arvicolinae	Microtus	sp	rt m3
40256	13	B2/L3	Rodentia	Cricetidae	Arvicolinae	Microtus	sp	lt m1 frag
40257	13	B2/L3	Rodentia	Cricetidae	Arvicolinae	Microtus	sp	molar frag
40258	13	B2/L3	Rodentia	Cricetidae	Arvicolinae	Microtus	sp	molar frag
40259	13	B2/L3	Rodentia	Cricetidae	Arvicolinae	Microtus	sp	molar frag
40260	13	B2/L3	Rodentia	Cricetidae	Arvicolinae	Microtus	sp	molar frag
40261	13	B2/L3	Rodentia	Cricetidae	Arvicolinae	Microtus	sp	molar frag
40262	13	B2/L3	Rodentia	Cricetidae	Arvicolinae	Microtus	sp	molar frag
40263	13	B2/L3	Rodentia	Cricetidae	Arvicolinae	Microtus	sp	molar frag

40264	13	B2/L3	Rodentia	Heteromyidae	Dipodomyinae	Dipodomys	sp	lt dp4
40265	13	B2/L3	Rodentia	Geomyidae	Thomomyinae	Thomomys	sp	rt P4
40266	13	B2/L3	Rodentia	Geomyidae	Thomomyinae	Thomomys	sp	lt m3
40267	13	B2/L3	Rodentia	Geomyidae	Thomomyinae	Thomomys	sp	lower molar
40268	13	B2/L3	Rodentia	Geomyidae	Thomomyinae	Thomomys	sp	molar frag
40269	13	B2/L3	Rodentia	Heteromyidae	Dipodomyinae	Dipodomys	sp	molar
40270	13	B2/L3	Rodentia	Heteromyidae	Dipodomyinae	Dipodomys	sp	molar
40271	13	B2/L3	Rodentia	Heteromyidae	Dipodomyinae	Dipodomys	sp	molar
40272	13	B2/L3	Rodentia	Heteromyidae	Dipodomyinae	Dipodomys	sp	molar frag
40273	13	B2/L3	Rodentia	Heteromyidae	Dipodomyinae	Dipodomys	sp	molar
40274	13	B2/L3	Rodentia	Heteromyidae	Dipodomyinae	Dipodomys	sp	molar
40275	13	B2/L3	Rodentia	Heteromyidae	Dipodomyinae	Dipodomys	sp	molar
40276	13	B2/L3	Rodentia	Heteromyidae	Dipodomyinae	Dipodomys	sp	molar
40277	13	B2/L3	Rodentia	Heteromyidae	Dipodomyinae	Dipodomys	sp	molar
40278	13	B2/L3	Rodentia	Heteromyidae	Dipodomyinae	Dipodomys	sp	molar
40279	13	B2/L3	Rodentia	Heteromyidae	Dipodomyinae	Dipodomys	sp	molar
40280	13	B2/L3	Rodentia	Heteromyidae	Dipodomyinae	Dipodomys	sp	molar
40284	13	B2/L3	Lagomorpha	Leporidae		Sylvilagus	audubonii	lt p3
40285	13	B2/L3	Lagomorpha	Leporidae		Sylvilagus	audubonii	lt p3
40286	13	B2/L3	Lagomorpha	Leporidae		Sylvilagus	audubonii	lt p3
40287	13	B2/L3	Lagomorpha	Leporidae		Sylvilagus	audubonii	lt p3
40288	13	B2/L3	Lagomorpha	Leporidae		Sylvilagus	audubonii	lt p3 frag
40289	13	B2/L3	Lagomorpha	Leporidae		Sylvilagus	sp	rt p3 frag
40290	13	B2/L3	Lagomorpha	Leporidae		Sylvilagus	sp	lt P2
40291	13	B2/L3	Lagomorpha	Leporidae		Sylvilagus	audubonii	rt p3 frag
40292	13	B2/L3	Lagomorpha	Leporidae		Sylvilagus	sp	lt p3 frag
40293	13	B2/L3	Lagomorpha	Leporidae		Sylvilagus	sp	m3
40294	13	B2/L3	Lagomorpha	Leporidae		Sylvilagus	sp	m3
40295	13	B2/L3	Lagomorpha	Leporidae		Sylvilagus	sp	lower lt tooth
40296	13	B2/L3	Lagomorpha	Leporidae		Sylvilagus	sp	lower lt tooth

40297	13	B2/L3	Lagomorpha	Leporidae		Sylvilagus	sp	lower lt tooth
40298	13	B2/L3	Lagomorpha	Leporidae		Sylvilagus	sp	lower lt tooth
40299	13	B2/L3	Lagomorpha	Leporidae		Sylvilagus	sp	lower rt tooth
40300	13	B2/L3	Lagomorpha	Leporidae		Sylvilagus	sp	lower rt tooth
40301	13	B2/L3	Lagomorpha	Leporidae		Sylvilagus	sp	lower rt tooth
40302	13	B2/L3	Lagomorpha	Leporidae		Sylvilagus	sp	lower tooth frag
40303	13	B2/L3	Lagomorpha	Leporidae		Sylvilagus	sp	lower tooth frag
40304	13	B2/L3	Lagomorpha	Leporidae		Sylvilagus	sp	lower tooth frag
40305	13	B2/L3	Lagomorpha	Leporidae		Sylvilagus	sp	lower tooth frag
40306	13	B2/L3	Lagomorpha	Leporidae		Sylvilagus	sp	lower tooth frag
40307	13	B2/L3	Lagomorpha	Leporidae		Sylvilagus	sp	lower tooth frag
40308	13	B2/L3	Lagomorpha	Leporidae		Sylvilagus	sp	lower tooth frag
40309	13	B2/L3	Lagomorpha	Leporidae		Sylvilagus	sp	lower tooth frag
40310	13	B2/L3	Lagomorpha	Leporidae		Sylvilagus	sp	lower tooth frag
40311	13	B2/L3	Lagomorpha	Leporidae		Sylvilagus	sp	lt P2
40312	13	B2/L3	Lagomorpha	Leporidae		Sylvilagus	sp	rt P2
40313	13	B2/L3	Lagomorpha	Leporidae		Sylvilagus	sp	rt P2 frag
40314	13	B2/L3	Lagomorpha	Leporidae		Sylvilagus	sp	upper lt tooth
40315	13	B2/L3	Lagomorpha	Leporidae		Sylvilagus	sp	upper rt tooth
40316	13	B2/L3	Lagomorpha	Leporidae		Sylvilagus	sp	upper lt tooth frag
40317	13	B2/L3	Lagomorpha	Leporidae		Sylvilagus	sp	upper rt tooth frag
40318	13	B2/L3	Lagomorpha	Leporidae		Sylvilagus	sp	upper tooth frag
40319	13	B2/L3	Lagomorpha	Leporidae		Sylvilagus	sp	upper tooth frag
40320	13	B2/L3	Lagomorpha	Leporidae		Sylvilagus	sp	upper tooth frag
40321	13	B2/L3	Lagomorpha	Leporidae		Sylvilagus	sp	upper tooth frag
40322	13	B2/L3	Lagomorpha	Leporidae		Sylvilagus	sp	upper tooth frag
40323	13	B2/L3	Lagomorpha	Leporidae		Sylvilagus	sp	upper tooth frag
40324	13	B2/L3	Lagomorpha	Leporidae		Sylvilagus	sp	upper tooth frag
40325	13	B2/L3	Lagomorpha	Leporidae		Sylvilagus	sp	upper tooth frag

40326	13	B2/L3	Lagomorpha	Leporidae		Sylvilagus	sp	upper tooth frag
40327	13	B2/L3	Lagomorpha	Leporidae		Sylvilagus	sp	upper tooth frag
40328	13	B2/L3	Lagomorpha	Leporidae		Sylvilagus	sp	upper tooth frag
40329	13	B2/L3	Lagomorpha	Leporidae		Sylvilagus	sp	upper tooth frag
40330	13	B2/L3	Lagomorpha	Leporidae		Sylvilagus	sp	upper tooth frag
40331	13	B2/L3	Lagomorpha	Leporidae		Sylvilagus	sp	upper tooth frag
40332	13	B2/L3	Lagomorpha	Leporidae		Sylvilagus	sp	upper tooth frag
40333	13	B2/L3	Lagomorpha	Leporidae		Sylvilagus	sp	lower tooth
40334	13	B2/L3	Lagomorpha	Leporidae		Sylvilagus	sp	upper tooth
40352	13	B2/L3	Rodentia	Cricetidae	Neotominae	Neotoma	sp	molar frag
40353	13	B2/L3	Rodentia	Sciuridae	Xerinae	Otospermophilus	?beecheyi	lt DP4
40354	13	B2/L3	Rodentia	Sciuridae	Xerinae	Otospermophilus	?beecheyi	lt M1/M2
40355	13	B2/L3	Rodentia	Sciuridae	Xerinae	Otospermophilus	?beecheyi	lt M1/M2
40357	13	B2/L3	Rodentia	Sciuridae	Xerinae	Otospermophilus	?beecheyi	rt DP4
40358	13	B2/L3	Rodentia	Sciuridae	Xerinae	Otospermophilus	?beecheyi	rt DP4
40359	13	B2/L3	Rodentia	Sciuridae	Xerinae	Otospermophilus	?beecheyi	rt M1/M2
40360	13	B2/L3	Rodentia	Sciuridae	Xerinae	Otospermophilus	?beecheyi	rt M3
40372	13	B2/L3	Rodentia	Sciuridae	Xerinae	Otospermophilus	?beecheyi	lt DP4
40373	13	B2/L3	Rodentia	Sciuridae	Xerinae	Otospermophilus	?beecheyi	lt dp4
40374	13	B2/L3	Rodentia	Sciuridae	Xerinae	Otospermophilus	?beecheyi	lt m1/m2
40375	13	B2/L3	Rodentia	Sciuridae	Xerinae	Otospermophilus	?beecheyi	rt dp4
40376	13	B2/L3	Rodentia	Sciuridae	Xerinae	Otospermophilus	?beecheyi	rt dp4
40377	13	B2/L3	Rodentia	Sciuridae	Xerinae	Otospermophilus	?beecheyi	rt dp4
40378	13	B2/L3	Rodentia	Sciuridae	Xerinae	Otospermophilus	?beecheyi	rt p4
40379	13	B2/L3	Rodentia	Sciuridae	Xerinae	Otospermophilus	?beecheyi	rt p4
40380	13	B2/L3	Rodentia	Sciuridae	Xerinae	Otospermophilus	?beecheyi	rt m1/m2
40381	13	B2/L3	Rodentia	Sciuridae	Xerinae	Otospermophilus	?beecheyi	rt m1/m2
40382	13	B2/L3	Rodentia	Sciuridae	Xerinae	Otospermophilus	?beecheyi	rt m3
40391	13	B2/L3	Eulipotyphla	Soricidae	Soricinae			partial rt dentary

40392	13	B2/L3	Eulipotyphla	Soricidae	Soricinae			rt M1/M2
40404	13	A3/L3	Rodentia	Cricetidae	Neotominae	Peromyscus	cf californicus	rt m1
40405	13	A3/L3	Rodentia	Cricetidae	Neotominae	?Peromyscus	sp	rt m1
40406	13	A3/L3	Rodentia	Cricetidae	Neotominae	Peromyscus	cf maniculatus	rt M1
40407	13	A3/L3	Rodentia	Cricetidae	Neotominae	?Peromyscus	sp	rt M1
40408	13	A3/L3	Rodentia	Cricetidae	Neotominae	Peromyscus	sp	rt m2
40409	13	A3/L3	Rodentia	Cricetidae	Neotominae	Peromyscus	cf maniculatus	lt M1
40410	13	A3/L3	Rodentia	Cricetidae	Neotominae	Peromyscus	sp	lt m2
40411	13	A3/L3	Rodentia	Cricetidae	Neotominae	Peromyscus	cf maniculatus	rt M1
40412	13	A3/L3	Rodentia	Cricetidae	Neotominae	Peromyscus	sp	rt m1
40413	13	A3/L3	Rodentia	Cricetidae	Neotominae	Peromyscus	sp	lt m1
40414	13	A3/L3	Rodentia	Cricetidae	Neotominae			rt M2
40415	13	A3/L3	Rodentia	Cricetidae	Neotominae	Peromyscus	sp	lt dentary w/ m2
40416	13	A3/L3	Rodentia	Cricetidae	Neotominae	Peromyscus	cf californicus	upper rt M2
40417	13	A3/L3	Rodentia	Cricetidae	Neotominae			lower molar
40418	13	A3/L1	Rodentia	Cricetidae	Neotominae	Peromyscus	sp	lt M1
40419	13	A3/L1	Rodentia	Cricetidae	Neotominae	Peromyscus	sp	rt m1
40420	13	A3/L1	Rodentia	Cricetidae	Neotominae	Peromyscus	sp	lt M1
40421	13	A3/L1	Rodentia	Cricetidae	Neotominae	Peromyscus	sp	rt m1
40422	13	A3/L1	Rodentia	Cricetidae	Neotominae	Peromyscus	sp	lt M2
40423	13	A3/L1	Rodentia	Cricetidae	Neotominae	Peromyscus	sp	lt M2
40424	13	A2/L1	Rodentia	Cricetidae	Neotominae	Peromyscus	sp	lt m1
40425	13	A2/L1	Rodentia	Cricetidae	Neotominae	Peromyscus	sp	rt M1
40426	13	A2/L1	Rodentia	Cricetidae	Neotominae	Peromyscus	sp	rt m2
40427	13	A2/L1	Rodentia	Cricetidae	Neotominae	?Peromyscus	sp	partial rt dentary
40428	13	A2/L1	Rodentia	Cricetidae	Neotominae	?Peromyscus	sp	rt maxilla frag

40429	13	B2/L1	Rodentia	Cricetidae	Neotominae	Peromyscus	sp	rt M1
40430	13	B2/L1	Rodentia	Cricetidae	Neotominae	?Peromyscus	sp	lt m2
40431	13	B2/L1	Rodentia	Cricetidae	Neotominae	Peromyscus	sp	lt M1
40432	13	B2/L1	Rodentia	Cricetidae	Neotominae	Peromyscus	sp	rt m2
40433	13	B2/L1	Rodentia	Cricetidae	Neotominae	?Peromyscus	sp	lt m1
40434	13	B2/L1	Rodentia	Cricetidae	Neotominae	Peromyscus	sp	lt m1
40435	13	B2/L1	Rodentia	Cricetidae	Neotominae	?Peromyscus	sp	rt m1
40436	13	B2/L1	Rodentia	Cricetidae	Neotominae	Peromyscus	sp	lt m1
40437	13	B2/L1	Rodentia	Cricetidae	Neotominae	?Peromyscus	sp	lt M2
40438	13	B2/L1	Rodentia	Cricetidae	Neotominae	?Peromyscus	sp	lt M2
40439	13	B2/L1	Rodentia	Cricetidae	Neotominae	Peromyscus	sp	lt M1
40440	13	B2/L1	Rodentia	Cricetidae	Neotominae	Peromyscus	sp	lt m2
40441	13	B2/L1	Rodentia	Cricetidae	Neotominae	Peromyscus	sp	rt m2
40442	13	B2/L1	Rodentia	Cricetidae	Neotominae	?Peromyscus	sp	lt maxilla frag
40443	13	B2/L1	Rodentia	Cricetidae	Neotominae	Peromyscus	sp	rt m1
40444	13	B2/L1	Rodentia	Cricetidae	Neotominae	Peromyscus	sp	lt m2
40445	13	B3/L1	Rodentia	Cricetidae	Neotominae	Peromyscus	cf californicus	lt M1
40446	13	B3/L1	Rodentia	Cricetidae	Neotominae	Peromyscus	sp	lt m1
40447	13	B3/L1	Rodentia	Cricetidae	Neotominae	Peromyscus	sp	lt m2
40448	13	A2/L2	Rodentia	Cricetidae	Neotominae	Peromyscus	sp	lt M1
40449	13	A2/L2	Rodentia	Cricetidae	Neotominae	Peromyscus	sp	lt m2
40450	13	A2/L2	Rodentia	Cricetidae	Neotominae	Peromyscus	cf maniculatus	rt m1
40451	13	A2/L2	Rodentia	Cricetidae	Neotominae	Peromyscus	sp	rt m1
40452	13	A2/L2	Rodentia	Cricetidae	Neotominae	Peromyscus	sp	lt m1
40453	13	A2/L2	Rodentia	Cricetidae	Neotominae	Peromyscus	sp	lt M1
40454	13	A2/L2	Rodentia	Cricetidae	Neotominae	Peromyscus	sp	lt m1
40455	13	A2/L2	Rodentia	Cricetidae	Neotominae	Peromyscus	sp	rt m2
40456	13	A2/L2	Rodentia	Cricetidae	Neotominae	Peromyscus	cf maniculatus	lt m1

40457	13	A2/L2	Rodentia	Cricetidae	Neotominae	Peromyscus	sp	rt m2
40458	13	A2/L2	Rodentia	Cricetidae	Neotominae	Peromyscus	sp	rt M1
40459	13	A2/L2	Rodentia	Cricetidae	Neotominae	Peromyscus	sp	lt M2
40460	13	A3/L2	Rodentia	Cricetidae	Neotominae	Peromyscus	cf maniculatus	lt M1
40461	13	A3/L2	Rodentia	Cricetidae	Neotominae	Peromyscus	sp	rt M1
40462	13	A3/L2	Rodentia	Cricetidae	Neotominae	Peromyscus	sp	rt M1
40463	13	A3/L2	Rodentia	Cricetidae	Neotominae	Peromyscus	sp	lt m1
40464	13	A3/L2	Rodentia	Cricetidae	Neotominae	Peromyscus	cf maniculatus	rt m1
40465	13	A3/L2	Rodentia	Cricetidae	Neotominae	Peromyscus	sp	lt m1
40466	13	A3/L2	Rodentia	Cricetidae	Neotominae	cf Peromyscus	maniculatus	rt m1
40467	13	A3/L2	Rodentia	Cricetidae	Neotominae	Peromyscus	sp	rt m1
40468	13	A3/L2	Rodentia	Cricetidae	Neotominae	Peromyscus	cf maniculatus	lt m1
40469	13	A3/L2	Rodentia	Cricetidae	Neotominae	Peromyscus	sp	lt m1
40470	13	A3/L2	Rodentia	Cricetidae	Neotominae	Peromyscus	sp	rt m1
40471	13	A3/L2	Rodentia	Cricetidae	Neotominae	Peromyscus	sp	lt m1
40472	13	A3/L2	Rodentia	Cricetidae	Neotominae	?Peromyscus	sp	lt dentary
40473	13	A3/L2	Rodentia	Cricetidae	Neotominae	Peromyscus	sp	lt m1
40474	13	A3/L2	Rodentia	Cricetidae	Neotominae			rt m1
40475	13	A3/L2	Rodentia	Cricetidae	Neotominae			partial rt m1
40476	13	A3/L2	Rodentia	Cricetidae	Neotominae	?Peromyscus	sp	partial lt M1
40477	13	A3/L2	Rodentia	Cricetidae	Neotominae			m1 frag
40478	13	A3/L2	Rodentia	Cricetidae	Neotominae			lt m2
40479	13	A3/L2	Rodentia	Cricetidae	Neotominae			lt m2
40480	13	A3/L2	Rodentia	Cricetidae	Neotominae	Peromyscus	sp	lt m2
40481	13	A3/L2	Rodentia	Cricetidae	Neotominae			rt m2
40482	13	A3/L2	Rodentia	Cricetidae	Neotominae			rt m2
40483	13	A3/L2	Rodentia	Cricetidae	Neotominae			lt m2
40484	13	A3/L2	Rodentia	Cricetidae	Neotominae	Peromyscus	sp	rt m2

40485	13	A3/L2	Rodentia	Cricetidae	Neotominae	Peromyscus	sp	lt m2
40486	13	A3/L2	Rodentia	Cricetidae	Neotominae	Peromyscus	sp	rt m2
40487	13	A3/L2	Rodentia	Cricetidae	Neotominae	Peromyscus	sp	rt m2
40488	13	B2/L2	Rodentia	Cricetidae	Neotominae	Peromyscus	sp	rt m1
40489	13	B2/L2	Rodentia	Cricetidae	Neotominae	Peromyscus	cf maniculatus	lt m1
40490	13	B2/L2	Rodentia	Cricetidae	Neotominae	Peromyscus	sp	lt m1
40491	13	B2/L2	Rodentia	Cricetidae	Neotominae	Peromyscus	sp	rt m1
40492	13	B2/L2	Rodentia	Cricetidae	Neotominae	Peromyscus	sp	lt m1
40493	13	B2/L2	Rodentia	Cricetidae	Neotominae	Peromyscus	sp	rt m1
40494	13	B2/L2	Rodentia	Cricetidae	Neotominae	Peromyscus	sp	lt m2
40495	13	B2/L2	Rodentia	Cricetidae	Neotominae	Peromyscus	sp	lt m2
40496	13	B2/L2	Rodentia	Cricetidae	Neotominae	Peromyscus	sp	rt m2
40497	13	B2/L2	Rodentia	Cricetidae	Neotominae	Peromyscus	sp	rt m2
40498	13	B2/L2	Rodentia	Cricetidae	Neotominae	cf Reithrodontomys	megalotis	rt m2
40499	13	B2/L2	Rodentia	Cricetidae	Neotominae	Peromyscus	sp	rt m3
40500	13	B2/L2	Rodentia	Cricetidae	Neotominae	Peromyscus	sp	lt M1
40501	13	B2/L2	Rodentia	Cricetidae	Neotominae	Peromyscus	sp	rt M1
40502	13	B2/L2	Rodentia	Cricetidae	Neotominae	Peromyscus	cf maniculatus	rt M1
40503	13	B2/L2	Rodentia	Cricetidae	Neotominae	cf Reithrodontomys	megalotis	rt M1
40504	13	B2/L2	Rodentia	Cricetidae	Neotominae	Peromyscus	sp	rt M3
40505	13	B2/L2	Rodentia	Cricetidae	Neotominae	?Peromyscus	sp	lt dentary frag
40506	13	B2/L2	Rodentia	Cricetidae	Neotominae	?Peromyscus	sp	lt maxilla
40507	13	B2/L2	Rodentia	Cricetidae	Neotominae	Peromyscus	cf californicus	lt maxilla frag
40508	13	B3/L2	Rodentia	Cricetidae	Neotominae	Peromyscus	sp	lt m1
40509	13	B3/L2	Rodentia	Cricetidae	Neotominae	cf Reithrodontomys	megalotis	lt m1
40510	13	B3/L2	Rodentia	Cricetidae	Neotominae	Peromyscus	sp	rt m1
40511	13	B3/L2	Rodentia	Cricetidae	Neotominae	Peromyscus	sp	rt m1
40512	13	B3/L2	Rodentia	Cricetidae	Neotominae	Peromyscus	sp	lt m2

40513	13	B3/L2	Rodentia	Cricetidae	Neotominae	Peromyscus	sp	rt m2
40514	13	B3/L2	Rodentia	Cricetidae	Neotominae	Peromyscus	sp	lt M1
40515	13	B3/L2	Rodentia	Cricetidae	Neotominae	Peromyscus	sp	rt M2
40516	13	B3/L2	Rodentia	Cricetidae	Neotominae	Peromyscus	sp	rt M2
40517	13	B2/L3	Rodentia	Cricetidae	Neotominae	Peromyscus	sp	lt m1
40518	13	B2/L3	Rodentia	Cricetidae	Neotominae	Peromyscus	sp	lt m1
40519	13	B2/L3	Rodentia	Cricetidae	Neotominae	Peromyscus	sp	rt m1
40520	13	B2/L3	Rodentia	Cricetidae	Neotominae	Peromyscus	sp	rt m1
40521	13	B2/L3	Rodentia	Cricetidae	Neotominae	Peromyscus	sp	rt m1
40522	13	B2/L3	Rodentia	Cricetidae	Neotominae	cf Onychomys	torridus	rt m1
40523	13	B2/L3	Rodentia	Cricetidae	Neotominae	Peromyscus	sp	lt m2
40524	13	B2/L3	Rodentia	Cricetidae	Neotominae	Peromyscus	sp	rt m2
40525	13	B2/L3	Rodentia	Cricetidae	Neotominae	Peromyscus	sp	rt m3
40526	13	B2/L3	Rodentia	Cricetidae	Neotominae	?Peromyscus	sp	molar frag
40527	13	B2/L3	Rodentia	Cricetidae	Neotominae	cf Onychomys	torridus	lt M1
40528	13	B2/L3	Rodentia	Cricetidae	Neotominae	Peromyscus	sp	lt M1
40529	13	B2/L3	Rodentia	Cricetidae	Neotominae	Peromyscus	sp	rt M1
40530	13	B2/L3	Rodentia	Cricetidae	Neotominae	Peromyscus	cf maniculatus	rt M1
40531	13	B2/L3	Rodentia	Cricetidae	Neotominae	cf Onychomys	torridus	rt M1
40532	13	B2/L3	Rodentia	Cricetidae	Neotominae	Peromyscus	sp	lt M2
40533	13	B2/L3	Rodentia	Cricetidae	Neotominae	Peromyscus	sp	lt M2
40534	13	B2/L3	Rodentia	Cricetidae	Neotominae	Peromyscus	sp	rt M2
40535	13	B2/L3	Rodentia	Cricetidae	Neotominae	Peromyscus	sp	lt m2
40539	13	A2/L1	Carnivora	Mustelidae	Mustelinae	Mustela	frenata	rt P4 frag
40540	13	B2/L1	Carnivora	Mustelidae	Mustelinae	Mustela	frenata	rt C1
40542	13	A2/L2	Carnivora	Mustelidae	Mustelinae	Mustela	frenata	lt p2
40543	13	A2/L2	Carnivora	Mustelidae	Mustelinae	Mustela	frenata	lt p3
40546	13	A3/L2	Carnivora	Mustelidae	Mustelinae	Mustela	frenata	lt p3
40547	13	A3/L2	Carnivora	Mephitidae		?Mephitis	mephitis	partial rt p2

40548	13	B2/L2	Carnivora	Mustelidae	Mustelinae	Mustela	frenata	rt c1
40551	13	B2/L2	Carnivora	Mustelidae	Mustelinae	Mustela	frenata	rt m2
40555	13	B2/L3	Carnivora	Mustelidae	Mustelinae	Mustela	frenata	lt P4
40557	13	B2/L3	Carnivora	Mephitidae		Mephitis	mephitis	lt P3
40560	13	B2/L3	Carnivora	?Mustelidae		?Mustela	frenata	tooth frag -M1?
40561	13	B2/L3	Carnivora	Mustelidae	Mustelinae	Mustela	frenata	rt P2
40562	13	B2/L3	Carnivora	Mustelidae	Mustelinae	Mustela	frenata	rt P2
42211	13	A2/L2	Rodentia	Sciuridae	Xerinae			lower tooth frag
42212	13	A2/L2	Rodentia	Sciuridae	Xerinae			upper tooth frag
42213	13	A2/L2	Rodentia	Sciuridae	Xerinae			lower tooth frag

Appendix Table 4.9.3: Destructively sampled fossils from Project 23 that yielded insufficient collagen for accelerator mass spectrometry.

Specimen number	**Deposit**	**Taxon**
P23-31032	14	*Sylvilagus audubonii*
P23-31035	14	*Sylvilagus audubonii*
P23-31039	14	*Sylvilagus audubonii*
P23-31043	14	*Sylvilagus audubonii*
P23-31052	14	*Sylvilagus audubonii*
P23-31055	14	*Sylvilagus bachmani*
P23-36331	7B	*Sylvilagus* sp.
P23-31114	14	*Otospermophilus* ?*beecheyi*
P23-33230	14	*Sylvilagus audubonii*
P23-33231	14	*Sylvilagus bachmani*
P23-31115	14	*Otospermophilus* ?*beecheyi*
P23-33234	14	*Microtus* sp.
P23-36572	13	*Otospermophilus* ?*beecheyi*
P23-37097	13	*Otospermophilus* ?*beecheyi*
P23-40643	14	*Otospermophilus* ?*beecheyi*
P23-40645	14	*Otospermophilus* ?*beecheyi*
P23-40646	14	*Sylvilagus* sp.

Appendix Table 4.9.4: List of 17 species used to inform average community-weighted trait estimates for each P23 deposit. Labels to the left of species names indicate their spatial and taxonomic group for species-pool sensitivity analysis. Label abbreviations are as follows: L = local, R = regional, C = continental, K = known, cf = tentative, E = estimated. Categories are hierarchical with local and known being the most exclusive spatial and taxonomic category respecitivy. For example, a "local" taxon will also be included in regional and continental species pools; however, a "regional" taxon will be included in regional and continental species pools but not local ones. The median value of six BioClim traits calculated across the contemporary range of each species is listed in addition to its average adult body mass, maximum value of maximum monthly temperature (Max_5), minimum value of minimum monthly temperature (Min_6), maximum value of mean annual precipitation (Max_12), and minimum value of mean annual precipitation (Min_12). See Methods for other BioClim variable definitions and trait explanations. Trait values of paleoclimate-limiting taxa (i.e., those with the lowest maximum temperature and precipitation values and/or highest minimum temperature and precipitation values) are underlined. In cases where identifications of paleoclimate-limiting species are uncertain (i.e., cf or estimated), asterisks indicate the next most limiting species known to occur in P23.

Species	**BIO1**	**BIO5**	**Max_5**	**BIO6**	**Min_6**	**BIO12**	**Max_12**	**Min_12**	**BIO13**	**BIO14**	**Mass (g)**
D. agilis (L, E)	15.95	32.67	43.08	0.54	-9.81	367	836	77	74	1	60.21
M. mephitis (C, K)	6.39	27.10	43.74	-12.71	-32.49	589	3347	58	92	19	2399.99
M. californicus (L, K)	14.47	31.43	45.66	1.35	-13.77	532	2039	58	102	2	57.42
M. frenata (C, K)	10.95	30.13	43.08	-6.67	-26.20	788	6070	81	106	20	190.03
N. merriami (R, E)	14.26	31.32	39.61	0.35	-14.00	513	1392	74	100	2	74.77
N. macrotis (L, K)	15.44	31.63	43.14	1.78	-13.81	388	1392*	69*	76	1	NA
O. torridus (R, cf)	17.48	36.38	45.66	1.45	-13.67	271	1125	48	40	4	21.68
O. beecheyi (L, K)	11.84	29.72	45.11	0.52	-13.84	611	3084	67	112	4	597.82
P. californicus (L, cf)	15.63	32.05	43.14	2.33	-11.87	377	1125	63	74	1	42.68

P. maniculatus (C, cf)	4.72	25.37	45.66	-14.54	-32.64	568	4236	46	90	18	19.98
R. megalotis (R, cf)	10.46	30.94	45.66	-7.82	-21.70	418	4266	46	75	10	10.72
S. latimanus (L, cf)	11.88	29.92	43.11	-0.58	-13.81	521.5	1991	65	96	4	62.46
S. ornatus (L, E)	15.70	32.55	43.08	2.22	-9.85	421	1696	73	83	1	5.31
S. gracilis (R, K)	11.76	31.62	45.66	-4.16	-21.76	372	3347	46	63	10	NA
S. audubonii (R, K)	14.27	32.71	45.66	-3.27	-21.76	379	2453	46	69	8	880.88
S. bachmani (L, K)	15.20	31.64	43.08*	2.07	-8.97	484	3084	54	97	1	714.53
T. bottae (R, K)	15.04	33.67	45.66	-1.39	-21.21	309	2134	46	55	6	122.7

Appendix Table 4.9.5: List of recent small mammal specimens examined for P23 fossil identifications. See McGuire (2011), Fox et al. (2019), and Fox (Chapter 3) for a list of comparative specimens used to quantitatively identify P23 fossil *Microtus*, *Sylvilagus*, and *Neotoma* respectively. MCZ = Harvard Museum of Natural History, LACM = Los Angeles County Museum of Natural History.

Museum Number	**Genus**	**Species**
MCZ-61195	*Chateodipus*	*C. baileyi*
MCZ-61507	*Chateodipus*	*C. baileyi*
MCZ-61190	*Chateodipus*	*C. baileyi*
MCZ-61187	*Chateodipus*	*C. baileyi*
MCZ-43619	*Chateodipus*	*C. californicus*
MCZ-9078	*Chateodipus*	*C. californicus*
MCZ-9439	*Chateodipus*	*C. fallax*
MCZ-20814	*Chateodipus*	*C. fallax*
MCZ-61173	*Chateodipus*	*C. pencillatus*
MCZ-61502	*Chateodipus*	*C. pencillatus*
MCZ-7727	*Chateodipus*	*C. pencillatus*
MCZ-7827	*Chateodipus*	*C. spinatus*
MCZ-18207	*Chateodipus*	*C. spinatus*
MCZ-12240	*Dipodomys*	*D. simulans*
MCZ-5191	*Dipodomys*	*D. simulans*
MCZ-12225	*Dipodomys*	*D. simulans*
MCZ-12236	*Dipodomys*	*D. simulans*
MCZ-9218	*Dipodomys*	*D. agilis*
MCZ-4862	*Dipodomys*	*D. agilis*
MCZ-5218	*Dipodomys*	*D. deserti*
MCZ-16846	*Dipodomys*	*D. deserti*
MCZ-4775	*Dipodomys*	*D. californicus*
MCZ-4771	*Dipodomys*	*D. californicus*
MCZ-4770	*Dipodomys*	*D. californicus*
MCZ-4776	*Dipodomys*	*D. californicus*
MCZ-4778	*Dipodomys*	*D. californicus*
MCZ-4777	*Dipodomys*	*D. californicus*
MCZ-4772	*Dipodomys*	*D. californicus*
MCZ-34771	*Dipodomys*	*D. heermanni*
MCZ-34772	*Dipodomys*	*D. heermanni*
MCZ-34773	*Dipodomys*	*D. heermanni*
MCZ-9148	*Dipodomys*	*D. heermanni*
MCZ-51448	*Dipodomys*	*D. meriami*
MCZ-18084	*Dipodomys*	*D. meriami*
MCZ-61455	*Dipodomys*	*D. meriami*

MCZ-61503	*Dipodomys*	*D. meriami*
MCZ-61527	*Dipodomys*	*D. meriami*
MCZ-5231	*Dipodomys*	*D. meriami*
MCZ-46468	*Dipodomys*	*D. meriami*
MCZ-30018	*Dipodomys*	*D. meriami*
MCZ-32401	*Dipodomys*	*D. microps*
MCZ-8426	*Dipodomys*	*D. panamintinus?*
MCZ-50896	*Dipodomys*	*D. panamintinus*
MCZ-43622	*Dipodomys*	*D_venustus*
MCZ-41326	*Mustela*	*M. erminea*
MCZ-41327	*Mustela*	*M. erminea*
MCZ-41358	*Mustela*	*M. erminea*
MCZ-41367	*Mustela*	*M. erminea*
MCZ-41370	*Mustela*	*M. erminea*
MCZ-41368	*Mustela*	*M. erminea*
MCZ-41365	*Mustela*	*M. erminea*
MCZ-41361	*Mustela*	*M. erminea*
MCZ-41360	*Mustela*	*M. erminea*
MCZ-B25	*Mustela*	*M. frenata*
MCZ-B37	*Mustela*	*M. frenata*
MCZ-10516	*Mustela*	*M. frenata*
MCZ-10515	*Mustela*	*M. frenata*
MCZ-41364	*Mustela*	*M. frenata*
MCZ-10013	*Mustela*	*M. nivalis*
MCZ-5532	*Mustela*	*M. nivalis*
MCZ-27132	*Mustela*	*M. nivalis*
MCZ-B9646	*Neotamias*	*T. merriami*
MCZ-B2345	*Neotamias*	*T. merriami*
MCZ-15554	*Neotamias*	*T. merriami*
MCZ-B4843	*Neotamias*	*T. merriami*
MCZ-19748	*Notiosorex*	*N. crawfordi*
MCZ-61210	*Notiosorex*	*N. crawfordi*
MCZ-61229	*Notiosorex*	*N. crawfordi*
LACM-727	*Onychomys*	*O. torridus*
LACM-1622	*Onychomys*	*O. torridus*
LACM-2641	*Onychomys*	*O. torridus*
LACM-2954	*Onychomys*	*O. torridus*
LACM-6596	*Onychomys*	*O. torridus*
LACM-20476	*Onychomys*	*O. torridus*
LACM-20714	*Onychomys*	*O. torridus*
LACM-50569	*Onychomys*	*O. torridus*

LACM-50570	*Onychomys*	*O. torridus*
LACM-50571	*Onychomys*	*O. torridus*
LACM-50736	*Onychomys*	*O. torridus*
LACM-50737	*Onychomys*	*O. torridus*
LACM-62785	*Onychomys*	*O. torridus*
LACM-63670	*Onychomys*	*O. torridus*
LACM-81179	*Onychomys*	*O. torridus*
LACM-86389	*Onychomys*	*O. torridus*
LACM-6593	*Onychomys*	*O. torridus*
MCZ-7673	*Perognathus*	*P. longimembris*
MCZ-18211	*Perognathus*	*P. longimembris*
MCZ-3268	*Perognathus*	*P. parvus*
MCZ-51706	*Perognathus*	*P. parvus*
LACM-286	*Peromyscus*	*P. boylii*
LACM-815	*Peromyscus*	*P. boylii*
LACM-942	*Peromyscus*	*P. boylii*
LACM-943	*Peromyscus*	*P. boylii*
LACM-960	*Peromyscus*	*P. boylii*
LACM-963	*Peromyscus*	*P. boylii*
LACM-964	*Peromyscus*	*P. boylii*
LACM-20403	*Peromyscus*	*P. boylii*
LACM-30204	*Peromyscus*	*P. boylii*
LACM-39740	*Peromyscus*	*P. boylii*
LACM-39741	*Peromyscus*	*P. boylii*
LACM-46211	*Peromyscus*	*P. boylii*
LACM-50688	*Peromyscus*	*P. boylii*
LACM-50872	*Peromyscus*	*P. boylii*
LACM-90391	*Peromyscus*	*P. boylii*
LACM-1511	*Peromyscus*	*P. californicus*
LACM-1521	*Peromyscus*	*P. californicus*
LACM-31624	*Peromyscus*	*P. californicus*
LACM-81331	*Peromyscus*	*P. californicus*
LACM-81335	*Peromyscus*	*P. californicus*
LACM-81336	*Peromyscus*	*P. californicus*
LACM-81337	*Peromyscus*	*P. californicus*
LACM-81338	*Peromyscus*	*P. californicus*
LACM-81339	*Peromyscus*	*P. californicus*
LACM-85370	*Peromyscus*	*P. californicus*
LACM-85373	*Peromyscus*	*P. californicus*
LACM-88186	*Peromyscus*	*P. californicus*
LACM-90044	*Peromyscus*	*P. californicus*

LACM-90045	*Peromyscus*	*P. californicus*
LACM-90046	*Peromyscus*	*P. californicus*
LACM-90350	*Peromyscus*	*P. californicus*
LACM-86413	*Peromyscus*	*P. californicus*
LACM-96108	*Peromyscus*	*P. californicus*
LACM-7587	*Peromyscus*	*P. crinitus*
LACM-7588	*Peromyscus*	*P. crinitus*
LACM-8115	*Peromyscus*	*P. crinitus*
LACM-8116	*Peromyscus*	*P. crinitus*
LACM-20482	*Peromyscus*	*P. crinitus*
LACM-20483	*Peromyscus*	*P. crinitus*
LACM-29016	*Peromyscus*	*P. crinitus*
LACM-29017	*Peromyscus*	*P. crinitus*
LACM-29018	*Peromyscus*	*P. crinitus*
LACM-29019	*Peromyscus*	*P. crinitus*
LACM-29020	*Peromyscus*	*P. crinitus*
LACM-29022	*Peromyscus*	*P. crinitus*
LACM-29023	*Peromyscus*	*P. crinitus*
LACM-29025	*Peromyscus*	*P. crinitus*
LACM-30211	*Peromyscus*	*P. crinitus*
LACM-39689	*Peromyscus*	*P. crinitus*
LACM-45551	*Peromyscus*	*P. crinitus*
LACM-106	*Peromyscus*	*P. eremicus*
LACM-414	*Peromyscus*	*P. eremicus*
LACM-415	*Peromyscus*	*P. eremicus*
LACM-419	*Peromyscus*	*P. eremicus*
LACM-3449	*Peromyscus*	*P. eremicus*
LACM-38238	*Peromyscus*	*P. eremicus*
LACM-39764	*Peromyscus*	*P. eremicus*
LACM-39766	*Peromyscus*	*P. eremicus*
LACM-45440	*Peromyscus*	*P. eremicus*
LACM-45441	*Peromyscus*	*P. eremicus*
LACM-46204	*Peromyscus*	*P. eremicus*
LACM-46976	*Peromyscus*	*P. eremicus*
LACM-69607	*Peromyscus*	*P. eremicus*
LACM-86416	*Peromyscus*	*P. eremicus*
LACM-6706	*Peromyscus*	*P. maniculatus*
LACM-6710	*Peromyscus*	*P. maniculatus*
LACM-6711	*Peromyscus*	*P. maniculatus*
LACM-31062	*Peromyscus*	*P. maniculatus*
LACM-63367	*Peromyscus*	*P. maniculatus*

LACM-63368	*Peromyscus*	*P. maniculatus*
LACM-63370	*Peromyscus*	*P. maniculatus*
LACM-63371	*Peromyscus*	*P. maniculatus*
LACM-63373	*Peromyscus*	*P. maniculatus*
LACM-63538	*Peromyscus*	*P. maniculatus*
LACM-63539	*Peromyscus*	*P. maniculatus*
LACM-63540	*Peromyscus*	*P. maniculatus*
LACM-83905	*Peromyscus*	*P. maniculatus*
LACM-83906	*Peromyscus*	*P. maniculatus*
LACM-86438	*Peromyscus*	*P. maniculatus*
LACM-86444	*Peromyscus*	*P. maniculatus*
LACM-86459	*Peromyscus*	*P. maniculatus*
LACM-86460	*Peromyscus*	*P. maniculatus*
LACM-86461	*Peromyscus*	*P. maniculatus*
LACM-49267	*Peromyscus*	*P. truei*
LACM-49268	*Peromyscus*	*P. truei*
LACM-49270	*Peromyscus*	*P. truei*
LACM-49272	*Peromyscus*	*P. truei*
LACM-49277	*Peromyscus*	*P. truei*
LACM-62656	*Peromyscus*	*P. truei*
LACM-62657	*Peromyscus*	*P. truei*
LACM-62660	*Peromyscus*	*P. truei*
LACM-62664	*Peromyscus*	*P. truei*
LACM-62667	*Peromyscus*	*P. truei*
LACM-87684	*Peromyscus*	*P. truei*
LACM-87685	*Peromyscus*	*P. truei*
LACM-87746	*Peromyscus*	*P. truei*
LACM-87748	*Peromyscus*	*P. truei*
LACM-90156	*Peromyscus*	*P. truei*
MCZ-41746	*Sorex*	*S. ornatus*
MCZ-20161	*Sorex*	*S. ornatus*
MCZ-13189	*Sorex*	*S. trowbridgii*
MCZ-9572	*Sorex*	*S. trowbridgii*
MCZ-9574	*Sorex*	*S. trowbridgii*
MCZ-9580	*Sorex*	*S. trowbridgii*
MCZ-9581	*Sorex*	*S. trowbridgii*
MCZ-34447	*Sorex*	*S. vagrans*
MCZ-34448	*Sorex*	*S. vagrans*
MCZ-34449	*Sorex*	*S. vagrans*
MCZ-34450	*Sorex*	*S. vagrans*
MCZ-7722	*Sorex*	*S. palustris*

MCZ-7779	*Sorex*	*S. palustris*
MCZ-34036	*Sorex*	*S. palustris*
MCZ-18443	*Spermophilus*	*S. beecheyi*
MCZ-43233	*Spermophilus*	*S. beecheyi*
MCZ-B5360	*Spermophilus*	*S. beecheyi*
MCZ-B9334	*Spermophilus*	*S. beecheyi*
MCZ-7977	*Spermophilus*	*S. beecheyi*
MCZ-11693	*Spermophilus*	*S. beecheyi*
MCZ-B9329	*Spermophilus*	*S. beecheyi*
MCZ-B5358	*Spermophilus*	*S. beecheyi*
MCZ-B9333	*Spermophilus*	*S. beecheyi*
MCZ-15595	*Spermophilus*	*S. beecheyi*
MCZ-29969	*Spermophilus*	*S. beecheyi*
MCZ-13313	*Spermophilus*	*S. beecheyi*
MCZ-13315	*Spermophilus*	*S. beecheyi*
MCZ-52879	*Spermophilus*	*S. beecheyi*
MCZ-B9308	*Spermophilus*	*S. beldingi*
MCZ-B9309	*Spermophilus*	*S. beldingi*
MCZ-B9310	*Spermophilus*	*S. beldingi*
MCZ-B9311	*Spermophilus*	*S. beldingi*
MCZ-B9315	*Spermophilus*	*S. beldingi*
MCZ-B8640	*Spermophilus*	*S. lateralis*
MCZ-B8447	*Spermophilus*	*S. lateralis*
MCZ-B8641	*Spermophilus*	*S. lateralis*
MCZ-B9318	*Spermophilus*	*S. lateralis*
MCZ-11698	*Spermophilus*	*S. lateralis*
MCZ-16835	*Spermophilus*	*S. tereticaudus*
MCZ-16838	*Spermophilus*	*S. tereticaudus*
MCZ-16839	*Spermophilus*	*S. tereticaudus*
MCZ-16829	*Spermophilus*	*S. tereticaudus*
MCZ-16833	*Spermophilus*	*S. tereticaudus*
MCZ-43217	*Tamias*	*T. amoenus*
MCZ-11705	*Tamias*	*T. amoenus*
MCZ-B9591	*Tamias*	*T. amoenus*
MCZ-B9589	*Tamias*	*T. amoenus*
MCZ-B4845	*Tamias*	*T. speciosus*
MCZ-B4846	*Tamias*	*T. speciosus*
MCZ-B4847	*Tamias*	*T. speciosus*
MCZ-12066	*Thomomys*	*T. bottae*
MCZ-12065	*Thomomys*	*T. bottae*
MCZ-B7826	*Thomomys*	*T. bottae*

MCZ-12153	*Thomomys*	*T. bottae*
MCZ-12279	*Thomomys*	*T. bottae*
MCZ-12280	*Thomomys*	*T. bottae*
MCZ-51206	*Thomomys*	*T. bottae*
MCZ-9196	*Thomomys*	*T. bottae*
MCZ-9151	*Thomomys*	*T. bottae*
MCZ-B9152	*Thomomys*	*T. bottae*
MCZ-B9170	*Thomomys*	*T. bottae*
MCZ-5377	*Thomomys*	*T. bottae*
MCZ-5375	*Thomomys*	*T. bottae*
MCZ-15621	*Thomomys*	*T. bottae*
MCZ-17087	*Thomomys*	*T. bottae*
MCZ-19736	*Thomomys*	*T. mazama*
MCZ-19733	*Thomomys*	*T. mazama*
MCZ-19734	*Thomomys*	*T. mazama*
MCZ-19735	*Thomomys*	*T. mazama*
MCZ-18331	*Thomomys*	*T. monticola*
MCZ-B9169	*Thomomys*	*T. monticola*
MCZ-19737	*Thomomys*	*T. monticola*
MCZ-19739	*Thomomys*	*T. monticola*
MCZ-B9157	*Thomomys*	*T. monticola*
MCZ-B9158	*Thomomys*	*T. monticola*
MCZ-B9159	*Thomomys*	*T. monticola*
MCZ-B9160	*Thomomys*	*T. monticola*
MCZ-4687	*Thomomys*	*T. talpoides*
MCZ-34015	*Thomomys*	*T. talpoides*
MCZ-34016	*Thomomys*	*T. talpoides*
MCZ-34017	*Thomomys*	*T. talpoides*
MCZ-B1429	*Thomomys*	*T. talpoides*
MCZ-B1430	*Thomomys*	*T. talpoides*
MCZ-B1431	*Thomomys*	*T. talpoides*
MCZ-B5672	*Thomomys*	*T. talpoides*
MCZ-18355	*Thomomys*	*T. townsendi*
MCZ-18336	*Thomomys*	*T. townsendi*
MCZ-18337	*Thomomys*	*T. townsendi*
MCZ-18338	*Thomomys*	*T. townsendi*

Appendix Table 4.9.6: Linear discriminant analysis classification results of fossil cricetid lower first molars based on 2D landmark data from Fox et al. (2020) and Fox (Chapter 3) for *Microtus* (n=60) and *Neotoma* (n=14) respectfully. Predicted group membership (PGM) results and posterior probabilities of group membership (PP) are listed for each specimen in each landmark dataset replicate (T1 and T2) of Fox (Chapter 3) and the first two dataset replicates of Fox et al. (2020) (i.e., datasets "Dinolite_NoTilt_EO_T1" and "Dinolite_NoTilt_EO_T2"). An additional 29 *Microtus* specimens from Deposit 14 were added to the Deposit 1 fossil dataset of Fox et al. (2020). Cross-validated predicted group membership accuracy of recent *Microtus* "training" species used to inform fossil species predictions is 86.2% and 82.6% for T1 and T2 respectively, and 84.9% and 83.4% for T1 and T2 respectively of recent *Neotoma* species. Underlined specimens indicate fossils recovered from the sampling effort of this study. Non-underlined fossils indicate specimens previously accessioned in LACMP23 collections. Fossils classified as *M. californicus* and *N. macrotis* in both data replicates of their respective studies were assigned a final identification as such while specimens classified as *M. californicus* and *N. macrotis* in one or neither replicate were assigned a final identification of "*Microtus* sp." or "*Neotoma* sp." Predicted occurrences of other species are not considered trustworthy, even when predicted in both analytical replicates, because counts of those species fall within the mean range of classification error of their respective study. That is, no species of *Microtus* predicted in both analytical replicates other than *M. californicus* account for more than 15.6% of the total fossil sample and therefore fall within the mean range of classification error of that study [100-(86.2 + 82.6)/2 = 15.6]. The same applies to species of *Neotoma* other than *N. macrotis*.

Number	**Deposit**	**Taxon**	**PGM T1**	**PP T1**	**PGM T2**	**PP T2**	**Final ID**
P23-04397	1	*Microtus*	*M. longicaudus*	0.660	*M. longicaudus*	0.851	*Microtus sp*
P23-05105	1	*Microtus*	*M. californicus*	1.000	*M. californicus*	1.000	*M. californicus*
P23-06214	1	*Microtus*	*M. californicus*	0.966	*M. californicus*	0.966	*M. californicus*
P23-09006	1	*Microtus*	*M. californicus*	0.966	*M. californicus*	0.965	*M. californicus*
P23-09372	1	*Microtus*	*M. californicus*	0.845	*M. californicus*	0.841	*M. californicus*
P23-09913	1	*Microtus*	*M. oregoni*	0.999	*M. oregoni*	0.987	*Microtus sp*
P23-10586	1	*Microtus*	*M. longicaudus*	1.000	*M. longicaudus*	1.000	*Microtus sp*
P23-13663	1	*Microtus*	*M. californicus*	0.988	*M. longicaudus*	0.696	*Microtus sp*
P23-18239	1	*Microtus*	*M. californicus*	0.656	*M. californicus*	0.777	*M. californicus*
P23-18804	1	*Microtus*	*M. californicus*	0.996	*M. californicus*	0.914	*M. californicus*
P23-21551	1	*Microtus*	*M. californicus*	1.000	*M. californicus*	0.723	*M. californicus*
P23-22460	1	*Microtus*	*M. californicus*	1.000	*M. californicus*	0.980	*M. californicus*
P23-22501	1	*Microtus*	*M. californicus*	0.992	*M. californicus*	0.818	*M. californicus*
P23-23118	1	*Microtus*	*M. californicus*	0.925	*M. californicus*	0.728	*M. californicus*

P23-23435	1	*Microtus*	*M. californicus*	1.000	*M. californicus*	1.000	*M. californicus*
P23-26491	1	*Microtus*	*M. californicus*	1.000	*M. californicus*	1.000	*M. californicus*
P23-28157	1	*Microtus*	*M. oregoni*	0.998	*M. oregoni*	0.983	*Microtus sp*
P23-28158	1	*Microtus*	*M. californicus*	0.999	*M. californicus*	0.933	*M. californicus*
P23-28159	1	*Microtus*	*M. townsendii*	0.977	*M. californicus*	0.849	*Microtus sp*
P23-28160	1	*Microtus*	*M. californicus*	1.000	*M. californicus*	1.000	*M. californicus*
P23-28225	1	*Microtus*	*M. longicaudus*	0.915	*M. longicaudus*	0.869	*Microtus sp*
P23-28268	1	*Microtus*	*M. californicus*	0.999	*M. californicus*	0.999	*M. californicus*
P23-28269	1	*Microtus*	*M. californicus*	0.995	*M. californicus*	0.941	*M. californicus*
P23-28270	1	*Microtus*	*M. californicus*	1.000	*M. californicus*	0.995	*M. californicus*
P23-28325	1	*Microtus*	*M. californicus*	0.993	*M. californicus*	0.978	*M. californicus*
P23-28326	1	*Microtus*	*M. californicus*	0.936	*M. longicaudus*	0.658	*Microtus sp*
P23-28327	1	*Microtus*	*M. californicus*	1.000	*M. californicus*	1.000	*M. californicus*
P23-28328	1	*Microtus*	*M. californicus*	1.000	*M. californicus*	1.000	*M. californicus*
P23-28607	1	*Microtus*	*M. californicus*	1.000	*M. californicus*	0.941	*M. californicus*
P23-28840	1	*Microtus*	*M. californicus*	1.000	*M. californicus*	1.000	*M. californicus*
P23-28841	1	*Microtus*	*M. californicus*	1.000	*M. californicus*	0.996	*M. californicus*
P23-31610	14	*Microtus*	*M. longicaudus*	0.763	*M. longicaudus*	0.838	*Microtus sp*
P23-31744	14	*Microtus*	*M. longicaudus*	0.927	*M. longicaudus*	0.929	*Microtus sp*
P23-31863	14	*Microtus*	*M. californicus*	0.470	*M. longicaudus*	0.707	*Microtus sp*
P23-31864	14	*Microtus*	*M. californicus*	0.997	*M. californicus*	0.815	*M. californicus*
P23-31866	14	*Microtus*	*M. californicus*	1.000	*M. californicus*	0.996	*M. californicus*
P23-31869	14	*Microtus*	*M. californicus*	1.000	*M. californicus*	0.970	*M. californicus*
P23-31870	14	*Microtus*	*M. californicus*	1.000	*M. californicus*	1.000	*M. californicus*
P23-32002	14	*Microtus*	*M. californicus*	0.668	*M. californicus*	0.897	*M. californicus*
P23-32003	14	*Microtus*	*M. montanus*	0.568	*M. montanus*	0.838	*Microtus sp*
P23-32004	14	*Microtus*	*M. californicus*	0.995	*M. californicus*	0.989	*M. californicus*
P23-32005	14	*Microtus*	*M. longicaudus*	0.965	*M. longicaudus*	0.571	*Microtus sp*
P23-32006	14	*Microtus*	*M. californicus*	0.658	*M. californicus*	0.632	*M. californicus*
P23-32008	14	*Microtus*	*M. townsendii*	0.927	*M. montanus*	0.820	*Microtus sp*

P23-32010	14	*Microtus*	*M. californicus*	1.000	*M. californicus*	1.000	*M. californicus*
P23-32011	14	*Microtus*	*M. montanus*	0.494	*M. montanus*	0.941	*Microtus sp*
P23-32013	14	*Microtus*	*M. longicaudus*	0.899	*M. longicaudus*	0.996	*Microtus sp*
P23-32038	14	*Microtus*	*M. longicaudus*	0.901	*M. longicaudus*	0.655	*Microtus sp*
P23-33956	14	*Microtus*	*M. californicus*	0.925	*M. californicus*	0.700	*M. californicus*
P23-34077	14	*Microtus*	*M. montanus*	0.565	*M. longicaudus*	0.826	*Microtus sp*
P23-34078	14	*Microtus*	*M. longicaudus*	0.731	*M. californicus*	0.958	*Microtus sp*
P23-34079	14	*Microtus*	*M. oregoni*	0.585	*M. californicus*	0.931	*Microtus sp*
P23-34080	14	*Microtus*	*M. longicaudus*	0.502	*M. longicaudus*	0.925	*Microtus sp*
P23-34174	14	*Microtus*	*M. montanus*	0.905	*M. montanus*	0.693	*Microtus sp*
P23-34175	14	*Microtus*	*M. californicus*	0.858	*M. californicus*	0.794	*M. californicus*
P23-34177	14	*Microtus*	*M. californicus*	0.999	*M. californicus*	0.953	*M. californicus*
P23-34178	14	*Microtus*	*M. oregoni*	0.990	*M. oregoni*	0.648	*Microtus sp*
P23-34231	14	*Microtus*	*M. montanus*	0.983	*M. montanus*	0.998	*Microtus sp*
P23-34232	14	*Microtus*	*M. townsendii*	0.768	*M. californicus*	0.997	*Microtus sp*
P23-36617	14	*Microtus*	*M. californicus*	0.584	*M. californicus*	0.999	*M. californicus*
P23-40158	13	*Neotoma*	*N. macrotis*	0.898	*N. fuscipes*	0.736	*Neotoma sp*
P23-40402	13	*Neotoma*	*N. macrotis*	0.757	*N. fuscipes*	0.718	*Neotoma sp*
P23-28509	1	*Neotoma*	*N. albigula*	0.597	*N. macrotis*	0.842	*Neotoma sp*
P23-31175	14	*Neotoma*	*N. albigula*	0.696	*N. albigula*	0.527	*Neotoma sp*
P23-31976	14	*Neotoma*	*N. macrotis*	0.911	*N. macrotis*	0.671	*N. macrotis*
P23-33922	14	*Neotoma*	*N. fuscipes*	0.643	*N. fuscipes*	0.932	*Neotoma sp*
P23-34168	14	*Neotoma*	*N. macrotis*	0.902	*N. fuscipes*	0.523	*Neotoma sp*
P23-35665	7B	*Neotoma*	*N. macrotis*	0.999	*N. macrotis*	0.918	*N. macrotis*
P23-35668	7B	*Neotoma*	*N. macrotis*	0.988	*N. macrotis*	0.99	*N. macrotis*
P23-35780	7B	*Neotoma*	*N. macrotis*	0.89	*N. macrotis*	0.961	*N. macrotis*
P23-35782	7B	*Neotoma*	*N. macrotis*	0.656	*N. macrotis*	0.842	*N. macrotis*
P23-35806	7B	*Neotoma*	*N. macrotis*	0.877	*N. macrotis*	0.871	*N. macrotis*
P23-35934	7B	*Neotoma*	*N. macrotis*	0.992	*N. macrotis*	0.996	*N. macrotis*
P23-36312	7B	*Neotoma*	*N. fuscipes*	0.968	*N. fuscipes*	0.725	*Neotoma sp*

Appendix Table 4.9.7: Average $\delta^{18}O$ estimates using the mean $\delta^{18}O$ value from Hendy et al. (2007) between the oldest and youngest calibrated date of each P23 deposit (top), linear interpolation of the Hendy et al. (2007) $\delta^{18}O$ dataset using the mean of the OxCal calibrated age distribution of each specimen per deposit (middle), and linear interpolation using the median of the OxCal calibrated age distribution of each specimen per deposit (bottom). See Methods for details about each calculation. Colors illustrate the rank-order of overall temperature differences between deposits based on averaged $\delta^{18}O$ values: Dark blue = coldest, light blue = second coldest, pink = second warmest, red = warmest.

Deposit climate estimates	**Deposit 1**	**Deposit 14**	**Deposit 13**	**Deposit 7B**
mean $\delta^{18}O$ of age range	2.052	2.088	2.042	2.038
interpolated $\delta^{18}O$ of means	2.029	2.253	1.986	1.868
interpolated $\delta^{18}O$ of medians	2.040	2.285	1.938	1.798

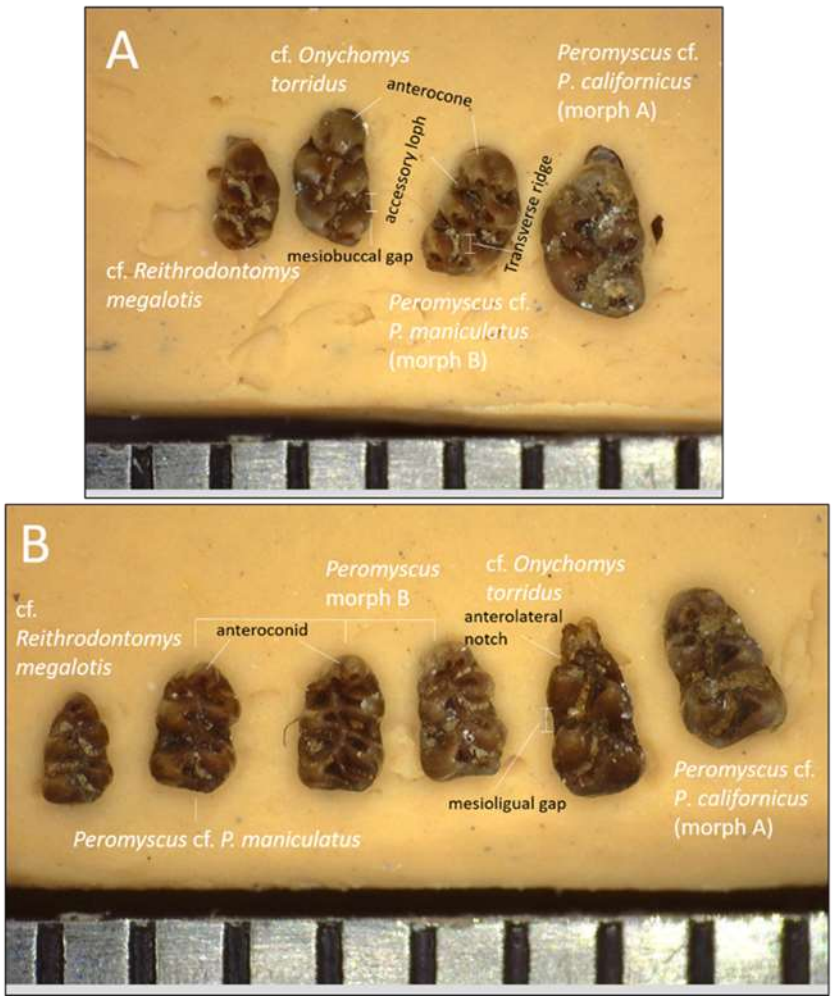

Appendix Figure 4.9.1: A) From left to right: LACMP23-40503 cf. *Reithrodontomys megalois* right M1; LACMP23-40527 cf. *Onychomys torridus* left M1 with anteriorly protruding anterocone; LACMP23-40502 *Peromyscus* cf. *P. maniculatus* right M1 with prominent anterobuccal accessory loph; LACMP23-31887 *Peromyscus* morph A. AB) From left to right: LACMP23-40509 cf. *Reithrodontomys megalois* left m1; LACMP23-40456 *Peromyscus* cf. *P. maniculatus* left m1 with a diminutive, undivided, anteroconid; LACMP23-40473 *Peromyscus* morph B left m1 with marked anteroconid division; LACMP23-40517 *Peromyscus* morph B left m1 with a divided, trefoil-like, anteroconid pattern; LACMP23-40522 cf. *Onychomys torridus* right m1 with a more anteriorly positioned anteroligual cusp and wider mesiolingual gap than referred *Peromyscus* specimens; LACMP23-40404 *Peromyscus* morph A right m1. Morph A includes the largest and most robust of the peromicine molars identified within Project 23.

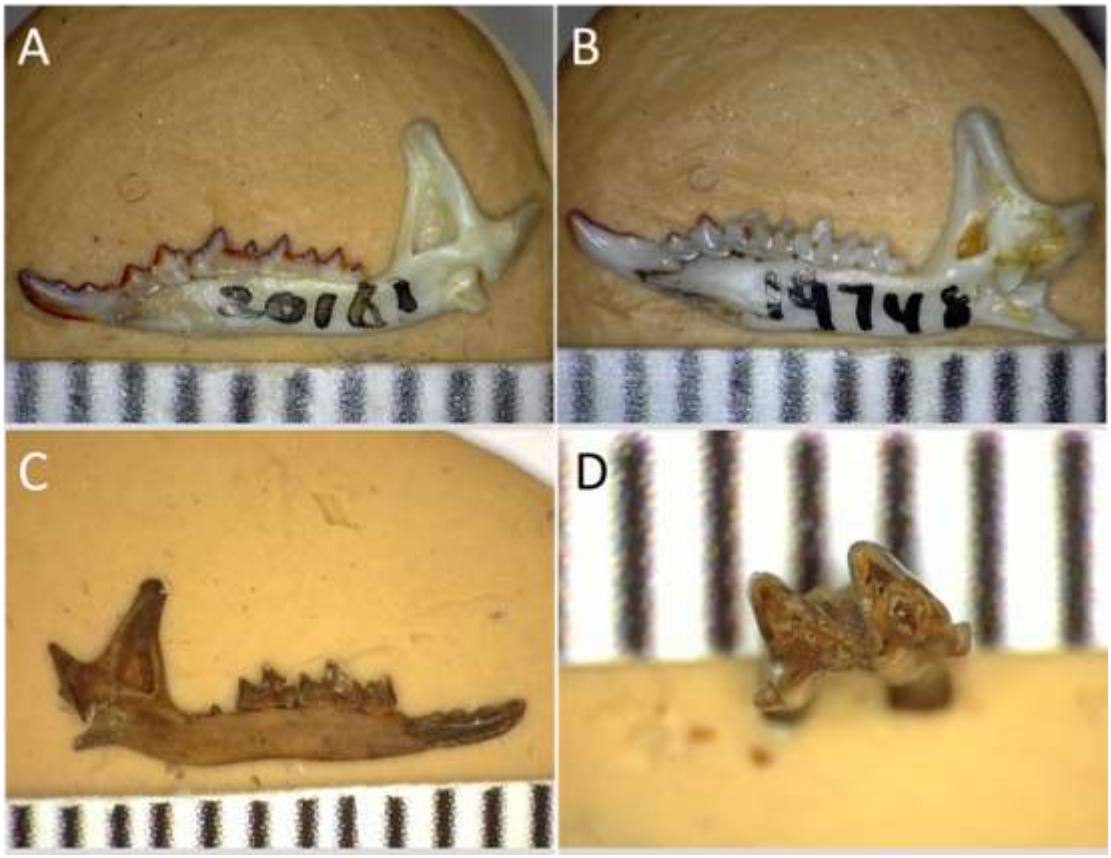

Appendix Figure 4.9.2: A) Right dentary of extant *Sorex ornatus* (MCZ-20161) with prominent enamel pigmentation, a relatively angular ramus, and a large mandibular foramen typical of all recent *Sorex* specimens examined (Appendix Table 4.9.5). B) Right dentary of extant *Notiosorex crawfordi* (MCZ-19748) exhibiting little enamel pigmentation, more curved ramus slopes, and a relatively small mandibular foramen typical of all recent *Notiosorex* specimens examined (Appendix 5). C) Fossil left dentary of LACMP23-31483 *Sorex* sp. from P23 Deposit 1 exhibiting posterior dentary characters consistent with extant *Sorex*. D) Occlusal view of LACMP23-35853 *Scapanus* cf. *S. latimanus* left m1/m2 from P23 Deposit 7B.

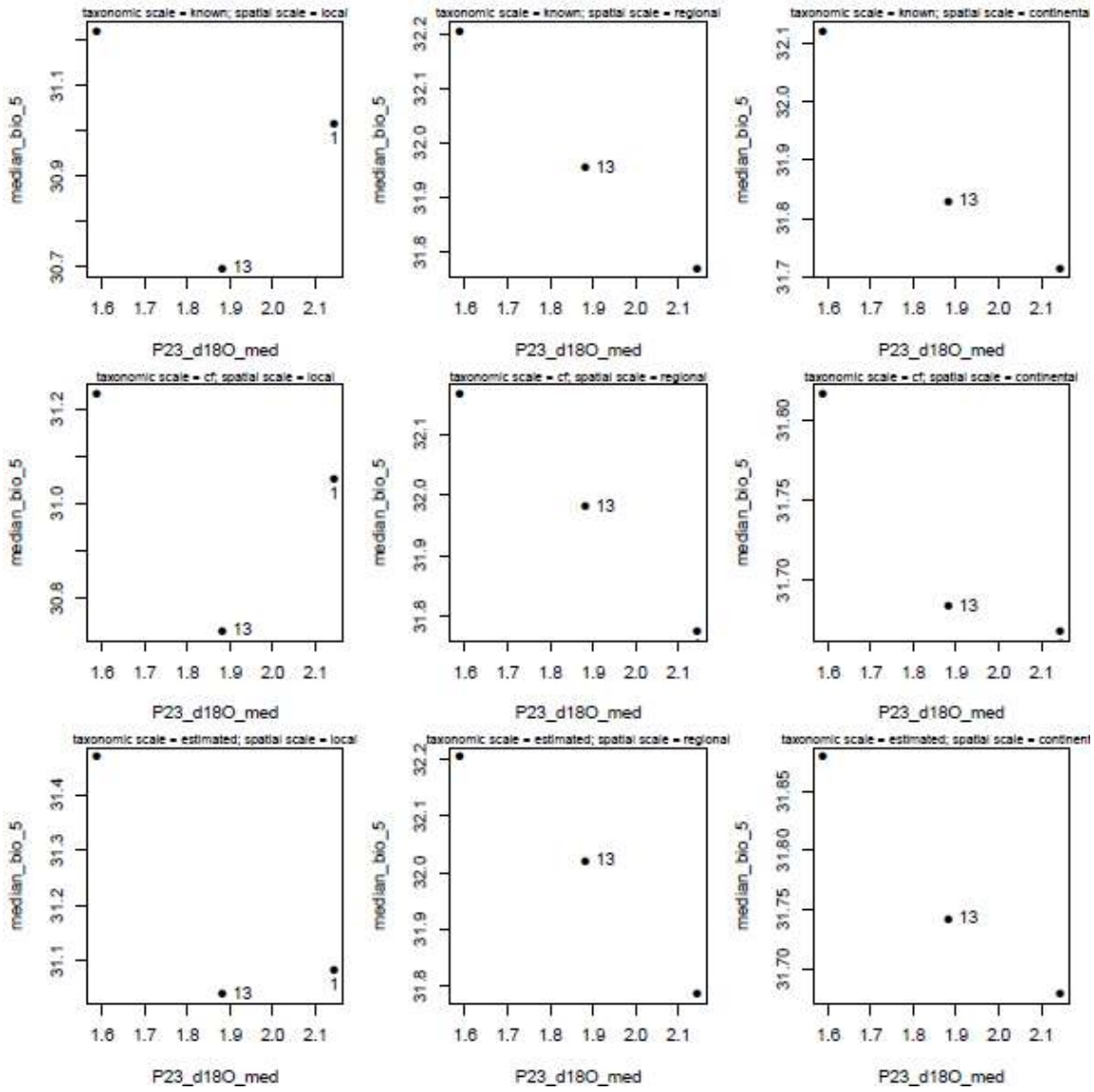

Appendix Figure 4.9.3: Results of nine spatial and taxonomic sensitivity simulations (see Methods) illustrating the relationship between average community-weighted temperature trait estimates, based on the median maximum temperature of the warmest month value (BIO5) across the range of each identified species, and median interpolated $\delta^{18}O$ climate estimates for P23 Deposits: 1, 13, and 7B. $\delta^{18}O$ climate and community trait data were calculated from Hendy et al. (2007) and Fick and Hijmans (2017) respectively.

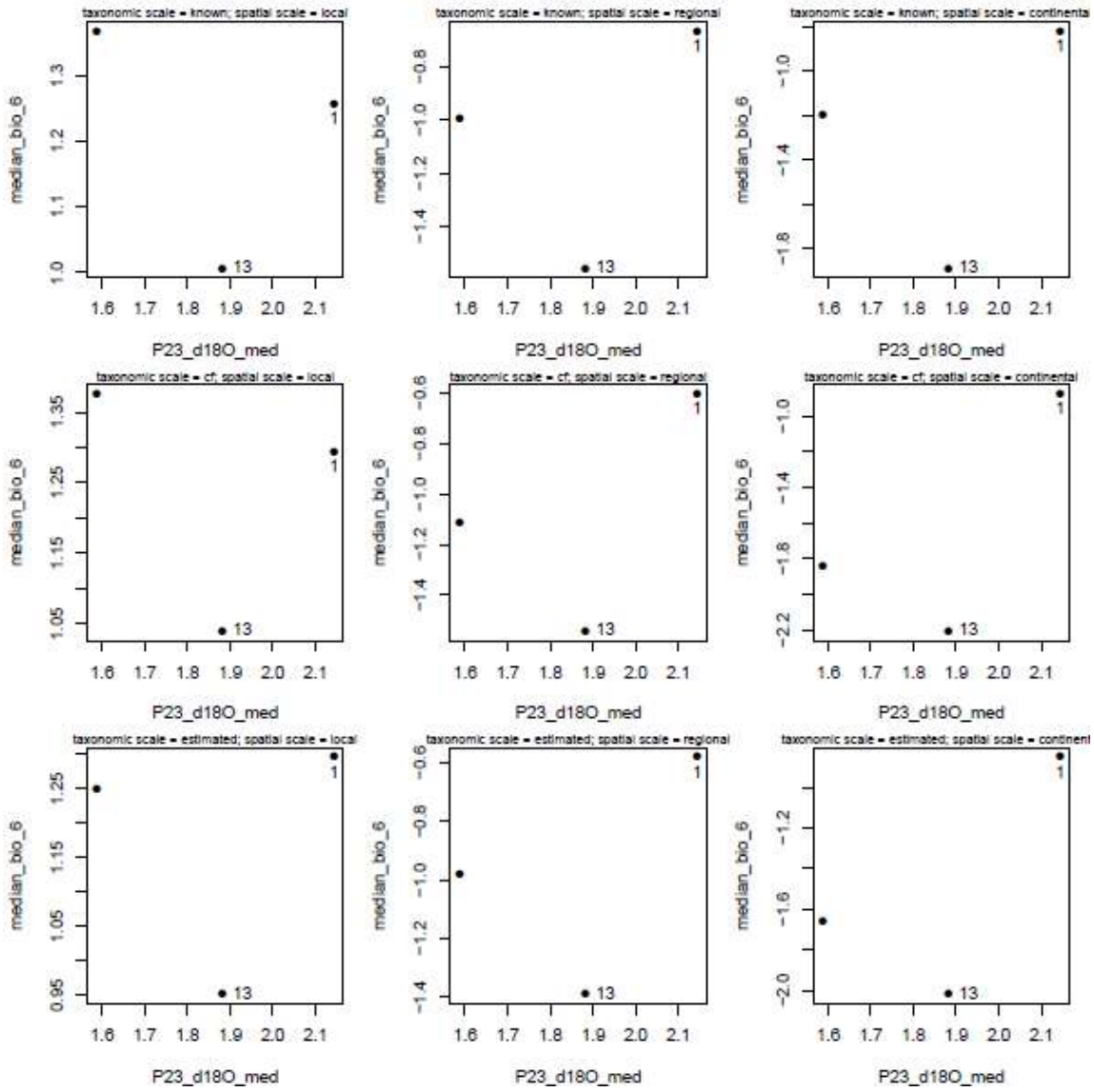

Appendix Figure 4.9.4: Results of nine spatial and taxonomic sensitivity simulations (see Methods) illustrating the relationship between average community-weighted temperature trait estimates, based on the median minimum temperature of the coldest month value (BIO6) across the range of each identified species, and median interpolated $\delta^{18}O$ climate estimates for P23 Deposits: 1, 13, and 7B. $\delta^{18}O$ climate and community trait data were calculated from Hendy et al. (2007) and Fick and Hijmans (2017) respectively.

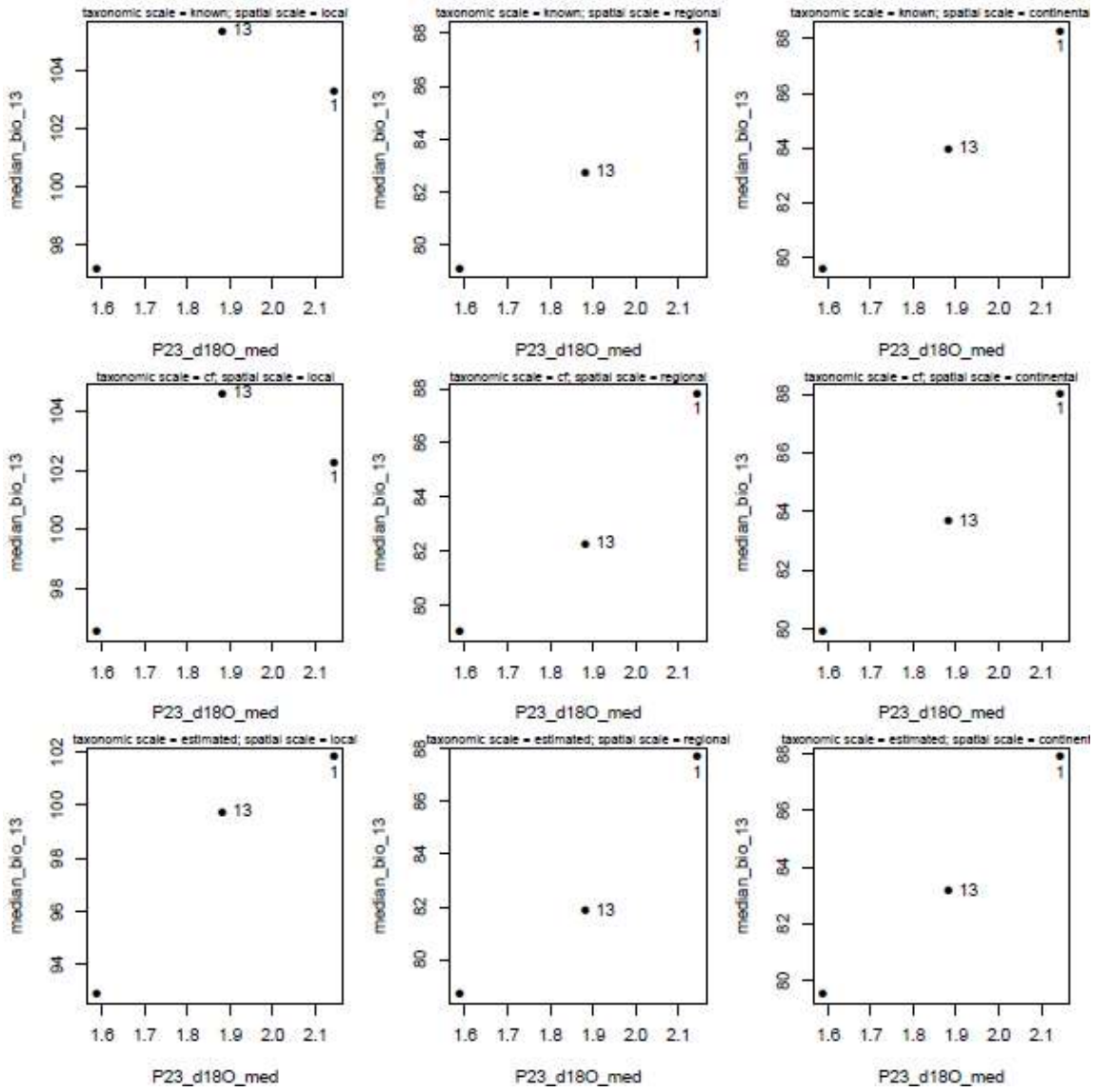

Appendix Figure 4.9.5: Results of nine spatial and taxonomic sensitivity simulations (see Methods) illustrating the relationship between average community-weighted precipitation trait estimates, based on the median precipitation of the wettest month value (BIO13) across the range of each identified species, and median interpolated δ18O climate estimates for P23 Deposits: 1, 13, and 7B. δ18O climate and community trait data were calculated from Hendy et al. (2007) and Fick and Hijmans (2017) respectively.

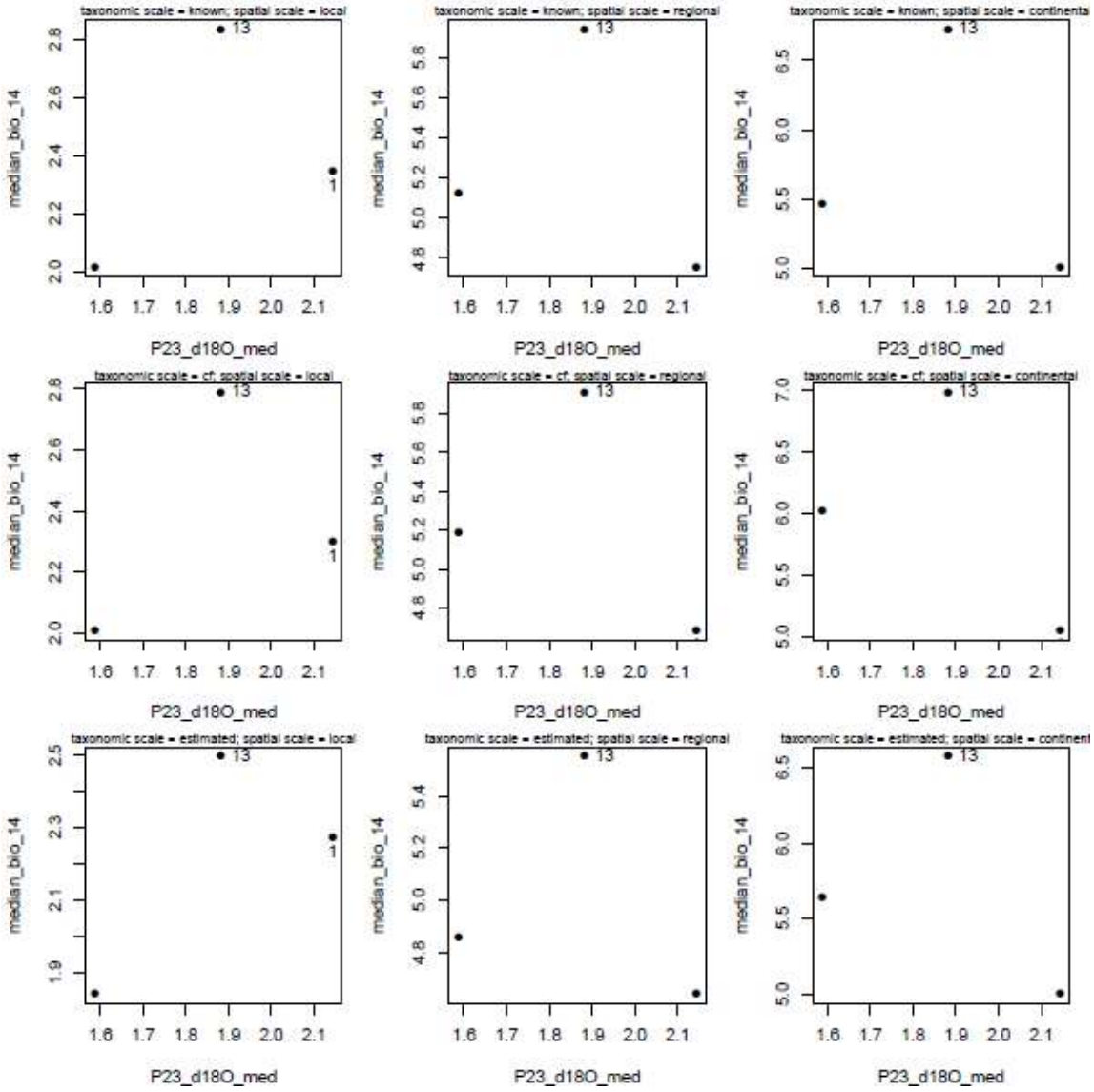

Appendix Figure 4.9.6: Results of nine spatial and taxonomic sensitivity simulations (see Methods) illustrating the relationship between average community-weighted precipitation trait estimates, based on the median precipitation of the driest month value (BIO14) across the range of each identified species, and median interpolated $\delta^{18}O$ climate estimates for P23 Deposits: 1, 13, and 7B. $\delta^{18}O$ climate and community trait data were calculated from Hendy et al. (2007) and Fick and Hijmans (2017) respectively.

Chapter 5: Radiocarbon and stable isotope analysis of fossil collagen reveals climate as the primary driver of small mammal niche dynamics over the last 50,000 years in the Los Angeles Basin, California

5.1 Abstract

Stable isotope analyses are useful for quantifying the realized niche of recent and fossil organisms and for evaluating niche changes in response to abiotic and biotic variables. However, contemporary systems lack the temporal extent to track niche responses to gradual or rare events such as non-anthropogenic environmental change and mass extinction. On the other hand, paleontological data are prone to time-averaging and incomplete stratigraphic records that can erase geologically rapid events and fine-scale patterns and processes. The ideal system for quantifying long-term drivers of organismal niche dynamics is therefore one with relatively complete biotic and temporal records preserved over millennia that capture significant periods of environmental and ecological change. The Rancho La Brea Tar Pits in Los Angeles, California, preserve millions of plant and animal fossils deposited throughout the last 50,000 years and are therefore well-suited for such analyses. I sampled over 100 specimens of small and mid-sized mammals, mostly sciurids and leporids, from Rancho La Brea to quantify their isotopic niche and track niche changes in response to long-term changes in climate and biotic interactions. Niches were quantified via stable carbon ($\delta^{13}C$) and nitrogen ($\delta^{15}N$) isotope analysis of fossil collagen. Further, each specimen was radiocarbon dated to track individual isotope ecology at precise points in time. Overall, sciurids and leporids exhibit different isotopic niches that appear to be facilitated by niche partitioning. Comparison of time-binned taxa before versus during and after the terminal Pleistocene extinction exhibit differences in $\delta^{13}C$ values and in $\delta^{13}C$, $\delta^{15}N$, niche breadth, suggesting that extinction-driven biotic reorganization impacted small mammal niches as well. However, when these data are evaluated continuously through time against high-resolution regional climate data, it is clear that climate is the primary driver of long-term isotopic niche changes in this system. These findings emphasize the importance of scale and data resolution when quantifying and interpreting (paleo)ecological patterns and processes.

5.2 Introduction

The extent to which various natural processes shape organismal niches is a fundamental question that has motivated ecological research over the past century (Hutchinson, 1957; Soberón & Nakamura, 2009). Such processes are difficult to measure, in part, because the relative impact of different abiotic (e.g., climate) and biotic (e.g., species interaction) effects on niches are difficult to disentangle and can be exacerbated by heterogeneity across spatial and temporal scales (Holt, 2009; Wiens, 2011). Contemporary experiments of niche-shaping variables may not have the temporal capacity to capture rare but important events (Holt, 2009), such as catastrophic disturbances and mass extinctions, or gradual events such as immigration/emigration and environmental change (Jackson & Overpeck, 2000). The late Quaternary fossil record can

bridge short-term observations of niche dynamics with natural processes operating on geologic timescales at a temporal precision not obtainable from pre-Quaternary data (i.e., 10^0–10^3 years; Jackson & Overpeck, 2000). Even so, abiotic and biotic drivers of niche dynamics are difficult to evaluate with the primary data available through paleoecological records, such as the presence and abundance of taxa at various points in space and time. However, geochemical techniques, such as stable isotope analysis, can be employed to better quantify the realized niche of recent and fossil organisms because these methods often record the ecological and environmental contexts in which individuals are found.

Stable isotope analysis of organic tissues (e.g., keratin, bone collagen, and tooth enamel) is a well-established tracer of ecological niche components including diet, the environment in which an organism lived, and interactions therein at various spatial and temporal scales (Cerling et al., 2003; Koch, 1998; Newsome et al., 2007). Two commonly used stable isotopes for evaluating ecological patterns and processes are carbon ($\delta^{13}C$) and nitrogen ($\delta^{15}N$). For example, $\delta^{13}C$ in consumer tissues reflects the types of organic materials eaten by an organism or its prey (e.g., plants with C_3, C_4, and CAM photosynthetic pathways), and will fluctuate in response to changes in temperature, precipitation, salinity, soil nutrients, and irradiance (Ehleringer & Monson, 1993; Koch, 1998; Kohn, 2010; Smith & Epstein, 1971; Tieszen, 1991). $\delta^{15}N$ also reflects aspects of temperature, precipitation, soil conditions, and salinity in addition to trophic position; organisms at higher trophic positions and those that consume more protein will exhibit enriched $\delta^{15}N$ signatures (Ambrose, 1991; Cormie & Schwarcz, 1996; Craine et al., 2015; Deniro & Epstein, 1981). Stable carbon and nitrogen isotope analysis of bone collagen and stable carbon and oxygen ($\delta^{18}O$) isotope analysis of tooth enamel are often used to infer past diet, biotic interactions, and to reconstruct paleoenvironments through fossils of medium and large-bodied mammals (e.g., Coltrain et al., 2004; Fox-Dobbs et al., 2008; Koch et al., 1998; Trayler et al., 2015). Similar research on small mammal fossils (e.g., rodents and lagomorphs) is less common, but is becoming more prevalent with increasing recognition of their utility for tracking fine scale paleoecological processes (e.g., Smiley et al., 2016). Small mammals exhibit small home ranges, fast metabolisms, short life spans, and tend to compartmentalize microhabitats (Cuenca-Bescós et al., 2009; Grayson, 2006; Smartt, 1977). Consequently, their stable isotope values generally reflect less spatial, temporal, and resource averaging than megafauna, and therefore can track local conditions with greater precision. For example, stable isotopes of leporid bone collagen and tooth enamel have been shown to exhibit significant relationships with temperature and precipitation, respectively, across space (Somerville et al., 2018) and time (Somerville et al., 2020). Several other studies within the last decade have quantified the isotopic niche of small mammal fossils – including those of leporids (Commendador & Finney, 2016; Feranec et al., 2010; Ugan & Coltrain, 2011), ground squirrels (Commendador & Finney, 2016; Feranec et al., 2010; McLean & Emslie, 2012), pocket gophers (Commendador & Finney, 2016), woodrats (McLean & Emslie, 2012), and other rats and mice (Terry, 2018; Tomé et al., 2020) – to evaluate their past responses to local environmental changes during the Quaternary.

Despite their demonstrated isotopic sensitivity to climate today (Smiley et al., 2016; Somerville et al., 2018), most paleontological studies published thus far find little or no linkage between small mammal isotope niches and paleoclimate (Feranec et al.,

2010; McLean & Emslie, 2012; Terry, 2018; Tomé et al., 2020) (but see Commendador & Finney, 2016). It has thus been suggested that neutral processes or community assembly may have a greater impact on small mammal niches than abiotic processes over extended time scales (Terry, 2018; Tomé et al., 2020). However, those inferences are generated from studies of temporally binned data. Although necessary when working with time-averaged records, and without individually dated specimens or semi-continuous temporal sequences, such binning can obscure geologically rapid events such as the decadal- to millennial-scale climatic oscillations known to have occurred throughout the late Quaternary (Hendy et al., 2002; Hendy & Kennett, 1999). To accurately assess the relative impacts of abiotic and biotic processes on small mammal niches, it may be necessary to examine continuous data over geologic time scales rather than time-binned or time-averaged data because much of the fine-scale processes impacting organismal niches may be lost while doing so. However, locating paleontological sites with the right conditions for such analyses is difficult. The ideal site must: a) preserve many individuals and exhibit excellent physical and geochemical fossil preservation (to obtain large isotopic sample sizes), and b) exhibit nearly continuous depositional sequences over millennial time scales (to track paleoecological patterns of a temporal length and resolution comparable to that of Quaternary paleoclimate datasets).

One site that meets the preservation requirements for semi-continuous, millennial-scale, isotopic analysis is Rancho La Brea (RLB), located in Los Angeles, California. Asphalt assemblages at RLB have yielded millions of well-preserved late Pleistocene and Holocene plant and animal fossils (Stock & Harris, 1992). Collectively, these deposits document a nearly complete temporal sequence of life in the Los Angeles Basin over the past 50,000 years (Fuller et al., 2014; Holden et al., 2017; O'Keefe et al., 2009), and are therefore well suited for evaluating past species-environment interactions and climate change responses. However, fossils assemblages of RLB are time-averaged due to asphaltic mixing, and there is extensive overlap in specimen ages within and among deposits (Fox, Chapter 4; Fuller et al., 2014, 2020; Holden et al., 2017; O'Keefe et al., 2009). This makes RLB a challenging site to evaluate fine scale paleoecological patterns at the assemblage level. On the other hand, RLB provides a unique opportunity to evaluate nearly continuous ecological patterns over geologic time if enough contemporaneous age and trait data are collected (i.e., via individually radiocarbon dated specimens) because the assemblages are not inhibited by incomplete depositional and stratigraphic events in the way most localities are. Thus, by gathering enough age and trait measurements, it is possible to track organismal niche dynamics at a temporal resolution unobtainable elsewhere. Stable isotope analyses have previously been conducted at RLB, but they largely focus on time-averaged data of mammalian megafauna (Coltrain et al., 2004; DeSantis et al., 2019; Feranec et al., 2009) (but see Fuller et al., 2020). It is therefore unsurprising that different studies of mammalian isotope ecology at RLB have generated dissimilar conclusions regarding the past ecologies and biotic interactions of certain taxa (Coltrain et al., 2004; DeSantis et al., 2019, 2020; Feranec et al., 2009; Valkenburgh et al., 2020). Even the magnitude and direction of environmental change in this area, a potentially major factor shaping species niches, is a topic of historical contention at this site based on different time-averaged paleoclimate proxies (Compton, 1937; Doyen & Miller, 1980; Johnson, 1977; Lamb,

1989; Warter, 1976). Though, recent work indicates that long-term environmental changes were likely subtle (Fox, Chapter 4; Holden et al., 2017).

To assess isotopic niche dynamics at a relatively fine temporal scale and resolution, I sample >100 small mammal individuals for radiocarbon dating and $\delta^{13}C$, $\delta^{15}N$, isotope analysis and evaluate their responses to changing abiotic and biotic conditions during the last 50,000 years. In doing so, I address the following questions:

1) Do different small mammal species partition niches at RLB?

2) Are intraspecific niches temporally stable, or do they change through time?

3) Are niche differences among taxa, and within taxa through time, driven by abiotic or biotic processes?

5.3 Methods

5.3.1 Sampling

To evaluate small mammal niches at RLB, 109 specimens were sampled for radiocarbon and $\delta^{13}C$, $\delta^{15}N$, analysis. Seventy-seven specimens were sampled from Project 23 Deposits 1, 7B, 13 and 14 at RLB as reported in Fox (Chapter 4). However, the age distribution of those specimens is restricted to Marine Isotope Stage 3 (MIS 3, ~60,000 to 26,000 years before present (BP); Meerbeeck et al., 2009; Siddall et al., 2008). To extend this temporal range, we sampled an additional 32 specimens from the Hancock collection at RLB, including specimens from Pits A, Bliss 29, 4, 10, 16, and Hancock specimens with no locality data that frequently yield MIS 1 and MIS 2 dates (i.e., from 26,000 BP to present) (O'Keefe et al., 2009). Our samples focused on craniodental and postcranial bone elements of cottontail rabbits (*Sylvilagus* spp.) and ground squirrels (*Otospermophilus* ?*beecheyi*) because they are the most abundant small mammal taxa at RLB that are large enough to produce enough collagen for radiocarbon and stable isotope analysis from isolated elements. *Sylvilagus* dentaries that retained lower third premolars (p3s) were further differentiated among the two species found at RLB – *S. audubonii* (desert cottontail) and S. *bachmani* (brush rabbit) – using the identification protocol of (Fox et al., 2019).

The same element of each specimen was sampled per deposit when possible to avoid resampling individuals. However, this was not always possible as specimens from certain deposits are more limited than others in the RLB collections. Given the taphonomic processes leading to fossilization (Behrensmeyer et al., 2000), the risk of resampling the same individual is likely low. Maximizing sample size was therefore prioritized over adhering to the "same element" rule. Similarly, specimens of adult individuals were preferentially sampled, but due to the higher representation of juvenile fossils at RLB relative to many other fossil sites (N. Fox personal observation, 2018; Miller, 1968), this was not always possible. Older juveniles were selected when it was not possible to sample adult specimens to mitigate preweaning effects that can marginally

enrich $\delta^{13}C$, $\delta^{15}N$, isotope values during nursing (Fuller et al., 2006; Jenkins et al., 2001). Due to this measure, and the fact that bulk isotopes of cortical bone collagen quantify diet averaged over the life of an organism (Hedges et al., 2007; Matsubayashi & Tayasu, 2019), any nursing effects on the isotopic niche of fossils analyzed here should be negligible.

5.3.2 Isotopic analysis

All specimens were radiocarbon dated using accelerator mass spectrometry (AMS) at the UC Irvine Keck Carbon Cycle AMS Laboratory with a National Electrostatics Corporation 0.5 MV 1.5SDH-1 Pelletron and modified 60-sample MCSNICS ion source (Southon & Santos, 2004). Fossils were sampled either in full or sectioned with a handheld Dremel rotary tool depending on the amount material available. Only specimens with initial bone weights >200 mg were selected for destructive analysis because anything lighter from RLB is unlikely to yield sufficient collagen for AMS (J. Southon, UC Irvine, personal communication). Fossils from RLB contain hydrocarbon contaminants due to their asphaltic depositional setting, but accurate radiocarbon dates (and stable isotope values) are attainable from bone collagen through petroleum removal techniques (Fox-Dobbs et al., 2006; Friscia et al., 2008; Fuller et al., 2014; Fuller et al., 2015; Marcus & Berger, 1984; O'Keefe et al., 2009). Specimens were prepared for AMS using the ultrafiltration procedure of Fuller et al. (2014) and ultimately analyzed as graphitized CO_2 acquired from ~2 mg of purified collagen. Following AMS, radiocarbon ages were calibrated in OxCal v.4.3.2 (Bronk Ramsey, 2009) using the IntCal13 calibration curve (Reimer et al., 2013). The mean of the Bayesian probability age distribution of each specimen was then used for paleoclimate comparisons described further below. A portion of collagen obtained from each sample was reserved for carbon ($\delta^{13}C$) and nitrogen ($\delta^{15}N$) isotope analysis to ensure quality of the radiocarbon date and quantify the dietary niche of each radiocarbon-dated specimen. Those isotopic ratios were measured from ~0.7 mg collagen aliquots combusted to CO_2 and N_2 using a Fisons NA 1500NC elemental analyzer and Finnigan Delta Plus isotope ratio mass spectrometer at a precision of ±0.1‰ and ± 0.2‰ for $\delta^{13}C$ and $\delta^{15}N$, respectively. Stable isotope values are reported in standard delta notation as δ in parts per thousand (per mil (‰)), where $\delta\ (‰) = 1000\ [(R_{sample}/R_{standard}) - 1]$ with international references Vienna Pee Dee Belemnite (VPDB) and atmospheric N_2 as standards for carbon and nitrogen, respectively.

5.3.3 Biotic and abiotic proxies

Biotic interactions are difficult to evaluate directly through the fossil record. Therefore, we use the terminal Pleistocene extinction event that occurred between ~18,000 and 10,000 years ago as a proxy for a major biotic disturbance. Abrupt community shifts occurred during that time due to the extinction of 72% of mammalian megafauna genera (Koch & Barnosky, 2006), which likely triggered a cascade of effects on the organization and function of other plants and animals (Gill et al., 2009; Johnson, 2009). To determine if small mammal niches were measurably impacted by those disturbances, we evaluate isotopic niches in two age bins based on the radiocarbon age of each specimen. One bin contains specimens deposited prior to these disturbances,

hereafter the pre-disturbance community, between 50,000 years ago until the end of the Last Glacial Maximum (~18,000 years ago), and the other contains the post-disturbance community encompassing specimens deposited between the deglacial period and historic times (~18,000 to ~500 years ago).

Because terminal Pleistocene extinctions were likely caused, at least in part, by abrupt climate change during the deglacial period (Koch & Barnosky, 2006), isotopic niche shifts between pre- and post-disturbance community cannot be attributed to biotic effects without first isolating climate effects. To discern the relative contribution of biotic and abiotic effects on small mammal niches among these communities, I measured the relationship between small mammal $\delta^{13}C$, $\delta^{15}N$, values and $\delta^{18}O$ climate data from Santa Barbara Basin ODP Hole 893A planktonic foraminifera (*Neogloboquadrina pachyderma*; Hendy et al., 2007). Those isotopes reflect regional sea surface temperature trends spanning the last >60 thousand years, which are comparable to the Greenland ice core records in direction, magnitude, and resolution (Hendy et al., 2002; Hendy & Kennett, 1999) (Fig. 5.1), and therefore function as a high-quality regional climate proxy for localities in southern California. I linearly interpolated $\delta^{18}O$ between the originally measured sample ages of the sediment core, and then extracted the inferred $\delta^{18}O$ at the mean OxCal-calibrated age of each RLB specimen to evaluate whether correlations occur between age-adjusted climate values and small mammal isotopic niches through time. However, isotopic niche correlations with climate do not rule out biotic effects either. For example, competitive interactions could cause different small mammal species to partition resources and track climate independently within their respective niche spaces. To address this, I examine the effects of regional climate and taxonomic variation on collagen $\delta^{13}C$ and $\delta^{15}N$ values to determine which has a greater impact on small mammal isotopic niches through time.

5.3.4 Statistical analysis

Interspecific isotopic niches are evaluated for significant differences in $\delta^{13}C$ and $\delta^{15}N$ among taxa overall (i.e., with time-averaged data) using Welch two-sample t-tests or Wilcoxon rank-sum tests in R [version 4.0.2, (R Core Team, 2020)] depending on the normality and homoscedasticity of data distributions. Niche differences within and among taxa in pre- versus post-disturbance communities are analyzed via $\delta^{13}C$ and $\delta^{15}N$ biplots with 68% confidence interval probability ellipses around isotopic convex hulls. Probability ellipses are included to estimate sampling effects among species and temporal communities, using the R package SIBER version 2.1.4 (Jackson et al., 2011). Finally, relationships among $\delta^{13}C$, $\delta^{15}N$, and climate ($\delta^{18}O$) are analyzed via linear models. I fit a linear model that originally included $\delta^{18}O$, taxon (i.e., *Sylvilagus* and *Otospermophilus*), and the interaction between the two variables against $\delta^{13}C$ and $\delta^{15}N$ separately. I then performed stepwise regression to determine which final combination of predictor variables best fits these data. Specimens with unmeasurable ages >50,000 years BP were omitted from analyses with temporal assumptions (i.e., disturbance community and climate/taxon analyses).

5.3.5 Expected results

If biotic interactions (e.g., resource partitioning) are the primary drivers of small mammal niches over millennial timescales, then I expect isotopic values of different small mammal species to be dissimilar, thus compartmentalizing different parts of the RLB microenvironment, because they occupy different niches today. Specifically, I expect ground squirrels to exhibit a broader isotopic niche than rabbits because contemporary ground squirrels tend to consume a wider variety of resources. *Otospermophilus beecheyi*, for example, prefer to consume oak and grass seeds today, but will switch to consume a variety of herbaceous vegetation, including fruits and flowers, depending on season – and even consumes carrion and animal prey occasionally (Smith et al., 2016). This species is therefore expected to exhibit a broader isotopic niche than cottontail rabbits, which largely consume grasses today (Chapman, 1974; Chapman & Willner, 1978). Within the two cottontail rabbit species identified at RLB, the desert cottontail typically inhabits relatively open and arid environments, while the brush rabbit inhabits environments with denser vegetation cover (Chapman, 1974; Chapman & Willner, 1978). Therefore, I expect $\delta^{13}C$, $\delta^{15}N$, values of the desert cottontail to be more positive than the brush rabbit overall if niche partitioning among sympatric species similarly shaped small mammal niches in the past. The rationale for this expectation is that C_4 and CAM photosynthetic plants generally occur in warmer/drier environments and exhibit more positive $\delta^{13}C$ values than C_3 plants (Ehleringer, 1978; Kohn, 2010; O'Leary, 1988). Even within C_3 plants, $\delta^{13}C$ values can fluctuate up to 6‰ due to changing environmental conditions. C_3 plants tend to exhibit more positive isotope values in warmer/drier environments due to increased stomatal closure with water stress which, in turn, decreases photosynthetic $\delta^{13}C$ discrimination (Kohn, 2010; Tieszen, 1991). $\delta^{15}N$ also tends to be more enriched in warmer, drier, and open systems than in cooler, wetter, and closed canopy systems (Amundson et al., 2003; Craine et al., 2015). In addition, I expect a directional shift in the isotopic signals of rabbits and squirrels to occur between pre- and post-disturbance communities due to food web restructuring after the megafauna extinction and/or ecological release from competition with megaherbivores (e.g., horses), which consumed similar vegetation across the RLB landscape (Fuller et al., 2020). Such shifts could be reflected as more positive or negative isotope values among communities, indicating a shift in resource consumption, or a shift in isotopic niche breadth indicating a change in consumed resource diversity/specialization before versus after these biotic disturbance events.

If climate change contributes to niche dynamics over extended timescales, then I expect to see a significant relationship between small mammal isotopic values and regional $\delta^{18}O$ through time. Specifically, I expect $\delta^{13}C$ and $\delta^{15}N$ to be more positive during warmer time periods overall, thus exhibiting a negative correlation with $\delta^{18}O$, than during cooler time periods using the same isotope theory rationale mentioned above. Further, if climate is the dominant shaper of niches in this system, I expect that $\delta^{18}O$ would have a stronger effect on $\delta^{13}C$ or $\delta^{15}N$ than taxon identity – in other words, while niche partitioning may cause the $\delta^{13}C$, $\delta^{15}N$, values to differ among taxa, the overall relationship with $\delta^{18}O$ should be stronger if climate primarily shapes isotopic niches through time. If small mammal niches are relatively stable through time, if these niches are largely shaped by neutral processes, or if the microclimate of RLB changed in a

dissimilar pattern to that of regional climate (e.g., was static while the regional climates show shifts), then I expect to see no statistically significant differences in isotopic niches among taxa, no directional change in niches among pre- and post-disturbance communities, and no correlations with regional climate through time.

5.4 Results

5.4.1 Samples, dates, and stable isotope values

Of the 109 specimens sampled, dates were obtainable from 85 specimens (Table 5.1). Twenty-two specimens yielded insufficient collagen for radiocarbon dating or stable isotope analysis (Appendix Table 5.9.1). Dates from Project 23 specimens are restricted to MIS 3 (>50,000 to ~30,000 calibrated years (cal.) BP; Fox, Chapter 4). However, the age range of specimens sampled from the Hancock collection is considerably broader, ranging from ~47,258 to ~2,377 cal. BP (43,700 to 2,375 radiocarbon years BP, Table 5.1), thus permitting analysis of isotopic niches from MIS 3 through MIS 1. Stable carbon and nitrogen isotopes were measured in 83 specimens, 77 of which are cottontail rabbits and ground squirrels. Stable isotope values of rabbits and squirrels range from -22.5‰ to -18.5‰ and 3.2‰ to 9.9‰ for $\delta^{13}C$ and $\delta^{15}N$, respectively. Isotope values of mesocarnivores (i.e., *Canis latrans*, coyote, n =2 and *Mustela frenata*, long-tailed weasel, n = 1) range from -20.2‰ to -17.0‰ and 10.4‰ to 12.3‰ for $\delta^{13}C$ and $\delta^{15}N$ respectively (Appendix Table 5.9.2). Samples of all taxa aside from rabbits and squirrels are too small to analyze statistically. Therefore, only the 77 leporid and sciurid specimens were evaluated for overall niche differences (48 and 29 rabbit and squirrel specimens respectively). Of the 77 rabbits and squirrels from which $\delta^{13}C$ and $\delta^{15}N$ were obtained, 70 yield measurable amounts of ^{14}C and are assigned a radiocarbon age (Table 5.1). Thus, 70 specimens were included in pre- versus post-disturbance community niche analysis. For age-calibration purposes, four of the 70 specimens yield mean calibrated age values beyond the measurable limit of OxCal. Therefore, the total number of rabbit and squirrel specimens included in calibrated age analyses with regional climate (Hendy et al., 2007) was 66 (40 rabbits and 26 squirrels).

5.4.2 Intra and interspecific niches

Wilcoxon rank-sum results show that both carbon and nitrogen isotopes are significantly different among time-averaged data of rabbits and squirrels (carbon: W = 1199, $p < 0.0001$; nitrogen: W = 497.5, $p = 0.037$; Fig. 5.2). Within rabbit species, carbon isotopes were significantly different between *S. audubonii* and *S. bachmani* (W = 102.5, $p = 0.023$; Fig. 5.2C) but nitrogen values were not (W = 88, $p = 0.151$; Fig. 5.2D). Carbon and nitrogen isotope niches are overall broader in fossil squirrels than rabbits, even though the rabbit niches are averaged across two species (Table 5.2; Fig. 5.3). Among time bins, post-disturbance communities (< 18,000 years BP) exhibited broader niche ellipses and were overall more $\delta^{13}C$-enriched than pre-disturbance communities in both taxa (Table 5.2; Fig. 5.3). Note that given the lack of dated samples from ~29,000 – 18,000 years BP, the pre-disturbance time bin encompasses a slightly larger period of

time than post-disturbance time bins: ~21,000 years of time averaging pre-disturbance and ~16,000 years post-disturbance

Stepwise regression indicates that no significant interaction occurs between foraminiferal $\delta^{18}O$ and taxon (i.e., rabbit versus squirrel) for either carbon ($p = 0.740$) or nitrogen ($p = 0.371$) isotope values. However, variation in $\delta^{13}C$ is significantly associated with both $\delta^{18}O$ and taxon (Fig. 5.4A). The combined model of $\delta^{18}O$ plus taxon best fits the carbon isotope data ($R^2 = 0.50$, $p < 0.0001$, $n = 66$; Fig. 5.4A). In the univariate models, more variation is explained by $\delta^{18}O$ than by taxon ($R^2 = 0.38$ and 0.29 for $\delta^{18}O$ and taxon, respectively), and examination of residuals of the univariate climate-only model indicates significant differences among taxa (Fig. 5.4B), again reinforcing the dual importance of climate and taxon. Neither $\delta^{18}O$ nor taxon explain significant variation in $\delta^{15}N$ (Fig. 5.4C), but taxon as a single variable is marginally significant ($p = 0.056$). Pooled rabbit and squirrel $\delta^{13}C$ and climatic $\delta^{18}O$ show similar patterns of change through time overall (Fig. 5.5).

5.5 Discussion

5.5.1 Overview

This study seeks to disentangle the biotic (resource partitioning) versus abiotic (climate) contributions to small mammal niche dynamics through time. While some resource partitioning is observed among taxa (Figs. 5.2 & 5.4), there is a stronger correlation between $\delta^{13}C$ and climate (Figs. 5.4 & 5.5). Overall, these data suggest that climate is the primary driver of isotopic niche changes in these species over the last 50,000 years.

5.5.2 Niche characterization

$\delta^{13}C$ values of -22.5‰ to -18.5‰ in RLB rodents and lagomorphs (Table 5.1; Figs. 5.2 & 5.3) are indicative of primarily C_3 diets overall. C_3 plants generally exhibit carbon isotope values of -35‰ to -20‰ (Kohn, 2010; O'Leary, 1988). Assuming a $\delta^{13}C$ tissue-diet trophic enrichment of 1‰ (DeNiro & Epstein, 1978), most small herbivores sampled in this study (75 of 78) consumed C_3 vegetation exclusively or near-exclusively (Table 5.1). It is notable that the three specimens exhibiting trophically adjusted $\delta^{13}C$ values of -19.8‰ to -19.5‰, possibly reflecting mixed C_3 and C_4/CAM plant diets (Kohn, 2010; O'Leary, 1988), are all Holocene in age (LACMHC-11584, LACMHC-143517, LACMV-4509 (Table 5.1)), even though sample sizes for the Holocene are much smaller than for the Pleistocene. Thus, no evidence of substantial C_4/CAM plant consumption is present in locally confined RLB taxa during the late Pleistocene. This contrasts with the mesopredator samples as one coyote (LACMP23-2046) of late Pleistocene age exhibits a $\delta^{13}C$ value indicative of a mixed C_3 and C_4/CAM diet (Appendix Table 5.9.2). Such age-resource offsets among taxa may reflect differences in late Pleistocene vegetative landscapes of the Los Angeles Basin at different spatial scales since contemporary coyote home ranges average around 1,000 ha and 4,000 ha for females and males, respectively, though ranges over 16,000 ha are not uncommon

(Bekoff, 1977). Conversely, desert cottontails, brush rabbits, and California ground squirrels usually exhibit home ranges of less than 5 ha (Boellstorff & Owings, 1995; Connell, 1954; Ingles, 1941). Similar patterns are observed among some RLB megafauna species. For example, fossil bison consumed more C_4 vegetation than fossil horses at RLB overall (Feranec et al., 2009). Such patterns were attributed to seasonal migration in bison and more localized ranges of horses (Feranec et al., 2009) given that the local environment of RLB during the late Pleistocene appears to have been dominated by C_3 vegetation based on isotopic analysis of other megafauna fossils (Coltrain et al., 2004). Finding exclusively C_3 diets in all locally confined small mammals with confirmed Pleistocene ages further supports that interpretation.

Unlike $\delta^{13}C$, $\delta^{15}N$ varies substantially among small herbivores, ranging from 3.2‰ to 9.9‰ (Table 5.1); the upper range overlaps with the observed $\delta^{15}N$ range of RLB mesocarnivores (Coltrain et al., 2004; Fuller et al., 2020). This variation could reflect microenvironmental changes in soil nutrients, salinity, temperature, and aridity through time (Ambrose, 1991; Amundson et al., 2003; Craine et al., 2015), or it could reflect eco-behavioral differences among individuals such as varying levels of coprophagy in rabbits (Ugan and Coltrain 2011; Commendador and Finney 2016) and facultative carnivory in squirrels (Smith et al. 2016). Similarly, enriched nitrogen isotope values are seen in larger RLB herbivores, and soil aridity during plant growing seasons has been suggested as a probable cause (Coltrain et al. 2004).

5.5.3 Interspecific niches

In addition to consumed resource variation among small herbivores and mesocarnivores, time-averaged carbon and nitrogen isotope values differ significantly among small herbivore taxa, with ground squirrels being more enriched in $\delta^{13}C$ and cottontail rabbits being more enriched in $\delta^{15}N$ (Fig. 5.2). Fossil squirrels exhibit broader isotopic niches than rabbits overall (Table 5.2; Fig. 5.3), thus following expectations of more variable resource consumption based on the contemporary ecologies of ground squirrels and cottontails (Chapman 1974; Chapman & Willner 1978; Smith et al. 2016). Within the two cottontail species found at RLB, significant differences in $\delta^{13}C$ also occur. Nitrogen isotopes do not vary significantly between rabbit species; however, values are more positive in desert cottontails than brush rabbits overall (Fig. 5.2). Such patterns are expected if these taxa partitioned niches in the past because contemporary individuals of ground squirrels tend to consume different resources than rabbits, and desert cottontails and brush rabbits often occupy different microhabitats (Chapman 1974; Chapman & Willner 1978; Smith et al. 2016). Indeed, similar isotopic patterns have been observed at the genus level between contemporary *Lepus* (hares) and *Sylvilagus*. Members of *Lepus* tend to occupy more open and arid environments than *Sylvilagus* and exhibit more enriched $\delta^{13}C$ and $\delta^{15}N$ across spatial gradients overall – consistent with expectations for taxa living in more open and arid systems (Somerville et al. 2018). Considering these data, similar niche partitioning among sympatric species may have occurred in the past with desert cottontails occupying more open sections of the RLB landscape and brush rabbits occupying more densely vegetated areas. However, rabbits tend to date older than squirrels in our sample (Table 5.1), and samples sizes among the two rabbit species are

highly unequal (Fig. 5.2) because fossils of the brush rabbit are rarer than those of the desert cottontail at RLB (Fox et al. 2019; Fox, Chapter 4). It is thus possible that these observed isotopic differences are due to sampling, age, and associated climate offsets among individuals and taxa rather than competitive interactions if niches are primarily driven by climate in this system.

5.5.4 Climate correlations

Statistically significant correlations between climate and $\delta^{13}C$ occur in squirrels and rabbits (Fig. 5.4A) suggesting that climate contributed to small mammal niche variation over the last 50,000 years. Such correlations were stronger with regional climate than with taxonomic factors, further suggesting that climate had a greater impact on small mammal niches than biotic effects such as competition and niche partitioning. Negative correlations between $\delta^{13}C$ and $\delta^{18}O$ (Figs. 5.4 & 5.5) match expectations of more enriched carbon values in warmer climates due to increased water stress in C_3 plants or increased abundance of C_4/CAM plants that generally thrive in warmer and drier growing conditions (Ehleringer, 1978; O'Leary, 1988; Smith & Epstein, 1971). Conversely, no relationship was observed between $\delta^{15}N$ and climate in any dataset (Fig. 5.4C). Such discrepancies could be due to different environmental, physiological, and behavioral process impacting carbon versus nitrogen assimilation and discrimination. For example, microenvironmental changes in soil aridity, nutrients, salinity, mycorrhizal processes, and vegetation over millennial timescales could affect these results (Ambrose, 1991; Amundson et al., 2003; Craine et al., 2015), and different foraging behaviors among individuals could also convolute these patterns. Such behaviors may include facultative carnivory in squirrels (Smith et al., 2016) that would enrich their $\delta^{15}N$ values and coprophagy in rabbits. Though, impacts of coprophagy on tissue $\delta^{15}N$ is poorly understood (Commendador & Finney, 2016; Somerville et al., 2018; Ugan & Coltrain, 2011).

5.5.5 Disturbance communities

Collectively, rabbits and squirrels both exhibit broader niches in post-disturbance communities than pre-disturbance communities (Table 5.2; Fig. 5.3). This could indicate that small mammals were able to consume a wider variety of resources after being released from competition with extinct megaherbivores such as *Equus occidentalis*, which consumed similar C_3 resources to rabbits and squirrels during the late Pleistocene (Fuller et al., 2020). Alternatively, given the strong signal of climate, a broader isotopic niche during the deglacial period versus the last glacial period could be explained by climate alone. The latter interpretation is supported by more variable regional climate conditions from 18,000 years ago to present than from 50,000 to 30,000 years ago as reflected in marine foraminiferal data (Fig. 5.1). Given the strength of correlation between $\delta^{13}C$ and $\delta^{18}O$, the effects of climate rather than competitive release or other trophic dynamics appear to be the primary driver of small mammal niche changes in this system.

5.5.6 Paleoenvironmental implications

Despite interpretations that late Pleistocene environments of RLB were largely similar to those of the Los Angeles Basin today (Dice, 1925; Doyen & Miller, 1980; Fox, Chapter 4; Holden et al., 2017; Johnson, 1977), perhaps indicating more buffered local microclimates than regional climate data suggest (e.g., Hendy et al., 2007), small mammal isotopic niches changed substantially through time. Such changes largely reflect regional climate patterns observed in the marine foraminiferal record off the Santa Barbara Basin. Indeed, patterns of rabbit and squirrel $\delta^{13}C$ closely mirror $\delta^{18}O$ values with similarly inverted peaks and valleys at analogous points in time (Fig. 5.5). These data suggest that the microclimate of RLB experienced by small mammals changed in a similar pattern, if not magnitude, to that of regional climate over the last 50,000 years. Such patterns are characterized by rapid climatic oscillations that fluctuated around a similar mean from 50,000 to ~35,000 years BP, steady cooling near the LGM from ~35,000 to ~17,000 years BP, and rapid high-magnitude warming after 17,000 years BP (Hendy et al., 2002; Hendy & Kennett, 1999) (Figs. 5.1 & 5.5).

Inferences of microclimate patterns at RLB are largely speculative for some time periods over the late Quaternary (Table 5.1; Fig. 5.5). For example, despite efforts to sample a broad range of dates and deposits, no dates were recovered between 29,000 and 18,000 years BP. Similarly, the RLB insect chronology dataset of Holden et al. (2017) had a conspicuous gap in ages between 26,000 and 16,000 years BP despite acquiring 182 dates and nearly continuous age distributions before and after MIS 2. Holden et al. (2017) suggested that temperatures during MIS 2 may have dropped below the threshold at which asphalt solidifies (observed at < 18 °C today) for longer periods of time, thus narrowing windows of entrapment. Although a limited sample of megafauna fossils date within MIS 2 (O'Keefe et al., 2009), lower ambient temperatures near the LGM could have disproportionately biased the entrapment of smaller and lighter animals such as insects, rodents, and lagomorphs that may not have generated enough pressure to become mired in the asphalt during those cooler climates. The apparent absence of microfauna dating to the time period immediately prior to and during the LGM may therefore signify substantially colder local conditions than at any other time throughout the last 50,000 years, which matches regional climate patterns and interpretations (Hendy et al., 2002; Hendy & Kennett, 1999) (Fig. 5.1).

5.5.7 Conclusions

When examining time-averaged and time-binned data, isotopic niche differences among taxa appear to be facilitated by biological effects such as niche partitioning (Fig. 5.2) or extinction-driven food web changes (Table 5.2; Fig. 5.3). Only when high-resolution age and climate data are examined is it clear that climate is the primary driver of long-term niche changes in this system (Figs. 5.4 & 5.5). This does not suggest that biological effects had no impact on small mammal niches. Indeed, most isotopic patterns observed among fossil taxa match resource partitioning expectations based on the ecologies of their extant representatives, and climate does not explain all the variation in these data (Fig. 5.4). It is not possible to determine whether the isotopic values of consumed resources changed through time or if the small mammals switched resources,

as stable isotopes of dated plant macrofossils are not evaluated here. Nevertheless, it is clear that age and associated climate offsets of individual specimens have a greater impact on stable isotope values than taxon-specific resource consumption or other biological effects in this system (Figs. 5.4 & 5.5). These findings have important implications for isotopic studies, and possibly studies of other traits, that use time-averaged paleontological data to interpret past biotic interactions and responses to climate change because sampling across geologically rapid events, if undetected, can lead to erroneous conclusions.

5.6 References

Ambrose, S. H. (1991). Effects of diet, climate and physiology on nitrogen isotope abundances in terrestrial foodwebs. *Journal of Archaeological Science*, *18*(3), 293–317. https://doi.org/10.1016/0305-4403(91)90067-Y

Amundson, R., Austin, A. T., Schuur, E. a. G., Yoo, K., Matzek, V., Kendall, C., Uebersax, A., Brenner, D., & Baisden, W. T. (2003). Global patterns of the isotopic composition of soil and plant nitrogen. *Global Biogeochemical Cycles*, *17*(1). https://doi.org/10.1029/2002GB001903

Behrensmeyer, A. K., Kidwell, S. M., & Gastaldo, R. A. (2000). Taphonomy and paleobiology. *Paleobiology*, *26*, 103–147. https://doi.org/10.1666/0094-8373(2000)26[103:TAP]2.0.CO;2

Bekoff, M. (1977). Canis latrans. *Mammalian Species*, *79*, 1–9. https://doi.org/10.2307/3503817

Boellstorff, D. E., & Owings, D. H. (1995). Home Range, Population Structure, and Spatial Organization of California Ground Squirrels. *Journal of Mammalogy*, *76*(2), 551–561. https://doi.org/10.2307/1382363

Bronk Ramsey, C. (2009). Bayesian Analysis of Radiocarbon Dates. *Radiocarbon*, *51*(1), 337–360. https://doi.org/10.1017/S0033822200033865

Cerling, T. E., Harris, J. M., & Passey, B. H. (2003). Diets of East African Bovidae Based on Stable Isotope Analysis. *Journal of Mammalogy*, *84*(2), 456–470. https://doi.org/10.1644/1545-1542(2003)084<0456:DOEABB>2.0.CO;2

Chapman, J. A. (1974). Sylvilagus bachmani. *Mammalian Species*, *34*, 1–4. https://doi.org/10.2307/3503777

Chapman, J. A., & Willner, G. R. (1978). Sylvilagus audubonii. *Mammalian Species*, *106*, 1–4.

Coltrain, J. B., Harris, J. M., Cerling, T. E., Ehleringer, J. R., Dearing, M.-D., Ward, J., & Allen, J. (2004). Rancho La Brea stable isotope biogeochemistry and its implications for the palaeoecology of late Pleistocene, coastal southern California. *Palaeogeography, Palaeoclimatology, Palaeoecology*, *205*(3), 199–219. https://doi.org/10.1016/j.palaeo.2003.12.008

Commendador, A. S., & Finney, B. P. (2016). Holocene environmental change in the eastern Snake River Plain of Idaho, USA, as inferred from stable isotope analyses of small mammals. *Quaternary Research*, *85*(3), 358–370. https://doi.org/10.1016/j.yqres.2016.03.008

Compton, L. V. (1937). Shrews from the Pleistocene of the Rancho La Brea asphalt. *University of California Press*, *24*, 85–90.

Connell, J. H. (1954). Home Range and Mobility of Brush Rabbits in California Chaparral. *Journal of Mammalogy*, *35*(3), 392–405. https://doi.org/10.2307/1375964

Cormie, A. B., & Schwarcz, H. P. (1996). Effects of climate on deer bone δ15N and δ13C: Lack of precipitation effects on δ15N for animals consuming low amounts of C4 plants. *Geochimica et Cosmochimica Acta*, *60*(21), 4161–4166. https://doi.org/10.1016/S0016-7037(96)00251-7

Craine, J. M., Brookshire, E. N. J., Cramer, M. D., Hasselquist, N. J., Koba, K., Marin-Spiotta, E., & Wang, L. (2015). Ecological interpretations of nitrogen isotope ratios of terrestrial plants and soils. *Plant and Soil*, *396*(1/2), 1–26.

Cuenca-Bescós, G., Straus, L. G., González Morales, M. R., & García Pimienta, J. C. (2009). The reconstruction of past environments through small mammals: From the Mousterian to the Bronze Age in El Mirón Cave (Cantabria, Spain). *Journal of Archaeological Science*, *36*(4), 947–955. https://doi.org/10.1016/j.jas.2008.09.025

DeNiro, M. J., & Epstein, S. (1978). Influence of diet on the distribution of carbon isotopes in animals. *Geochimica et Cosmochimica Acta*, *42*(5), 495–506. https://doi.org/10.1016/0016-7037(78)90199-0

Deniro, M. J., & Epstein, S. (1981). Influence of diet on the distribution of nitrogen isotopes in animals. *Geochimica et Cosmochimica Acta*, *45*(3), 341–351. https://doi.org/10.1016/0016-7037(81)90244-1

DeSantis, L. R. G., Crites, J. M., Feranec, R. S., Fox-Dobbs, K., Farrell, A. B., Harris, J. M., Takeuchi, G. T., & Cerling, T. E. (2019). Causes and Consequences of Pleistocene Megafaunal Extinctions as Revealed from Rancho La Brea Mammals. *Current Biology*, *29*(15), 2488-2495.e2. https://doi.org/10.1016/j.cub.2019.06.059

DeSantis, L. R. G., Feranec, R. S., Fox-Dobbs, K., Harris, J. M., Cerling, T. E., Crites, J. M., Farrell, A. B., & Takeuchi, G. T. (2020). Reply to Van Valkenburgh et al. *Current Biology*, *30*(4), R151–R152. https://doi.org/10.1016/j.cub.2020.01.011

Dice, L. R. (1925). Rodents and lagomorphs of the Rancho la Brea deposits. *Carnegie Institution of Washington*, *349*, 119–130.

Doyen, J. T., & Miller, S. E. (1980). Review of Pleistocene darkling ground beetles of the California asphalt deposits (Coleoptera: Tenebrionidae, Zopheridae). *Pan-Pacific Entomologist*, *56*(1), 1–10.

Ehleringer, J. R. (1978). Implications of quantum yield differences on the distributions of C3 and C4 grasses. *Oecologia*, *31*(3), 255–267. https://doi.org/10.1007/BF00346246

Ehleringer, J. R., & Monson, R. K. (1993). Evolutionary and Ecological Aspects of Photosynthetic Pathway Variation. *Annual Review of Ecology and Systematics*, *24*(1), 411–439. https://doi.org/10.1146/annurev.es.24.110193.002211

Feranec, R. S., Hadly, E. A., & Paytan, A. (2009). Stable isotopes reveal seasonal competition for resources between late Pleistocene bison (*Bison*) and horse (*Equus*) from Rancho La Brea, southern California. *Palaeogeography, Palaeoclimatology, Palaeoecology*, *271*(1), 153–160. https://doi.org/10.1016/j.palaeo.2008.10.005

Feranec, R. S., Hadly, E. A., & Paytan, A. (2010). Isotopes reveal limited effects of middle Pleistocene climate change on the ecology of mid-sized mammals. *Quaternary International*, *217*(1), 43–52. https://doi.org/10.1016/j.quaint.2009.07.018

Fox, N. S., Takeuchi, G. T., Farrell, A. B., & Blois, J. L. (2019). A protocol for differentiating late Quaternary leporids in southern California with remarks on Project 23 lagomorphs at Rancho La Brea, Los Angeles, California, USA. *PaleoBios*, *36*, 1–20.

Fox-Dobbs, K., Leonard, J. A., & Koch, P. L. (2008). Pleistocene megafauna from eastern Beringia: Paleoecological and paleoenvironmental interpretations of stable carbon and nitrogen isotope and radiocarbon records. *Palaeogeography, Palaeoclimatology, Palaeoecology*, *261*(1), 30–46. https://doi.org/10.1016/j.palaeo.2007.12.011

Fox-Dobbs, K., Stidham, T. A., Bowen, G. J., Emslie, S. D., & Koch, P. L. (2006). Dietary controls on extinction versus survival among avian megafauna in the late Pleistocene. *Geology*, *34*(8), 685–688. https://doi.org/10.1130/G22571.1

Friscia, A. R., Van Valkenburgh, B., Spencer, L., & Harris, J. (2008). Chronology and Spatial Distribution of Large Mammal Bones in Pit 91, Rancho la Brea. *PALAIOS*, *23*, 35–42.

Fuller, B. T., Fahrni, S. M., Harris, J. M., Farrell, A. B., Coltrain, J. B., Gerhart, L. M., Ward, J. K., Taylor, R. E., & Southon, J. R. (2014). Ultrafiltration for asphalt removal from bone collagen for radiocarbon dating and isotopic analysis of Pleistocene fauna at the tar pits of Rancho La Brea, Los Angeles, California. *Quaternary Geochronology*, *22*, 85–98. https://doi.org/10.1016/j.quageo.2014.03.002

Fuller, B. T., Fuller, J. L., Harris, D. A., & Hedges, R. E. M. (2006). Detection of breastfeeding and weaning in modern human infants with carbon and nitrogen stable isotope ratios. *American Journal of Physical Anthropology*, *129*(2), 279–293. https://doi.org/10.1002/ajpa.20249

Fuller, B. T., Harris, J. M., Farrell, A. B., Takeuchi, G. T., & Southon, J. R. (2015). Sample Preparation for Radiocarbon Dating and Isotopic Analysis of Bone from Rancho La Brea. *Natural History Museum of Los Angeles County Science Series*, *42*, 151–167.

Fuller, B. T., Southon, J. R., Fahrni, S. M., Farrell, A. B., Takeuchi, G. T., Nehlich, O., Guiry, E. J., Richards, M. P., Lindsey, E. L., & Harris, J. M. (2020). Pleistocene paleoecology and feeding behavior of terrestrial vertebrates recorded in a pre-LGM asphaltic deposit at Rancho La Brea, California. *Palaeogeography, Palaeoclimatology, Palaeoecology*, *537*, 109383. https://doi.org/10.1016/j.palaeo.2019.109383

Gill, J. L., Williams, J. W., Jackson, S. T., Lininger, K. B., & Robinson, G. S. (2009). Pleistocene Megafaunal Collapse, Novel Plant Communities, and Enhanced Fire Regimes in North America. *Science*, *326*(5956), 1100–1103. https://doi.org/10.1126/science.1179504

Grayson, D. K. (2006). The Late Quaternary biogeographic histories of some Great Basin mammals (western USA). *Quaternary Science Reviews*, *25*(21), 2964–2991. https://doi.org/10.1016/j.quascirev.2006.03.004

Hedges, R. E. M., Clement, J. G., Thomas, C. D. L., & O'Connell, T. C. (2007). Collagen turnover in the adult femoral mid-shaft: Modeled from anthropogenic radiocarbon tracer measurements. *American Journal of Physical Anthropology*, *133*(2), 808–816. https://doi.org/10.1002/ajpa.20598

Hendy, I. L. (2007). *Santa Barbara Basin ODP893A Planktonic Stable Isotope Data*. IGBP PAGES/World Data Center for Paleoclimatology Data Contribution Series # 2007-080. NOAA/NCDC Paleoclimatology Program, Boulder CO, USA.

Hendy, I. L., & Kennett, J. P. (1999). Latest Quaternary North Pacific surface-water responses imply atmosphere-driven climate instability. *Geology*, *27*(4), 291–294. https://doi.org/10.1130/0091-7613(1999)027<0291:LQNPSW>2.3.CO;2

Hendy, I. L., Kennett, J. P., Roark, E. B., & Ingram, B. L. (2002). Apparent synchroneity of submillennial scale climate events between Greenland and Santa Barbara Basin, California from 30–10ka. *Quaternary Science Reviews*, *21*(10), 1167–1184. https://doi.org/10.1016/S0277-3791(01)00138-X

Holden, A. R., Southon, J. R., Will, K., Kirby, M. E., Aalbu, R. L., & Markey, M. J. (2017). A 50,000 year insect record from Rancho La Brea, Southern California: Insights into past climate and fossil deposition. *Quaternary Science Reviews*, *168*, 123–136. https://doi.org/10.1016/j.quascirev.2017.05.001

Holt, R. D. (2009). Bringing the Hutchinsonian niche into the 21st century: Ecological and evolutionary perspectives. *Proceedings of the National Academy of Sciences*, *106*(Supplement 2), 19659–19665. https://doi.org/10.1073/pnas.0905137106

Hutchinson, G. E. (1957). Concluding remarks. *Cold Spring Harbor Symposium*, *22*, 415–427.

Ingles, L. G. (1941). Natural History Observations on the Audubon Cottontail. *Journal of Mammalogy*, *22*(3), 227–250. https://doi.org/10.2307/1374949

Jackson, A. L., Inger, R., Parnell, A. C., & Bearhop, S. (2011). Comparing isotopic niche widths among and within communities: SIBER - Stable Isotope Bayesian Ellipses in R: Bayesian isotopic niche metrics. *Journal of Animal Ecology*, *80*(3), 595–602. https://doi.org/10.1111/j.1365-2656.2011.01806.x

Jackson, S. T., & Overpeck, J. T. (2000). Responses of plant populations and communities to environmental changes of the late Quaternary. *Paleobiology*, *26*(sp4), 194–220. https://doi.org/10.1666/0094-8373(2000)26[194:ROPPAC]2.0.CO;2

Jenkins, S. G., Partridge, S. T., Stephenson, T. R., Farley, S. D., & Robbins, C. T. (2001). Nitrogen and carbon isotope fractionation between mothers, neonates, and nursing offspring. *Oecologia*, *129*(3), 336–341. https://doi.org/10.1007/s004420100755

Johnson, C. N. (2009). Ecological consequences of Late Quaternary extinctions of megafauna. *Proceedings of the Royal Society B: Biological Sciences*, *276*(1667), 2509–2519. https://doi.org/10.1098/rspb.2008.1921

Johnson, D. L. (1977). The late Quaternary climate of coastal California: Evidence for an ice age refugium. *Quaternary Research*, *8*(2), 154–179.

Koch, P. L. (1998). Isotopic Reconstruction of Past Continental Environments. *Annual Review of Earth and Planetary Sciences*, *26*(1), 573–613. https://doi.org/10.1146/annurev.earth.26.1.573

Koch, P. L., & Barnosky, A. D. (2006). Late Quaternary Extinctions: State of the Debate. *Annual Review of Ecology, Evolution, and Systematics*, *37*(1), 215–250. https://doi.org/10.1146/annurev.ecolsys.34.011802.132415

Koch, P. L., Hoppe, K. A., & Webb, S. D. (1998). The isotopic ecology of late Pleistocene mammals in North America: Part 1. Florida. *Chemical Geology*, *152*(1), 119–138. https://doi.org/10.1016/S0009-2541(98)00101-6

Kohn, M. J. (2010). Carbon isotope compositions of terrestrial C3 plants as indicators of (paleo)ecology and (paleo)climate. *Proceedings of the National Academy of Sciences*, *107*(46), 19691–19695. https://doi.org/10.1073/pnas.1004933107

Lamb, R. V. (1989). *The nonmarine mollusks of Pit 91, Rancho La Brea, southern California, and their paleoecologic and biogeographic implications.* [Master's thesis]. California State University, Northridge.

Marcus, L. F., & Berger, R. (1984). The significance of radiocarbon dates for Rancho La Brea. In P. S. Martin & R. G. Klein (Eds.), *Quarternary extinctions: A prehistoric revolution* (pp. 159–183). The University of Arizona Press.

Matsubayashi, J., & Tayasu, I. (2019). Collagen turnover and isotopic records in cortical bone. *Journal of Archaeological Science*, *106*, 37–44. https://doi.org/10.1016/j.jas.2019.03.010

McLean, B. S., & Emslie, S. D. (2012). Stable isotopes reflect the ecological stability of two high-elevation mammals from the late Quaternary of Colorado. *Quaternary Research*, *77*(3), 408–417. https://doi.org/10.1016/j.yqres.2012.02.001

Miller, G. J. (1968). On the age distribution of *Smilodon Californicus* Bovard from Rancho La Brea. *Contributions in Science*, *131*, 1–17.

Newsome, S. D., Rio, C. M. del, Bearhop, S., & Phillips, D. L. (2007). A niche for isotopic ecology. *Frontiers in Ecology and the Environment*, *5*(8), 429–436. https://doi.org/10.1890/060150.1

O'Keefe, F. R., Fet, E., & Harris, J. (2009). Compilation, Calibration, and Synthesis of Faunal and Floral Radiocarbon Dates, Rancho La Brea, California. *Contributions in Science*, *518*, 1–16.

O'Leary, M. H. (1988). Carbon Isotopes in Photosynthesis. *BioScience*, *38*(5), 328–336. https://doi.org/10.2307/1310735

R Core Team. (2020). *R: A language and environment for statistical computing. R Foundation for Statistical Computing* (Version 4.0.2) [Computer software]. https://www.R-project.org/

Reimer, P. J., Bard, E., Bayliss, A., Beck, J. W., Blackwell, P. G., Ramsey, C. B., Buck, C. E., Cheng, H., Edwards, R. L., Friedrich, M., Grootes, P. M., Guilderson, T. P., Haflidason, H., Hajdas, I., Hatté, C., Heaton, T. J., Hoffmann, D. L., Hogg, A. G., Hughen, K. A., … Plicht, J. van der. (2013). IntCal13 and Marine13 Radiocarbon Age Calibration Curves 0–50,000 Years cal BP. *Radiocarbon*, *55*(4), 1869–1887. https://doi.org/10.2458/azu_js_rc.55.16947

Siddall, M., Rohling, E. J., Thompson, W. G., & Waelbroeck, C. (2008). Marine isotope stage 3 sea level fluctuations: Data synthesis and new outlook. *Reviews of Geophysics*, *46*(4). https://doi.org/10.1029/2007RG000226

Smartt, R. A. (1977). The ecology of late Pleistocene and recent *Microtus* from south-central and southwestern New Mexico. *The Southwestern Naturalist*, *22*(1), 1–19. https://doi.org/10.2307/3670460

Smiley, T. M., Cotton, J. M., Badgley, C., & Cerling, T. E. (2016). Small-mammal isotope ecology tracks climate and vegetation gradients across western North America. *Oikos*, *125*(8), 1100–1109. https://doi.org/10.1111/oik.02722

Smith, B. N., & Epstein, S. (1971). Two Categories of 13C/12C Ratios for Higher Plants. *Plant Physiology*, *47*(3), 380–384. https://doi.org/10.1104/pp.47.3.380

Smith, J. E., Long, D. J., Russell, I. D., Newcomb, K. L., & Muñoz, V. D. (2016). Otospermophilus beecheyi (Rodentia: Sciuridae). *Mammalian Species*, *48*(939), 91–108. https://doi.org/10.1093/mspecies/sew010

Soberón, J., & Nakamura, M. (2009). Niches and distributional areas: Concepts, methods, and assumptions. *Proceedings of the National Academy of Sciences*, *106*, 19644–19650. https://doi.org/10.1073/pnas.0901637106

Somerville, A. D., Froehle, A. W., & Schoeninger, M. J. (2018). Environmental influences on rabbit and hare bone isotope abundances: Implications for paleoenvironmental research. *Palaeogeography, Palaeoclimatology, Palaeoecology*, *497*, 91–104. https://doi.org/10.1016/j.palaeo.2018.02.008

Somerville, A. D., Nelson, B. A., Punzo Díaz, J. L., & Schoeninger, M. J. (2020). Rabbit bone stable isotope values distinguish desert ecoregions of North America: Data from the archaeological sites of Pueblo Grande, La Ferreria, and La Quemada. *Journal of Archaeological Science*, *113*, 105063. https://doi.org/10.1016/j.jas.2019.105063

Southon, J. R., & Santos, G. M. (2004). Ion Source Development at Kccams, University of California, Irvine. *Radiocarbon*, *46*(1), 33–39. https://doi.org/10.1017/S0033822200039321

Stock, C., & Harris, J. M. (1992). Rancho La Brea: A record of Pleistocene life in California. *Science Series*, *37*, 1–113.

Terry, R. C. (2018). Isotopic niche variation from the Holocene to today reveals minimal partitioning and individualistic dynamics among four sympatric desert mice. *Journal of Animal Ecology*, *87*(1), 173–186. https://doi.org/10.1111/1365-2656.12771

Tieszen, L. L. (1991). Natural variations in the carbon isotope values of plants: Implications for archaeology, ecology, and paleoecology. *Journal of Archaeological Science*, *18*(3), 227–248. https://doi.org/10.1016/0305-4403(91)90063-U

Tomé, C. P., Smith, E. A. E., Lyons, S. K., Newsome, S. D., & Smith, F. A. (2020). Changes in the diet and body size of a small herbivorous mammal (hispid cotton rat, *Sigmodon hispidus*) following the late Pleistocene megafauna extinction. *Ecography*, *43*(4), 604–619. https://doi.org/10.1111/ecog.04596

Trayler, R. B., Dundas, R. G., Fox-Dobbs, K., & Van De Water, P. K. (2015). Inland California during the Pleistocene—Megafaunal stable isotope records reveal new paleoecological and paleoenvironmental insights. *Palaeogeography, Palaeoclimatology, Palaeoecology*, *437*, 132–140. https://doi.org/10.1016/j.palaeo.2015.07.034

Ugan, A., & Coltrain, J. (2011). Variation in collagen stable nitrogen values in black-tailed jackrabbits (*Lepus californicus*) in relation to small-scale differences in climate, soil, and topography. *Journal of Archaeological Science*, *38*(7), 1417–1429. https://doi.org/10.1016/j.jas.2011.01.015

Valkenburgh, B. V., Clementz, M. T., & Ben-David, M. (2020). Problems with inferring a lack of competition between Rancho La Brea dire wolves and sabertooth cats based on dental enamel. *Current Biology*, *30*(4), R149–R150. https://doi.org/10.1016/j.cub.2020.01.009

Van Meerbeeck, C. J., Renssen, H., & Roche, D. M. (2009). How did Marine Isotope Stage 3 and Last Glacial Maximum climates differ? – Perspectives from equilibrium simulations. *Climate of the Past*, *5*, 33–51.

Warter, J. K. (1976). Late Pleistocene plant communities–evidence from the Rancho La Brea tar pits. In J. Latting (Ed.), *Plant Communities of Southern California* (pp. 32–39). California Native Plant Society Special Publication No. 2.

Wiens, J. J. (2011). The niche, biogeography and species interactions. *Philosophical Transactions of the Royal Society B: Biological Sciences*, *366*(1576), 2336–2350. https://doi.org/10.1098/rstb.2011.0059

5.7 Tables

Table 5.1: Carbon ($\delta^{13}C$) and nitrogen ($\delta^{15}N$) isotope values, and/or radiocarbon ages (^{14}C age) and radiocarbon age uncertainties (+/-), of all 80 rabbit (*Sylvilagus*) and squirrel (*Otospermophilus*) specimens from which either or both were obtained. $\delta^{18}O$ values reflect *Neogloboquadrina pachyderma* $\delta^{18}O$ data from Hendy et al. (2007) linearly interpolated to the mean calibrated age of each specimens' Bayesian probability age distribution analyzed in OxCal v.4.3.2 using the IntCal13 calibration curve (Reimer et al. 2013). $\delta^{18}O$ values are only generated for specimens with measurable calibrated ages (i.e., < ~50,000 years BP) from which $\delta^{13}C$ and $\delta^{15}N$ values were also obtained (n = 66).

UCIAMS	LACM	Deposit	Taxon	$\delta^{13}C$ (‰)	$\delta^{15}N$ (‰)	^{14}C age (BP)	+/-	Collagen yield (%)	C:N (atomic)	$\delta^{18}O$ (‰)
216772	V-4516	No data	*Otospermophilus*	-20.7	3.8	2375	15	4.7	3.2	0.52
223494	HC-143517	No data	*Sylvilagus*	-18.8	6.2	2650	25	4.2	3.3	0.42
223493	HC-11584	Pit 10	*Otospermophilus*	-18.5	9.9	4505	20	6.6	3.3	0.62
216760	HC-11534	Pit 10	*Otospermophilus*	-20.8	3.6	5925	20	3.5	3.3	0.49
223528	V-4509	Pit 10	*Otospermophilus*	-18.6	4.4	6155	25	3.0	3.3	0.31
216761	HC-11587	Pit 10	*Otospermophilus*	-21.1	5.9	11105	25	2.1	3.3	1.44
216766	HC-142767	No data	*Sylvilagus*	-22.0	7.6	13990	40	1.9	3.4	2.71
216767	HC-142772	No data	*Sylvilagus*	-21.9	4.9	14390	40	1.9	3.4	2.70
223513	P23-40634	P23-14	*Sylvilagus*	-21.3	7.2	25830	140	3.1	3.3	2.50
198298	P23-33235	P23-14	*Otospermophilus*	-20.9	7.0	26310	150	2.3	3.4	2.45
223587	P23-40642	P23-14	*Otospermophilus*	-20.3	6.4	26710	110	4.0	3.3	2.31
223516	P23-40637	P23-14	*Sylvilagus*	-20.9	7.9	26780	160	2.7	3.3	2.27
223515	P23-40636	P23-14	*Sylvilagus*	-	-	27200	160	0.5	NA	NA
223524	V-2641	P23-14	*Sylvilagus*	-20.9	7.2	28090	180	1.6	3.3	1.95
223529	V-4519	No data	*Otospermophilus*	-19.3	9.4	28370	180	2.0	3.3	1.88
217078	V-2174	Pit 16	*Sylvilagus*	-22.3	8.2	28500	240	1.3	3.4	2.38
216765	HC-142766	Pit 16	*Sylvilagus*	-21.3	8.4	28600	240	2.6	3.4	2.23
216771	V-2173	Pit 16	*Sylvilagus*	-22.5	6.9	30320	290	1.7	3.3	2.19

198206	P23-33228	P23-1	*Otospermophilus*	-20.7	6.4	30480	290	2.9	3.9	2.14
223526	V-2737	No data	*Sylvilagus*	-21.2	8.1	30540	240	2.6	3.2	1.92
198302	P23-33228	P23-1	*Otospermophilus*	-20.2	6.7	30870	270	3.1	3.3	1.58
216780	V-4531	Pit 16	*Otospermophilus*	-21.4	4.5	30900	320	1.6	3.4	1.44
216781	P23-35670	P23-7B	*Otospermophilus*	-21.5	6.6	30970	320	5	3.3	1.58
216779	V-4524	No data	*Otospermophilus*	-20.7	5.3	31000	320	2.1	3.4	1.62
223507	P23-39818	P23-13	*Sylvilagus*	-22.2	6.4	31230	270	3.3	3.5	1.65
216773	V-4520	No data	*Otospermophilus*	-20.4	6.3	31340	330	1.9	3.3	1.70
223525	V-2644	Pit 4	*Sylvilagus*	-21.1	8.6	31460	260	2.6	3.3	1.47
198207	P23-33229	P23-1	*Otospermophilus*	-20.9	8.5	31830	340	2.4	3.4	2.26
223508	P23-39822	P23-13	*Sylvilagus*	-21.1	9.4	31980	280	2.7	3.4	2.30
198201	P23-17139	P23-1	*Otospermophilus*	-20.4	7.6	32500	370	1.3	3.3	1.42
223509	P23-39825	P23-13	*Otospermophilus*	-21.2	6.2	32660	300	4.5	3.3	1.57
198295	P23-31113	P23-14	*Otospermophilus*	-20.8	8.8	33070	350	1.2	3.4	1.70
198203	P23-26592	P23-1	*Otospermophilus*	-21	4.0	33100	620	1.1	3.4	1.76
223505	P23-39811	P23-13	*Sylvilagus*	-21.9	7.3	33260	320	2.0	3.4	1.65
223499	P23-36896	P23-13	*Sylvilagus*	-21.5	4.2	33590	340	3.8	3.3	1.85
191099	P23-28903	P23-1	*Sylvilagus*	-21.1	9.1	33830	480	1.2	3.3	1.73
223498	P23-36859	P23-13	*Otospermophilus*	-21.2	8.7	34800	390	5.0	3.4	2.40
191097	P23-22009	P23-1	*Sylvilagus*	-22.4	6.7	35150	580	1.1	3.6	2.27
223500	P23-36907	P23-13	*Otospermophilus*	-21.0	3.7	35230	410	1.9	3.4	2.38
223501	P23-36910	P23-13	*Otospermophilus*	-21.2	3.9	35270	410	5.5	3.4	2.41
191102	P23-31423	P23-1	*Sylvilagus*	-21.3	7.3	35420	580	1.5	3.5	2.32
191096	P23-18270	P23-1	*Sylvilagus*	-22.5	4.5	35440	580	1.7	3.5	2.15
216770	HC-142779	Pit A	*Sylvilagus*	-22.1	6.9	35740	570	0.95	3.4	2.28
191095	P23-5233	P23-1	*Sylvilagus*	-21.3	8.4	35750	610	2.7	3.3	2.33
191100	P23-30238	P23-1	*Sylvilagus*	-21.5	7.3	35780	600	1.2	3.6	2.07
223527	V-2751	No data	*Sylvilagus*	-21.3	4.5	35870	450	1.6	3.3	2.23

198202	P23-20172	P23-1	*Otospermophilus*	-21.4	4.4	35900	560	1.5	3.4	2.25
191098	P23-25476	P23-1	*Sylvilagus*	-21.4	7.4	36050	630	1.4	3.4	2.23
198204	P23-30796	P23-1	*Otospermophilus*	-21.1	3.8	36160	910	1.2	3.3	2.24
223506	P23-39812	P23-13	*Sylvilagus*	-21.2	8.2	36260	470	3.5	3.3	1.87
216764	HC-142764	Pit 16	*Sylvilagus*	-21.0	6.9	36350	620	2.5	3.4	1.44
198205	P23-33227	P23-1	*Otospermophilus*	-20.7	7.0	36580	610	3.2	3.7	1.60
223517	P23-40638	P23-14	*Sylvilagus*	-21.4	7.2	36870	500	1.1	3.4	1.94
216763	HC-142763	Pit 16	*Sylvilagus*	-21.4	7.6	36880	660	2.6	3.4	1.90
223522	P23-40644	P23-14	*Sylvilagus*	-	-	38490	610	0.4	NA	NA
223585	P23-35541	P23-13	*Sylvilagus*	-21.4	5.2	39220	460	2.7	3.3	2.05
223497	P23-36693	P23-13	*Sylvilagus*	-22.0	7.0	39240	670	1.3	3.5	2.31
198294	P23-28902	P23-1	*Sylvilagus*	-20.9	5.5	39700	810	0.8	3.5	2.03
223496	P23-36572	P23-13	*Otospermophilus*	-20.9	6.2	40640	800	1.9	3.5	1.52
216768	HC-142773	Pit A	*Sylvilagus*	-21.8	7.8	41000	1100	1.1	3.4	1.89
216784	P23-36332	P23-7B	*Sylvilagus*	-21.7	5.6	41500	1200	1.7	3.2	1.73
216783	P23-35774	P23-7B	Leporidae	-21.6	4.9	42600	1400	2.5	3.3	2.10
216769	HC-142778	Pit A	*Sylvilagus*	-21.3	5.2	42900	1400	1.4	3.4	1.81
216762	HC-130857	Bliss 29	*Otospermophilus*	-21.2	4.5	43700	1600	2.7	3.4	1.97
223502	P23-36989	P23-13	*Sylvilagus*	-21.4	7.2	44000	1200	4.2	3.5	1.92
191101	P23-31269	P23-1	*Sylvilagus*	-20.5	8.1	46200	2200	2	3.3	1.63
217079	P23-36331	P23-7B	*Sylvilagus*	-21.4	6.6	46200	2400	1.2	3.3	1.75
223503	P23-37612	P23-13	*Sylvilagus*	-21.4	5.7	46200	1600	3.0	3.4	1.88
198296	P23-31118	P23-14	*Otospermophilus*	-19.3	3.2	47400	2000	0.7	3.5	NA
223504	P23-37651	P23-13	*Otospermophilus*	-20.1	6.8	47400	1800	4.3	3.4	NA
223519	P23-40640	P23-14	*Sylvilagus*	-	-	49400	2400	0.3	NA	NA
223518	P23-40639	P23-14	*Sylvilagus*	-21.7	6.9	49800	2500	1.1	3.3	NA
216785	P23-36336	P23-7B	*Sylvilagus*	-22.1	5.3	50200	3500	1	3.3	NA
191103	P23-31033	P23-14	*Sylvilagus*	-21.7	8.5	>47800	NA	0.8	3.5	NA
191104	P23-31036	P23-14	*Sylvilagus*	-22.3	7.3	>49900	NA	1.8	5.6	NA

191105	P23-31056	P23-14	*Sylvilagus*	-21.7	7.3	>49900	NA	1.1	4.0	NA
223523	P23-40647	P23-14	*Sylvilagus*	-21.0	9.6	>49900	NA	1.8	3.4	NA
191242	P23-31031	P23-14	*Sylvilagus*	-21.1	4.3	>50800	NA	1.1	3.5	NA
223514	P23-40635	P23-14	*Sylvilagus*	-21.6	6.2	>51700	NA	1.7	3.3	NA
-	P23-31115	P23-14	*Otospermophilus*	-19.0	7.1	-	NA	0.7	3.4	NA

Table 5.2: SIBER summary statistics defined in Jackson et al. (2011) of isotopic niches illustrated in Figure 5.3. TA = convex hull area, SEA = standard ellipse area, SEA_c = corrected standard ellipse area (adjusted for groups with small sample sizes).

	Sylvilagus Pre-LGM	*Sylvilagus* Post-LGM	*Otospermophilus* Pre-LGM	*Otospermophilus* Post-LGM
TA	7.38	4.25	11.49	9.60
SEA	1.91	7.71	3.20	8.75
SEA_c	1.96	15.42	3.34	11.67

5.8 Figures

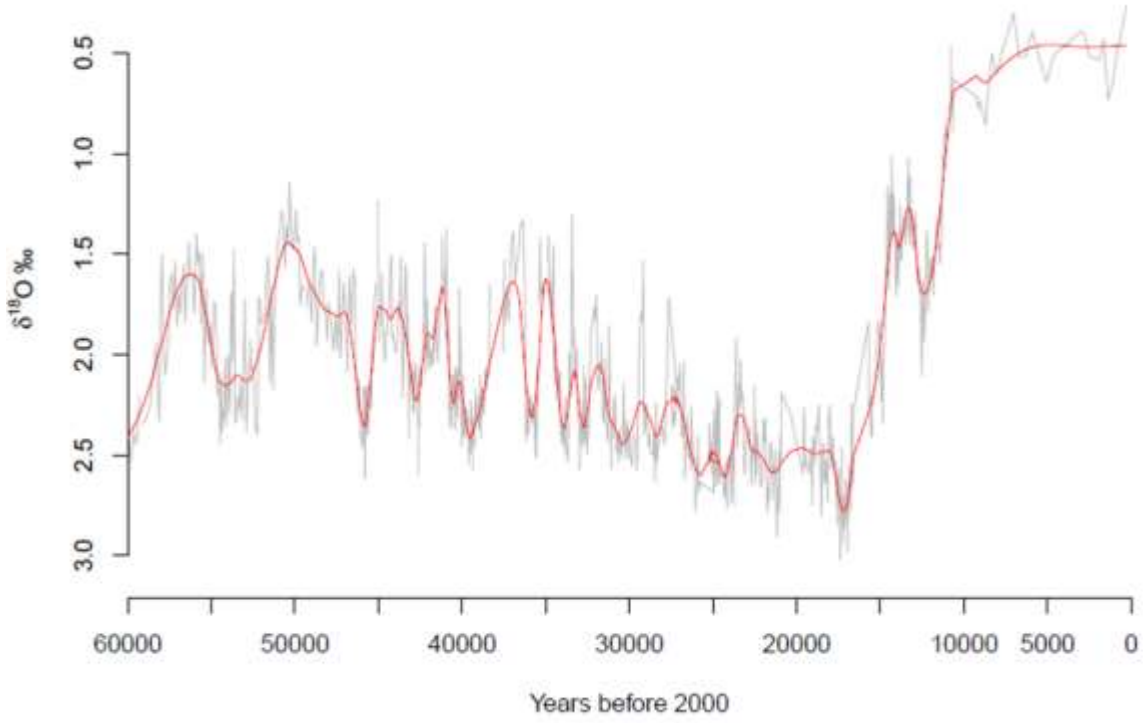

Figure 5.1: Marine foraminifera (*Neogloboquadrina pachyderma*) $\delta^{18}O$ climate record from Santa Barbara Basin ODP Hole 893A (Hendy et al., 2007). A locally estimated scatterplot smoothing (LOESS) polynomial (red line) is fitted over the original data (gray line) with a smoothing parameter $\alpha = 0.05$.

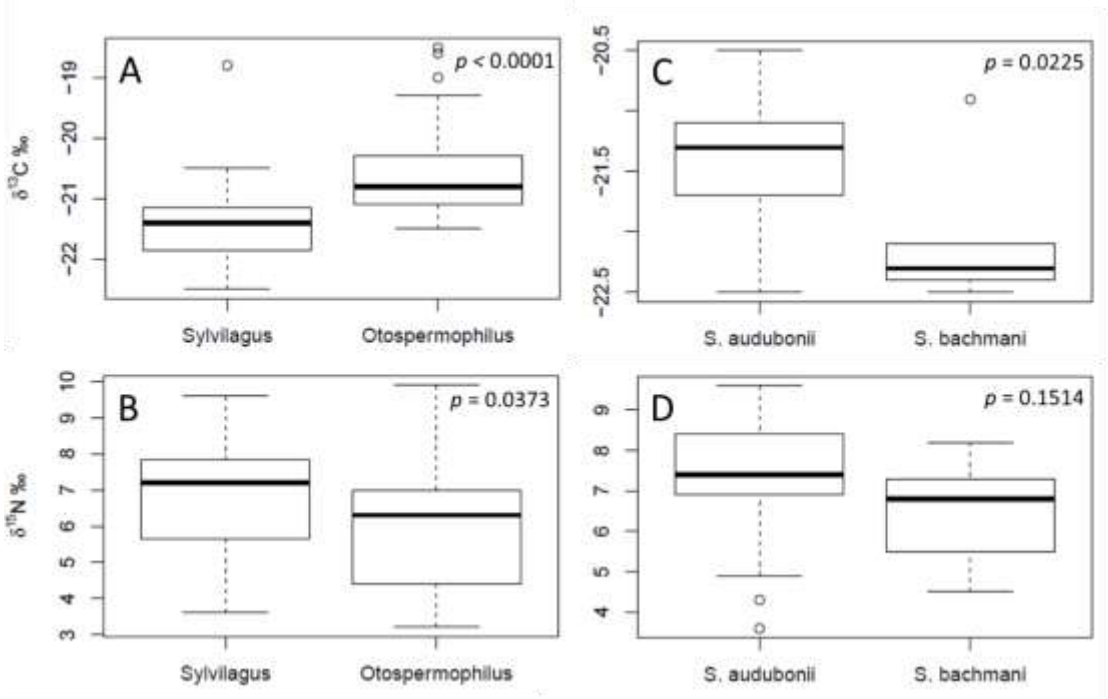

Figure 5.2: Boxplots of time-averaged stable isotopes with Wilcoxon rank-sum test significance values. A) Carbon isotope differences between *Sylvilagus* spp. (n = 48) and *Otospermophilus* ?*beecheyi* (n = 29), B) nitrogen isotope differences between *Sylvilagus* spp. (n = 48) and *Otospermophilus* ?*beecheyi* (n = 29), C) carbon isotope differences between a subset of *Sylvilagus* specimens identified as *Sylvilagus audubonii* (n = 21) and S. *bachmani* (n = 6), D) nitrogen isotope differences between *Sylvilagus audubonii* (n = 21) and S. *bachmani* (n = 6).

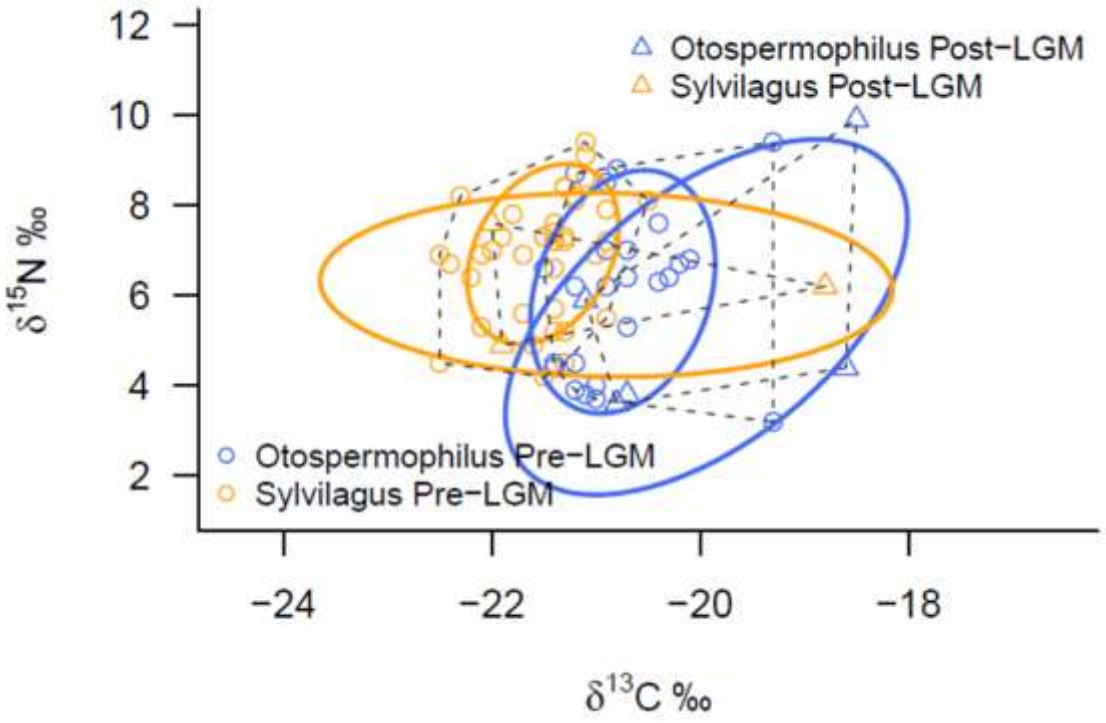

Figure 5.3: Carbon and nitrogen isotope niches of squirrels (*Otospermophilus*) and rabbits (*Sylvilagus*) depicting convex hulls (dashed lines) and 68% confidence interval ellipses generated in the R package SIBER. Pre-LGM communities contain specimens dating prior to the Last Glacial Maximum (~50,000 to 26,000 calibrated years BP, n = 62). Post-LGM communities contain specimens dating after the Last Glacial Maximum (< 18,000 years BP, n = 8). No sampled specimens date within the LGM (~26,000 to 18,000 years BP).

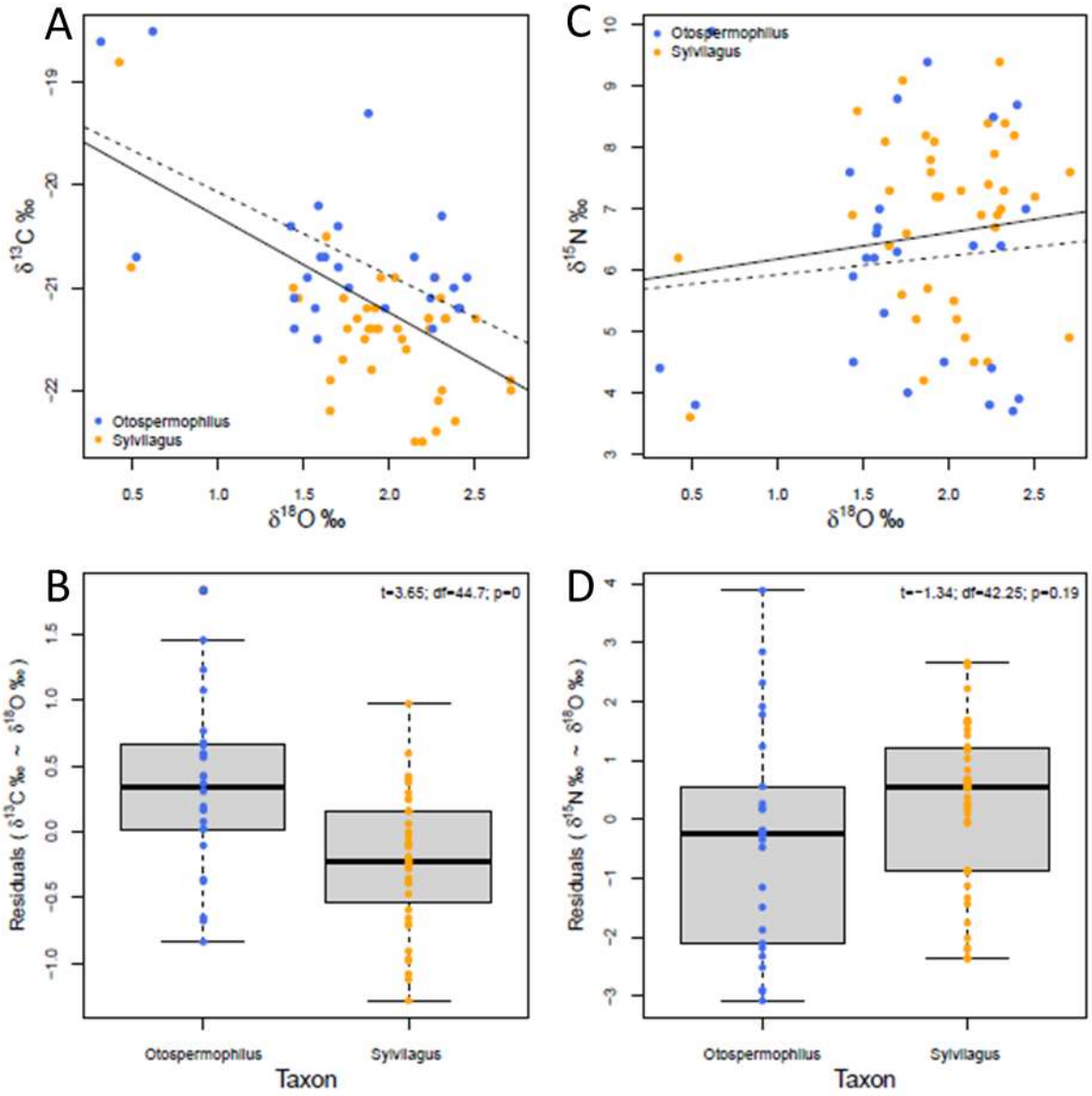

Figure 5.4: The relationship between isotope niche and climate. A) and C) show the relationship between small mammal $\delta^{13}C$ and $\delta^{15}N$, respectively, and $\delta^{18}O$ from the Santa Barbara Basin ODP Hole 893A planktonic foraminifera climate dataset of (Hendy et al., 2007) linearly interpolated to the calibrated age of each specimen. In both panels, the dashed line indicates the fitted relationship between $\delta^{13}C$ or $\delta^{15}N$ and $\delta^{18}O$ from the final model which includes taxon as an independent variable. The solid line indicates the fitted relationship between $\delta^{13}C$ or $\delta^{15}N$ and $\delta^{18}O$ from a linear model that just includes $\delta^{18}O$ as the independent variable. B) and D) indicate the residuals from climate-only models, plotted by taxon. Model summary statistics for A) are – climate-only: $R^2 = 0.38$, $t = -6.231$, $p = <0.0001$; climate + taxon: $R^2 = 0.50$, t (climate) = -5.873, p (climate) = <0.0001, t (taxon) = -3.924, p (taxon) = 0.0002. C) climate-only: $R^2 = 0.02$, $t = 1.105$, $p = 0.273$; climate + taxon: $R^2 = 0.05$, t (climate) = 0.771, p (climate) = 0.444, t (taxon) = -1.450, p (taxon) = 0.152.

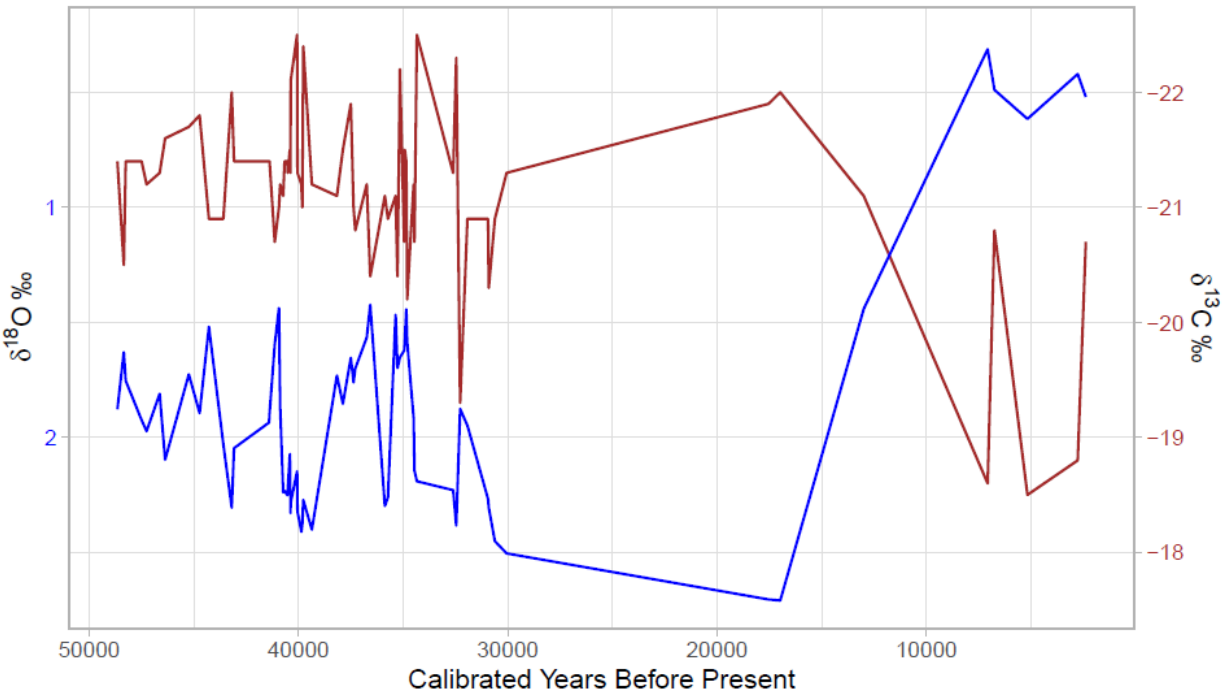

Figure 5.5: Pooled *Sylvilagus* and *Otospermophilus* $\delta^{13}C$ (brown) and *Neogloboquadrina pachyderma* $\delta^{18}O$ (blue), shown in Figure 4A, plotted through time against the OxCal calibrated age of each specimen (n = 66). The y-axes are inverted, with lower $\delta^{18}O$ values reflecting warmer temperatures than more positive values.

5.9 Appendix

Table 5.9.1: Twenty-two destructively sampled fossils from RLB that yielded insufficient collagen for isotopic analysis.

LACM number	Deposit	Taxon
P23-31032	14	*Sylvilagus*
P23-31035	14	*Sylvilagus*
P23-31039	14	*Sylvilagus*
P23-31043	14	*Sylvilagus*
P23-31052	14	*Sylvilagus*
P23-31055	14	*Sylvilagus*
P23-36331	7B	*Sylvilagus*
P23-31114	14	*Otospermophilus*
P23-33230	14	*Sylvilagus*
P23-33231	14	*Sylvilagus*
P23-36572	13	*Otospermophilus*
P23-37097	13	*Otospermophilus*
P23-40643	14	*Otospermophilus*
P23-40645	14	*Otospermophilus*
P23-40646	14	*Sylvilagus*
HC-11541	Pit 10	*Sylvilagus*
HC-130889	Pit A	*Otospermophilus*
HC-142770	No data	*Sylvilagus*
HC-142782	Pit A	*Sylvilagus*
HC-142783	Pit A	*Sylvilagus*
V-2645	Pit 4	*Sylvilagus*
V-4522	No data	*Otospermophilus*

Table 5.9.2: Carbon ($\delta^{13}C$) and nitrogen ($\delta^{15}N$) isotope values, and/or radiocarbon ages (^{14}C age) and radiocarbon age uncertainties (+/-), of all seven non-leporid or sciurid specimens sampled.

UCIAMS	LACM	Deposit	Taxon	$\delta^{13}C$ (‰)	$\delta^{15}N$ (‰)	^{14}C age (BP)	+/-	Collagen yield (%)	C:N (atomic)
198208	P23-33233	P23-14	*Neotoma*	-21.1	8.2	25620	160	1.4	3.8
198297	P23-33232	P23-14	*Thomomys*	-21.6	3.9	28600	210	0.6	3.6
223520	P23-40641	P23-14	*Neotoma*	-	-	28750	190	0.5	NA
198200	P23-11485	P23-1	*Canis latrans*	-19.9	11.1	35050	510	2	3.5
198199	P23-2046	P23-1	*Canis latrans*	-17.0	12.3	35770	550	2.6	3.3
216782	P23-35691	P23-7B	*Mustela frenata*	-20.2	10.4	38750	840	3.1	3.2
-	P23-33234	P23-14	*Microtus*	-22.2	5.6	-	NA	0.5	3.4